# Investigation of novel therapeutic strategies in B cell and antibody mediated disease

**Dr Gemma Deborah Banham**

**Pembroke College, Cambridge**

**Department of Medicine, University of Cambridge**

**Supervisor: Dr Menna Clatworthy**

**May 2018**

***This dissertation is submitted for the degree of Doctor of Philosophy***

**Summary**

**Investigation of novel therapeutic strategies in B cell and antibody mediated disease**

**Dr Gemma Deborah Banham**

Terminally differentiated B cells are responsible for antibody generation, a key component of adaptive immunity. IgG antibodies play an important role in defence against infection but can be pathogenic in some autoimmune diseases and in solid organ transplantation. In addition to antibody generation, there is increasing interest in the antibody-independent functions of B cells, including their ability to regulate immune responses via the production of IL10.

In this thesis I firstly explored the therapeutic potential of belimumab, an anti-BLyS antibody, in an experimental medicine study in kidney transplant recipients. The rationale for this study was based on published studies showing that B cells activate alloreactive T cells and secrete human leukocyte antigen (HLA) and non-HLA antibodies that negatively affect graft function and survival, but may also play a protective role by regulating alloimmune responses promoting transplant tolerance. B-Lymphocyte Stimulator (BLyS) is a cytokine that promotes B cell activation and survival. We performed the first randomized controlled trial using belimumab as early maintenance immunosuppression in kidney transplantation. In belimumab-treated subjects, we demonstrate a reduction in naïve and activated memory B cells, plasmablasts, IgG transcripts in peripheral blood and new antibody formation as well as evidence of reduced CD4 T cell activation and of a skewing of the residual B cell compartment towards an IL10-producing regulatory phenotype. This experimental medicine study highlights the potential of belimumab as a novel therapeutic agent in transplantation.

In the second part of my project I performed a preclinical study investigating the potential efficacy of bromodomain inhibitors in reducing antibody-mediated immune cell activation. Immune complexed antigen can activate mononuclear phagocytes (MNP), comprising macrophages and dendritic cells (DCs), via ligation of Fc gamma receptors (FcγR), that bind the Fc region of IgG. FcγR-dependent MNP activation results in profound changes in gene expression that mediate antibody effector function in these cells. The resulting inflammatory response can be pathological in the setting of autoimmune diseases, such as systemic lupus erythematosus and in antibody-mediated rejection in transplantation. BET proteins are a family of histone modification 'readers' that bind acetylated lysine residues within histones and function as a scaffold for the assembly of complexes that regulate gene transcription. Bromodomain inhibitors (I-BET) selectively inhibit the transcription of a subset of inflammatory genes in macrophages following toll-like receptor stimulation. Since MNPs

make a key contribution to antibody-mediated pathology, we sought to determine the extent to which I-BET inhibits macrophage and DC activation by IgG.

We show that I-BET delays phagolysosome maturation associated with build-up of immune complex (IC) whilst selectively inhibiting IC induced cytokine production. I-BET changed MNP morphology, resulting in a less adherent phenotype, prompting an assessment of its impact on DC migration. In vitro, in a three-dimensional collagen matrix, IgG-IC induced augmentation of DC chemotaxis to chemokine (C-C motif) ligand 19 (CCL19) was abrogated by the addition of I-BET. In vivo, two photon imaging showed that systemic I-BET treatment reduced IC-induced dermal DC mobilisation. Tissue DCs and transferred DC also had reduced migration to draining lymph nodes following I-BET treatment. These observations provide mechanistic insight into the potential therapeutic benefit of I-BET in the setting of antibody-associated inflammation.

**Contents**

**Preface**

This dissertation is the result of my own work and includes nothing which is the outcome of work done in collaboration, except as declared in the Preface and specified in the text.

This dissertation is not substantially the same as any that I have submitted, or is being concurrently submitted for a degree of diploma or other qualification at the University of Cambridge or any other University or similar institution except as declared in the Preface and specified in the text.

I further state that no substantial part of my dissertation has already been submitted, or is being concurrently submitted for any such degree, diploma or other qualification at the University of Cambridge or any other University or similar institution except as declared in the Preface and specified in the text.

My dissertation does not exceed the prescribed word limit (and is approximately 50000 words long excluding references).

……

Gemma Deborah Banham

May 2018

**List of commonly used abbreviations**

| | |
|---|---|
| 2D | two-dimensional |
| 3D | three-dimensional |
| A/I | activatory to inhibitory ratio |
| ABMR | antibody mediated rejection |
| ADCC | antibody dependent cellular cytotoxicity |
| ADPR | ADP ribose |
| anti-dsDNA | anti-double stranded DNA |
| APRIL | a proliferation-inducing ligand |
| Arp2/3 | actin-related proteins 2 and 3 |
| ATG | anti-thymocyte globulin |
| BAFF | B cell activating factor |
| BAFF-R | B cell activating factor receptor |
| BCMA | B cell maturation protein A |
| BCR | B cell receptor |
| BET | bromodomain and extraterminal domain |
| BLyS | B Lymphocyte Stimulator |
| BMDC | bone marrow derived dendritic cells |
| BMDM | bone marrow derived macrophages |
| BPAR | biopsy proven acute rejection |
| Breg | regulatory B cells |
| CFSE | carboxyfluorescein succinimidyl ester |
| cADPR | cyclic ADP ribose |
| CCL19 | chemokine (C-C motif) ligand 19 |
| CCR7 | C-C chemokine receptor type 7 |
| cDC | conventional DC |
| CDK9 | cyclin-dependent kinase 9 |
| CDR | complementarity determining regions |
| CFA | complete Freund's adjuvant |
| CIA | Collagen induced arthritis |
| CLR | C-type lectin receptors |
| CMV | cytomegalovirus |
| CpG | CpG oligodeoxynucleotides |
| CUC | Clinical Unit Cambridge |
| CXCL12 | C-X-C Motif Chemokine Ligand 12 |
| DAG | diacylglycerol |
| DAMPs | damage associated molecular patterns |
| DC | dendritic cell |
| DCD | donated after circulatory death |
| DNA | deoxyribonucleic acid |
| DSA | donor specific anti-HLA antibody |
| EAE | experimental autoimmune encephalomyelitis |
| EC | ethics committee |
| EDIL3 | EGF-like repeats and discoidin I-like domains 3 |
| EGFP | enhanced green fluorescent protein |

| | |
|---|---|
| ESRF | end-stage renal failure |
| EYFP | enhanced yellow fluorescent protein |
| Fab | fragment antigen binding |
| Fc | fragment crystallizable |
| FcRn | neonatal Fc receptor |
| FCS | fetal calf serum |
| FcγR | Fc gamma receptor |
| FDR | False Discovery Rate |
| FITC | fluorescein isothiacyanate |
| GCP | good clinical practice |
| GDNF | glial cell-derived neurotrophic factor |
| GM-CSF | Granulocyte-macrophage colony-stimulating factor |
| GSK | GlaxoSmithKline |
| GWAS | genome wide association studies |
| H&E | Hematoxylin and Eosin |
| HLA | human leucocyte antigen |
| I-BET | Bromodomain inhibitor |
| IC | immune complex |
| ICOS | inducible costimulator |
| ICOS | inducible T cell costimulator |
| IFA | Incomplete Freund's Adjuvant |
| IFN | interferon |
| Ig | immunoglobulin |
| IL | interleukin |
| iNOS | inducible nitrous oxide synthase |
| IP | intraperitoneal |
| IP3 | inositol trisphosphate |
| IRB | Institutional review board |
| IRF1 | interferon regulatory factor 1 |
| ITAM | immunoreceptor tyrosine-based activation motif |
| ITIM | immunoreceptor tyrosine-based inhibition motif |
| IV | intravenous |
| IVIG | intravenous immunoglobulin |
| JAM1 | junctional adhesion molecule 1 |
| JNK | c-Jun N-terminal kinase |
| KO | knockout |
| LCMV | lymphocytic choriomeningitis virus |
| LT | lymphotoxin |
| Mcl1 | myeloid cell leukaemia 1 |
| M-CSF | macrophage colony-stimulating factor |
| Mek | mitogen-activated protein extracellular signal-related kinase |
| MFI | Geometric mean fluorescence intensity |
| MHC | Major-histocompatibility-complex |
| MICA | MHC class I related chain A |
| MITT | modified intention to treat |
| MMF | mycophenolate mofetil |

| | |
|---|---|
| MMP | matrix metalloproteinase |
| MMRM | mixed model for repeated measures |
| MNP | including mononuclear phagocyte |
| MoDC | monocyte derived DC |
| MOG | myelin oligodendrocyte glycoprotein |
| NF-κB | nuclear factor kappa B |
| NLR | nucleotide oligomerization domain (NOD)-like receptor |
| NSM | non-switched memory |
| NTN | nephrotoxic nephritis |
| On-Trt | On-Treatment |
| OVA | ovalbumin |
| OVA-647 | ovalbumin conjugated to alexa flour 647 |
| OVA-IC | immune complexed ovalbumin |
| PAMPs | pathogen associated molecular patterns |
| PAS | Periodic acid–Schiff |
| PBMC | peripheral blood mononuclear cells |
| PBS | phosphate buffered saline |
| PC1 | principal component 1 |
| PC2 | principal component 2 |
| pDC | plasmacytoid DC |
| PGE2 | prostaglandin E2 |
| PI3K | phosphoinositide 3-kinase |
| PIB | phorbol 12-myristate 13-acetate, ionomycin and brefeldin A |
| PK | pharmacokinetic |
| PKC | protein kinase C |
| PLCγ | phospholipase Cγ |
| PMA | phorbol 12-myristate 13-acetate |
| Post-Trt | Post-Treatment |
| PP | per protocol |
| P-TEFb | positive transcription elongation factor |
| QC | quality control |
| RAP | reporting and analysis plan |
| RCT | randomised controlled trial |
| RNA | ribonucleic acid |
| RNA Pol II | RNA-polymerase II |
| rtPCR | reverse transcription polymerase chain reaction |
| SC | subcutaneous |
| sI-BET | significantly suppressed by I-BET |
| siRNA | small interfering RNA |
| SLE | systemic lupus erythematosis |
| SLO | secondary lymphoid organ |
| SM | switched memory |
| SNEC | secondary necrotic cell-derived material |
| SNPs | single nucleotide polymorphisms |
| Syk | Spleen tyrosine kinase |
| T1 | transitional type 1 |

| | |
|---|---|
| T2 | transitional type 2 |
| T3 | transitional type 3 |
| TACI | transmembrane activator and CAML interactor |
| TCMR | T cell mediated rejection |
| Tfh | T follicular helper cells |
| TGF-b | transforming growth factor beta |
| TLO | tertiary lymphoid organ |
| TLR | toll like receptor |
| TNF-α | tumour necrosis factor alpha |
| TrB | transitional B cells |
| Treg | regulatory T cell |
| WASP | Wiskott–Aldrich syndrome protein |

**Summary: Investigation of novel therapeutic strategies in B cell and antibody mediated disease**

Terminally differentiated B cells are responsible for antibody generation, a key component of adaptive immunity. IgG antibodies play an important role in defence against infection but can be pathogenic in some autoimmune diseases and in solid organ transplantation. In addition to antibody generation, there is increasing interest in the antibody-independent functions of B cells, including their ability to regulate immune responses via the production of IL10.

In this thesis I firstly explored the therapeutic potential of belimumab, an anti-BLyS antibody, in an experimental medicine study in kidney transplant recipients. The rationale for this study was based on published studies showing that B cells activate alloreactive T cells and secrete human leukocyte antigen (HLA) and non-HLA antibodies that negatively affect graft function and survival, but may also play a protective role by regulating alloimmune responses promoting transplant tolerance. B-Lymphocyte Stimulator (BLyS) is a cytokine that promotes B cell activation and survival. We performed the first randomized controlled trial using belimumab as early maintenance immunosuppression in kidney transplantation. In belimumab-treated subjects, we demonstrate a reduction in naïve and activated memory B cells, plasmablasts, IgG transcripts in peripheral blood and new antibody formation as well as evidence of reduced CD4 T cell activation and of a skewing of the residual B cell compartment towards an IL10-producing regulatory phenotype. This experimental medicine study highlights the potential of belimumab as a novel therapeutic agent in transplantation.

In the second part of my project I performed a preclinical study investigating the potential efficacy of bromodomain inhibitors in reducing antibody-mediated immune cell activation. Immune complexed antigen can activate mononuclear phagocytes (MNP), comprising macrophages and dendritic cells (DCs), via ligation of Fc gamma receptors (FcγR), that bind the Fc region of IgG. FcγR-dependent MNP activation results in profound changes in gene expression that mediate antibody effector function in these cells. The resulting inflammatory response can be pathological in the setting of autoimmune diseases, such as systemic lupus erythematosus and in antibody-mediated rejection in transplantation. BET proteins are a family of histone modification 'readers' that bind acetylated lysine residues within histones and function as a scaffold for the assembly of complexes that regulate gene transcription. Bromodomain inhibitors (I-BET) selectively inhibit the transcription of a subset of inflammatory genes in macrophages following toll-like receptor stimulation. Since MNPs make a key contribution to antibody-mediated pathology, we sought to determine the extent to which I-BET inhibits macrophage and DC activation by IgG.

We show that I-BET delays phagolysosome maturation associated with build-up of immune complex (IC) whilst selectively inhibiting IC induced cytokine production. I-BET changed MNP morphology, resulting in a less adherent phenotype, prompting an assessment of its impact on DC migration. *In vitro*, in a three-dimensional collagen matrix, IgG-IC induced augmentation of DC chemotaxis to chemokine (C-C motif) ligand 19 (CCL19) was abrogated by the addition of I-BET. *In vivo*, two photon imaging showed that systemic I-BET treatment reduced IC-induced dermal DC mobilisation. Tissue DCs and transferred DC also had reduced migration to draining lymph nodes following I-BET treatment. These observations provide mechanistic insight into the potential therapeutic benefit of I-BET in the setting of antibody-associated inflammation.

**Chapter 1: Introduction**

### 1.1 B cell development and function

#### 1.1.1 B cells and antibody

The immune system is comprised of an innate, rapidly responding component and an adaptive component. The latter is characterised by a capacity to adapt antigen-specific receptors to enhance immune responses as they develop and exhibit memory of previous exposure. B cells are the central mediators of humoral adaptive immunity. B cells are lymphocytes characterised by the surface expression of a B cell receptor (BCR), a membrane bound antigen-binding immunoglobulin (Ig) coupled with a signal transduction moiety. Immunoglobulins are made up of two heavy and two light chains, each of which contain variable and constant domains (Figure 1)(Janeway CA Jr 2001). The crystal structure of the immunoglobulin domain reveals β strands which form a characteristic β sheet fold (Bork 1994). The fragment antigen binding (Fab) region is made up of one constant and one variable domain from each light and heavy chain. Hypervariable regions known as complementarity determining regions (CDR) are found in the loops that extend between the β sheet structures. Three CDR are found on each of the light ($V_L$) and heavy ($V_H$) chains of the variable domains. CDR are responsible for binding to antigen; variation in CDR largely determines the binding affinity of specific antibody-antigen combinations and allows for a broad range of antibody specificities (Sela-Culang 2013).

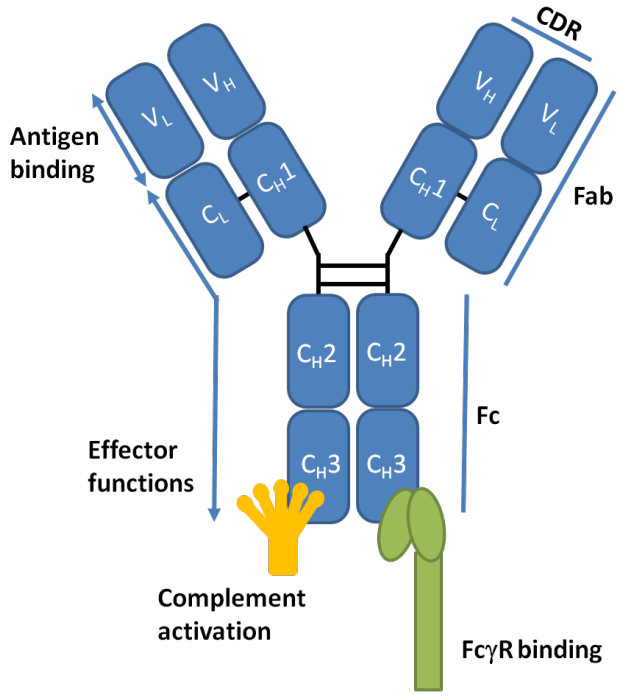


*Figure 1: Antibody structure. Immunoglobulins are made up of two heavy (H) and two light (L) chains, each of which contain variable ($V_H$, $V_L$) and constant ($C_H$, $C_L$) domains. CDR complementarity determining regions, Fab fragment antigen binding region, Fc fragment crystallizable region*

The antibody constant domain allows for common effector functions, for example through binding of the fragment crystallizable (Fc) region to Fc receptors, receptors for Ig expressed on both innate and adaptive immune cells, and complement proteins. B cells are most widely known as the precursors to terminally differentiated B cells, known as plasma cells that secrete immunoglobulins, also known as antibodies, in response to activation following recognition of antigen via their BCR (Janeway CA Jr 2001). B cells can produce antibodies reactive not only to protein and peptide antigens (T-dependent antigens) but also to carbohydrate/polysaccharide antigens (T-independent antigens). Secreted antibodies are able to directly neutralize pathogens or toxins. They can also bind complement and activate it via the classical and alternative pathways (Karsten 2012). The resultant complement cascade can lead to direct lysis of microbes, phagocytosis of microbes opsonised by complement fragments e.g. C3b and induction of inflammation via secretion of anaphylotoxins e.g. C5a, with resultant recruitment of antibody, complement and mononuclear phagocytes to the site of infection.

B cells have other effector functions besides antibody production which can influence the development of both humoral and cellular immune responses. B cells perform antigen presentation (Rodriguez-Pinto 2005) and organize the structure of lymphoid tissues, regulating lymphangiogenesis (Angeli 2006). B cells derived lymphotoxin (LT) and tumour necrosis factor alpha (TNFα) are important regulators of steady state lymphangiogenesis, supporting the development of follicular dendritic cells (Fu 1998) and regulating the development of secondary (Gonzalez 1998, Tumanov 2002) and tertiary lymphoid organs (Weyand 2005). B cells control lymph node remodelling during acute immune responses via provision of LT; lymph node expansion following murine lymphocytic choriomeningitis virus (LCMV) was reduced in B cell deficient mice, inhibited by B cell depletion of wild type mice and restored in B cell deficient mice by B cell reconstitution (Kumar 2010). B cells also control the final steps of development of gut associated lymphoid tissues through LT and TNF signalling (Tumanov 2004) and direct interactions with Peyer's patch stroma (Golovkina 1999) (reviewed in (Shen 2015)). B cell interactions with subepithelial dendritic cells in Peyer's patches are critical for effective IgA mucosal responses against oral antigens and gut commensals (Reboldi 2016).

B cells can be subdivided into 'effector' and 'regulatory' B cells depending on their cytokine profile (Figure 2)(Lund 2008). The environment in which a B cell is activated determines the cytokines they produce and the resultant immune response. Dendritic cells activated by toll like receptor (TLR) ligands secrete interleukin (IL)-12, promoting the differentiation of Th1 T cells. These Th1 cells provide help to naïve B cells, inducing the transcription factor T-bet and differentiation to a B effector 1 cell fate (Be1), prompting the release of the cytokines associated with type 1 immune responses, for example interferon γ (IFN-γ) and IL-12. These B cells go on to present antigen to naïve

T cells promoting further Th1 differentiation, leading to a positive feedback loop, amplifying Th1 responses (Harris 2005a). In contrast, T cell help delivered by Th2 T cells promotes the IL-4 dependent differentiation of B cells into B effector 2 cells (Be2) that produce type 2 associated cytokines, for example IL-2, IL-4 and IL-13 (Harris 2005b). Under certain circumstances signals delivered by TLR ligands, CD40 crosslinking or antigen induce differentiation of B cells into IL-10 producing regulatory B cells (Rosser 2015).

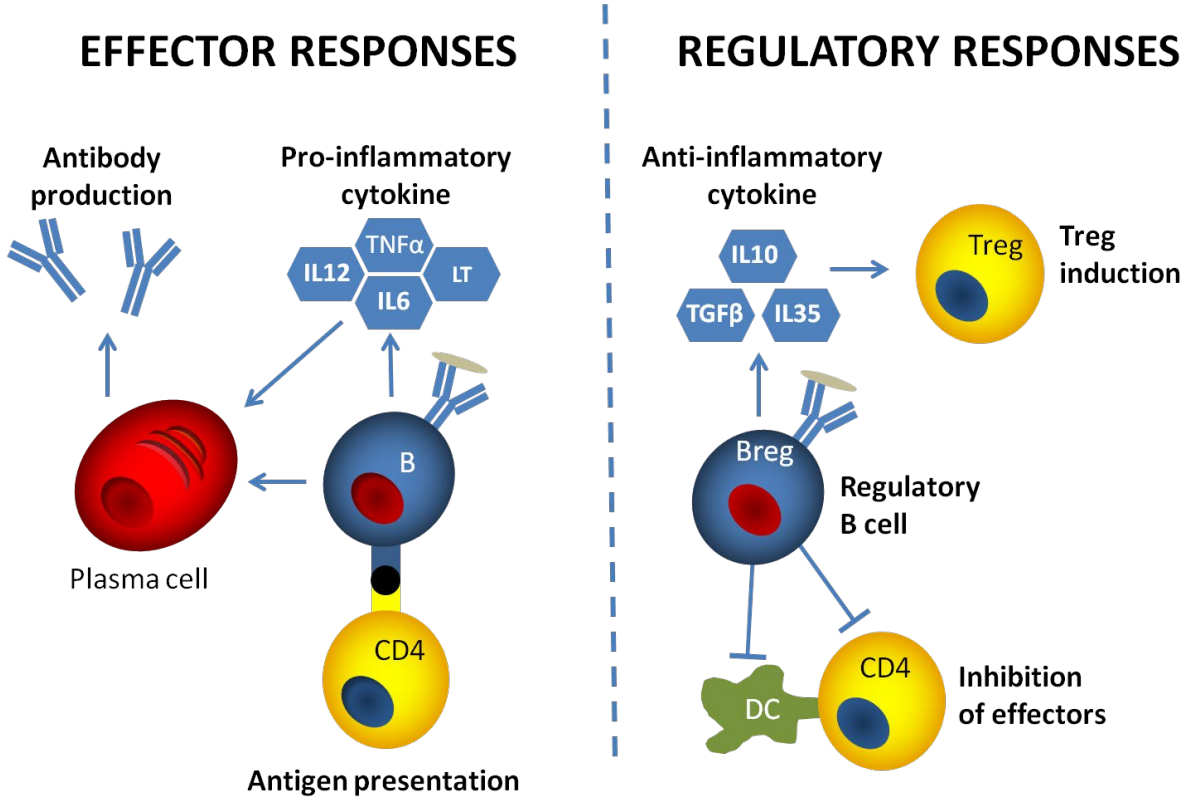


*Figure 2: B cell effector and regulatory functions. B cells have important roles as both effectors and regulators. Effector functions include antibody production, antigen presentation and secretion of pro-inflammatory cytokines, including IL-6, that can activate T cells. Regulatory B cells are a recently described subset which inhibit T-cell responses via the production of IL-10. There are also thought to be regulatory B cells which act independently of IL-10, utilising contact mediated suppression and release of other anti-inflammatory cytokines for example TGF-$\beta$ and IL-35. Regulatory B cells are also able to induce expansion of regulatory T cell populations.*

B cell effector responses are of great importance in the host defence against pathogens however, over-active or inappropriate effector responses can be pathogenic in the setting of autoimmunity, and undesirable when causing allo-immunity following transplantation. Tight regulation is therefore required to enable appropriate cellular responses; often achieved through systems involving a balance of activatory and inhibitory signalling.

### 1.1.2 B cell subsets and activation

The B cell lineage comprises of two subtypes, B1 and B2 cells. B1 cells reside primarily within the pleural and peritoneal cavity in mice and are capable of producing low affinity natural antibodies to T-independent antigens as a first line of defence. A human equivalent population has been identified in umbilical cord blood and adult peripheral blood (Griffin 2011). B2 cells are generated within the bone marrow. They develop from pro-B cells to pre-B cells to immature B cells that exit the bone marrow, entering the periphery migrating to the spleen where they go through several transitional stages (T1, T2) prior to reaching maturity (Loder 1999).

Mature B cells can be divided into two subgroups: marginal zone B cells that are responsible for T independent responses, resident within the marginal zone of the spleen, an area specialized to filter blood borne antigens and follicular B cells responsible for T-dependent responses. Follicular B cells internalise antigen bound via their BCR, undergo activation and traffic to the border between the B cell follicle and T cell zone of secondary lymphoid organs, where they can present antigen to CD4+ T cells in the context of class II major histocompatibility complex (MHC) molecules. Activated, but not naïve B cells, express co-stimulation molecules required to provide the second signal needed for T cell activation. B cell activation is generally dependent on T cell help so in many cases an alternative innate antigen presenting cell, for example a dendritic cell, is required to provide the initial activating signal to CD4+ helper T cells. B cell antigen presentation is optimised to amplify high affinity antigen-specific responses.

Following this B-T cell interaction, a proportion of B cells become short lived extra-follicular plasmablasts and the remainder enter the germinal centre; here antibody encoding genes are modified by class switch recombination and somatic hypermutation. Class switch recombination induces changes in the constant region of the heavy chain resulting in different antibody isotypes without inducing changes in the variable region that would affect antigen specificity (Stavnezer 2008). Naïve B cells express only IgM. As they undergo maturation they co-express IgD. Class-switch recombination following antigen encounter renders cells capable of producing IgG, IgA or IgE, each having defined effector functions. During somatic hypermutation, mutations are induced within the CDR which alter binding specificity and affinity of the resultant BCR. These B cells then undergo clonal selection, competing for limited antigen and survival signals offered by follicular dendritic cells. Only those with the highest affinity for antigen will survive to become long lived memory B cells or plasma cells (Rajewsky 1996). A subset of CD4+ T cells known as T follicular helper (Tfh) cells are characterised by expression of the transcription factor Bcl6 (Nurieva 2009), located within B cell follicles and are essential for the development and maintenance of germinal centre B cells (Crotty 2011). A small proportion of plasma cells arising from the germinal centre become established as

long-lived non-proliferative plasma cells in the bone marrow, secreting high affinity class switched antibodies and enabling a heightened antibody response on re-challenge with the previously encountered antigen (Radbruch 2006).

B1 B cells and marginal zone B cells form an important part of the early innate immune response. They have the capacity to respond to antigens and inflammatory stimuli rapidly, terminally differentiating into short lived plasmablasts within three days of particulate bacterial antigen exposure (Martin 2001). Follicular B cells form an important part of the adaptive immune response, generating short-lived plasmablasts within three to five days, followed by long-lived memory B cells and bone marrow resident plasma cells that produce high affinity antibodies and are critical for rapid, specific and heightened secondary immune responses on rechallenge (Slifka 1998, Bernasconi 2002, Nutt 2015).

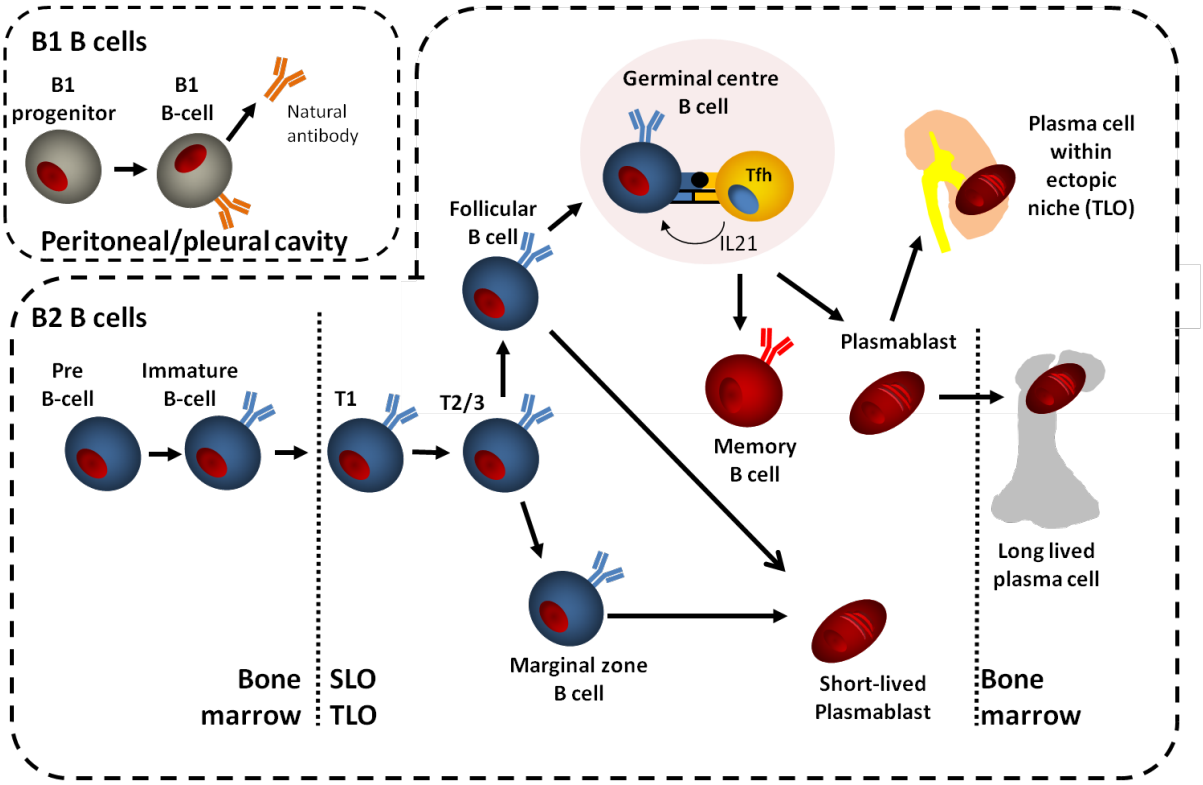


*Figure 3: B cell development, based on figure from (Clatworthy 2011), permission for reprinting granted by John Wiley and Sons. A minor B-cell population, known as B1 cells, are found mainly in the pleural and peritoneal cavities and produce low affinity natural antibodies independent of T cell help. The majority of peripheral B cells are referred to as B2 cells and are produced in the bone marrow. B2 cells pass through several stages of maturation as they exit from the bone marrow and pass into the periphery. Following antigen encounter, B cells obtain T-cell help and enter the germinal center where they undergo class switch recombination and affinity maturation. They compete for limited*

*antigen and survival signals offered by follicular dendritic cells, with only those with the highest affinity for antigen surviving to become long lived memory B cells or plasmablasts. Tfh are critical for germinal center formation, providing both contact and cytokine (IL-21) signals for germinal center B cells. Some plasmablasts find a suitable niche for long-term survival within bone marrow and tertiary lymphoid organs (TLO) within inflamed tissue, for example rejecting allografts.*

### 1.1.3 B cell development and tolerance

As B cells mature they pass through multiple tolerance checkpoints, set periods of time where their fate can be influenced and determined, allowing for regulation of self reactive B cell clones resulting in an immunologically tolerant B cell compartment. Mechanisms of tolerance include clonal deletion, receptor editing, clonal anergy, and competition for extrinsic factors (Goodnow 2005). The first checkpoint occurs at the pre-B cell stage and requires expression of a pre-BCR. Induction of recombination activating genes (RAG1 and RAG2) initiates V(D)J recombination, enabling the developing B cell to produce heavy and light chain Ig receptors and form a functional BCR. Before exiting the bone marrow, immature B cells must pass through a central tolerance checkpoint (immature checkpoint). The strength of BCR signalling determines whether cells are allowed to progress (positive selection) or whether they undergo receptor editing or apoptosis (Tiegs 1993, Tussiwand 2009). Those expressing a non autoreactive receptor with an appropriate level of antigen binding receive optimal BCR signalling (tonic or basal BCR signalling) and are positively selected. Those expressing low levels of BCR may rearrange their light chain in an attempt to produce a more efficient BCR. Those expressing a BCR with high affinity for self antigen expressed in the bone marrow undergo receptor editing; RAG 1 and RAG2 are switched off only once a receptor that is not autoreactive is produced, allowing the immature B cell to be positively selected to exit the bone marrow. Cells that fail to be positively selected die by apoptosis. Peripheral tolerance mechanisms operate to control autoreactive cells reaching the periphery. Immature B cells that undergo positive selection and migrate from the bone marrow to the spleen are known as transitional B cells (TrB) and can be further subdivided into transitional type 1 (T1), transitional type 2 (T2) and transitional type 3 (T3) subsets. A further tolerance checkpoint occurs at the transitional to follicular stage. In contrast to central tolerance that is dependent on BCR binding affinity alone, the stringency of this peripheral tolerance checkpoint can be modulated by the cytokine BLyS as described in detail below.

B cells may become activated when they encounter antigen that binds to their cognate BCR. The result of this interaction is dependent on the affinity of the antigen for the BCR, and the environmental context. The BCR signal transduction moiety is composed of the transmembrane proteins Igα (CD79a) and Igβ (CD79b), which signal via immunoreceptor tyrosine-based activation

motifs (ITAMs) located within their cytoplasmic domains (Clark 1992). The B cell co-receptor complex comprised of CD19, CD21 (CR2), and CD81 provides additional non-antigen specific signals that modulate BCR signal transduction (Fearon 1995). The B cell may receive additional co-activating and inhibitory signals that determine the net activation threshold and control the extent to which BCR cross-linking drives B cell activation (Poe 2001, Nitschke 2005), including signals through TLR (Lanzavecchia 2007). In murine B cells, generation of T-dependent antigen-specific antibody responses requires activation of TLRs in B cells in addition to CD4+ T-cell help (Pasare 2005). B cells may also receive activating signals from cytokines including BLyS (Mackay 2003).

## 1.2 B cells and antibody in disease

### 1.2.1 Immune complexes in disease

When the immune response is directed against self-antigens autoimmune disease can result. Systemic lupus erythematosus (SLE) is an archetypal example of an autoimmune disease caused by the deposition of IgG immune complexes in tissues including the kidneys but also other tissues for example skin. Antinuclear antibodies and immune complex deposits can be identified by immunofluorescence, for example when they are deposited within the kidney (Toong 2011, Tsokos 2011). Patient's with SLE display impaired phagocytosis of apoptotic debris (Herrmann 1998), leading to an accumulation of apoptotic cells in patient blood, germinal centres and inflamed tissues (Emlen 1994, Munoz 2010). Dying cells are prone to progress to secondary necrosis, exposing autoantigens which form immune complexes with circulating antinuclear autoantibodies. Deposited immune complexes activate plasmacytoid DCs, leading to the release of type 1 interferons that activate DCs and autoreactive B and T cells (Ronnblom 2008). An interferon-inducible gene expression signature in peripheral blood cells distinguishes those with SLE from controls and is associated with severe disease (Baechler 2003). Undigested secondary necrotic cell-derived material (SNEC) is captured by follicular dendritic cells within germinal centres, driving selection of autoreactive B cells. Deposited immune complexes activate complement, causing inflammation which attracts neutrophils and macrophages which bind via their Fc$\gamma$ receptors. SNEC-containing immune complexes are cleared by blood-borne mononuclear phagocytes resulting in the secretion of inflammatory cytokines; potentiating inflammation and organ damage leading to further cell death and establishment of chronic inflammation (Munoz 2010).

Other examples of antibody mediated diseases include Goodpasture's Syndrome where antibodies to type IV collagen deposit within the kidneys and lungs (Bolton 1996), rheumatoid arthritis (Korganow 1999) and autoimmune thyroid disease (Nielsen 2004).

### 1.2.2 Antibody mediated pathology in kidney transplantation

Antibodies forming following kidney transplantation have a deleterious role. Those who receive organs from HLA-antibody incompatible donors and have donor specific anti-HLA antibodies (DSA) at the time of transplantation have increased rates of graft loss, with risk of antibody mediated rejection (ABMR) correlated with the peak HLA-DSA strength (Lefaucheur 2010). Historically, transplantation in the setting of a positive crossmatch and preformed antibodies was often associated with hyperacute rejection (Patel 1969, Jeannet 1970). Desensitisation regimes that aim to reduce DSA prior to HLA-incompatible transplantation improve outcomes allowing successful transplantation across HLA antibody barriers with improved survival outcomes compared to remaining on dialysis or the deceased donor waiting list (Montgomery 2011), though the popularity of HLA-incompatible transplantation has decreased as the living donor kidney paired exchange scheme has grown.

Recipients developing donor specific HLA-antibodies following transplantation have reduced survival of their grafts due to the development of chronic ABMR (Wiebe 2012). Those who develop antibody mediated vascular rejection are nine times more likely to lose their grafts than those experiencing T cell mediated rejection without vascular inflammation (Lefaucheur 2013). Allograft rejection is generally classified according to Banff histological criteria with recent revisions incorporating our increasing understanding of ABMR (Haas 2014, Haas 2016).

The presence of non-HLA antibodies has also been associated with worsened graft outcomes. The presence of antibodies against MHC class I–related chain A (MICA) antigens is associated with increased rates of allograft rejection and reduced allograft survival (Zou 2007). The graft loss associated with anti-MICA antibodies appears to occur early in the post-transplantation period, a typical feature of rejection mediated by preformed antibodies. A subset of patients with severe allograft dysfunction associated with accelerated hypertension in the absence of anti-HLA antibodies were found to have antibodies against the angiotensin II type I ($AT_1$) receptor (Dragun 2005).

### 1.3 Regulatory B cells

The last decade has brought increasing evidence for existence of B cells with a regulatory phenotype. Regulatory B cells (Breg) act primarily via secretion of the anti-inflammatory cytokine IL-10, but may also exert regulatory signals via other mechanisms including induction of regulatory T cells (Treg), contact mediated suppression and release of other cytokines including transforming growth factor beta (TGF-β) and IL-35 (Rosser 2015).

Initial reports of B cells with regulatory capacity came in murine models. Mice deficient in B cells are unable to recover from experimental autoimmune encephalomyelitis (EAE) (Wolf 1996), indicating a role for B cells in regulation of the immune response. Recovery is dependent on IL-10 release from autoantigen reactive B cells; mice with IL-10 deficiency restricted to B cells experience a severe non remitting form of EAE with an increased pro-inflammatory cytokine response to autoantigen, with rescue of the defect by transfer of B cells from normal mice that had recovered from EAE (Fillatreau 2002). The first use of the phrase regulatory B cells came in 2002, with description of a subset CD1d$^{hi}$ Bregs that inhibited progression of intestinal inflammation in a murine colitis model (Mizoguchi 2002). Soon after came a report of prevention and treatment of collagen induced arthritis (CIA) with transfer of IL-10 secreting B cells isolated from arthritogenic splenocytes (Mauri 2003).

There is debate in the scientific community regarding the phenotype and origin of B cells with regulatory capacity, compounded by lack of a lineage-specific transcription factor to aid reliable identification. Identification of Bregs is therefore generally characterised by their capacity to secrete IL-10, although this may not capture all Breg. Breg have been identified within several different subsets of B cells in mice and men (summarised in table 1). One of the difficulties with identification and classification of Breg is that detection generally requires *ex vivo* stimulation. Stimulation may alter surface receptor expression hindering classification and the response may differ depending on the precise stimuli used. Alterations in the *in vivo* environment, as a result of inflammation and changes in gut microbiome, are known to influence Breg development (Rosser 2014). TIM-1 has been suggested as a murine marker for Breg, expressed by a large proportion of IL-10 secreting B cells including transitional, marginal zone, follicular and CD1d(hi)CD5+ B cells. Treatment with an anti-TIM antibody induced IL-10 producing TIM-1+ Breg and prolonged cardiac allograft survival (Ding 2011). Recently, a small case series has identified TIM+ Breg in humans, altered in number and function in systemic sclerosis patients (Aravena 2017). A transcriptomic analysis by Sun et al. highlighted CD9 as a robust marker of IL-10 competent Breg and their progenitors, allowing for the identification and study of cells capable of producing IL-10 without altering their phenotype by *ex vivo* stimulation (Sun 2015a). CD9+ B cells ameliorate inflammation in a Th1 cell mediated model of contact hypersensitivity (Sun 2015a) and in an allergic asthma model driven by Th2 and Th17 T cell responses (Braza 2015). Use of IL-10 reporter mice has allowed the identification of IL-10 secreting cells *in vivo* and identified plasmablasts as the predominant source of IL-10 during EAE (Matsumoto 2014). A subset of Bregs characterised by the production of IL-35 and expression of plasma cell markers has been described that ameliorate the response in EAE (Shen 2014). Treatment of mice with IL-35 induces IL-10 and IL-35 producing Breg *in vivo* and inhibits experimental uveitis (Wang 2014).

IL-10 producing B cells are enriched in a number of subsets in humans, particularly in transitional (CD24/CD38high)(Blair 2010) and memory B cell (CD24high/CD27+) (Iwata 2011) subsets. Van de Veen et al. utilised a whole genome expression analysis approach to characterise IL-10 producing Br1 Breg cells, which included CD27- naïve B cells and CD27+ memory B cells and were enriched within the CD73-CD25+CD71+ B cell compartment (van de Veen 2013). To date a Breg specific transcription factor has not been identified. Breg may originate from a common or shared progenitor. Given the reports of Breg in multiple compartments, it is possible that a Breg phenotype is inducible, with the ability of a B cell to acquire regulatory capacity not based on the expression of a specific Breg lineage but rather its context, influenced by the B cell's environment (Mauri 2015).

| Subset | Surface markers (mouse) | Surface markers (human) | Mechanism of suppression | References |
|---|---|---|---|---|
| B10 | CD5+CD1dhi | CD24hiCD27+ | IL-10, suppress effector CD4+ T cells, monocytes and DC | (Yanaba 2008, Iwata 2011) |
| Transitional 2-marginal zone precursor (T2-MZP) | CD19+CD21hi CD23hiCD24hi | - | IL-10, Treg induction, suppress effector CD4+ and CD8+ T cells | (Evans 2007, Blair 2009) |
| Immature cells | | CD19+CD24hiCD38hi | IL-10, Treg induction, inhibit Th1 and Th17 responses | (Blair 2010, Flores-Borja 2013) |
| Marginal zone (MZ) cells | CD19+CD21hi CD23− | - | IL-10, induction of T cell IL10 | (Gray 2007) |
| Plasma cells | CD138+MHC-11lo B220+ | - | IL-10, IL-35 | (Shen 2014) |
| Plasmablasts | CD138+CD44hi | CD19+CD24hiCD27int | IL-10 | (Matsumoto 2014) |
| Tim-1+ B cells | Tim-1+CD19+ | - | IL-10, suppress effector CD4+ T cells | (Ding 2011) |
| Br1 | - | CD19+CD25hiCD71hi | IL-10, IgG4 | (van de Veen 2013) |
| CD9+ B cells | CD19+CD9+ | - | IL-10, cell contact | (Braza 2015, Sun 2015a) |
| PD-L1hi B cells | PD-L1hi | - | PD-L1, regulate Tfh function | (Khan 2015) |

Table 1: Breg subsets in mouse and man, adapted from (Rosser 2015); use with permission from Elsevier.

It is clear that Breg can influence the development and recovery from autoimmunity in animal models (Fillatreau 2002, Mizoguchi 2002, Mauri 2003). Evidence for Breg involvement in autoimmune disease pathogenesis is mounting and manipulation of the Breg compartment may prove to be a useful therapeutic option (Mauri 2017). Breg are functionally impaired in SLE (Blair

2010) and rheumatoid arthritis (Flores-Borja 2013). Claudia Mauri's group recently showed that the defect in SLE patients was due to failure of the normal regulatory feedback loop between plasmacytoid DC (pDC) and Breg, hypothesised to be secondary to increased exposure to IFN-α (Menon 2016). In healthy volunteers, pDC drive the differentiation of immature B cells into CD24+CD38hi Breg cell and plasmablasts by IFN-α release and CD40 engagement, and these Breg limit IFN-α release from the pDC via IL-10 release. However in SLE patients, pDCs promoted plasmablast differentiation but failed to induce Breg cells, leading to a loss in functional Breg and an increase in autoantibody producing plasmablasts.

A number of lines of evidence suggest that regulatory B cells may be important in transplantation, regulating the immune response to the transplanted organ (Stolp 2014). The pathogenic roles of B cells in transplantation are well established. As the precursors to antibody secreting cells, B cells are responsible for the production of DSA and non-HLA antibodies that are associated with development of acute and chronic ABMR and poor graft outcomes (Dragun 2005, Zou 2007, Loupy 2013). B cells also act as antigen presenting cells, presenting allo-antigen to CD4+ T cells resulting in T cell mediated rejection (TCMR) and produce pro-inflammatory cytokines including IL-6 (Barr 2012) that can activate T cells driving TCMR. In addition, IL-6 promotes B cell differentiation into antibody-forming plasma cells, contributes to the plasma cell niche (Kometani 2015), enhances Tfh cell development critical for germinal centre responses, and inhibits the generation of regulatory T cells (Jordan 2017). With these pathogenic B cell effector functions in mind, we began an open label randomised controlled trial where patients received two doses (day 0 and 7) of the B cell depleting agent rituximab or the anti-CD25 agent daclizumab, with a steroid free maintenance regime of tacrolimus and mycophenolate mofetil (MMF) (Clatworthy 2009). Surprisingly, rituximab was associated with an excess rate of TCMR (5/6 (83%) biopsy proven acute rejection (BPAR) in the rituximab group versus 1/7 (14%) in the daclizumab group ($p=0.01$)), leading to early cessation of the study. We hypothesised that the increased incidence of TCMR may in part have been due to inadvertent depletion of Breg. Two further randomised controlled trials have been conducted using a single dose of rituximab at induction in combination with a maintenance regime of tacrolimus, MMF and corticosteroids. A study by Tyden and colleagues (Tyden 2009) found no significant difference in TCMR at 6 months (8/68 (11.7%) in the rituximab group versus 12/68 (17.6%) in the placebo group; p=0.31), with similar rates of ABMR, TCMR and DSA at three years and worryingly a significantly increased mortality rate in the rituximab treated group (8/68 versus 0/68; p=0.006), with 6 cases being due to myocardial infarction/cardiac arrest (Tyden 2012). A study by van den Hoogan and colleagues used an identical regime to Tyden et al. and found no overall benefit of rituximab (BPAR 23/138 (16.7%) in the rituximab group versus 30/142 (21.2%) in the placebo group;

p=0.25) with no excess mortality at a median follow up of 4 years. A subgroup analysis suggested potential benefit in those with increased immunological risk; immunologically high-risk patients (PRA >6% or re-transplant) not receiving rituximab had a significantly higher incidence of rejection (13/34, 38.2%) compared to other treatment groups (rituximab-treated immunologically high-risk patients, and rituximab- or placebo-treated immunologically low-risk (PRA ≤ 6% or first transplant) patients (17.9%, 16.4% and 15.7%, p = 0.004) (van den Hoogen 2015). Rituximab induction in the setting of cardiac transplantation is associated with accelerated cardiac allograft vasculopathy, with an increase seen in the percent change from baseline atheroma volume at 1 year measured by intravascular ultrasound (6.8 ± 8.2% rituximab group versus 1.9 ± 4.4% placebo (p=0.0019)) (Chandraker 2016).

An enrichment of B cell transcripts in peripheral blood mononuclear cells (PBMC), together with increased proportions of regulatory B cells in drug-free 'tolerant' kidney transplant recipients and a change in the balance of activated and regulatory T cells support the notion that B cells are a key player in the regulation of peripheral tolerance (Newell 2010, Pallier 2010, Chesneau 2014). Further support for a Breg role comes from immunophenotyping of those who do and do not experience rejection. Kidney transplant recipients with a higher number of TrB cells have a reduced frequency of rejection (Shabir 2015). The balance of pro-inflammatory (for example IL-6, TNFα) and anti-inflammatory cytokines released from B cells is thought to be a factor in maintaining peripheral immune tolerance. Compared with TrB cells from patients with stable kidney graft function, TrB cells from patients with graft rejection displayed a reduced IL-10/TNFα ratio, did not inhibit *in vitro* expression of Th1 cytokines by T cells, and abnormally suppressed expression of Th2 cytokines. Furthermore, in patients with graft dysfunction, a low IL-10/TNFα ratio in TrB associated with poor graft outcomes after 3 years of follow-up (Cherukuri 2014). Patients with rejection following ABO incompatible transplantation had fewer $CD24^{high}/CD27^{+}$ memory B cells, a subset enriched for B10 Breg (Schlosser 2016).

### 1.4 BAFF/BLyS

#### 1.4.1 BLyS control of B cell development and tolerance

BLyS (also known as B cell activating factor belonging to the TNF family (BAFF) and tumor necrosis factor ligand superfamily member 13B) is expressed as a membrane bound type II transmembrane protein on various cell types including macrophages, monocytes, dendritic cells and bone marrow stromal cells. It can be cleaved to a soluble form. BLyS binds to three receptors, BAFF receptor (BAFF-R), transmembrane activator and CAML interactor (TACI) and B cell maturation protein A (BCMA), binding to BAFF-R with high affinity and to BCMA and TACI with lower affinity. TACI and BCMA, but not BAFF-R, also bind the related TNF family cytokine APRIL (a proliferation-inducing ligand; also known as tumor necrosis factor ligand superfamily member 13 (TNFSF13)).

BAFF-R is the most widely expressed, being found on all human peripheral B cells, as well as on human splenic naïve, memory and marginal zone B cells. BCMA and TACI are upregulated during B cell differentiation with TACI expression paralleling that of the memory marker CD27 (Darce 2007). BCMA expression is limited to antibody secreting B cells and is critical for the survival of long-lived plasma cells (Avery 2003, O'Connor 2004). Signalling through the APRIL-BCMA axis within the bone marrow induces expression of the anti-apoptotic factor myeloid cell leukaemia 1 (Mcl1), which is essential for the survival of all antibody secreting cells (Peperzak 2013). Splenic plasma cells were sustained at near normal frequency in BCMA deficient mice with normal levels of Mcl1 indicating an alternative BCMA independent survival pathway.

B cells become dependent on BLyS signalling through BAFF-R at the transitional T1 stage and mice deficient in BLyS have reduced mature B cells within peripheral lymphoid systems, with near complete absence of follicular and marginal zone B cells (Schiemann 2001). A similar phenotype is shown in A/WySnJ mice that have a disrupted BAFF-R locus (Thompson 2001). Human BAFF-R deficiency is associated with adult onset antibody deficiency syndrome (Warnatz 2009). In contrast to the murine BLyS mutants, the human deficiency shows a late onset with variable penetrance and does not inevitably lead to a clinically overt immunodeficiency.

BLyS is also important for maintenance of the germinal centre response; germinal centre B cells downregulate TACI following IL-21 mediated signalling with resultant reduction in surface bound BLyS. Tfh act as a local source of BLyS within the germinal centre that is required for normal affinity maturation and the persistence of high affinity germinal centre B cells (Goenka 2014). In addition, BLyS contributes to the plasma cells niche, selectively enhancing the survival of plasmablasts generated from human memory cells (Avery 2003). Mice overexpressing BLyS have marked B cell

expansion, with splenomegaly and lymphadenopathy, and develop autoimmune manifestations including an SLE like disorder characterised by circulating immune complexes, hypergammaglobulinemia, anti-double stranded DNA (anti-dsDNA) autoantibodies and immunoglobulin deposition within the kidneys (Mackay 1999, Gross 2000, Khare 2000).

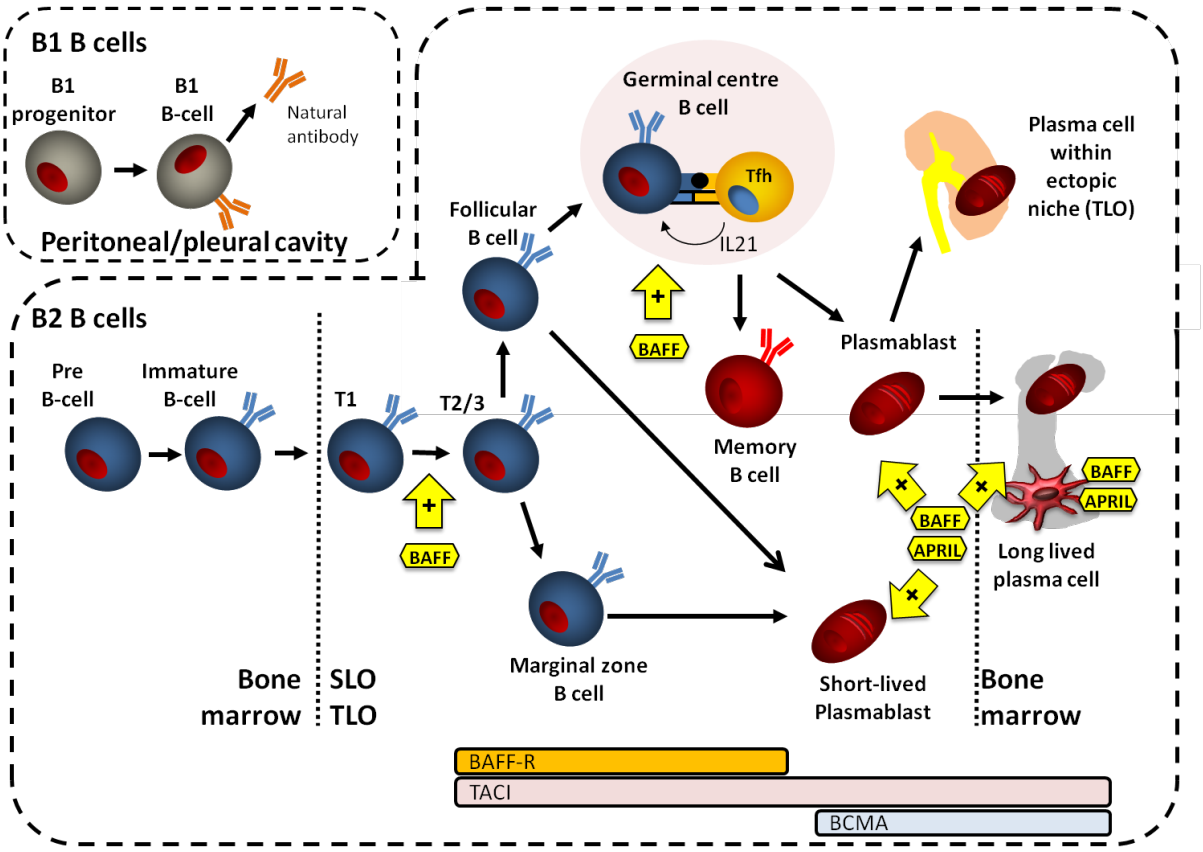


*Figure 4: BAFF/BLyS control of B cell development, based on (Inaba 2016) and (Clatworthy 2011). BAFF-R is expressed on B cells as they mature through the T1 stage; B cells become dependent on BLyS signalling at the T1/T2 checkpoint. BLyS is important in maintaining the germinal centre response, with local production by Tfh. Plasma cells are supported by a niche which provides necessary survival signals including BAFF and APRIL, which both bind to the BAFF receptors, BCMA and TACI. Targeting of the plasma cell pool may therefore require dual blockade of BAFF and APRIL.*

BLyS signalling downstream of the BAFF-R activates the alternative nuclear factor kappa B (NF-κB) pathway, leading to upregulation of anti-apoptotic members of the Bcl-2 family and degradation of pro-apoptotic proteins such as Bim (Craxton 2005). TACI and BCMA signal via the classical NF-κB and Mek (mitogen-activated protein extracellular signal-related kinase) pathways leading to increased expression of anti-apoptotic proteins and downregulation of pro-apoptotic proteins, and through the JNK/p38 (c-Jun N-terminal kinase) pathway, driving class-switching (Bossen 2006). TACI and BAFF-R are both able to drive isotype switching through class switch recombination in response to

BLyS although induction of IgA switching appears dependent on TACI and class switching in response to APRIL is solely mediated by TACI (Castigli 2005b). Polymorphisms in TNFRSF13B, the gene encoding TACI, have been associated with human common variable immunodeficiency and IgA deficiency, diseases characterised by impaired class switching (Castigli 2005a, Salzer 2005).

TACI may also have regulatory roles in B cell homeostasis; mice deficient in TACI have increased B cell numbers, with expanded populations of Tfh and germinal centre B cells following T dependent immunisation, secondary to up-regulation of inducible costimulator (ICOS) ligand on TACI-deficient B cells. However, these mice display defective antigen-specific antibody responses resulting from significantly reduced numbers of antibody-secreting cells (Ou 2012). TACI regulates the survival of plasmablasts and is required for efficient plasma cell differentiation in response to T independent antigens (Mantchev 2007).

There is feedback between BCR and BAFF-R signalling. BCR signalling leads to generation of p100, a substrate for the alternative NF-κB pathway utilised by BAFF-R; BLyS mediated NF-κB signalling promotes survival. This underpins the dependency of B cells beyond the transitional stage for BLyS; T1 cell lipid rafts contain insufficient cholesterol to generate p100 and are subject to negative selection. BCR signalling in late transitional and follicular B cells generates sufficient p100 to support BLyS-mediated survival signals (Stadanlick 2008). Levels of BLyS can influence stringency of peripheral B cell negative selection at the transitional to follicular checkpoint; low levels lead to increased competition for signalling and negative selection of autoreactive B cells whereas excess BLyS facilitates escape from negative selection with survival of autoreactive clones that would otherwise have undergone anergy or deletion (Lesley 2004, Thien 2004).

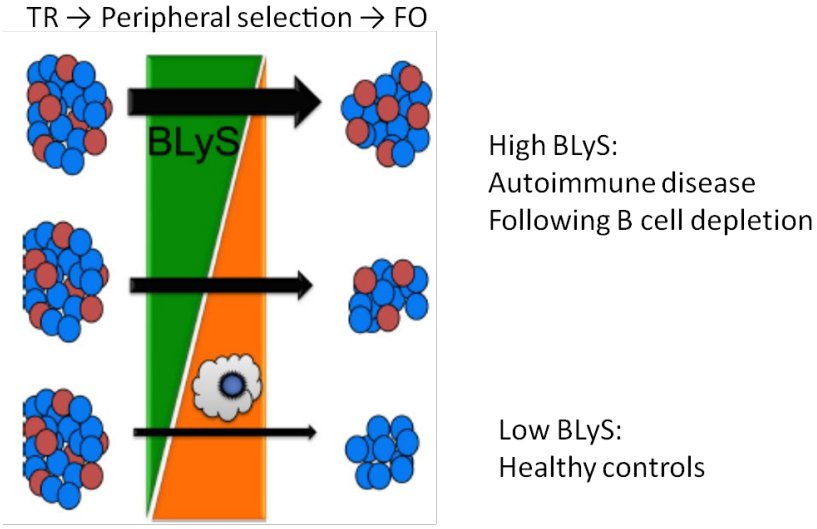

*Figure 5: The level of soluble BLyS (green) controls the stringency of peripheral B cell negative selection (orange) at the transitional to follicular (TR→FO) checkpoint. In the presence of high soluble BLyS levels, B cell clones normally subject to deletion (red cells) are permitted to enter the FO B cell pool. Under BLyS limited conditions a range of TR B cell clones normally capable of maturing (blue cells) do not survive. Adapted from (Parsons 2010); reprinted with permission from Elsevier.*

### 1.4.2 BLyS in disease

Increased levels of circulating BLyS have been identified in patients with autoimmunity (Jonsson 2005, Bosello 2008, Steri 2017) and may be associated with the development or maintenance of autoreactive B cells. A rise in serum BLyS can also be seen following B cell depleting therapy (Vallerskog 2007, Bloom 2009) which may contribute to the increased incidence of secondary autoimmunity seen following alemtuzumab treatment for multiple sclerosis (Thompson 2010), and increased levels of DSA and ABMR following alemtuzumab induction therapy in the setting of renal transplantation (Bloom 2009). A polymorphism in TNFSF13B, the gene encoding BLyS, has been associated with autoimmunity risk in a recent genome wide association study (Steri 2017). The causal variant was identified as an insertion–deletion variant, GCTGT→A (in which A is the risk allele), that yielded a shorter transcript which escaped microRNA inhibition and increased production of soluble BLyS, which in turn led to an increase in B cells and immunoglobulin.

### 1.4.3 BLyS and transplantation

Numerous studies have associated elevated serum BLyS levels in renal transplant recipients with a heightened humoral immune response. Patients with increased serum BLyS have a significantly increased risk of developing *de novo* DSA (Thibault-Espitia 2012) and increased presence and severity of transplant glomerulopathy (Sango 2016). We have shown in an HLA antibody incompatible cohort that increased levels of serum BLyS measured pre-transplant are associated with an increased frequency of ABMR (Banham 2013). Alterations in receptors for BLyS may also be important; Thibault-Espitia and colleagues detected an inverse correlation between serum and transcript levels of BLyS and expression levels of the receptors BAFF-R and TACI, and showed that stable patients with high BAFF-R levels had a higher risk of developing graft dysfuction (Thibault-Espitia 2012). Tertiary lymphoid organs (TLO) may form within the allograft in the setting of chronic antibody mediated rejection. Here, BLyS may be an important local factor maintaining the niche. Indeed, BLyS protein and transcript levels were found to be overexpressed in chronically rejected grafts when compared with normal kidneys and lymph nodes (Thaunat 2008). BLyS has been detected by immunohistochemistry in renal allograft acute rejection and interstitial fibrosis/tubular

atrophy biopsies, correlating with C4d staining (Xu 2009), a marker of complement activation and hallmark of antibody mediated rejection.

Furthermore, animal models of transplantation give further evidence of a pathogenic role for BLyS in alloimmunity and highlight the potential for therapeutic intervention. In a murine cardiac allograft model, mice with a mutation in the BAFF-R or with a targeted deletion of BLyS, showed prolonged cardiac allograft survival compared to wild-type or TACI deficient controls (Ye 2004). The effect of BLyS was shown to influence the T cell compartment in addition to the B cell compartment; binding of BLyS to BAFF-R expressed by a subset of primarily CD4+ T cells provided co-stimulation leading to T cell activation and allo-proliferation *in vitro* and *in vivo*. In a murine islet cell allograft model, BLyS blockade followed by a short course of rapamycin allowed for long term survival of MHC-disparate allografts (Parsons 2012). Induction therapy with rapamycin was necessary, but not sufficient, for the achievement of this long-term graft survival, which was associated with absence of DSA, impaired T cell activation, increased regulatory T cells and a regulatory cytokine milieu with low IL-2, high IL-5, high IL-10, and low IFN-γ production. Use of atacicept, a recombinant TACI-Ig fusion protein that blocks both BLyS and APRIL, prevented early DSA formation and ABMR development in a T cell depletion induced nonhuman primate ABMR model, although increased T cell rejection findings were observed, likely secondary to graft prolongation (Kwun 2015). Belimumab (Benlysta; GlaxoSmithKline, Rockville, MD, USA), a humanised anti-BLyS IgG1 antibody, is licensed for use in patients with SLE (Furie 2011, Navarra 2011). BLyS inhibition, used as monotherapy, had little impact on HLA antibody titres in sensitised subjects on the transplant waiting list (Naji , Mujtaba 2016), but to date this axis has not been targeted in human transplant recipients.

### 1.5 Fc gamma receptors (FcγRs)

#### 1.5.1 FcγRs determine antibody effector function

Many of the effects of IgG antibodies are mediated by cross-linking FcγRs, surface glycoproteins that bind IgG immune complexes, and are expressed by most immune cells, including mononuclear phagocytes. There are several different types of FcγR in mice and men that differ in their expression and binding affinity to different classes of IgG. FcγR are important in promoting and regulating the immune and inflammatory responses to immune complex (Nimmerjahn 2008). The human receptors comprise of 3 classes; FcγRI, FcγRII and FcγRIII (Figure 6). The murine receptors are simpler with an analogous FcγR1 and FcγRIIb but only two activatory low affinity receptors, FcγRIII which is similar in structure to human FcγRIIa and FcγRIV which is a homolog of FcγRIIIa.

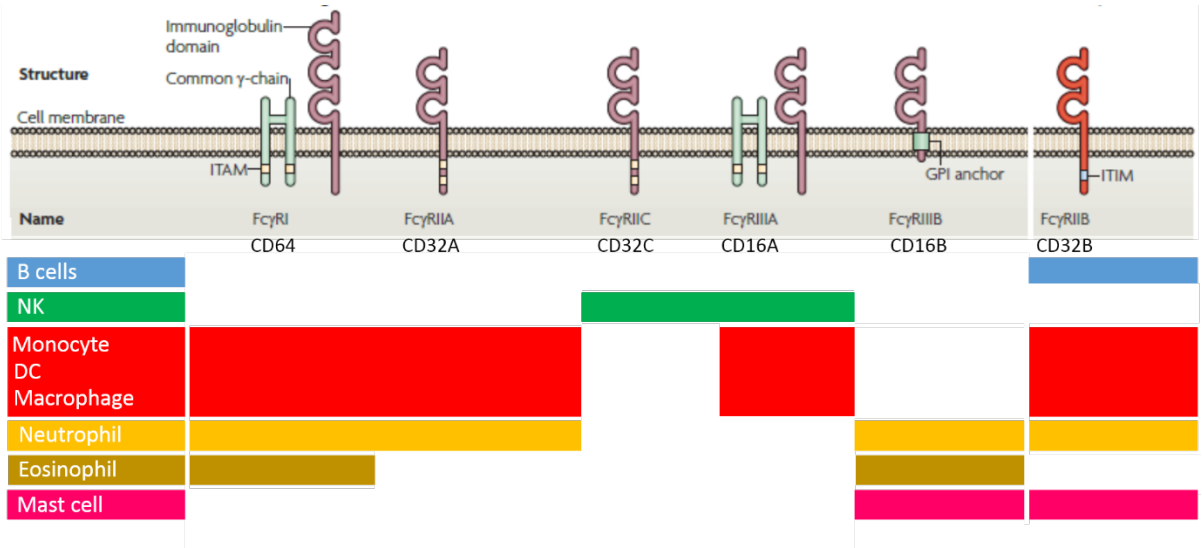


*Figure 6: Human FcγR expression (adapted from (Smith 2010), copyright © 2010, reprinted with permission from Springer Nature). Cell specific FcγR expression is shown, with each immune cell subset represented by a different colour block.*

FcγRII has three isoforms, A, B and C and FcγRIII has two, A and B. With the exception of FcγRIIb, these receptors are all activatory, containing immunoreceptor tyrosine-based activatory motifs (ITAM) within the cytoplasmic domain of the receptor (FcγRIIa and FcγRIIc) or in the associated FcR common γ-chain (FcγRI and FcγRIIIa). FcγR1 is a high affinity receptor that can bind monomeric IgG. The low affinity receptors FcγRII and FcγRIII bind immune complexes and mediate many of the effector functions of antibody. FcγRIIb, in contrast contains immunoreceptor tyrosine-based inhibitory motifs (ITIM) within its cytoplasmic tail and acts as the sole inhibitory FcγR. The ratio of binding to activatory and inhibitory receptors, known as the A/I ratio, determines the activation threshold of a particular cell. Cytokines differentially regulate the expression of the two opposing FcγR systems; IFN-γ increases monocyte FcγRIIa expression and reduces FcγRIIb expression whereas IL-4 increases FcγRIIb whilst reducing FcγRIIa (Pricop 2001). Mutations or polymorphisms affecting the expression or function of FcγR have been associated with the balance between susceptibility to infection and autoimmunity in mice and men (Smith 2010).

B cells and plasma cells only express the inhibitory receptor, FcγRIIb. Crosslinking of FcγRIIb to the BCR increases the B cell activation threshold, regulating antibody production and reducing B cell mediated antigen presentation to T cells. Cross linking of FcγRIIb in the absence of BCR ligation in mature B cells and terminally differentiated plasma cells can induce apoptosis via non ITIM mediated signalling pathways (Nitschke 2005, Smith 2010). Mononuclear phagocytes express both activatory and inhibitory FcγRs.

### 1.5.2 FcγR signalling

The interaction between pathogen bound IgG and activatory FcγR on macrophages mediates pathogen clearance via phagocytosis and antibody dependent cellular cytotoxicity (ADCC). Crosslinking of activatory FcγR leads to phosphorylation of ITAMs, activation of the signalling molecule spleen tyrosine kinase (Syk) and the initiation of an activating signal cascade. This results in activation of various downstream targets including phosphoinositide 3-kinase (PI3K) and phospholipase Cγ (PLCγ) which lead to increased intracellular calcium levels and stimulation of the RAS–RAF–MAPK (mitogen activated protein kinase)-pathway. Downstream signalling events are triggered resulting in changes in the actin cytoskeleton leading to phagocytic cup formation, production of pro-inflammatory cytokines and chemokines as well as oxidative burst and ADCC (Nimmerjahn 2008). This inflammatory response assists in pathogen clearance but can potentially propagate tissue inflammation in the case of autoimmunity. Kidney resident macrophages detect and scavenge circulating IC and trigger a FcγRIV-dependent inflammatory response leading to the recruitment of monocytes and neutrophils. IC uptake is dependent on the unique anatomical position of kidney macrophages that are situated in close apposition to endothelial cells that transport circulating IC to them (Stamatiades 2016). FcγRIIb inhibits IC-induced pro-inflammatory cytokine production in macrophages (Clatworthy 2004). FcγRIIb may have an additional, non-inhibitory role in macrophage function by mediating endocytosis and non-inflammatory clearance of immune complexes from arthritic joints by macrophages (van Lent 2003).

## 1.6 Mononuclear phagocytes

Monocytes, macrophages and DCs are professional phagocytes and antigen presenting cells found in most tissues, forming a network of immune sentinels specifically positioned to detect and respond to invading micro-organisms (Geissmann 2010), playing a pivotal role in the generation of an adaptive immune response. Mononuclear phagocytes express a range of immune receptors that recognise pathogen associated molecular patterns (PAMPs) and damage associated molecular patterns (DAMPS), known as pattern recognition receptors, including TLRs, C-type lectin receptors (CLR), scavenger receptors and nucleotide oligomerization domain (NOD)-like receptors (NLRs) in addition to the activatory FcγR receptors FcγRIIa and FcγRIIIa and the inhibitory receptor FcγRIIb.

Monocytes circulate in the blood prior to entering tissues where they differentiate into macrophages or DC. Inflammatory monocytes are preferentially recruited to areas of inflammation, produce inflammatory cytokines and contribute to local and systemic inflammation. Resident monocytes enter tissues under steady state conditions (Gordon 2014).

### 1.6.1 Macrophages are tissue resident mononuclear phagocytes specialised for phagocytosis

Macrophages reside within tissues throughout the body, positioned to ingest and process foreign materials, dead cells and debris, and recruit additional macrophages from the circulation and stimulate lymphocytes during infection or following injury. The majority are maintained through self renewal, derived from embryonic precursors (Schulz 2012, Hashimoto 2013, Ginhoux 2014)**.** Tissue-specific factors drive highly specialized macrophage functions irrespective of their ontological origin (Epelman 2014)**.** Phagocytosis of pathogens by macrophages initiates the innate immune response and sets in motion the adaptive response. Pathogen bound IgG binds to activatory FcγR on macrophages, facilitating pathogen clearance via phagocytosis and ADCC as described above. Phagocytosis of IgG immune complexes initiates a similar inflammatory response (Gordan 2015). Phagocytosis can also be triggered following binding of complement opsonised pathogens to complement receptors, though the signalling downstream of receptor binding differs as does the resultant inflammatory response, with FcγR induced phagocytosis but not complement receptor mediated phagocytosis being tightly coupled to the generation of inflammatory metabolites (Aderem 1999).

Macrophage phagocytosis does not always induce inflammation. Indeed macrophages induce immune tolerance toward self through removal of dying cells that have undergone apoptosis, without activating proinflammatory responses (Savill 1997, Kono 2008). Tissue macrophages also suppress inflammation mediated by inflammatory monocytes, thereby ensuring that tissue homeostasis is restored following infection or injury. Defects in apoptotic cell clearance are implicated in the pathogenesis of SLE (Munoz 2005, Munoz 2010). Historically, macrophages have been classified into classically activated M1 macrophages that secrete proinflammatory cytokines in response to pathogens and alternatively activated M2 macrophages that have anti-inflammatory functions and regulate wound healing and fibrosis. This nomenclature has lost popularity given that there is a range of macrophage activation states, with marked plasticity of macrophage populations in response to environmental cues; favouring classification on a spectrum according to macrophage function in host defence, wound healing or immune regulation (Mosser 2008).

### 1.6.2 Dendritic cells are specialised for antigen internalisation, migration to draining lymph nodes and presentation of antigen to T cells

DCs display a number of receptors, including FcγR, that enable internalisation of antigen and presentation to T cells (Banchereau 1998). Presentation of processed antigen to T cells may lead to T cell activation, if appropriate co-stimulatory signals are also provided by mature DC (Hawiger 2001). DC's reside in an immature state in peripheral tissues where they act as sentinels to induce

protective immunity against incoming danger. When levels of captured self-antigen are low, or in the absence of appropriate co-stimulatory signalling, DCs contribute to the clearance of dying cells and provide tolerogenic signals to T cells (Hawiger 2001, Steinman 2003), maintaining homeostasis to self antigens. In steady state, heterogenous populations of DCs are localised to distinct anatomical sites according to their unique homing properties (Merad 2013). However during infection, and in the context of autoimmunity, DCs play a pivotal role in the activation of CD4 and CD8 T cells. DC maturation may be induced following activatory FcγR ligation (van Montfoort 2012), as well as through signalling induced by TLR ligands, CD40 ligation and pro-inflammatory cytokines (Roake 1995, Reis e Sousa 2006). FcγRIIb inhibits FcγR-dependent internalization and presentation of antigen and exerts a basal level of inhibition to DC maturation in the presence of ICs, providing an important tolerance checkpoint (Boruchov 2005). Microarray analysis of unstimulated and IC-activated bone marrow derived DC (BMDC) reveals a gene expression profile associated with effective T cell activation, dependent on the presence of activating FcγR and regulated by FcγRIIb. FcγRIIb-deficient DCs have an improved capacity to activate naïve T lymphocytes, displaying enhanced FcγR-dependent Ag presentation. *In vivo* induction of CD8+ T cell expansion was increased in mice selectively lacking FcγRIIb on DC (CD11cCre X FcγRIIb fl/fl mice) compared to wildtype controls (van Montfoort 2012).

Dendritic cells can broadly be divided into plamacytoid DC (pDC) and conventional DC (cDC) (Merad 2013). Plasmacytoid DC represent a small subset of DCs, with poor antigen presenting capacity, but that produce large quantities of type I interferon on recognition of foreign nucleic acids by TLR7 and 9, particularly important in the antiviral response. All other subsets of DCs can be grouped together as cDC; cDC are uniquely specialized in processing exogenous antigen for presentation to T cells and T cell priming and are best characterized further by their location. Non lymphoid tissue cDC's represent 1-5% of tissue resident cells, depending on the organ in question, and consist of two major subsets: CD103+CD11b- and CD11b+ cDCs. Skin resident DC can be divided into langerhans cells and dermal DC (Kaplan 2010). Langerhans cells are the only MHC II expressing cells within the epidermis; those that are transiting through the dermis or that have migrated to skin-draining lymph nodes can be identified based on expression of Langerin (CD207), EpCam and CD11b and the absence of CD8 and CD103 expression. Dermal DC express CD103 but not EpCam, CD11b or CD8 and can be divided into Langerin+ and Langerin- subsets. Dermal DC migrate to skin draining lymph nodes in the steady state and in response to infection, and are able to present antigen acquired in the periphery to T cells. Non lymphoid tissue DCs that have migrated to tissue draining lymph nodes through the lymphatics are known as tissue migratory DC (Randolph 2005) in contrast to blood-borne lymphoid organ resident DCs. In the steady state, tissue migratory DC migrate through afferent lymphatics to T

cell areas of lymph nodes, carrying antigens phagocytosed in the periphery; this process is increased several fold following DC maturation in response to inflammatory signals. Most of these stimuli trigger downstream signalling pathways that activate NF-κB and induce proinflammatory gene expression. In contrast to steady-state tissue migratory cDCs, those that migrate in response to inflammation also produce inflammatory cytokines and upregulate costimulatory molecules such as CD40, CD80 and CD86, as well as MHC class II, optimising the DC for antigen presentation enabling it to drive adaptive immunity; the nature of the immune response being guided by the specific maturation signal received, the DCs ontogeny and environmental modifiers which determine whether the DC becomes immunogenic or tolerogenic (Reis e Sousa 2006). Lymphoid organ resident DCs reside permanently in lymphoid tissues including lymph nodes, mucosal associated lymphoid tissues such as Peyer's patches and the spleen and mainly consist of CD8+ and CD11b+ subsets (Merad 2013).

### 1.6.3 Control of dendritic cell migration

The control of DC migration is complex since the process of migration relies both on a cell's intrinsic capacity to migrate as well as signals guiding migration from the surrounding environment. DC maturation induces a switch in chemokine receptor expression, to allow migration of DC from peripheral tissue where they capture antigen to the lymph nodes where they can stimulate T cells. Immature DC express chemokine receptor 1 (CCR1), chemokine receptor 2 (CCR2), chemokine receptor 5 (CCR5) and chemokine (C-X-C motif) receptor 1 (CXCR1), allowing them to respond to their respective ligands which are chemokines produced at inflammatory sites. Maturation, induced by stimulation with LPS or TNFα, leads to upregulation of chemokine receptor 7 (CCR7) and chemokine (C-X-C motif) receptor 4 (CXCR4) and downregulation of CXCR1, CCR1 and CCR5 (Sallusto 1998), allowing mature DC to undergo CCR7 dependent migration to draining lymph nodes. Mice deficient in CCR7 have similar numbers of DCs in their peripheral organs to wild type mice, but show reduced mobilisation of DC from dermal tissues in response to contact sensitisation induced by fluorescein isothiacyanate (FITC) skin painting (Forster 1999), indicating that CCR7 is not required for recruitment of DC progenitors to the skin and mucosal surfaces but is required for mobilisation in response to external stimuli. Activating FcγR-crosslinking by preformed IC or autoantibody containing serum provides a similar maturation signal inducing upregulation of CCR7, and this process is inhibited by FcγRIIb (Clatworthy 2014a).

Various signalling modules act downstream of CCR7 ligation, leading to multiple points of regulation of DC migratory responses such as chemotaxis and migratory speed (Figure 7; reviewed in (Randolph 2008)). The Rho family of GTPases act as an intermediate in the signalling pathway leading to

activation of the actin binding protein cofilin, which may regulate the basal migratory speed of DCs but not DC chemotaxis (Riol-Blanco 2005). CCR7 signalling also induces activation of PI3K, protein kinase C (PKC) and NF-κB, which are important for activation and survival of cells and phospholipase Cβ2 (PLCβ2) which breaks down plasma membrane lipids into diacylglycerol (DAG) and the calcium second messenger, inositol trisphosphate (IP3), leading to the release of intracellular calcium from stores in the endoplasmic reticulum, with effects on chemotaxis. Cdc42 and Rac, but not RhoA GTPases, coordinate actin polarization, cytoskeletal rearrangement, cell polarity, and ultimately motility in a c-Jun N-terminal kinase (JNK) dependent pathway (Iijima 2005).

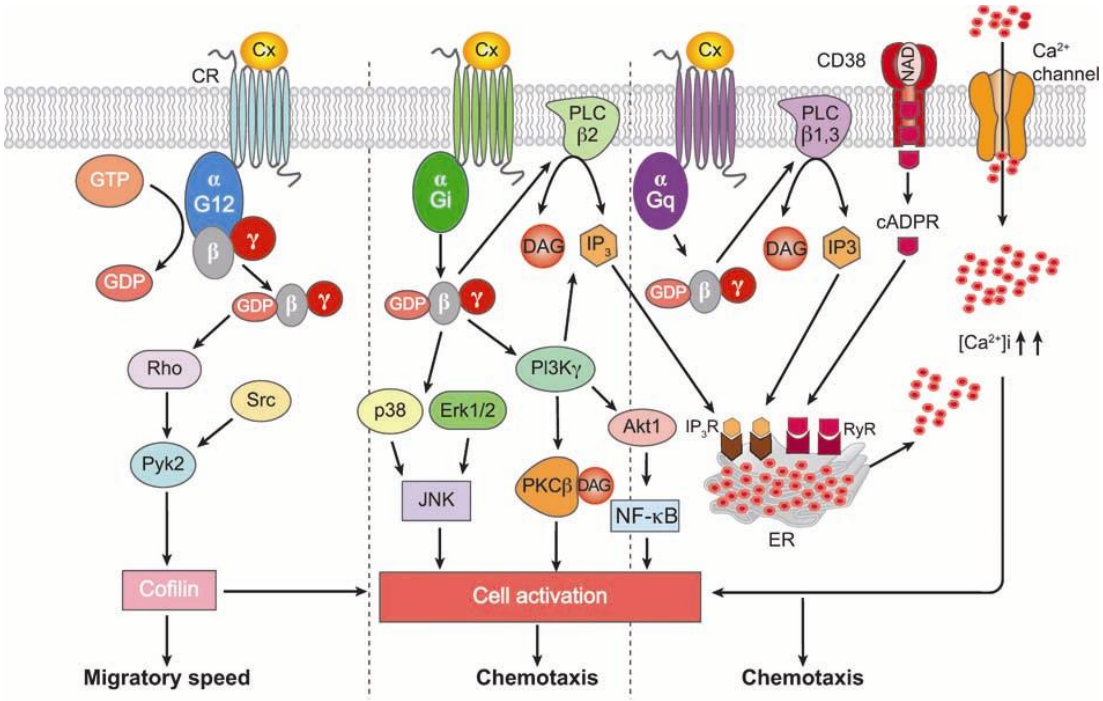


Randolph GJ, et al. 2008.
Annu. Rev. Immunol. 26:293–316

*Figure 7: Various signalling pathway modules regulate distinct migratory responses induced by chemokines through CCR7 (Randolph 2008). Reproduced with permission from the Annual Review of Immunology, Volume 26 © 2008 by Annual Reviews, http://www.annualreviews.org. Upon agonist binding trimeric G proteins consisting of α, β, and γ subunits are uncoupled and a series of signal transduction events ensue that result in cell activation followed by enhanced motility. At least two non-overlapping independent signalling modules are activated upon CCR7 ligation.*

Migrating DCs secrete matrix metalloproteinases (MMPs) to facilitate movement through the extracellular matrix and across basement membranes (Ratzinger 2002). MMP release is also inhibited by FcγRIIb (Clatworthy 2014a). Prostaglandin E2 (PGE2), present at sites of inflammation induces DC migration by inducing MMP-9 which is required in addition to CCR7 for the migration of

mature DC to draining lymph nodes (Yen 2008). Mast cells are able to induce Langerhans cell migration from the skin to the draining lymph nodes following IgE mediated activation *in vivo* via a histamine dependent mechanism (Jawdat 2004). The cysteinyl leukotriene pathway also promotes DC migration. Migration of DC from skin to lymph nodes was reduced in mice lacking the leukotriene C4 transporter MRP1, and restored by exogenous cysteinyl leukotrienes. *In vitro*, these cysteinyl leukotrienes promoted optimal chemotaxis to chemokine (C-C motif) ligand 19 (CCL19), but not to other related chemokines, suggesting that triggering of DC by cysteinyl leukotrienes is required for maximal chemotaxis towards CCL19 (Robbiani 2000). Activation of DC, induces the downregulation of E-cadherin which permits their detachment from the epidermis (Schwarzenberger 1996) and the upregulation of various adhesion molecules including integrins (Price 1997) and CD44 (Weiss 1997), which facilitate migration. The absence of junctional adhesion molecule 1 (JAM1) expression by DCs facilitates their migration to lymph nodes (Cera 2004); it is unclear whether JAM1 supports prolonged cell–cell interactions, impeding the passage of DC across the lymphatic endothelium, or whether the increase in DC migration that is observed in the absence of JAM1 is associated with the positive regulation of $\beta_1$-integrin expression by JAM1 (Mandell 2005), since $\beta_1$-integrins mediate the interaction of DCs with extracellular-matrix components and may favour retention of DCs in the periphery. Although integrins are not required for interstitial migration of DC (Lammermann 2008), they are required for the transendothelial migration of DC (Maddaluno 2009, Gunawan 2015).

CD38, a glycoprotein expressed on the surface of mononuclear phagocytes and other immune cells, is an ecto-enzyme, meaning that its active site is located on the outside of the cell, positioning it to respond to substrates found within the extracellular matrix. CD38 catalyses a reaction using NAD+ substrate, leading to the formation of the metabolites ADP ribose (ADPR) and cyclic ADP ribose (cADPR) that induce calcium flux via modulation of the cADPR- and ADPR-activated plasma membrane channel TRPM2. CD38 regulates the migration of DC precursors from the blood to peripheral sites and controls the migration of mature DCs from sites of inflammation to lymph nodes; mice lacking CD38 have impaired T cell dependent antibody responses. CD38 and cADPR modulate calcium mobilization in chemokine-stimulated DCs and are required for the chemotaxis of immature and mature DCs to CCL2, CCL19, CCL21, and C-X-C Motif Chemokine Ligand 12 (CXCL12) (Partida-Sanchez 2004). Of note, inflammatory signals and bacterial products that induce DC maturation and CCR7 expression often also induce upregulation of CD38.

Cell migration requires the dynamic interaction between a cell and the substratum on which it is attached and over which it migrates. In order to migrate, cells must acquire a special asymmetry, enabling them to turn intracellularly generated forces into net cell body translocation, leading to forward propulsion (Lauffenburger 1996). Lamellipodia and filopodia are membrane projections that

can extend reversibly into three dimensions around the cell in response to migratory stimuli, driven by actin polymerisation. Once the membrane protrusion has become adherent to the substratum, a contractile force is required to move the cell body forward; this may be driven by myosin interactions with actin filaments. Rapid migration requires efficient mechanisms to release adhesions at the rear of the cell, in order to allow the cell to move forward (Figure 8).

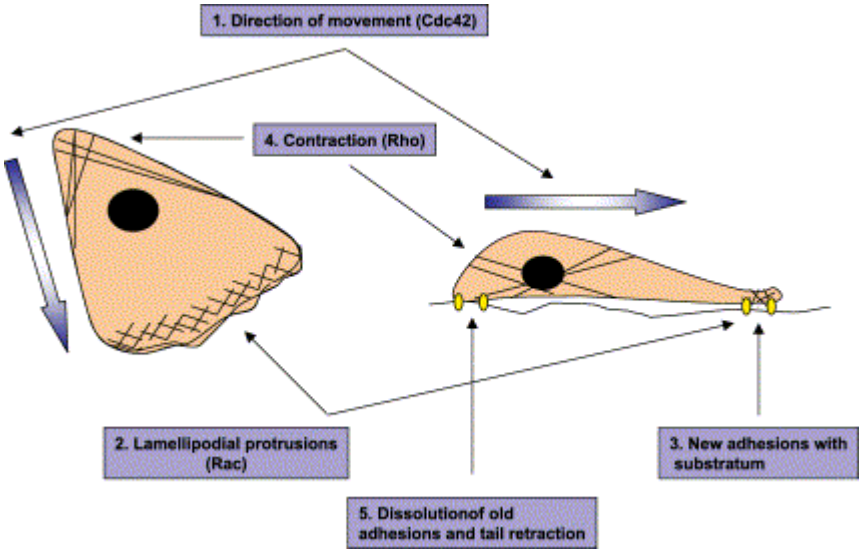


*Figure 8: Reprinted from (Raftopoulou 2004) with permission from Elsevier. A migrating cell (seen from the top and side). A migrating cell needs to perform a coordinated series of steps to move. Cdc42 regulates the direction of migration, Rac induces membrane protrusion at the front of the cell through stimulation of actin polymerization and integrin adhesion complexes, and Rho promotes actin:myosin contraction in the cell body and at the rear.*

All these steps involve the assembly, the disassembly or the reorganization of the actin cytoskeleton, and each must be coordinated both in space and time to generate productive, net forward movement. Alterations in DC migration can therefore be induced by modification of the process of actin polymerisation. A complex of 7 proteins known as actin-related proteins 2 and 3 (Arp2/3) complex regulates the assembly of new actin filaments at the leading edge of moving cells. Vinculin is a cytoplasmic actin-binding protein that eukaryotic cells use to strengthen adhesions and promote cell spreading and lamellipodial extension. Assembly of vinculin-containing focal complexes at the leading edge allows transient adhesion of the cytoskeletal network to the extracellular matrix, enabling development of traction force and forward movement of the cell. Vinculin selectively recruits Arp2/3 to the leading edge of the lamellipodium, coupling the actin polymerization machinery to adhesion complexes to promote membrane protrusion (Craig 2003). Although vinculin seems to restrain migration in two-dimensional (2D) tissue culture systems, it is required for the generation of traction forces necessary for effective directional migration in three-dimensional (3D)

collagen systems that may more closely mimic the *in vivo* environment (Thievessen 2015). Proteins of the Wiskott–Aldrich syndrome protein (WASP) family bind directly to Arp2/3 and stimulate its ability to promote nucleation of new actin filaments. Murine DC deficient in WASP exhibited defects of attachment and detachment to fibronectin coated surfaces *in vitro*, leading to impaired net translocation and displayed impaired DC homing *in vivo* in a FITC paint hypersensitivity model (de Noronha 2005). Upstream of the WASP family members, receptor tyrosine kinases, G-protein-coupled receptors, PI3K and the Rho family of GTPases receive and transduce the signals that lead to actin nucleation through WASP-Arp2/3 action. The Rho family includes Rho, which regulates the assembly of contractile, actin:myosin filaments as well as Rac and Cdc42 that appear to regulate the polymerization of actin to form peripheral lamellipodial and filopodial protrusions *(Nobes 1995, Raftopoulou 2004)*. Dock8 is a guanine nucleotide exchange factor that has been shown to activate the GTPase Cdc42 in mouse DCs and be critical for interstitial DC migration (Harada 2012, Krishnaswamy 2015, Eisenbarth 2016); DOCK8 mutations are associated with combined immunodeficiency in humans (Zhang 2009). Inhibitory signalling to the Arp2/3 complex mediated by a protein known as Arpin, provides a mechanism for directional persistence of migration and the ability for cells to steer (Dang 2013). Gadkin (also known as Ap1ar) negatively regulates Arp2/3 function (Maritzen 2012); it's loss impaired DC migration *in vitro* but not *in vivo*, suggesting compensatory mechanisms (Schachtner 2015). PI3K also controls the directionality of movement by controlling F-actin spatial localisation and leukocyte polarity towards chemoattractant (Rickert 2000). The signalling adaptor Eps8 is an actin capping protein involved in the formation of a dense actin meshwork, essential for sustaining persistent and extended cell protrusions required for effective DC migration (Frittoli 2011).

Although integrins are required for movement of leukocytes over two-dimensional surfaces, three-dimensional movement within tissues is integrin independent, and reliant on forces generated from actin-network expansion, with myosin-II dependent contractility required for squeezing through narrow gaps (Lammermann 2008).

DC are the only type of antigen presenting cell that have the capacity to stimulate the activation of naïve T cells, initiating a primary adaptive immune response. Naïve T cells collect in paracortical regions of lymph nodes and the spleen, migrating to these locations directly from the vasculature, not passing through peripheral tissues. Re-location of DC to lymph nodes increases their likelihood of encountering naïve CD4 T cells that express antigen receptors recognising the presented antigen peptide, and may potentially promote autoimmune T cell activation if autoantigen-containing immune complexes have been internalised (Figure 9). DC migration is also important once a DC reaches the lymph node; after establishing initial contact between their dendrites and naïve T cells,

mature DC migrate towards contacted lymphocytes and tightly entrap the T cells within a complex net of membrane extensions. DCs from *Rac1*−/− or *Rac2*−/− mice show severe alterations in dendrite formation, defective migration *in vivo* and impaired T cell priming *(Benvenuti 2004).*

ICs also contribute to relocation of DC by driving lymph node lymphangiogenesis, in a VEGF-A dependent process, controlled by FcγRIIb (Clatworthy 2014b).

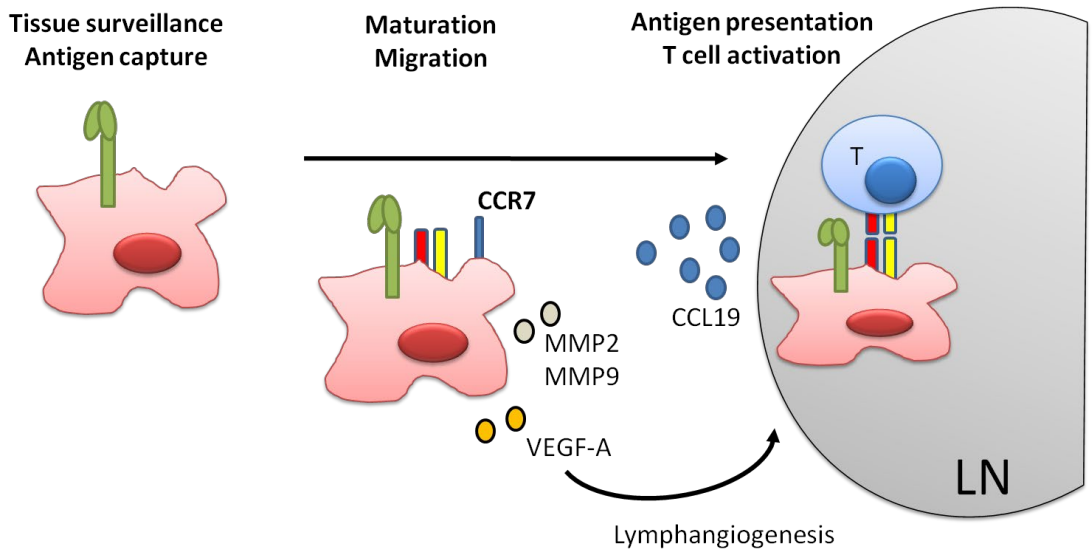


*Figure 9: Maturation of DC facilitates relocation and drives phenotypic change to meet altered functional requirements. FcγR expressed on the surface of DC (shown in green) recognise and bind the Fcγ portion of immunoglobulin, providing a pathway for the specific uptake of opsonized antigen. DC migrate from the periphery where they capture antigen to lymph nodes where they encounter T cells, following maturation signals inducing upregulation of the CCR7 receptor (shown in blue). DC expressing CCR7 are able to migrate towards a gradient of CCL19 which directs them to lymph nodes where they are more likely to encounter T cells expressing the TCR that recognises their internalised antigen. Upon maturation DC also secrete matrix metalloproteinases, promoting break down of the extracellular matrix facilitating forward migration and VEGF-A, supporting lymphangiogenesis. Once within the lymph node, DC present antigen in the context of MHC II (shown in red) to cognate T cells and provide co-stimulation signals, via ligation of co-stimulatory receptors with their respective ligands (shown in yellow), promoting T cell activation.*

### 1.6.4 Cell specific influence on autoimmunity

DC specific effects play an important role in autoimmune disease. Collagen induced arthritis (CIA) (Yilmaz-Elis 2014) and nephrotoxic nephritis (NTN)(Sharp 2013) are murine models of antibody mediated autoimmune disease, where FcγRIIb expressed on myeloid cells rather than on B cells is

protective. Despite their comparable anti-mouse collagen autoantibody titers, full FcγRIIb knockout (KO), but not B cell-specific FcγRIIb KO mice showed a significantly increased incidence and severity of disease compared with wild-type (WT) control mice when immunized with bovine collagen. Following immunisation with chicken collagen, disease incidence was significantly increased in pan-myeloid and full FcγRIIb KO mice but not in B cell-specific KO mice, compared with WT control mice; with an increase in disease severity only seen in full FcγRIIb KO mice. This suggests that anti-mouse collagen autoantibodies are a prerequisite for the development of CIA but their presence is insufficient for disease development, with FcγRIIb on myeloid effector cells controlling susceptibility by modulating the threshold for downstream Ab effector pathways (Yilmaz-Elis 2014). In a similar study, selective deletion of FcγRIIb from B cells did not increase susceptibility to NTN compared with WT mice, despite presence of increased antibody titres, but mice lacking FcγRIIb on myeloid cells had exacerbated disease. Where there was a lack of FcγRIIb on circulating myeloid cells, expression of FcγRIIb on intrinsic renal cells provided an additional level of protection from Ab-mediated glomerulonephritis (Sharp 2013).

SLE is an autoimmune disease characterised by the deposition of IgG immune complexes and so B cells are clearly of great importance to disease pathogenesis. Mice with B cells but not secreted Ig have severe disease indicating that both antibody dependent and independent functions are important (Chan 1999). B cells act as antigen presenting cells (Giles 2015) and prime autoreactive T cells (Chan 1998). The immune response to deposited immune complex determines the degree of tissue damage and disease progression, with T cells and MNP playing an important role (Bagavant 2009). DCs contribute to T cell pathogenicity following disease initiation, influencing tissue damage and are also an important source of BLyS (Teichmann 2010). The inducible T cell costimulator (ICOS) co-receptor stimulates Tfh cell differentiation in lymphoid tissue, supporting the germinal centre response. Local triggering of the ICOS coreceptor by CD11c+ myeloid cells drives organ inflammation in lupus prone mice by protecting Tfh and effector CD8+ T cells within inflamed tissues from apoptosis by signalling through the PI3K-Akt pathway, promoting cell proliferation and survival, with minimal effect on autoantibody titres (Teichmann 2015). Blockade of ICOS signalling could modulate pathogenic T cell responses, offering potential to attenuate destructive organ inflammation, regardless of the nature of the disease initiating event.

### 1.7 Treatment strategies for antibody mediated disease

#### 1.7.1 Current strategies

Several strategies exist for treating antibody mediated disease (Figure 10) including non-specific immunosuppressive regimes using corticosteroids, or other disease modifying agents for example

alkylating drugs such as cyclophosphamide, or anti-proliferative drugs such as methotrexate, azathioprine and mycophenolate mofetil. The development of more specific monoclonal antibodies has greatly impacted the treatment of autoimmune diseases. These include antibodies which target pro-inflammatory cytokines, for example TNFα (infliximab, adalimumab, etanercept) and IL-6 (tocilizumab), or are cytotoxic to B cells, causing their depletion via complement or antibody mediated cellular toxicity, for example rituximab and alemtuzumab. Belimumab, a monoclonal antibody blocking BLyS has shown some efficacy in SLE (Furie 2011, Navarra 2011, Manzi 2012) and is being trialled for other indications (see chapter 3). Direct removal of antibody via plasmapheresis can be used in some acute presentations where rapid control of disease is required, for example in Goodpasture's Syndrome (Bolton 1996).

Intravenous immunoglobulin (IVIG) is a preparation of human polyclonal IgG derived from pooled plasma samples, widely used in the treatment of autoimmune disease (Nimmerjahn 2007a) and in transplantation, in the setting of desensitisation prior to HLA-incompatible transplantation and as a treatment for ABMR (Jordan 2006). IVIG is hypothesised to have multiples modes of action including competition with pathogenic IgG for activating FcγRs, blocking access to these receptors and inhibiting immune cell activation; upregulation of the inhibitory receptor FcγRIIb; high dose IgG saturation of the neonatal Fc receptor (FcRn), disrupting FcRn mediated recycling of pathogenic IgG from acidic lysosomal vesicles, resulting in increased lysosomal degradation and rapid clearance of IgG; neutralisation of antigen via Fab mediated binding and inhibition of complement activation (Nimmerjahn 2007a, Clatworthy 2011).

Treatments focussed on increasing regulation of the immune response offer promise for autoimmune disease and transplantation (Wood 2012), for example by inducing or indeed transferring *ex vivo* manipulated tolerogenic DC (Morelli 2007, Hilkens 2013), Treg (Riley 2009, Miyara 2014), mesenchymal stem cells or Breg (Wang 2014). The One Study is a cooperative project, aiming to trial the use of cell based therapies in human renal transplantation (Geissler 2012).

Activation of Fcγ receptors induces signalling that leads to the transcription of pro-inflammatory cytokines. Small molecules for example PI3K inhibitors that interfere with cell signalling are in development and may be beneficial in treating autoimmune disease (Banham-Hall 2012). Activation of B cells and mononuclear phagocytes by cytokines or antibodies requires gene transcription in these cells. Using small drug molecules to target epigenetic modifications that regulate transcription may offer an alternative mechanism for controlling the inflammatory response.

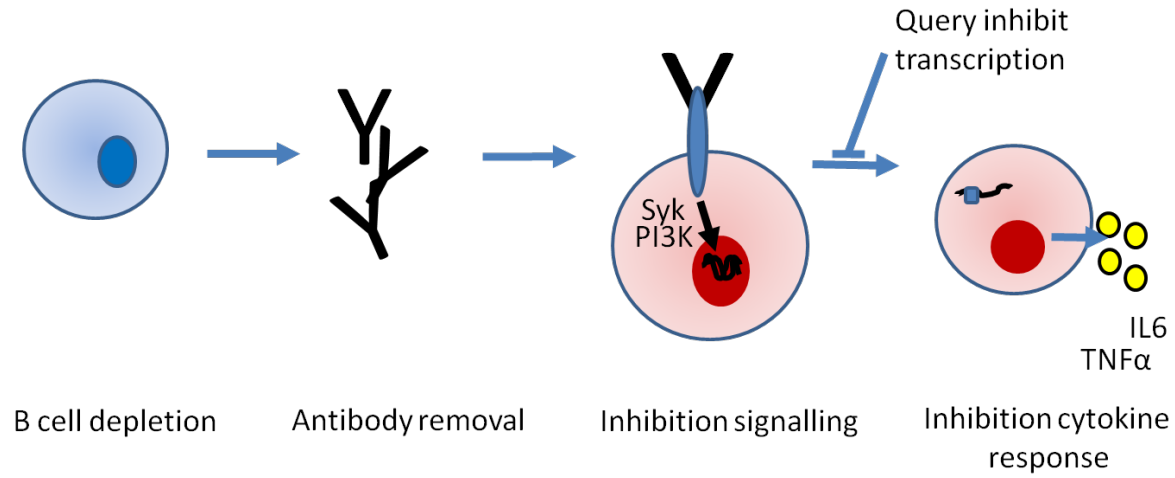


*Figure 10: Therapeutic options for antibody mediated disease. Current commonly used therapies include B cell depleting drugs for example rituximab and alemtuzumab; removal of preformed antibodies using plasmapheresis; and inhibition of downstream cytokines for example TNF$\alpha$ (infliximab, etanercept, adalimumab), IL-6 (tocilizumab) and IL1 (anakinra). Newer strategies in development with potential for use in autoimmune disease include those targeting intracellular signalling pathways, for example PI3K and Syk inhibitors and epigenetic modulators that inhibit the transcription of pro-inflammatory cytokines.*

### 1.7.2 Epigenetic modulation and bromodomain inhibition

Epigenetic marks are heritable post translational changes applied to deoxyribonucleic acid (DNA) or associated histones that do not affect the DNA sequence itself but have marked effects on chromatin structure, determining the likelihood of gene transcription due to changes in accessibility to the cell's transcription machinery. Histones are globular proteins which associate with DNA and have flexible N-terminal tails which can be covalently modified, for example by acetylation or methylation (Bannister 2011). Histones that are heavily acetylated have an open chromatin structure, are more accessible to RNA polymerases and are generally transcriptionally active (Struhl 1998).

Bromodomains are highly conserved, left twisted bundles of four α-helices, linked by diverse loop regions, forming a hydrophobic pocket that recognises acetylated lysine residues (Dhalluin 1999). In humans, there are estimated to be 56 bromodomains encoded in 42 proteins (Sanchez 2009). The bromodomain and extra-terminal domain (BET) family are a group of proteins that contain two mutually related bromodomain motifs (BD1 and BD2) and an extra-terminal domain and function as chromatin readers. They bind to acetylated lysine residues, acting as scaffolds for the assembly of

protein complexes critical for gene transcription, for example the positive transcription elongation factor (P-TEFb) complex (LeRoy 2008). They regulate gene transcription via controlling the recruitment of transcription factors, transcriptional co-activators and transcriptional co-repressors. In mammals the BET family includes BrdT, Brd2, Brd3 and Brd4. Transgenic mice that overexpress Brd2 develop B cell lymphomas and transplantable leukaemia (Greenwald 2004), suggesting an important role for BET proteins in the expansion and maintenance of lymphocytes with potential implications for autoimmune disease. Brd4 reads inducible acetylation marks at H4K5, H4K8 and H4K12 on primary response gene promotors, recruiting pTEFb (a complex formed by cyclin-dependent kinase 9 (CDK9) and its activator cyclin T1 which phosphorylates RNA-polymerase II (RNA Pol II) via CDK9, resulting in elongation of transcription, initiating a switch from basal RNA polymerase transcription of immature unspliced transcripts to productive transcription of protein coding mRNA (Hargreaves 2009) (Figure 11).

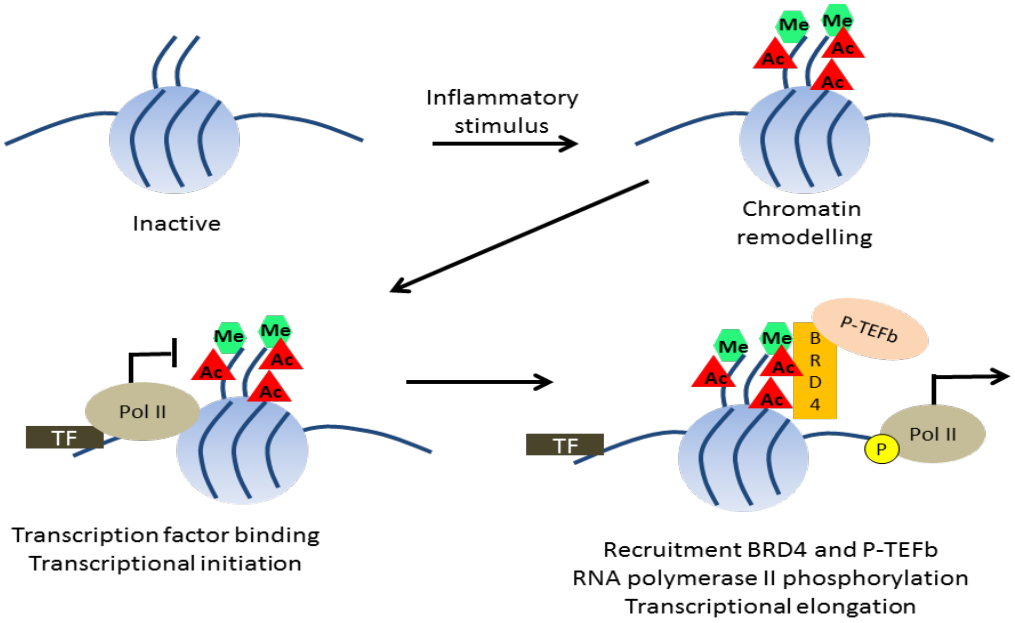


*Figure 11: BRD4 recruits P-TEFb and initiates gene transcription. Based on (Schaefer 2014). Inflammatory stimuli induce epigenetic changes, for example histone acetylation (illustrated as red triangles labelled Ac) and methylation (illustrated as green circles labelled Me), which lead to chromatin remodelling. Transcription factor binding sites (represented by rectangles marked TF) become exposed resulting in initiation of transcription. Induced acetylation of histones H3 and H4 (H3/H4Kac) recruits BRD4 and P-TEFb to chromatin. P-TEFb phosphorylates RNA polymerase II (Pol II) (indicated by a yellow circle labelled P), releasing it from a paused state, resulting in elongation of mature RNA.*

In addition, BET proteins regulate transcription of inflammatory genes at other levels. Brd4 is associated with regulating nuclear factor kappa beta (NF-κB) inducible responses (Figure 12). Binding of Brd4 to the acetylated lysine-310 residue of the RelA subunit of NF-κB is essential for the recruitment of Brd4 to the promoters of NF-κB target genes and subsequent coactivation of NF-κB. Brd4 further recruits CDK9 to phosphorylate RNA Pol II, activating the transcriptional activity of NF-κB (Huang 2009). BET family proteins have also been shown to have roles in regulating cell division with dysregulation associated with malignancy (Belkina 2012).

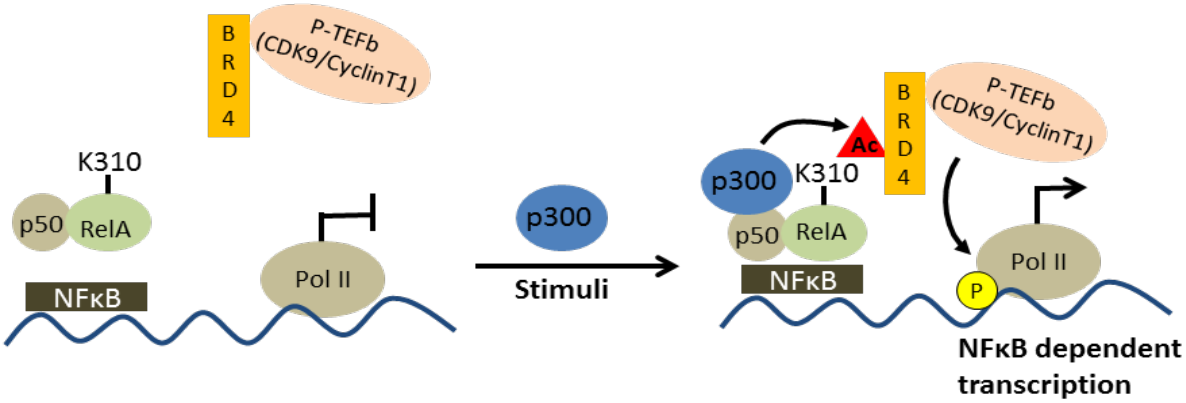


*Figure 12: Brd4 enhances transcriptional activation of NF-κB and the expression of a subset of NF-κB responsive inflammatory genes in an acetylated lysine-310-dependent manner. Following inflammatory stimuli, p300 acetylates RelA at the lysine-310 (K310) residue, triggering the recruitment of Brd4. Brd4 further recruits CDK9 to phosphorylate RNA Pol II, activating the transcriptional activity of NF-κB. Brd4 is also recruited to the promoters of a subset of NF-κB target genes during the activation of NF-κB.*

Stimulus-dependent acetylation of RelA at lysine-310 by p300 triggers the recruitment of Brd4 to the promoter via its bromodomains. Brd4 further activates CDK9 to phosphorylate the carboxyl-terminal domain of RNA Pol II and facilitates transcription of NF-κB target genes (Huang 2009).

The potential of BET proteins as a therapeutic target resulted in the development of BET-inhibitors, including the GlaxoSmithKline (GSK) compound I-BET762 (Nicodeme 2010) and JQ-1 (Filippakopoulos 2010), small molecules that mimic acetylated histones and interfere with their binding to BET proteins (Figure 13). Bromodomain inhibitors bind to the bromodomains of BRD4, preventing them from binding to acetyl-lysine modifications. In the absence of BRD4 recruitment, P-TEFb is unable to dock and phosphorylate RNA polymerase II, leading to a failure to initiate gene transcription. These compounds are currently in early clinical trials for cancer (Andrieu 2016a). I-BET151 is a compound

that retains BET selectivity but is optimised pharmacokinetically for *in vivo* use and has potential for oral chronic dosing (Dawson 2011, Mirguet 2012, Seal 2012).

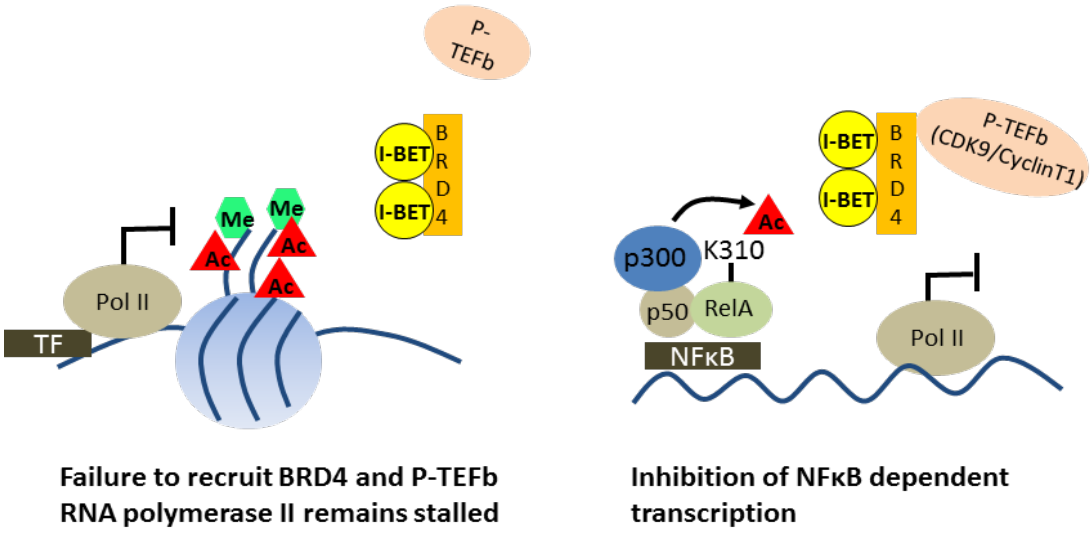


*Figure 13: Bromodomain inhibitors prevent BRD4 binding to acetylated lysine residues. I-BET bind to the bromodomains of BRD4, blocking their interaction with acetylated lysine residues. In the absence of BRD4 binding, P-TEFb is not recruited and RNA polymerase II remains stalled. I-BET selectively inhibits secondary response genes, including NF-κB and its target genes, that require* stimulation induced *chromatin remodelling prior to recruitment of* RNA polymerase II.

Selectivity of bromodomain inhibitors is in part based on the baseline epigenetic state of genetic loci. Affected genes generally have low levels of baseline H4 acetylation, H3K4 methylation, prior polymerase II recruitment and CpG, and belong to a group known as secondary response genes. Secondary response genes require new protein synthesis prior to induction, with formation of an initiation complex and recruitment of RNA polymerase for transcription. Genes affected by I-BET also have a greater reduction in BET recruitment following I-BET treatment compared to those not affected by treatment. In contrast, primary response genes initiate the early response, have higher levels of baseline H4 acetylation, H3K4 methylation, CpG and RNA polymerase II recruitment and are poised for immediate transcriptional activation and therefore are less dependent on BET protein recruitment for transcription. This does not explain all the differential selectivity of gene targets to I-BET; knockdown of BET genes with small interfering RNA (siRNA) suppressed the expression of Tnf that was resistant to I-BET762 treatment suggesting an additional mechanism independent of interaction with acetylated histones (Nicodeme 2010).

Super-enhancers are genomic regions with high numbers of enhancers identified by a concentrated region with high amounts of chromatin modification (Whyte 2013, Heinz 2015). Brown and

colleagues have described changes that occur in the endothelial cell epigenome associated with inflammation (Brown 2014) (Figure 14). Stimulation with TNFα prompted a dramatic and rapid NF-κB guided global redistribution of BRD4 away from basal endothelial super-enhancers to new inflammatory super-enhancers despite persistent histone hyperacetylation, leading to swings in transcriptional initiation and elongation and the transcription of key inflammatory genes. BRD4 is required to communicate enhancer remodelling to RNA Pol II, with the majority of enhancer bound BRD4 found within a small number of these super-enhancer regions. Bromodomain inhibition impedes NF-κB directed reorganisation of super-enhancers, suppressing super-enhancer dependent proinflammatory gene transcription, demonstrated by *in vivo* inhibition of atherogenesis, a pathogenic process dependent on inflammatory endothelial activation (Brown 2014).

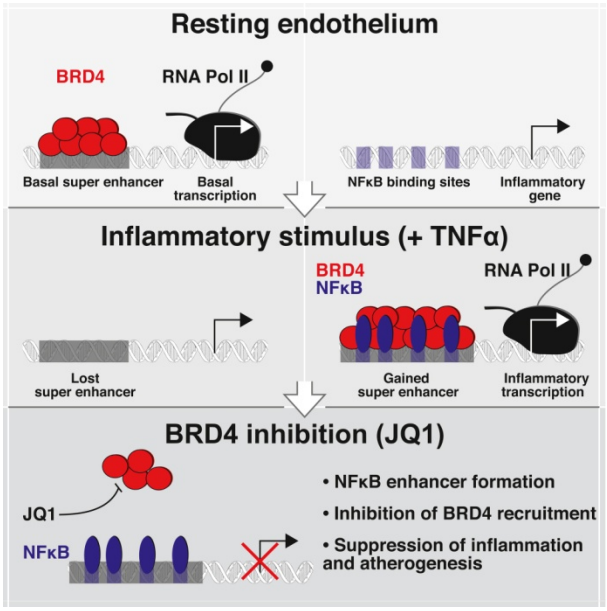


*Figure 14: Graphical abstract from (Brown 2014), reprinted with permission of Elsevier.*

Bromodomain inhibitors have been shown to selectively inhibit genes associated with inflammation following murine BMDM treatment with LPS *in vitro* and protect mice from LPS induced septic shock *in vivo* (Nicodeme 2010, Belkina 2013). Reanalysis of the Nicodeme et al. data set (Nicodeme 2010) shows that the LPS induced inflammatory response in murine macrophages can be explained by redistribution of super-enhancers, with preferential I-BET151 mediated inhibition of gene transcription driven by proinflammatory super-enhancers compared to those driven by typical enhancers (Brown 2014).

I-BET151 has also been shown to have effects on inflammatory responses in primary human monocytes. I-BET151 inhibited TLR4- and TNF-induced IFN responses and IFN-stimulated gene expression by both diminishing IFN-β expression and by suppressing transcriptional responses to

IFN-β. I-BET151 inhibited responses to cytokines (IFN-β, IFN-γ, IL-4, and IL-10) that activate the JAK-STAT signalling pathway, by inhibiting cytokine-induced transcription of STAT targets in a gene-specific manner without affecting STAT activation or recruitment, suggesting potential for effects on monocyte polarisation and inflammatory diseases (Chan 2014). Bromodomain inhibition inhibits the maturation of DC and enhances their tolerogenic properties (Toniolo 2015, Schilderink 2016). I-BET151 treated murine BMDC and human monocyte derived DC (MoDC) show reduced LPS induced expression of co-stimulatory molecules, reduced cytokine production and reduced T cell activation. Treatment of BMDC with I-BET151 did not affect their ability to polarise ovalbumin specific CD4+ CD62L+ naïve T cells towards Th1, Th2, or Th17 phenotype, but increased induction of Foxp3 expressing Treg with suppressive properties (Schilderink 2016). Similarly, JQ-1 impairs LPS-induced MoDC maturation, via a mechanism dependent on inhibition on LPS induced STAT5 phosphorylation and nuclear accumulation. JQ1 inhibited the expression of cytokines and cell surface markers associated with MoDC maturation leading to a decreased ability of MoDC to induce CD4+ and CD8+ T cell proliferation, reduced T-cell-mediated pro-inflammatory cytokine production and inhibition of Th1 polarization with maintained ability to induce Th2 cells and Tregs (Toniolo 2015).

BET proteins are expressed ubiquitously in mammalian tissues so inhibition may have effects on multiple lineages of cells. Effects on T cell differentiation have been shown with effects on multiple lineages. Treatment of naïve CD4+ T cells with a BET inhibitor during the first two days of differentiation had long lasting effects on subsequent gene expression and cytokine production and inhibited the ability of antigen-specific T cells, differentiated under Th1 but not Th17 conditions *in vitro*, to induce pathogenesis in an adoptive transfer model of EAE (Bandukwala 2012). The BET inhibitor JQ1 was reported by Mele and colleagues to have a selective effect on human and murine Th17 cell differentiation *in vitro*, directly regulating production of effector cytokines such as IL-17, IL-23 and granulocyte-macrophage colony-stimulating factor (GM-CSF). Therapeutic dosing inhibited EAE, a model induced by immunizing mice with myelin oligodendrocyte glycoprotein (MOG) peptide. *In vitro* stimulation of T cells obtained from the cervical lymph nodes of JQ1-treated EAE animals with MOG peptide produced normal levels of IFN-γ but reduced IL-17, suggesting a specific effect on Th17 cells (Mele 2013). Collagen induced arthritis was also inhibited by treatment with JQ1, although the mechanism of inhibition was not elicited in this study. JQ1 treated *in vitro* expanded antitumor T cells showed enhanced persistence and antitumour effects in murine models, maintaining features of stem cell–like and central memory T cells (Kagoya 2016).

The innate immune response is critical in determining the response to tissue injury and whether this results in repair or fibrosis. JQ1 suppresses innate inflammatory and profibrotic transcriptional networks robustly enriched for NF-κB and TGF-β signalling in heart failure, improving outcomes in

mice with pre-established heart failure from chronic pressure overload and following induction of massive anterior myocardial infarction (Duan 2017). Bromodomain inhibition has also shown benefit in animal models of renal (Xiong 2016, Zhou 2017), lung (Tang 2013) and liver (Ding 2015, Zhubanchaliyev 2016) fibrosis.

The broad range targets for bromodomain inhibition means that it is likely that effects on multiple pathways contribute to inhibition of inflammatory responses. Beatriz Suarez-Alvarez and colleagues show that JQ1 reduces inflammation in multiple models of renal injury; unilateral ureteric obstruction, anti-glomerular basement membrane antibody induced nephrotoxic nephritis and angiotensin II induced renal damage (Suarez-Alvarez 2017). Common findings included reduced proinflammatory mediators and reduced infiltration of inflammatory macrophages/monocytes. JQ1 was shown to inhibit direct BRD4 binding to proinflammatory gene promotors including those for CCL2, CCL5 and IL6, inhibit canonical NF-κB pathway activation, reducing RelA nuclear levels in the injured kidneys across models, and target IL-17 production suggesting an effect on Th17 immune responses. JQ1 has also been shown to attenuate the progression of proteinuria and nephritis and improve survival in a MRL-lpr murine lupus model, with reduced levels of pro-inflammatory cytokines, BAFF and serum anti-dsDNA antibodies and reduced immune complex-mediated activation of human monocytes *in vitro* by JQ1 (Wei 2015).

Targeting of integral pathways, for example the NF-κB pathway, may allow use of this class of drug in a broad range of inflammatory conditions, irrespective of the initial cause of injury. However, some argue that lack of specificity may limit use, and there is ongoing interest in developing new compounds with improved selectivity. The first bromodomain (BD1) functions to anchor the activated Brd4/transcription protein complex to target genes in chromatin through binding to lysine-acetylated histone H4 (Zhang 2012), whereas the second bromodomain (BD2) of Brd4 is dedicated to interaction with lysine-acetylated transcription factors and p-TEFb (Schroder 2012). Selective inhibition of BD1 of BET proteins, with the newly described bromodomain inhibitor MS402, inhibits primarily Th17 cell differentiation with a little or almost no effect on Th1 or Th2 and Treg cells and prevents and ameliorates T-cell transfer-induced colitis in mice by blocking Th17 cell overdevelopment (Cheung 2017). Genomic sequencing analysis of BET inhibitor treated murine Th17 cells confirmed a more selective effect of MS402 over JQ1; MS402 was similarly effective in releasing Brd4 genomic occupancy at Th17 signature genes and super-enhancers but had fewer effects than JQ1 at housekeeping genes.

The timing of treatment may be critical in determining the effect on host immunity and whether beneficial host innate immune responses are affected. The Nos2 gene encoding inducible nitrous

oxide synthase (iNOS) is activated during infection with the intracellular organism Listeria. Inhibition of BET proteins by JQ1 treatment strongly reduced nitrous oxide production and immunity of mice to Listeria monocytogenes and influenza virus. JQ1 also exacerbated the colitogenic activity of dextran sodium sulfate where the host inflammatory response is protective (Wienerroither 2014).

**1.8 Hypotheses:**

1. Belimumab (an anti-BLyS antibody), given in conjunction with standard maintenance immunosuppression, will reduce B cell activation and antibody generation and B cell production of pro-inflammatory cytokine in renal transplant recipients

2. Bromodomain inhibition will selectively inhibit FcγR-mediated MNP activation, providing a novel therapeutic strategy in IgG-immune complex-associated inflammation.

**1.9 Aims of the project:**

i. To perform an experimental medicine study in human kidney transplant recipients in order to characterise B cell activation post-renal transplant, and to determine if BLyS neutralisation is a useful therapeutic strategy to modulate B cell cytokine production, antibody formation and T cell activation in this clinical context.

ii. To undertake pre-clinical studies in human and mouse cells *in vitro*, and to perform *in vivo* murine experiments, to determine if and how bromodomain inhibitors modulate:
    a. immune complex uptake and processing by macrophages and their generation of cytokines and chemokines.
    b. FcγR-mediated dendritic cell migration and activation by IgG immune complexes.

**Chapter 2: Materials and Methods**

### 2.1 BEL114424 clinical trial

The clinical study was a collaborative project with clinicians, scientists and statisticians from Addenbrooke's Hospital, the University of Cambridge and GSK all being critical for its design, implementation and completion. The human biological samples were sourced ethically and their research use was in accord with the terms of the informed consents under an institutional review board (IRB)/ethics committee (EC) approved protocol.

#### 2.1.1 Study design

In this phase IIA, randomised, double-blind, sponsor unblind study (BEL114424; clinical trials.gov identifier NCT01536379; EudraCT number 2011-006215-56), subjects were recruited between September 2013 and February 2015 at a single UK transplant centre (Addenbrooke's Hospital, Cambridge). Subjects were randomised 1:1 to receive 7 doses of intravenous (IV) belimumab 10mg/kg or placebo (0.9% sodium chloride solution) by at days 0, 14, 28 followed by 4-weekly doses through to week 20, in addition to basiliximab (20mg IV days 0 and 3), tacrolimus (0.15mg/kg daily: target trough level 6-10μg/L first 6 months post transplantation, 5-8μg/L thereafter), mycophenolate mofetil (500mg twice daily) and prednisolone (20mg daily initially, weaning to 5mg daily in month 1-2). Patients received infection prophylaxis with nystatin (1st month), co-trimoxazole (months 1-6) and valganciclovir (months 1-6), and were followed for 12 months.

#### 2.1.2 Study patients

Patients aged 18 to 75 years receiving a kidney transplant were eligible for inclusion. Exclusion criteria included donor age <5 or >70 years, ABO blood type incompatibility, 0-0-0 HLA mismatch, a positive T and/or B cell cross-match, and previous recipient exposure to B cell targeted therapy (full eligibility criteria are in the study protocol available at www.gsk-clinicalstudyregister.com/study/114424#ps).

Initial study recruitment was slower than anticipated and my feedback on the recruitment process guided changes to the study protocol to allow targets to be met. Addenbrooke's hospital specialises in transplanting kidneys donated after circulatory death (DCD). The majority of DCD donors did not meet initial tight donor exclusion criteria in view of their age and comorbidities; an amendment was sought to widen eligibility criteria (protocol amendment 4, dated 16 October 2013). The original protocol excluded DCD donors aged > 60 years old, or > 50 if they had died from a stroke, had a history of high blood pressure, or had a serum creatinine greater than 135μmol/L at the time of donation. We felt that including all DCD donors <70 would not impact on the quality of the study but may substantially improve recruitment.

Due to the nature of deceased donor transplantation there was often a restricted time window for gaining informed consent, compounded by the fact that this was a time of heightened emotions, not ideally suited to complex decision-making, where standard procedures required to facilitate timely transplantation took precedent. I observed a wide range of attitudes and risk behaviours towards clinical trials in patients with end stage kidney disease and placed high importance on ensuring that I maintained focus on protecting potentially vulnerable research participants. The trial involved a complex protocol with frequent sampling and dosing which was not well received by many patients who wished to receive their transplant and return to follow-up at local centres as soon as possible. The patient information sheet was lengthy and could not be shortened due to legal restraints. My experience consenting patients highlighted areas of common misunderstanding and guided minor amendments. The practicalities of obtaining and processing samples for multiple mechanistic studies and coordinating required study staff proved particularly challenging out of hours; a pharmacy out of hours rota was finalised to facilitate out of hours recruitment. Due to these challenges, recruitment was slower than initially anticipated and an additional centre at Guy's Hospital was added to the study in August 2014. Study recruitment was completed in February 2015 with all subjects consented at Addenbrooke's Hospital.

**2.1.3 Study endpoints**

Co-primary endpoints were safety and efficacy measured by change in naïve B cells from baseline to Week 24, a biomarker of functional BLyS neutralisation validated in patients with SLE (Navarra 2011). Safety was measured via capture of adverse events and serious adverse events, classified using the Medical Dictionary for Regulatory Activities.

Secondary and exploratory endpoints included pharmacodynamics, immunological biomarkers (e.g. regulatory B cells, assessment of peripheral blood transcriptional profiles, and non-HLA antibodies) and clinical endpoints.

**2.1.4 Study oversight**

The study was designed by the sponsor, GSK, in close collaboration with principal investigators at Addenbrooke's Hospital. The study was approved by the local Research Ethics Committee and all patients provided written informed consent.

**2.1.5 Statistical analysis (Led by Mr Don Shanahan, GSK):**

Primary analyses were undertaken using a pre-specified modified intention to treat (MITT) population including all patients randomised who received at least one infusion of study drug.

Secondary and exploratory biomarker outputs were undertaken using a pre-specified per protocol (PP) population that included all MITT subjects who received at least five infusions of study drug, were followed up beyond week 24 and received no prohibited medications or plasma exchange (referred to as PP1 population in the study reporting and analysis plan (RAP)).

No formal statistical hypotheses were defined in the RAP. For the primary and secondary biomarker endpoints, a mixed model for repeated measures (MMRM) approach was used to produce adjusted mean differences between belimumab and placebo with corresponding 95% confidence intervals. The MMRM approach used fixed categorical effects of treatment, visit, donor organ status (coded as live donor, donated after brain death, donated after circulatory death) and treatment-by-visit interaction and fixed continuous covariates of baseline values and baseline values-by-visit interaction. A compound symmetry variance structure was used to model the within-patient errors, shared across treatments.

All post hoc analyses are labelled as such. Analyses were performed using SAS version 9.3 except for transcriptomic and protein microarray analyses, which were performed using R version 3.3.1. I recreated graphs for publication using Prism software. For exploratory analyses outside of the RAP, analysis was performed in Prism and the approach verified by the statistics team lead by Mr Don Shanahan, GSK. Data integrity was checked according to GSK internal procedures.

The target sample size of 20 evaluable subjects was calculated to achieve a reduction in naïve B cell count from baseline to 24 weeks, based on naïve B cell data from a previous trial of belimumab in SLE (BLISS-76) (Stohl 2012) and n=93 renal transplant recipients at the Cambridge Transplant Unit (unpublished data). Interim re-estimations of sample size were performed in November 2014 and February 2015.

**2.1.6 Visit windows**

Assessments were assigned to visit windows (slots) according to the date of assessment (for study schedule see study protocol). For adverse events the on-treatment phase commenced from the start of the first infusion of belimumab/placebo and ended 28 days after the last dose. The post-treatment phase began the following day. For other primary and secondary endpoints, the on-treatment phase ended 35 days after the last dose to allow incorporation of the On-Trt Week 24 visit on day 168 +/- 7 days.

The visit slotting intervals for the Pre-Treatment and On-Treatment (On-Trt) phases for biomarker endpoints were as follows:

| Week | Day relative to first infusion | Day | Visit Window |
|---|---|---|---|
| Baseline | ≤0 | ≤0 | ≤0 |
| On-Trt Week 4 | 28 | 28 - 27 Days or + 14 Days | Days 1 to 42 |
| On-Trt Week 8 | 56 | 56 - 13 Days or + 14 Days | Days 43 to 70 |
| On-Trt Week 12 | 84 | 84 - 13 Days + 42 Days | Days 71 to 126 |
| On-Trt Week 24 | 168 | 168 - 41 Days +7 Days | Days 127 to 175 |

The visit slotting intervals for the Post-Treatment (Post-Trt) phase for biomarker endpoints were as follows:

| Week | Day relative to (last infusion + 35 Days) | Day relative to last infusion | Day | Visit Window |
|---|---|---|---|---|
| Post-Trt Week 12 | 84 | 119 | 84 – 83 Days or + 56 Days | Days 1 to 140 |
| Post-Trt Week 28 | 196 | 231 | 196 – 55 Days or + 154 Days | Days 141 to 350 |

If more than one assessment fell within the same visit window, the assessment nearest to the scheduled time point was used. If two assessments were equally close, the latter was used. Samples for transcriptomic and protoarray analysis were collected at baseline, at week 24 (+/- 7 days) and at week 52 (+/- 7 days) according to the study schedule, irrespective of the last dose of study drug given, so data for these endpoints are presented without window fitting. On-treatment samples for the B cell stimulation assay were limited so the last available on-treatment result is displayed ('Last On-Trt').

### 2.1.7 Immunophenotyping

Immunophenotyping was performed by flow cytometry with absolute cell numbers calculated using TBNK counts.

Sample processing, acquisition and blinded gating was performed by the GSK Clinical Unit Cambridge (CUC) team and QUEST; analysis of exploratory biomarker outputs was performed by Dr Gemma Banham with data integrity checks performed by Ms Adele Gibson, GSK.

### 2.1.8 BEL114424 B cell stimulation assays

B cell stimulation assays were performed by Dr Gemma Banham in collaboration with Ms Adele Gibson, GSK.

For validation studies PBMC were isolated from human whole blood from healthy volunteers collected into Lithium Heparin Vacutainer tubes (BD Biosciences) (Blood Donation Units at GSK, Stevenage and GSK CUC Addenbrooke's, Cambridge). Blood was diluted and layered on to 15ml Ficoll-Paque (GE Healthcare) in 50ml Accuspin tubes and centrifuged at 800g for 20mins without breaking. The mononuclear layer at the interface was harvested, washed and counted. For freezing, cell pellets were resuspended in freezing medium A (60:40 fetal calf serum (FCS):RPMI), followed by an equivalent volume of freezing medium B (80:20 FCS:DMSO added dropwise), to make a final concentration of 1 x $10^7$ cells per ml. Cells were transferred to cryovials in 1ml aliquots and frozen at -80$^0$C, and transferred to liquid nitrogen storage one week later until ready to be used.

For the BEL114424 Breg assay, frozen PBMC samples were used from specified trial timepoints. These samples were processed following venepuncture by the GSK CUC according to standard operating procedures, in line with the BEL114424 study protocol and stored in liquid nitrogen until ready to be used.

Frozen peripheral blood mononuclear cells were thawed, washed and resuspended in RPMI, supplemented with 1% L-glutamine (Gibco), 1% penicillin/streptomycin (Gibco) and 10% heat inactivated FCS (PAA Labs), and plated in flat bottom 48 well plates at a concentration of 1x$10^6$ cells in 200µl. Cells were incubated at 37°C in a 5% CO2 humidified incubator for 48 hours with stimuli applied as described. CpG DNA Oligodeoxynucleotides (100nM; Hycult Biotech) and CD40L (1µg/ml; R&D Systems) were added at the beginning of the 48 hour incubation period (48 hour stimulation) or just for the last 5 hours (5 hour stimulation). Phorbol 12-myristate 13-acetate (PMA) (50ng/ml; Sigma-Aldrich), ionomycin (500ng/ml; Sigma-Aldrich) and brefeldin A (5µg/ml; BioLegend) (PIB) were added for the last 5 hours of culture. Following stimulation the cells were harvested, washed in FACS buffer (phosphate buffered saline (PBS) with 1% FCS and 0.1% NaN3), blocked with human FcX Trustain block (BioLegend), then stained with a surface antibody panel, followed by live dead discrimination using fixable aqua dead cell dye (Invitrogen), fixed and stored overnight at 4°C prior to permeabilization (Invitrogen) and intracellular staining prior to acquisition using a flow cytometer.

Antibodies used are listed in Appendix 2.

### 2.1.9 B cell stimulation assays on healthy controls

These assays were performed by Mr. Joseph Chadwick, GSK with guidance from Dr Gemma Banham and Ms Adele Gibson.

CD19+CD27+ memory B cells were enriched from PBMCs of 16 healthy donors using a human memory B cell isolation kit (Miltenyi Biotec) and cultured *in vitro* in the presence of CpG (100nM; Hycult Biotech) and CD40L (1µg/ml; R&D Systems) with 0 to 200ng/ml BLyS (GSK) for 48 hours. Phorbol 12-myristate 13-acetate (PMA) (50ng/ml; Sigma-Aldrich), ionomycin (500ng/ml; Sigma-Aldrich) and brefeldin A (5µg/ml; BioLegend) were added for the last 5 hours of culture and IL-6 and IL-10 quantified by flow cytometry. In 7 of these healthy donors, 15nM belimumab (GSK) was added in addition to 100ng/ml BLyS.

### 2.1.10 Transcriptomic analysis

Performed by Dr Shaun Flint (University of Cambridge/GSK) and Dr Paul Lyons, University of Cambridge.

RNA was extracted from whole blood or from purified leukocyte subsets in Professor Smith's laboratory (University of Cambridge), as described previously (Lyons 2007), and hybridised to Human Gene ST 2.1 microarrays (Affymetrix). Microarray data are available in the ArrayExpress database (http://www.ebi.ac.uk/arrayexpress) under accession number E-MTAB-5906.

Lysates (CD4+ T-cell) and PaxGene tubes (whole blood) were stored at -80°C until required. RNA was extracted from CD4+ T-cell lysates using an AllPrep Kit (Qiagen) and from whole blood using the PAXgene system (Qiagen). RNA was processed and hybridised to Human Gene ST 2.1 microarrays (Affymetrix) according to the manufacturer's instructions.

Affymetrix CEL files were imported into R/Bioconductor, normalised and summarised at the transcript cluster level using the oligo package (rma function, target = "core"). Transcript clusters were annotated using Ensembl biomaRt and manufacturer's own annotation and Affymetrix control probes were removed. Non-protein coding probes were also removed.

Weighted gene coexpression network analysis (WGCNA) was undertaken of the whole blood gene expression data using the WGCNA package in R/Bioconductor. One of the resulting whole blood gene expression modules was identified as representing a B-cell transcriptional programme on the basis of a unique overlap of module genes with the Gene Ontology class 'GO:0050853 BCR signalling pathway'. Module expression was determined as the value of the first principal component

calculated from module gene expression, along standard analysis lines for WGCNA and using functions in the WGCNA package.

Differential gene expression analyses were performed using the limma package in R/Bioconductor. The model incorporated time-point and treatment group interaction terms and accounted for the repeated measures nature of the analysis (study participants contributed gene expression samples at three different timepoints) using the duplicateCorrelation function. Contrasts were defined for differential expression at baseline, 24 weeks and 52 weeks (Belimumab – Placebo at each timepoint). Estimates were adjusted using the eBayes function.

Where there was more than one transcript cluster per gene, differential expression was summarised into a single gene measure using the mean log-fold change. Immunoglobulin coding genes were identified from their Ensembl Biotype annotation. Cell cycle genes were identified using the Gene Ontology class 'GO:0007049 Cell cycle'.

#### 2.1.11 ProtoArray® (Invitrogen) protein microarrays

Assay run by Thermo Fisher, analysis performed by Dr Shaun Flint, GSK

Serum samples were stored at -80°C until required. ProtoArray® Human Protein Microarray 5.1 slides were blocked in blocking buffer (50 mM HEPES, 200 mM NaCl, 0.01% Triton X-100, 25% glycerol, 20 mM reduced glutathione, 1.0 mM DTT, 1X Synthetic Block) at 4 °C for 1 hour. After blocking, arrays were rinsed once with freshly prepared PBST buffer (1X PBS, 0.1% Tween 20, and 1 X Synthetic Block). Arrays were then probed with a 1:500 dilution of each sample diluted in 5 mL of PBST buffer. Arrays were incubated for 90 minutes at 4°C in QuadriPERM 4-well trays (Greiner) with gentle agitation. After incubation, slides were washed five times (5 minutes per wash) in 5 ml PBST Buffer in 4-well trays. An Alexa Fluor®647-conjugated goat anti-human IgG antibody diluted in 5 ml PBST buffer to a 1.0 µg/ml final concentration was added to each array and allowed to incubate with gentle shaking at 4°C for 90 minutes. After incubation, the secondary antibody was removed, and arrays were washed as described above. Arrays were dried by spinning in a table top centrifuge equipped with a plate rotor at 200x gravity for 2 minutes. Arrays were then scanned using a Tecan PowerScanner™ fluorescent microarray scanner.

GenePix 7 software was used to overlay the mapping of human proteins in the array list file to each array image with a fixed feature size of 130 um (diameter). After aligning each of the 48 subarrays using spots from the AlexaFluor®-conjugated and murine antibodies printed in each subarray, the features were resized by the GenePix software to best fit the feature. Pixel intensities for each spot

on the array were determined. Arrays were normalised and a signal for each spot on the array calculated by subtracting the local background signal. Microarray hybridisation and these initial processing steps were performed by ThermoFisher.

After removing data from control group spots and TNFSF13B (as bound by belimumab) the signal from duplicate spots was combined (mean) to give one value per unique antigen. This dataset was used to define a global threshold for 'significant' antibody binding (10,750) by maximising the signal-to-noise ratio for the comparison of number of antigen with a signal above threshold in samples at baseline (no immunosuppression) versus Week 24 (maximal immunosuppression). This approach avoided defining a threshold based on the parameter of interest (treatment group), relying on the biologically plausible hypothesis that there would be differences in circulating auto-/allo-antibody pre- and post-transplant.

This threshold was used to determine whether an individual antigen specificity had significant antibody binding (yes/no). New antigenic specificities post-transplant were defined as antigenic specificities with significant binding at week 24 post-transplant not observed at baseline (week 0). Patient serum was hybridised to ProtoArray (Invitrogen) protein microarrays according to manufacturer's instructions.

### 2.2 Investigation of the effect of bromodomain inhibitors on FcγR mediated MNP activation

The human biological samples used were sourced ethically and their research use was in accord with the terms of the informed consents under an institutional review board/ethics committee approved protocol.

#### 2.2.1 Generation of macrophages from murine bone marrow

Femurs and tibiae from C57BL/6 mice were removed and separated from the surrounding muscle tissue by blunt dissection. Intact bones were disinfected in 70% ethanol. The bone ends were cut with sterile scissors and the marrow flushed with sterile PBS using a 23G needle. Cells were spun at 1300rpm for 5 minutes then re-suspended in RPMI 1640 media supplemented with 1% penicillin-streptomycin and 10% FCS (all Sigma) in 10cm petri dishes (one leg per petri dish in 5ml media). To promote differentiation to a macrophage phenotype recombinant murine macrophage colony-stimulating factor (M-CSF) (Peprotech; final concentration 10ng/ml) was added to the media. Media was supplemented on day 3 and changed on day 6 and cells seeded in 6, 12, or 24 well culture plates at an appropriate density suitable for individual experiments when displaying morphology consistent with a mature state (day 3-6)

### 2.2.2 Generation of bone marrow derived dendritic cells from murine bone marrow

Femurs and tibiae were processed as above. The cells obtained from each mouse were resuspended in 60ml RPMI 1640 media supplemented with 1% penicillin-streptomycin and 10% FCS (all Sigma) in a 75cc tissue culture flask. To promote differentiation to a dendritic cell phenotype recombinant murine granulocyte-macrophage colony-stimulating factor (GM-CSF) (Peprotech; final concentration 20ng/ml) was added to the media. Non adherent cells were removed with half the media on day 3, and the media replaced with murine GM-CSF (Peprotech; final concentration 40ng/ml). Non adherent cells were removed on day 6 and plated in appropriate tissue culture plates for use in media supplemented with murine GM-CSF (Peprotech; final concentration 20ng/ml). Cells were used between days 7 to 10.

### 2.2.3 Generation of human monocyte derived macrophages

The human biological samples used were sourced ethically and their research use was in accord with the terms of the informed consents under an IRB/EC approved protocol. ”Leukocyte “cones” were obtained from the National Blood Service (Cambridge, UK). Cell fractions were separated using Histopaque 1077 (Sigma-Aldrich, Gillingham, UK) and the monocyte layer retrieved. Cells were cultured in cRPMI with 0.1 mcg/ml MCSF (Peprotech, London, UK) and were supplemented every 72 hr for 5-10 days. Adherent cells were lifted with a cell scraper. Mature macrophages were identified according to their distinctive forward/side scatter profile on flow cytometry.

### 2.2.4 Reconstitution of I-BET 151

I-BET151 was supplied by GSK. For *in vitro* assays, a stock solution of 10mM was prepared in DMSO (Sigma), and further diluted to desired concentrations in cell culture medium prior to addition to cells. For *in vivo* studies, I-BET151 was dosed at 30mg/kg and prepared by dissolving in normal saline containing 5% (v/v) DMSO and 10% (w/v) Kleptose HPB.

### 2.2.5 Flow cytometry

Cells were stained for flow cytometry according to standard protocols, briefly summarised here.

1. Adherent cells were scraped off cell culture plates using the plunger of a suitably sized syringe and collected in a 12x75 mm round bottomed FACS tube. Following centrifugation for 5 minutes at 1300 rpm at 4$^{o}$C, supernatants were discarded and the cell pellet agitated to achieve a single cell suspension in a volume of approximately 100 µL.

2. Non-specific Fc-mediated staining was inhibited by adding 1µl normal mouse serum to each tube and incubating for 15 minutes on ice prior to staining with specific antibodies.
3. For directly conjugated antibodies (see appendices), an appropriate quantity of each primary antibody was added and the cells incubated on ice in the dark for 45-60 minutes. Staining for CCR7 was performed at room temperature.
4. Cells were washed with PBS (2ml/tube) and centrifuged at 1300rpm for 5 minutes at 4°C. The supernatant was discarded and the pellet re-suspended
5. Step 4 repeated.
6. Cells were then stained for viability using LIVE/DEAD® Fixable Aqua Dead Cell Stain Kit (Life Technologies; #L34957) according to the manufacturer's instructions.
7. Cells were fixed in FACS FICS (PBS containing 1% formaldehyde, 0.02% sodium azide, 2% glucose)
8. FACS was performed using a BD LSRFortessaTM (Becton Dickinson) flow cytometer. Data were analysed with FlowJo software (Tree Star).

Antibodies used are listed in the appendices

### 2.2.6 Preparation of immune complexes for *in-vitro* stimulation

LPS-free ovalbumin (OVA; Hyglos GmbH) was mixed in the following quantities with rabbit anti-OVA (Sigma) and PBS and incubated at 37 °C for 60 minutes:

To stimulate 0.5-1 x$10^6$ macrophages in a volume of 300µl in a 24 well plate:

0.4µl of 1mg/ml solution of OVA

4µl of rabbit anti-OVA (3-5mg/ml)

7.8µl of PBS

For phagocytosis assays where half the amount of OVA-conjugate (Ovalbumin-647 (Invitrogen) or Ovalbumin-FITC (Invitrogen)) and rabbit anti-OVA were used to avoid oversaturation of the assay.

### 2.2.7 Phagocytosis of immune complexes

The phagocytic ability of macrophages treated with I-BET151 or DMSO was assessed using a flow cytometry based phagocytosis assay. Bone marrow derived macrophages (BMDM) were fed ovalbumin conjugated to alexa flour 647 (OVA-647) that had been opsonized with rabbit anti-ovalbumin immunoglobulin (IC; prepared as described above). Cells were harvested at defined time

points and washed to remove free IC. Phagocytosis was assessed via flow cytometry following desired surface and viability staining. The percentage of cells containing phagocytic material were quantified using an untreated control to set the positive gate. In addition the geometric mean fluorescence in the alexa flour 647 channel of all live cells and phagocytic index (geometric mean fluorescence of live phagocytic cells) were calculated to quantify phagocytosis.

Phagocytic degradation products were identified by substituting OVA-647 for DQ-OVA (Invitrogen), a conjugate that exhibits bright green fluorescence only after proteolytic degradation.

### 2.2.8 Phagocytosis of apoptotic cells

Thymi of C57BL/6 mice were removed and passed through a 70μm cell strainer. Thymocytes were labelled with cell tracker orange (ThermoFIsher) according to the manufacturer's instructions, then rendered apoptotic via treatment with dexamethasone (Sigma; 1μM for 17 hours). Phagocytosis was assessed via flow cytometry and confocal microscopy.

### 2.2.9 Confocal microscopy

Murine BMDM were isolated from bone marrow and grown as described above. When mature, they were seeded onto glass cover slips sterilised in 70% ethanol prior to placing in 24 well culture plates. For assessment of immune complex phagocytosis, immune complexes were prepared as described above, and added to culture wells at defined time points prior to fixation of cells and staining. Staining was performed as follows:

1. Cells were washed with RPMI to remove free IC
2. Cells were fixed to cover slips by incubation with FACS FICS for 15minutes.
3. Cells were blocked and permeabilised in blocking buffer made from 0.1M TRIS, 1%BSA, 0.1% Triton X-100, 1% normal goat serum (goat secondary antibodies used)
4. Cells were incubated at room temperature with primary antibodies diluted in blocking buffer for 1-3 hours.
5. Following washing with 0.1M TRIS, cells were incubated at room temperature for 1-2 hours with appropriate secondary antibodies diluted in blocking buffer.
6. Slides were incubated with phalloidin diluted in blocking buffer for 45-60 minutes
7. Following a further wash, cover slips were mounted onto slides using VectaShield Hardset Mounting Medium with DAPI (Vector Labs #H1500)
8. Images were acquired using a Zeiss 710 or 780 confocal microscope and analysed using Imaris software.

For quantification of cell adhesion cells, following permeabilization, cells were stained with phalloidin alone and mounted using VectaShield Hardset Mounting Medium with DAPI (Vector Labs #H1500).

Antibodies used are listed in the appendices

**2.2.10 Cytokine measurement**

TNF-α and IL-6 concentrations in culture supernatants were measured by ELISA (Duokit DY410 (TNFα); DY206 (IL6); R&D Systems) according to the manufacturer's instructions. MCP3 levels were measured by ELISA (Peprotech #900-K123) according to the manufacturer's instructions. Multiplex cytokine analysis on cell supernatants was performed by the Addenbrooke's Hospital Core Biochemical Assay Laboratory using the MesoScale Discovery assay system (IFN-γ, IL-1 beta, IL-2, IL-4, IL-5, IL-6, KC-GRO,IL-10, IL-12 & TNF alpha).

**2.2.11 Mice**

Wild-type C57BL/6 were obtained from Jackson Laboratories (Margate, UK) as were transgenic mice expressing enhanced yellow fluorescent protein (EYFP) under the control of the CD11c promoter (Lindquist 2004), enhanced green fluorescent protein (EGFP) under the control of the human ubiquitin C promoter (Schaefer 2001), and enhanced cyan fluorescent protein (ECFP) mice under the control of chicken beta actin promotor (Barnden 1998). Ovalbumin (OVA)-specific, MHC class II-restricted alpha beta T cell receptor (TCR) transgenic mice (OTII mice)(Barnden 1998) were also purchased from Jackson Laboratories (Margate, UK). FcγRIIb-deficient mice on a C57BL/6 background (Bolland 2000) were kindly provided by Jeff Ravetch (Rockefeller University, New York) and Silvia Bolland (National Institutes of Health, NIAID, Bethesda, MD).

Mice were maintained in specific-pathogen-free conditions at a Home Office-approved facility in the UK. All animal studies were ethically reviewed and carried out in accordance with Animals (Scientific Procedures) Act 1986 and the GSK Policy on the Care, Welfare and Treatment of Animals.

**2.2.12 Tissue dissociation of murine kidneys**

Immediately following terminal procedure mouse kidneys were perfused with PBS. Organs were minced through a 70 μm cell strainer, digested in 1mg/ml collagenase A, 1mg/ml DNase I (both Roche, Burgess Hill, UK) and 2% heat inactivated FCS (Sigma-Aldrich, Gillingham, UK) in PBS for 20 minutes, before red blood cell lysis and staining for flow cytometry.

**2.2.13 RNA extraction from murine kidneys**

Samples of murine kidney were submerged after harvest in RNAlater™ Stabilization Solution (Invitrogen, UK), stored at 4$^{o}$C for 24 hours prior to storage at -80$^{o}$C, until ready for further processing. After thawing, tissue was removed from the RNAlater solution and homogenised in lysis buffer using Precellys®homogenisation technology (Bertin, France) and RNA extracted using PureLink RNA Mini Kit (Invitrogen, UK) according to manufacturer's instructions.

### 2.2.14 Reverse Transcriptase Polymerase Chain Reaction

Tissue sections or cell suspensions were lysed in RNA lysis buffer. Subsequent RNA extraction was performed using Ambion RNA PureLink Kit (Life Technologies, Paisley, UK) and yields analysed using Nanodrop spectrophotometry (Thermo-Scientific, Loughborough, UK). Complementary DNA synthesis was undertaken using High Capacity RNA to cDNA (Life Technologies, Paisley, UK) and BioRad (Hemel Hempstead, UK) PCR machine. RT-PCR was performed using Taqman reagents (Thermo-Fisher, Paisley, UK) on the Viia 7 PCR machine (Life Technologies, Paisley, UK). For primers see Materials and Methods Appendix. Gene expression relative to GAPDH/HPRT was calculated using 2-ΔCT for DMSO and I-BET treated samples individually (Schmittgen 2008).

### 2.2.15 Experimental protocol for murine bone marrow derived macrophage transcriptomic study

BMDM were prepared from C57BL/6 mice as described above. BMDM treated with or without ovalbumin (OVA) or immune complexed ovalbumin (OVA-IC) in the presence of 3.3μm I-BET 151 or DMSO control for 1 hour, 4 hours and 14 hours. I-BET or DMSO was added 30 minutes prior to the addition of stimulus. RNA was extracted using Ambion PureLink RNA Mini Kits according to the manufacturer's instructions.

Samples were sent to Cambridge Genomics Service and assessed for concentration and quality using a SpectroStar (BMG Labtech, Aylesbury, UK) and a Bioanalyser (Agilent Technologies, Cheadle, UK).

Array processing (Cambridge Genomic Services, University of Cambridge):
Microarray experiments were performed at Cambridge Genomic Services, University of Cambridge, using a species specific Gene 2.1 ST Array Plate (Affymetrix, Wooburn Green, UK) in combination with WT PLUS amplification kit (Affymetrix) according to the manufacturer's instructions. Briefly, 100ng Total RNA was amplified along with inline PolyA spike in control RNA, using the WT PLUS amplification kit (Affymetrix). Successfully amplified samples were labelled using the GeneChip WT terminal labelling kit (Affymetrix) using the in line hybridization controls. Plate arrays were processed on the GeneTitan instrument (Affymetrix) using the GeneTitan Hybridization,

Wash and Stain kit (Affymetrix). Samples were hybridized to the array, washed, stained and scanned using the array specific parameters provided by Affymetrix. Finally, basic visual quality control was performed using Command Console Viewer (Affrymetrix) prior to bioinformatic quality control.

### 2.2.16 Bioinformatics

Bioinformatic analysis was performed by Dr John Ferdinand.
After scanning the files generated by the scanner (CEL files) were loaded in R using the oligo package from Bioconductor (Carvalho 2010). No background correction or normalisation was applied at this stage. To assess the quality of the data, plots of the control probes were generated along with boxplots, MA plots and intensity distribution plots. The raw data was then processed using the RMA method (Irizarry 2003). The data was background corrected, normalised using quantile and summarized. Once the data had been processed, comparisons were performed using the limma package with results corrected for multiple testing using False Discovery Rate (FDR) testing (Ritchie 2015). Further analysis of normalised data was performed including Gene Set Enrichment Analysis (Subramanian 2005) and weighted correlation network analysis (Langfelder 2008).

### 2.2.17 *In vitro* transwell migration assay

Bone marrow derived dendritic cells were stimulated with IC for 16-24 hours in the presence of I-BET151 or DMSO control. Following stimulation, cells were washed and re-suspended in serum free media. Migration was assessed in a three hours transwell migration assay through 8μm pore semipermeable membranes (Corning Life Sciences), by calculating the proportion of live cells that passed through the membrane.

### 2.2.18 *In vitro* 3D chemotaxis assay

Bone marrow derived dendritic cells derived from transgenic mice expressing a fluorescent tag were stimulated with IC for 16-24 hours in the presence of I-BET151 or DMSO control. After washing, cells were counted, resuspended to a concentration of 10-15 x $10^6$ cells/ml and incorporated within a 1.5mg/ml bovine collagen gel loaded into a μ-Slide Chemotaxis chamber (Ibidi, Germany) as per manufacturer's instructions. A chemokine gradient of CCL19 (Peprotech, UK) was applied where indicated.

Composition of 1.5mg/ml bovine collagen I gel (for total volume 300μl)

- 20μl 10x Minimum Essential Media Eagle (MEM; Sigma)
- 20μl water

- 10µl 7.5% sodium bicarbonate solution (Sigma)
- 50µl RPMI 1640
- 150µl 3mg/ml bovine collagen I (Sigma)
- 50µl cell suspension (10-15 x $10^6$ cells/ml) in RPMI

Cell movement was imaged using time lapse confocal microscopy using a Zeiss LSM 780 inverted confocal microscope (Zeiss, Germany), with stacked images taken every 45-60 seconds, for a period of 2-4 hours. Image analysis was performed using the surface tracking function within Imaris software (Bitplane, Switzerland).

**2.2.19 *In vivo* models**

All procedures were conducted in accordance with the United Kingdom Animals (Scientific Procedures) Act 1986

**a) Accelerated nephrotoxic nephritis**

In the established model, female C57BL/6 mice are pre-immunized by intraperitoneal (IP) injection with 0.2 mg sheep IgG in a 50:50 mix of saline and complete Freund's adjuvant (CFA) (Sharp 2013). Due to constraints of our home office licence, we attempted to induce disease, giving this injection subcutaneously. Five days later, the mice were injected intravenously via the tail vein with 0.2 ml nephrotoxic polyclonal sheep anti mouse glomerular basement membrane antibody (kind gift from Ruth Tarzi, Imperial College, London).

Mice were monitored for the development of nephritis by collecting urine obtained when passed spontaneously upon handling. Mice were monitored daily for any weight loss and haematuria and/or proteinuria measured by dipstick and the experiments terminated if the mice showed signs of ill health. Mice were sacrificed at day 14 (or earlier if dictated my clinical phenotype) and kidneys and blood (post-mortem cardiac bleed) taken for analysis. Kidney samples taken for histological analysis in formalin (subsequent Hematoxylin and Eosin (H&E) and Periodic acid–Schiff (PAS)) or snap frozen and stored at -80 degrees Celsius for future RNA analysis or stored for future immunofluorescence staining following incubation in 0.05 M phosphate buffer containing 0.1 M L-lysine, pH 7.4, 2 mg/mL $NaIO_4$ and 10 mg/mL paraformaldehyde (12 hours), washing in phosphate buffer and dehydration in 30% sucrose in phosphate buffer (12 hours) and snap freezing in OCT. Blood urea and urine albumin creatinine ratios were quantified by Addenbrooke's Hospital Core Biochemical Assay Laboratory.

**b) In vivo migration assay: FITC paint**

Wild type C57BL/6 mice were treated with intraperitoneal injection of I-BET151 (30mg/kg) or solvent control. Dermal DCs were labelled by FITC painting, followed by local administration of IC to induce DC migration (as in (Clatworthy 2014a)). Forty eight hours later, the number of FITC+ MHC class II high CD11c+ cells in draining and non-draining LN was quantified by flow cytometric analysis of disrupted lymph nodes. Lymph nodes were disrupted by homogenizing through a 70-µm cell strainer (BD Falcon), and digested in PBS containing DNase I (1mg/mL; Roche, Burgess Hill, UK), collagenase A (1mg/mL; Roche, Burgess Hill, UK), and 2% FCS (Sigma-Aldrich, Gillingham, UK) at room temperature for 20 min.

**c) In vivo migration assay: DC transfer**

Fluorescently labelled BMDC (GFP or CFP) were stimulated with IC for 24 hours in the presence of I-BET151 or DMSO. Cells were then washed in PBS to remove non-internalised IC and I-BET151/DMSO and injected subcutaneously in the flank or footpad (depending on the lymph node harvested) of a recipient C57BL/6. Draining and non-draining lymph nodes were harvested 48-72 hours following DC transfer and fluorescently labelled DC's quantified via flow cytometry.

**d) In vivo migration assay: Intravital imaging of dermal DCs by two photon microscopy (performed with Dr. Menna Clatworthy)**

CD11c EYFP mice were injected intraperitoneally with DMSO or I-BET at a dose of 30mg/kg, followed 2 hours later by subcutaneous injection of 50 µl of 0.1mg/ml OVA solution to one hind footpad and 50 µl of OVA-IC solution (5µg OVA; 150µg rabbit anti ova) to the contralateral footpad. Nineteen hours later following intravenous injection Qdot® 655 probe (Invitrogen Molecular Probes) to delineate dermal vasculature, mice were anaesthetised with isoflurane. Footpad dermal DCs were imaged using a Leica multiphoton microscope; a time-lapse sequence was generated by imaging stacks of the footpad every 45 seconds for up to 1 hour. Image analysis was performed using the surface tracking function within Imaris software version 7.4 (Bitplane, Switzerland).

**e) Intravenous Immune complex**

C57/BL6 mice were injected intraperitoneally with DMSO or I-BET at a dose of 30mg/kg. A second dose was given 24 hours later, followed by an intravenous dose of Immune complexes (6.5µg of ovalbumin opsonised with 63.75 µg of rabbit anti ova prepared as detailed above) via tail vein injection. Mice were sacrificed 60 minutes later, organs flushed with cold PBS and digested and stained for flow cytometry analysis or placed in RNA later for RNA extraction. In a modification for a repeat experiments, mice were injected with intravenous CD45 immediately prior to schedule 1, to allow identification of intravascular lymphocytes within kidney tissue.

### f) Intraperitoneal Immune complex

C57/BL6 mice were injected intraperitoneally with DMSO or I-BET at a dose of 30mg/kg. A second dose was given 24 hours later, followed by an intraperitoneal dose of Immune complexes (6.5µg of ovalbumin-647 opsonised with 63.75 µg rabbit anti ova as detailed above). Mice were sacrificed 4 hours later, and peritoneal lavage performed with 6ml ice cold supplemented with 2% FCS. Flow cytometric analysis of 3ml of peritoneal lavage fluid was performed.

## 2.2.20 Image Analysis

Both *in vitro* and *in vivo* migration movies were processed using Imaris software (Version 7.4). The surface tool was used to track individual DC and track statistics exported into Microsoft Excel and plotted in GraphPad Prism. The standalone version of Ibidi's Chemotaxis and Migration Tool (Ibidi, Germany) was used to visualise tracks for the *in vitro* movies. Definitions of calculated parameters are shown below; i is the index of different single cells numbered from 1 to n ($1 \leq i \leq n$).

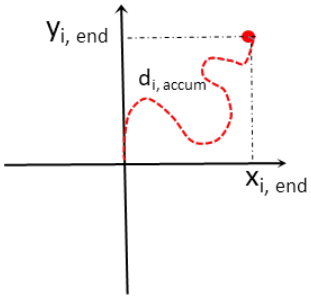


Track displacement x ($x_{i,\,end}$)= displacement of track in x axis

Track displacement y ($y_{i,\,end}$)= displacement of track in y axis

Track displacement length = length of straight line between cell start and end point (euclidean distance)

Track length = accumulated distance ($d_{i,\,accum}$)

The x forward migration index ($x_{FMI}$) and $y_{FMI}$ represent the efficiency of the forward migration of cells, in relation to the x- or y- axis. The larger the index on an axis, the stronger the chemotactic effect is on this axis.

$$x_{FMI} = \frac{1}{n}\sum_{i=1}^{n}\frac{x_{i,end}}{d_{i,accum}}$$

$$y_{FMI} = \frac{1}{n}\sum_{i=1}^{n}\frac{y_{i,end}}{d_{i,accum}}$$

The center of mass ($M_{end}$) represents the averaged point of all cell endpoints. The x and y values indicate the direction in which the group of cells primarily traveled.

$$M_{end} = \frac{1}{n}\sum_{i=1}^{n}(x_{i,end}, y_{i,end})$$

### 2.2.21 DC:T cell co-culture assay

BMDC were differentiated *in vitro* and plated in 96 well round bottomed plates at a density of 50000 cells per well in RPMI media supplemented with 1% penicillin-streptomycin and 10% FCS. DMSO or I-BET was added 30 minutes prior to addition of OVA or OVA-IC as indicated and cells were washed three times with tissue culture media five hours later. Meanwhile, a single cell OVA specific lymphocyte suspension was produced by mashing spleens from OTII mice through 70μm cell strainers. Following red blood cell lysis, CD4+ T cells were labelled with biotinylated anti-CD4 antibody (1:200) and isolated using magnetic activated cell sorting. CD4+ T cells were then labelled with carboxyfluorescein succinimidyl ester (CFSE; eBiosciences) according to manufacturer's instructions. CFSE labelled CD4+ T cells were washed three times and then co-cultured with the prepared DC at a ratio of 5:1 cells. T cell proliferation and activation was assessed 96 hours later via flow cytometry.

### 2.2.22 Data analysis

Graphs were compiled using GraphPad Prism. $P<0.05$ was taken to be statistically significant, annotated on figures as *NS $p>0.05$; *$p<0.05$; **$p<0.01$; ***$p<0.001$; ****$p<0.0001$.*

**Appendix 1: Murine antibodies**

| Antigen | Fluorophore | Clone | Species/Isotype | Supplier | Product number | Dilution |
|---|---|---|---|---|---|---|
| **Antibodies for flow cytometry:** | | | | | | |
| CCR7 | PE | 4B12 | Rat/IgG2a, κ | Biolegend | 120106 | 1:100 |
| CD103 | PE | M290 | Rat/IgG2a, κ | BD Biosciences | 557495 | 1:200 |
| CD11b | eFluor® 450 | M1/70 | Rat/IgG2b, κ | Biolegend | 101224 | 1:200 |
| CD11c | eFluor® 450 | N418 | Armenian hamster/IgG | eBioscience | 48-0114-82 | 1:200 |
| CD11c | PE | N418 | Armenian hamster/IgG | eBioscience | MA5-16878 | 1:200 |
| CD11c | PECy7 | N418 | Armenian hamster/IgG | Biolegend | 117318 | 1:200 |
| CD16/32 | PECy7 | 2.4G2 | Rat/IgG2b, κ | BD Biosciences | 560829 | 1:200 |
| CD16/32 | PE | 2.4G2 | Rat/IgG2b, κ | BD Biosciences | 553145 | 1:200 |
| CD19 | PE | eBio1D3 (1D3) | Rat/IgG2a, κ | eBioscience | 12-0193-83 | 1:200 |
| CD19 | PECy7 | eBio1D3 (1D3) | Rat/IgG2a, κ | eBioscience | 25-0193-82 | 1:200 |
| CD19 | PERCP Cy5.5 | 6D5 | Rat/IgG2a, κ | Biolegend | 115534 | 1:200 |
| CD19 | BV785 | 6D5 | Rat/IgG2a, κ | Biolegend | 115543 | 1:200 |
| CD25 | PERCP Cy5.5 | PC61.5 | Rat/IgG1, λ | eBioscience | 45-0251-82 | 1:200 |
| CD3 | BV605 | 17A2 | Rat/IgG2b, κ | Biolegend | 100237 | 1:200 |
| CD3 | BV785 | 17A2 | Rat/IgG2b, κ | Biolegend | 100231 | 1:200 |
| CD3e | PERCP Cy5.5 | 145-2C11 | Armenian hamster/IgG | eBioscience | 45-0031-82 | 1:200 |
| CD32b | APC | AT130-2 | Mouse/IgG2a, κ | eBioscience | 17-0321-82 | 1:200 |
| CD4 | PECy7 | GK1.5 | Rat/IgG2b, κ | eBioscience | 25-0041-82 | 1:200 |
| CD4 | APC | GK1.5 | Rat/IgG2b, κ | eBioscience | 17-0041-82 | 1:200 |
| CD40 | APC | HM40-30 | Armenian hamster/ IgM, κ | eBioscience | 17-0402-82 | 1:200 |
| CD45 | FITC | 30-F11 | Rat/IgG2b, κ | eBioscience | 11-0451-85 | 1:200 |
| CD45 | UV395 | HI30 | Mouse/IgG1, κ | BD Biosciences | 56427 | 1:200 |
| CD45.2 | APC-eFluor® 780 | 104 | Mouse/IgG2a, κ | eBioscience | 47-0454-82 | 1:200 |
| CD69 | BV605 | H1.2F3 | Armenian Hamster/IgG1, λ3 | BD Biosciences | 563290 | 1:200 |
| CD80 | PECy7 | 16-10A1 | Armenian hamster/IgG | eBioscience | 25-0801-82 | 1:200 |
| CD86 | FITC | GL1 | Rat/IgG2a, κ | eBioscience | 11-0862-82 | 1:200 |

| | | | | | | |
|---|---|---|---|---|---|---|
| CD86 | PE | GL1 | Rat/IgG2a, κ | eBioscience | 12-0862-83 | 1:200 |
| CD8α | ef450 | 53-6.7 | Rat/IgG2a, κ | eBioscience | 48-0081-82 | 1:200 |
| CX3CR1 | PE | SA011F11 | Mouse/IgG2a, κ | Biolegend | 149006 | 1:200 |
| EpCAM | APC | G8.8 | Rat/IgG2a, κ | eBioscience | 17-5791-82 | 1:200 |
| F4/80 | FITC | BM8 | Rat/IgG2a, κ | eBioscience | 11-4801-85 | 1:200 |
| F4/80 | BV605 | BM8 | Rat/IgG2a, κ | Biolegend | 123133 | 1:200 |
| Ly-6C | PERCP Cy5.5 | HK1.4 | Rat/IgG2c, κ | eBioscience | 45-5932-80 | 1:200 |
| Ly-6G (Gr-1) | PECy7 | RB6-8C5 | Rat/IgG2b, κ | eBioscience | 25-5931-82 | 1:200 |
| Ly-6G (Gr-1) | APC-eFluor® 780 | RB6-8C5 | Rat/IgG2b, κ | eBioscience | 47-5931-82 | 1:200 |
| MHC Class II-1 | eFluor® 450 | AF6-120.1 | Mouse/IgG2a, κ | eBioscience | 48-5320-82 | 1:200 |
| MHC Class II (I-A/I-E) | BV650 | M5/114.15.2 | Rat/IgG2b, κ | Biolegend | 107641 | 1:400 |
| MHC Class II (I-A/I-E) | A700 | M5/114.15.2 | Rat/IgG2b, κ | eBioscience | 56-5321-82 | 1:200 |
| **Antibodies for immunohistochemistry:** | | | | | | |
| anti Rab5 | NA | C8B1 | Rabbit/IgG | Cell signalling technology | 3547 | 1:100 |
| anti Rab7 | NA | D95F2 | Rabbit/IgG | Cell signalling technology | 9367 | 1:100 |
| anti-EEA1 | NA | C45B10 | Rabbit/IgG | Cell signalling technology | 3288 | 1:100 |
| Rat anti LAMP1 | NA | Unknown | Rat | Kind gift from Matthew Seaman, University of Cambridge | | 1:250 |
| F4/80 | FITC | BM8 | Rat/IgG2a, κ | EBioscience | 11-4801-85 | 1:100 |
| Goat anti Rabbit | Alexa Fluor™ 647 | | Goat/IgG | Invitrogen | A21244 | 1:300 |
| Goat anti Rat | Alexa Fluor™ 647 | | Goat/IgG | Invitrogen | A21247 | 1:300 |

**Appendix 2: Human antibodies**

| Antigen | Fluorophore | Clone | Isotype | Supplier | Product Number | Dilution |
|---|---|---|---|---|---|---|
| CD27 | FITC | O323 | Mouse/IgG1, κ | Biolegend | 302806 | 1:100 |
| CD16 | ef450 | CB16 | Mouse/IgG1, κ | EBioscience | 48-0168-41 | 1:200 |
| CD19 | APC Cy7 | SJ25C1 | Mouse/IgG1, κ | BD Biosciences | 557791 | 1:25 |
| CD24 | PerCP-Cy5.5 | ML5 | Mouse/IgG2a, κ | Biolegend | 311116 | 1:20 |
| CD25 | PE Cy7 | BC96 | Mouse/IgG1, κ | Biolegend | 302612 | 1:20 |
| CD3 | AmCyan | SK7 | Mouse/IgG1, κ | BD Biosciences | 339186 | 1:20 |
| CD3 | APC-Cy7 | HIT3a | Mouse/IgG2a, κ | Biolegend | 300318 | 1:100 |
| CD3 | AF488 | HIT3a | Mouse/IgG2a, κ | Biolegend | 300320 | 1:100 |
| CD32A | unconjugated | | Polyclonal | R&D | AF1330 | 1:100 |
| CD38 | BV421 | HIT2 | Mouse/IgG1, κ | Biolegend | 303526 | 1:200 |
| CD71 | PERP Cy5.5 | CY1G4 | Mouse/IgG2a, κ | Biolegend | 334114 | 1:20 |
| CD73 | BV421 | AD2 | Mouse/IgG1, κ | Biolegend | 344008 | 1:20 |
| IgD | PE Cy7 | IA6-2 | Mouse/IgG2a, κ | BD Biosciences | 561314 | 1:100 |
| IgD | APC | IA6-2 | Mouse/IgG2a, κ | Biolegend | 348222 | 1:100 |
| IL10 | PE | JES3-9D7 | Rat/IgG1, κ | BioLegend | 501404 | 5µl/test |
| IL10 | PE | JES3-19F1 | Rat/IgG1, κ | BioLegend | 506804 | 5µl/test |
| IL6 | APC | MQ2-13A5 | Rat/IgG1, κ | BioLegend | 501112 | 5µl/test |
| Rat IgG1, κ | APC | RTK2071 | Rat/IgG1, κ | BioLegend | 400412 | 5µl/test |
| TNFα | APC | MAb11 | Mouse/IgG1, κ | BioLegend | 502912 | 5µl/test |

**Appendix 3: Other stain reagents**

| Antigen | Fluorophore | Supplier | Product Number | Dilution |
|---|---|---|---|---|
| Ovalbumin | Alexa Fluor™ 647 | Invitrogen | O34784 | As described |
| Ovalbumin | FITC | Invitrogen | O23020 | As described |
| DQ™ Ovalbumin | | Invitrogen | D12053 | As described |
| LIVE/DEAD™ Fixable Aqua Dead Cell Stain Kit | | Invitrogen | L34957 | 1:300 |
| 123count eBeads™ Counting Beads | | eBioscience | 01-1234-42 | 25000-50000 beads/test |
| Zombie UV™ Fixable Viability Dye | | Biolegend | 423107 | 1:500 |
| Zombie Aqua™ Fixable Viability Dye | | Biolegend | 423101 | 1:500 |
| QDot 655 probe | | Invitrogen Molecular Probes | | 1:5 |
| CFSE | | eBioscience | 65-0850-84 | 5µM final concentration |
| Phalloidin | Alexa Fluor™ 568 | Invitrogen | A12380 | 1:100 |
| Phalloidin | Alexa Fluor™ 647 | Invitrogen | A22287 | 1:50 |

**Chapter 3: A phase two randomised controlled trial of belimumab in kidney transplant recipients demonstrates comparable safety and an increase in regulatory B cells**

### 3.1. Chapter summary

There is an increasing appreciation of the complex but important role of B cells in determining transplant outcomes. Activated B cells can present antigen to alloreactive T cells and secrete HLA and non-HLA antibodies that negatively affect graft function and survival. In contrast, B cells can regulate alloimmune responses and have been implicated in transplant tolerance. There is currently a significant unmet need in transplantation for immunosuppressants that inhibit B cell effector functions whilst promoting regulation.

BLyS is a cytokine that promotes B cell activation and survival, and has not previously been targeted in kidney transplant recipients. We performed the first randomized controlled trial using belimumab, an anti-BLyS antibody, as early maintenance immunosuppression in kidney transplantation, performing comprehensive immunological characterization of the impact of BLyS neutralization on the peripheral B cell compartment. We demonstrate a reduction in naïve and in activated memory B cells, a reduction in plasmablasts, IgG transcripts in peripheral blood and in new antibody formation in belimumab-treated subjects. Furthermore, we present evidence of reduced CD4 T cell activation and of a skewing of the residual B cell compartment towards an IL10-producing regulatory phenotype following belimumab treatment.

This trial provides a blueprint for proof of concept experimental medicine studies in transplantation, a field which has struggled to deliver randomised controlled trials (RCTs) using new immunosuppressants, in contrast to the field of autoimmunity. We recruited a relatively small number of patients to deliver information on safety, but performed intensive mechanistic studies on patient samples to generate robust data on relevant immunological readouts, providing the confidence to pursue this therapeutic target in future studies.

A manuscript containing this work was accepted on 20th April 2018 for publication in the Lancet (Banham 2018)(See Appendix A).

## 3.2 Background

### 3.2.1 Rationale for a study of belimumab in renal transplantation

In the UK, 913 people per million population require renal replacement therapy (MacNeill 2016). Renal transplantation offers the best treatment for most patients, optimising quantity and quality of life (Tonelli 2011). Despite advances in immunosuppressive regimes, long-term transplant function remains variable. Current immunosuppressive regimens carry an increased risk of infection but limit T cell activation such that TCMR occurs in less than 25% of kidney transplant recipients and is largely treatable. In contrast, there remain significant challenges in the field of humoral alloimmunity. *De-novo* DSA and some non-HLA antibodies are associated with ABMR and allograft loss (Dragun 2005, Zou 2007, Loupy 2013). Furthermore, sensitised patients with pre-formed DSA have an elevated risk of acute and chronic ABMR, both of which reduce graft survival (Bentall 2013). B cells influence the immune response to the allograft through their capacity to produce antibodies, act as antigen presenting cells and secrete cytokines (Clatworthy 2011).

Belimumab is a monoclonal antibody that binds soluble BLyS, a B cell survival factor, with high affinity, inhibiting its biological activity. We hypothesised that belimumab would reduce B cell activation and the associated allo-immune response. Since clinical end-points such as ABMR are rare, we sought to perform a small, mechanistic experimental study to assess the impact of BLyS inhibition on peripheral lymphocyte subsets as well as on standard transplant outcome parameters. The aim was to obtain safety and biomarker data to assess the potential for efficacy and safety of belimumab treatment in preventing allograft rejection.

### 3.2.2 Recruitment of subjects to a phase two randomised controlled trial

We conducted a phase 2 double-blind (sponsor unblind) randomised placebo-controlled trial (BEL114424; clinical trials.gov identifier NCT01536379; EudraCT number 2011-006215-56), to assess the safety and potential efficacy of belimumab, in addition to standard of care immunosuppression post-kidney transplantation. Subjects were randomised 1:1 to receive seven doses of belimumab 10mg/kg or placebo (0.9% sodium chloride solution) by intravenous infusion at days 0, 14, 28 followed by four-weekly doses through to week 20, in addition to standard of care immunosuppression and were followed for twelve months post-transplant (Figure 15; further details in materials and methods).

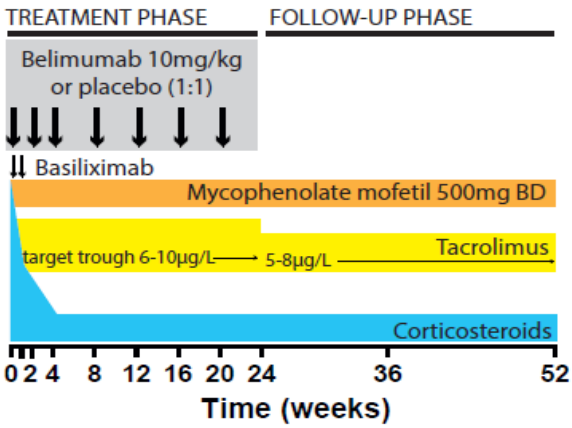


*Figure 15: BEL114424 Treatment schedule. Schematic showing the timing of study infusions alongside standard of care induction (basiliximab) and maintenance immunosuppression (mycophenolate mofetil, tacrolimus and corticosteroids).*

A target sample size of twenty evaluable subjects (those with a week 24 assessment) was calculated to achieve a reduction in naïve B cell count from baseline to 24 weeks, based on naïve B cell data from a previous trial of belimumab in SLE (BLISS-76) (Stohl 2012) and n=93 renal transplant recipients at the Cambridge Transplant Unit (unpublished data). Interim re-estimations of sample size were performed in November 2014 and February 2015 by unblinded statisticians at GSK.

The clinical study was a collaborative project with clinicians, scientists and statisticians from Addenbrooke's Hospital, the University of Cambridge and GlaxoSmithKline all being critical for its completion. I had an instrumental role in getting the trial up and running; recruiting and consenting all study patients, coordinating study team members and overseeing adverse event reporting. In addition, with oversight from the Clatworthy lab, I worked alongside Adele Gibson and Robbie Henderson at the GSK Experimental Medicine Unit to design and validate a regulatory B cell assay, with subsequent optimisation for use in the clinical study. In collaboration with Adele Gibson, I was responsible for running the assay on clinical study samples in a blinded fashion. I led the analysis of this part of the study and was fully involved in the wider BEL114424 study analysis and reporting, the only non-GSK employee included in the primary study analysis team.

### 3.3 Development and validation of a regulatory B cell assay in human peripheral blood

The experimental plan for B cell phenotyping and B cell stimulation assays was developed in the Clatworthy Lab. The assay was optimised and validated with Adele Gibson, GSK Experimental Medicine Unit, Stevenage, UK. Data included is reported in a GSK internal report entitled 2016N273645_00 Development and validation of a Regulatory B cell Assay in Human Peripheral Blood.

Given the increasing evidence that regulatory B cells may be beneficial for the alloimmune response, we wished to determine the effect of belimumab treatment on this subset. No prior studies using belimumab had specifically looked at the effect of the drug on Breg or B cell cytokine production. We designed a regulatory B cell assay to align with published studies (Iwata 2011, Cherukuri 2014), optimised the assay to maximise detection of this rare population with limited frozen PBMC samples and thoroughly validated it prior to use in a clinical setting at the GlaxoSmithKline Clinical Unit Cambridge, using limited frozen PBMC samples stored from study timepoints, under good clinical practice (GCP) conditions.

A two stage assay was performed. Stimulation of PBMC for 5 hours allowed for detection of circulating Breg, cells producing intracellular stored cytokines for which they are pre-programmed to synthesise. A longer stimulation with CpG/CD40L for 48 hours, with addition of PIB for the last 5 hours, allows the additional detection of precursor Breg cells that have the capacity to produce IL-10 with appropriate stimulation (pro-Bregs).

### 3.3.1 Optimisation of experimental controls to allow definition of cytokine secreting B cells

48 hours post-stimulation, we noted that cells changed in shape and size resulting in a change in autofluorescence. We therefore adopted an approach of using different controls for the 5 hour and 48 hour assays. For the 48 hour assay, we used a sample stimulated for 48 hours with CD40L and CpG, with BFA only added for the last 5 hours to set the IL-10 gate since a negligible number of B cells secrete IL-10 in the absence of additional stimulation with PMA and ionomycin. In contrast, IL-6 secreting cells could be detected following this stimulus; an isotype control antibody was therefore used in place of the IL-6 antibody to set the IL-6 gate (Figure 16). For the 5 hour assay we used a BFA only control to set the IL10 gate and an IL-6 isotype control to set the IL6 gate.

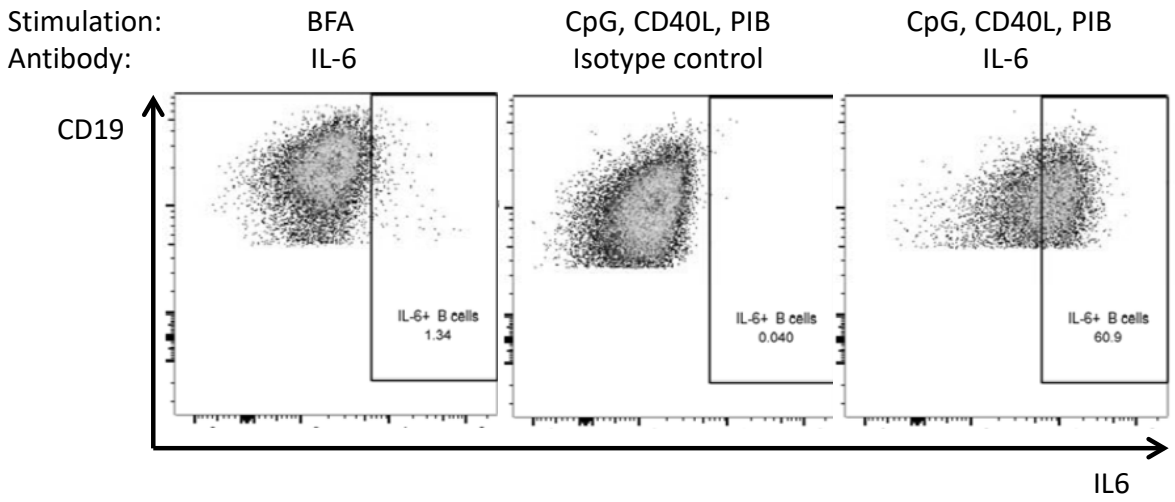


*Figure 16: Use of an IL6 isotype control (middle) was better than stimulation with BFA only (left) for setting a gate for IL6 secreting B cells following full in-vitro stimulation for 48 hours (right).*

Full examples of gating can be seen in section 3.4.10.

### 3.3.2 Optimisation of flow cytometry staining panel

Initial experiments measured intracellular IL-10, IL-6 and TNF-α. A decision was made to drop TNF-α from the final panel since our stimulation conditions produced high levels of TNF-α across donors, with little inter donor variability. We noted that the expression of many surface markers, for example CD27, changed following 48 hours of stimulation, meaning that it was not possible to categorise cells into memory subsets following stimulation (data not shown). Given that inclusion of these surface markers on 48 hour stimulated cells was felt to be unhelpful, a change to the surface staining panel was proposed in response to the van de Veen et al. publication suggesting enrichment of Bregs in a B cell subset identified with the surface markers $CD73^{-}CD25^{+}CD71^{+}$ (van de Veen 2013). Different surface staining antibody panels were investigated to establish whether there was any effect on IL-10 or IL-6 detection (Figure 17).

A

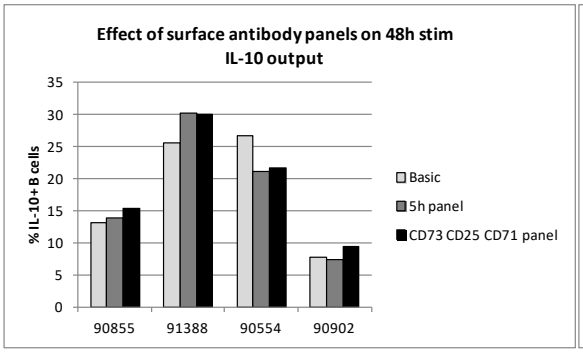


B

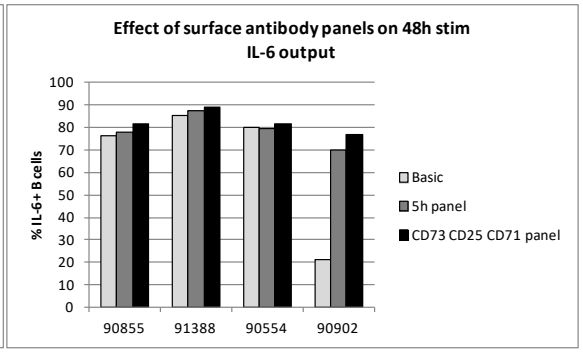

*Figure 17: Effect of different surface staining panels on IL-10 and IL-6 detection following 48h stimulation. 48h stimulated PBMCs were surface labelled with different antibody panels. '5hr panel' refers to the standard panel used in all prior studies; 'Basic' panel refers to just CD3-FITC and CD19-APC-Cy7; 'CD73 CD25 CD71 panel' refers to staining with CD3-FITC, CD71-PerCP-Cy5.5, CD25-PE-Cy7, CD19-APC-Cy7 and CD73-BV421. Cytokine detection shown from 4 individual donors. IL-10 detection shown in panel A, IL-6 detection shown in panel B.*

With the exception of one outlier for IL-6 detection (Figure 17b), quantification of IL-I0 and IL-6, was similar, independent of the surface staining panel used. Confirming published results, B cells in the $CD73^{-}CD25^{+}CD71^{+}$ subset were found to have the highest proportion of IL-10+ cells, followed by the $CD73^{+}CD25^{+}CD71^{+}$ subset (Figure 18).

A strong correlation between the percentage of $CD73^{-}CD25^{+}CD71^{+}$ B cells in a resting sample and the percentage that go on to produce IL-10 following 48 hour stimulation was found (Figure 19c). Following stimulation CD25 and CD71 expression increases (Figure 19b) but a correlation remained between the % of $CD73^{-}CD25^{+}CD71^{+}$ B cells and the % of B cells that produce IL-10 (Figure 19d). Therefore, we included these markers in the surface staining panel for the 48 hour stimulus and stained an aliquot of cells prior to stimulation.

*Figure 18: IL-10 production of subsets of B cells expressing different combinations of CD73, CD25 and CD71. PBMC samples from three donors were stimulated for 48 hours with CD40L and CpG, with PIB added in the last 5 hours. Following stimulation cells were stained for surface CD19, CD73, CD25, CD71, and CD3 and intracellular IL-10 and IL-6. The percentage of CD19+ cells expressing IL-10 within different surface marker subsets was quantified.*

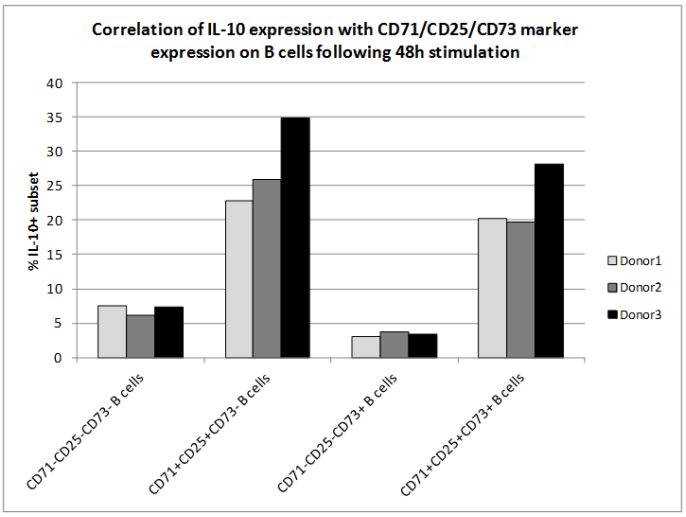


a)

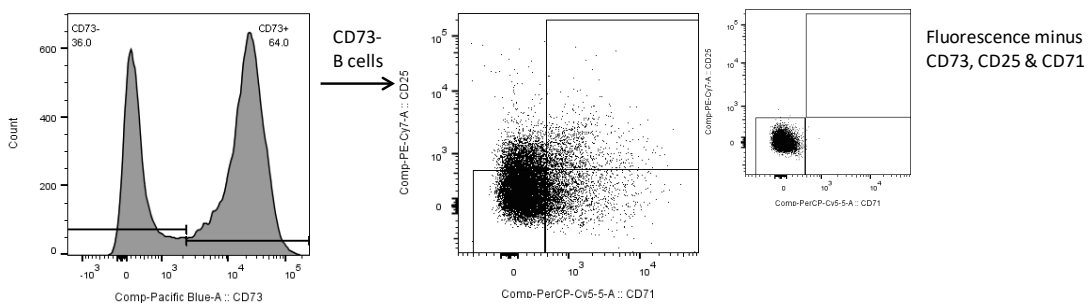

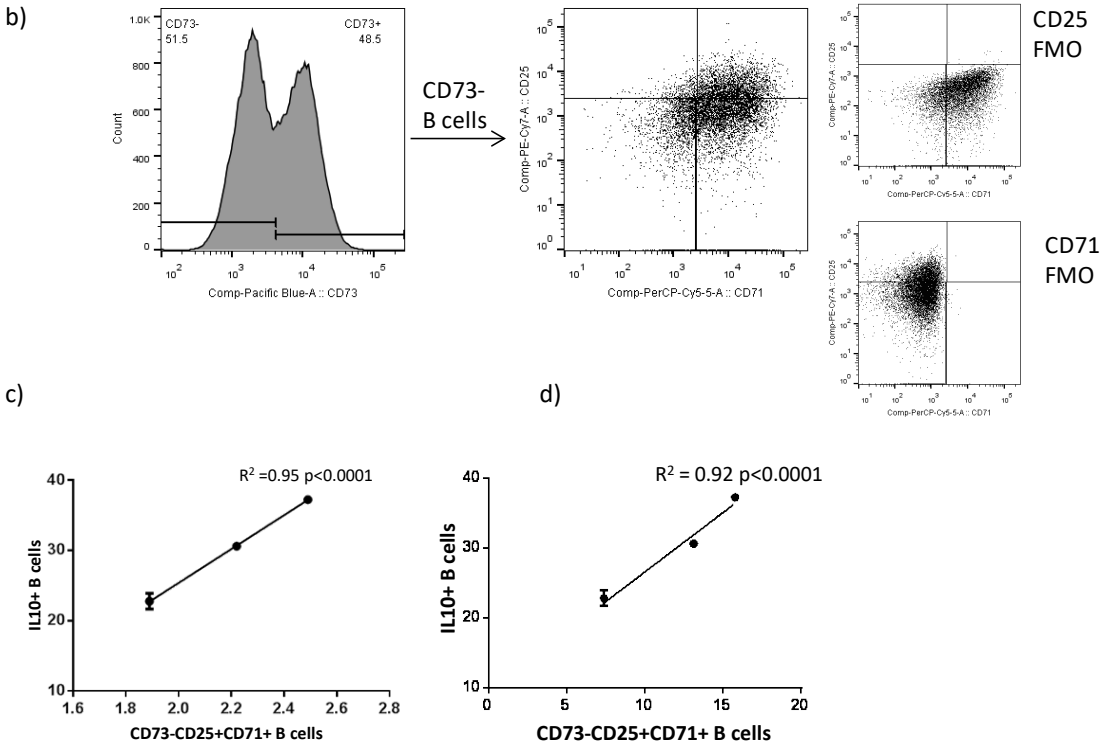


*Figure 19: Staining of CD73-CD25+CD71+ B cells and correlation with IL10+ B cells following stimulation. Frozen PBMC samples from 3 donors were surface stained following thawing with antibodies recognising CD19, CD73, CD25, CD71, CD3. Cells from the same thawed aliquots were stimulated for 48h followed by surface staining and intracellular staining for IL-10 and IL-6. Representative surface staining, from one donor, (gated on CD19+ CD3- live singlets) to identify CD73-CD25+CD71+ B cells is shown for freshly thawed cells (a) and for 48h stimulated cells (b). IL-10 positive B cells were quantified and correlated with the freshly thawed surface staining (c) and stimulated surface staining (d). c and d show mean +/- standard error of the mean with linear regression analysis*

### 3.3.3 Transfer of assay to CUC to enable processing of trial samples under good clinical practice conditions

Prior to running the BEL114424 study samples, we transferred the assay to the GSK CUC. Assay transfer was assessed by carrying out the assay on samples from the same bleed in several donors (Figure 20). The 5h assay showed similar % IL-10+ B cells from two donors with the third donor showing higher levels of IL-10 producing cells at the CUC. IL-6+ B cells were greater in the CUC assay (Figure 20a). At 48h, both % IL-10 and IL-6+ B cells were similar in three donors with greater variability in one donor (Figure 20b). This donor had low cell recovery on thawing in the CUC assay

which may have affected performance. Given that differing reagent stocks and flow cytometers were used at the different sites, the variability seen was judged to be acceptable.

a)

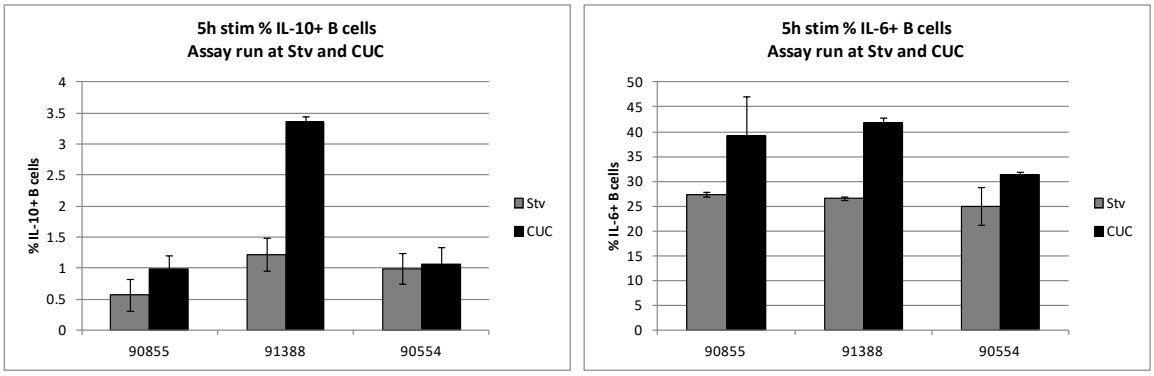


b)

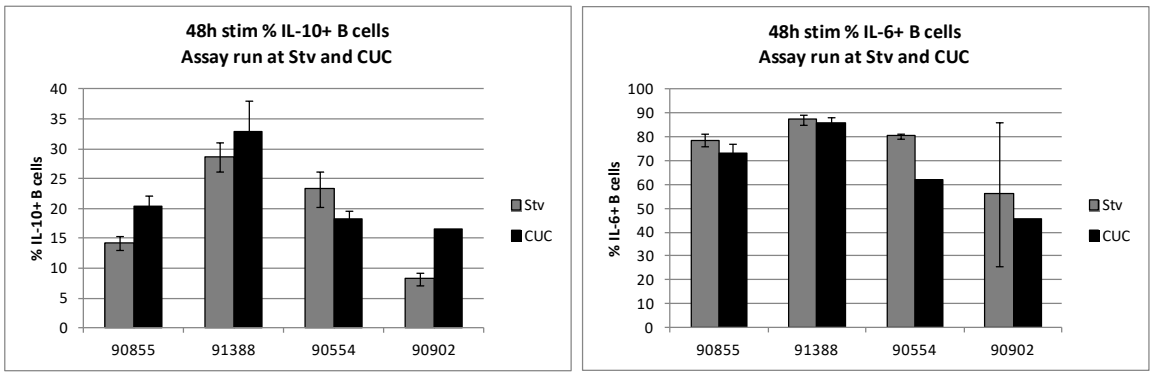


*Figure 20: Comparison of IL-10 and IL-6 production from samples run at Stevenage and CUC, Addenbrooke's site. PBMC samples from several donors, prepared and frozen at Stevenage were assayed at Stevenage and other vials from same bleed transferred and assayed at CUC. IL-10 and IL-6 producing B cells were identified following 5h stimulation (a) and 48h stimulation (b). n=3 replicates for each donor with mean +/- SD displayed.*

### 3.4 BEL114424 study analysis

#### 3.4.1 Reference to source data at GSK

The BEL114424 study results were analysed by the BEL114424 study analysis team, of which I was an integral part. Analysis were defined prior to study unblinding as part of a statistical analysis plan. All *post hoc* analyses are marked as such.

Raw data is referenced from the following internal GSK reports and electronic laboratory notebook entries.

2016N276025_00 BEL114424 Clinical Pharmacology Study Report

2017N310877_00 Regulatory B cell exploratory flow cytometry analysis for belimumab in renal transplant study BEL114424 report – Gemma Banham, Adele Gibson

2017N317074_00 Analysis of BLyS receptors and B cell activation markers for belimumab in renal transplant study BEL114424 – Gemma Banham, Adele Gibson, Shaun Flint

N59855-1: Exploratory analysis of whole blood, CD4+ T-cell and CD14+ monocyte gene expression data from BEL114424 – Shaun Flint, Katie Foster, Robbie Henderson

N59855-2: Pre-processing, QC and normalisation of whole blood, CD4+ T-cell and CD14+ monocyte gene expression data from BEL114424 - Shaun Flint

N59855-3: A description of the pre-processing steps and plot generation using exploratory flow cytometry data from BEL114424 to support the publication plan - Shaun Flint, Adele Gibson

N59855-4: Additional exploratory analysis of whole blood gene expression data from BEL114424 - Shaun Flint (work done in collaboration with Dr Paul Lyons, University of Cambridge)

N59855-6: An exploratory analysis of ProtoArray auto/allo-antibody data from BEL114424 (Belimumab in renal transplantation). Shaun Flint

N60700-62: Figures and statistical analyses of final project report "Assessing the impact of BLyS neutralisation on the cytokine profile of memory B cells as an immunosuppressive therapy for renal transplantation". Joseph Chadwick

2017N339717_00: Analysis of IL-6/IL-10 cytokine profile following BLyS stimulation and neutralisation by belimumab in memory B cells from healthy donors. Joseph Chadwick, Katie Foster.

**3.4.2 Study populations**

Two hundred and sixty patients admitted to Addenbrooke's Hospital for a renal transplant between September 2013 and February 2015 were screened for study inclusion. Of these, 105 did not meet inclusion criteria for the study and 82 were unable to be approached for consent due to logistical reasons including unavailability of study staff or study drug, insufficient time to gain informed consent and the recipient being resident out of region. Forty-five subjects were approached and made an informed choice not to participate in the study; 30 subjects were consented for inclusion in the study however the transplant did not proceed in four due to donor organ unsuitability and one subject was found to be ineligible on screening. An additional 43 subjects were screened at Guy's Hospital between August 2014 and February 2015, with 18 found to be ineligible, 24 unable to

participate due to logistical reasons and one refusing consent. The reasons for subjects not meeting inclusion criteria are shown in Table 2.

A total of 28 subjects were randomised to the study, with 25 going on to receive a transplant and at least one infusion of study drug. This made up the modified intention to treat (MITT) population that was used for the analysis of the co-primary outcomes; safety and a change in naïve B cells from baseline to Week 24. Secondary and exploratory biomarker outputs were undertaken using a pre-specified per protocol population (PP) that included all MITT subjects who received at least five infusions of study drug, were followed up beyond week 24 and received no prohibited medications or plasma exchange (referred to as PP1 population in study protocol). Figure 21 shows a consort 2010 flow diagram (Moher 2001) describing the enrolment, randomisation and follow up populations.

**Table 2: Reasons for subjects not meeting inclusion criteria.**

| Reason not meeting inclusion criteria | Number |
|---|---|
| Donor characteristic | 36 |
| Alternative immunosuppression planned | 21 |
| 0-0-0 mismatch | 16 |
| HLAi or ABOi transplant | 15 |
| Other disease/condition judged unsuitable by PI | 12 |
| Prior therapy | 8 |
| Transplant other than kidney | 3 |
| Recipient hepatitis | 3 |
| Donor hepatitis | 2 |
| Recipient unable to consent due to learning difficulties | 2 |
| Recipient HIV+ | 2 |
| Drug sensitivity | 1 |
| Prior malignancy | 1 |
| Poor venous access | 1 |
| **Total** | **123** |

The two treatment groups were similar in terms of their baseline characteristics (Table 3). The majority were receiving their first renal transplant and were of low immunological risk. A single subject (subject 5) in the belimumab treatment group was found to have a positive flow cytometry cross-match with donor specific antibodies to DP1 and DP6 at baseline. This subject was receiving a second transplant and known to be sensitized against multiple HLA DP antigens. The HLA DP type of the donor was not known at the time of transplantation, and T and B lymphocyte CDC cross-match tests were negative. Both the donor DP type and flow cytometry cross-match result became

available following transplantation. Had this information been available the subject would have been deemed ineligible for the study and given lymphocyte depleting induction therapy in view of his increased immunological risk.

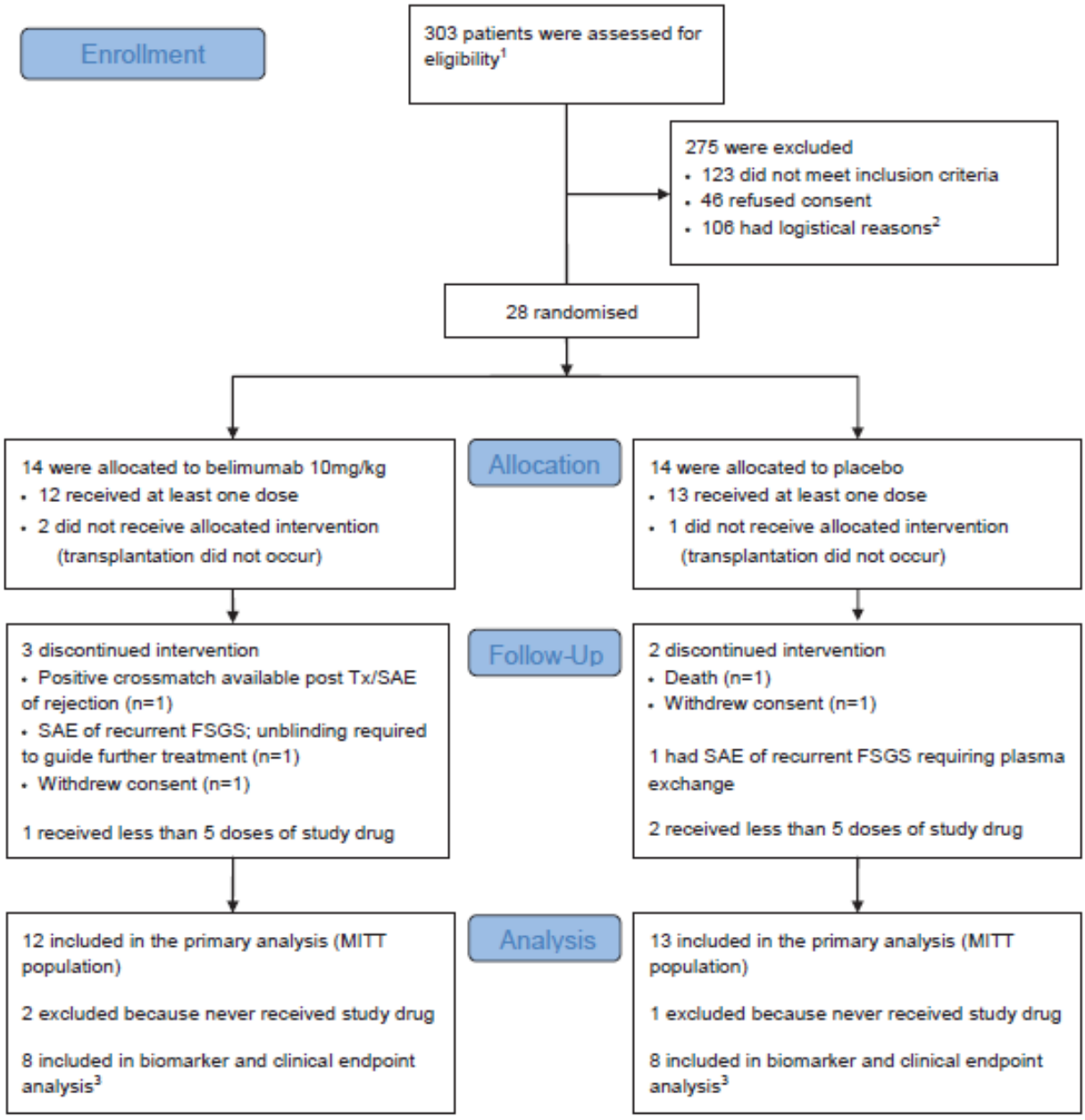


*Figure 21: BEL114424 study enrolment, randomisation and follow-up. The randomised treatment was given in addition to standard immunosuppression consisting of basiliximab, mycophenolate mofetil, tacrolimus and corticosteroids.* [1]260 at Addenbrooke's Hospital, Cambridge (28 randomised); 43 at Guy's and St Thomas' NHS Foundation Trust, London (0 randomised). [2]Logistical reasons included unavailability of study staff or study drug, insufficient time for consent and recipient resident out of region. [3]The pre-specified per protocol (PP) population used for biomarker and clinical endpoint analysis consisted of all subjects in the modified intention to treat (MITT) population who received at

least five infusions of study drug, no prohibited medications or plasma exchange and at least 24 weeks follow-up. FSGS Focal Segmental Glomerulosclerosis, SAE Serious Adverse Event

| Baseline demographic data, n | Placebo (n=13) | Belimumab 10mg/kg (n=12) |
|---|---|---|
| Age (years), Mean (SD) | 51.0 (14.0) | 54.3 (11.0) |
| Range | 24-73 | 32-72 |
| Sex, n (%) | | |
| - Female | 4 (31) | 7 (58) |
| - Male | 9 (69) | 5 (42) |
| Race, n (%) | | |
| -White/Caucasian | 12 (92) | 11 (92) |
| -Asian | 1 (8) | 1 (8) |
| Mean number (SD) of HLA-A/B/DR mismatches | | |
| -HLA-A | 1.7 (0.5) | 1.8 (0.5) |
| -HLA-B | 0.9 (0.6) | 1.1 (0.3) |
| -HLA-DR | 0.6 (0.5) | 0.8 (0.6) |
| Number of previous kidney transplants, n (%) | | |
| -0 | 11 (85) | 11 (92) |
| -1 | 2 (15) | 1 (8) |
| Pre-transplant renal replacement modality, n (%) | | |
| -None | 3 (23) | 2 (17) |
| -Haemodialysis | 7 (54) | 7 (58) |
| -Peritoneal dialysis | 3 (23) | 3 (25) |
| HLA antibody at baseline (MFI>2000), n (%) | | |
| -Non-DSA | 5 (38) | 3 (25) |
| -DSA [1] | 0 | 1 (8) |
| Donor type, n (%) | | |
| -Living | 3 (23) | 4 (33) |
| -Donation after circulatory death | 7 (54) | 5 (42) |
| -Donation after brain death | 3 (23) | 3 (25) |
| Donor age (years) | | |
| Mean (SD) | 52.9 (8.8) | 58.3 (8.1) |
| Range | 37-68 | 47-69 |
| Donor creatinine-last value prior to transplant (µmol/L) | | |

| | | |
|---|---|---|
| Mean (SD) | 64.8 (17.5) | 84.3 (30.7) |
| Median (Min, Max) | 66.0 (37-92) | 78.0 (51-167) |

*Table 3: Baseline demographics. [1]One subject randomised to belimumab had a positive pre-transplant MHC class II flow crossmatch (fulfilling an exclusion criterion but unknown at the time of enrolment and transplant).*

### 3.4.3 Belimumab pharmacokinetics and effect on circulating free BLyS

Belimumab pharmacokinetic (PK) parameters were similar to those observed in previous studies in SLE (Navarra 2011) and were not affected by end-stage renal failure (ESRF) (Figure 22).

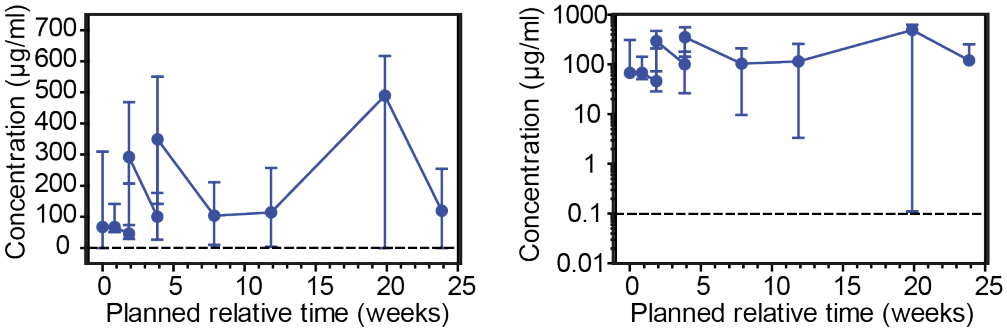


*Figure 22: Pharmacokinetic profile of belimumab. Median serum concentration of belimumab over time (left panel linear scale; right panel logarithmic scale). The lower limit of detection of 100ng/ml is marked with a dotted line. Error bars indicate range. PK population that consisted of all subjects randomised to belimumab treatment that were treated with at least one dose and had a PK sample that was analysed.*

Belimumab effectively removed circulating BLyS and levels remained suppressed up to week 12 post-treatment, rebounding thereafter (Figure 23).

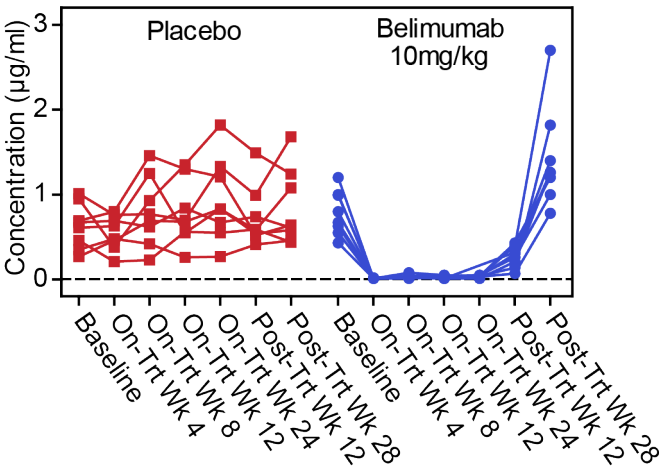

*Figure 23: Serum BLyS levels. Serial measurements of serum BLyS concentration (µg/ml) in individual subjects.*

### 3.4.4 Belimumab and placebo groups demonstrate comparable safety with adverse events consistent with that expected for the study population and known safety profile of belimumab

A key goal of this study was to determine the safety of belimumab in combination with standard transplant immunosuppression, in patients with ESRF. Belimumab has previously been used in patients with autoimmune diseases, in combination with steroids, and in some cases, an anti-proliferative agent (for example azathioprine, MMF or methotrexate) but is has not been trialled alongside an immunosuppression regime including induction therapy with CD25 blockade and triple maintenance immunosuppression (tacrolimus, MMF and prednisolone) in patients with ESRF at baseline, a condition known to be associated with a heightened susceptibility to infection (Vanholder 1993). It was therefore critical to assess the safety of the drug in this setting and this formed a co-primary endpoint for the study. We observed similar rates of adverse events in the placebo and belimumab treatment groups, during both the on treatment and post treatment periods (Table 4). Post-transplant infection was an important end-point, particularly given its association with an increased risk of rejection and allograft loss (von Willebrand 1986, Almond 1993, Reinke 1994, Bohl 2007). After 6 and 12 months follow-up, we observed similar rates of serious infection in belimumab and placebo groups (1/12 (8%) and 5/13 (38%) respectively during the 6 month on-treatment phase; 0/13 (0%) and 2/13 (15%) during the 6 months post-treatment follow-up phase). We also found no excess frequency of viral infection (BK virus or cytomegalovirus (CMV)) in belimumab-treated subjects. There were no new diagnoses of malignancy in either group within during the follow up period and one death, from a cardiovascular cause, in the placebo group. In summary, belimumab was not associated with an excess risk of infection or malignancy when used with standard transplant immunosuppression.

| | **On treatment [1]** | | **Post-treatment** | |
|---|---|---|---|---|
| | **Number (%) Subjects** | | **Number (%) Subjects** | |
| | **Placebo (n=13)** | **Belimumab (n=12)** | **Placebo (n=13)** | **Belimumab (n=12)** |
| Any adverse event (AE) | 10 (77) | 11 (92) | 9 (69) | 10 (83) |
| Any serious AE (SAE) | 7 (54) | 5 (42) | 2 (15) | 2 (17) |
| Any severe AE | 6 (46) | 8 (67) | 3 (23) | 3 (25) |
| Deaths [2] | 1 (8) | 0 | 0 | 0 |
| Most common AE [3] | | | | |
| - Leukopenia | 4 (31) | 4 (33) | 3 (23) | 3 (25) |

| | | | | |
|---|---|---|---|---|
| - Diarrhoea | 3 (23) | 5 (42) | 1 (8) | 1 (8) |
| - Urinary tract infection [4] | 3 (23) | 4 (33) | 1 (8) | 2 (17) |
| - Anaemia [5] | 4 (31) | 3 (25) | 0 | 1 (8) |
| - Lower respiratory tract infection [6] | 2 (15) | 2 (17) | 2 (15) | 0 |
| - Dyspepsia[7] | 2 (15) | 2 (17) | 2 (15) | 0 |
| - Nasopharyngitis | 2 (15) | 1 (8) | 1 (8) | 2 (17) |
| - Alanine aminotransferase increased | 2 (15) | 2 (17) | 0 | 0 |
| - Diabetes Mellitus[8] | 1 (8) | 1 (8) | 0 | 2 (17) |
| - Endoscopic evidence upper GI inflammation[9] | 2 (15) | 1 (8) | 0 | 0 |
| - Dizziness | 0 | 2 (17) | 0 | 1 (8) |
| - Vomiting | 0 | 2 (17) | 0 | 0 |
| Infections | | | | |
| - All | 7 (54) | 5 (42) | 8 (62) | 6 (50) |
| - Serious infections (n≥1) | 5 (38) | 1 (8) | 2 (15) | 0 |
| - Severe infections (n≥1) | 5 (38) | 2 (17) | 3 (23) | 0 |
| - Opportunistic infections | 3 (23) | 2 (17) | 3 (23) | 3 (25) |
| - BK viraemia | 2 (15) | 1 (8) | 1 (8) | 1 (8) |
| - BK viraemia-associated nephropathy | 0 | 1 (8) | 1 (8) | 0 |
| - Cytomegalovirus (CMV) viraemia[10] | 1 (8) | 0 | 1 (8) | 2 (17) |
| Malignant neoplasm | 0 | 0 | 0 | 0 |
| Depression/Suicide/Self injury | 0 | 0 | 0 | 0 |
| Post infusion systemic reaction[11] | 0 | 1 (8) | NA | NA |
| Recurrence of focal segmental glomerulonephritis[12] | 1 (8) | 1 (8) | 0 | 0 |
| Hypogammaglobulinemia of grade ≥3 (<4.0g/L) | 2 (15) | 3 (25) | 0 | 0 |

*Table 4. Safety findings during on-treatment and post-treatment phases, by treatment group. [1]The on-treatment phase commenced from the start of the first infusion of study drug and ends 28 days after the last dose. The post-treatment phase begun the following day. [2]Death due to fatal myocardial infarction and acute cardiac failure. [3]Includes all AEs (by grouped MedDRA preferred terms) occurring in more than one subject during the study not including opportunistic infections (listed separately), ordered by overall frequency. [4]Grouped preferred terms include urinary tract infection, Escherichia urinary tract infection, urinary tract infection enterococcal and urosepsis. [5]Grouped preferred terms include anaemia, anaemia vitamin B12 deficiency and iron deficiency anaemia. [6]Grouped preferred terms include pneumonia and lower respiratory tract infection. [7]Grouped preferred terms include dyspepsia and gastrooesophageal reflux disease. [8]Grouped preferred terms include diabetes mellitus and type two diabetes mellitus; one post treatment AE was*

*worsening of diabetes, onset on treatment, in context of steroids for SAE (colitis). [9]Grouped preferred terms include oesophagitis, duodenal ulcer, duodenitis and ulcerative gastritis. [10]Grouped preferred terms include cytomegalovirus test positive, cytomegalovirus viraemia, culture positive (verbatim term CMV). [11]The infusion reaction reported was mild, settled spontaneously and did not recur on subsequent infusions. [12]Grouped preferred terms include focal segmental glomerulosclerosis (FSGS) and glomerulonephritis (recurrence of FSGS verbatim term). NA denotes not applicable.*

### 3.4.5 Belimumab and placebo groups demonstrate comparable clinical outcomes: acute rejection, allograft function and survival

B cell depletion with the anti-CD20 antibody rituximab has been associated with increased TCMR (Clatworthy 2009) and cardiac allograft vasculopathy (Chandraker 2016). Since belimumab also depletes some B cell subsets, we sought to confirm that its use was not associated with an increase in alloimmune responses. The frequency of TCMR (including episodes classified as borderline according to the BANFF 2009 criteria (Sis 2010)) was similar in belimumab (n=1/12 (16.7%)) and placebo-treated subjects (n=3/13 (23%), Table 5). One subject was randomised to the belimumab group but withdrawn from the study due to a positive B lymphocyte flow cytometry cross-match (an exclusion criterion), the results of which became available post-transplant (donor specific antibodies to DP1 and DP6). This subject was receiving a second transplant and known to be sensitized against multiple HLA DP antigens. The HLA DP type of the donor was not known at the time of transplantation, and T and B lymphocyte CDC cross-match tests were negative. Both the donor DP type and flow cytometry cross-match result became available following transplantation. Had this information been available the subject would have been deemed ineligible for the study and given lymphocyte depleting induction therapy in view of his increased immunological risk. This subject experienced Banff IIA acute cellular rejection with features suspicious for early humoral rejection (day 6) associated with a rise in the titre of DP DSA and development of de novo DSA to HLA-A11 and HLA-B18. A further biopsy (day 34) demonstrated overt antibody mediated rejection. They were withdrawn from the study following a single dose of belimumab and the rejection responded to treatment with methylprednisolone, plasma exchange and anti-thymocyte globulin. Overall, transplant function at one year, graft and patient survival were not negatively impacted by the addition of belimumab to standard of care immunosuppression (Table 4 & 5).

| Clinical outcome data[1], n | Placebo (n=8) | | Belimumab 10mg/kg (n=8) | |
|---|---|---|---|---|
| Acute transplant rejection by week 52[2], n (%) | | | | |
| - Borderline, not treated | 2 (25) | | 0 | |
| - Borderline, treated | 1 (12.5) | | 0 | |
| - Type IIa, treated | 0 | | 1 (12.5) | |
| Cumulative HLA class I (MFI >500)[3] | Sub 22 | Sub 28 | Sub 8 | Sub 27 |
| Before treatment | 39612 | 20046 | 127392 | 4894 |
| On treatment Wk 2 | 24658 | 14731 | 56453 | 4493 |
| On treatment Wk 4 | 26129 | 21466 | 33810 | 3438 |
| On treatment Wk 8 | 28930 | 19528 | 34420 | 4632 |
| On treatment Wk 12 | 26709 | 26500 | 25985 | 6320 |
| On treatment Wk 24 | 23152 | 18376 | 26491 | 8103 |
| Post treatment week 28 | 19204 | 18892 | 24607 | 4349 |
| Cumulative HLA class II (MFI >500)[3] | Sub 4 | | Sub 1 | |
| Before treatment | 2382 | | 16009 | |
| On treatment Wk 2 | 916 | | 9305 | |
| On treatment Wk 4 | 1211 | | 12346 | |
| On treatment Wk 8 | 768 | | 12553 | |
| On treatment Wk 12 | 606 | | 10540 | |
| On treatment Wk 24 | 577 | | 13408 | |
| Post treatment week 28 | 785 | | 9075 | |
| Graft survival, n (%) | 8 (100) | | 8 (100) | |
| Creatinine at 52 weeks (µmol/L) | | | | |
| Mean (SD) | 142.5 (65.7) | | 110.6 (43.6) | |
| Median (Min, Max) | 114 (86-282) | | 94 (68-201) | |
| eGFR at 52 weeks (ml/min/1.73m$^2$), | | | | |
| Mean (SD) | 53.00 (22.10) | | 57.42 (15.08) | |
| Median (Min, Max) | 54.03 (20.41-86.63) | | 56.77 (30.25-81.93) | |

*Table 5: BEL114424 clinical outcomes. [1]Clinical outcome data described for the per protocol population. [2]Acute rejection was defined on biopsy according to Banff 2009 criteria: Acute antibody mediated rejection (Grade I, II or III) or acute T cell mediated rejection (Borderline, Type IA, Type IB, Type IIA, Type IIB, Type III). An additional subject randomised to belimumab had a positive pre-*

*transplant MHC class II flow crossmatch (fulfilling an exclusion criterion but unknown at the time of enrolment and transplant). They experienced Type IIA acute cellular rejection (day 6) and grade II antibody mediated rejection (day 34). They were withdrawn once the crossmatch was recognised following a single dose of belimumab. [3]Cumulative HLA class I and class II MFI calculated by summing the normalised MFI values for any single antigen bead with a value above the level of detection (500). An additional subject in the belimumab group underwent adoptive transfer of donor HLA-specific allosensitization following kidney transplantation from a highly sensitized donor, as described in (Maxfield 2015). SD standard deviation, n number of subjects, HLA human leukocyte antigen, MFI mean fluorescence intensity measured by Luminex assay, DSA Donor specific antibody, Min minimum, Max maximum, and eGFR estimated glomerular filtration rate.*

### 3.4.6 Belimumab targets naïve and activated B cells whilst sparing memory B cells

BLyS is known to support the survival of transitional and naïve B cells (Mackay 2003). The second co-primary endpoint for the study was the change from in naïve B cells from baseline to Week 24, a biomarker of functional BLyS neutralisation validated in patients with SLE (Navarra 2011). We observed a reduction in the number and proportion of naïve B cells in belimumab-treated subjects (Figure 24). In line with the statistical analysis plan, analysis of the primary endpoints was performed on the MITT population (Figure 24A). The magnitude of the treatment effect was diluted in this small study by those subjects who did not receive multiple doses of the randomised study drug; when only the PP population is considered there was a more marked difference in the change in naïve B cells from baseline to Week 24 (Figure 24C).

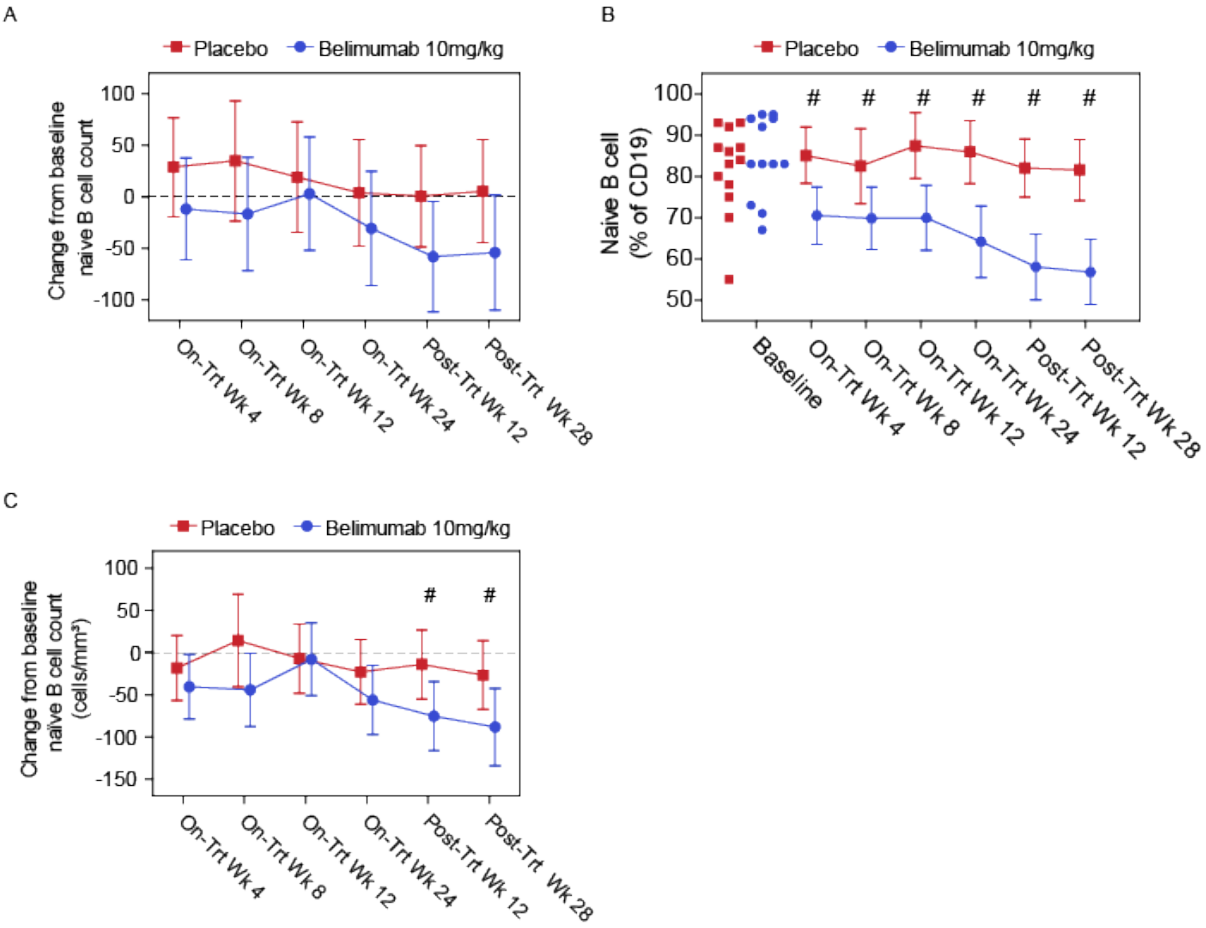


*Figure 24: Belimumab affects naïve B cells. Panel A shows the adjusted mean (95% CI) change from baseline in* naïve *(CD20+CD27-) B cell count, by visit and treatment (MITT population). Panel B shows* naïve *(CD20+CD27-) B cells expressed as a percentage of B cells by visit and treatment group (MITT population), with raw values at baseline for comparison and adjusted mean estimate +/- 95% confidence intervals at subsequent timepoint. Panel C shows the adjusted mean (95% CI) change from baseline in* naïve *(CD20+CD27-) B cell count, by visit and treatment (PP population). # indicates that the 95% confidence interval of the treatment difference does not include zero.*

Belimumab treatment altered the composition of the B cell compartment, with naïve B cells being depleted the most compared to baseline levels (Figure 25).

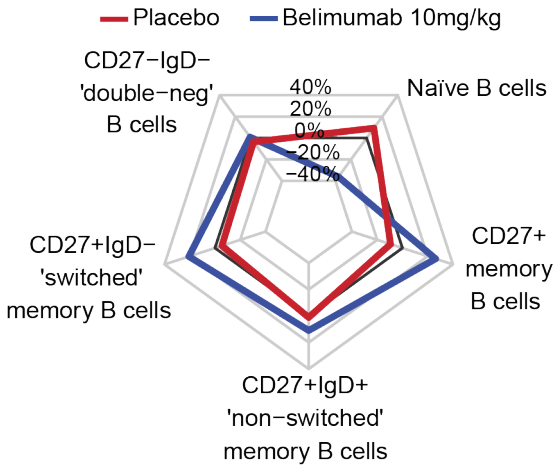


*Figure 25: Belimumab alters the B cell compartment. Median difference from baseline at week 24 in the labelled B cell populations by treatment group (PP population), with each population expressed as a percentage of B cells.*

In contrast, memory B cells were spared (Figure 26A) such that the proportion of memory B cells was increased (Figure 26B). In contrast to the effect of belimumab on the total memory pool, activated memory B cells were decreased, assessed using two different markers of activation, CD95 (Figure 26C & D) and CD21 (Figure 29)

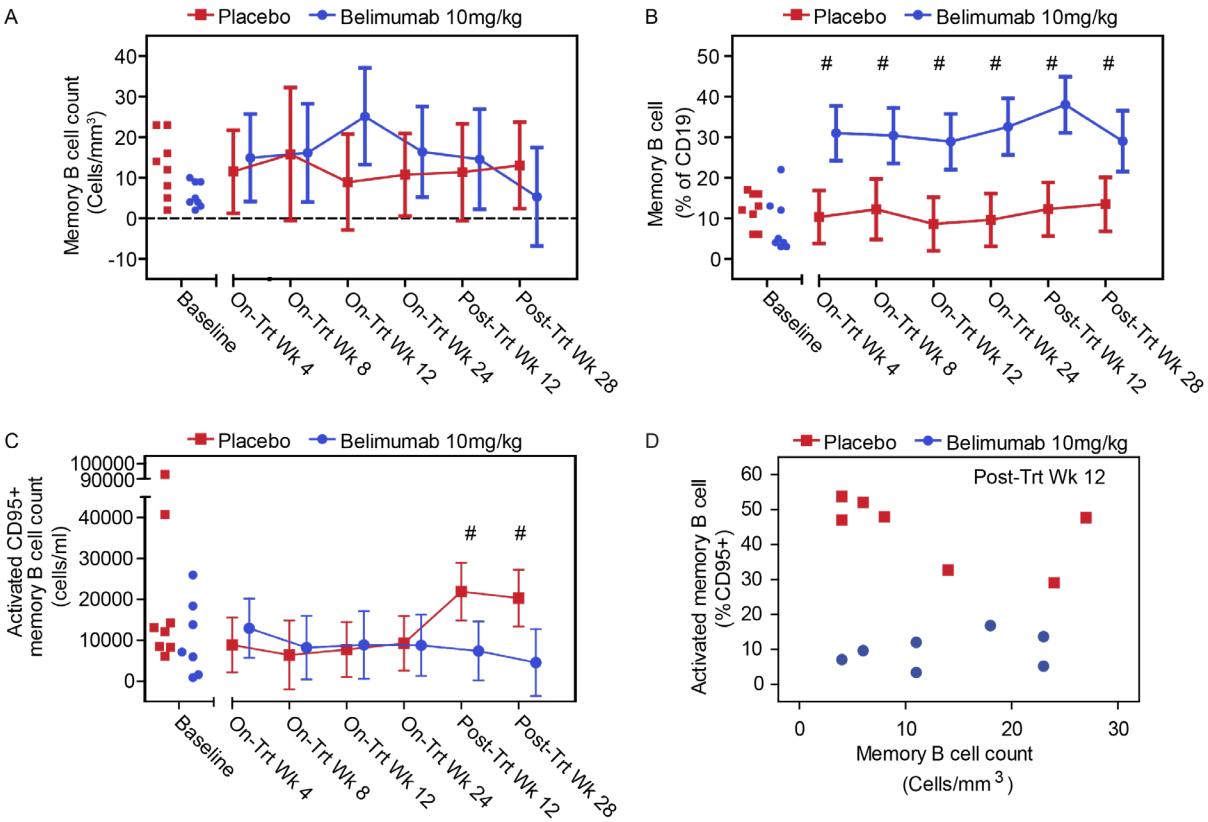

*Figure 26: Belimumab spares memory B cells. Panel A shows the memory (CD20+CD27+) B cell count, by visit and treatment. Panel B shows memory (CD20+CD27+) B cells expressed as a percentage of B cells by visit and treatment group. Panel C shows activated memory (CD95+CD27+) B cell count (cells/ml) by visit and treatment group. Panel D shows the relationship between memory B cell count (cells/mm$^3$) and activated memory B cell (CD95+CD27+) percentage at the post treatment week 12 timepoint for individual subjects labelled by treatment group. A-C show PP population with raw values displayed at baseline for comparison, with adjusted mean estimate +/- 95% confidence intervals at subsequent timepoints. # indicates that the 95% confidence interval of the treatment difference does not include zero. D shows data for individual PP subjects labelled by treatment group. A, B and D are post hoc analyses.*

A low proportion of naïve B cells expressed the CD95 activation marker. The proportion expressing CD95 was not impacted by belimumab treatment but absolute numbers of CD95+ naive B cells decreased, reflecting the reduction in naïve B cells seen (Figure 27a). There was a clear decrease in the proportion of switched memory, non-switched memory and to a lesser degree double negative cells that were CD95+ positive from week 4 through to 36, with reductions in absolute numbers of these cells at week 36 and 52 (Figure 27b-d).

Activation of B cells is associated with reduction of surface expression of the complement receptor CD21. A high proportion of memory B cells were CD21+ at baseline in both treatment groups (Figure 28). In the placebo group, a number of subjects sharply downregulated CD21+ at week 24 and 36 on non-switched memory B cells (Figure 28b) and to a lesser degree switched memory B cells (Figure 28c). In the belimumab group this effect was attenuated and delayed (Figure 28b-c). In the belimumab group compared to the placebo group, absolute counts of activated CD21 negative naïve B cells were reduced from week 4 onwards, in the most part due to reduced naïve B cell numbers (Figure 28a). Absolute counts of activated CD21 negative non-switched and switched memory populations were reduced at week 36 and 52 in belimumab compared to placebo group (Figure 28b-c), despite the increased proportion of memory cells seen at these timepoints.

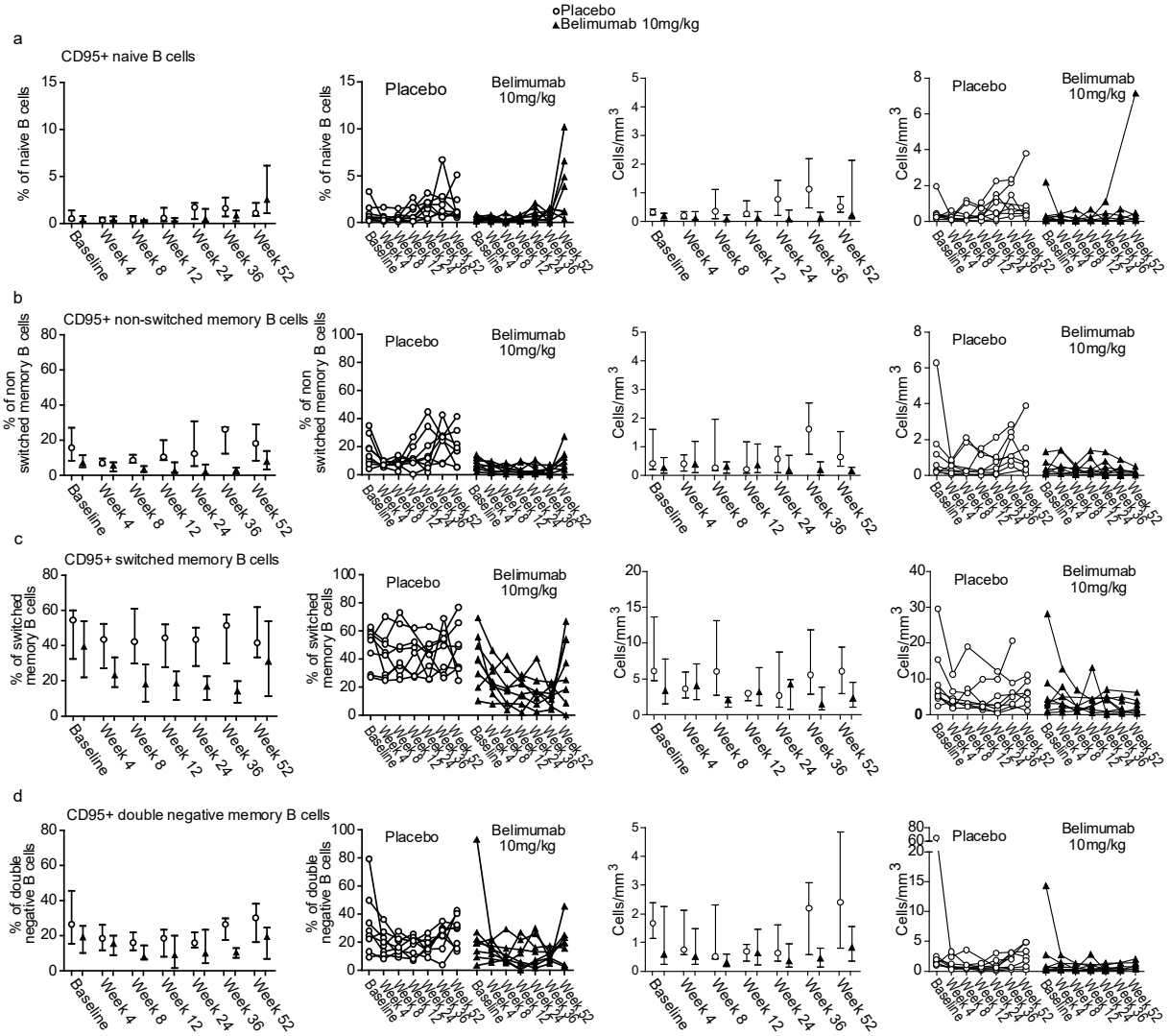


*Figure 27: Expression of the activation marker CD95 on B cell memory subsets. Graphs show the percentage of each subset expressing CD95 and absolute counts of CD95+ cells within each subset a) naïve B cells (CD19+CD27-IgD+) b) non-switched memory B cells (CD19+CD27+IgD+) c) switched memory B cells (CD19+CD27+IgD-) d) double negative memory B cells (CD19+CD27-IgD-). 1st and 3rd column plots show medians with interquartile range. 2nd and 4th column plots show individual subject values over time.*

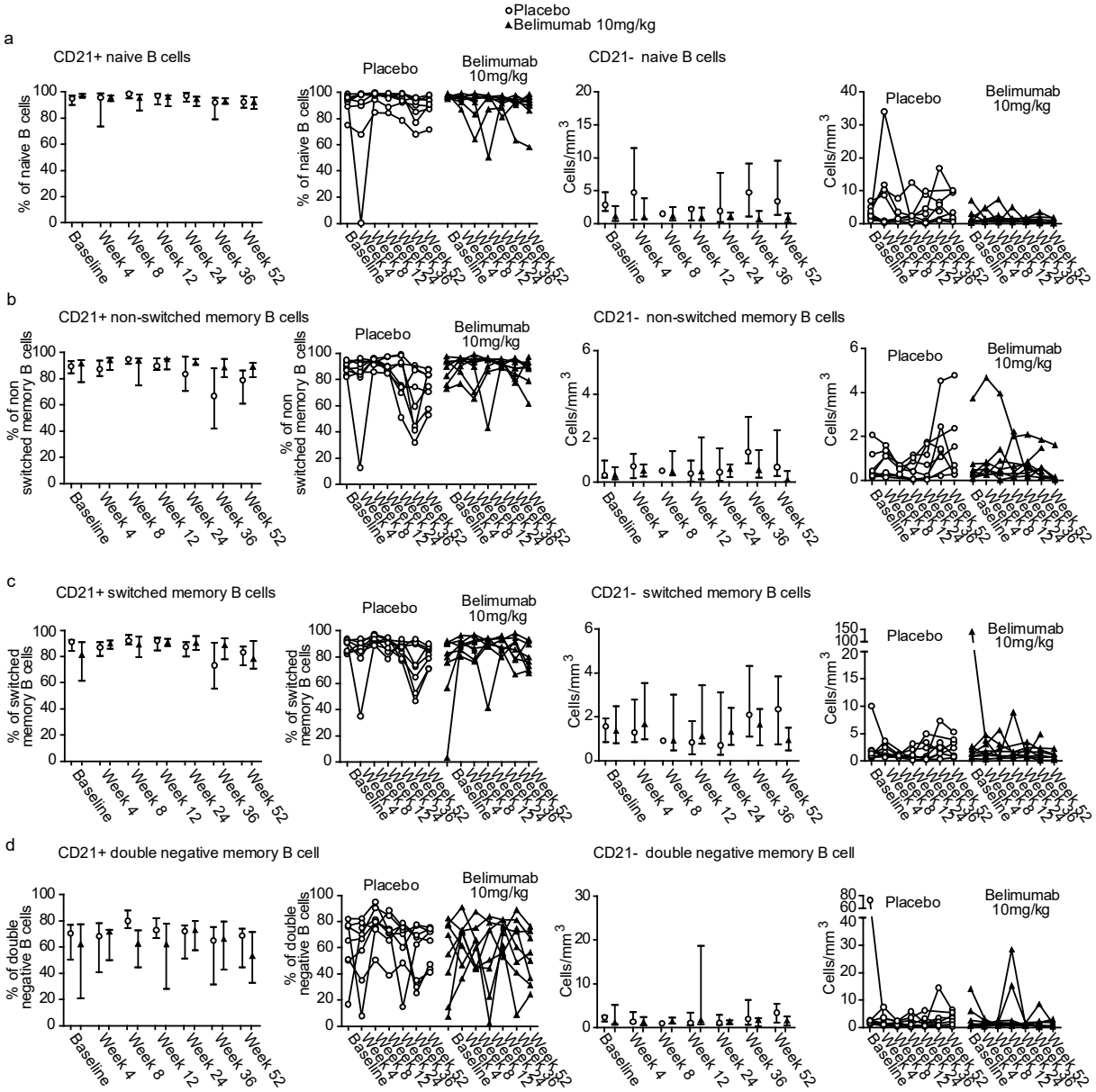


*Figure 28: Expression of the activation marker CD21 on B cell memory subsets. Graphs show the percentage of each subset expressing CD21 and absolute counts of CD21- cells within each subset a) naïve B cells (CD19+CD27-IgD+) b) non-switched memory B cells (CD19+CD27+IgD+) c) switched memory B cells (CD19+CD27+IgD-) d) double negative memory B cells (CD19+CD27-IgD-). 1st and 3rd column plots show medians with interquartile range; 2nd and 4th column plots show individual subject values over time.*

### 3.4.7 Belimumab alters BLyS receptor expression

The BLyS receptor TACI is normally expressed at high levels on the surface of CD27+ memory B cells (Darce 2007). Levels of TACI on memory B cells were markedly reduced throughout the treatment

period in belimumab treated subjects compared with controls (Figure 29), with similar effects seen in total memory, non-switched memory and switched memory populations (Figure 30).

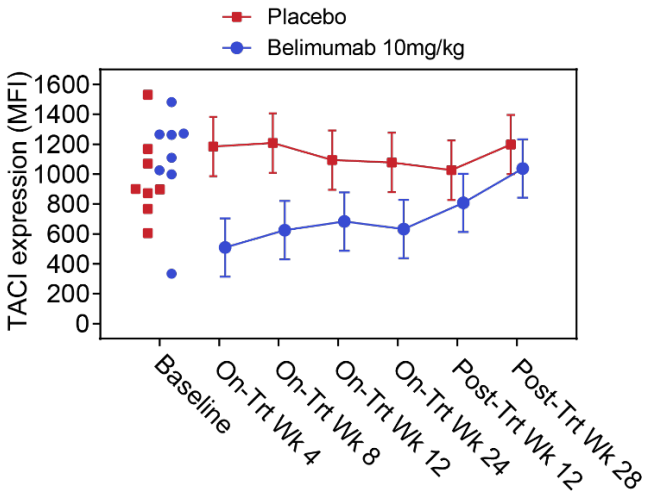


*Figure 29: TACI expression on memory B cells is a strong pharmacodynamic marker of belimumab action. Geometric mean fluorescence intensity (MFI) of TACI staining on CD19+CD27+ memory B cells. PP population; raw values displayed at baseline for comparison, with adjusted mean estimate +/- 95% confidence intervals at subsequent timepoint. Note % confidence interval of the treatment difference not calculated for this endpoint.*

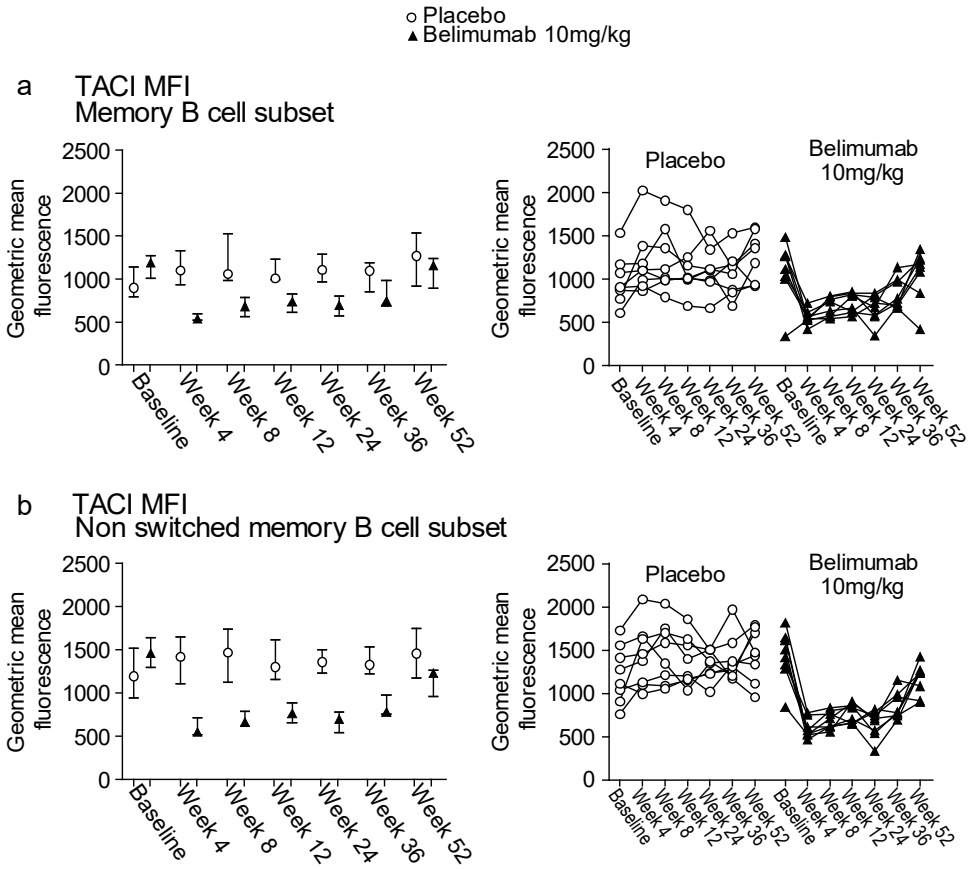

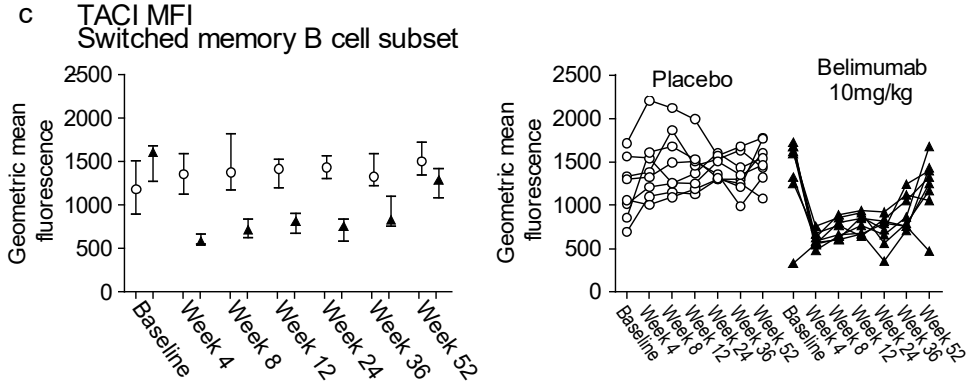


*Figure 30: TACI receptor expression. MFI of TACI staining on a) memory B cells (CD19+CD27+) b) non-switched memory B cells (CD19+CD27+IgD+) c) switched memory B cells (CD19+CD27+IgD-). Left plots show medians with interquartile range. Right plots show individual subject values over time.*

Further characterisation of BLyS receptor expression was performed. There was a trend towards an increase in BAFFR expression in memory but not naïve B cells, with a clear difference between the treatment groups at Week 36 (Figure 31).

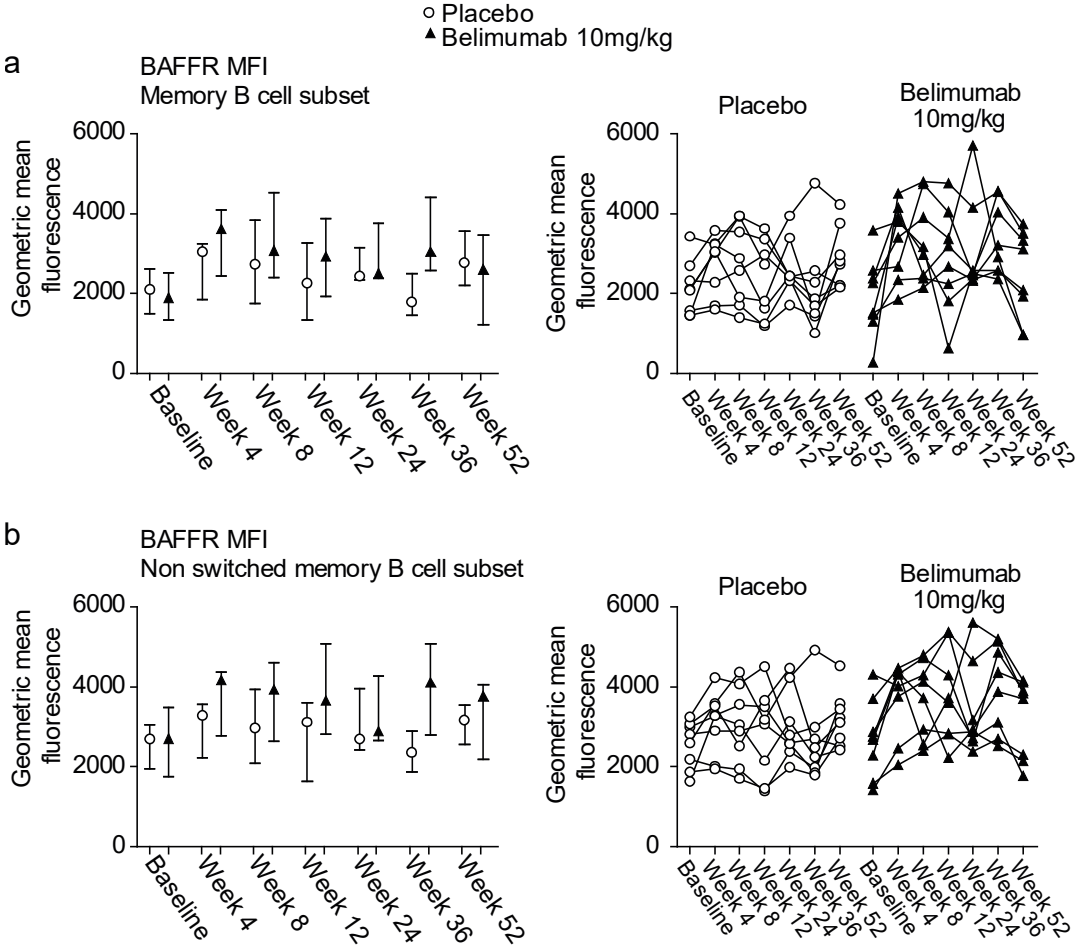

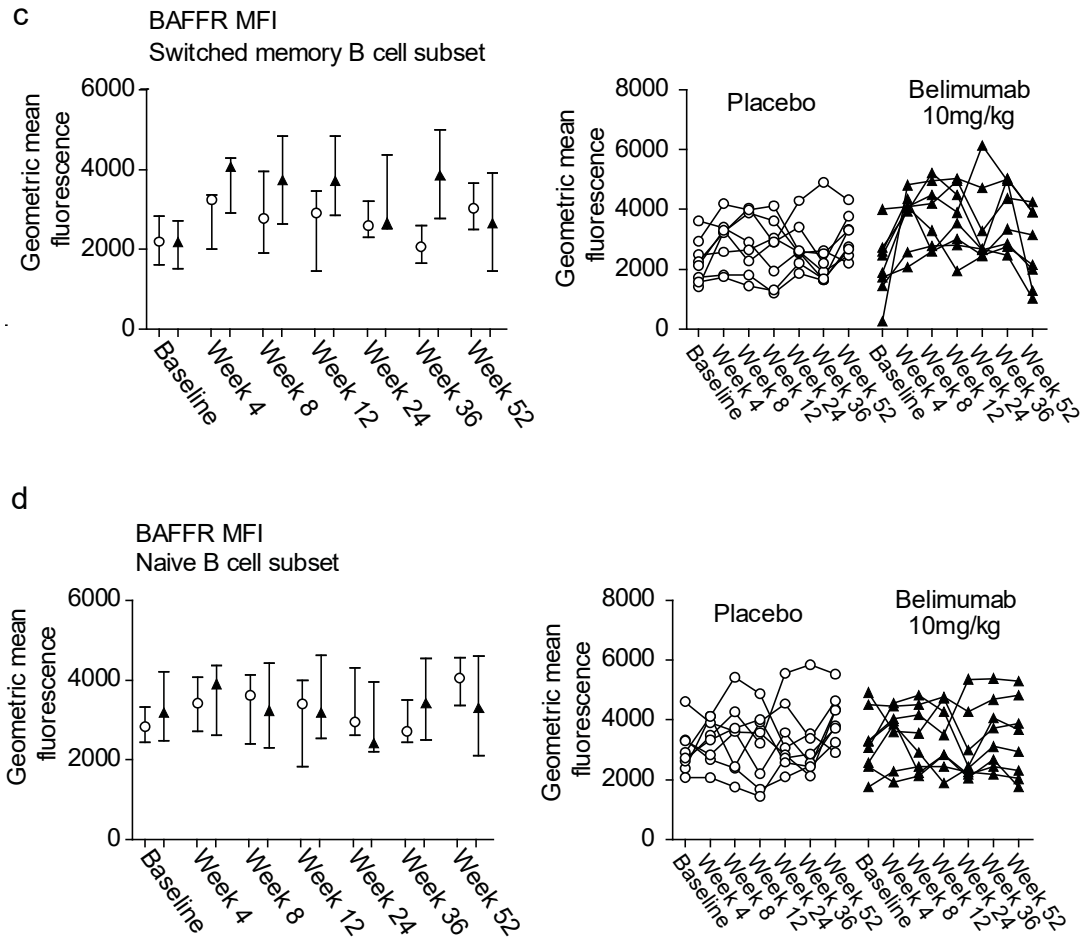


*Figure 31: BAFFR receptor expression. MFI of BAFFR staining on a) memory B cells (CD19+CD27+) b) non-switched memory B cells (CD19+CD27+IgD+) c) switched memory B cells (CD19+CD27+IgD-) d) naïve B cells (CD19+CD27-IgD+). Left plots show medians with interquartile range. Right plots show individual subject values over time.*

There was no clear treatment effect on BCMA expression on plasmablasts, however plasmablast numbers were low throughout the treatment period so few samples were suitable for analysis (Figure 32).

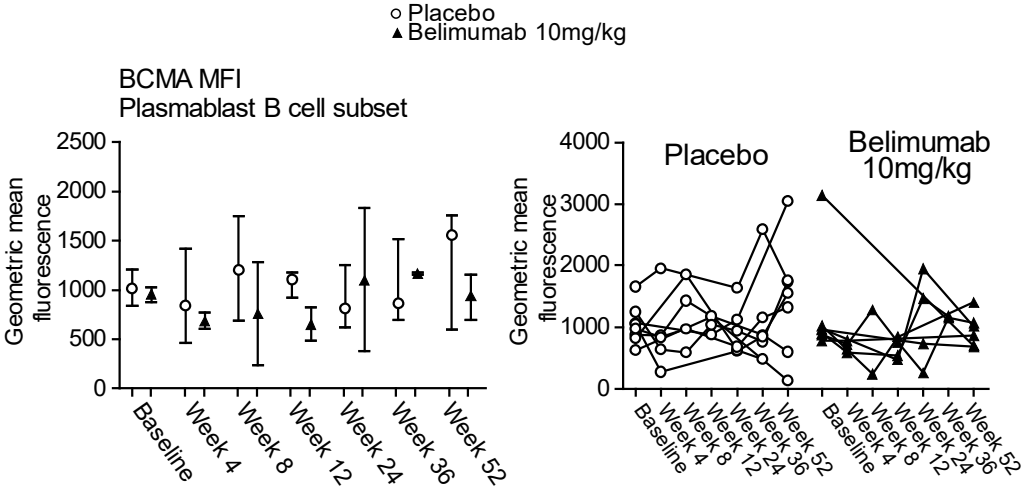

*Figure 32: BCMA receptor expression. MFI of BCMA staining on plasmablasts (CD19+CD27+CD38+). Left plot shows medians with interquartile range. Right plots show individual subject values over time.*

### 3.4.8 Belimumab impacts antibody producing cells

There was also a reduction in circulating CD19+CD27+CD38hi plasmablasts measured by flow cytometry (Figure 33).

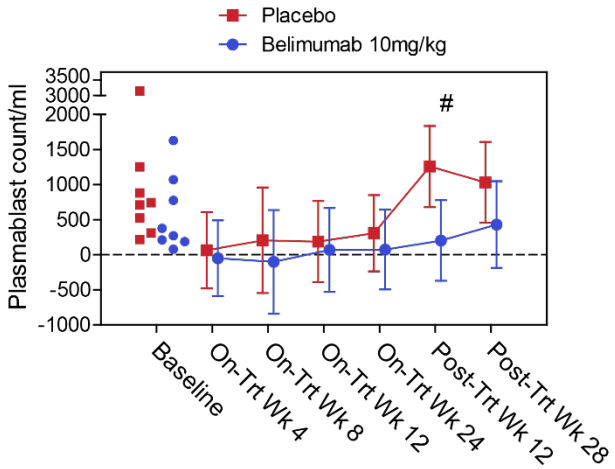


*Figure 33. Belimumab leads to a reduction in circulating plasmablasts. Adjusted mean (95% CI) of plasmablast (CD19+CD27+CD38+) count/ml. PP population with raw values displayed at baseline for comparison, with adjusted mean estimate +/- 95% confidence intervals at subsequent timepoints. # indicates that the 95% confidence interval of the treatment difference does not include zero*

In order to further understand the potential impact of belimumab on B cell activation and differentiation into antibody-secreting cells, we assessed the whole blood transcriptome. Using a differential expression analysis approach, we compared whole blood gene expression in belimumab treated subjects compared to controls. Immunoglobulin coding genes were among the most differentially expressed. Figure 34A shows fold-change and unadjusted p-values at week 52. The distribution of differential gene expression for the whole transcriptome was symmetrical, indicating no global changes in gene expression (Figure 34A upper panel). In contrast, the volcano plot showing only immunoglobulin probes demonstrate a clear difference with lower expression of these transcripts in the belimumab 10 mg/kg group, compared with the placebo group (Figure 34A lower panel), although sample numbers were too small to demonstrate statistical significance for this comparison. In support of this observation, a weighted gene co-expression network analysis identified a B cell gene expression module (Figure 34B), the expression of which was attenuated in

belimumab-treated subjects (Figure 34C). The most attenuated genes in this module coded for immunoglobulin, suggesting a strong effect on antibody-secreting cells (Figure 34D).

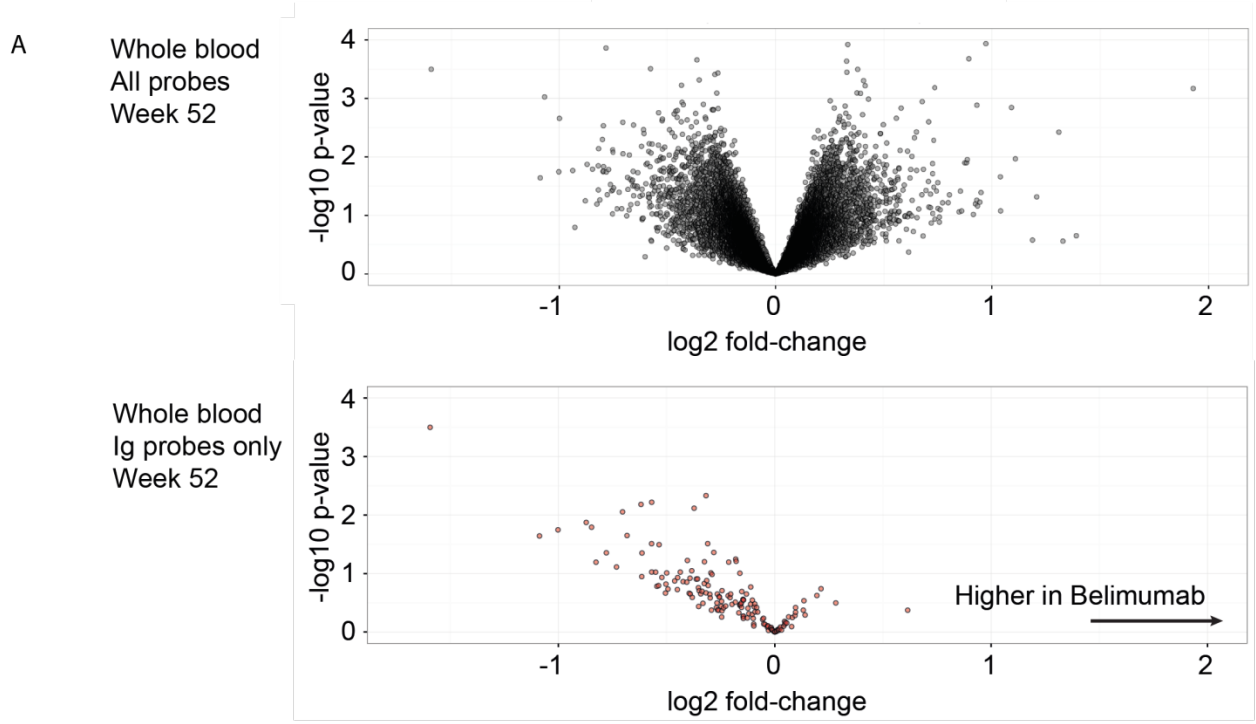


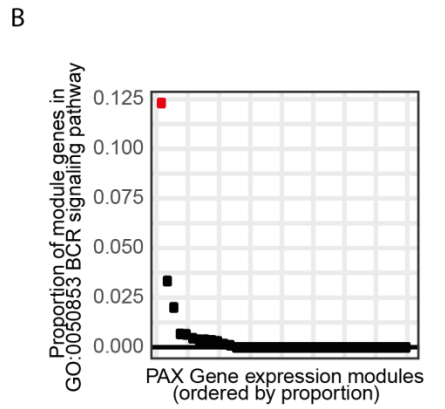


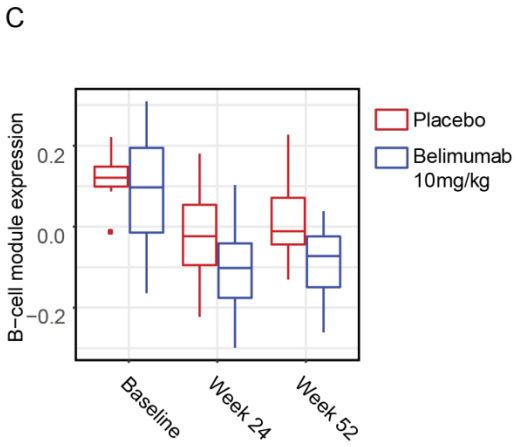


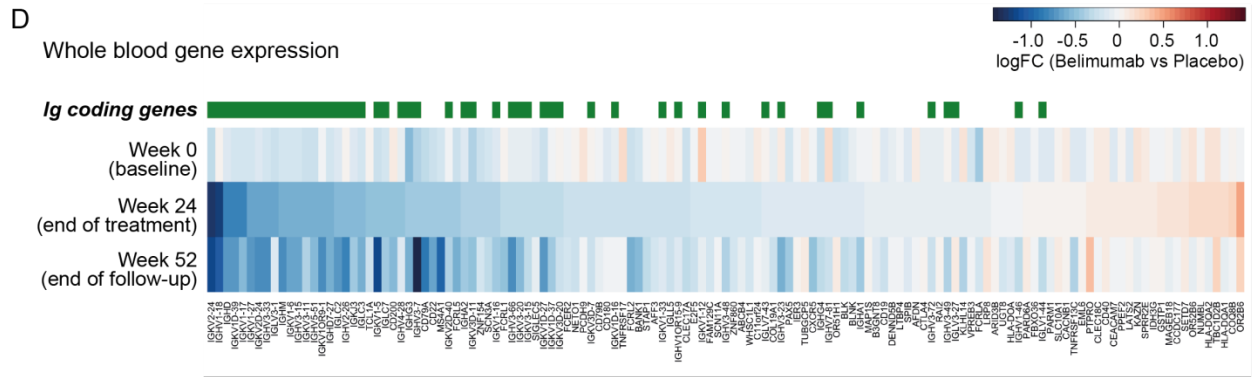

*Figure 34: Belimumab reduces the transcription of immunoglobulin coding genes. Panel A shows volcano plots demonstrating differentially regulated genes in belimumab vs placebo treated subjects at week 52. The upper panel shows all probes on the microarray; the lower panel shows only immunoglobulin coding probes. Panel B shows proportion of module genes within each module identified during weighted correlation network analysis of whole blood RNA in the GO:0050853 BCR signalling pathway. A single module (coloured red) was enriched for BCR signalling and analysed further for the effects of belimumab treatment. Panel C shows expression (arbitrary units) of this expression module by treatment group at baseline, end of on-treatment phase (Week 24) and end of follow-up (Week 52). Horizontal lines correspond to median and interquartile ranges. Panel D shows a heat map of differential gene expression (Belimumab versus Placebo groups) for genes in the B cell module at baseline, Week 24 and Week 52. Genes are ordered by fold-change at Week 24 and immunoglobulin-coding transcripts are highlighted. Colour corresponds to $log_2$-fold change, with blue indicating higher expression in Placebo relative to Belimumab. Analysis performed on MITT population at baseline and PP thereafter.*

### 3.4.9 Belimumab treatment inhibits new non-HLA antibody production but study underpowered to detect changes in HLA antibodies

Eight study participants had detectable anti-HLA antibodies (non donor-specific) at transplantation (3/12 in the belimumab group and 5/13 in the placebo group, Table 3). Belimumab treatment was associated with a reduction in HLA antibody titre post-transplant in some subjects (Figure 35). Two patients recruited to the study developed de novo DSA during follow-up; both had been withdrawn following a single dose of belimumab for reasons unrelated to antibody development. Subject 5 was withdrawn due to a positive cross-match; subject 13 withdrew consent for study drug (Figure 35C).

Non-HLA autoantibodies can also have a deleterious effect on allograft function (Dragun 2005, Zhang 2016). Antibodies against MHC class I–related chain A (MICA) antigens are associated with renal allograft rejection and reduced allograft survival, particularly amongst those well matched for HLA antigens (Zou 2007). One patient in each treatment group had positive anti-MICA antibodies at baseline; subject 19 received one dose of placebo and had positive levels throughout the first year post transplant; in contrast subject 27 received 5 doses of belimumab and antibody levels fell below the positive threshold. Subject 13 received a single dose of belimumab and developed *de novo* anti-MICA antibodies in addition to low titre *de novo* DSA. The small numbers of subjects with positive anti-MICA antibodies prevents us from being able to draw firm conclusions, however this data suggests that belimumab may be beneficial in reducing non-HLA antibodies.

A

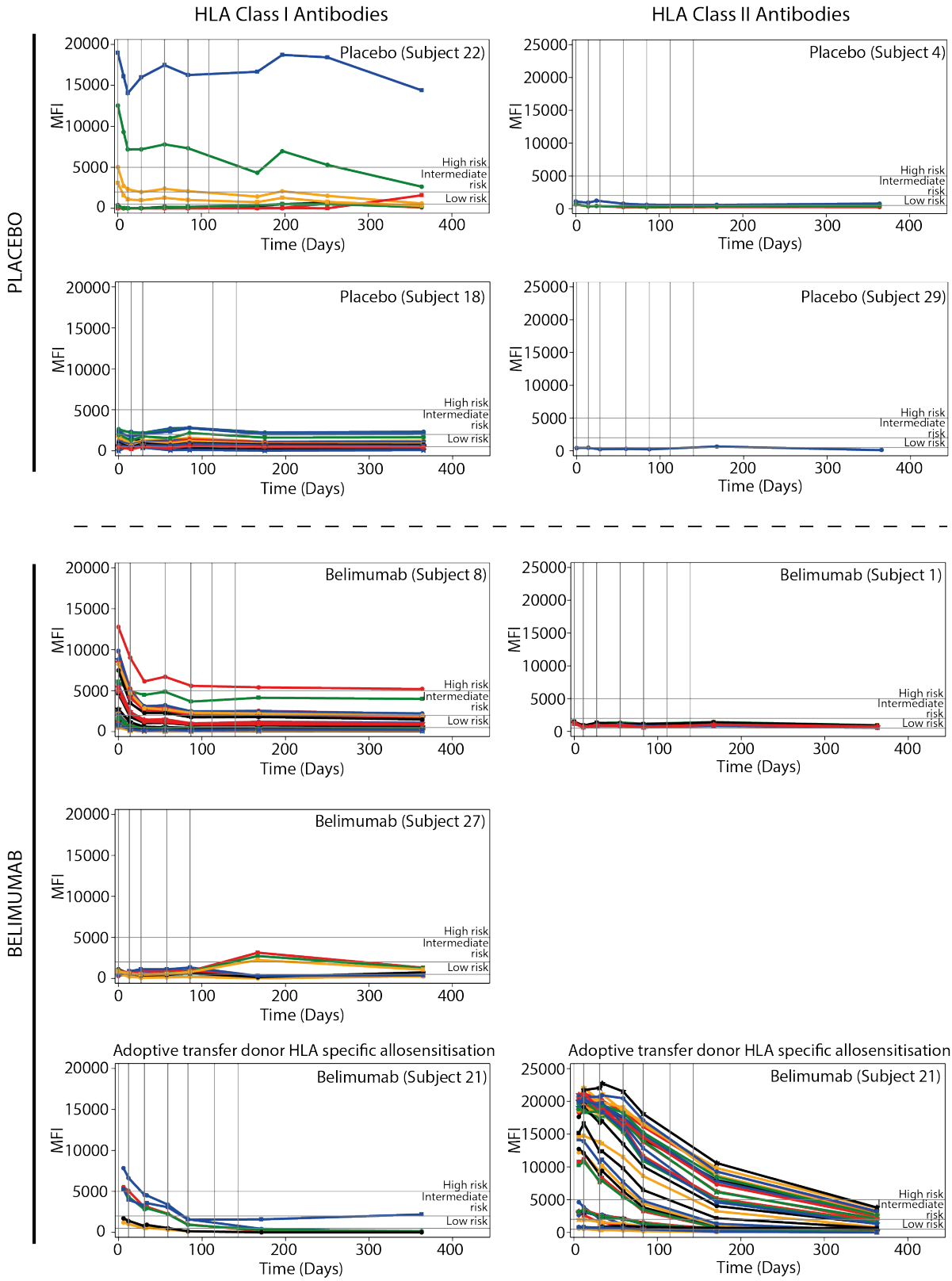
HLA Class I Antibodies
HLA Class II Antibodies
PLACEBO
BELIMUMAB
Placebo (Subject 22)
Placebo (Subject 4)
Placebo (Subject 18)
Placebo (Subject 29)
Belimumab (Subject 8)
Belimumab (Subject 1)
Belimumab (Subject 27)
Adoptive transfer donor HLA specific allosensitisation
Belimumab (Subject 21)
Adoptive transfer donor HLA specific allosensitisation
Belimumab (Subject 21)
MFI
Time (Days)
High risk
Intermediate risk
Low risk

B

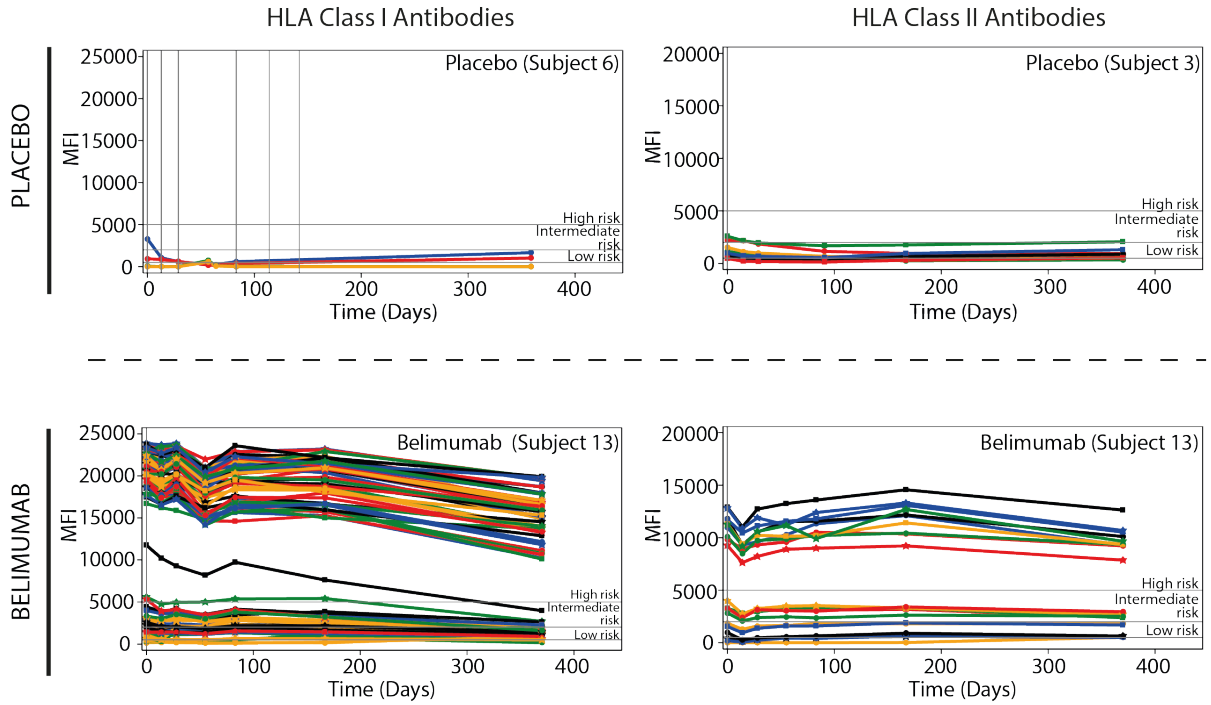


C

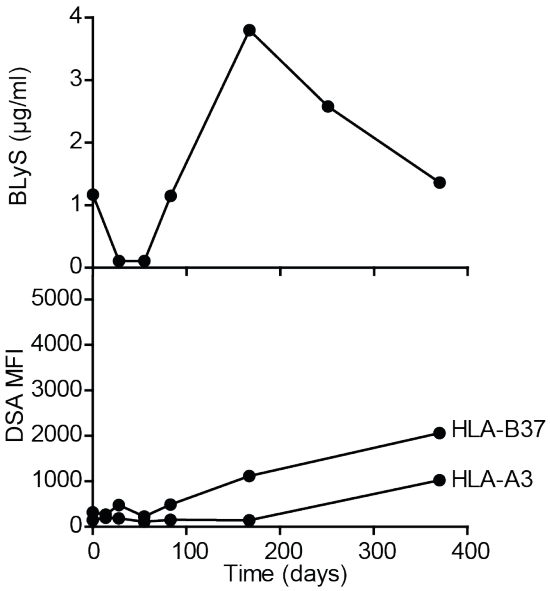


*Figure 35: Serum samples before and after treatment were screened for HLA antibodies using Luminex HLA class I and class II antibody detection beads (LABScreenTM Mixed, One Lambda) and HLA antibody specificities were determined using Luminex single antigen HLA-specific antibody detection beads (LABScreen Single Antigen HLA Class I and Class II, One Lambda). The normalized mean fluorescence intensity (MFI) for each single antigen bead with an MFI above the detection limit of 500 at any timepoint is shown in individuals from the per protocol population (A) and those not in*

*the per protocol population (B). Risk categories refer to the clinical interpretation assigned to MFI levels by the Histocompatibility and Immunogenetics laboratory for donor specific HLA antibodies. Vertical lines show when doses of study drug were received. Subject 6 received plasma exchange for FSGS between days 31 and 64. Subjects 3 and 13 withdrew consent for study drug following a single dose. Adoptive transfer donor HLA specific allosensitization as described in (Maxfield 2015). Panel C shows the relationship between serum BLyS and de-novo donor-specific HLA antibody over time for subject 13 who received a single dose of belimumab on day 0 prior to withdrawal of consent for study drug. Serum was sampled for BLyS levels at Day 0, week (W) 4, W8, W16, W24, W36 and W52 within time windows specified in the study protocol. The first increase in serum BLyS was detected at W24 (day 167), with a fall in levels thereafter to baseline by W52 (day 370). Antibodies were measured using Luminex single antigen HLA-specific antibody detection beads (LABScreen Single Antigen HLA Class I and Class II, One Lambda); donor specificity was determined manually by comparison of donor and recipient HLA-types. A low MFI MHC class I B37 antibody became detectable at W24 (day 167), and a further A3 antibody at W52 (day 370), the latter in the context of a falling serum BLyS level.*

*De novo* HLA and non-HLA IgG autoantibodies can have a deleterious effect on allograft function (Dragun 2005, Sigdel 2012, Jackson 2015). In order to sensitively measure the ability of belimumab to inhibit the development of *de novo* IgG antibodies, we tested serum taken at time zero and week 24 for antibody binding to a human protein array. This demonstrated that the addition of belimumab to standard of care immunosuppression significantly reduced *de novo* IgG antibody formation (Figure 36).

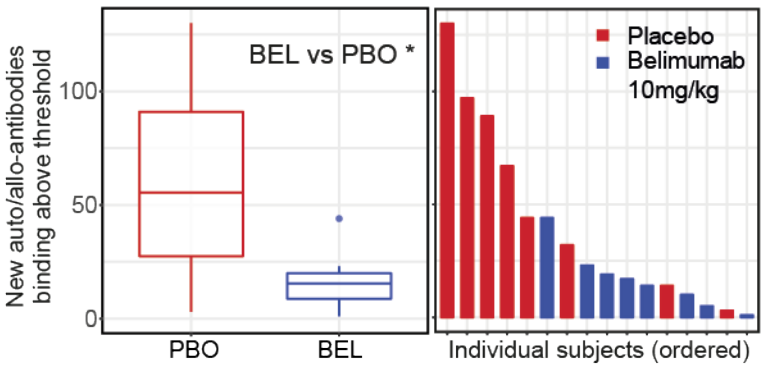


*Figure 36: Belimumab reduces new non-HLA antibody generation. The number of unique ProtoArray antigen specificities with significant antibody binding at Week 24 but not baseline. Horizontal lines on boxplot (left) correspond to median and interquartile ranges. Individual patient data shown (right), ordered by number. Patients are coloured by treatment group. The Wilcoxon rank-sum test was used to compare the belimumab treatment group (BEL) and placebo treatment group (PBO); * denotes p<0.05.*

In addition to effects on *de novo* antibodies, we also observed an effect on pre-formed non-HLA antibodies that have been implicated in allograft damage; at week 24 we saw reduced IgG specific for kidney antigens (Li 2009) following belimumab treatment (Figure 37A,B), and a significant reduction in anti-EDIL3 (EGF-like repeats and discoidin I-like domains 3) antibodies (Figure 37C), an endothelial cell-specific antibody associated with post-transplant glomerulopathy (Jackson 2015). The presence of antibodies to glial cell-derived neurotrophic factor (GDNF) at the time of transplantation has been associated with more severe chronic allograft injury (interstitial fibrosis and tubular atrophy) on 24 month biopsies (Sigdel 2012); we observed a reduction in the number of subjects with detectable anti-GDNF antibodies at week 24 compared with time 0 in the belimumab group (6/8 and 2/8 at time 0 and 24 weeks respectively), in contrast to the placebo group (6/8 and 6/8 at time 0 and week 24 respectively) (Figure 37D). Together, these data emphasise that belimumab modulates a clinically important aspect of B cell function post-transplant.

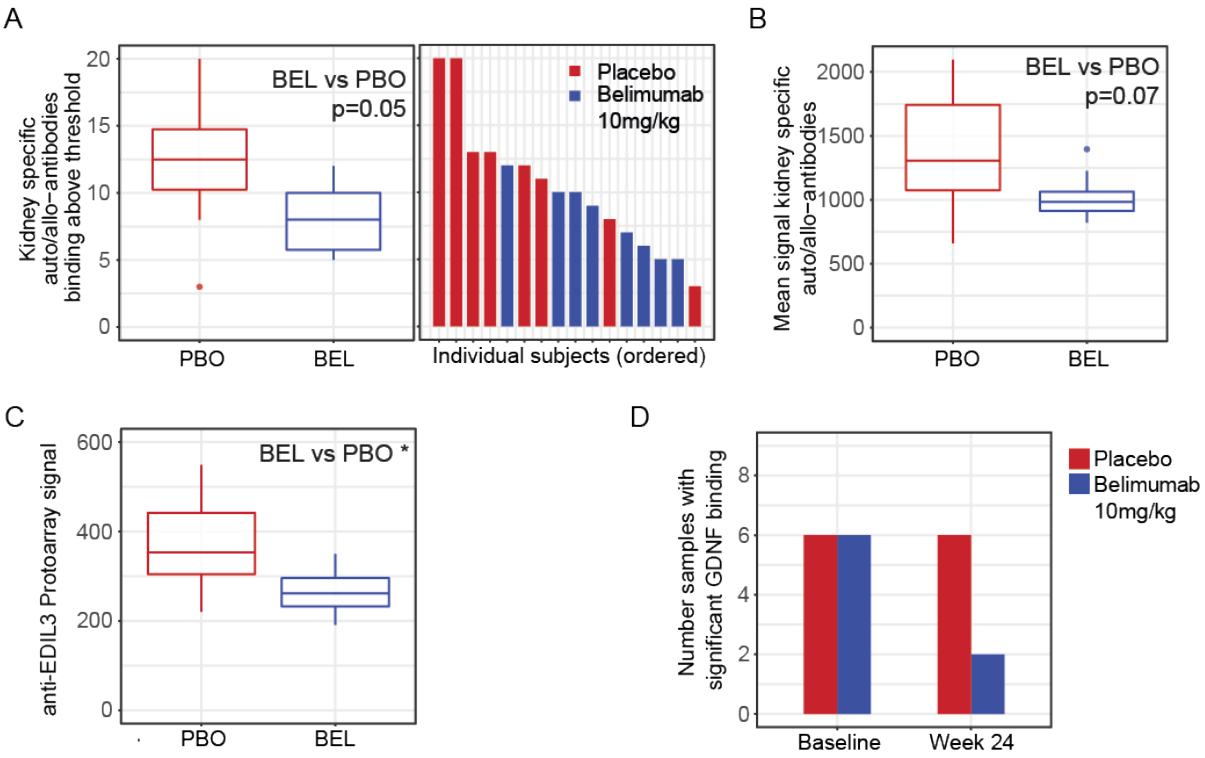


*Figure 37: Belimumab reduced pre-formed kidney specific antibodies. The number (A) and mean protoarray signal (B) of kidney specific unique ProtoArray antigen specificities (defined in (Li 2009)) with significant antibody binding at Week 24. In A, horizontal lines on boxplot (left) corresponds to median and interquartile ranges. Individual patient data shown (right), ordered by number. Patients are coloured by treatment group. Panel C shows the distribution of the mean protoarray signal from two antigens on the array annotated to EDIL3 (BC053656.1; BC030828.1) by treatment group at week 24. Panel D shows the number of subjects in each treatment group with above threshold*

*protoarray binding to GDNF at baseline and week 24. PP population; Eight subjects were tested at each timepoint for both treatment groups. Horizontal lines on boxplots correspond to median and interquartile ranges. The Wilcoxon rank-sum test was used to compare the belimumab treatment group (BEL) and placebo treatment group (PBO) in post-hoc analyses; * denotes p<0.05; exact p values displayed where p ≥ 0.05.*

### 3.4.10 Belimumab treatment skews the residual B cell compartment towards an IL10-producing regulatory phenotype

IL-10 producing B cells are enriched within transitional and memory subsets and associated with favourable outcomes in renal transplantation (Cherukuri 2013, Cherukuri 2014, Chesneau 2014, Shabir 2015). We observed a reduction in the number of transitional B cells following belimumab treatment (Figure 38A) with maintenance of memory B cells (Figure 38B).

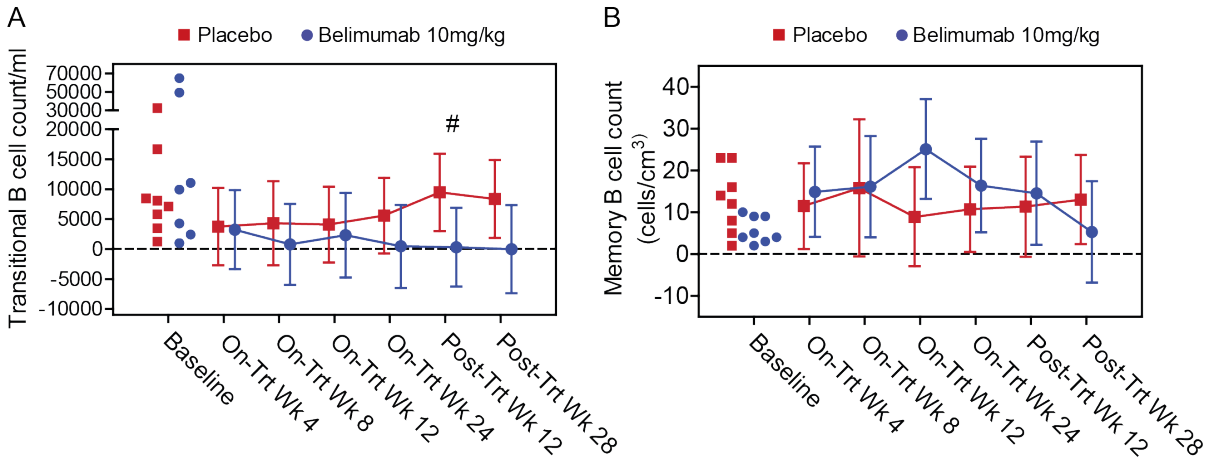


*Figure 38: Belimumab reduced transitional B cells but not memory B cells. A shows the transitional ($CD24^{br}CD38^{br}IgD^{+}$) B cell count/ml. B shows the memory ($CD20^{+}CD27^{+}$) B cell count (cells/$cm^3$). PP population. Raw values shown at baseline with adjusted mean estimate +/- 95% confidence intervals at subsequent timepoints. # indicates that the 95% confidence interval of the treatment difference does not include zero.*

In order to further assess the effect on the regulatory B cell compartment, we sought to address how belimumab treatment affects B cell cytokine production post-transplant. PBMC were stimulated *ex vivo* with CpG and CD40L, and B cell IL-10 and IL-6 production assessed. Prior validation work with healthy controls showed that surface marker expression was not altered significantly by a short 5 hour stimulation (data not shown). We were therefore able to quantify the cytokine production of subsets of B cells, based on their surface marker expression. Figure 39 shows representative flow cytometry plots to demonstrate the gating strategy used to define cytokine positive cells and

memory subsets. At week 12 post-transplant, subjects receiving belimumab had a reduction in IL-6-producing B cells and an increase in IL-10+ B cells (Figure 40A, B), skewing the cytokine ratio toward a more regulatory profile compared with controls (Figure 40C). This skewing of cytokine production towards IL-10 was observed in both transitional and memory B-cell subsets (Figure 40D).

IL-10 and IL-6 producing B cells were found within naïve (CD19+CD27-IgD+), transitional B (TrB) (CD19+CD24hiCD38hiIgD+), CD24+CD27+ memory (CD19+CD24+CD27+), switched memory (SM) (CD19+CD27+IgD-) and non-switched memory (NSM) (CD19+CD27+IgD+) subsets. Examining the surface markers expressed by B cells stained for intracellular cytokines revealed changes associated with belimumab treatment. In placebo-treated subjects, naïve B cells make up the majority of IL6+ B cells but a lesser proportion of IL10+ B cells (median 82.02% vs 51.12% at 12 week post treatment; Figure 41a). At 12 weeks post treatment, a reduced proportion of the IL-10 and IL-6 producing B cells from those treated with belimumab had a naïve phenotype and there was a concomitant rise in the proportion with a memory phenotype (Figure 41a).

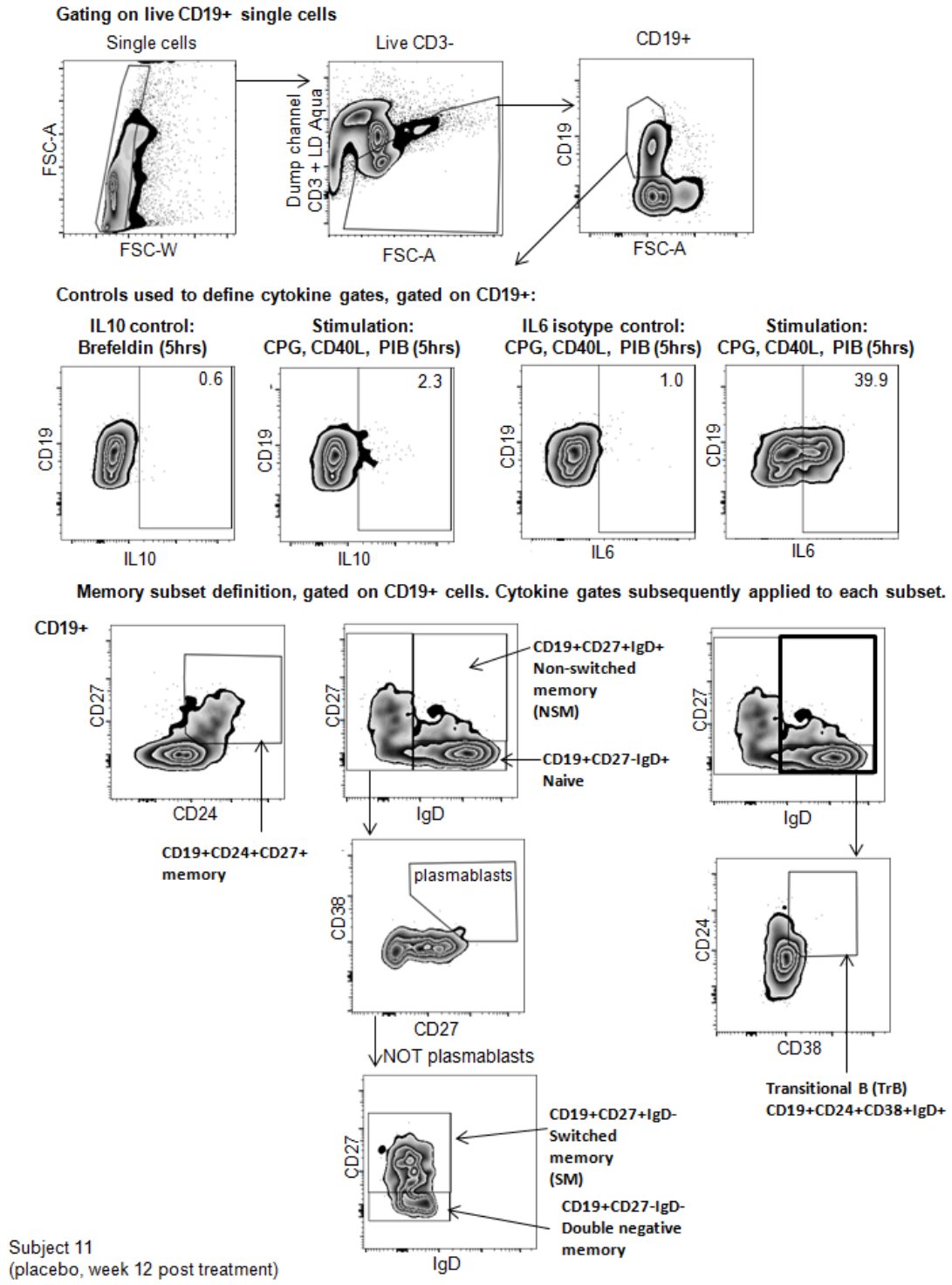


*Figure 39: Representative flow cytometry plots from 5 hour stimulation assay showing gating strategy used to define cytokine positive cells and memory subsets. The same cytokine gates were applied to each memory subset. Zebra plots are computed using equal probability contouring with the last 2% of events shown as dots.*

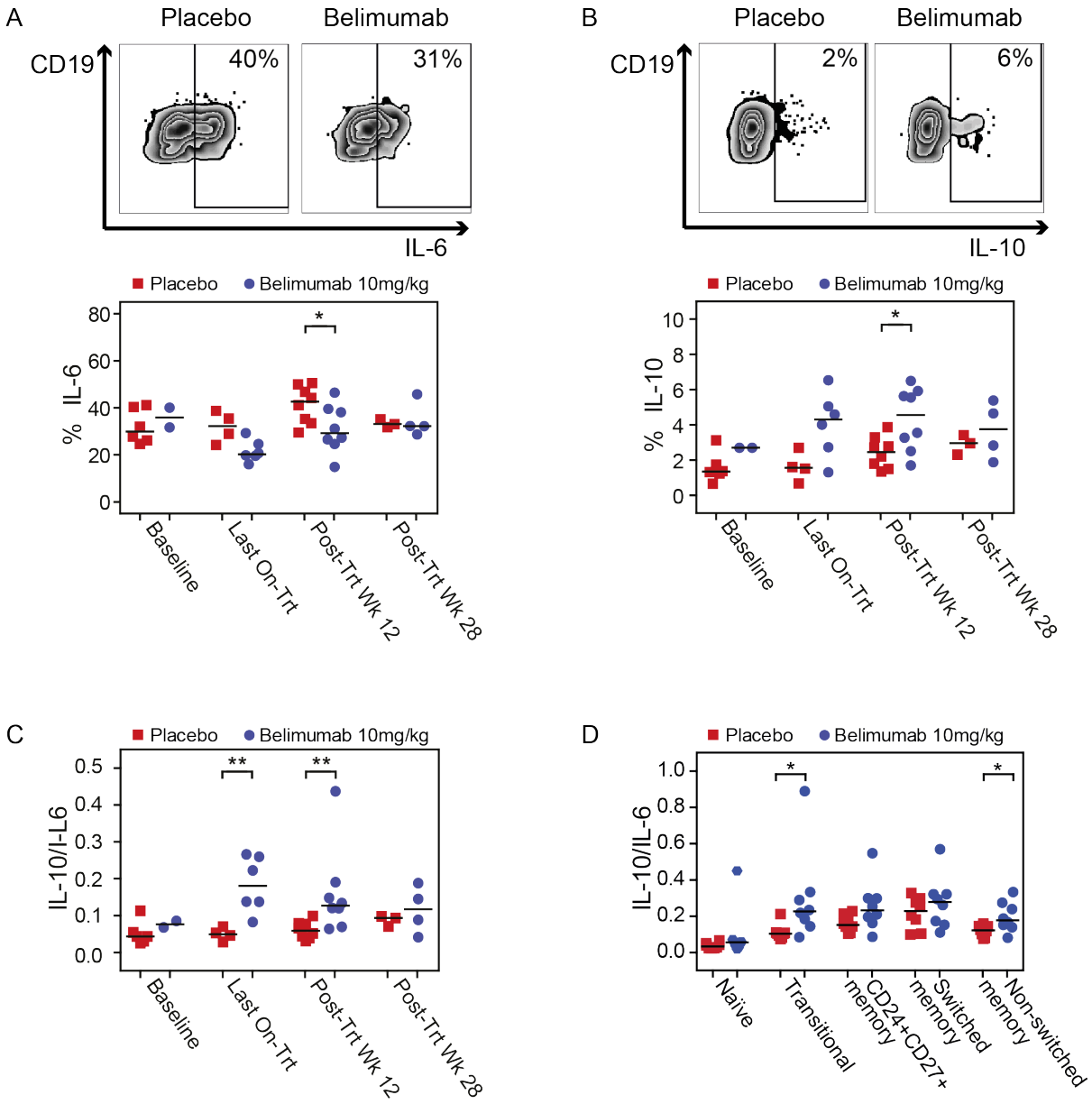


*Figure 40: Belimumab treatment increases circulating regulatory B cells. PBMC were stimulated ex vivo for 5 hours and intracellular cytokine production quantified by flow cytometry (Panel A-D). Individual data points represent individual subjects with horizontal lines signifying the median for each treatment group. Wilcoxon rank-sum tests were performed to compare samples by treatment and visit. Panel A shows representative flow cytometry plots for IL-6 (upper) and the percentage of CD19+ B cells expressing IL-6 (lower). Panel B shows representative flow cytometry plots for IL-10 (upper) and the percentage of CD19+ B cells expressing IL-10 by treatment group and timepoint (lower). Panel C shows the calculated ratio of IL-10/IL-6 with higher values indicating a more anti-inflammatory cytokine milieu. Panel D shows the IL-10/IL-6 ratio for individual subsets of naïve (CD27-), transitional (CD24hiCD38hiIgD+), CD24+CD27+ memory, switched memory (CD27+IgD-), and non-switched memory (CD27+IgD+) B cells at post treatment Wk 12. PP population. P-values*

*calculated using Wilcoxon rank-sum tests. * denotes p<0.05, ** p<0.01. All analyses were performed post hoc.*

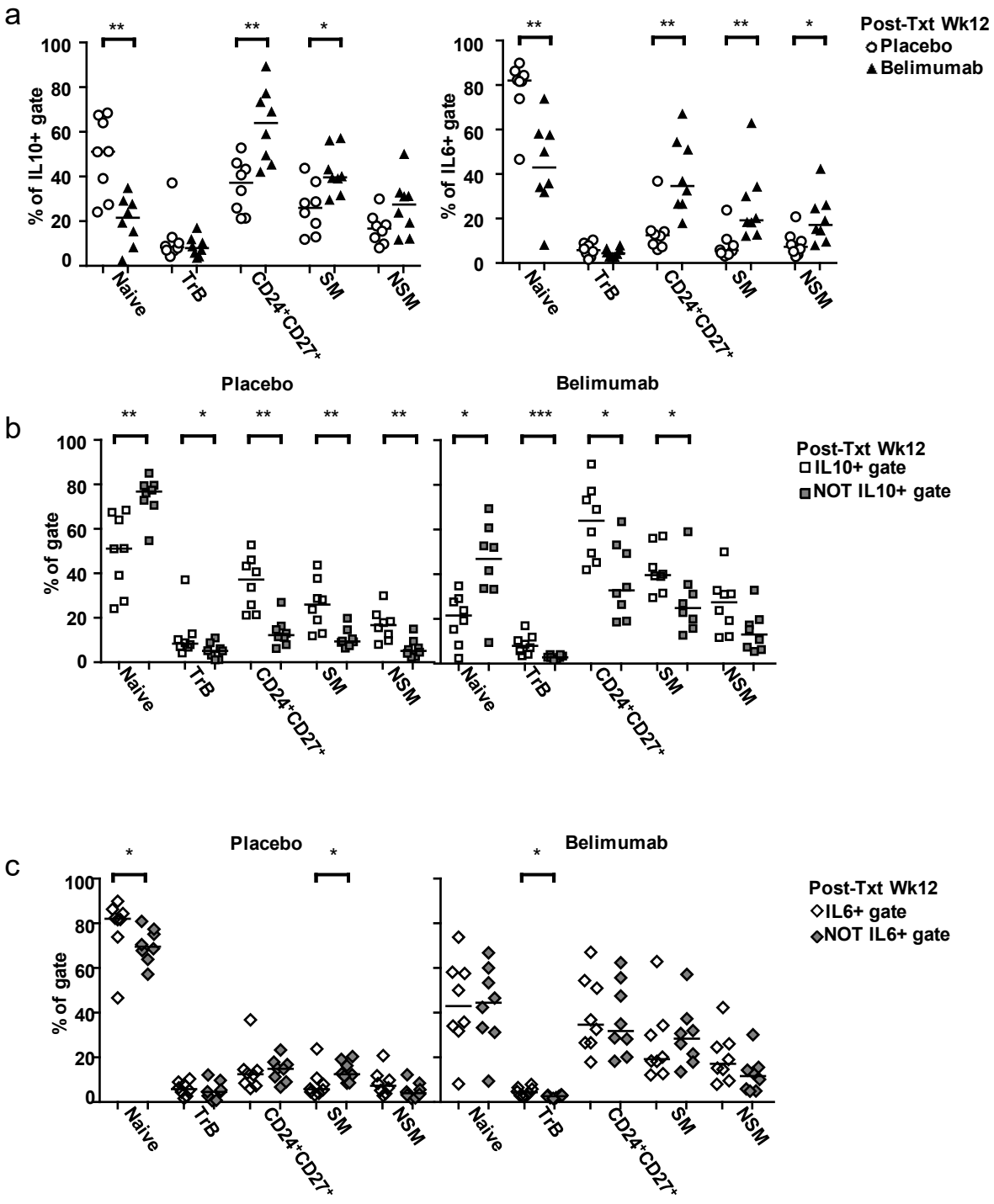


*Figure 41: Post hoc backgating analysis of 5 hour stimulated samples shows that cytokine producing B cells are depleted for naïve B cells and enriched for memory B cells following belimumab treatment. a) Phenotype of CD19+IL10+ and CD19+IL6+ cells at 12 weeks post treatment. b) IL10+ B cells are enriched for TrB and memory B cells, whilst naïve B cells are under-represented. Comparison of IL10*

*producing and NOT IL10 producing cells at 12 weeks post treatment. c) IL6+ B cells are enriched for naïve B cells in placebo treated subjects. The proportion of naïve B cells in the peripheral blood falls following belimumab treatment. Comparison of IL6 producing and NOT IL6 producing cells at 12 weeks post treatment. PP population. P values calculated using two-tailed mann whitney tests. * denotes p<0.05, ** denotes p<0.01, *** denotes p<0.001. All analyses were performed post hoc. Naïve (CD27); TrB Transitional (CD24hiCD38hiIgD+); SM switched memory (CD27+IgD-); NSM Non-switched memory (CD27+IgD+).*

Comparing the profile of B cells in the cytokine secreting and non-secreting populations gives an indication as to whether belimumab treatment effects on the regulatory B cell compartment mirrors that seen as a whole. The differences between the phenotype of IL10+ and NOT IL10+ populations were similar in the belimumab and placebo treatment groups at 12 weeks post treatment. IL10+ B cells were enriched for transitional B cells and CD24+CD27+, switched and non-switched memory cells in both treatment groups, representing a greater proportion in the IL10+ gate compared to the NOT IL10+gate in these subsets. In contrast, naïve B cells were under-represented in the IL10+ gate (Figure 41b). IL6+ B cells were predominantly comprised of naïve B cells in placebo treated subjects and naïve B cells were over-represented in placebo IL6+ cells compared to the NOT IL6+ cells. The proportion of naïve B cells fell to similar levels of IL6+ and NOT IL6+ cells following belimumab treatment (Figure 41c).

To explore whether the effect of belimumab treatment on the regulatory compartment went beyond changing the proportion of cells from each subset, by altering the cytokine profile of the resultant B cell compartment, the ratio of IL10/IL6 producing B cell subsets were examined. Following belimumab treatment there was a trend for increased IL10 production relative to IL6 across multiple B cell subsets including TrB and memory subsets (Figure 42). A summary of treatment effect across subsets at post treatment week 12 is shown in Figure 40D. During the 'on treatment' period, there was a strong negative correlation between the percentage of CD19+ cells that were naïve and the percentage that produce IL-10, but not with the percentage that produce IL-6 (Figure 43). There was a strong positive correlation between percentage of CD19+ cells that were of a memory phenotype and the percentage that produce IL-10 but not with the percentage that produce IL-6 (Figure 44 (CD19+CD27+); Figure 45 (CD19+CD24+CD27)). There was no correlation between cytokine production and the proportion of transitional B cells (Figure 46). These strong reciprocal correlations between the proportion of naïve and memory B cells with the proportion of IL-10 producing cells suggesting the importance of the phenotype of the circulating B cells in determining their regulatory capacity.

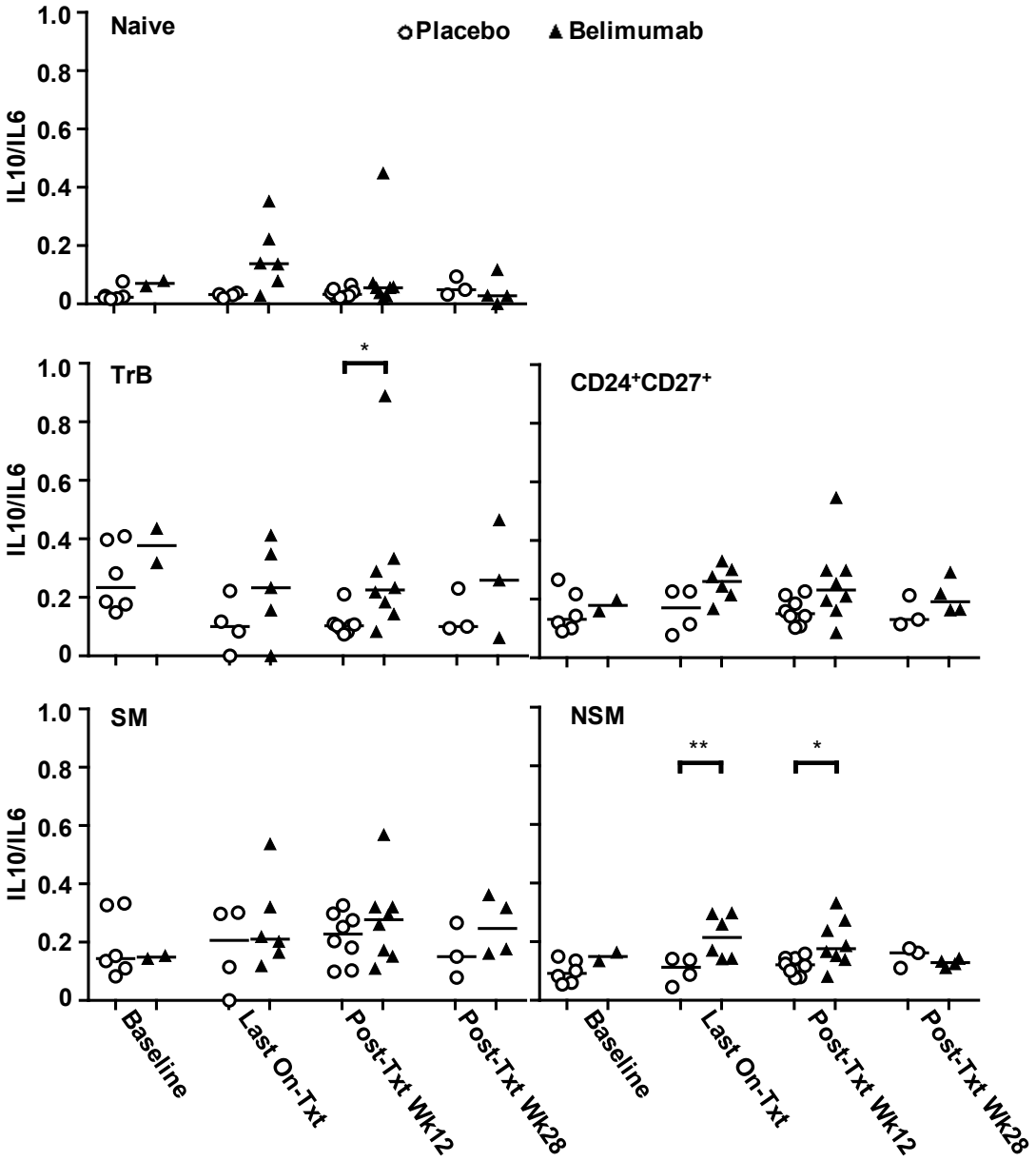


*Figure 42: Belimumab appears to have a general effect across subsets of skewing cytokine production towards IL10 relative to IL6. Ratio of the percentage of cells secreting IL10 to the percentage of cells secreting IL6 (IL10/IL6) following a 5 hour stimulation. The subset displayed is denoted in the top left of each graph. Due to the low frequency of TrB cells, replicate files were concatenated to increase the TrB event number to improve the accuracy of cytokine reporting. PP population. P values calculated using two-tailed mann whitney tests. * denotes p<0.05, ** denotes p<0.01. All analyses were performed post hoc. TrB transitional B, SM switched memory, NSM non switched memory.*

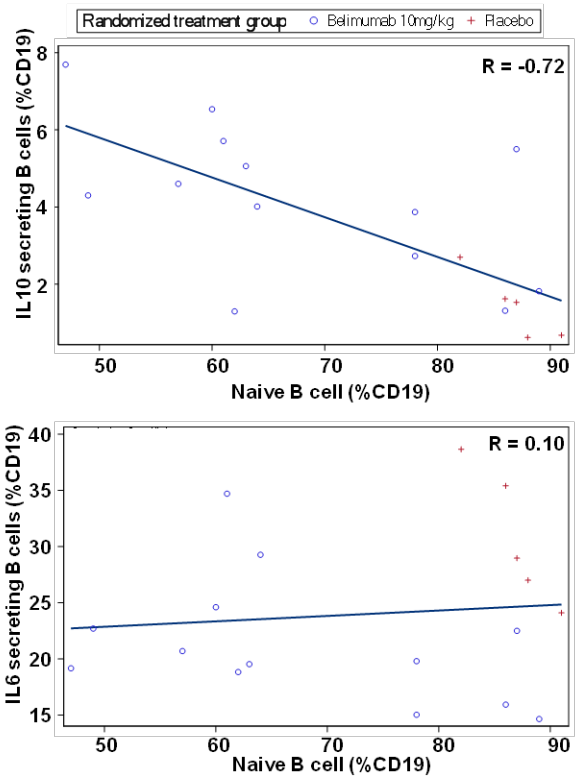


*Figure 43: Correlation between naïve B cells and IL-10 secreting B cells (top) and IL-6 secreting B cells (bottom). All readings collected during the on treatment phase are shown and colour coded by treatment group. Cytokine data taken from 5 hour stimulation. PP population, post hoc analysis. R = pearson correlation coefficients*

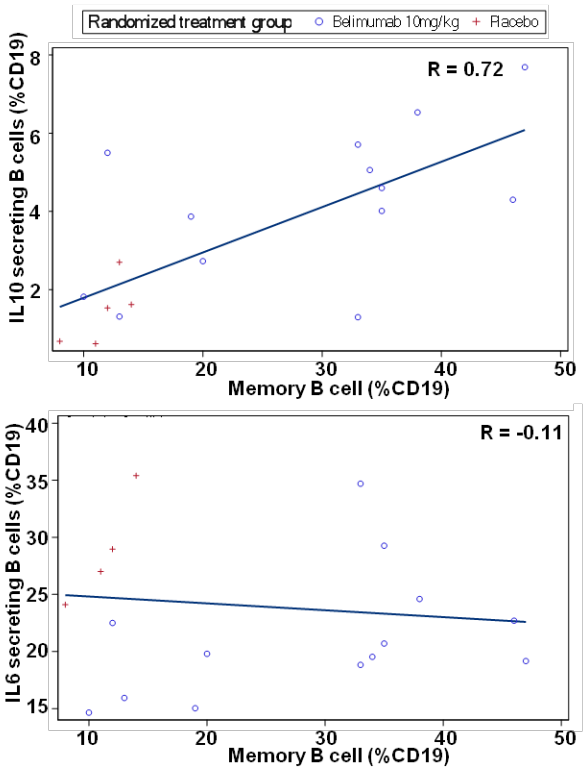


*Figure 44: Correlation between memory B cells (CD19+CD27+) and IL-10 secreting B cells (top) and IL-6 secreting B cells (bottom). All readings collected during the on treatment phase are shown and colour coded by treatment group. Cytokine data taken from 5 hour stimulation. PP population, post hoc analysis. R = pearson correlation coefficients*

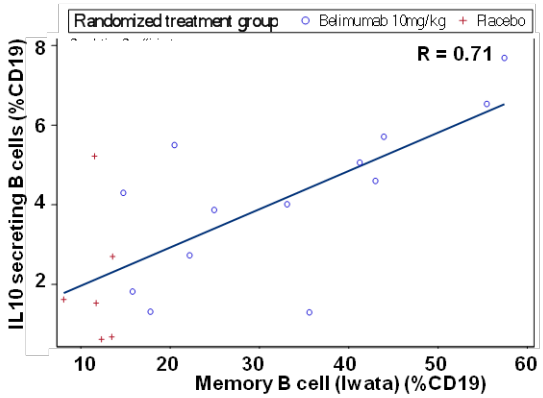


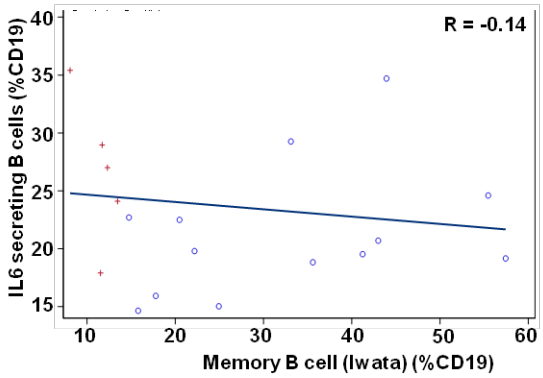


*Figure 45: Correlation between memory B cells (CD19+CD24+CD27+) and IL-10 secreting B cells (top) and IL-6 secreting B cells (bottom). All readings collected during the on treatment phase are shown and colour coded by treatment group. Cytokine data taken from 5 hour stimulation. PP population, post hoc analysis. R = pearson correlation coefficients*

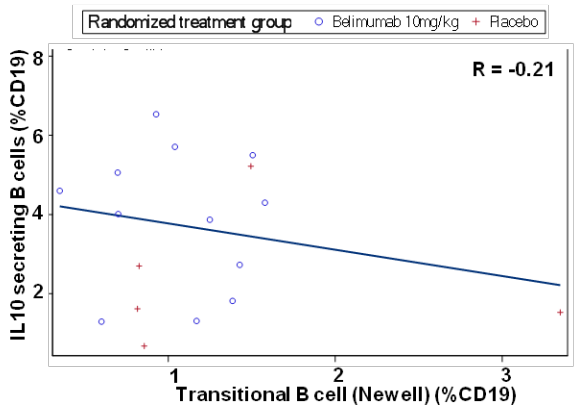


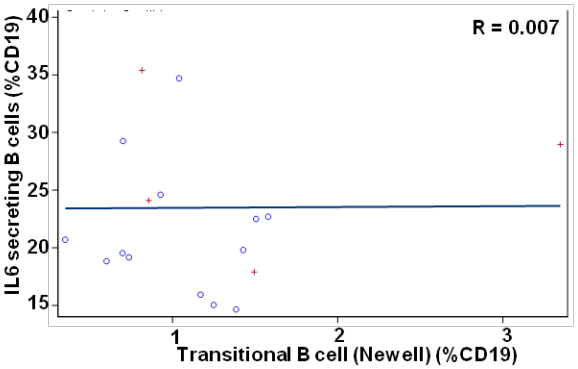


*Figure 46: Correlation between Transitional B cells (CD19+CD24b+CD38b+IgD+) and IL-10 secreting B cells (top) and IL-6 secreting B cells (bottom). All readings collected during the on treatment phase are shown and colour coded by treatment group. Cytokine data taken from 5 hour stimulation. PP population, post hoc analysis. R = pearson correlation coefficients*

The impact of belimumab on the circulating regulatory B cell compartment can therefore be summarised as follows. In placebo-treated subjects, naïve B cells make up the majority of IL-6+ B cells but a lesser proportion of IL-10+ B cells. Depletion of naïve B cells with belimumab is associated with a reduction in the proportion of IL-6 secreting B cells but a rise in the proportion of IL-10

producing B cells. Belimumab appears to impact the regulatory capacity of the B cell compartment in two ways. It causes a reduction in the proportion of naïve B cells that have a low IL10/IL6 ratio, with a concomitant increase in the proportion of memory B cells that have a higher IL10/IL6 ratio. In addition, belimumab appears to have a general effect across subsets of skewing cytokine production towards IL-10 relative to IL-6.

Some B cells may not produce IL-10 in their current state, but have the capacity to produce IL-10 in the right environmental context. A more prolonged period of *ex vivo* stimulation identified these Breg progenitors in addition to circulating Breg. Figure 47 shows representative plots demonstrating the gating strategy in a 48 hour stimulation assay. In this assay, subjects in the belimumab group had fewer IL-6 producing B cells than subjects in the placebo group with no difference in IL-10 producing B cells, indicating maintenance of Breg progenitors with resultant cells less likely to produce pro-inflammatory cytokines (Figure 48).

IL-10 producing regulatory B cells are enriched in the CD73-CD25+CD71+ B cell subset (van de Veen 2013). This subset was quantified in freshly thawed PBMCs and following 48 hour stimulation with CpG and CD40L, with the addition of PMA, ionomycin and brefeldin A during the last 5 hours. Proportions of CD73-CD25+CD71+ B cells were similar in those treated with belimumab and placebo. In both treatment groups, levels fell during the first 8 weeks on treatment, however this likely represents downregulation of surface CD25 expression following basiliximab treatment (Wang 2009) and therefore cannot be interpreted as a reduction in the CD73-CD25+CD71+ B cell subset (Figure 49a, b). CD73-CD25+CD71+ B cells from those treated with belimumab had a more regulatory phenotype during the 8 to 24 week on treatment period, with a greater proportion producing IL-10 relative to IL-6 following stimulation (Figure 49c).

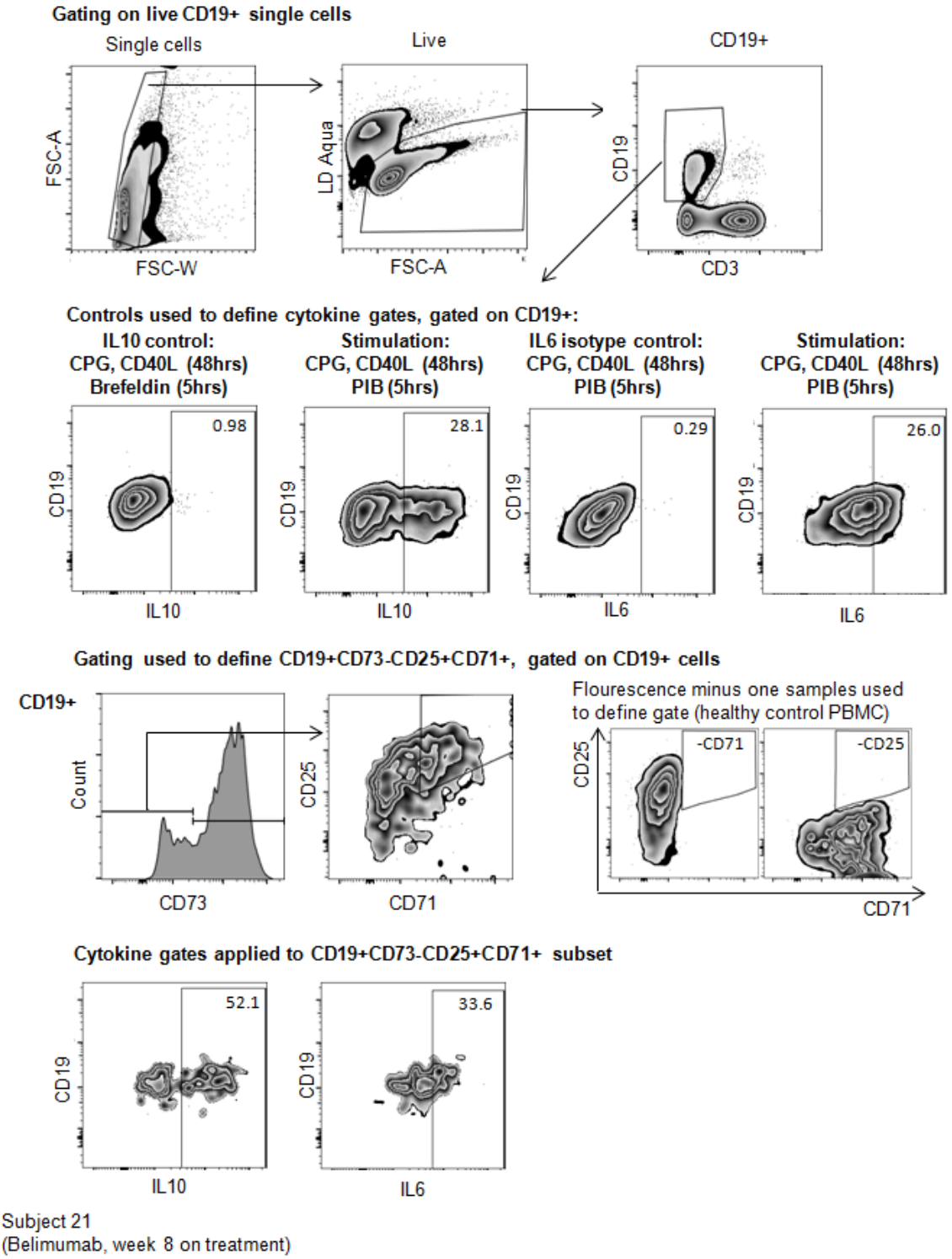


*Figure 47: Representative gating for CD73-CD25+CD71+ B cells stained following stimulation for 48 hours with CpG and CD40L with PMA, Ionomycin and Brefeldin added during the last five hours.*

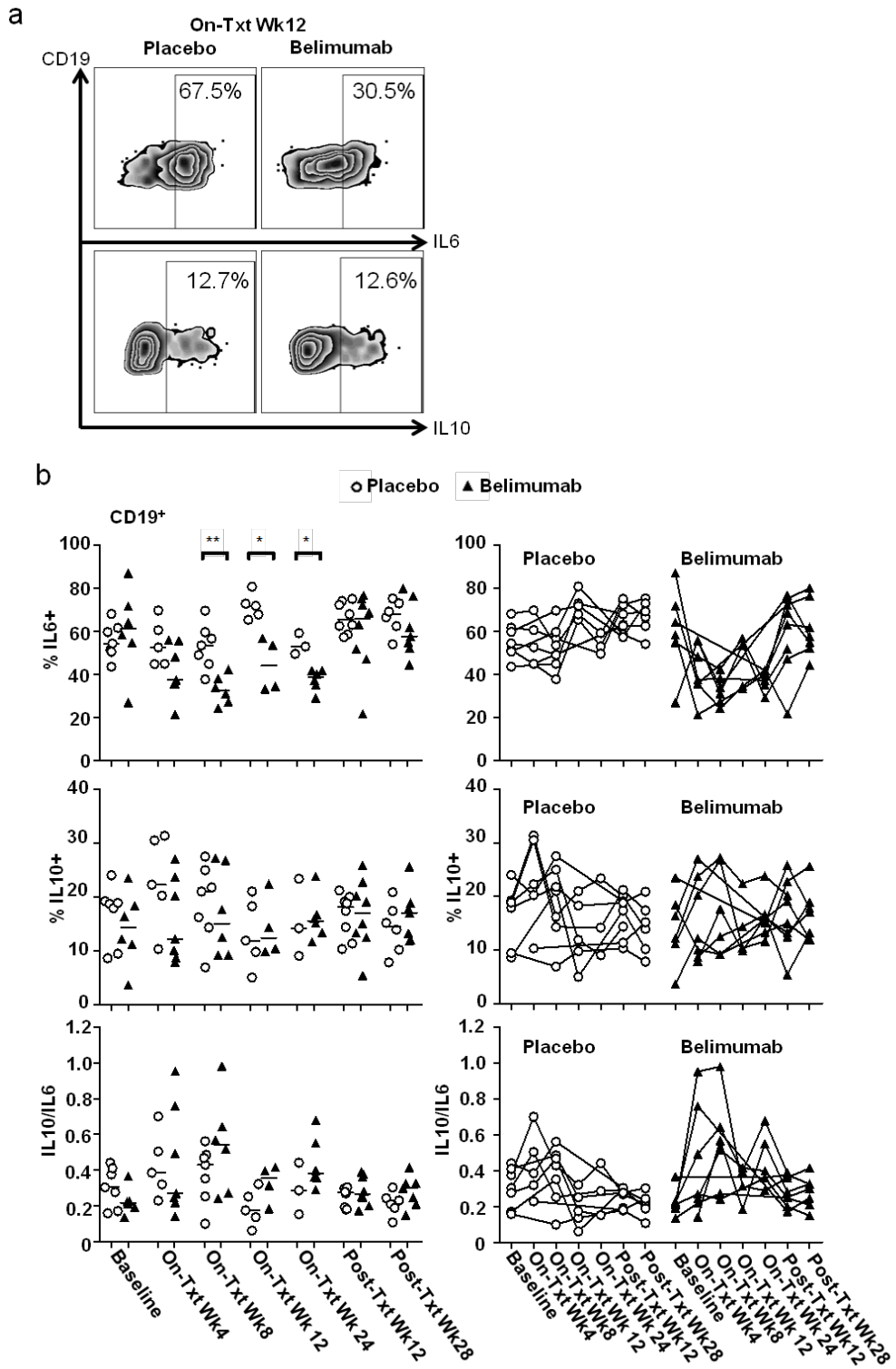


*Figure 48: Belimumab treated subjects maintain cells capable of producing IL10 on 48 hour stimulation (Breg progenitors) with a reduction in the proportion of cells secreting pro-inflammatory IL6. a) Representative flow cytometry plots gated on live CD19+ cells. Zebra plots are computed using equal probability contouring with the last 2% of events shown as dots. b) Percentage of CD19+ cells secreting IL-6 (IL6+) and IL-10 (IL10+) following a 48 hour stimulation and the ratio of IL10+ to IL6+ (IL10/IL6). Each point represents an individual subject; in the plots on the left the median of each*

*treatment group is shown by a horizontal line. The plots on the right show changes in individual subjects over time. PP population. P values calculated using two-tailed mann whitney tests. * denotes p<0.05, ** denotes p<0.01. All analyses were performed post hoc.*

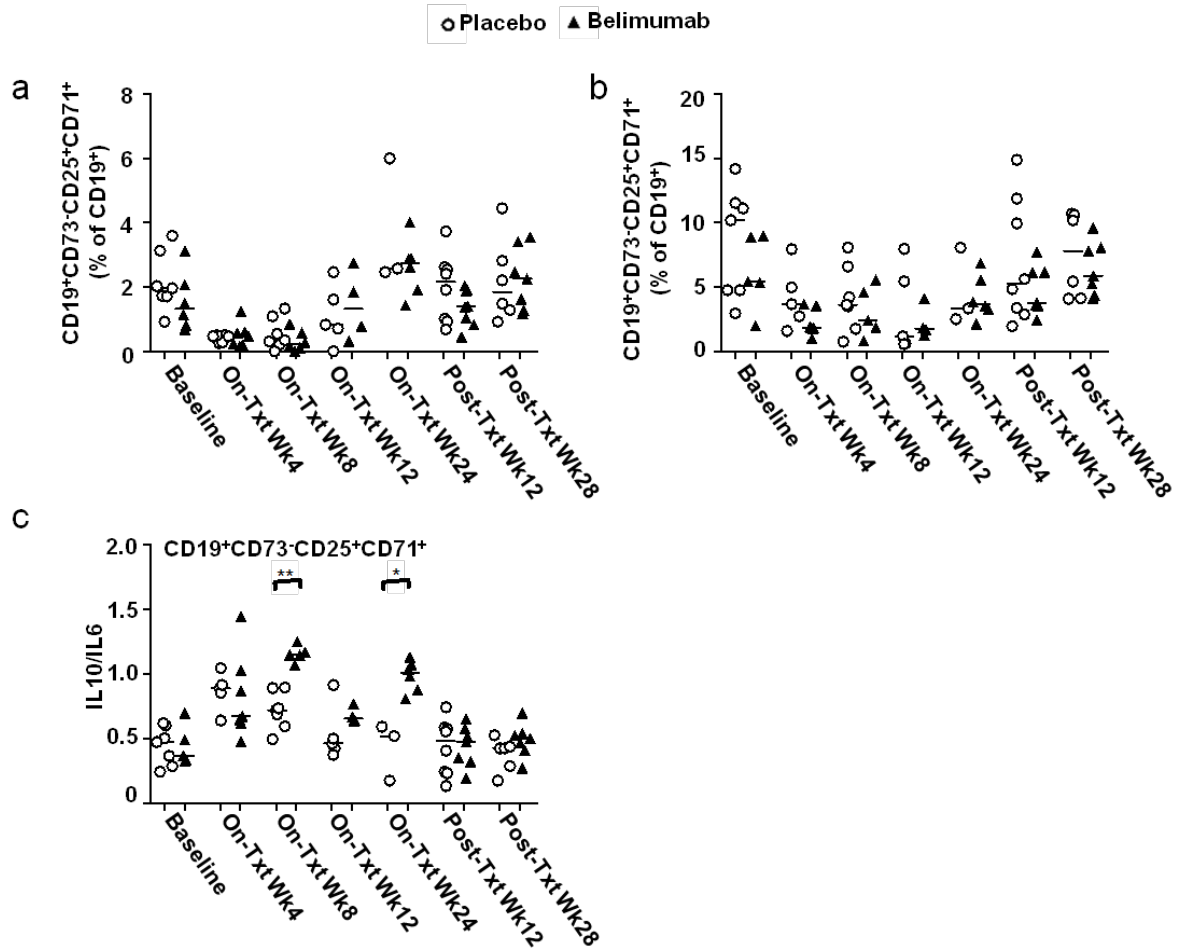


*Figure 49: CD73-CD25+CD71+ B cell analysis. a) Stained prior to stimulation. b) Stained following stimulation for 48 hours with CpG and CD40L with PMA, Ionomycin and brefeldin added during the last five hours. c) Ratio of percentage of CD19+CD73-CD25+CD71+ cells producing IL10 to the percentage producing IL6 (IL10/IL6). PP population. P values calculated using two-tailed mann whitney tests. * denotes p<0.05, ** denotes p<0.01. All analyses were performed post hoc.*

### 3.4.11 Memory B cell IL-10/IL-6 Ratio is BLyS Dependent

To confirm that the effect of belimumab on B cell cytokine production was B cell intrinsic we cultured human memory B cells from healthy controls with BLyS in the presence or absence of belimumab. This demonstrated that BLyS stimulation significantly decreased B cell IL-10 relative to IL-6, indicating a more inflammatory milieu, and that this effect was blocked in the presence of BLyS neutralisation by belimumab (Figure 50).

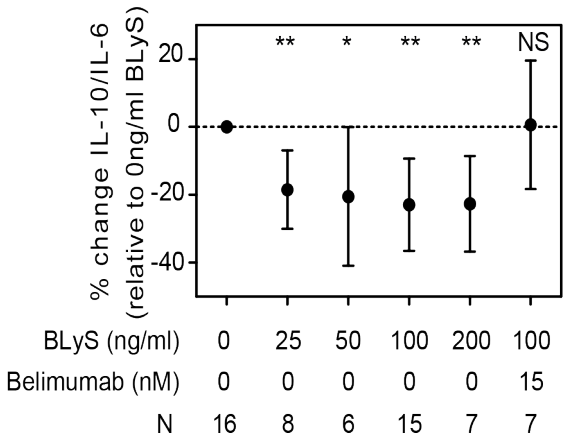


*Figure 50: Memory B cell IL-10/IL-6 Ratio is BLyS Dependent. PBMC from healthy volunteers enriched for CD27+ memory B cells and stimulated for 48 hours with increasing quantities of BLyS and in the presence or absence of belimumab. This figure shows the IL-10/IL-6 ratio (relative to 0ng/mL BLyS) in the different experimental conditions indicated. N, number of healthy volunteers tested for each experimental condition. T-tests were performed to determine whether the mean percentage change from baseline differed significantly from 0 for each experimental condition. * denotes p<0.05, ** denotes p<0.01. Experiments performed by Joseph Chadwick, GSK Experimental Medicine Unit.*

**3.4.12 Belimumab inhibits T cell proliferation**

We also investigated whether T cell activation was altered by belimumab treatment, since B cells are potent antigen presenting cells (Yuseff 2013) and IL-6 is known to augment T cell activation (Jordan 2017) whilst IL-10 can regulate T cell responses (Maynard 2008). There was no difference in the number of circulating T cells by treatment (Figure 51A, B) but transcriptomic analysis of purified circulating CD4 T cells revealed reduced cell cycle gene expression in belimumab-treated subjects suggesting that BLyS neutralisation may also inhibit T cell proliferation. Figure 51C shows volcano plots demonstrating no differences in the expression of cell cycle genes (WHITFIELD_CELL_CYCLE_G2_M gene list from MSigDb v5.1) at baseline (top panel) but a co-ordinated reduction in this geneset in subjects treated with belimumab 10 mg/kg compared with the placebo group at week 24 (bottom panel). Furthermore, numerous genes from this geneset were present in the list of genes most downregulated in the belimumab group relative to the placebo group at week 24.

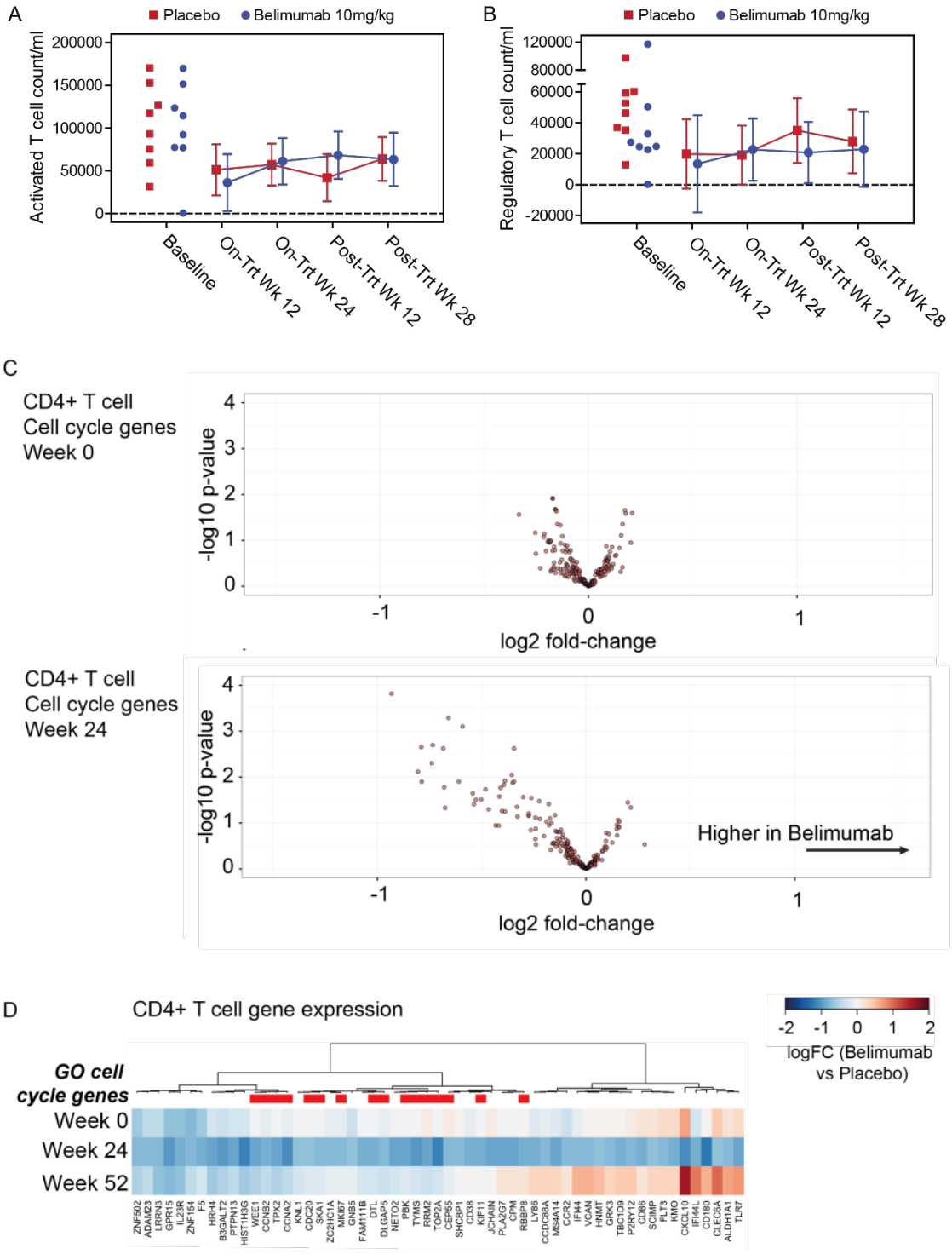


*Figure 51: Belimumab inhibits T cell cell cycle genes. Panel A shows activated T cell (CD4+CD25hiCD45RA-IL 7Rhi) count/ml. Panel B shows regulatory T cell (CD4+CD25hiIL-7Rlo) count/ml. Raw values shown at baseline with adjusted mean estimate +/- 95% confidence intervals, obtained from the same MMRM model as used for the primary endpoint, at subsequent timepoints.*

*Weeks 4 and 8 excluded due to known effects of basiliximab on CD25 surface expression. Panel C shows volcano plots demonstrating differentially regulated CD4+ T cell cell cycle genes in belimumab vs placebo treated subjects at week 0 (upper) and week 24 (lower). Panel D shows a heatmap of differential gene expression in blood CD4+ T-cells for the most downregulated genes at Week 24 in the Belimumab group relative to Placebo, ordered by fold-change at Week 24. Cell-cycle genes (GO:0007049) are highlighted. Colour corresponds to log2-fold change, with blue indicating higher expression in Placebo relative to Belimumab. Panels A-B use the PP population and panels C-D uses the MITT population for baseline and PP population thereafter. P-values in Panels A-D were calculated using Wilcoxon rank-sum tests and in Panel E using student's t-test*

**3.5 Discussion**

A key goal of this study was to determine the safety of belimumab in combination with standard transplant immunosuppression, in patients with ESRF. Although belimumab has previously been used in patients with SLE with renal involvement, it has not been used in patients with established ESRF. ESRF confers an increased risk of infection (Vanholder 1993), with impaired humoral immunity and reduced antibody vaccine responses (Eleftheriadis 2014). An added concern was the concomitant immunosuppression burden, which was significantly greater than that used in previous trials. Despite this burden of immunosuppression in an immunocompromised patient group, we observed no excess infections with the addition of belimumab.

Secondary and mechanistic end-points in this study provide evidence for beneficial effects of belimumab post-transplantation. In particular, despite depletion of B cell subsets known to contain regulatory B cells, the residual B cell compartment post-belimumab treatment demonstrated an increased capacity to produce the immunoregulatory cytokine IL-10 relative to IL-6. Since B cells are the major source of IL-6 in secondary lymphoid organs (Barr 2012), this observation is significant and of potential benefit in transplantation; IL-6 promotes B cell differentiation into antibody-forming plasma cells, contributes to the plasma cell niche (Kometani 2015), enhances T follicular helper cell development – cells critical for the germinal centre response, whilst inhibiting the generation of regulatory T cells (Jordan 2017). Indeed, an IL-6R antagonist has been used to treat patients with chronic ABMR (Choi 2017). We provide novel insights into the mechanism of action of belimumab, identifying for the first time the maintenance of a beneficial Breg subset on belimumab treatment, likely to be relevant in the setting of autoimmunity where belimumab use is common.

We present transcriptomic and protein microarray data suggesting that BLyS neutralisation reduced antibody-forming cells and resulted in a lower incidence of *de novo* non-HLA autoantibody formation post-transplant, both of which might positively affect transplant outcomes (Dragun 2005, Jackson

2015, Zhang 2016). Whether these effects were due to a reduction in B cell IL-6 production, or a direct effect of BLyS neutralisation on plasma cell survival (Benson 2008), was not addressed. Our study also highlights the role of BLyS in memory B cell activation, raising the possibility that belimumab may have utility in sensitised transplant subjects with pre-formed memory B cells. Finally, there was also a decrease in T cell proliferation markers demonstrating the potential for belimumab to impact both cellular and humoral alloimmunity.

Our study has several limitations; the sample size was not powered for clinical efficacy. We used belimumab in combination with non-lymphocyte depleting induction therapy (basiliximab), rather than thymoglobulin or alemtuzumab, agents that previously associated with an increase in serum BLyS (Bloom 2009). Whether belimumab would have the same pro-regulatory effect on the reconstituted B cell pool when used in combination with lymphocyte-depletion remains to be determined. Of note, we observed a rebound in serum BLyS following cessation of belimumab. Although this was not associated with any clinically overt effects, it raises the question of whether belimumab should be administered for a more extended period post-transplant. Belimumab is now available in a subcutaneous formation (Stohl 2017) which would make it easier to administer in an outpatient basis.

**Chapter 4: Bromodomain inhibitors modulate FcγR mediated macrophage activation, suggesting therapeutic potential in immune complex-mediated disease**

## Chapter 4: Bromodomain inhibitors modulate FcγR mediated macrophage activation, suggesting therapeutic potential in immune complex-mediated disease

### 4.1 Chapter summary

Immune complexed antigen can activate MNP via ligation of FcγR. FcγR-dependent MNP activation results in profound changes in gene expression that mediate antibody effector function in these cells. The resulting inflammatory response can be pathological in the setting of autoimmune diseases, such as systemic lupus erythematosus and in antibody-mediated rejection in transplantation. BET proteins are a family of histone modification 'readers' that bind acetylated lysine residues within histones and function as a scaffold for the assembly of complexes that regulate gene transcription. Bromodomain inhibitors (I-BET) selectively inhibit the transcription of a subset of inflammatory genes in macrophages following toll-like receptor stimulation. Since MNPs make a key contribution to antibody-mediated pathology, we sought to determine the extent to which I-BET inhibits macrophage activation by IgG.

Following FcγR stimulation of BMDM we detected changes in the expression of 1779 genes in the presence of DMSO, but only 172 genes in the presence of I-BET, suggesting that I-BET significantly attenuates IC-induced changes in gene expression. Numerous immune pathways induced by OVA-IC were downregulated by I-BET, including cytokine-chemokine signalling and cell adhesion pathways as well as antigen presentation pathways. Many of the LPS inducible genes that were significantly suppressed by I-BET (sI-BET) are also induced by IC and similarly suppressed by I-BET. Bromodomain inhibitors reduce FcγR expression on macrophages and dendritic cells *in vitro* and *in vivo*, potentially lowering their capacity to respond to IC. I-BET delays phagolysosome maturation associated with build-up of phagocytosed immune complex within BMDM and DC, whilst selectively inhibiting IC induced cytokine production, potentially promoting non-inflammatory clearance of ICs by tissue-resident cells.

We also showed efficacy of I-BET in murine models of IgG mediated inflammation. I-BET reduced spleen size following immune complex peritonitis and caused accumulation of phagocytosed IC within macrophages and neutrophils, with a trend towards reduced neutrophil recruitment in the peritoneal exudate. In response to circulating IC, I-BET reduced recruitment of mononuclear phagocytes to the kidney, reducing pro-inflammatory gene expression.

These findings support the hypothesis that bromodomain inhibition may be of benefit in the setting of antibody mediated disease, attenuating the immune response to deposited immune complex.

### 4.2 Background

IgG antibodies propagate inflammation in a number of autoimmune diseases and in organ transplantation. Many of their cellular effects are mediated by cross-linking FcγRs, surface glycoproteins that bind IgG immune complexes, and are expressed by most immune cells, including MNPs. FcγRs may be activating (in humans, FcγRIIA, IIIA, IIIB), or inhibitory (FcγRIIB) and their relative expression sets the activation threshold for a cell encountering IC (Nimmerjahn 2007b, Smith 2010). IgG-opsonised cargo may be phagocytosed by MNPs in an FcγR-dependent manner and degraded, in the case of macrophages, or processed for antigen presentation in the case of DCs. FcγR cross-linking in macrophages also results in the production of inflammatory cytokines, that assist in pathogen clearance but can potentially propagate tissue inflammation in autoimmunity. Deficiency or dysfunction of the inhibitory receptor FcγRIIB results in susceptibility to SLE in both mice and humans (Bolland 2000, Floto 2005, Kono 2005, Brownlie 2008, Smith 2010, Boross 2011), identifying the importance of this pathway in disease pathogenesis.

FcγR-dependent MNP activation results in profound changes in gene expression that mediate antibody effector function in these cells, including changes in genes associated with cytokine production, co-stimulation, antigen presentation and cell migration. Epigenetic marks such as DNA methylation and histone modifications control the expression of these genes. BET proteins (BRD2, BRD3 and BRD4) govern the assembly of histone acetylation-dependent chromatin complexes required for gene transcription (LeRoy 2008). Given the pivotal role of BET proteins in transcriptional regulation, small molecule compounds that inhibit binding of acetylated histones to BET proteins (I-BET) have been developed as potential anti-cancer and anti-inflammatory drugs (Prinjha 2012).

Treatment options in autoantibody-mediated disease such as SLE remain limited. B cell-targeted therapy may reduce antibody generation, but limiting FcγR-associated immune cell activation by existing autoantibodies remains an unmet need. I-BET have shown some utility in animal models of autoimmunity (Bandukwala 2012) including those with a proven antibody-dependent component, such as collagen-induced arthritis (Mele 2013) and selectively inhibit the transcription of a subset of inflammatory genes in macrophages following TLR4 stimulation (Nicodeme 2010, Belkina 2013).

Since MNPs make a critical contribution to antibody-mediated inflammation, we sought to determine the impact of I-BET on FcγR-mediated macrophage activation by IgG IC.

## 4.3 Results

### 4.3.1 I-BET inhibits gene expression induced by FcγR cross-linking in bone marrow derived macrophages

We first sought to gain a global overview of the extent to which changes in gene expression induced by FcγR cross-linking were altered by I-BET. We performed a transcriptomic analysis using affymetrix microarray analysis. BMDM were stimulated with IC (IgG-opsonised ovalbumin (OVA)) or control protein (OVA alone), as described previously (Clatworthy 2014a), with I-BET or DMSO solvent control added 30 minutes prior to the stimulus (Figure 52).

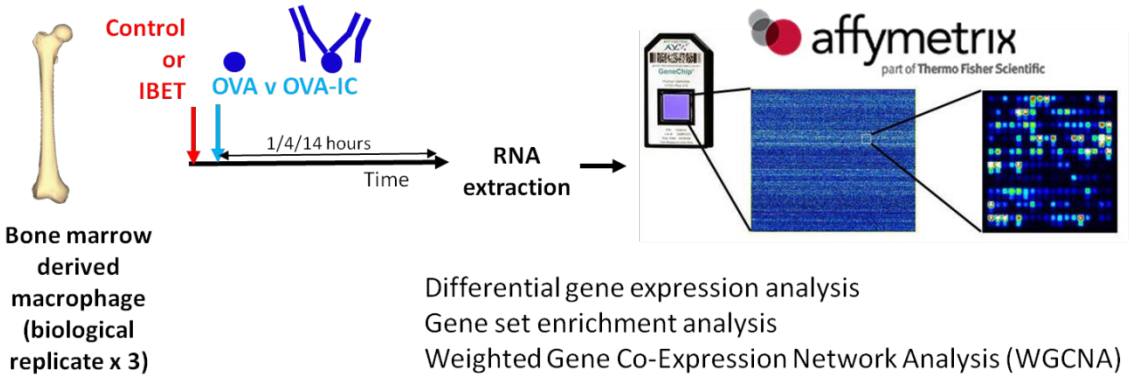


*Figure 52: Schematic describing experimental setup for microarray experiment. BMDM were stimulated with OVA-IC or OVA in the presence or absence of I-BET. RNA was extracted and transcriptomic analysis using an affymetrix microarray system was performed.*

Microarray analysis was performed by Dr John Ferdinand (post-doctoral fellow, Clatworthy Lab). Of the samples analysed one was rejected at the quality control (QC) stage, since it was a clear outlier with technical issues (Figure 53). Principal component analysis across the whole dataset showed that the greatest influence on the cell transcriptome was drug treatment, i.e. the presence or absence of I-BET (Figure 54). The second principal component separated samples that underwent stimulation for one hour from those stimulated for four hours or longer. This can be explained by the fact that these samples were prepared in an independent experiment at a different time.

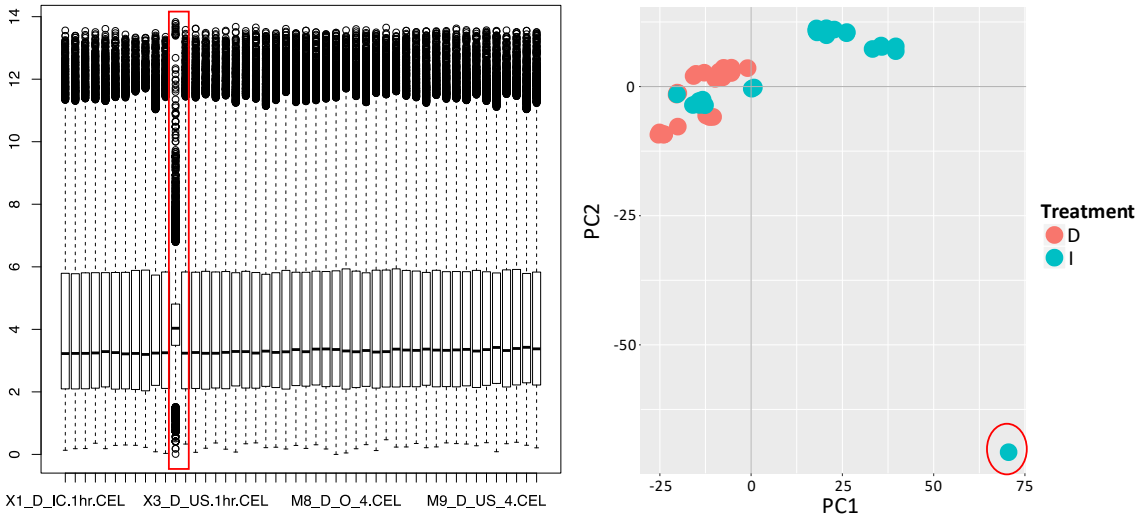


*Figure 53: QC plots identifying sample that failed QC. Boxplot of intensity (left); principal component plot (right). PC1 principal component 1; PC2 principal component 2; D DMSO; I I-BET.*

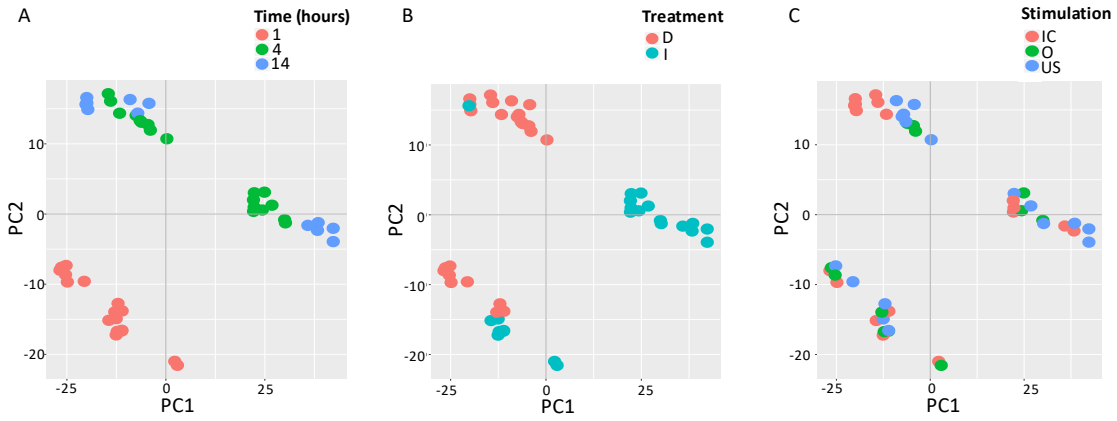


*Figure 54: Principal component plots of whole dataset coloured by timepoint (A), treatment (B) and stimulation (C). PC1 principal component 1; PC2 principal component 2; D DMSO; I I-BET; IC OVA-IC; O OVA; US unstimulated.*

Few changes were observed following OVA-IC stimulation at one hour. The principal component determining differential expression was the biological replicate from which the sample was derived. The second principal component was the drug treatment given prior to stimulation, with minimal effect of the stimulation itself (Figure 55A-C). At this early timepoint, few genes were differentially regulated when comparing the samples treated with OVA-IC and those treated with OVA in the presence of DMSO (Figure 55D)

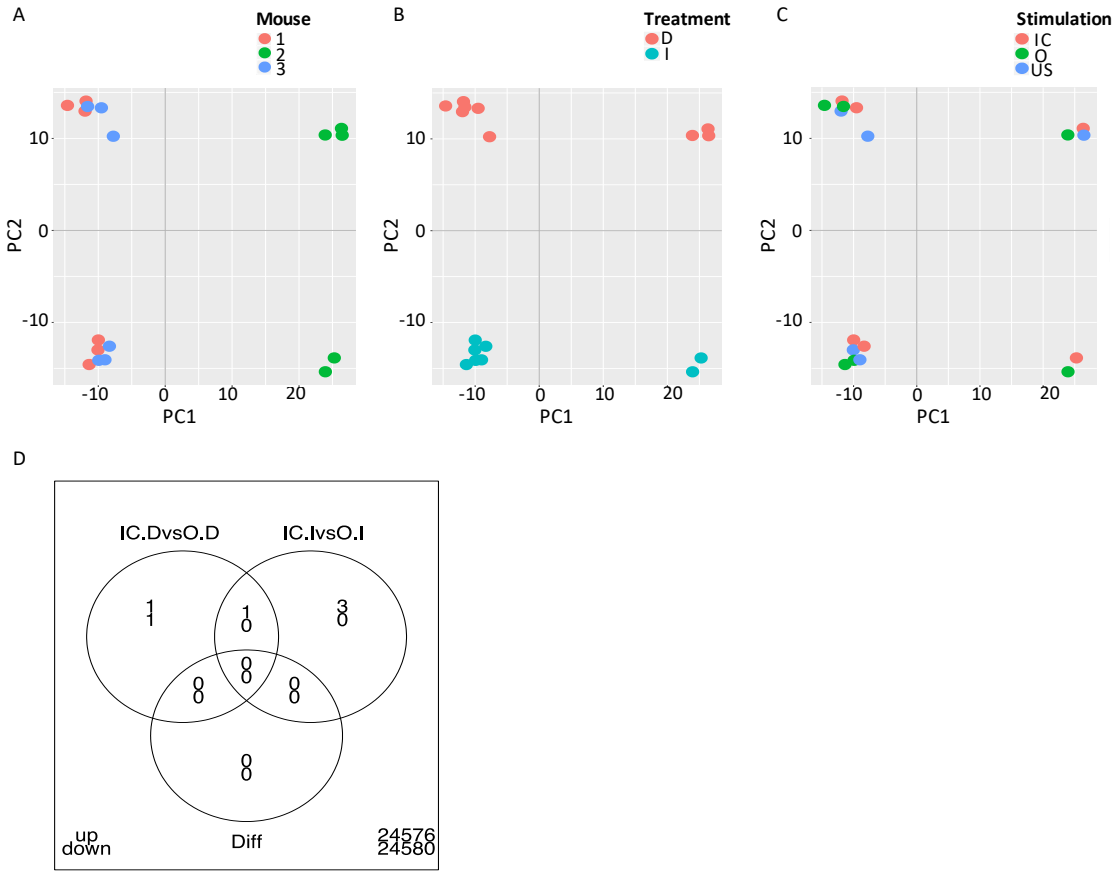


*Figure 55: Minimal effect of IC following one hour stimulation. Principal component plots of 1 hour dataset coloured by mouse (A), treatment (B) and stimulation (C). Venn diagram (D) describing genes differentially expressed (padj < 0.05 either direction) by immune complex in the presence of DMSO (IC.D vs O.D) and I-BET (IC.I vs O.I) and the effect of I-BET on IC stimulation (Diff). PC1 principal component 1; PC2 principal component 2; D DMSO; I I-BET; IC OVA-IC; O OVA; US unstimulated.*

Treatment of cells with I-BET for 1 hour did induce changes in the transcriptome; 389 genes were upregulated and 398 genes downregulated following the addition of I-BET to cells treated with OVA alone. Geneset enrichment analysis identified downregulation of immune pathways including cytokine and chemokine signalling, JAK-STAT and myc signalling pathways (Figure 56).

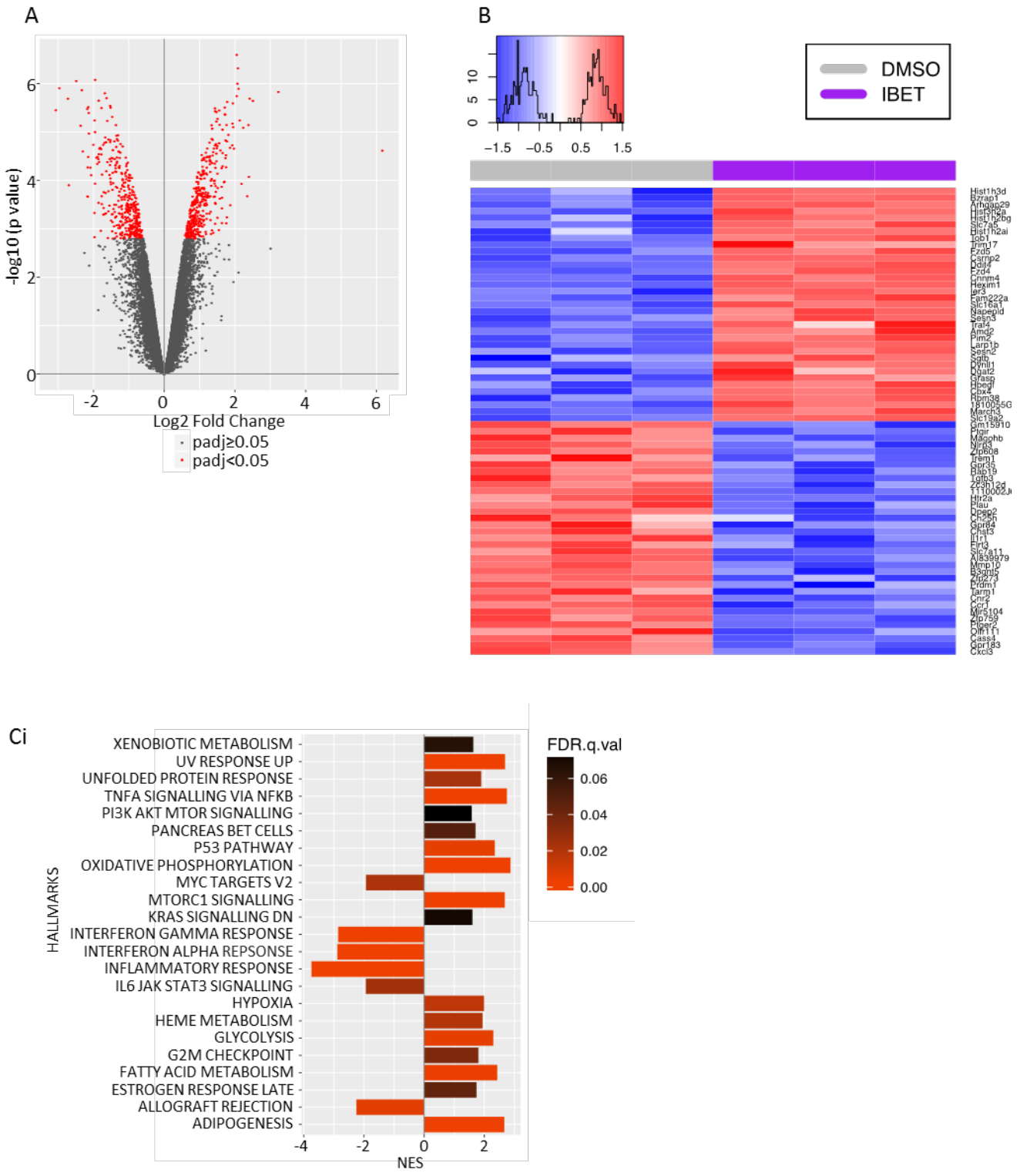
A
-log10 (p value)
Log2 Fold Change
padj≥0.05
padj<0.05
B
DMSO
IBET
Ci
HALLMARKS
XENOBIOTIC METABOLISM
UV RESPONSE UP
UNFOLDED PROTEIN RESPONSE
TNFA SIGNALLING VIA NFKB
PI3K AKT MTOR SIGNALLING
PANCREAS BET CELLS
P53 PATHWAY
OXIDATIVE PHOSPHORYLATION
MYC TARGETS V2
MTORC1 SIGNALLING
KRAS SIGNALLING DN
INTERFERON GAMMA RESPONSE
INTERFERON ALPHA REPSONSE
INFLAMMATORY RESPONSE
IL6 JAK STAT3 SIGNALLING
HYPOXIA
HEME METABOLISM
GLYCOLYSIS
G2M CHECKPOINT
FATTY ACID METABOLISM
ESTROGEN RESPONSE LATE
ALLOGRAFT REJECTION
ADIPOGENESIS
NES
FDR.q.val

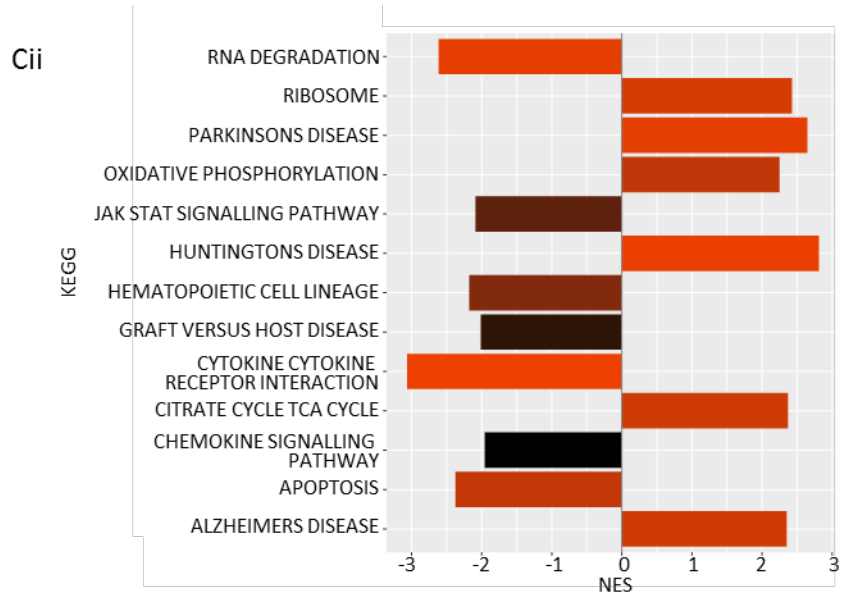


*Figure 56: I-BET induces changes in the transcriptome in the absence of FcγR crosslinking. A. Volcano plot showing the fold change and statistical significance of differential expression in the presence of I-BET (I-BET OVA vs DMSO OVA). B. Heat map showing the 35 top upregulated and downregulated genes. C. Gene set enrichment analysis using the Hallmark (i) and Kegg genesets (ii).*

Following a four hour stimulation with IC, many more changes in gene expression were induced; the principal determinant being drug treatment, followed by stimulation condition. No differential gene expression was observed between those samples treated with OVA and media alone (Figure 57D); therefore we used the OVA treated samples for statistical comparisons with OVA-IC. Following FcγR stimulation we detected changes in the expression of 1779 genes in the presence of DMSO. With the addition of I-BET, only 172 genes were differentially expressed, suggesting that I-BET significantly attenuates IC-induced changes in gene expression (Figure 57E). Volcano plots showing the effect of adding IC in the presence and absence of I-BET (Figure 57 F-G) and a scatter plot demonstrating the interaction (Figure 58) demonstrate the impact of I-BET. The significance of the effect of I-BET on FcγR induced changes can be assessed by looking at the interaction of the effect of IC and the effect I-BET i.e. the effect of I-BET on the effect of IC stimulation, calculated using a difference of differences approach ((IC.D vs O.D) minus (IC.I vs O.I)) in limma (Ritchie 2015). Of the 1779 genes impacted by OVA-IC, only 20 were found to be significantly impacted by the addition of I-BET with a threshold of $p_{adj}<0.05$ (Figure 57E), however the small number of samples processed limits the power for such an observation.

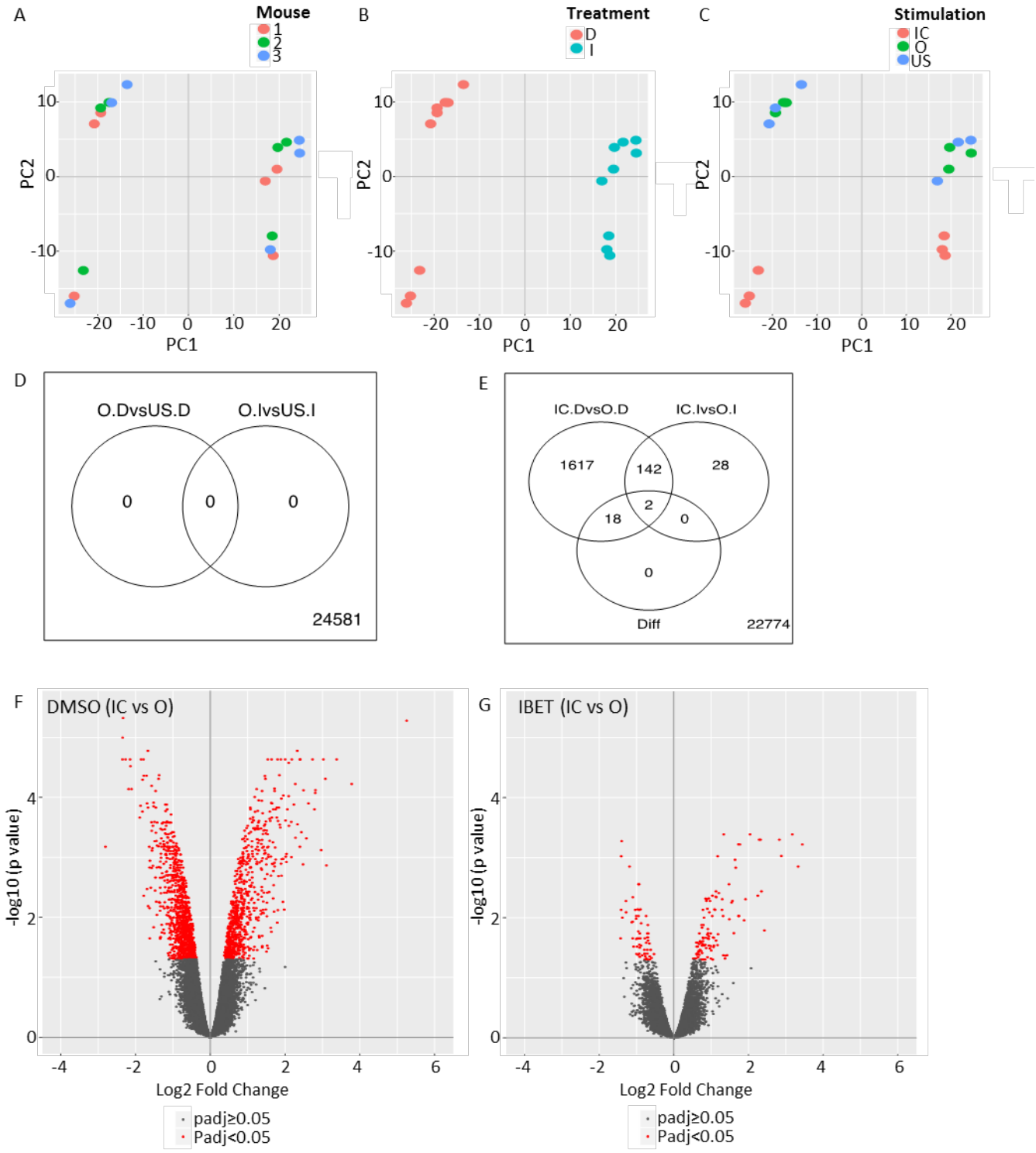


*Figure 57: I-BET dampens IC induced differential expression. Principal component plots of 4 hour dataset coloured by mouse (A), treatment (B) and stimulation (C). Venn diagram describing genes differentially expressed (padj < 0.05 either direction) by OVA vs US (D) and OVA-IC vs OVA (E) in the presence of DMSO and I-BET. Diff indicates the effect of I-BET on IC stimulation and is calculated as the difference of the difference. Volcano plots showing the fold change and statistical significance of IC dependent differential expression in the presence of DMSO (F) and I-BET (G). PC1 principal*

*component 1; PC2 principal component 2; D DMSO; I I-BET; IC OVA-IC; O OVA; US unstimulated.*

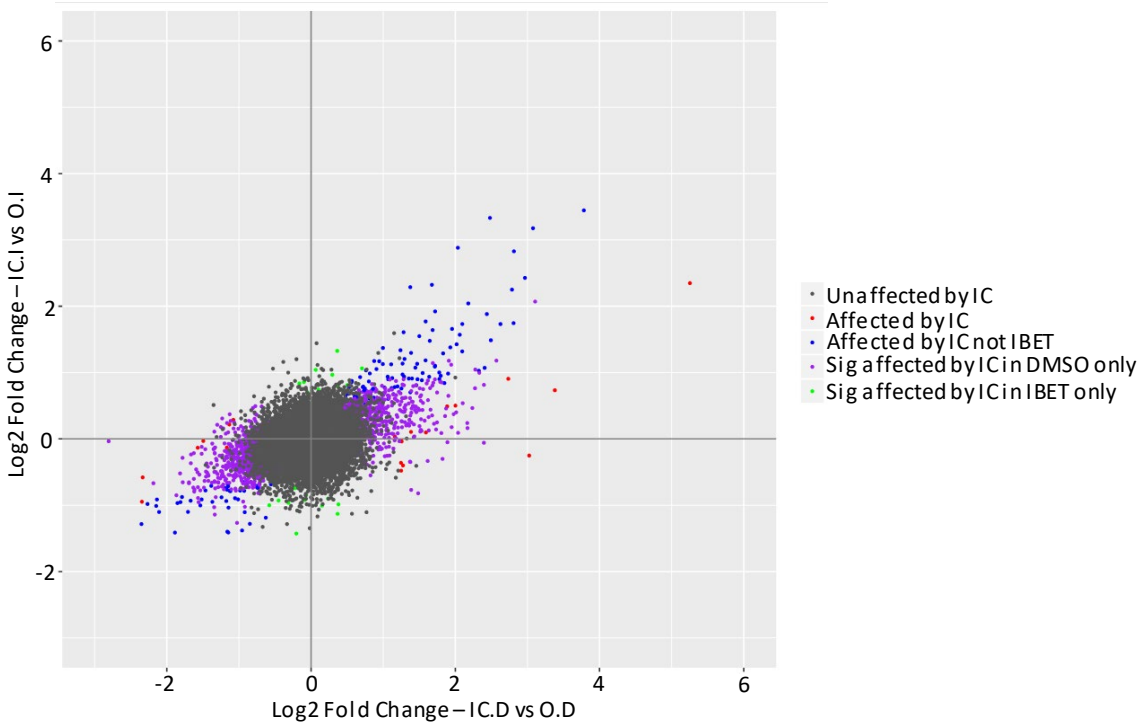


*Figure 58: Scatter plot demonstrating OVA-IC induced differential expression in the presence of DMSO (x axis) and I-BET (y axis). Genes are coloured based on the interaction, with genes differentially expressed on addition of OVA-IC and significantly impacted by I-BET coloured in red.*

The 75 top differentially regulated genes (ordered by adjusted p value) are shown in the heatmap in Figure 59. The bottom cluster of genes are upregulated with OVA-IC in the presence of DMSO; with quenching of the effect with the addition of I-BET. In order to identify pathways of genes impacted by the addition of I-BET, we performed gene set enrichment analysis (Figure 60). Numerous immune pathways induced by OVA-IC were downregulated by I-BET, including cytokine-chemokine signalling and cell adhesion pathways as well as antigen presentation pathways. Pathways that were upregulated by the addition of I-BET included pathways involving DNA and RNA remodelling.

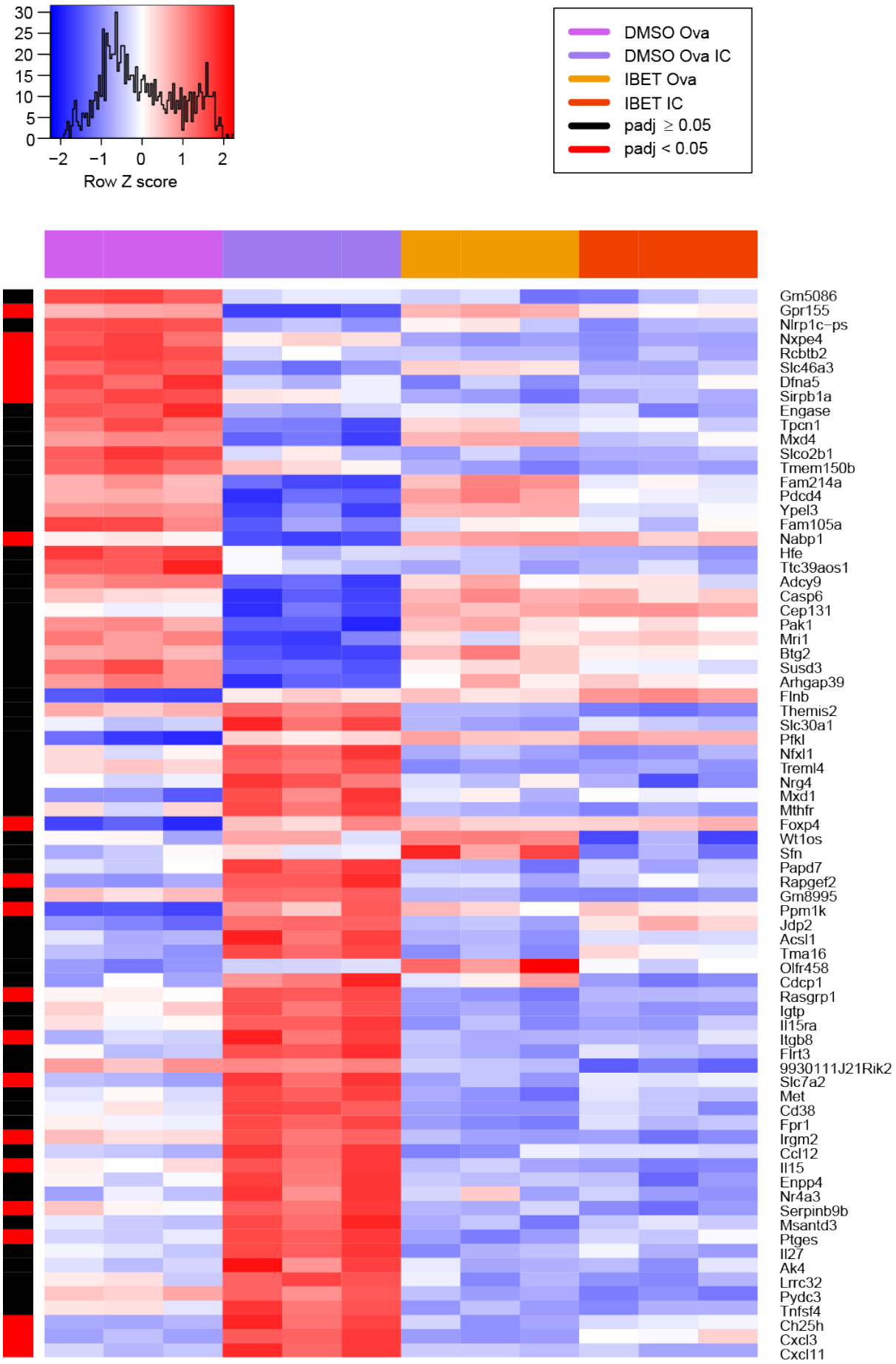
30
25
20
15
10
5
0
−2
−1
0
1
2
Row Z score
DMSO Ova
DMSO Ova IC
IBET Ova
IBET IC
padj ≥ 0.05
padj < 0.05
Gm5086
Gpr155
Nlrp1c−ps
Nxpe4
Rcbtb2
Slc46a3
Dfna5
Sirpb1a
Engase
Tpcn1
Mxd4
Slco2b1
Tmem150b
Fam214a
Pdcd4
Ypel3
Fam105a
Nabp1
Hfe
Ttc39aos1
Adcy9
Casp6
Cep131
Pak1
Mri1
Btg2
Susd3
Arhgap39
Flnb
Themis2
Slc30a1
Pfkl
Nfxl1
Treml4
Nrg4
Mxd1
Mthfr
Foxp4
Wt1os
Sfn
Papd7
Rapgef2
Gm8995
Ppm1k
Jdp2
Acsl1
Tma16
Olfr458
Cdcp1
Rasgrp1
Igtp
Il15ra
Itgb8
Flrt3
9930111J21Rik2
Slc7a2
Met
Cd38
Fpr1
Irgm2
Ccl12
Il15
Enpp4
Nr4a3
Serpinb9b
Msantd3
Ptges
Il27
Ak4
Lrrc32
Pydc3
Tnfsf4
Ch25h
Cxcl3
Cxcl11

*Figure 59 : Heatmap showing 75 top differentially regulated genes (ordered by adjusted p value). The p value demonstrated refers to the diff comparison, showing genes for which I-BET significantly impacts on the effect of OVA-IC*

*A*

.

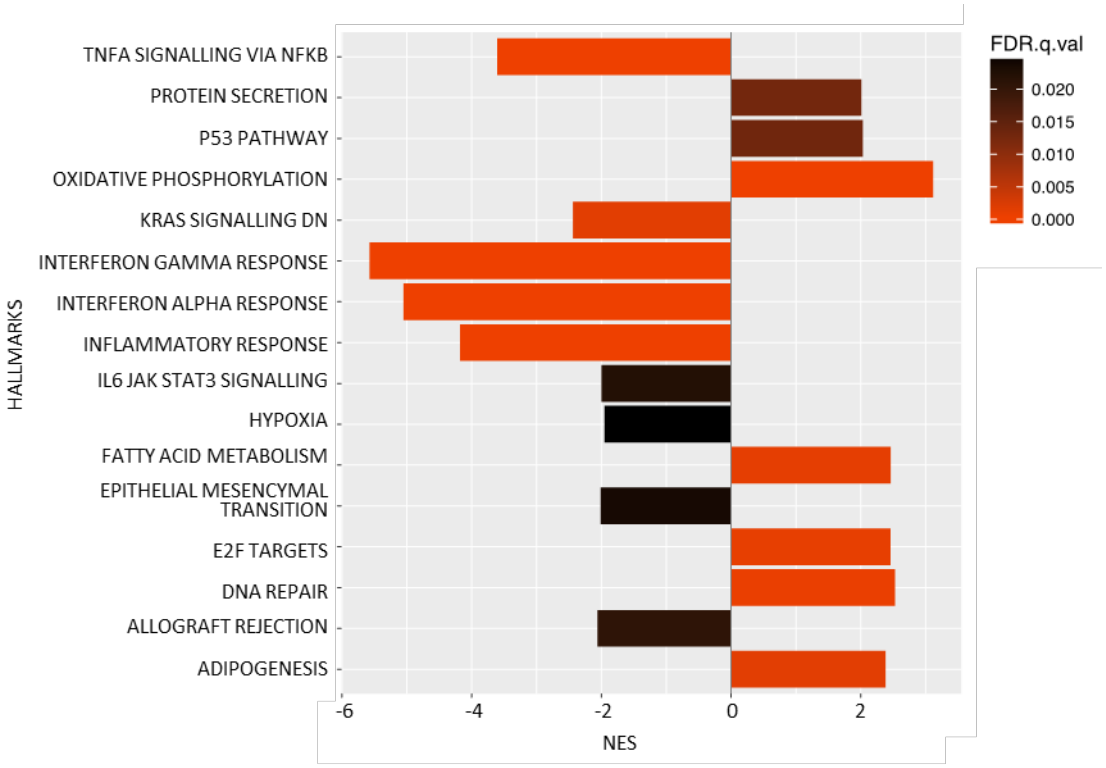


*B*

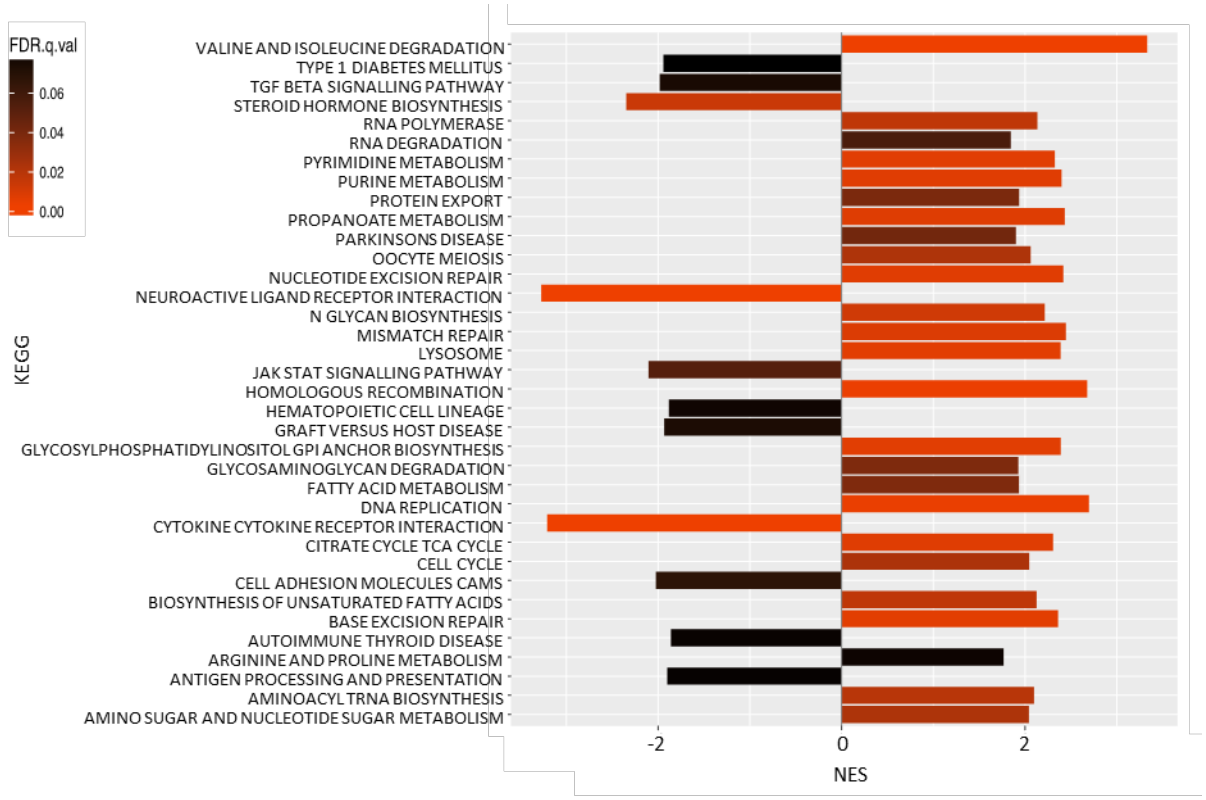


*Figure 60: Geneset enrichment analysis of genes for which I-BET significantly impacts on the effect of*

*OVA-IC. Hallmark genesets (A) and Kegg genesets (B) filtered to show pathways with FDR q value < 0.1. A negative NES indicates a pathway which is down regulated as a result of I-BET in IC stimulation.*

I-BET is known to impact LPS induced change in BMDM (Nicodeme 2010). We compared our dataset with the Nicodeme et al. dataset (deposited in Gene Expression Omnibus (GEO) database under the accession number GSE21764). Many of the LPS inducible genes that were significantly suppressed by I-BET (sI-BET) are also induced by IC and similarly suppressed by I-BET (Figure 61). This is illustrated by a heatmap showing a similar pattern of gene expression following IC treatment in the presence and absence of I-BET (Figure 61A) and the corresponding scatter plot (Figure 61B) where the majority of genes lie between the x axis and the line of equivalent gene expression, indicating that the log fold change following IC stimulation is positive in the absence of I-BET and suppressed by the addition of I-BET.

A

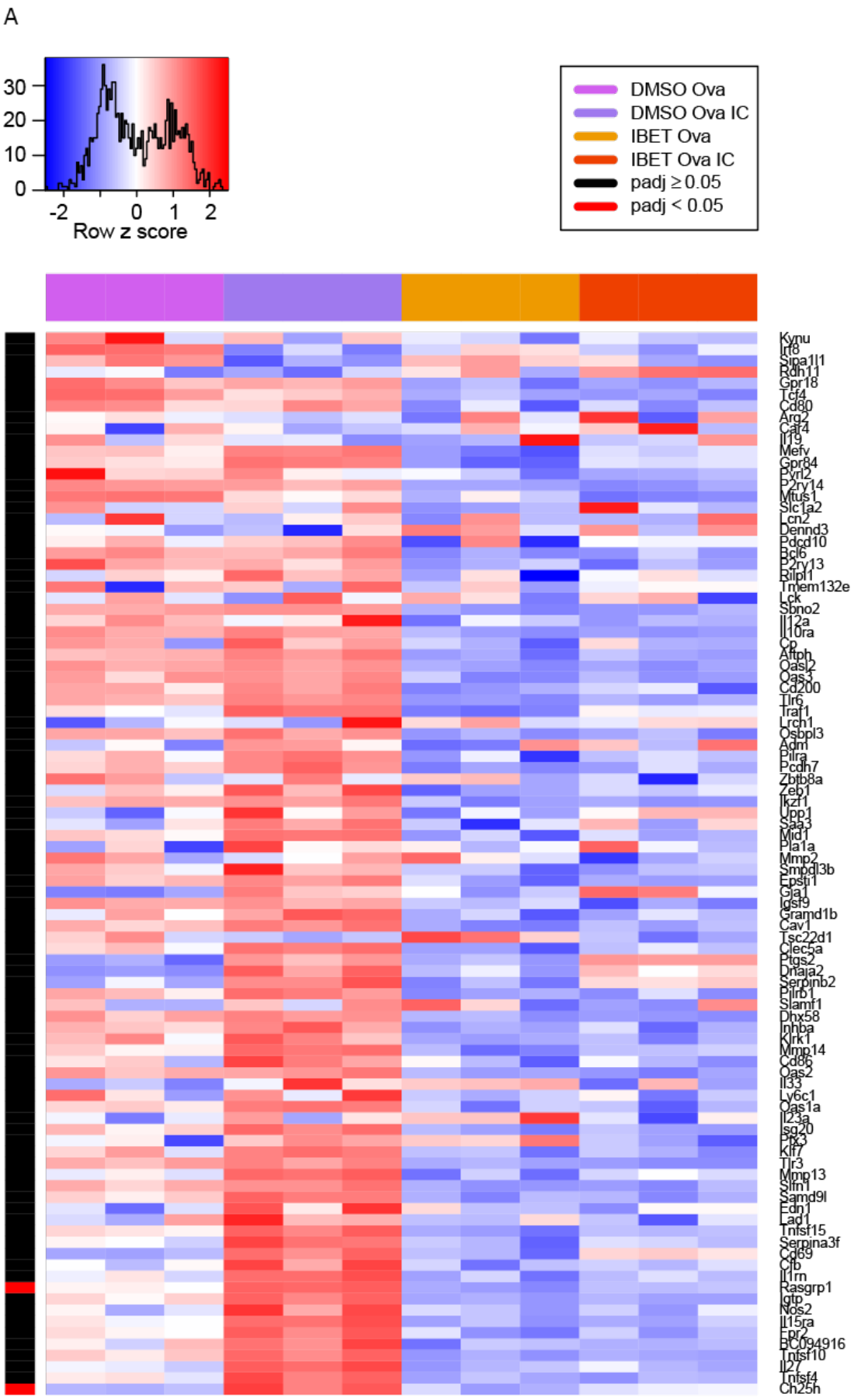
30
20
10
0
-2
0
1
2
Row z score
DMSO Ova
DMSO Ova IC
IBET Ova
IBET Ova IC
padj ≥ 0.05
padj < 0.05
Kynu
Irf8
Sipa1l1
Rdh11
Gpr18
Tcf4
Cd80
Arg2
Cat4
Il19
Mefv
Gpr84
P2ry12
P2ry14
Mtus1
Slc1a2
Lcn2
Dennd3
Pdcd10
Bcl6
P2ry13
Rilpl1
Tmem132e
Lck
Sbno2
Il12a
Il10ra
Cp
Aftph
Oasl2
Oas3
Cd200
Tlr6
Traf1
Lrch1
Osbpl3
Adm
Pilra
Pcdh7
Zbtb8a
Zeb1
Ikzf1
Vpp1
Saa3
Mid1
Pla1a
Mmp2
Smpdl3b
Epsti1
Gja1
Igsf9
Gramd1b
Cav1
Tsc22d1
Clec5a
Ptgs2
Dnaja2
Serpinb2
Pilrb1
Slamf1
Dhx58
Inhba
Klrk1
Mmp14
Cd86
Oas2
Il33
Ly6c1
Oas1a
Il23a
Isg20
Pik3
Klf7
Tlr3
Mmp13
Slfn1
Samd9l
Edn1
Lad1
Tnfsf15
Serpina3f
Cd69
Cfb
Il1rn
Rasgrp1
Igtp
Nos2
Il15ra
Epr2
BC094916
Tnfsf10
Il27
Tnfsf4
Ch25h

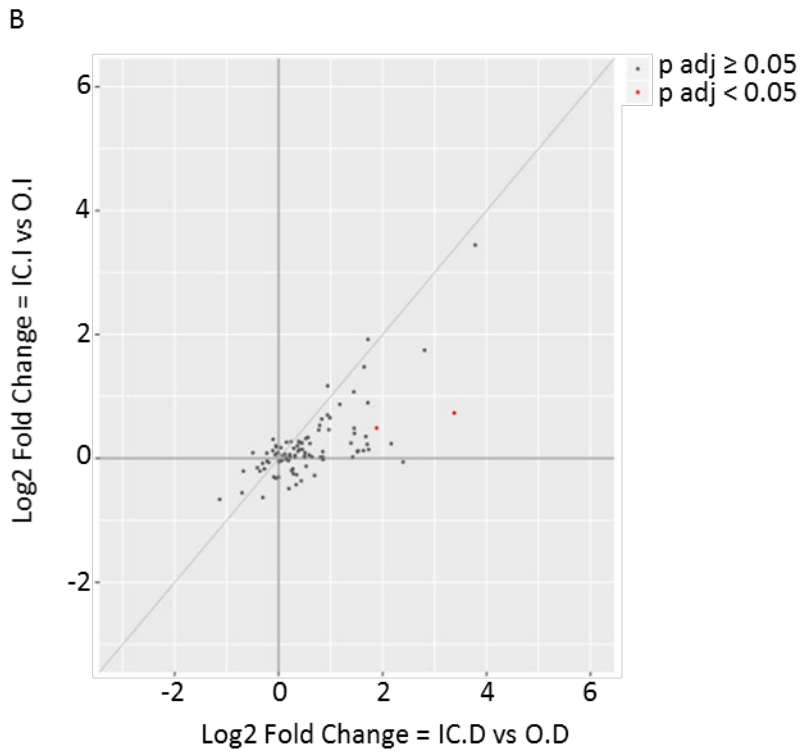


*Figure 61: I-BET has similar effect on IC-induced change as LPS-induced change. Heatmap (A) and scatter plot (B) showing the effect of FcγR crosslinking in the presence and absence of I-BET on those genes significantly impacted by I-BET following a 4 hour LPS stimulation* (Nicodeme 2010). The p value demonstrated refers to the diff comparison, showing genes for which I-BET significantly impacts on the effect of OVA-IC.

I-BET suppressed the IC induced transcriptional changes in numerous transcription factors (Figure 62), which may suggest an impact on superenhancer remodelling (Whyte 2013).

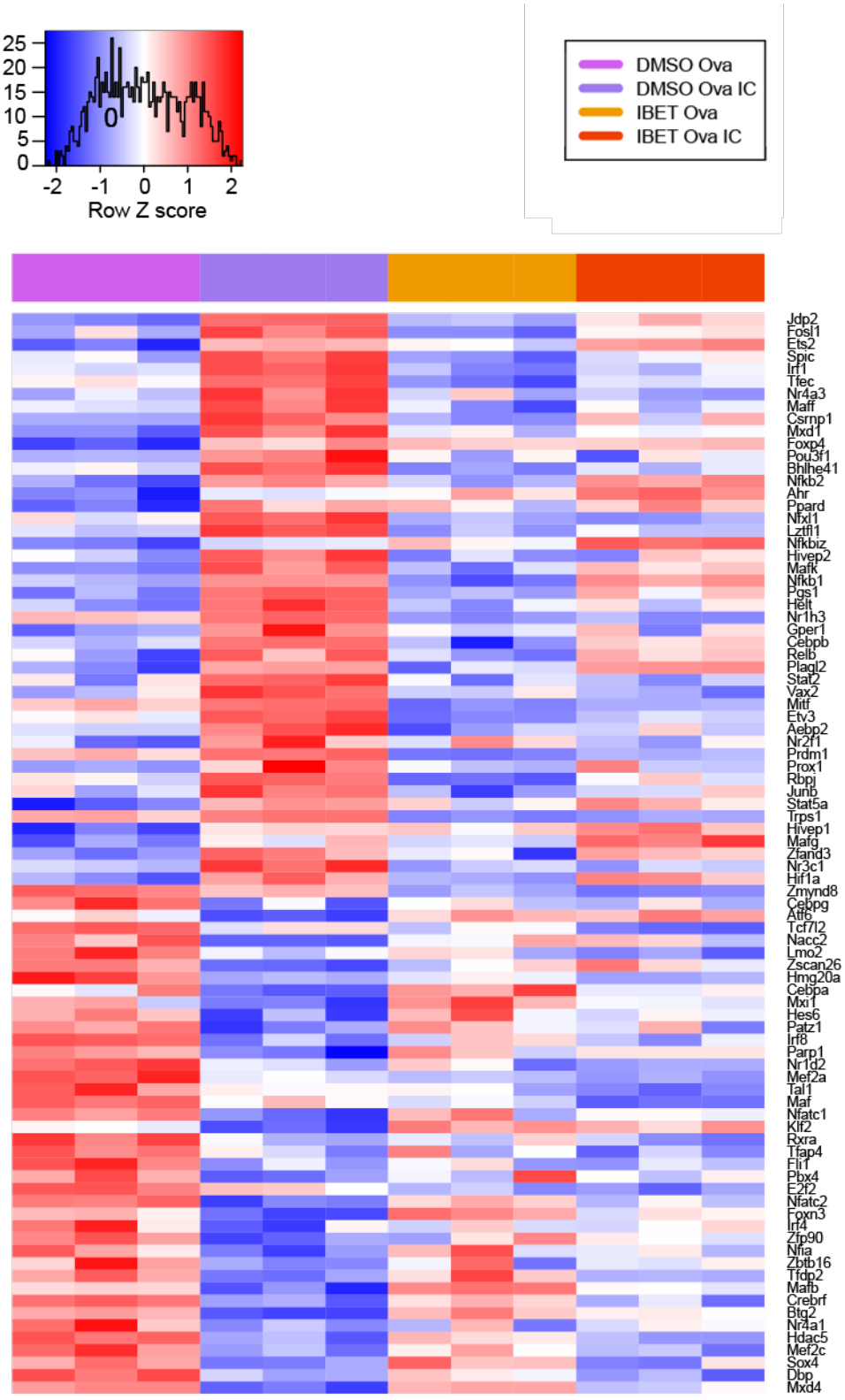


*Figure 62: Heatmap showing transcription factors differentially expressed following addition of OVA-IC.*

### 4.3.2 Bromodomain inhibitors reduce FcγR expression on macrophages and dendritic cells, lowering their capacity to respond to IC.

Our transcriptomic analysis showed that I-BET reduces the expression of FcγR genes (Figure 63A, B). Genes encoding activatory receptors and the inhibitory receptor FcγRIIb were affected. We performed reverse transcription polymerase chain reaction (rtPCR) analysis to confirm the changes in gene expression, and found a significant reduction in the expression of genes encoding FcγRIIb and the activatory receptors FcγRIII and FcγRIV (Figure 63C).

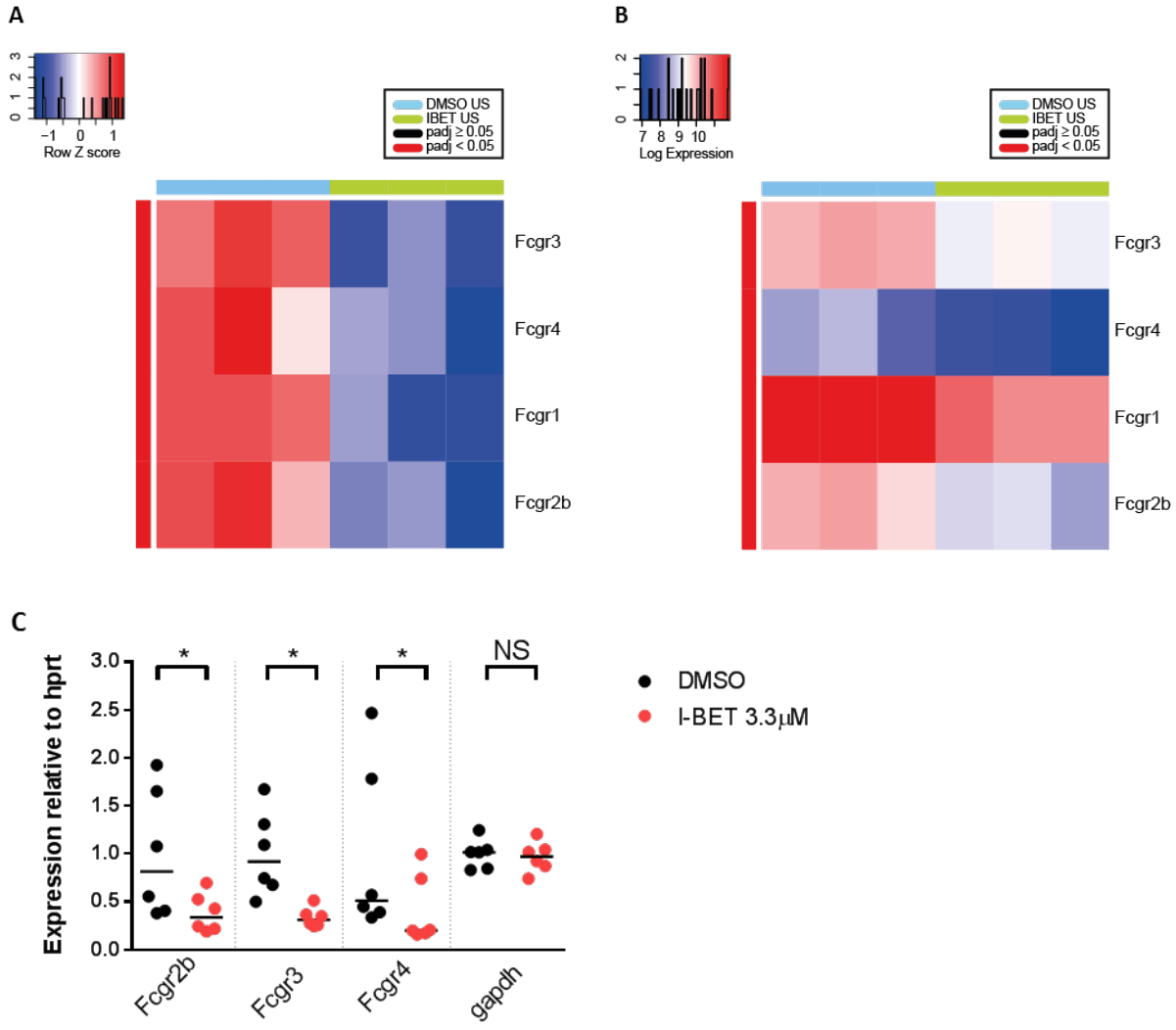


*Figure 63: I-BET reduces FcγR expression. Heatmaps showing row Z scores (A) and log expression (B) of FcγR genes in BMDM treated with DMSO or I-BET for four hours in the absence of additional stimuli. rtPCR confirmed reduced expression of FcγR genes following I-BET treatment (C). Groups compared using Wilcoxon matched-pairs signed rank test.*

We confirmed reduced FcγR expression following *in vitro I-BET treatment* at the protein level using flow cytometry. Initial experiments were performed using a 24G2 antibody that reacts specifically with a common non-polymorphic epitope on the extracellular domains of the murine FcγRIII (CD16) and FcγRII (CD32) receptors and is hence unable to distinguish between the activatory and inhibitory receptors. We observed reduced antibody binding with increasing concentrations of I-BET in murine bone marrow derived (Figure 64A) and peritoneal (Figure 64B) macrophages. At the time of later experiments, performed with bone marrow derived dendritic cells, a FcγRIIb (CD32b) specific antibody was available. I-BET treatment led to a reduction of CD32b in a concentration dependent manner (Figure 64Ci); with no effect on total CD16 and CD32 expression in these experiments. Human monocyte-derived macrophages also demonstrated a reduction in FcγR expression with I-BET treatment, particularly FcγRIII (Figure 64D)

A) Bone marrow derived macrophages

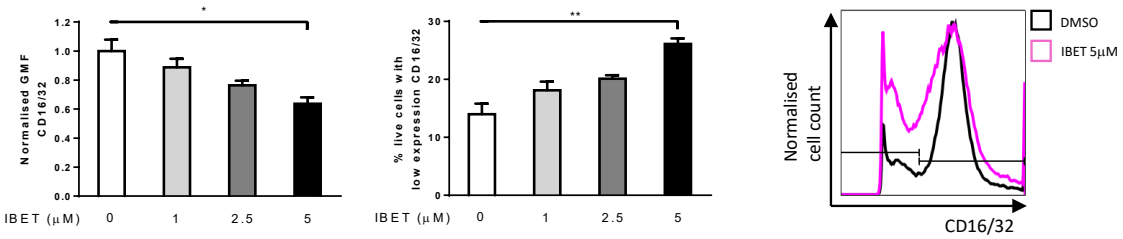


B) Peritoneal macrophages

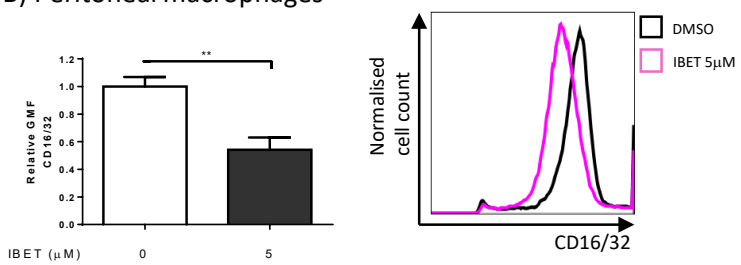


C) Bone marrow derived dendritic cells

i)

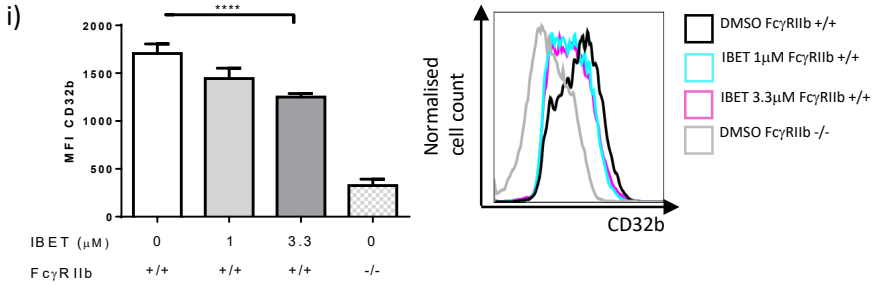

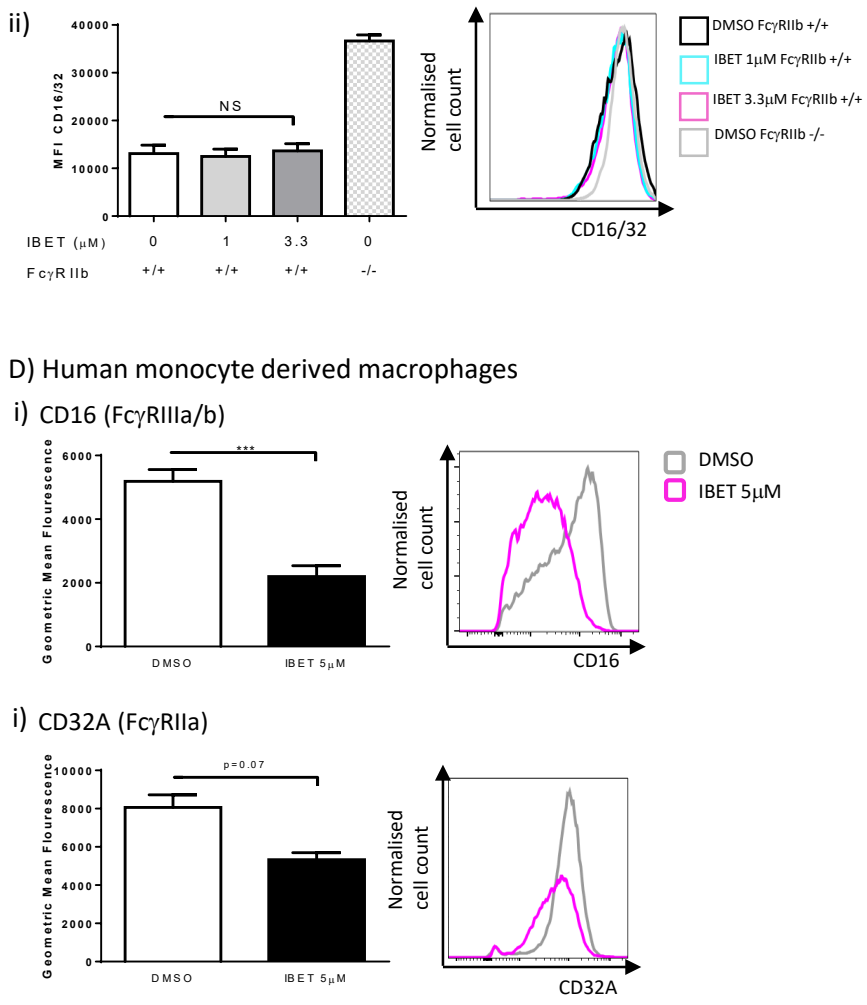


*Figure 64: I-BET151 reduces surface expression of murine and human Fcγ receptors. Surface CD16 and CD32 expression measured on murine BMDM (A) and peritoneal macrophages (B) treated with I-BET151 or DMSO for 14-24 hours. Geometric mean fluorescence of 24G2 antibody which binds to a common epitope on CD16 and CD32 (*CD16/32*) normalised to average reading in DMSO replicates for individual replicates. A. Results of two independent experiments shown. Differences between means significantly different by one-way ANOVA. B. Results of three independent experiments shown. Mean +/- standard error of the mean displayed; means compared using paired t test. C. Surface CD32b (i) and combined CD16 and CD32 (CD16/32) (ii) expression measured on murine bone marrow derived dendritic cells differentiated from FcγRIIb-/- and wildtype mice, treated with I-BET151 or DMSO for 12-16 hours; results from 3 independent experiments; mean +/- standard error of the mean displayed; differences between means compared by one-way ANOVA test. D. Human monocyte derived macrophages were differentiated in culture. Surface staining was performed on two donors following 24 hours treatment with DMSO or I-BET151. Plots show representative histograms and mean +/- standard error of the mean of geometric mean fluorescence for CD16 (a) and CD32A (b). Means compared using student t test.*

Our *in vitro* studies and transcriptomic analyses suggest that I-BET inhibits both activatory and inhibitory FcγR. The relative effect on different receptors may influence the activatory to inhibitory (A/I) ratio which determines the activatory threshold of cells. We also looked at the expression of FcγR on splenocytes in mice treated systemically with I-BET for a period of 3 days (mice used in FITC paint experiments in chapter 5). There was no change in the expression of FcγRIIb, the only FcγR expressed on B cells. However, in mononuclear phagocytes, we detected a significant reduction in combined CD16 and CD32 staining with only a marginal effect on CD32b, suggesting a greater effect on activatory FcγR expression, shifting the A/I ratio towards a less inflammatory state (Figure 65).

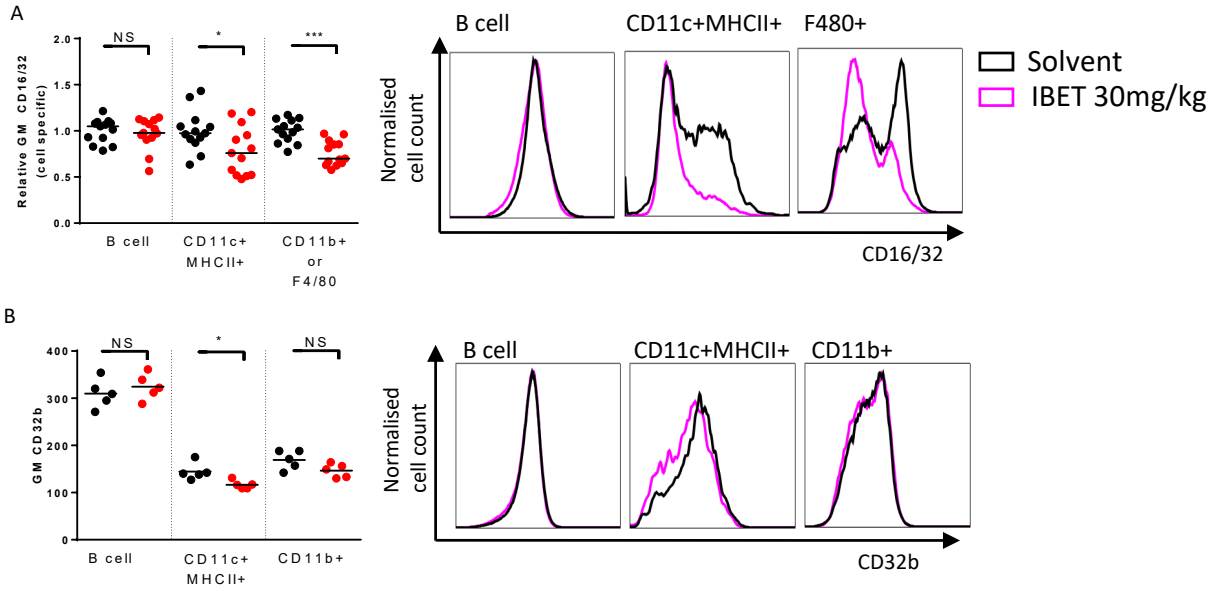


*Figure 65: In vivo treatment with I-BET for 3 days results in decreased FcγR expression on splenic B cells, DCs and macrophages. Plots show geometric mean fluorescence intensity for 24G2 antibody which binds to a common epitope on CD16 and CD32 (CD16/32) (A) and CD32A (B) with representative histograms. Data from four independent experiments; points represent individual mice; median values compared using mann whitney tests. NS p>0.05; *p<0.05; ***p<0.001.*

### 4.3.3 I-BET151 leads to accumulation of phagocytic material within MNP

We hypothesised that I-BET151 treatment would inhibit Fc-mediated phagocytosis. However, we observed increased phagocytic material within cells treated with I-BET151 at a 16-24 hour time point, as evidenced by a significantly increased geometric mean fluorescence for OVA 647 and an increase in phagocytic index (Figure 66). This effect on phagocytosis was concentration dependent (Figure 66B). A similar result was seen with OVA alone suggesting that the effect of I-BET151 on antigen internalisation may not be specific to FcγR mediated phagocytosis but may be due to more generalised effects on endocytosis.

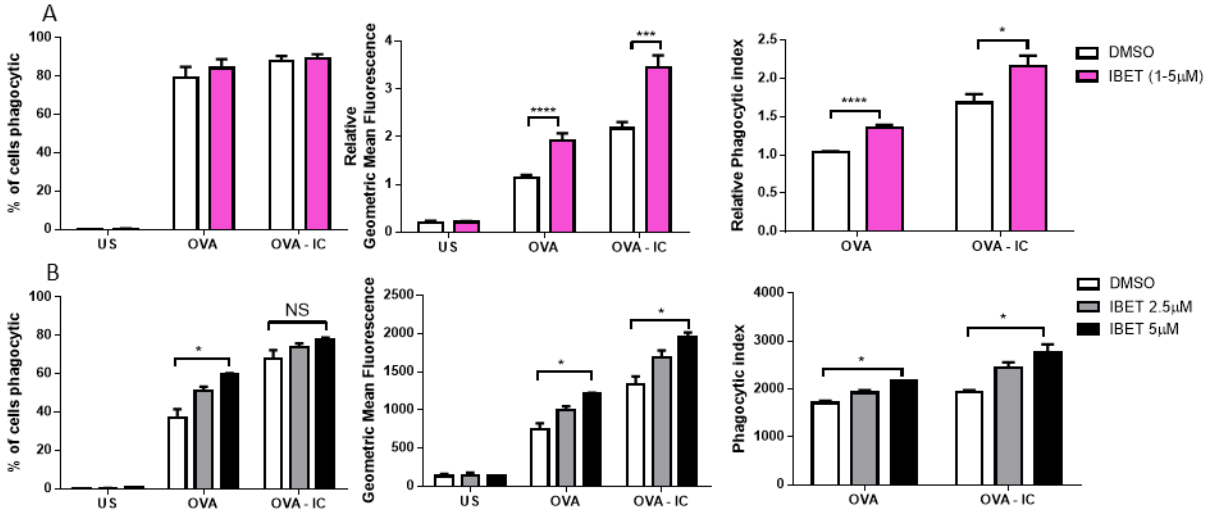


*Figure 66: I-BET151 increases phagocytic material within cells at a late time point in a concentration dependent manner. Murine BMDM were stimulated with OVA or OVA-IC in the presence of absence of I-BET151. Panel A shows the results of five independent experiments. Geometric mean fluorescence of OVA 647 has been normalised to average reading in DMSO treated OVA replicates to allow comparison between individual experiments. Differences between means significant by student t tests. Panel B shows a single experiment where cells were stimulated for 24 hours. Differences between means significant by one way ANOVA test. NS p>0.05; *p<0.05; ***p<0.001; ****p<0.0001.*

The increase in phagocytic material within cells treated with I-BET151 compared to DMSO only became apparent at later time points, with the phagocytic index separating two hours after OVA-IC uptake. This suggests that I-BET151 effects the processing and degradation of material rather than its uptake (Figure 67A). A similar pattern was seen when cells were fed immune complexes of DQ-OVA, a conjugate that only fluoresces following proteolytic degradation. I-BET151 caused an increase in the degradation products within phagocytic cells in a dose dependent manner, suggesting an impact in processing after the point at which DQ-OVA degradation products produce fluorescence (Figure 67B, 68). The action of I-BET was opposite to the effect of increasing the activation of cells by knocking out the inhibitory FcγRIIb receptor (Figure 68). Mice lacking FcγRIIb had lower levels of DQ degradation products within cells at a late timepoint compared to wildtype mice, likely due to more rapid clearance. I-BET treatment increased accumulation of DQ degradation products in FcγRIIb-/- mice to similar levels seen in wildtype DMSO treated mice.

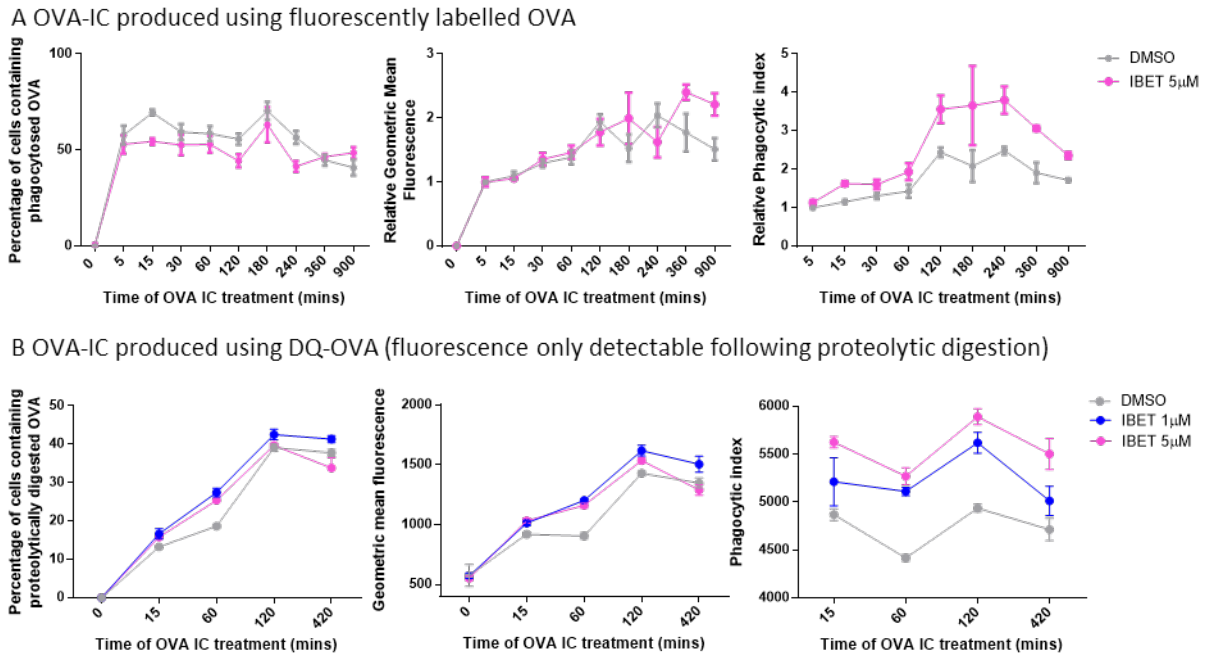


*Figure 67: I-BET151 leads to defect in the clearance of proteolytically cleaved phagocytic material within cells. Murine BMDM were stimulated with IC in the presence or absence of I-BET151. IC present within cells was measured at various time points (results from 4 independent experiments shown). B) Immune complexes were made from DQ-OVA, a protein that only upon proteolytic digestion releases fragments that exhibit fluorescence. I-BET151 causes an accumulation of degraded immune complex (results from single representative experiment shown).*

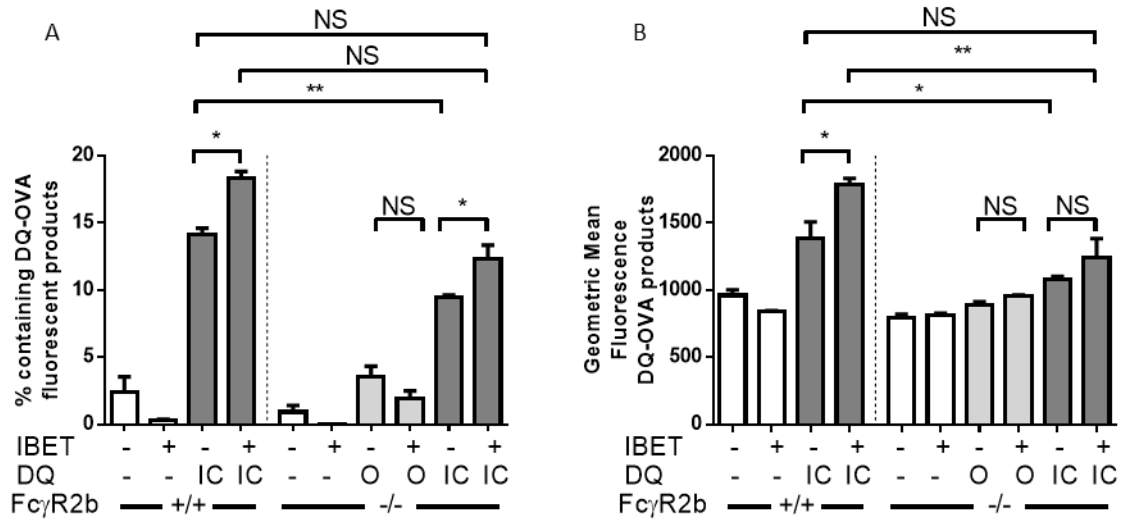


*Figure 68. Murine bone marrow derived dendritic cells derived from* FcγRIIb-/- and wildtype mice *were stimulated for 12 hours with IC made from DQ-OVA (DQ-IC) or DQ-OVA control (DQ-O) in the presence or absence of I-BET 3.3μM.*

*Results from single experiment; Mean +/- standard error of the mean displayed; means compared using unpaired t test (NS p>0.05; *p<0.05; **p<0.01).*

The effect of I-BET on phagocytosis is not limited to immune complexes. I-BET caused an increase in the presence of apoptotic cell debris within macrophages at a four hour time point (Figure 69).

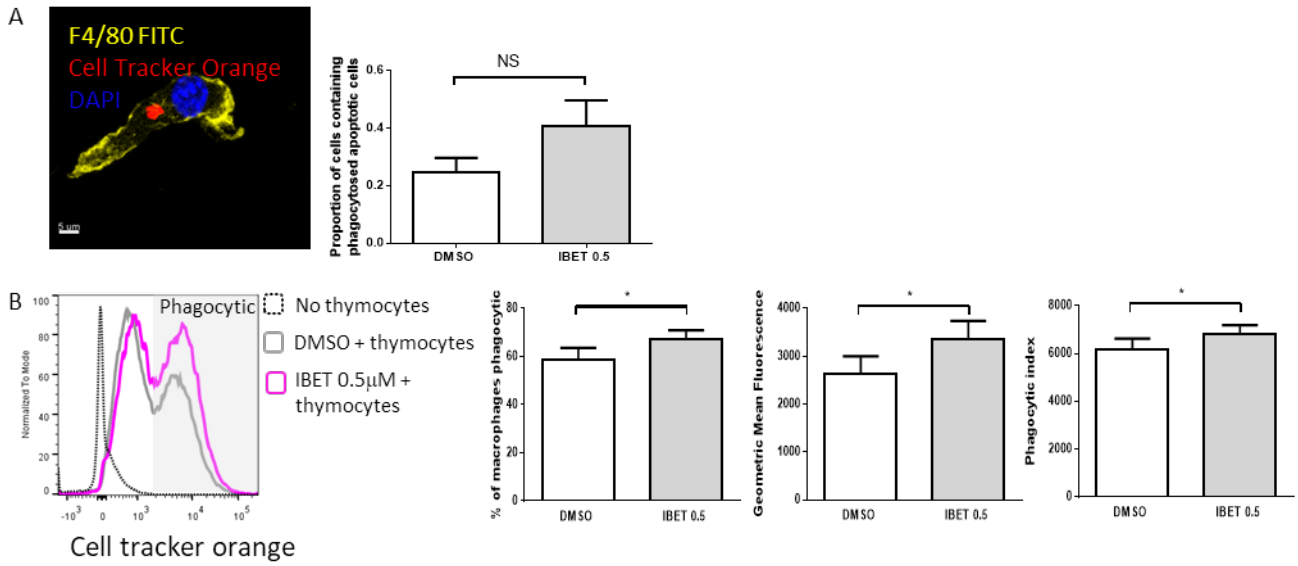


*Figure 69: I-BET151 has similar effect on macrophage phagocytosis of apoptotic cells. Murine thymocytes labelled with cell tracker orange and rendered apoptotic by dexamethasone treatment were fed to murine BMDM that had been pre-treated for 17 hours with DMSO or I-BET151 0.5μM and phagocytosis was measured by confocal microscopy (A) and flow cytometry (B) 4 hours later. Phagocytic macrophages shown as percentage of F4/80 positive live cells. Means compared with unpaired student t tests (NS p>0.05; *p<0.05).*

### 4.3.4 I-BET151 delays phagosome maturation

In order to further explore the effects of I-BET151 on phagocytosed antigen, we investigated the kinetics of phagosome maturation by staining cells for early and late endosome and lysosome markers (Figure 70). At early time points there was no difference in the co-localisation of the early endosome marker RAB5 with IC between control and I-BET151 treated cells. At later time points there was loss of RAB5 staining in DMSO treated cells and loss of co-localisation with vesicles containing IC, however in I-BET151 treated cells there was retained RAB5 co-localisation with IC containing vesicles. Similar results were seen at a late time point with EEA1, another marker of early endosomes. Both DMSO and I-BET151 treated macrophages show co-localisation of IC with RAB7, a marker of late endosomes at an early time point. At later time points, DMSO treated cells had

reduced RAB7 staining with limited co-localisation with IC whereas I-BET151 treated cells retain RAB7 with ongoing co-localisation with IC, suggesting a delay in phagolysosome maturation. I-BET151 treated cells do acquire LAMP1, a marker of mature lysosomes, at later timepoints so there is not a complete blockage of phagosome maturation.

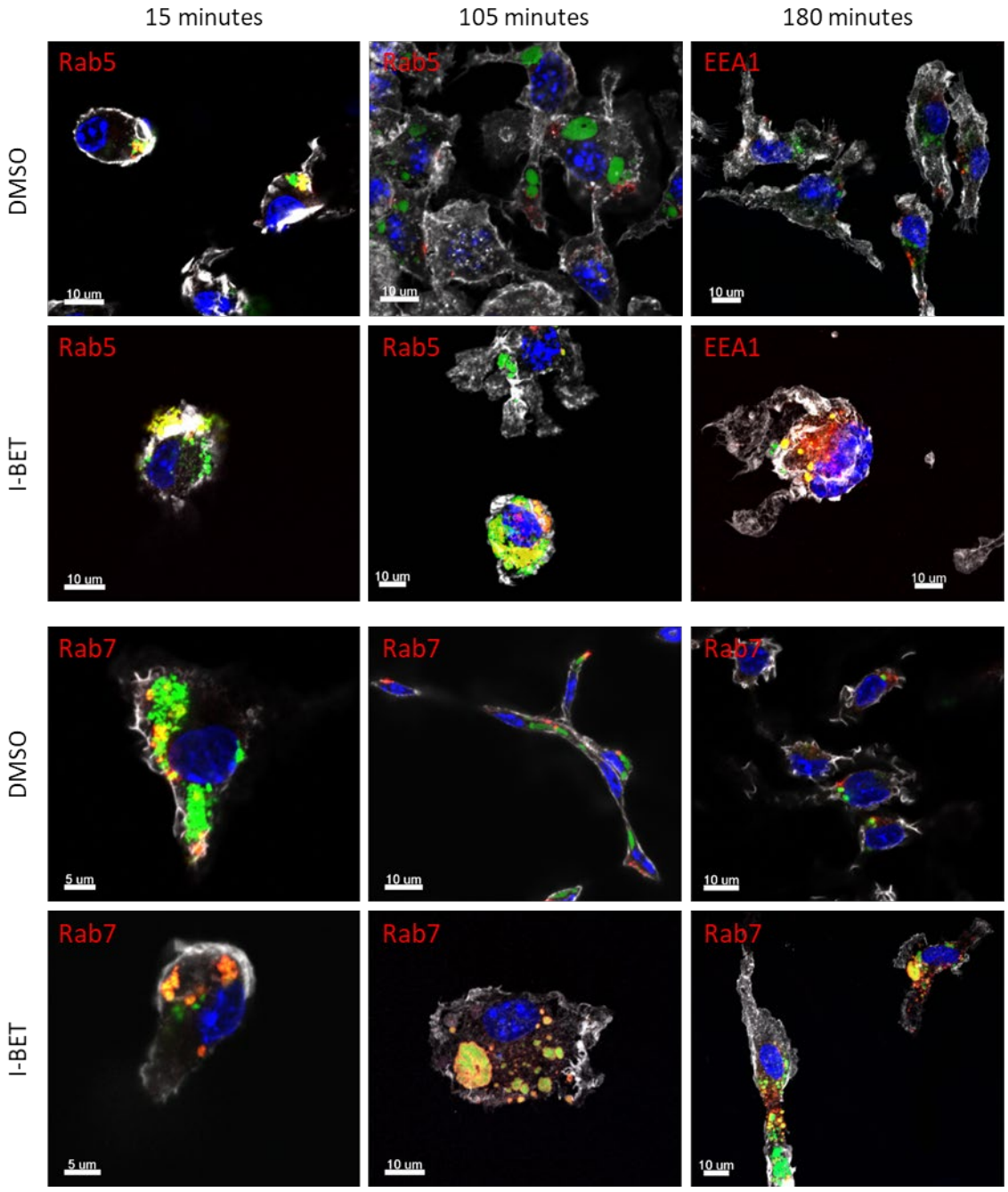

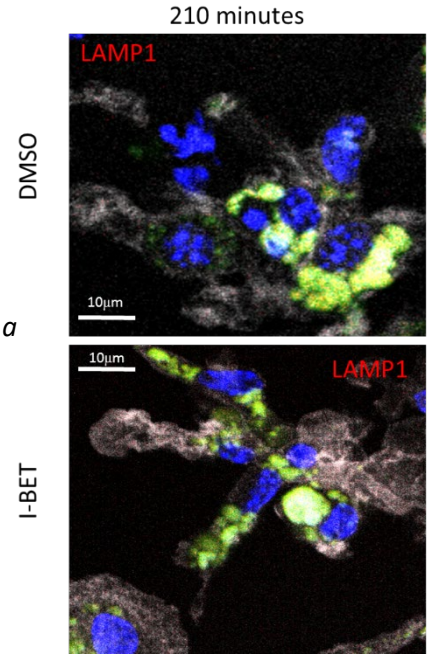


*Figure 70: I-BET151 delays phagosome maturation. Murine BMDM were adhered to cover slips and treated with DMSO or I-BET151 2.5μM for 15hours prior to IC addition. Cells were fixed at defined time periods following addition of IC and stained for Rab5, EEA1, Rab7. Staining for LAMP1 was done in different experiment where I-BET 3.3μM was used. Rab5, Rab7, EEA1, LAMP1 (red) as labelled. Phalloidin (white) was used to stain the actin cytoskeleton; DAPI (blue); IC (green).*

### 4.3.5 I-BET selectively inhibits cytokine production in response to IC stimulation

GSEA demonstrated that I-BET significantly down-regulated IC-induced enrichment of genes involved in cytokine-cytokine receptor interactions (Figure 60). Numerous chemokine and cytokine genes were induced by FcγR crosslinking and inhibited by I-BET (Figure 71A). To further assess the impact of I-BET on IC-induced cytokine and chemokine production, we used a multiplex cytokine analysis kit to test supernatants obtained from macrophage cultures. MCP3, also known as CCL7 is a chemokine that attracts monocytes to sites of inflammation. It binds to the chemokine receptors CCR1, 2, and 3. I-BET151 inhibits the OVA-IC induced increase in MCP3 transcript in BMDM in a concentration dependent manner (Figure 71Bi). As with LPS stimulation (Nicodeme 2010), there was no effect on TNFα production (Figure 71Bii). Cytokine analysis on the supernatants from one experiment showed a trend towards a reduction in IC-induced IL10 and KC/Gro production with I-BET treatment (Figure 71Biii-iv). IL6 was not detectable in the supernatants from BMDM treated with IC (data not shown); however *Il6* RNA was measurable by qPCR. We observed a rise in *Il6* transcripts one hour following FcγR crosslinking in the absence of I-BET; with inhibition of the response to baseline levels with the addition of I-BET (Figure 71Bv). A similar trend was seen in RNA extracted 4 hours following stimulation. Treatment of BMDC with I-BET151 throughout a period of immune complex stimulation, but not one hour prior to stimulation, reduced IL6 and MCP3 production (Figure 71C)

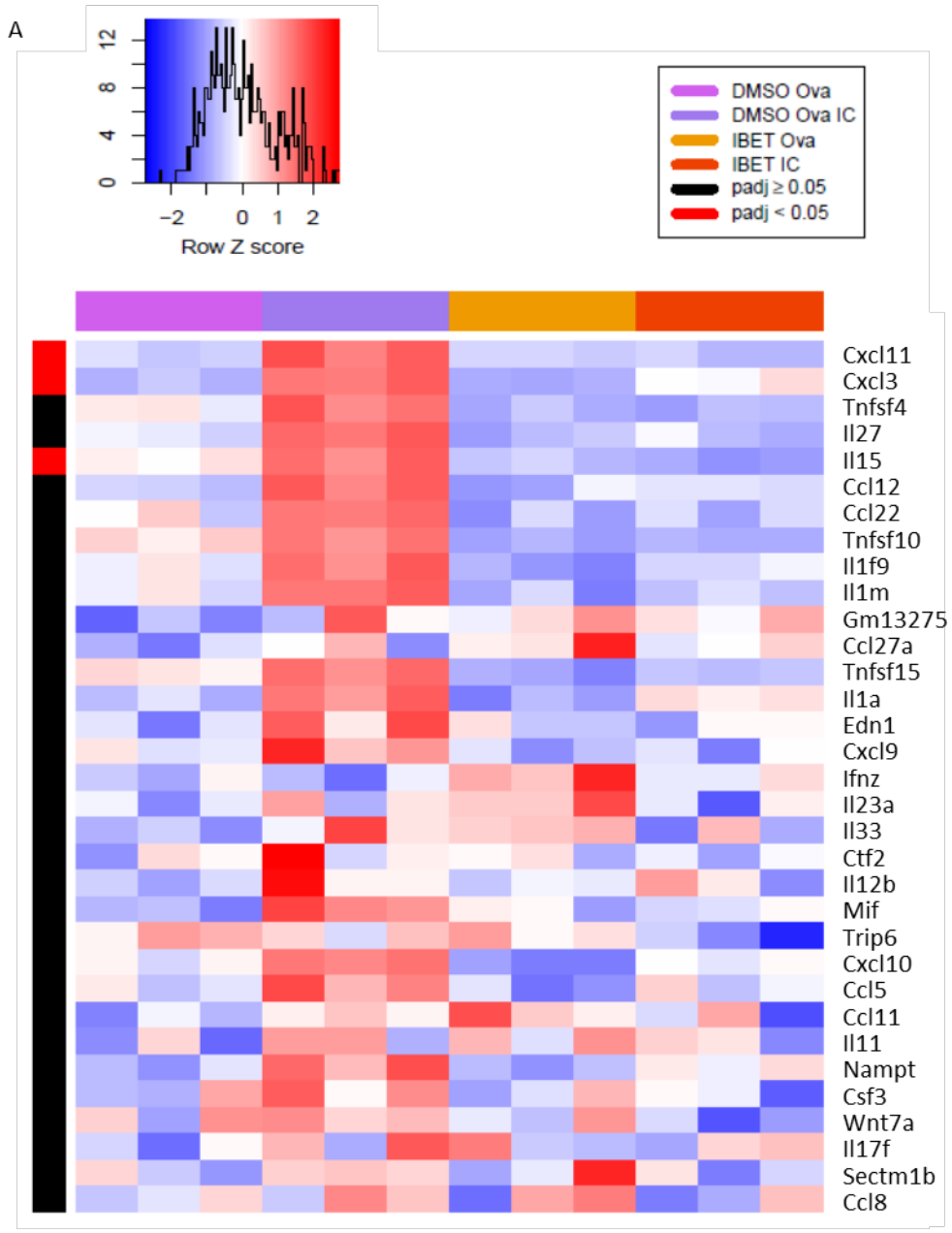
A
0
4
8
12
−2
0
1
2
Row Z score
DMSO Ova
DMSO Ova IC
IBET Ova
IBET IC
padj ≥ 0.05
padj < 0.05
Cxcl11
Cxcl3
Tnfsf4
Il27
Il15
Ccl12
Ccl22
Tnfsf10
Il1f9
Il1m
Gm13275
Ccl27a
Tnfsf15
Il1a
Edn1
Cxcl9
Ifnz
Il23a
Il33
Ctf2
Il12b
Mif
Trip6
Cxcl10
Ccl5
Ccl11
Il11
Nampt
Csf3
Wnt7a
Il17f
Sectm1b
Ccl8

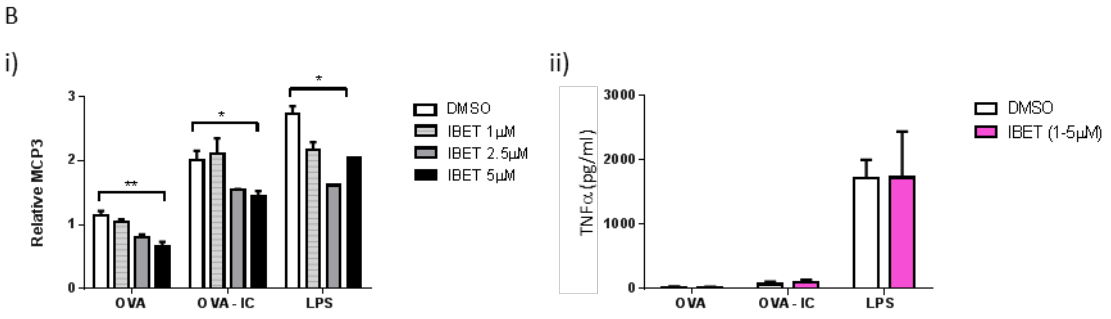
B
i)
Relative MCP3
0
1
2
3
**
*
*
OVA
OVA - IC
LPS
DMSO
IBET 1μM
IBET 2.5μM
IBET 5μM
ii)
TNFα (pg/ml)
0
1000
2000
3000
OVA
OVA - IC
LPS
DMSO
IBET (1-5μM)

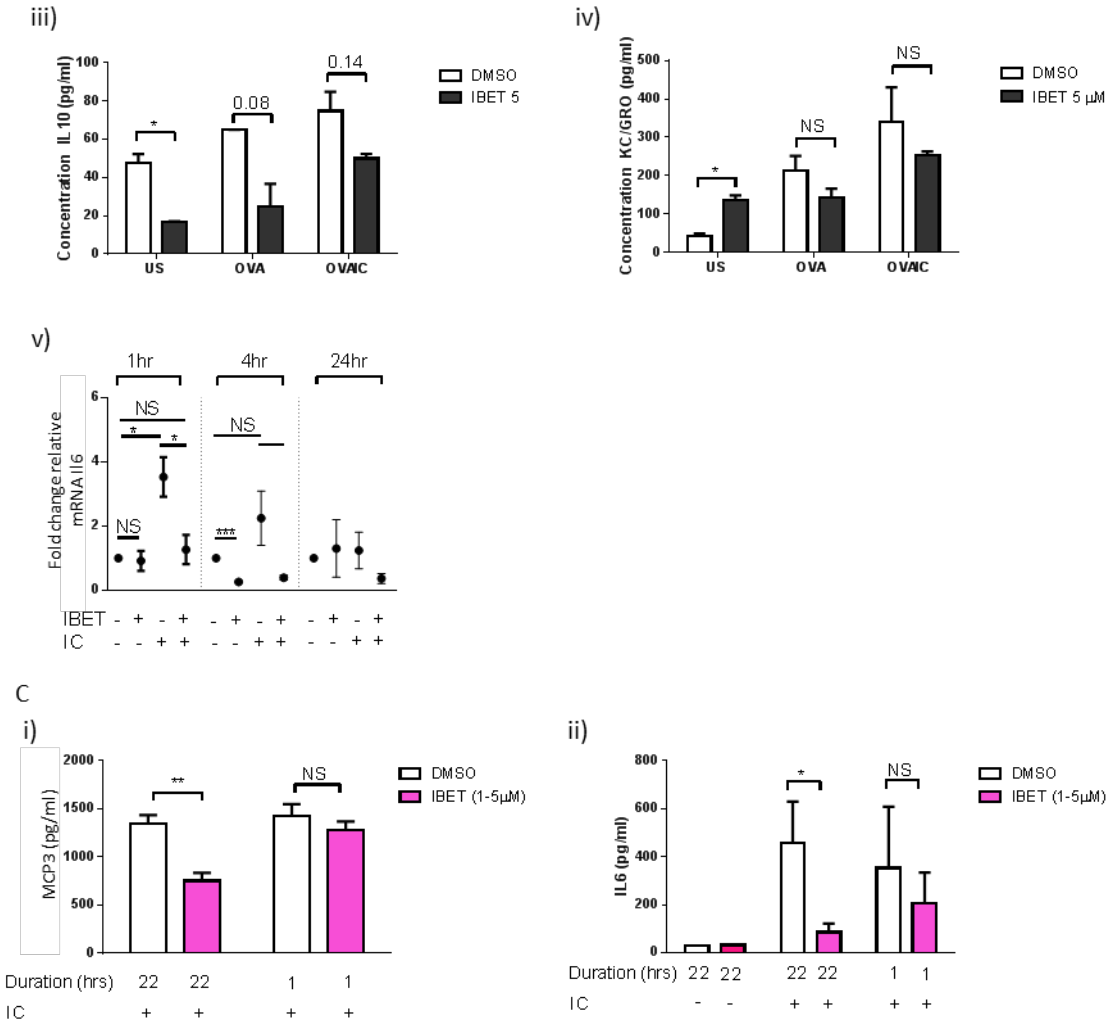


*Figure 71: I-BET151 selectively inhibits cytokine release in response to immune complex stimulation. A Heat map showing cytokine genes most impacted by I-BET. Murine BMDM were stimulated in the labelled conditions and RNA extracted for transcriptomic analysis following 4 hours stimulation. Genes ranked* by *log fold change of the difference of the difference ((IC.D vs O.D) minus (IC.I vs O.I)) representing the effect of I-BET on the effect of IC stimulation; the p value demonstrated refers to the diff comparison, showing genes for which I-BET significantly impacts on the effect of OVA-IC. Bi-iv), immune complexed OVA (OVAIC) or LPS in the presence of I-BET151 or DMSO for 24 hours. Supernatants were collected and stated cytokines assayed via ELISA (i-ii; results from three independent experiments) or MesoScale Discovery Multiplex Assay (iii-iv; single experiment). iv) RNA was extracted from BMDM stimulated for the documented times and Il6 transcript levels quantified by qPCR. C: Murine bone marrow derived dendritic cells were treated with I-BET151 or DMSO for one hour prior to or throughout IC stimulation. Supernatants were collected and stated cytokines assayed via ELISA (results from four independent experiments). P values calculated by one way ANOVA (Ai) or student t test (other). NS p>0.05; *p<0.05; **p<0.01.*

### 4.3.6 Failure to induce accelerated nephrotoxic nephritis without the use of IP CFA

In order to determine the effect of I-BET151 on an *in vivo* model of IC-mediated inflammation, we sought to establish the nephrotoxic nephritis model. In this model of IC-mediated glomerulonephritis, sheep are immunised with ground up mouse glomeruli and their serum harvested following the development of sheep anti-mouse glomeruli antibodies. Mice are pre-sensitised with an IP injection of sheep IgG mixed with CFA and produce anti-sheep IgG antibodies. When mice are subsequently given IV nephrotoxic serum, sheep anti-mouse glomerular antibodies deposit in glomeruli forming IC with preformed anti-sheep IgG results in a glomerulonephritis (Figure 72).

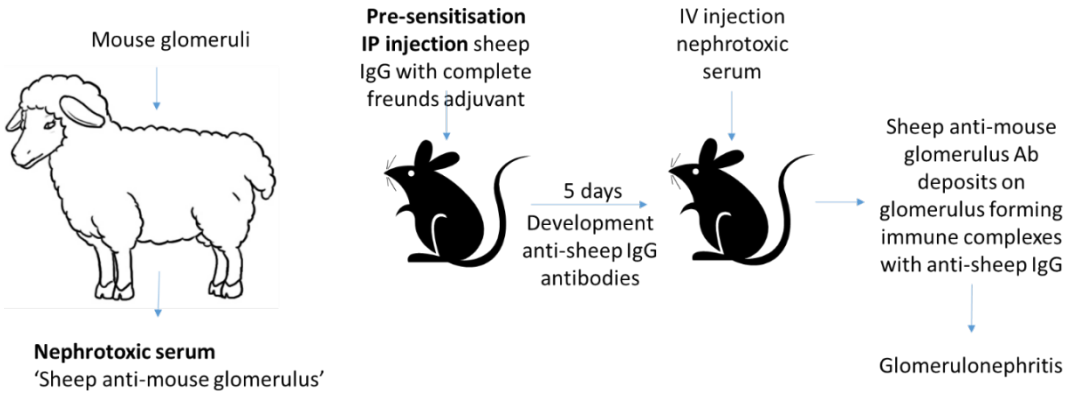


*Figure 72: Established model of accelerated nephrotoxic nephritis*

There are increasing regulations surrounding the use of CFA and under the terms of our home office animal licence we are unable to give CFA via the IP route. I therefore attempted to adapt the established model by substituting IP CFA for subcutaneous (SC) CFA. Despite the use of increasing doses of nephrotoxic serum, mice developed only minimal proteinuria (Figure 73a, c), had normal blood urea nitrogen values (Figure 73b) and no histological features of established glomerulonephritis. Mice deficient in FcγRIIb are known to be more susceptible to accelerated nephrotoxic nephritis. We therefore attempted to induce disease in mice with one null allele for FcγRIIb that show intermediate expression of the inhibitory receptor. Although a number of these mice developed greater amounts of proteinuria compared to wild type mice (Figure 73d), there was still no glomerulonephritis evident on histological examination. An experienced histopathologist found one lesion consistent with non-specific focal segmental glomerulosclerosis in one mouse but was unable to detect any glomerular thrombosis or crescents that are diagnostic of established disease.

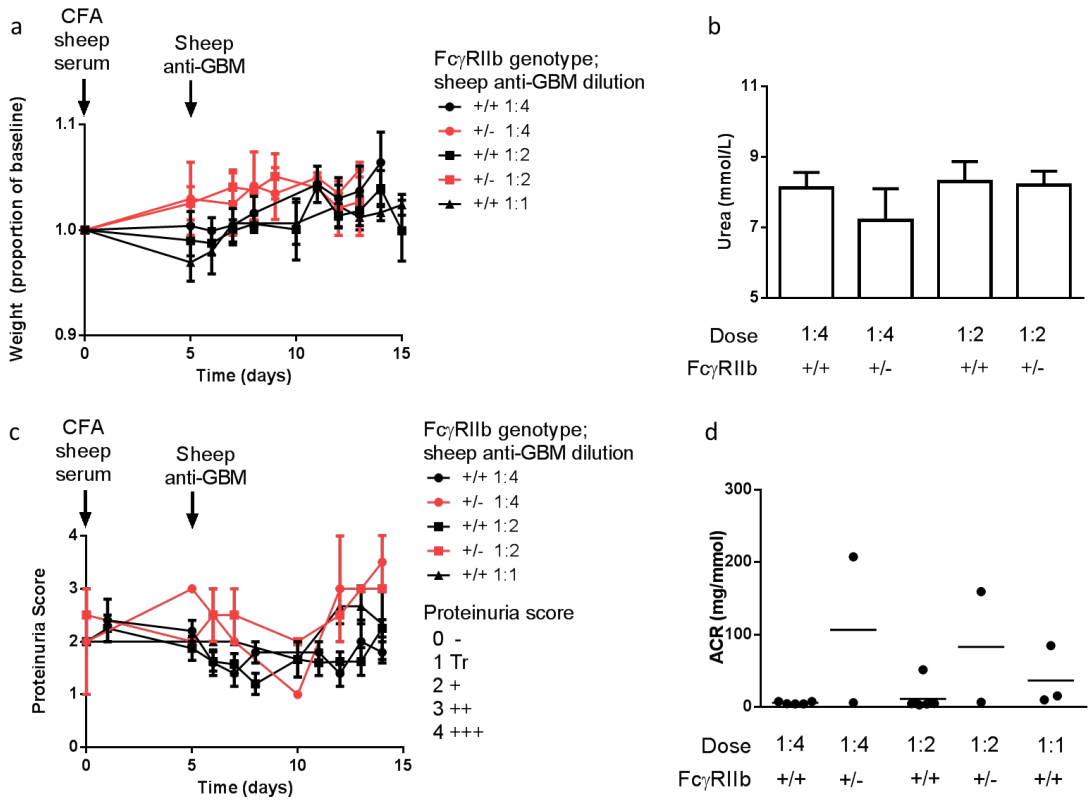


*Figure 73: Attempts to induce accelerated nephrotoxic nephritis. Female C57BL/6 mice were given an IV tail injection of sheep anti-mouse glomerular basement membrane five days following SC injection of sheep IgG in CFA. They were monitored for weight loss (a) and proteinuria (c) and sacrificed 14-15 days following initial CFA injection with collection of blood for urea measurement (b) and urine for proteinuria quantification by albumin creatinine ratio (ACR) (d).*

Concerned that the mice were not developing sufficient anti-sheep IgG due to the absence of CFA, we decided to boost the immune response prior to giving nephrotoxic serum by the use of an IP injection of Incomplete Freund's Adjuvant (IFA) seven days following initial SC sheep IgG/CFA. Unfortunately these mice developed anaphylaxis minutes following injection of nephrotoxic serum so the experiment was terminated (Figure 74). We therefore sought alternative models to assess the effects of I-BET on FcγR-mediated macrophage activation *in vivo*.

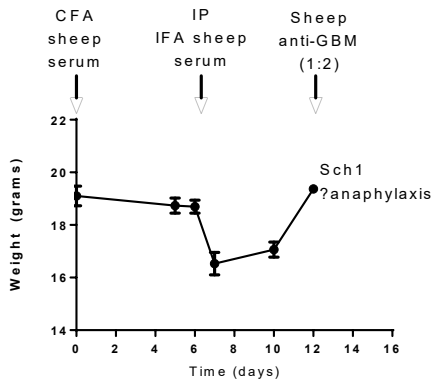


*Figure 74: Boosting sensitisation to Sheep IgG resulted in anaphylaxis on subsequent injection of anti-mouse glomerular sheep serum extract.*

### 4.3.7 I-BET reduces spleen size following immune complex peritonitis and leads to accumulation of phagocytosed IC *in vivo*

In order to assess the impact of I-BET on the immune complex mediated pathology *in vivo* we studied two alternative models. Firstly, we used a model of immune complex peritonitis, enabling us to study acute neutrophil recruitment and also assess the phagocytic properties of infiltrating immune cells (Figure 75)

A

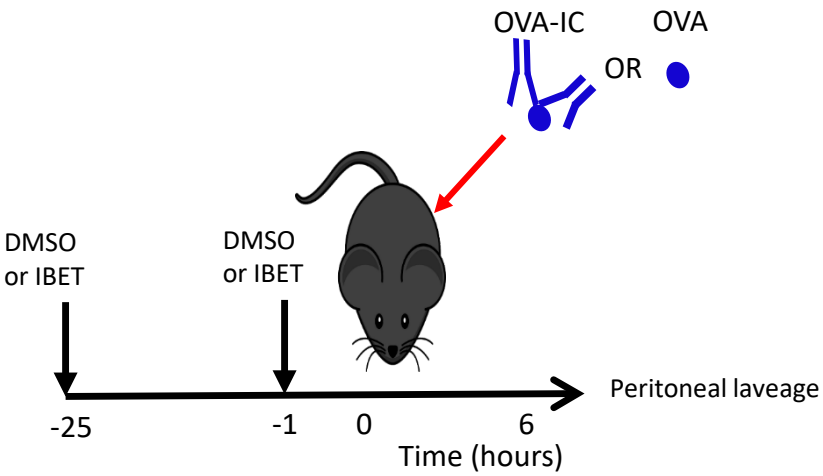

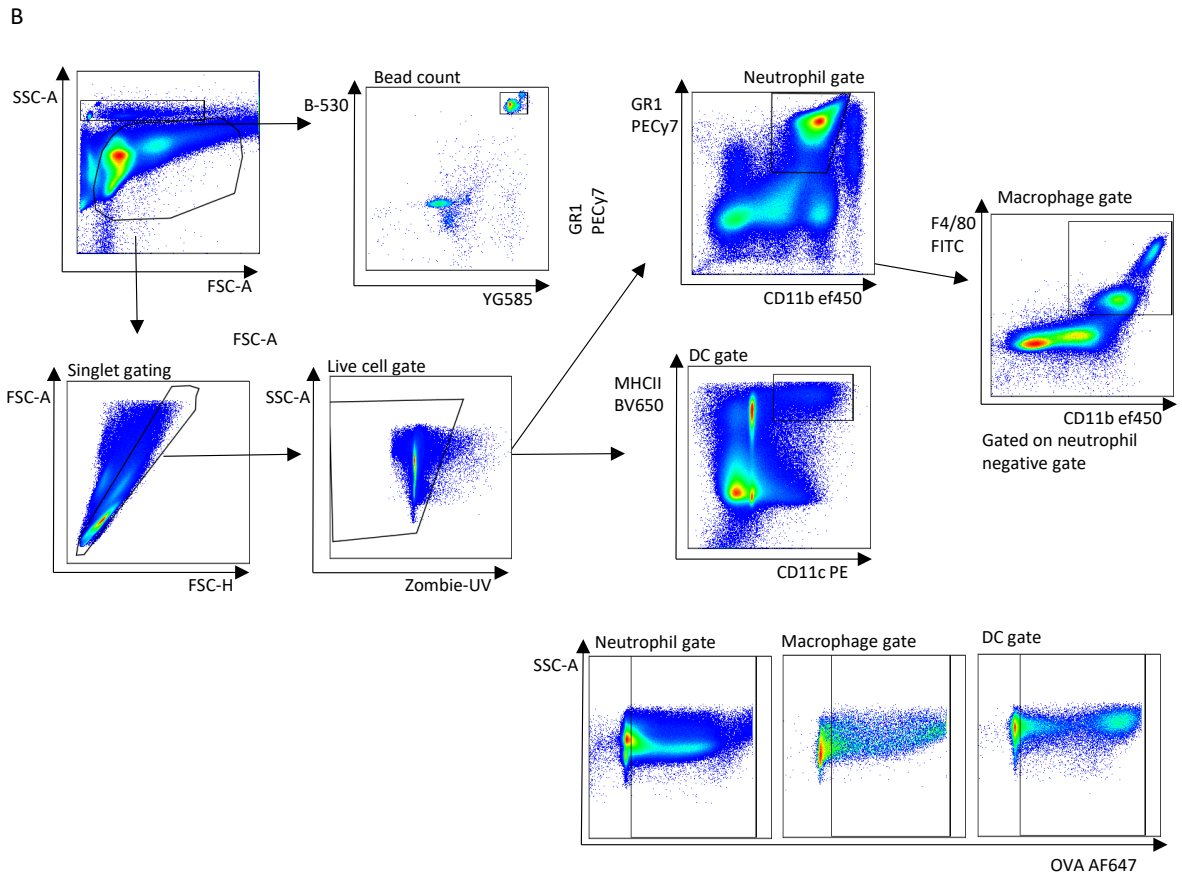


*Figure 75: Experimental procedure (A) and gating strategy (B) for an intraperitoneal immune complex peritonitis model. Mice were given immune complexed OVA or OVA control by intraperitoneal injection and culled 6 hours later with peritoneal lavage for quantification of inflammatory cell recruitment and assessment of phagocytosis.*

We observed a trend towards increased spleen size in control mice treated with intraperitoneal immune complex; I-BET treated mice had smaller spleens that DMSO treated mice receiving the same stimulus (Figure 76A). Within the peritoneal exudate there was a significant increase in neutrophils following immune complex instillation compared to OVA control. There were trends towards reduced cell recruitment in I-BET treated animals but these did not reach statistical significance (Figure 76B). Neutrophils (Figure 76C), macrophages (Figure 76D) and dendritic cells (Figure 76E) phagocytosed variable amounts of immune complexed and soluble OVA. There were no differences in any of these subsets in the proportion of cells containing phagocytosed material at four hours, however mirroring our *in vitro* findings, macrophages from animals treated with I-BET contained more phagocytosed OVA and OVA-IC. Neutrophils were able to phagocytose OVA-IC but not OVA; with levels accumulating to greater amounts in I-BET treated animals (Figure 76C).

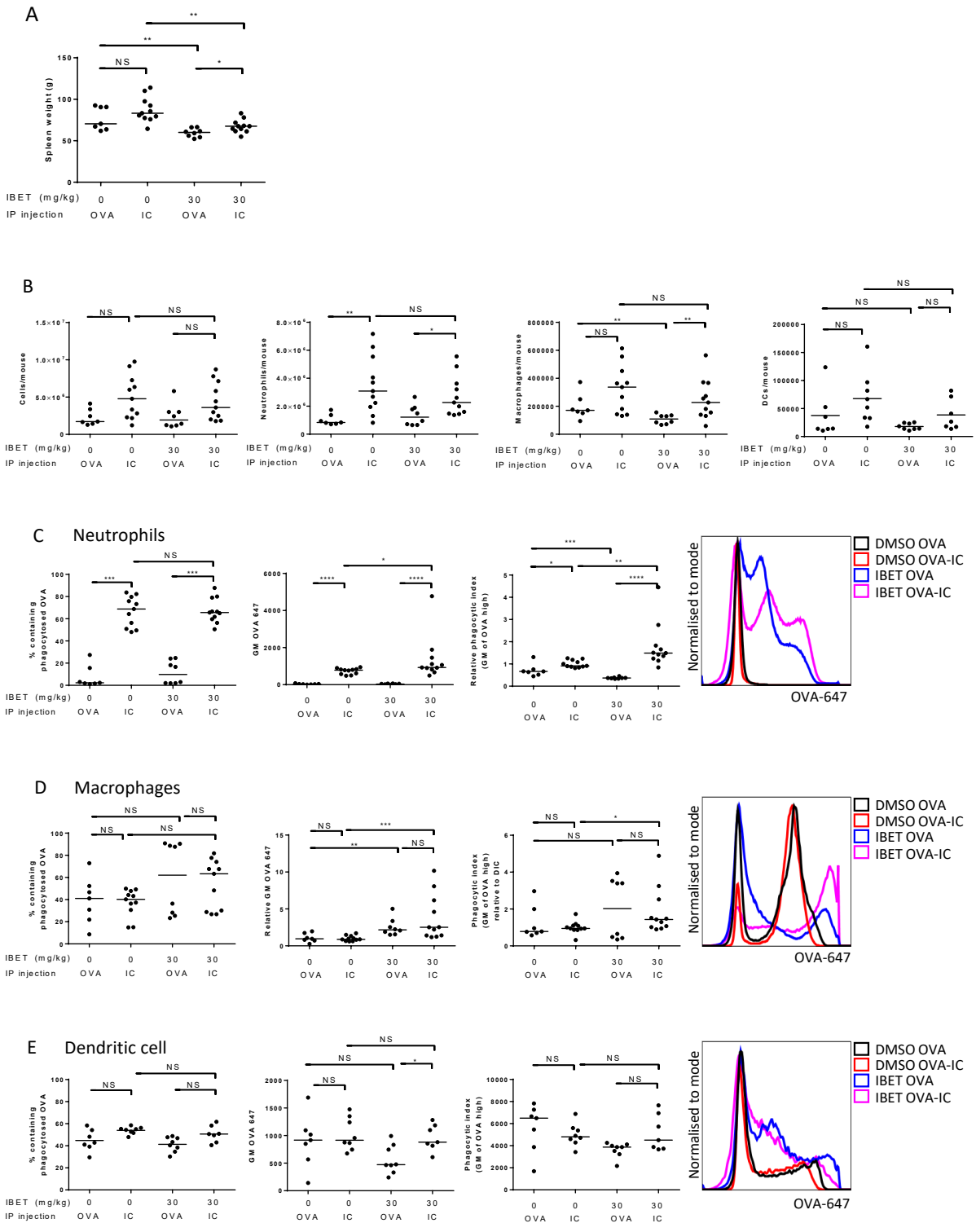


*Figure 76: I-BET treated phagocytes accumulate immune-complexed and soluble antigen in vivo. Spleen weight (A), peritoneal lavage cell composition (B), OVA-647 uptake in neutrophils (C), macrophages (D) and dendritic cells (E). For each population, the percentage of cells containing phagocytosed OVA is reported along with the geometric mean fluorescence for OVA-647, phagocytic index (the geometric mean fluorescence of the OVA+ gate) and representative histograms showing*

*OVA fluorescence. Mann-Whitney tests are used to compare medians (NS p>0.05; *p<0.05; **p<0.01; ***p<0.001; ****p<0.0001). Results from three independent experiments; relative values are reported where the combining values from independent experiments directly was not possible due to interexperimental variation in OVA fluorescence.*

### 4.3.8 I-BET reduces recruitment of mononuclear phagocytes to the kidney and reduces pro-inflammatory gene expression in response to circulating immune complex

We utilised an intravenous immune complex model in order to investigate the response of kidney resident mononuclear phagocytes to circulating immune complex, as used previously (Stamatiades 2016) (Figure 77). The experiment was repeated twice; on the first occasion the kidneys were flushed with cold PBS prior to harvest to remove intravascular cells, in the second experiment intravascular labelling of CD45+ cells was used. The results in both experiments were similar; pooled data is shown with the individual data points coloured according to whether intravascular labelling was used.

Mice treated with I-BET showed a trend towards reduced neutrophil recruitment one hour following injection of circulating immune complex (Figure 77A). CX3CR1 positive tissue resident MNPs can be classified according to their MHCII and Ly6C staining which has been described as a 'waterfall' (Tamoutounour 2012); newly extravasated cells express Ly6C but low levels of MHC II and those that have been present for longer, 'mature' tissue resident MNP, lose their Ly6C expression and acquire MHCII. I-BET treated mice had a more mature mononuclear phagocyte composition, with a lower proportion and number of newly extravasated and intermediate MNPs compared to solvent treated mice, irrespective of whether they received circulating immune complex or soluble antigen (Figure 78C).

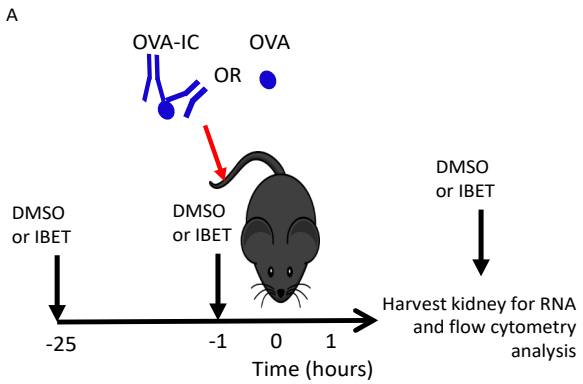

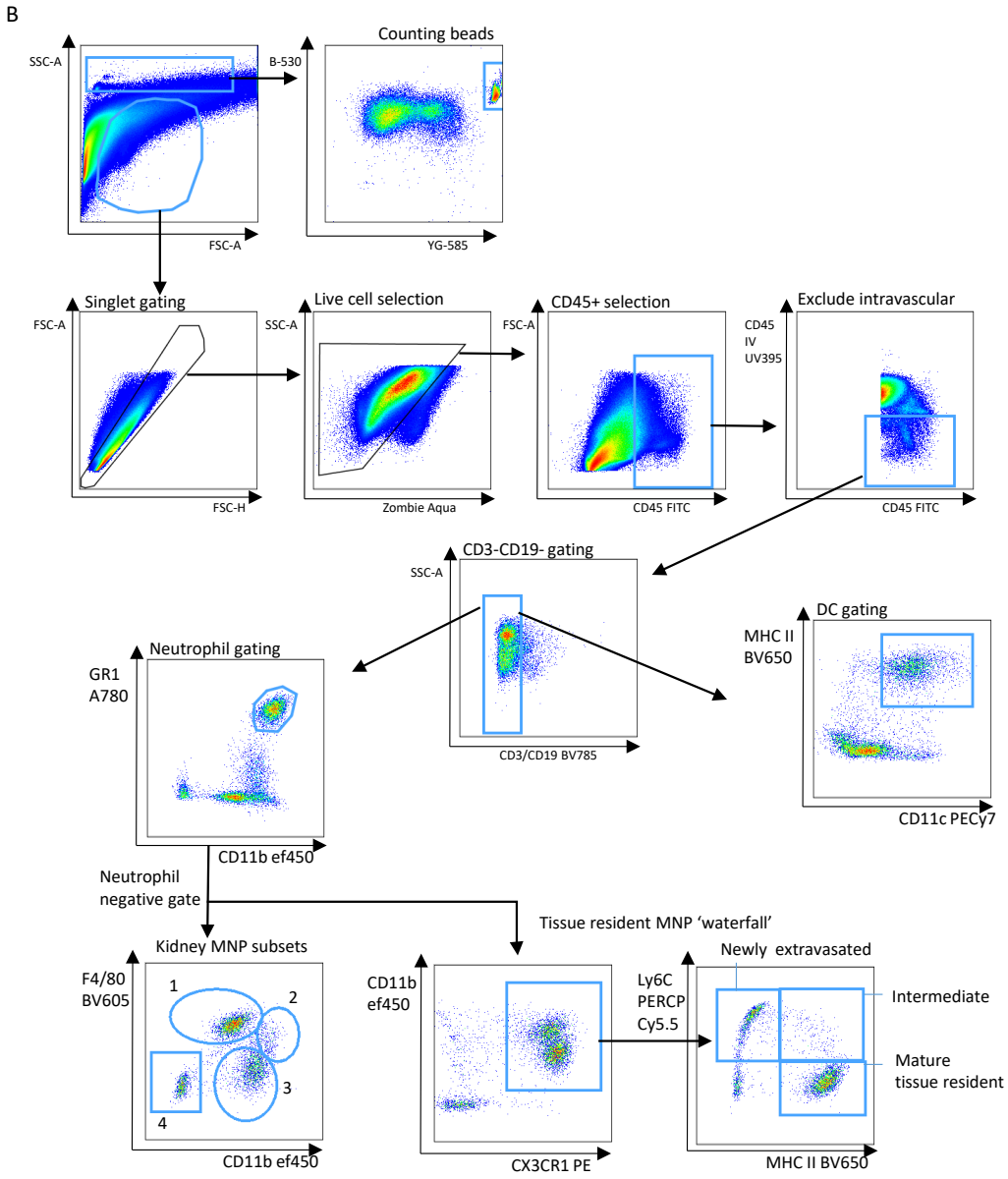


*Figure 77. Experimental procedure for* an intravenous immune complex model *(A). Experiment performed twice; on the second occasion mice were given an intravenous injection of CD45 immediately prior to schedule one to label intravascular cells.* B. Representative gating strategy used in the second experiment.

Alternatively, tissue resident MNPs can be classified into subsets 1 to 4 according to their CD11b and F4/80 expression (Berry 2017) (Figure 78D). The MNP1 subset of F4/80$^{hi}$ CD11b$^{int}$ cells expresses high levels of CD11c, MHC II, CX3CR1 and Clec9A, largely consistent with a cDC phenotype. These cells may either be mature and well-differentiated tissue-resident macrophages or DCs originally of monocyte origin, or perhaps derived from an embryonic precursor. The MNP2 subgroup of CD11b$^{hi}$ F4/80$^{int}$ cells are a heterogeneous group that may reflect different maturational states of extravasated monocytes. They are the predominant cells that phagocytose immune complex *in vivo*.

The MNP3 subgroup express MHC II, CD11b and CD103, and represent monocyte-derived macrophages with low level F4/80 expression. These cells correlate broadly with newly extravasated Ly6C$^{hi}$ MHC$^{lo}$ monocyte population in the waterfall gating schema. I-BET treated animals had an increase in F4/80 bright tissue resident MNP1 subset, with a reduction in the number of CD11b positive MNP2 and 3 subset tissue resident MNPs (Figure 78D); in keeping with the observations seen using alternative gating. The reduced influx of newly extravasated monocytes following I-BET treatment was associated with a reduction in the transcription of pro-inflammatory genes on FcγR crosslinking (Figure 78E).

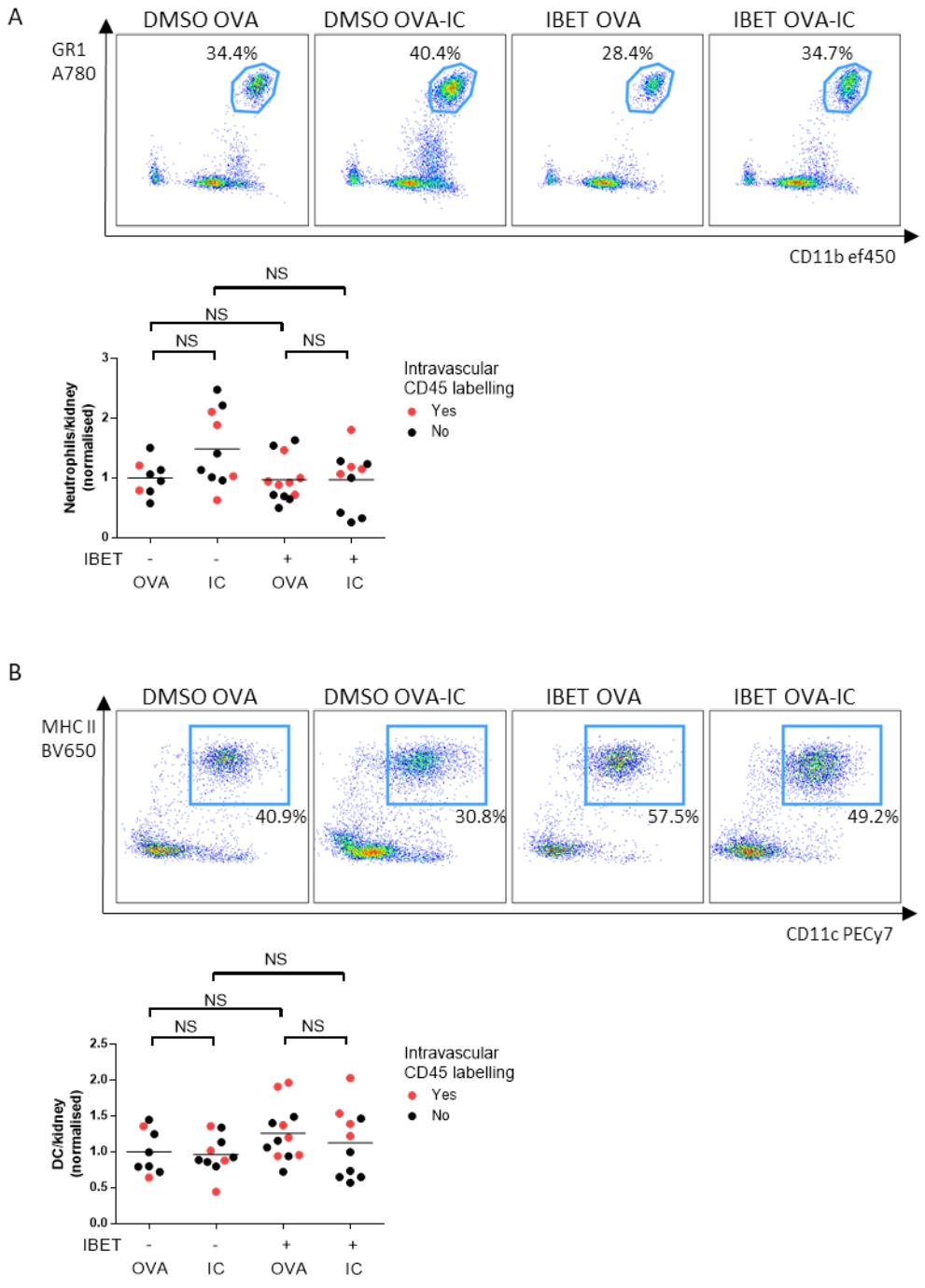

C

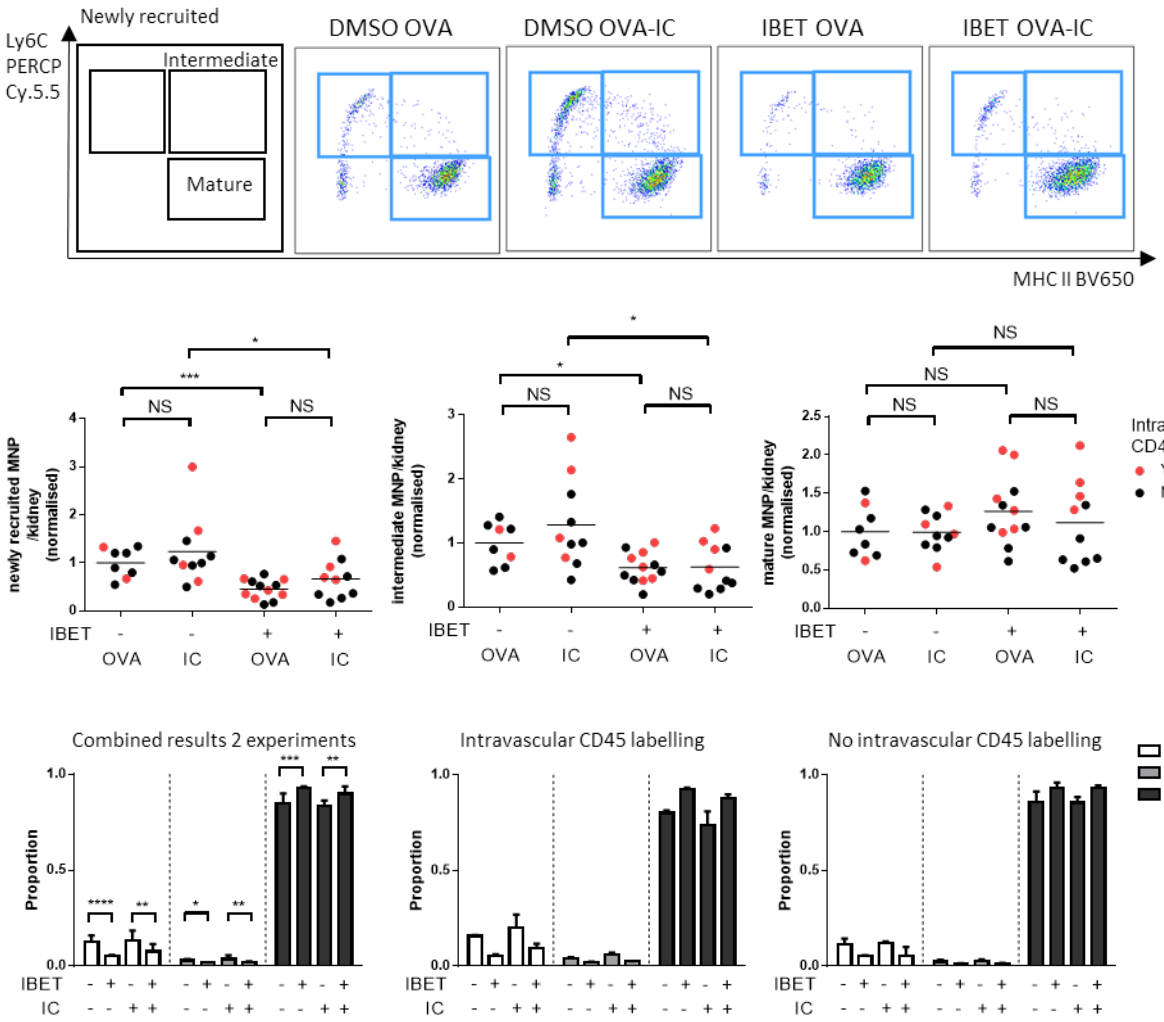
Newly recruited
Ly6C
PERCP
Cy.5.5
Intermediate
Mature
DMSO OVA
DMSO OVA-IC
IBET OVA
IBET OVA-IC
MHC II BV650
newly recruited MNP /kidney (normalised)
intermediate MNP/kidney (normalised)
mature MNP/kidney (normalised)
NS
IBET
OVA
IC
Intravascular CD45 labelling
Yes
No
Combined results 2 experiments
Intravascular CD45 labelling
No intravascular CD45 labelling
Proportion
Newly recruited
Intermediate
Mature

D

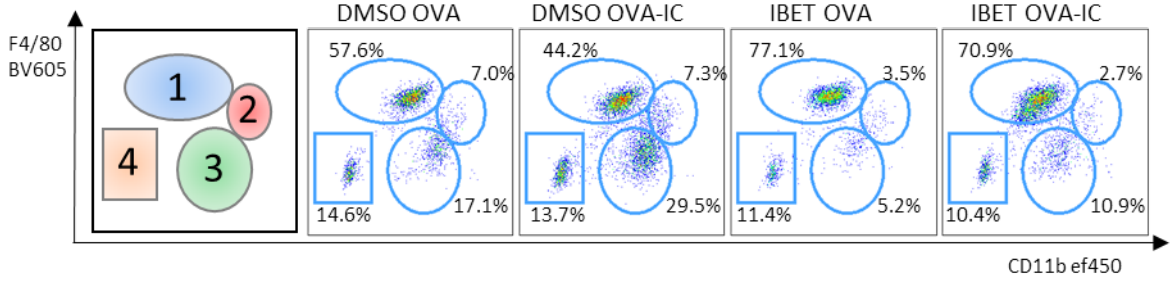
F4/80
BV605
1
2
3
4
DMSO OVA
DMSO OVA-IC
IBET OVA
IBET OVA-IC
57.6%
7.0%
14.6%
17.1%
44.2%
7.3%
13.7%
29.5%
77.1%
3.5%
11.4%
5.2%
70.9%
2.7%
10.4%
10.9%
CD11b ef450

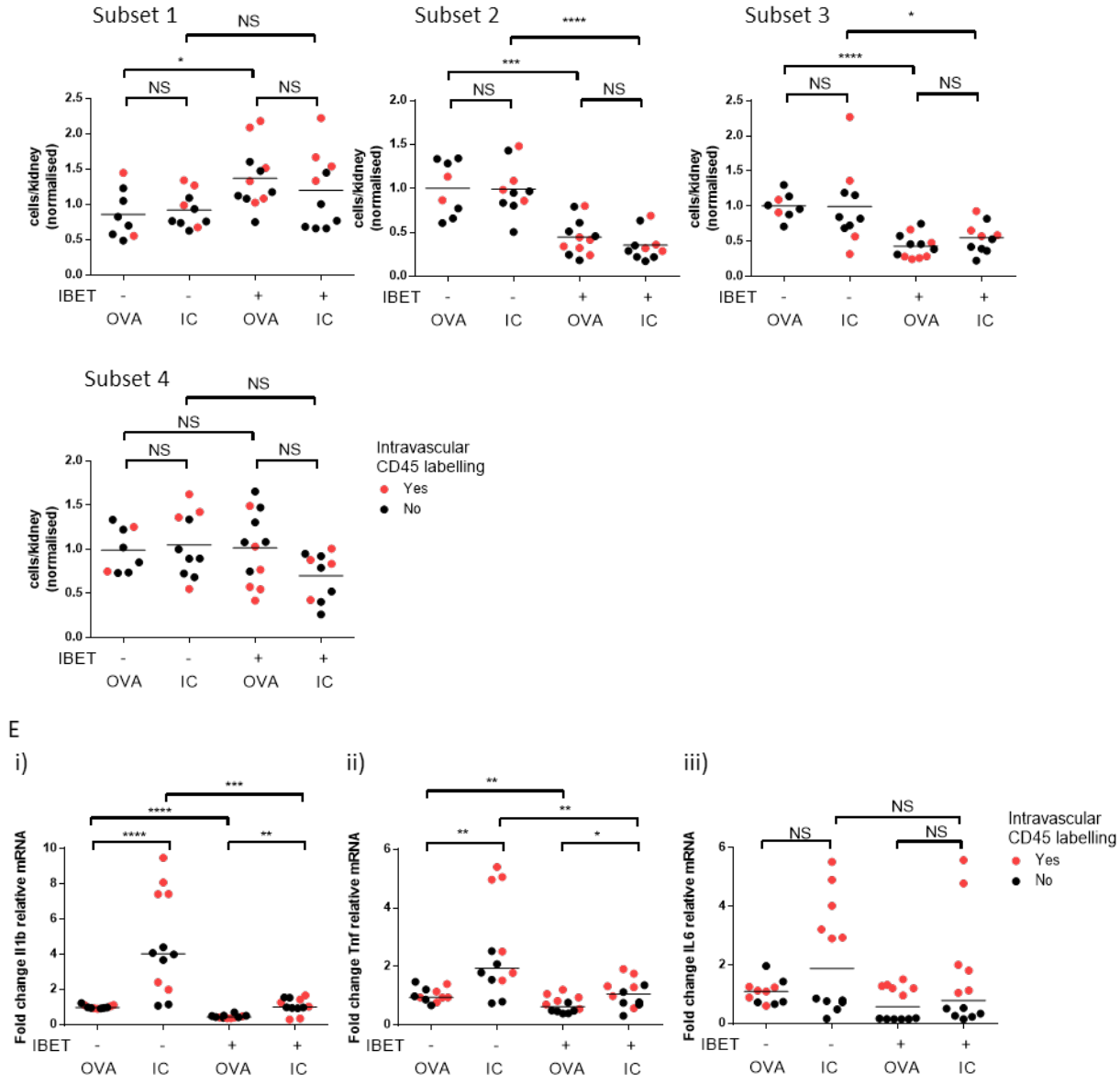


*Figure 78: I-BET reduces recruitment of mononuclear phagocytes to the kidney and reduces pro-inflammatory gene expression in response to soluble immune complex. Representative plots and summary data showing neutrophil recruitment (A), DC (B), MNP classified according to MHCII and Ly6C expression (C), and CD11b and F4/80 expression (D). E. qPCR in total kidney tissue for Il1β (i), Tnfα (ii) and Il6 (iii). Results from two independent experiments; data points coloured according to experiment; Mann-Whitney tests used to compare medians (NS p>0.05; *p<0.05; **p<0.01; ***p<0.001; ****p<0.0001). Median with interquartile range shown in C; statistics not performed on individual experiment results due to limited data points.*

### 4.4 Discussion

Given the effect of I-BET on MNP inflammatory responses to LPS, we hypothesised that I-BET may inhibit macrophage and DC activation by IgG, thus reducing antibody-mediated inflammation. Here we show I-BET inhibits the expression of many genes induced by FcγR crosslinking in murine BMDM, including genes involved in immune pathways identified by gene set enrichment analysis, such as TNFα signalling via NFκB, IFNα and IFNγ signalling, cytokine-chemokine signalling, cell adhesion pathways and antigen presentation. We also identified similarities in the effect of I-BET on IC-mediated gene expression to that observed in LPS simulated macrophages treated with I-BET (Nicodeme 2010); many of the LPS inducible genes significantly suppressed by I-BET were also induced by IC and similarly suppressed by I-BET, giving further evidence for a potential role for I-BET in the treatment of autoantibody-mediated disease.

Current therapies for antibody-mediated autoimmune diseases are imperfect, with treatment-resistance and frequent disease relapse. There are established therapies that inhibit autoantibody production, principally by depleting or inhibiting B cells, but few treatments that modulate MNP responses to IC. Our data show that I-BET reduced FcγR expression on macrophages and dendritic cells, potentially lowering their capacity to respond to IC. We identified reduced expression of both activatory and inhibitory FcγR *in vitro*, however *in vivo* studies suggested a greater effect on activatory receptors leading to a reduction in the A/I ratio and an increase in the activation threshold of MNPs encountering IgG immune complexes. This would suggest that even if autoantibodies were present, in the presence of I-BET, they may not cause inflammation due to this change in activation threshold. Of note, the A/I ratio is also known to determine Fcγ receptor-facilitated T cell activation by dendritic cells (van Montfoort 2012).

Furthermore, we show that I-BET leads to altered macrophage phagocytosis, with accumulation of phagocytosed IC and degradation products within cells associated with reduced inflammatory cytokine production. This would potentially promote non-inflammatory clearance of ICs by tissue-resident cells, again of benefit therapeutically.

Bromodomain inhibitors have been shown to have marked anti-inflammatory effects in numerous *in vivo* models, and have been associated with protection from autoimmune and inflammatory disease (Nicodeme 2010, Bandukwala 2012, Belkina 2013, Mele 2013, Brown 2014, Fu 2014, Meng 2014, Zhang 2015). The cellular mechanisms and immunological pathways mediating these anti-inflammatory effects are likely to be multifactorial and individual studies have focussed on different aspects of the immune response. In an adoptive transfer model of EAE, treatment with I-BET762

inhibited the ability of antigen-specific T cells, differentiated under Th1 but not Th17 conditions *in vitro*, to induce pathogenesis with reduced recruitment of macrophages consistent with decreased GM-CSF production by central nervous system infiltrating T cells (Bandukwala 2012). In a different study, inhibition of EAE and CIA was attributed to inhibition of Th17 mediated pathology (Mele 2013). Zhang et al. also showed JQ1 associated amelioration of CIA but attributed reduced joint inflammation and damage to effects on fibroblast-like synoviocytes, showing BRD4 silencing associated reductions in pro-inflammatory cytokine production from TNF-α stimulated rheumatoid arthritis fibroblast-like synoviocytes associated with reduced migration and invasion behaviour (Zhang 2015). Bromodomain inhibitors reduce levels of proinflammatory cytokines, protecting mice from endotoxin induced death and sepsis (Nicodeme 2010, Belkina 2013) and reduce the inflammatory response and bone destruction in experimental periodontitis (Meng 2014). JQ1 treatment inhibited the immune complex-mediated activation of human monocytes *in vitro* and attenuated murine lupus development *in vivo,* increasing survival in MRL-lpr mice, reducing serum concentrations of BAFF, IL1β, IL6, IL17, and IFNγ and augmenting IL10 (Wei 2015). Reductions in BAFF and IL6 levels alongside increased IL10 were also seen following *in vitro* culture of murine splenocytes and human monocytes stimulated with IC, bringing into question whether the effects of bromodomain inhibition may overlap with those of belimumab. Furthermore, the effects of bromodomain inhibition are not limited to immune cells; inhibition of type one diabetes was shown to be due to a dual effect inducing an anti-inflammatory phenotype in pancreatic macrophages mediated via effects on NFκB target genes and eliciting regeneration of pancreatic beta cells, with minimal effect on the transcriptome of CD4+ T cells infiltrating the pancreas and within draining lymph nodes (Fu 2014).

The capacity of bromodomain inhibitors to supress the macrophage inflammatory response to TLR4 stimulation is well established (Nicodeme 2010, Belkina 2013) and thought to occur due to remodelling of the enhancer landscape, with development of thousands of *de novo* enhancers. Many of these enhancers reside in super-enhancer regions, with loss of a subset of pre-existing enhancers (Kaikkonen 2013). Transcription of super-enhancer associated RNAs is dynamically induced at most of the key genes driving innate immunity and inflammation (Hah 2015). The selectivity of I-BET for pro-inflammatory genes is thought to arise from inhibition of NF-κB directed reorganisation of super-enhancers leading to suppressed super-enhancer dependent proinflammatory gene transcription (Brown 2014), a process of regulation distinct from that which coordinates constitutive expression of housekeeping genes.

The redistribution of super-enhancers is not limited to TLR4 stimuli and has been described following a wide variety of stimuli in human macrophages. GM-CSF stimulated monocytes were incubated with IFNγ (acute inflammation model), IL4 (alternative acute inflammation model) or a combination of TNF, prostaglandin E2 and Pam3CyS (chronic inflammation model) for 72 hours prior to assessment of histone modifications by CHIP-seq (Schmidt 2016). Schmidt and colleagues defined a transcriptional and epigenetic regulator network distinct to human inflammation associated macrophage activation that was distinct from the network seen in human somatic tissues and murine tissue resident macrophages. The inflammation associated network was characterised by a more globally permissive histone modification state, with both common and stimulus specific regulatory elements.

Epigenetic modifications induced by FcγR crosslinking have also been described. Chromatin remodelling of the Il10 promotor locus is responsible for inducing high levels of IL-10 secretion by macrophages stimulated in the presence of immune complexes. FcγR crosslinking results in rapid and enhanced activation of two MAPKs, ERK and p38. Activation of ERK leads to the phosphorylation of serine 10 on histone H3 at the Il10 gene, making the promoter more accessible to transcription factors generated in response to p38 activation. Immune complex stimulation alone was sufficient to activate ERK, modifying the Il10 locus to make it more accessible; however additional TLR signals from the addition of LPS were required to activate transcription factors that bind to the Il10 promotor, increasing IL10 production (Lucas 2005). The chromatin precipitation studies used in this study only allow detection of phosphorylation and acetylation at specified gene loci of interest (the Sp1 and STAT3 binding regions of the Il10 promotor in addition to a control region and the IL-12p40 promotor). It is likely that FcγR crosslinking induces more widespread epigenetic changes, which may influence the subsequent immune response and determine susceptibility to modulation by drugs including bromodomain inhibitors. Such changes might significantly influence the activation of macrophages by subsequent stimuli, so called trained immunity (Cheng 2014, Saeed 2014). We therefore propose a more comprehensive study of the epigenetic changes induced by FcγR crosslinking, detailed in chapter 6, and wish to determine which of these changes are impacted by I-BET.

The vast majority of single nucleotide polymorphisms (SNPs) associated with disease susceptibility in autoimmune disease in genome wide association studies (GWAS) are found in non-coding regions of the genome, localising preferentially within gene regulatory regions in immune cells (Farh 2015). Aberrant regulation of immune responses due to dysregulated gene expression may underpin susceptibility to autoimmune disease. Interactions between genetic susceptibility and epigenetic

changes caused by environmental factors may be responsible for inducing autoimmune disease. Processes controlling epigenetic modifications, superenhancer remodelling and the regulation of gene expression may offer new therapeutic targets, with potential to signpost inflammation associated targets (Tough 2017)

Our work suggests that I-BET inhibits the immune complex associated macrophage inflammatory response, similarly to its known effect on LPS driven inflammation. FcγR crosslinking induces multiple changes in gene expression in macrophages, impacting a number of inflammation associated pathways. We show that I-BET treatment alters the expression of FcγR, potentially modifying the A/I ratio and threshold for cell activation. Changes in the cytokine milieu are known to differentially effect FcγR expression (Liu 2005). The degree of change in expression of activatory and inhibitory receptors varied across our experiments with a reduced A/I ratio following I-BET treatment *in vivo*; perhaps due to additional indirect effects of altered cytokine expression.

A more detailed analysis of the epigenetic changes induced is required to fully understand I-BET targeting; however given the large number of inflammation associated genes impacted it is likely to involve reorganisation of super-enhancers. Our *in vivo* models further support the hypothesis that bromodomain inhibition may be of benefit in the setting of antibody mediated disease. Following administration of intravenous immune complex, I-BET treated animals recruited fewer newly extravasated monocytes to their kidneys compared to solvent treated controls, associated with a reduction in the transcription of pro-inflammatory genes. This suggests that I-BET may attenuate the immune response to deposited immune complex, for example in SLE or in the setting of donor specific antibody following renal transplantation, and may be a useful therapeutic tool alongside treatments that target B cells and antibody production itself.

**Chapter 5: Bromodomain protein inhibitors modulate FcγR-mediated DC migration, suggesting therapeutic potential in immune complex-mediated disease**

## Chapter 5: Bromodomain protein inhibitors modulate FcγR-mediated DC migration, suggesting therapeutic potential in immune complex-mediated disease

### 5.1 Chapter summary

Here, we explored the potential of BET protein inhibitors to limit FcγR-mediated DC activation and migration. We show that I-BET reduced the upregulation of many genes in MNP following IgG IC stimulation, including those associated with DC maturation and antigen presentation. We also observed a reduction in activating FcγR expression on I-BET treated DCs, reducing their susceptibility to IgG-mediated activation. I-BET treatment changed MNP morphology and resulted in a less adherent phenotype, prompting an assessment of its impact on DC migration. *In vitro*, in a 3D collagen matrix, IgG-IC induced augmentation of DC chemotaxis to CCL19 was abrogated by the addition of I-BET. In keeping with this, we observed that I-BET treatment inhibited the upregulation of CCR7 associated with FcγR cross-linking. *In vivo*, two photon imaging showed that systemic I-BET treatment reduced IC-induced dermal DC mobilisation. These tissue DCs also had reduced migration to draining lymph nodes. We confirmed a DC-intrinsic effect on IgG IC-induced migration by transferring I-BET-treated DCs into the skin and tracking their subsequent trafficking to lymph nodes. Together, our data confirm that I-BET has a substantial impact on FcγR-mediated DC activation and migration, and highlight the therapeutic potential of bromodomain protein inhibitors in antibody-mediated diseases, such as SLE.

## 5.2 Background

Almost all tissues contain a network of DCs, poised to detect and respond to local immune challenges, including deposited IgG IC. DCs act as important antigen presenting cells that may activate CD4 T cells, and determine whether these cells become tolerogenic or immunogenic (Banchereau 1998, Steinman 2012). This fate decision is dependent on the presence of co-stimulatory signals present on mature DCs (Hawiger 2001, Steinman 2003). DC maturation may be driven by stimuli such as TLR ligation and by activating FcγR cross-linking (Roake 1995, Reis e Sousa 2006). In addition to a requirement for maturation, tissue-resident DCs must be geographically re-located from peripheral tissues to lymph nodes to permit interactions with T cells (Sallusto 1998, Cyster 1999, Forster 1999, Randolph 2005). Most DCs enter tissues via the lymphatic vessels that drain peripheral tissues. The processes that govern this migratory pathway are therefore key regulators of the induction of immune responses. Central to DC migration is the expression of the chemokine receptor CCR7 and its interaction with CCL19 and CCL21, chemokines expressed by lymphatic endothelial cells that guide DCs to the T cell zone of lymph nodes (Sallusto 1998, Forster 1999). Other factors that facilitate this process include the production of MMPs, particularly MMP-2 and MMP-9 (Ratzinger 2002, Yen 2008), that allow movement through the extracellular matrix and across basement membranes. Indeed, pharmacological inhibition (Lebre 1999), antibody neutralization (Kobayashi 1999), or genetic deletion of MMPs (Ratzinger 2002, Ichiyasu 2004, Yen 2008) reduces DC migration.

Of note, abnormalities in monocytes and DCs have been observed in patients with SLE (Blanco 2001, Decker 2006, Ding 2006, Crispin 2012) and engagement of activating FcγRs on tissue DCs by autoantibody-containing IC in SLE leads to the upregulation of CCR7, and stimulates DC migration to draining lymph nodes (Clatworthy 2014a). Furthermore, the lupus-associated polymorphism in human *FCGR2B* (rs1050501) (Willcocks 2010) that results in receptor dysfunction (Floto 2005, Kono 2005), is associated with increased CCR7 expression on DCs following IgG IC stimulation (Clatworthy 2014a), driving enhanced migration to the T cell zone of lymph nodes, propagating autoimmunity and inflammation. Therefore, IgG IC-driven DCs migration may represent a useful therapeutic target in autoimmune diseases.

DC activation by IgG IC requires substantial changes in gene expression (Dhodapkar 2007). Bromodomain inhibition with JQ1 is known to inhibit LPS-induced STAT5-dependent DC maturation (Toniolo 2015), leading to reduced co-stimulatory molecule expression and IL12 production, and decreased ability of DC to induce T cell proliferation in an allogeneic system. Here, we explored the potential of BET protein inhibitors to limit FcγR-mediated DC activation and migration.

### 5.3 Results

#### 5.3.1 I-BET alters mononuclear phagocyte morphology and adhesion

We noted that compared to BMDM treated with DMSO *in vitro*, those treated with I-BET tended to float, being less adherent to tissue culture plastic, with more cells noted to float in the culture supernatant when examined via light microscopy. Analysis of these cells using a viability strain showed that similar proportions were alive compared to adherent cells treated with DMSO alone (Figure 79).

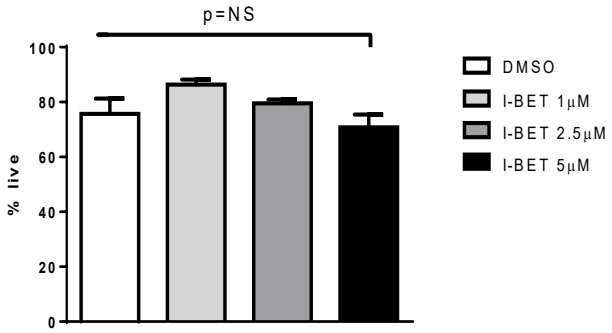


*Figure 79: I-BET151 does not affect viability at concentrations up to 5μM. BMDM were treated with DMSO or I-BET151 for 16-24 hours, prior to assessment of viability using Live Dead Aqua viability dye. Results combined from three independent experiments; p value calculated using one way ANOVA test*

Examination of BMDM treated with I-BET151 using confocal microscopy, staining the actin cytoskeleton with phalloidin, revealed changes in cell morphology consisted with the observation of decreased adherence to cell culture plates. I-BET treated cells appeared more rounded and were less adherent to cover slips (Figure 80).

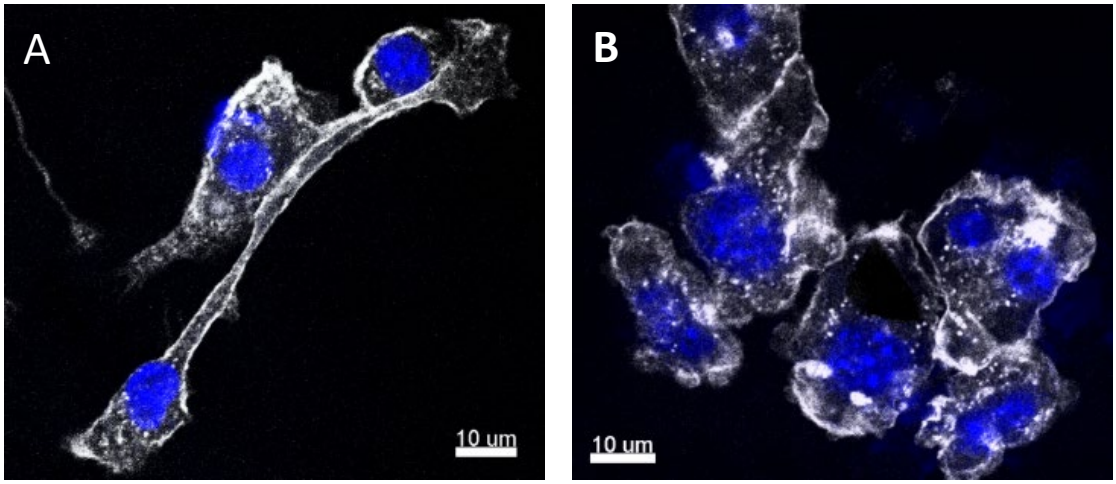


*Figure 80: I-BET causes rounding of BMDM. Representative images of BMDM treated with DMSO (A) or I-BET151 5μM (B). DAPI stain shown in blue; phalloidin in white*

Treatment with I-BET151 at a concentration of 5μM for 14 or 24 hours significantly reduced the adhesion of BMDM *in vitro* (Figure 81A, B). Fewer cells were adherent to cover slips following treatment, shown by significantly reduced numbers of cell nuclei per high power field examined (Figure 81Aiv; Biv). Cells were smaller in surface area and volume and more rounded in appearance, demonstrating increased sphericity (Figure 81Av-vii; Bv-vii). Phalloidin stains F-actin and can hence be used to image the actin cytoskeleton of cells. With increasing concentrations of I-BET151, there was a reduction in the actin contacts made with cover slips, with less dense phalloidin staining shown on maximum projection imaging. Treatment with DMSO alone induced some changes in cell morphology. Cells treated for only one hour and then given DMSO free media for 23 hours prior to fixation had greater phalloidin staining with clear demonstration of actin around each nucleus (Figure 81Ci). Treatment for one hour with I-BET151 at a concentration of 1μM or 5μM was sufficient to induce changes in adhesion, with reduced cell nuclei and phalloidin stain volume per high power field (Figure 81Civ-v), with no apparent change in average cell volume (Figure 81Cvi).

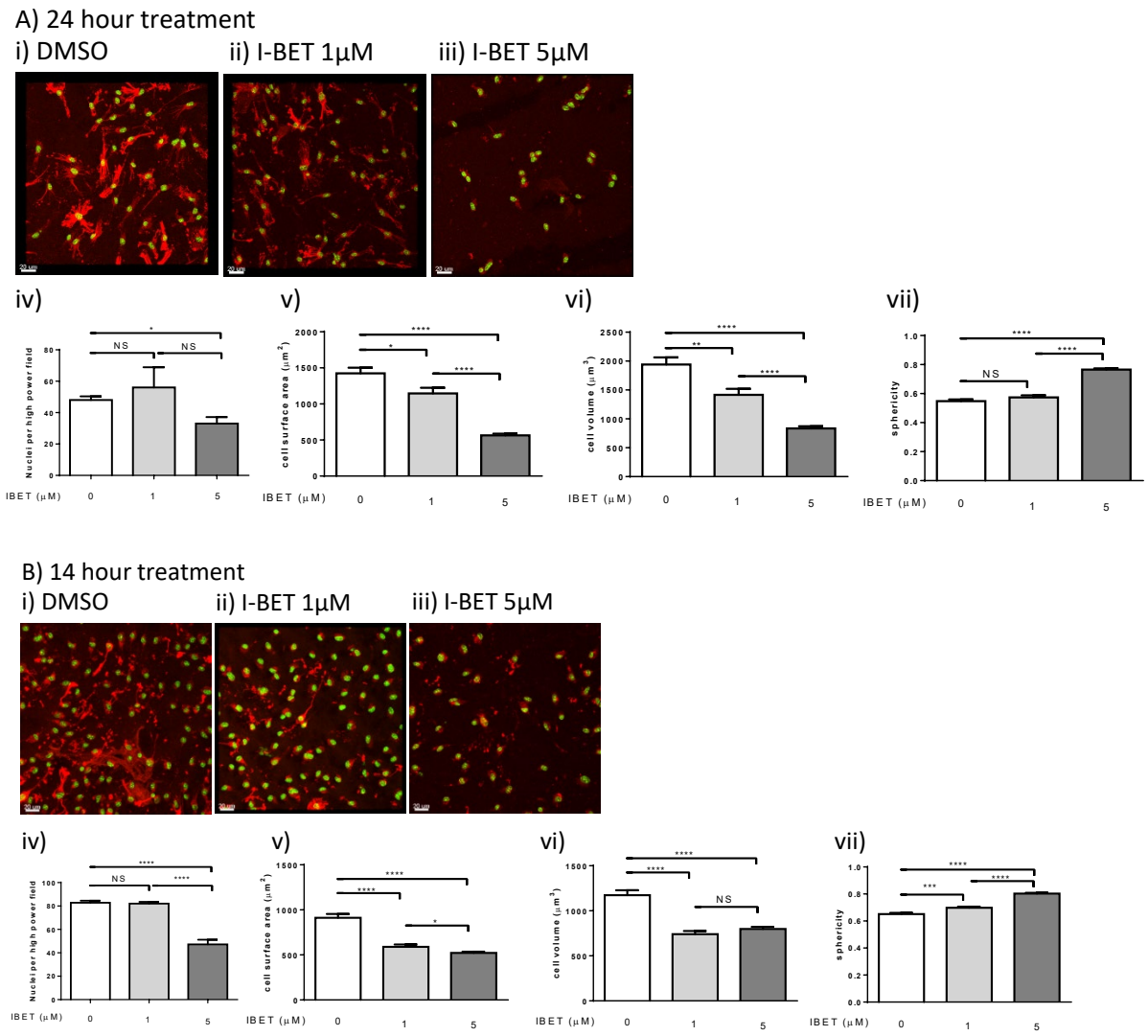

C) 1 hour treatment followed by 23 hour media alone

i) DMSO ii) I-BET 1µM) iii) I-BET 5µM

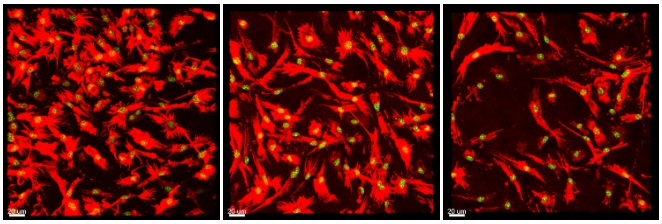

iv) v) vi)

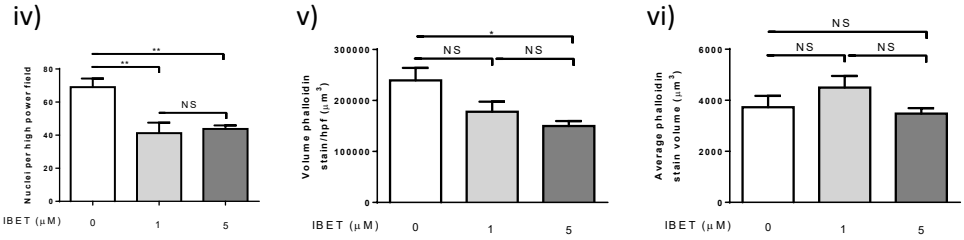


*Figure 81: I-BET reduces adhesion of BMDM. BMDM were allowed to stick down to cover slips then treated with DMSO (i), I-BET151 1µM (i) or I-BET151 5 µM (iii) for 24 hours (A) or 14 hours (B), fixed, stained with phalloidin 568 (red) and DAPI (green) and imaged by confocal microscopy (maximum projection images shown). In C, DMSO (i), I-BET151 1µM (i) or I-BET151 5 µM (iii) were present for only the first hour of 24 hour culture. Adhesion was quantified by counting the number of nuclei per high power field (iv). Morphology was quantified by cell surface area (Av; Bv), cell volume (Avi; Bvi) and cell sphericity (Avii; Bvii). In C, a high proportion of overlapping cells made it difficult to add surfaces to individual cells, so the phalloidin volume per high power field was quantified as a measure of cell volume (Cv); average cell volume was calculated by dividing the phalloidin cell volume by the number of nuclei per high power field (Cvi). Five high power fields imaged per condition; means compared using unpaired student t tests (NS p>0.05; *p<0.05; **p<0.01; ***p<0.001; ****p<0.0001).*

We were interested in whether this observation of decreased mononuclear phagocyte adhesion would impair the ability of dendritic cells to migrate, a process dependent on adhesion molecule expression. We confirmed that I-BET induced similar changes in cell morphology and adherence in bone marrow derived dendritic cells, with reduced cell surface area and volume, increased cell sphericity and reduced adhesion to tissue culture plastic (Figure 82).

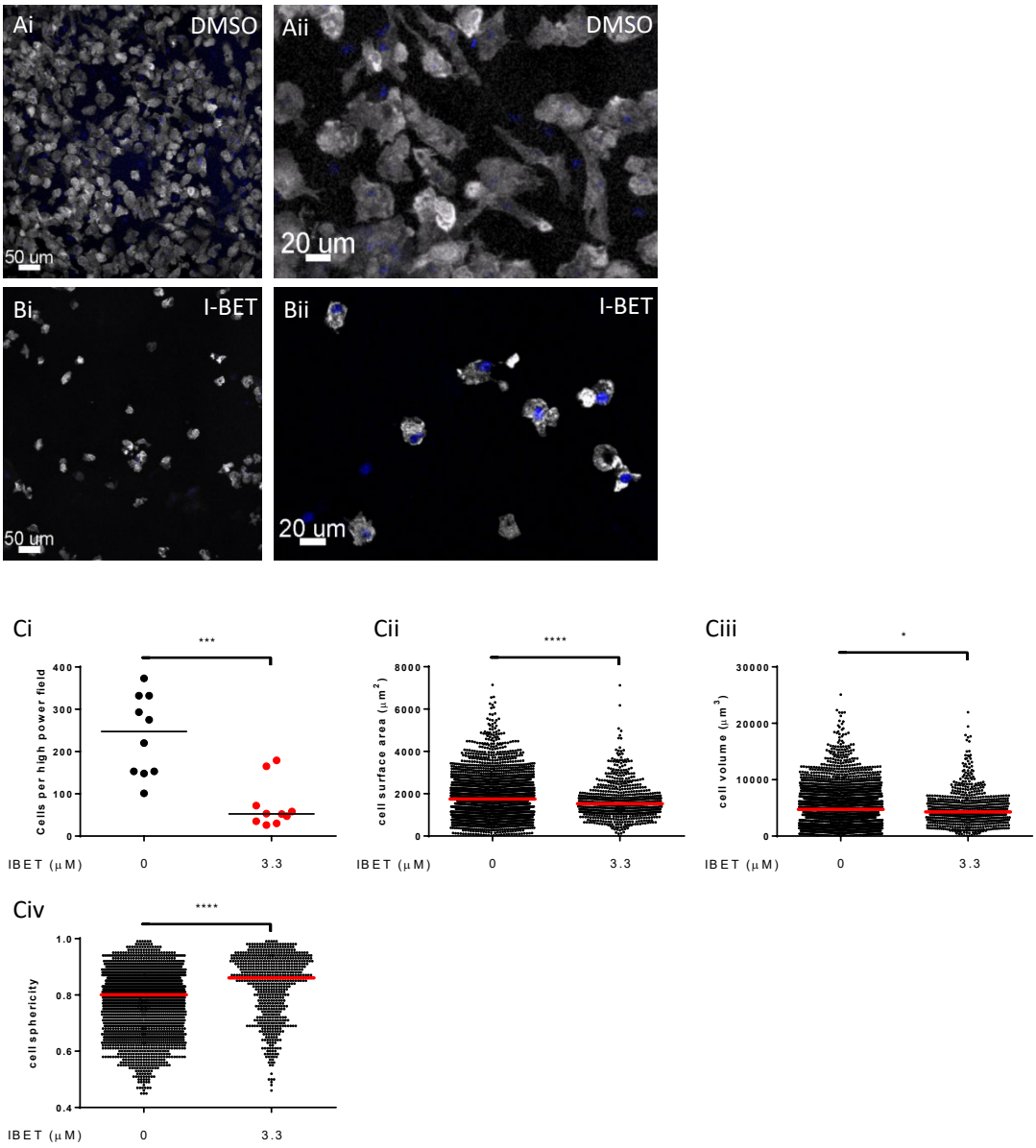


*Figure 82: I-BET reduces adhesion of BMDC. Representative images of bone marrow derived dendritic cells allowed to stick down to cover slips then treated with DMSO (A) or I-BET151 3.3μM (B) for 15 hours fixed, stained with phalloidin 568 (white) and DAPI (blue) and imaged by confocal microscopy (x25 lens high power field maximum projection image with 50μm scale bar (i); magnified with 20μm scale bar in (ii)). Quantification of cells from 10 high power fields per condition was performed by applying surfaces using Imaris software (C) with quantification of number of cells per high power field (i), cell surface area (ii), cell volume (iii) and cell sphericity (iv). Means compared using unpaired student t tests (NS p>0.05; *p<0.05; ***p<0.001; ****p<0.0001).*

### 5.3.2 I-BET alters expression of genes involved in cell adhesion and migration

Multiple gene pathways are involved in the process of DC adhesion and migration, including those coding for chemokine receptors and ligands, such as CCL19 and CCR7, matrix metalloproteinases, genes involved in prostaglandin and cysteinyl leukotriene signalling, adhesion molecules, and genes involved in regulation of the actin cytoskeleton, for example the Rac family of GTPases. We undertook transcriptomic analysis of BMDM treated with I-BET or DMSO control. Gene set enrichment analysis identified that I-BET treatment alone caused downregulation of multiple immune pathways including those involved in regulation of the actin cytoskeleton, leukocyte transendothelial migration and chemokine signalling pathways (Figure 83). Numerous chemokine receptors in additional to some chemokine ligands, were significantly downregulated following I-BET treatment (Figure 84)

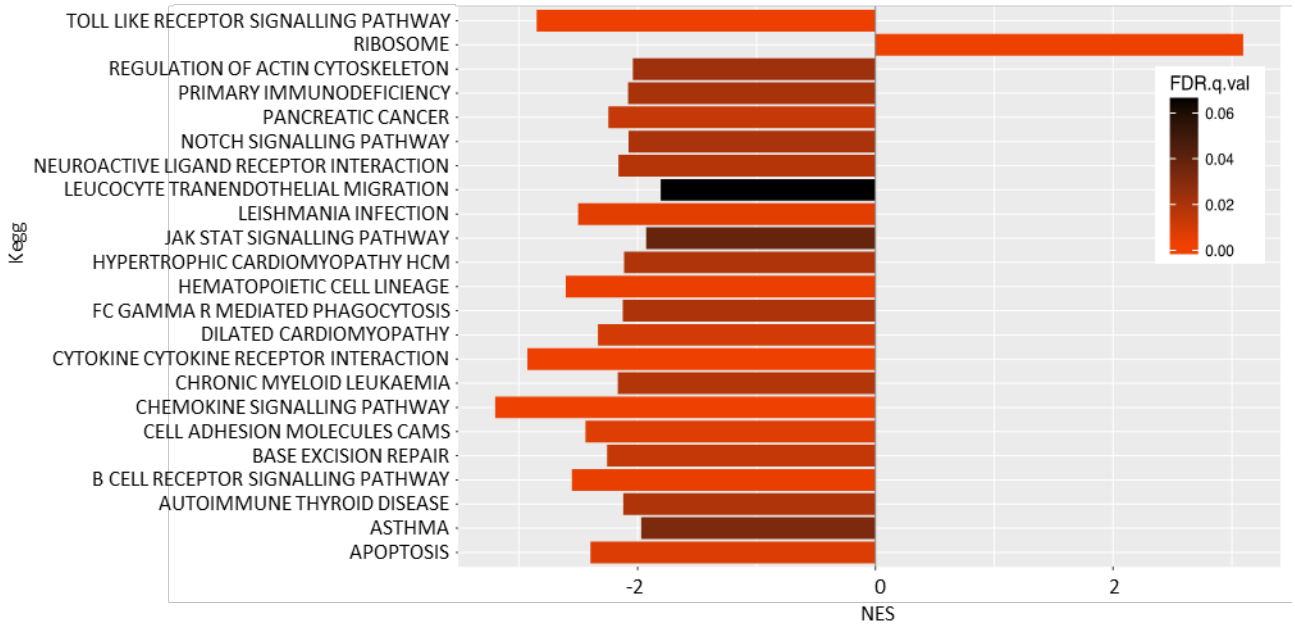


*Figure 83: Gene set enrichment analysis of genes differentially expressed following the treatment of BMDM with I-BET for 4 hours, using Kegg pathway terms. Genes ranked based on 1/p value with sign of log fold change. Pathways filtered to show those with a FDR q value < 0.1. Normalised enrichment score (NES) indicates pathways down regulated as a result of I-BET treatment.*

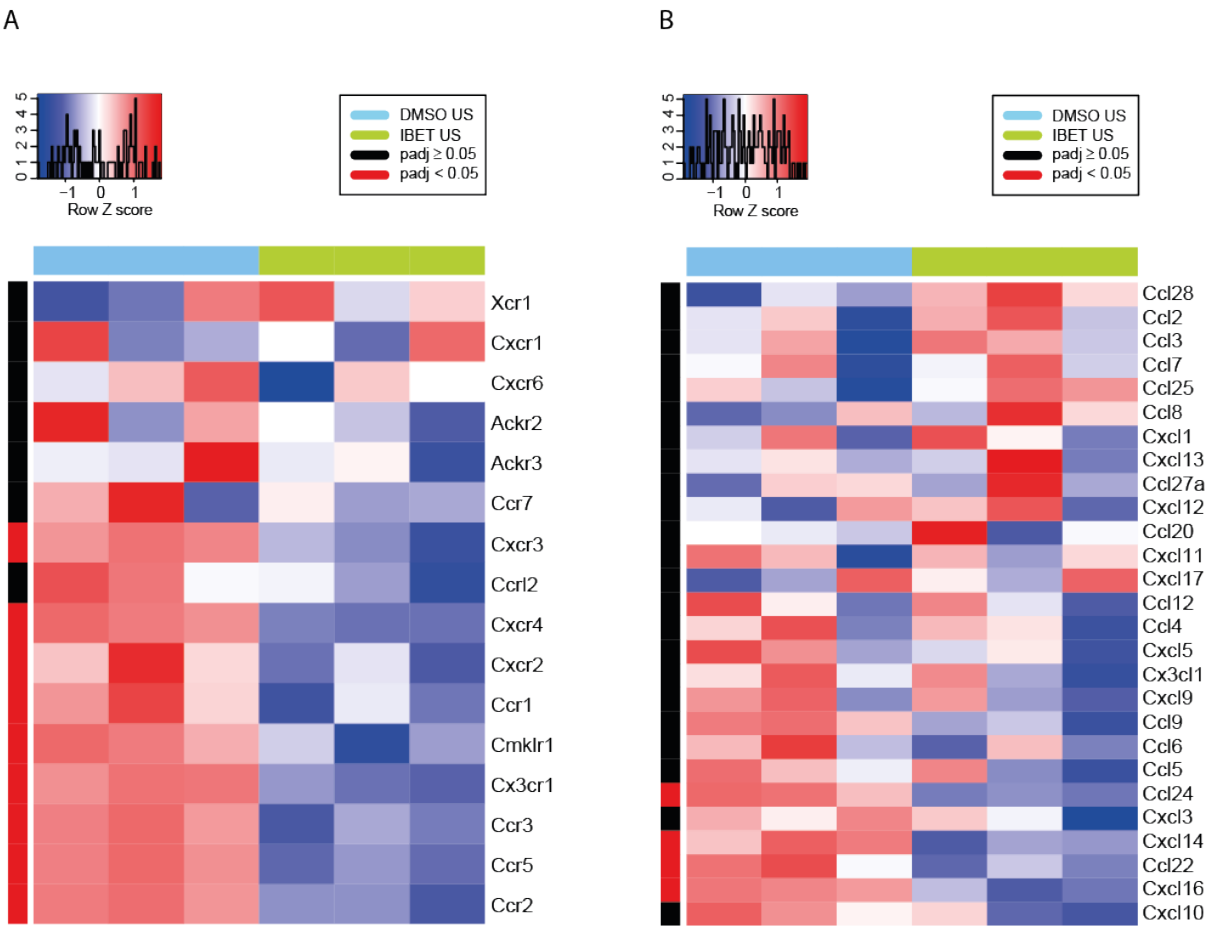


*Figure 84: Heatmap showing differential expression of chemokine receptor (left) and ligand (right) genes following a 4 hour treatment with I-BET*

Numerous pathways implicated in DC migration were significantly affected by the addition of I-BET (Figure 85). Genes encoding the cysteinyl leukotriene receptor 1 and 2 (*Cysltr1, Cysltr2*), prostaglandin E receptor 2 (*Ptger2*), integrin subunit alpha 4 (*Itga4*), platelet-activating factor receptor (*Ptafr*), PI3K catalytic subunit gamma (*Pik3cg*) and dedicator of cytokinesis 8 (*Dock8*) were all significantly downregulated with I-BET treatment. Other genes with functions in DC migration also appeared to be downregulated with I-BET treatment, though didn't reach statistical significance, for example genes encoding the small Rho family GTPases *Cdc42*, *RhoA*, *Rac1* and *Rac2*, components of the Arp2/3 complex (*Arpc2*, *Arpc5*, *Actr2*, *Actr4*), integrin subunit beta 2 (*Itgb2*), *Eps8*, *CCR7* and MMP9. Vinculin (*Vcl*) and adaptor related protein complex 1 associated regulatory protein (*Ap1ar*, a negative regulator of the Arp2/3 complex) were significantly upregulated following I-BET treatment.

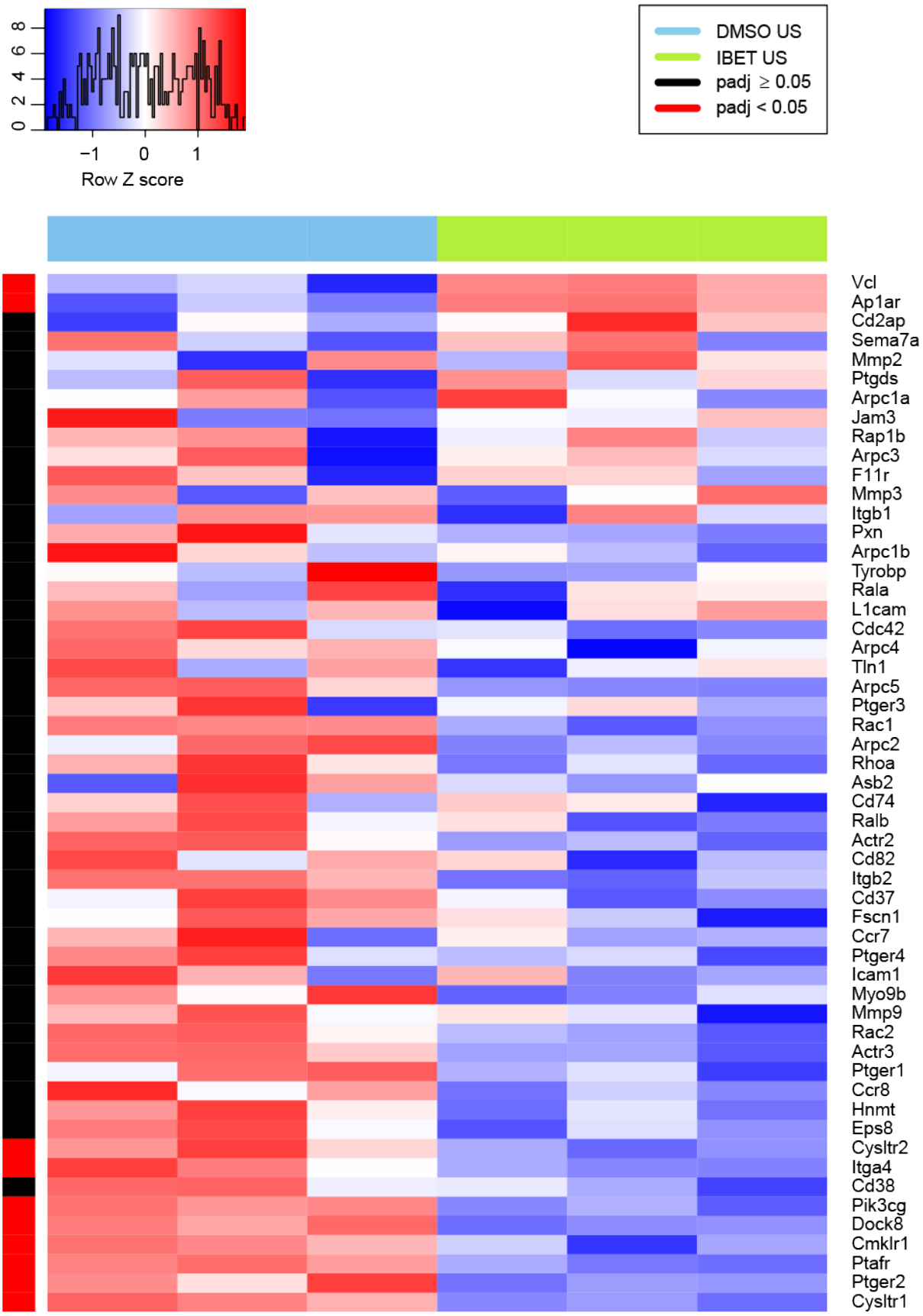


*Figure 85: Heatmap showing differential expression of genes implicated in DC migration following a 4 hour treatment with I-BET or DMSO*

A further analysis was performed on BMDM treated with OVA or OVA-IC for four hours, in the presence or absence of I-BET (Figure 86). *Ccr7* is upregulated by the addition of OVA-IC only in the absence of I-BET. The prostaglandin receptor genes (*Ptger1*, *Ptger2* and *Ptger4*) appear to be downregulated in the presence of I-BET; prostaglandin signalling is known to be important for the induction of *Mmp9*, which also appears to be downregulated by I-BET. I-BET downregulated leukotriene receptor genes, critical for the leukotriene mediated induction of capacity for DC to migrate towards CCL19. Additionally, I-BET downregulates the expression of the Rac family of GTPases (*Rac1* and *Rac2*) and the adhesion molecules integrin alpha 4 (*Itga4*), as well as both integrin beta 1 (*Itgb1*) and CD38 (*Cd38*), that are upregulated in response to FcγR crosslinking in the absence of I-BET.

### 5.3.3 Effect of I-BET on CCR7 protein expression unclear

We measured the expression of surface CCR7 on bone marrow derived dendritic cells using flow cytometry. We saw significant interexperiment variability; on some occasions I-BET clearly inhibited IC dependent CCR7 upregulation as suggested by the microarray analysis (Figure 87A upper panel results type A) whereas in others I-BET caused a concentration dependent increase in CCR7 expression (Figure 87A lower panel results type B), irrespective of whether IC was added. Figure 87B shows summary data from multiple experiments. Overall there was a trend towards increased CCR7 expression following I-BET treatment but this did not reach statistical significance. We queried whether the I-BET used may have been contaminated with LPS but variability was seen with fresh stocks and did not impact on results from alternative experiments run at the same time.

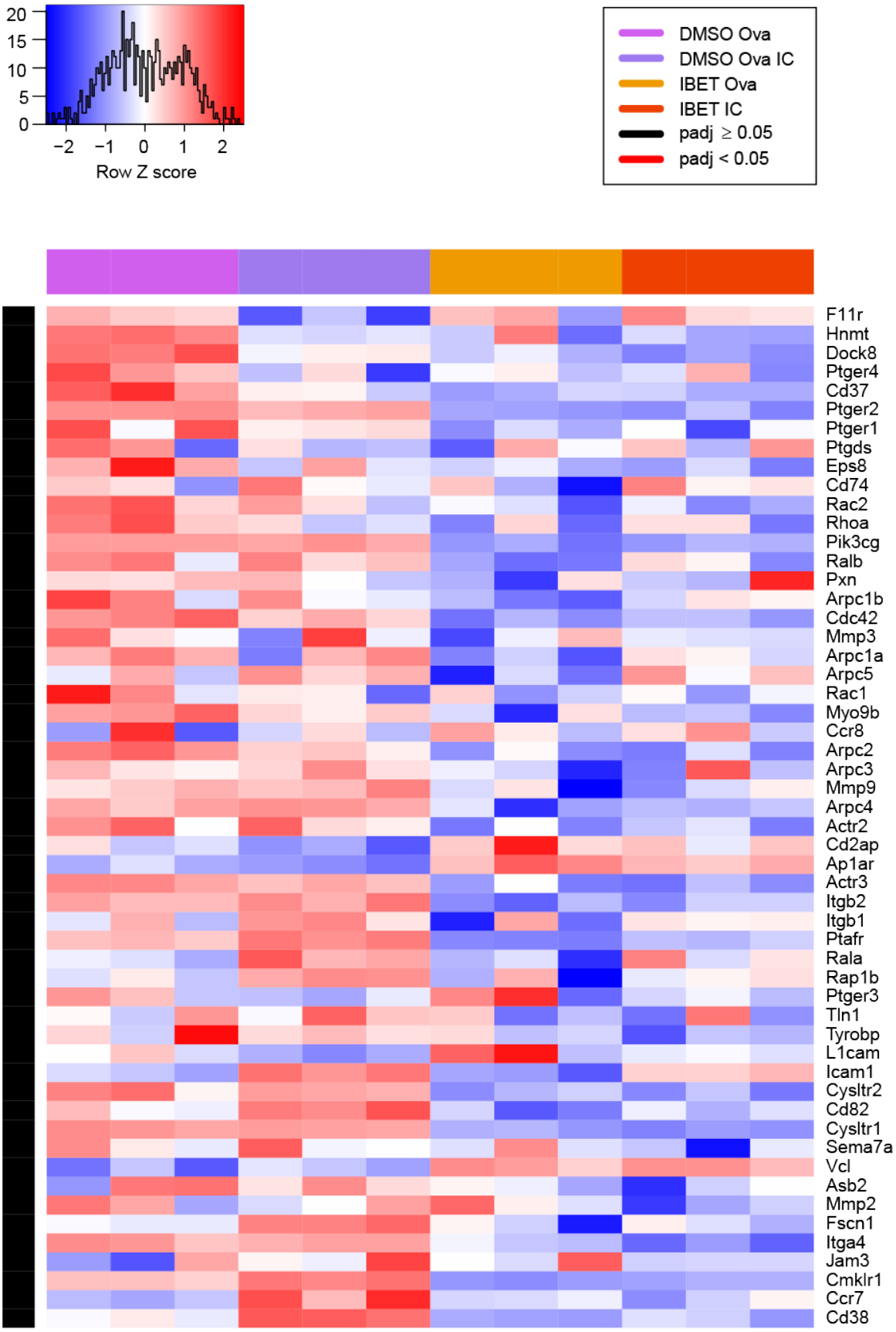


*Figure 86: Heatmap showing differential expression of genes implicated in DC migration following a 4 hour treatment with I-BET or DMSO plus OVA or immune complexed OVA. The p value demonstrated*

*refers to the diff comparison, showing genes for which I-BET significantly impacts on the effect of OVA-IC*

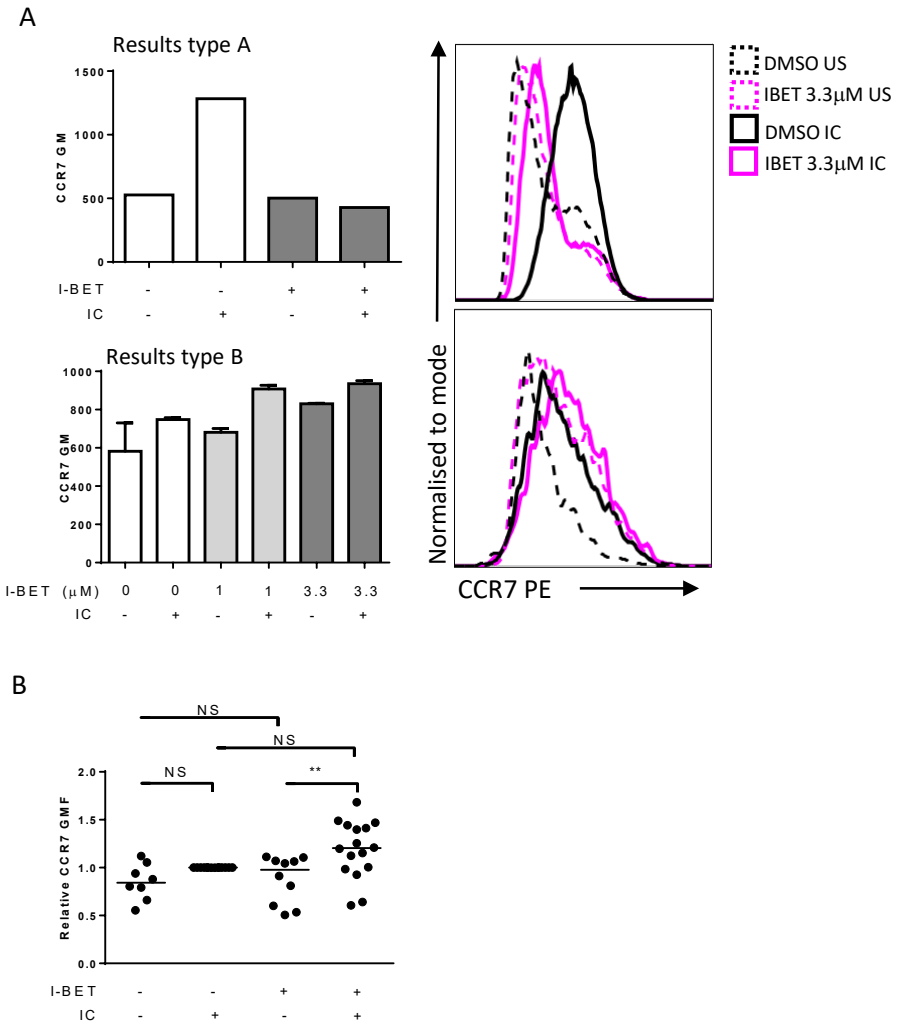


Figure 87: Surface CCR7 expression measured by flow cytometry. A: results from two representative experiments showing the different trends seen. B: Summary data from 14 independent experiments; each individual point represents the mean of technical replicates (up to three) within each experimental. I-BET was used at a concentration of 3.3μM in all but two experiments where it was additionally used at a concentration of 1μM (displayed by a separate point). Stimulation overnight in all but two experiments where it was only four hours. Groups compared using Wilcoxon matched-pairs signed rank test (*NS p>0.05; **p<0.01)*.

### 5.3.4 I-BET151 inhibits CCL19 guided migration *in vitro*

Due to the changes seen in cell morphology and adhesion, we hypothesised that I-BET151 would impact cell migration, a process that is also dependent on actin polymerisation. Initially we quantified cell migration in a simple transwell migration assay (Figure 88). We observed variation

between assays in the proportion of cells migrating, with a trend towards reduced migration following I-BET treatment (Figure 88B). The effect of I-BET appeared more marked when cells were exposed to a chemokine gradient (Figure 88C).

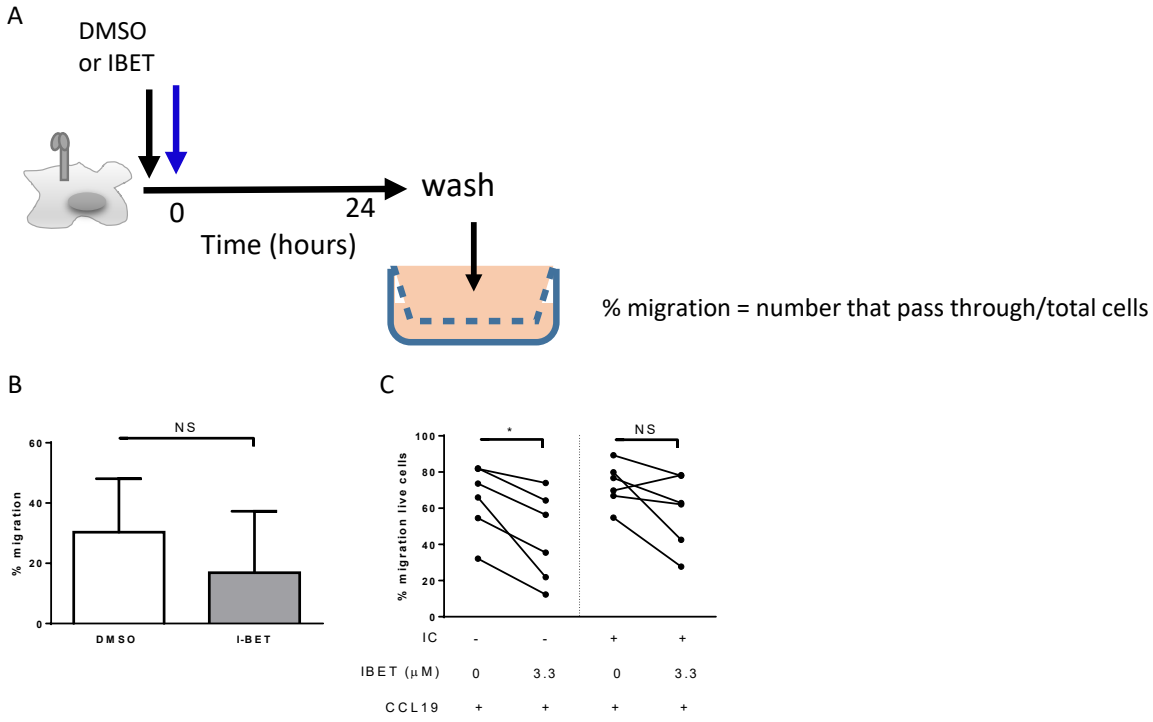


*Figure 88: Effect of I-BET on a transwell migration assay. BMDC were stimulated for 24 hours with OVA-IC in the presence of DMSO or I-BET151. Following washing their migration was assessed in a transwell migration assay (A). B shows results from of four experiments (I-BET used at a concentration of between 1 and 5 μM).; p NS via Mann-Whitney test. C shows results from single experiment where cells were exposed to a gradient of CCL19 (nM). P values calculated Wilcoxon matched-pairs signed rank test (NS p>0.05; *p<0.05).*

Due to concerns regarding the simplicity of this assay and its relevance to migration *in vivo*, along with concerns regarding its reproducibility, we went on to quantify the migration of dendritic cells in a 3D collagen matrix. Bone marrow was collected from fluorescently tagged reporter mice and differentiated into dendritic cells *in vitro* according to our standard protocol. Cells were treated with OVA-IC in the presence of DMSO or I-BET, then loaded into a collagen gel, which was allowed to set within an Ibidi® μ-Slide chemotaxis slide. Cell migration was imaged using time lapse confocal microscopy and cell movement tracked by applying surfaces to the images using Imaris image analysis software (Figure 89). FcγR crosslinking in the absence of I-BET led to an increase in CCL19 guided chemotaxis with increased forward migration parallel to the chemokine gradient and increased track displacement. I-BET treatment appeared to dampen chemokine directed movement,

with trends suggesting reduced deviation of the average cell centre of mass, reduced average forward migration index and reduced track displacement.

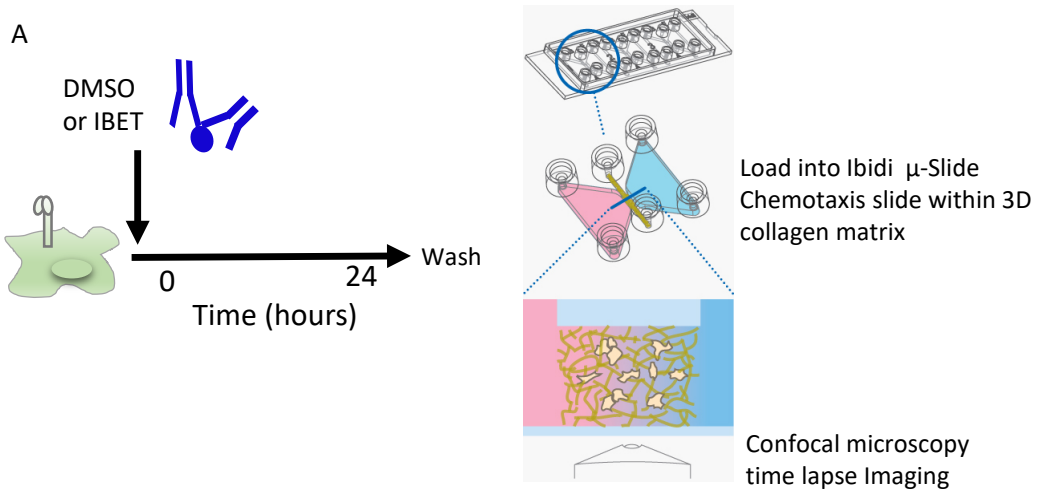


Bi) DMSO

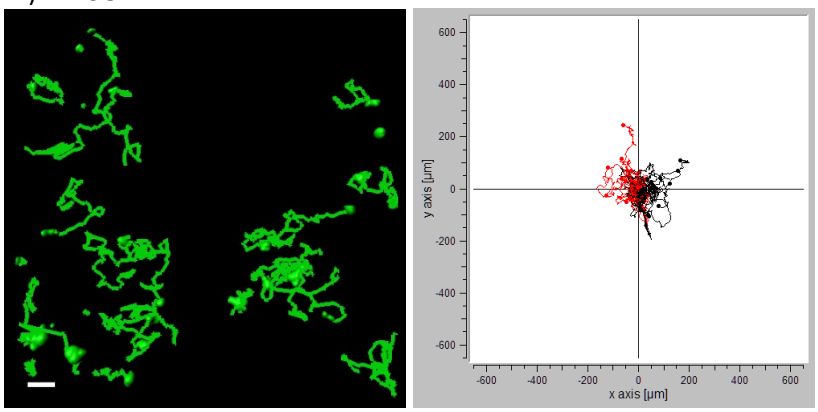


Bii) DMS0; CCL19 gradient

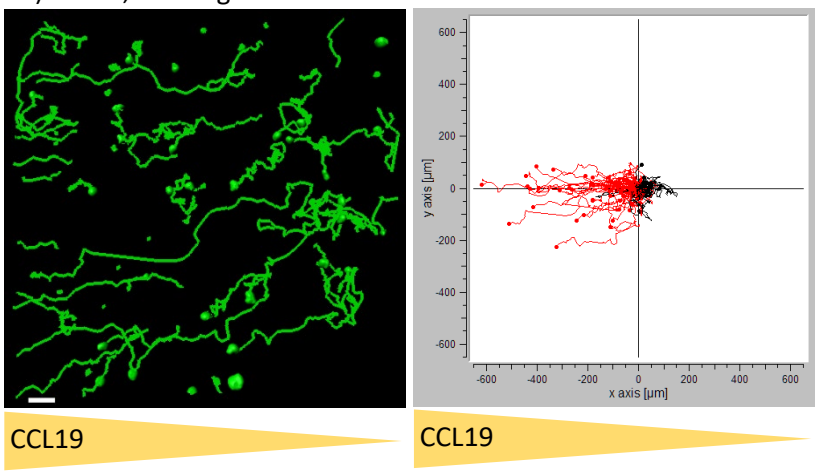

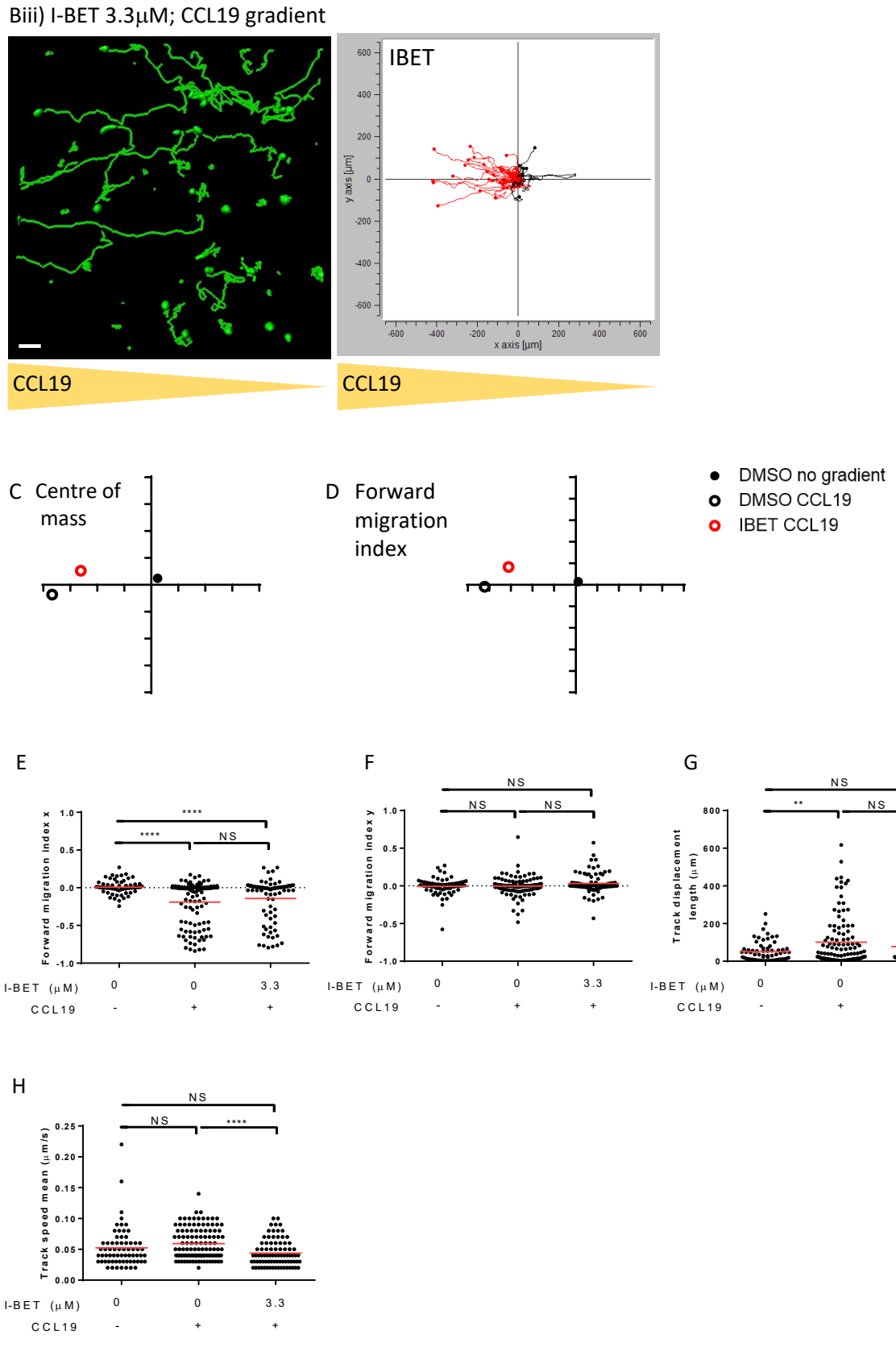


*Figure 89*: An *in vitro* model of CCL19 guided migration. *Bone marrow derived dendritic cells were stimulated for 24 hours with OVA-IC in the presence of DMSO or I-BET151 (3.3µM). Following*

*washing their migration was assessed in a 3D collagen matrix (A). B shows representative images following migration for 2 hours 43min (left) and the migration tracks of individual cells from two independent experiments (right), tracked using surfaces within Imaris image analysis software and plotted using the Ibidi Chemotaxis and Migration tool. Red tracks indicate cells with a negative final displacement in the x axis plane. I) DMSO treated cells in the absence of a chemokine gradient; ii) DMSO treated cells in the presence of a chemokine gradient; iii) I-BET treated cells in the presence of a chemokine gradient. The average centre of mass (C) and forward migration index parallel and perpendicular to the chemokine gradient (D) were calculated for the labelled conditions. Quantification of forward migration in the direction parallel to the chemokine gradient (E) and perpendicular to the chemokine gradient (F), track displacement length (G) and mean track speed (H). Results combined from of two independent experiments; red line indicates mean; p values calculated using unpaired student t tests (NS p>0.05; **p<0.01; ****p<0.0001).*

The Ibidi® µ-Slide chemotaxis slide allows concurrent imaging of three windows containing a collagen gel and therefore three chemokine gradients. We further optimised the assay by combining cells derived from two differently labelled fluorescent mice (Figure 90). This allowed us to test the migration of DMSO and I-BET treated cells, each with a different fluorescent tag within the same collagen matrix. Inconsistencies in the setting of collagen can affect the ease with which a cell can migrate through the gel; the optimisation therefore not only doubled the number of conditions that we were able to test in a single experiment, but also had the additional benefit of removing any inconsistencies related to the collagen itself, since cells were exposed to the same collagen matrix. In the absence of a chemokine gradient (Figure 90B), I-BET treated cells displayed increased random movement with increased track displacement, total track length and speed. However, chemokine directed migration (Figure 90C), was impeded in the presence of I-BET, demonstrated by reduced displacement of the average centre of mass (Figure 90D), reduced track displacement parallel to the chemokine gradient (Figure 90F), with a trend towards a reduced forward migration index parallel to the chemokine gradient (Figure 90E, G). This reduction in chemokine directed movement was observed despite an I-BET induced increase in overall movement, indicated by increased track length (Figure 90K) and speed (Figure 90L, M).

A

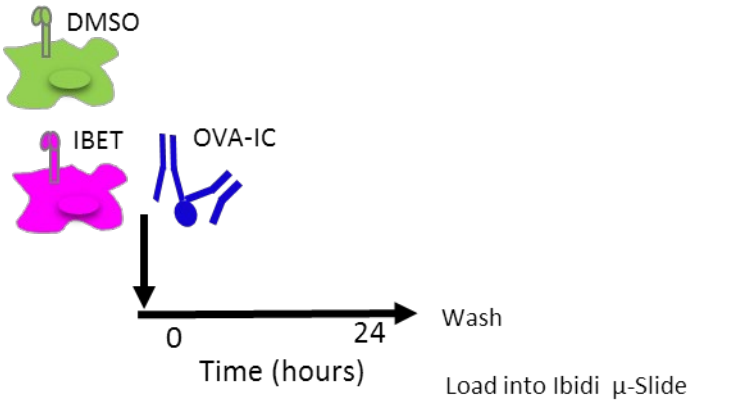


Wash

Load into Ibidi µ-Slide Chemotaxis slide within 3D collagen matrix

Time lapse Imaging using confocal microscopy

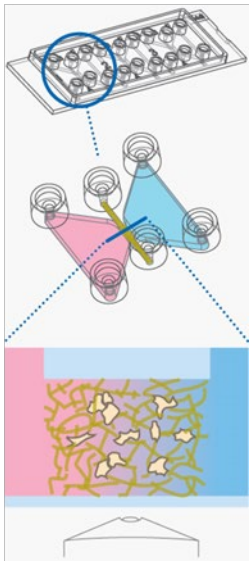

B i) ii) iii)

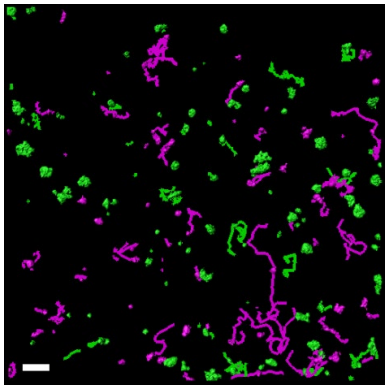

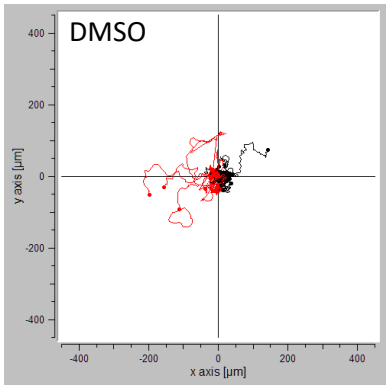


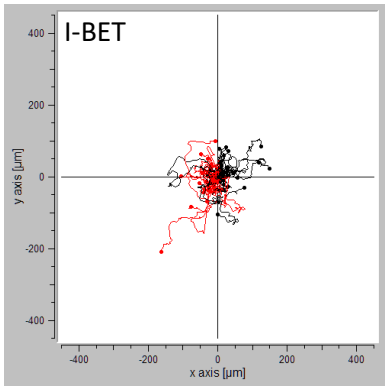


C i) ii) iii)

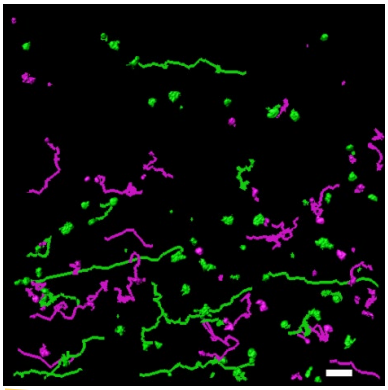

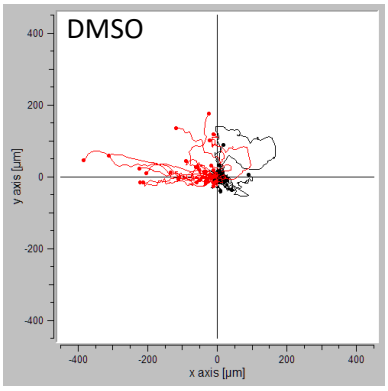


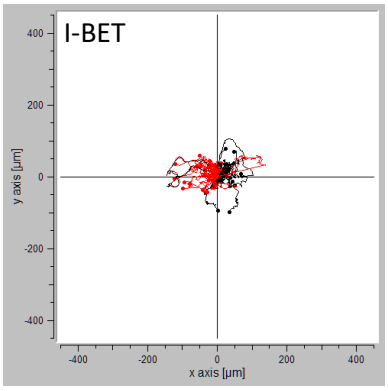


CCL19 CCL19 CCL19

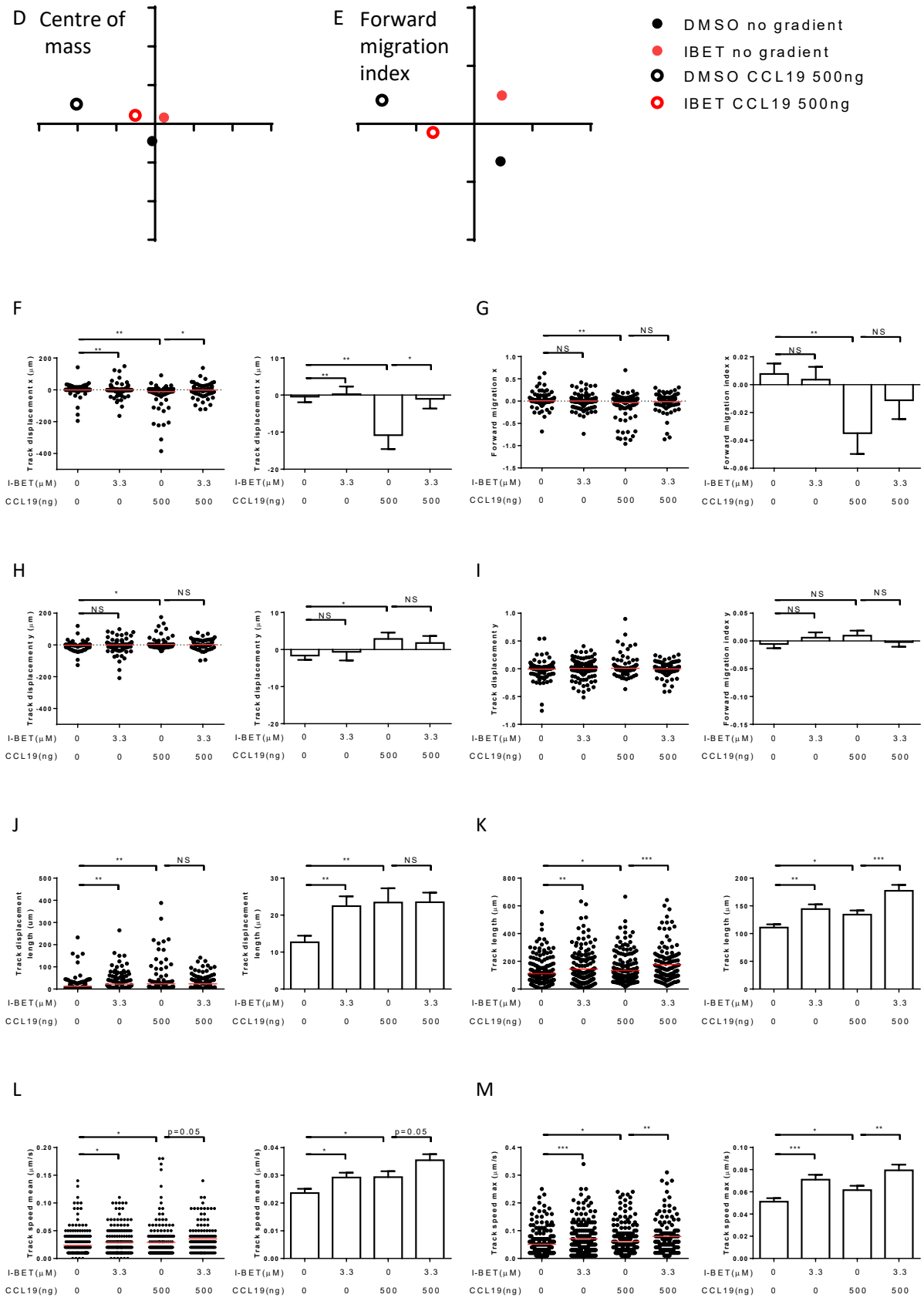
D Centre of mass
E Forward migration index
DMSO no gradient
IBET no gradient
DMSO CCL19 500ng
IBET CCL19 500ng
F
G
H
I
J
K
L
M
Track displacement x (µm)
Track displacement y (µm)
Forward migration x
Forward migration index x
Forward migration index y
Track displacement
Track displacement length (µm)
Track length (µm)
Track speed mean (µm/s)
Track speed max (µm/s)
I-BET(µM) 0 3.3 0 3.3
CCL19(ng) 0 0 500 500
NS
p=0.05

*Figure 90: I-BET151 inhibits CCL19 guided migration in vitro. BMDC were stimulated for 24 hours with OVA-IC in the presence of DMSO (GFP labelled) or I-BET151 3.3µM (RFP or CFP labelled). Following washing their migration was assessed in a 3D collagen matrix (A). B shows migration in the absence of a chemokine gradient with C showing migration in the presence of a 500ng CCL19 gradient (greatest to the left of the image. i) representative image following imaging for 2 hours, scale bar 50µm, ii) migration tracks of DMSO treated cells iii) migration tracks of I-BET treated cells. The average centre of mass (D) and forward migration index parallel and perpendicular to the chemokine gradient (E) were calculated for the labelled conditions. Individual cell data and means are shown for track displacement$_{x\ axis}$ (F), forward migration$_{x\ axis}$ (G), track displacement$_{y\ axis}$ (H), forward migration$_{y\ axis}$ (I), track displacement length (J), track length (K), mean track speed (L) and maximum track speed (M). Data from two independent experiments. Red lines indicate the mean; boxplots show mean and standard error of the mean. P values calculated using unpaired student t test (NS p>0.05; *p<0.05; **p<0.01; ***p<0.001).*

### 5.3.5 I-BET151 inhibits dendritic cell mobilisation and migration *in vivo*

Using two photon microscopy, with time lapse imaging of the movement of dermal DC within the hind footpad of mice expressing eYFP in CD11c+ cells (Figure 91), we showed that I-BET inhibits DC mobilisation in response to FcγR crosslinking. Imaging was performed in FcγRIIb null (FcγRIIb-/-) and wildtype C57B/6 (FcγRIIb+/+) mice; with pairs of age and sex matched mice imaged on the same day, one treated with I-BET and one treated with solvent control. In solvent treated mice, FcγR crosslinking by OVA-IC led to increased dermal DC movement with increased track length (Figure 91Bi, Bii, Ci, Cii). In FcγRIIb-/- mice the effect of crosslinking of activatory FcγR was abrogated in I-BET treated animals; track length and displacement were reduced following I-BET treatment (Figure 91Bii, iii) and an increase in cell migration speed was seen only in the absence of I-BET treatment (Figure 91Biv, v). In FcγRIIb+/+ mice, I-BET treatment actually led to an increase in mean track speed (Figure 91Cv), though movement was restricted and inefficient resulting in increased cumulative track length (Figure 91Cii) but reduced track displacement (euclidean distance) (Figure 91Ciii).

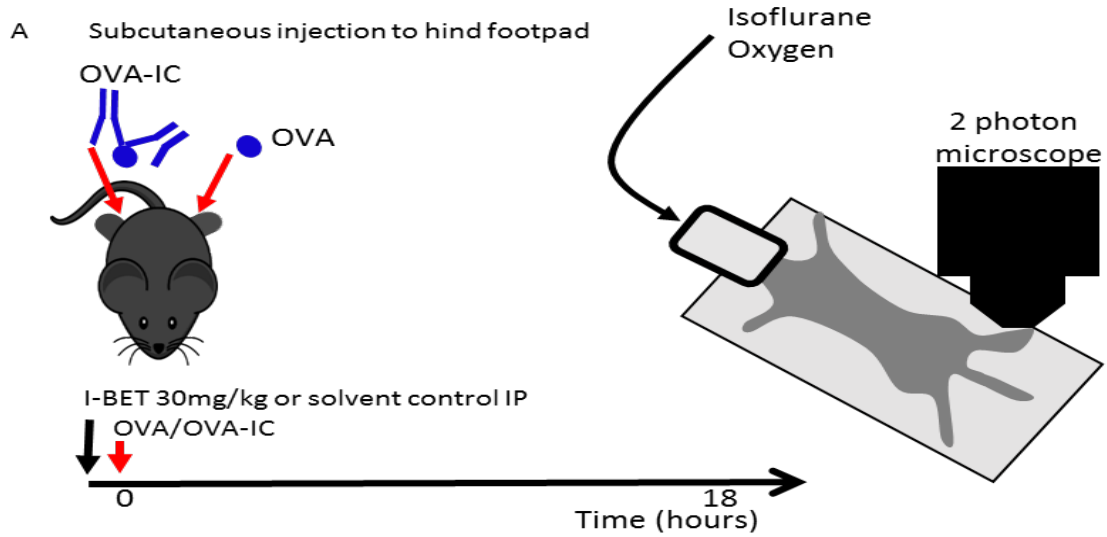
A
Subcutaneous injection to hind footpad
OVA-IC
OVA
Isoflurane
Oxygen
2 photon
microscope
I-BET 30mg/kg or solvent control IP
OVA/OVA-IC
0
18
Time (hours)

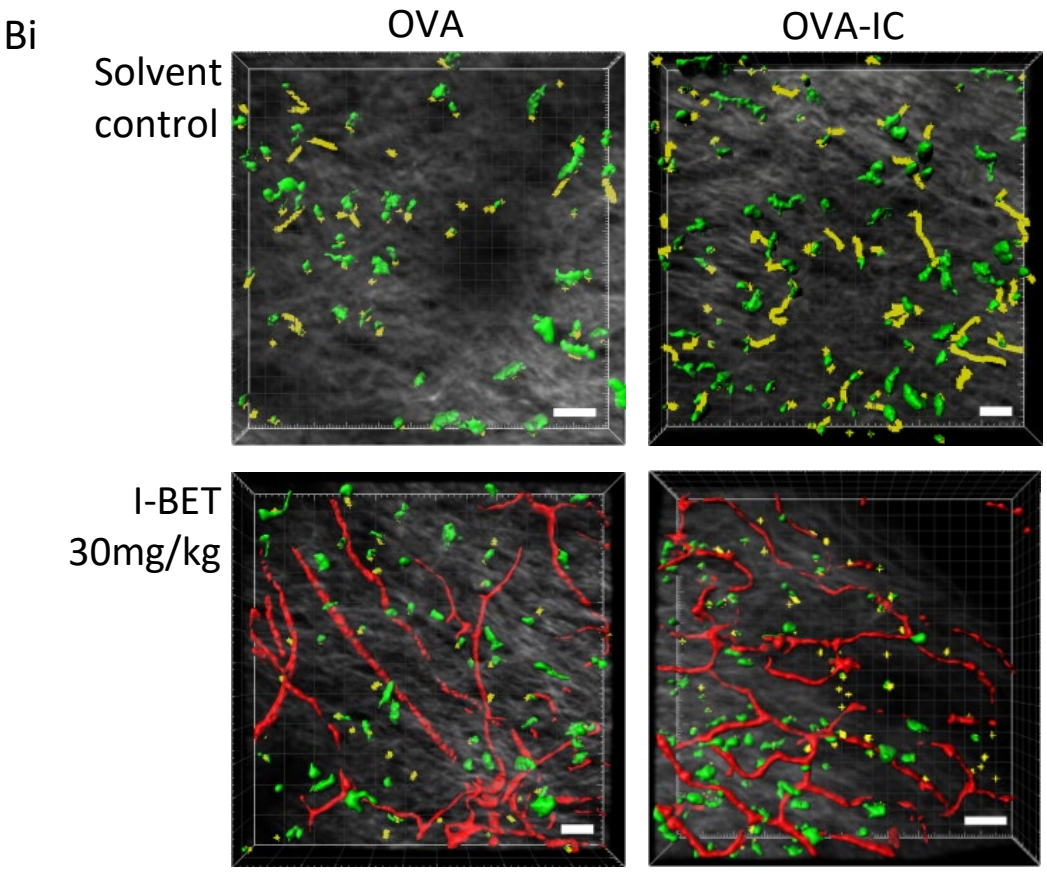
Bi
OVA
OVA-IC
Solvent
control
I-BET
30mg/kg

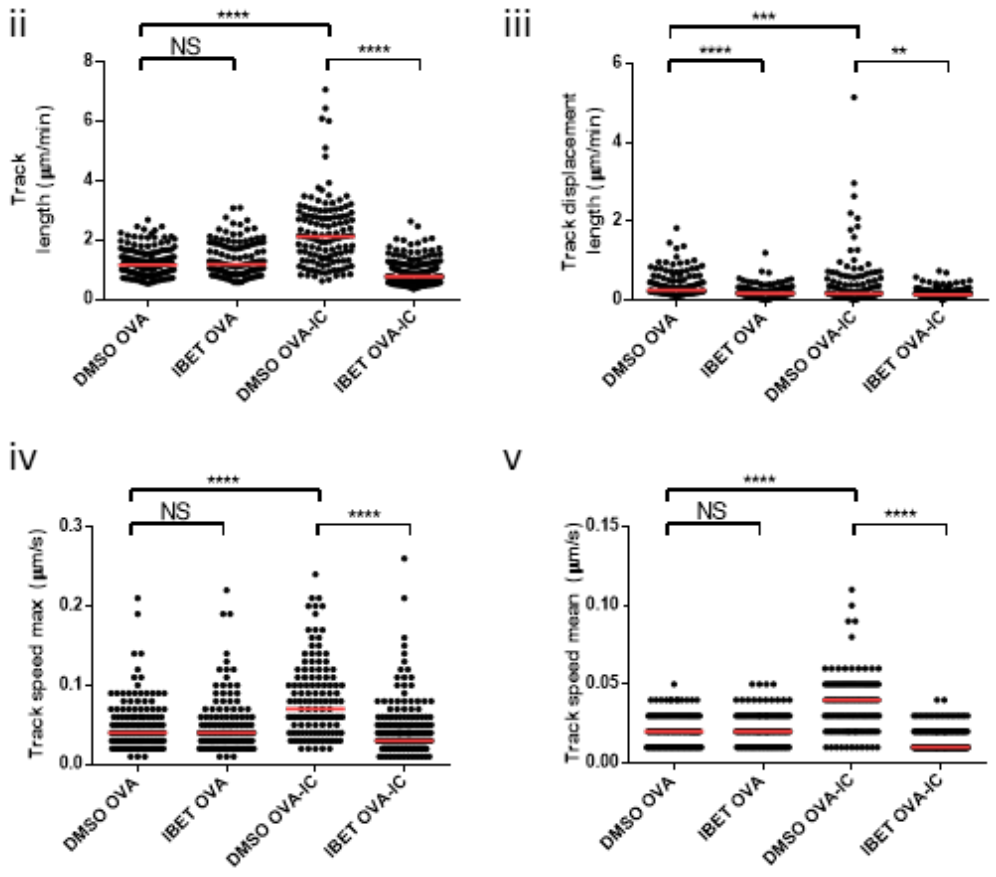
ii
iii
iv
v
Track length (µm/min)
Track displacement length (µm/min)
Track speed max (µm/s)
Track speed mean (µm/s)
NS
****
***
**
DMSO OVA
IBET OVA
DMSO OVA-IC
IBET OVA-IC

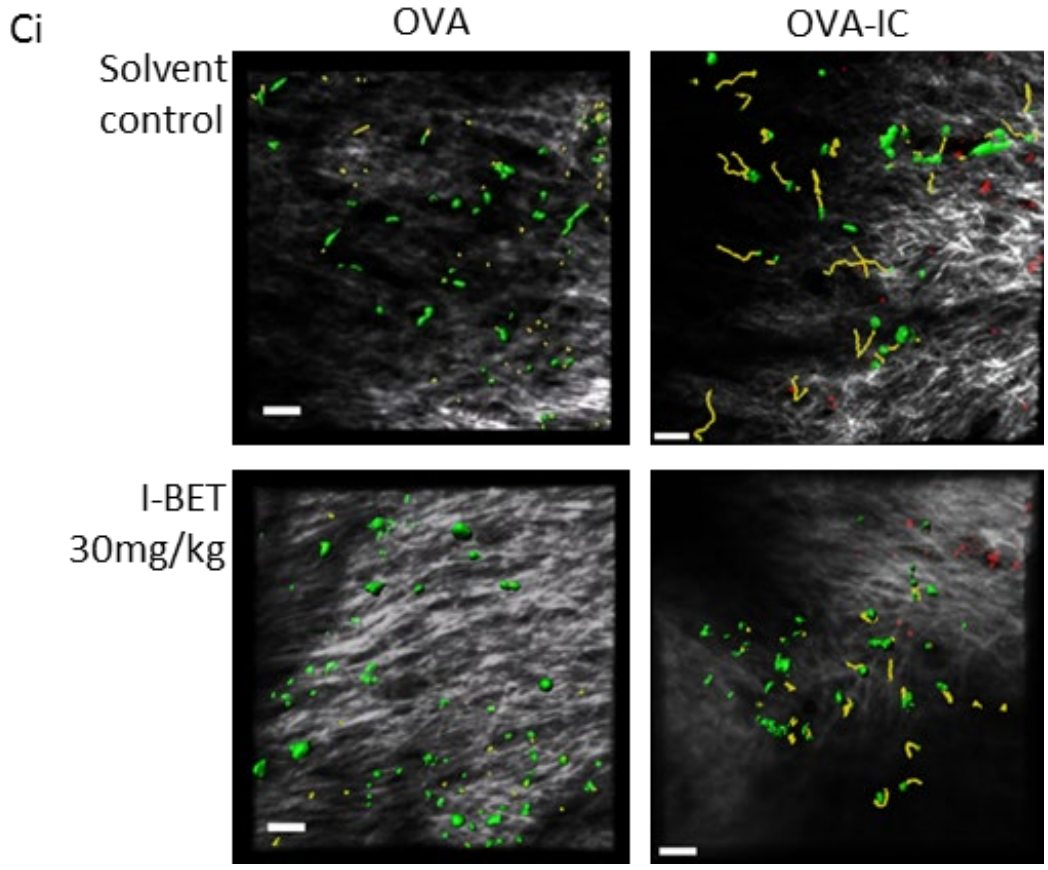
Ci
OVA
OVA-IC
Solvent control
I-BET 30mg/kg

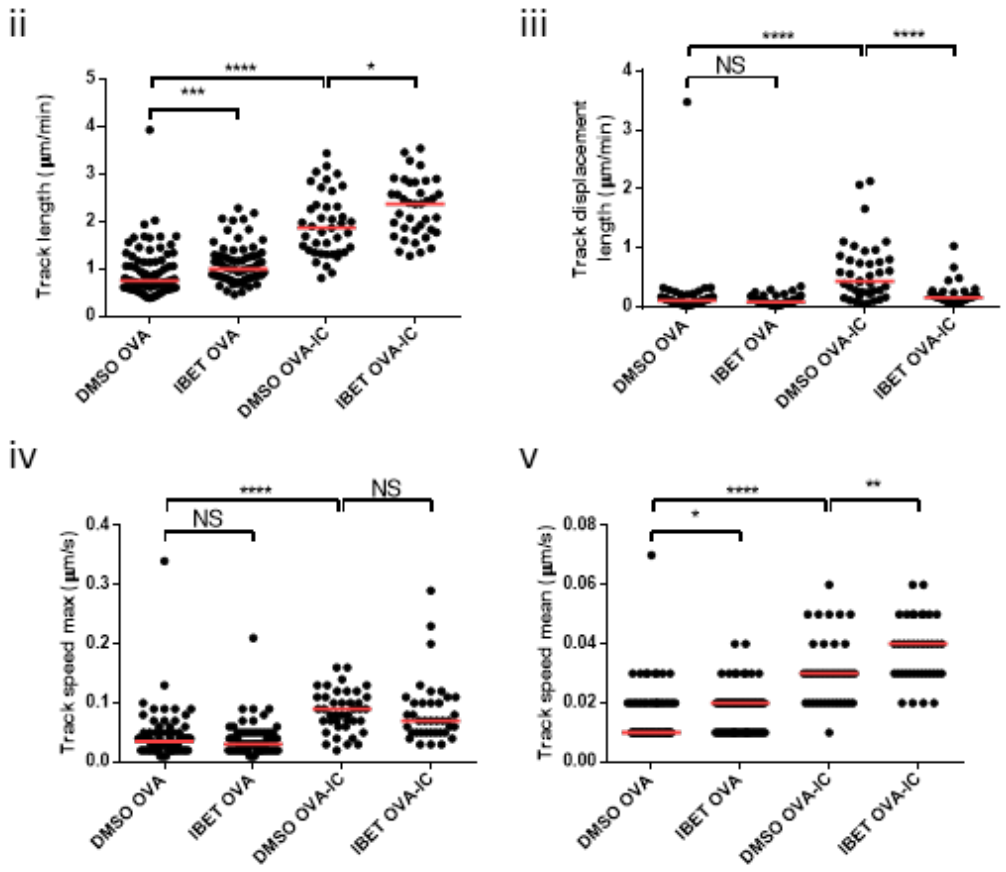


*Figure 91: I-BET inhibits DC migration in vivo in wildtype and* FcγRIIb-/- mice. *A shows the experimental set up; following treatment with I-BET or solvent control, mice were injected with OVA in one hind footpad and OVA-IC in the contralateral footpad, with imaging under isoflurane anaesthesia 18 hours later. B shows results from a representative experiment (1 of 2) using a pair of* FcγRIIb -/- mice. C shows results from a pair of wildtype BLK/6 mice. i) Dermal DC in the field of view were surface mapped and tracked in Imaris image analysis software. DC visible at the end of imaging are shown in green alongside *representative tracks (yellow) and 50µm scale bar; blood vessels were visualised via intravenous injection of Qdot probe, with surface mapping in Imaris software applied to the end time slice (shown in red (note injection and visualisation not successful in all mice)). Track length (ii), track displacement length (iii), maximum track speed (iv) and mean track speed (v) were quantified using surface tracking in Imaris image analysis software. Track lengths were calculated per minute imaged to account for differences in track duration. Red bars indicate medians; treatment groups were compared using Mann Whitney tests (NS p>0.05; *p<0.05; **p<0.01; ****p<0.0001).*

Immune complexes stimulate dermal dendritic cell migration to lymph nodes in a CCR7 and FcγR dependent manner (Clatworthy 2014a). In order to determine if I-BET151 has an effect on dendritic cell migration *in vivo*, we topically administered FITC to the skin in order to label dermal DCs,

stimulated them with IC, and harvested draining lymph nodes 48 hours later, as described in (Clatworthy 2014a) (Figure 92 & 93). I-BET151 reduced the number of migrating DCs identified in lymph nodes following IC stimulation. We observed no obvious systemic side effects in mice treated with I-BET 30mg/kg over a 48 hour period, with no difference in weight from those treated with a solvent control (Figure 93C). We found reduced numbers (Figure 92D) and proportion (Figure 92B, E) of FITC+, MHC class II high, CD11c+ dendritic cells in the draining and non draining lymph nodes of I-BET treated animals, compared to those treated with a solvent control, with similar effects on both dermal and Langerhans DC's.

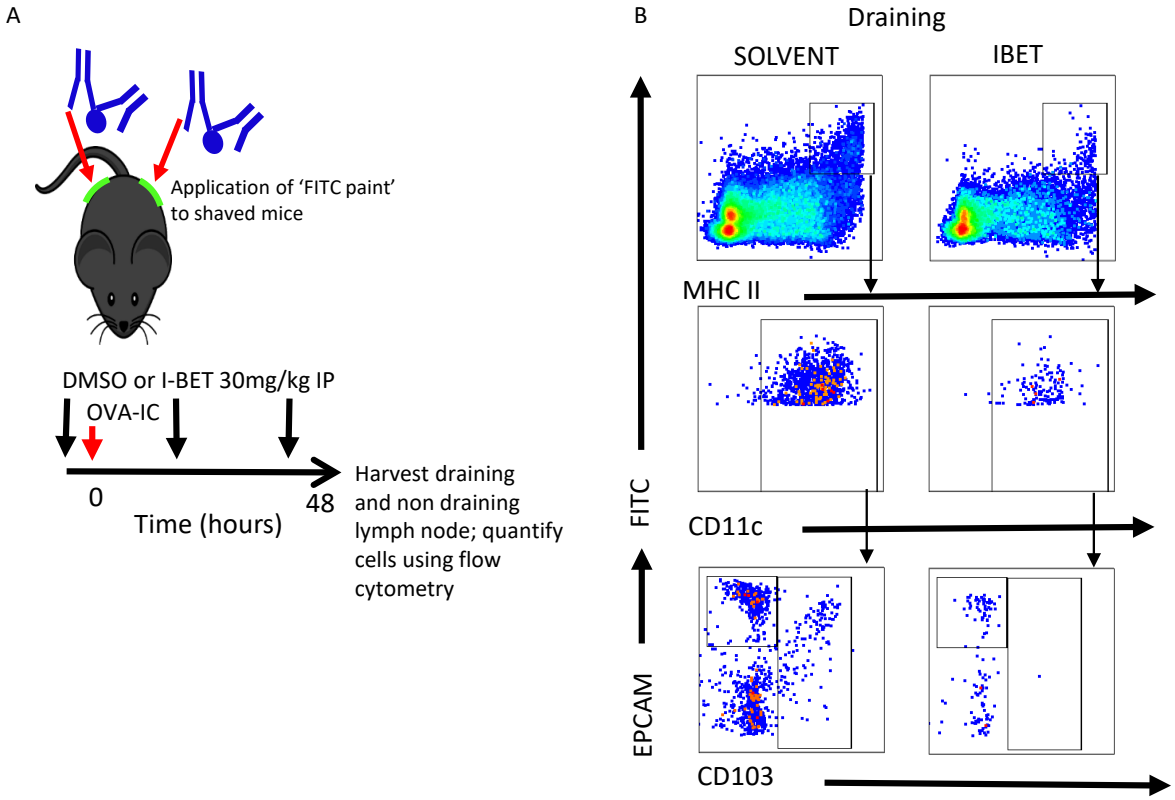


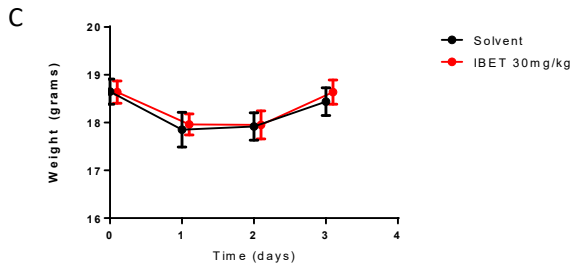

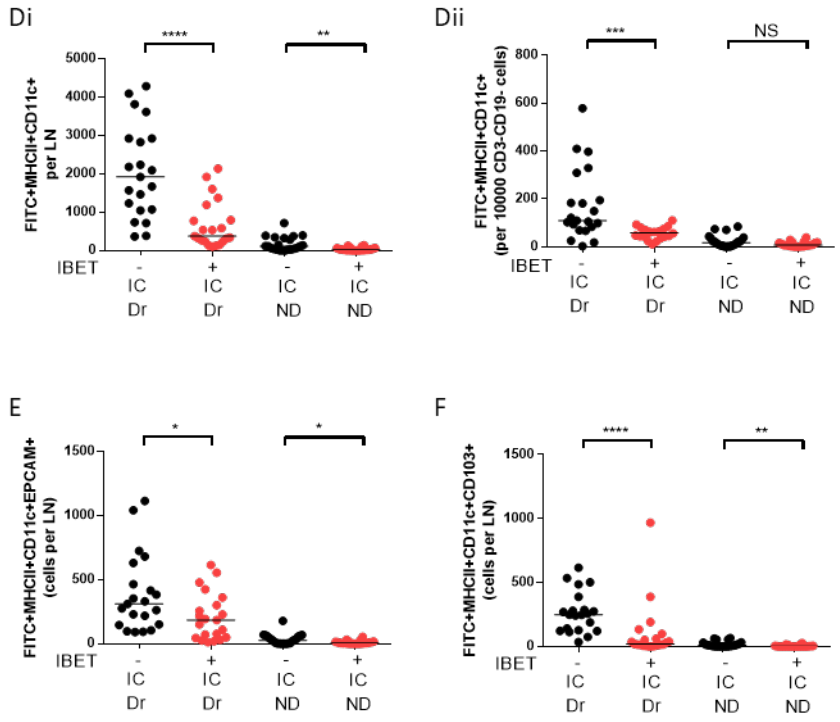


*Figure 92: I-BET inhibits DC migration in an in vivo FITC paint model. A shows the experimental set up. B shows representative flow cytometry plots. Summary of results showing animal weight (C), FITC+MHCII+CD11c+ DC numbers per lymph node (Di) and per 10000 CD3-CD19- cells (Dii), FITC+MHCII+CD11c+ EPCAM+ Langerhan DC (E) and FITC+MHCII+CD11c+CD103+ dermal DC (F). Data from 4 independent experiments. Line displays median value. P values calculated using Mann-Whitney tests (NS p>0.05; *p<0.05; **p<0.01; ***p<0.001; ****p<0.0001). Dr draining lymph node. ND non draining lymph node.*

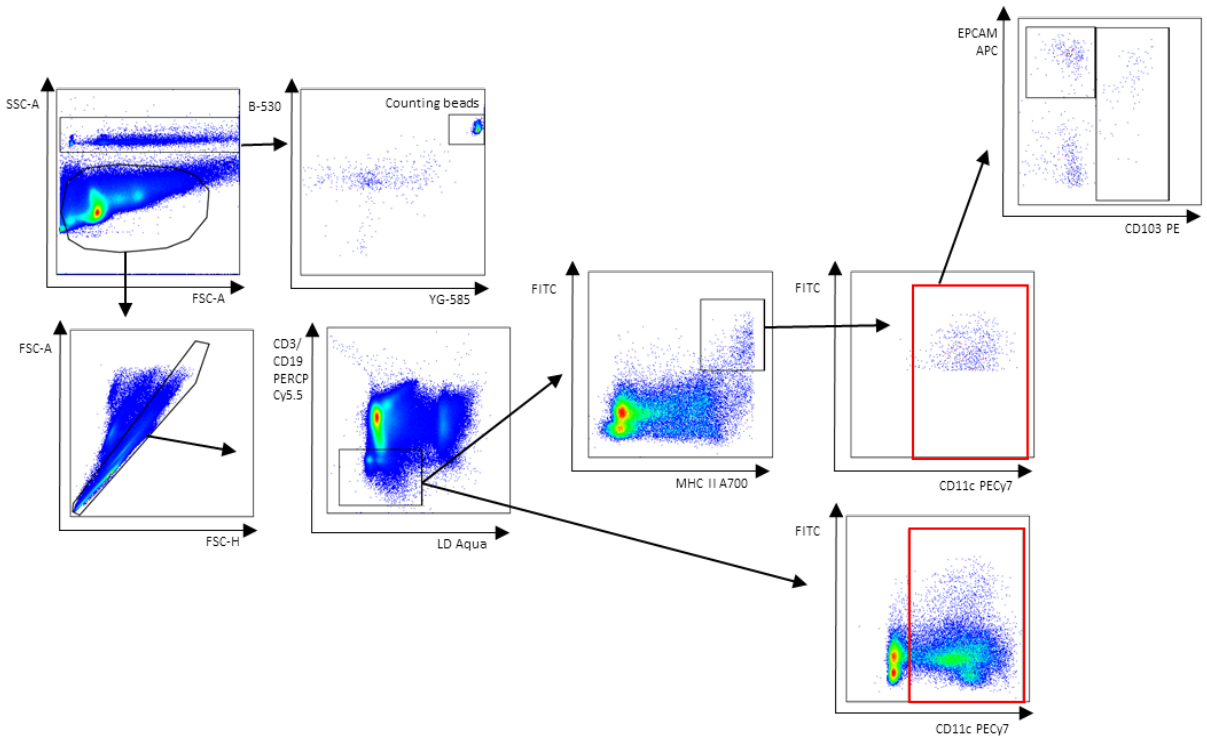


*Figure 93: Representative plots of gating strategy used in FITC paint experiment*

We noted that mice treated with systemic I-BET151 for the 48 hour period used in our FITC paint model, had smaller lymph nodes. This associated with reduced live cell numbers when quantified by flow cytometry, suggesting a change in DC lymph node homeostasis (Figure 94).

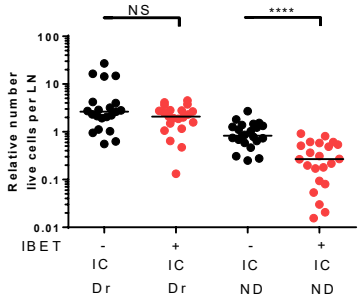


*Figure 94: I-BET reduces lymph node size. Quantification of lymph node cell number following FITC painting. The non draining lymph nodes in I-BET treated mice were macroscopically smaller and contained fewer cells. Results from four independent experiments. Line displays median value; groups compared using Mann Whitney test (NS p>0.05; ****p<0.0001).*

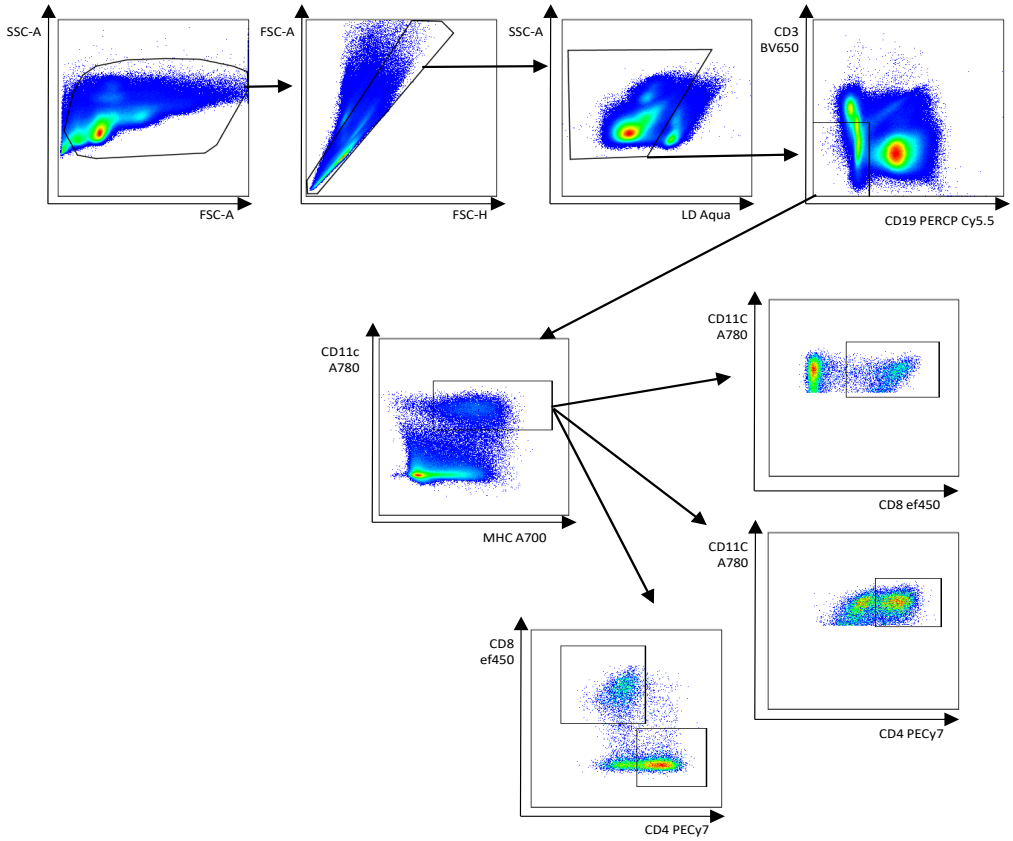


*Figure 95: Representative gating strategy used for quantification of splenic DC subsets*

Analysis of spleens by flow cytometry (Figure 95 & 96) revealed a reduction in the number of lymphoid organ resident DC (Figure 96B), with a specific loss of $CD8^+$ cDC in mice treated with I-BET151, leading to a reduced proportion and number of this subset (Figure 96C). There was relative preservation of $CD4^+$ DC (Figure 96D).

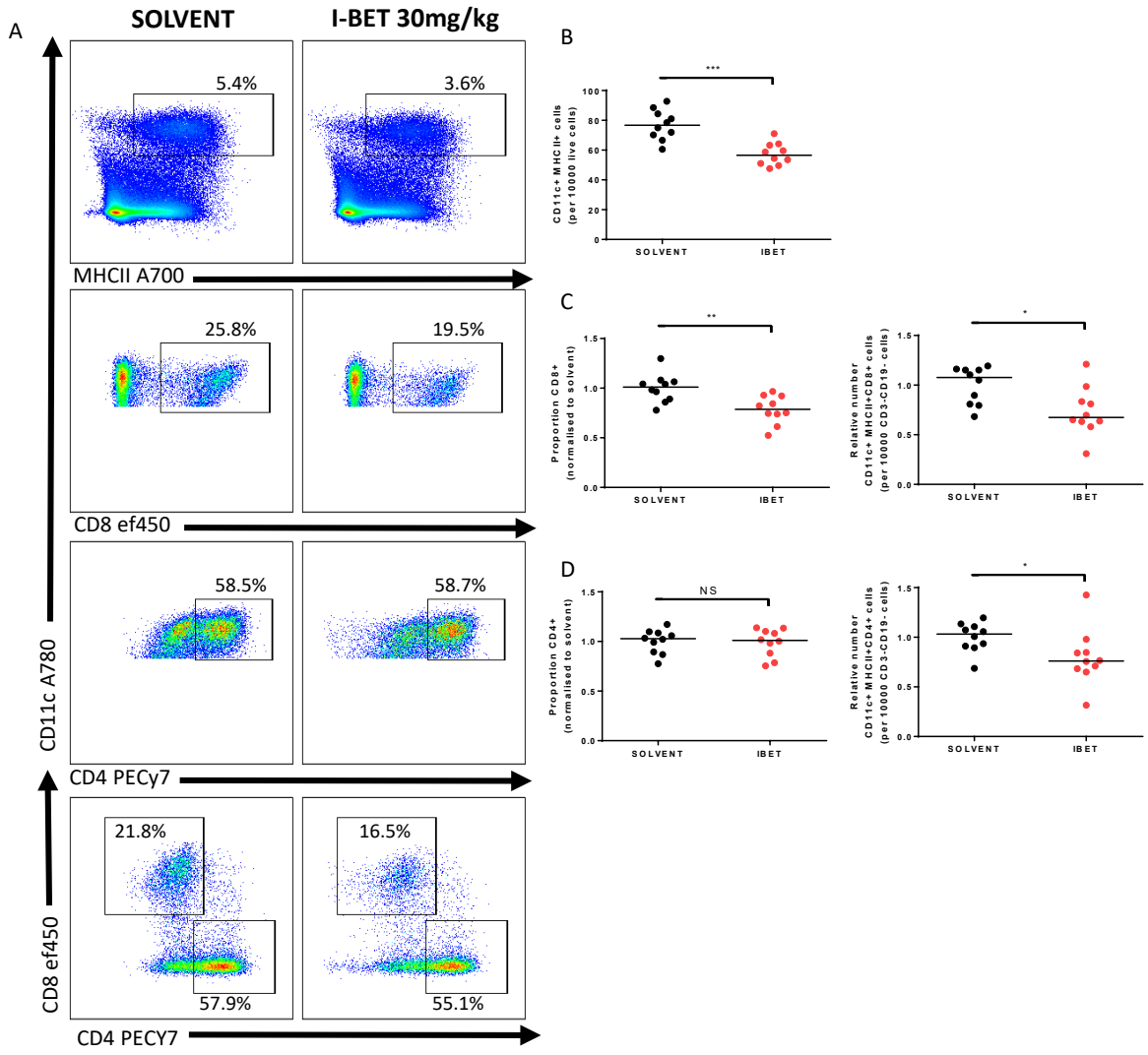


*Figure 96: I-BET reduces the number of splenic DCs with preferential reduction in CD8+ DC. Results from two independent FITC paint experiments shown. Panel A shows representative plots with quantification of DC number (B), CD8 (C) and CD4 (D) expression. Lines represent medians; groups compared using Mann-Whitney tests (NS p>0.05; *p<0.05; **p<0.01; ***p<0.001). Where relative counts shown; results normalised to the mean solvent value in each individual experiment.*

We next wished to explore whether the effect of I-BET was DC intrinsic since systemic treatment of animals with I-BET may have effects on other cell populations as well as chemokine gradients. We transferred GFP expressing DC, stimulated with OVA-IC *in vitro* in the presence or absence of I-BET to wild type C57BL/6 mice and quantified the number of GFP+ DC in the draining and non draining lymph nodes 48 hours later (Figure 97 & 98). We observed a trend towards reduced migration of I-BET treated DC, however there was marked variation in the number of GFP+ DC detected in different mice within the same experiment, who received the same amount of fluorescently labelled DC. We were therefore unable to rule out bias caused by variation in injection technique.

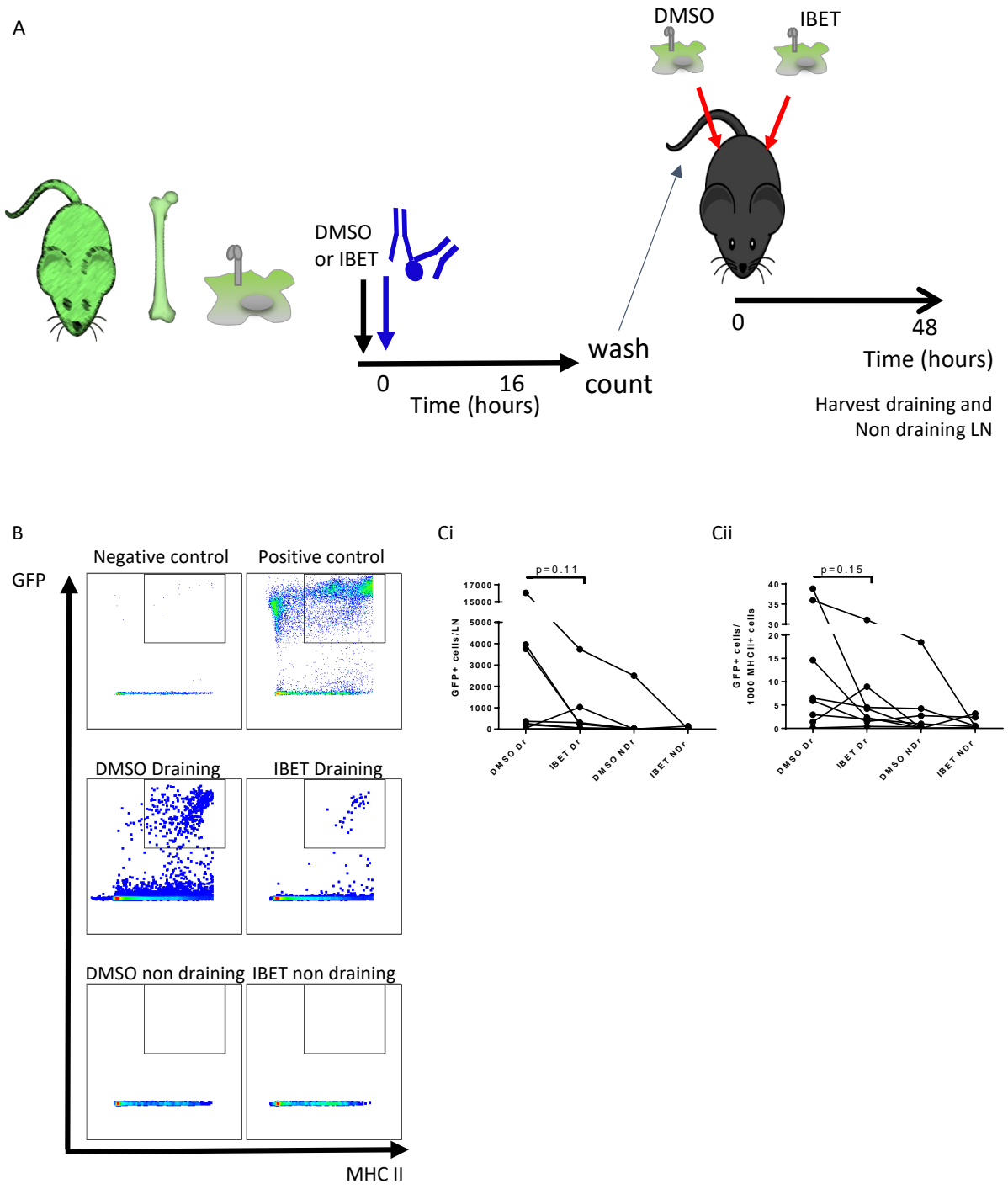


*Figure 97: I-BET inhibition of DC migration appears to be DC intrinsic in a cell transfer model. A shows the experimental set up. B shows representative flow cytometry plots gated on live CD3-CD19- singlets. Positive control made by mixing GFP positive DC with homogenised lymph node suspension in vitro. Summary of results showing GFP+ cells per lymph node (Ci) and per 10000 MHCII+ cells (Cii). P values calculated using Mann-Whitney test.*

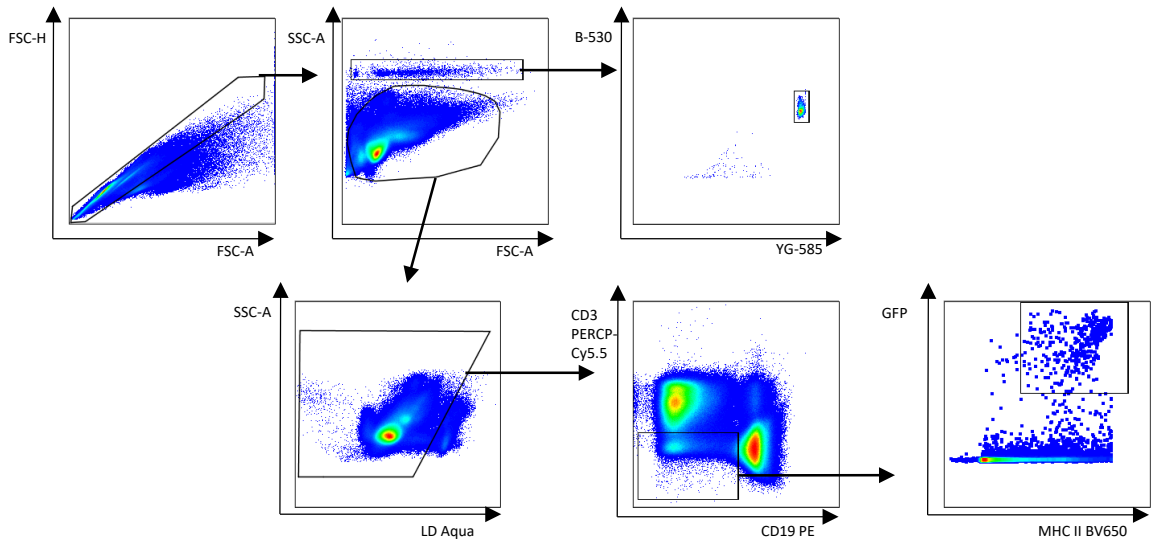


*Figure 98: Representative plots of gating strategy used in GFP DC cell transfer experiment*

We optimised the experiment using DC differentiated from multiple mouse strains, each expressing a different fluorescent reporter protein (GFP and cyan-fluorescent protein (CFP) mice). This allowed us to transfer a mix of I-BET and solvent treated DC and quantify the numbers reaching each lymph node; each lymph node would serve as its own control, removing any bias caused by differences in injection efficiency (Figure 99 & 100). The GFP signal was brighter than the CFP signal used; so GFP cells were treated with I-BET to maximise the chance of detection. A sample of the transferred cell mix was stained to ensure that an equal mix of DMSO and I-BET treated cells were transferred (Figure 99B). We observed a significant reduction in the proportion of I-BET treated DC reaching the LN (Figure 99C, D).

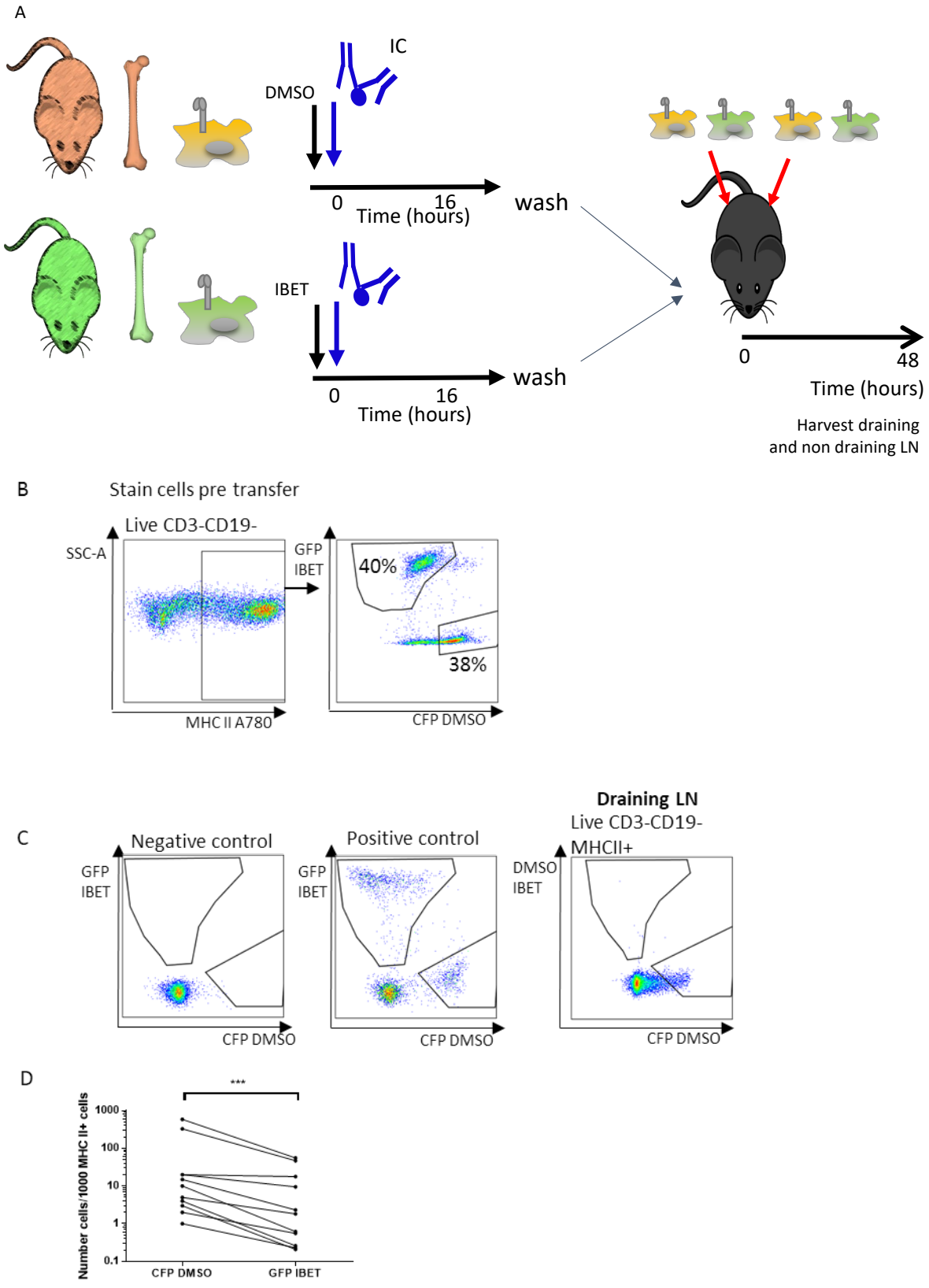


*Figure 99: I-BET inhibition of DC migration is DC intrinsic in an optimised cell transfer model. A shows the experimental set up. B shows representative flow cytometry plot demonstrating staining of the transferred DC mixture, gated on live CD3-CD19- cells. C shows representative flow cytometry plots of*

*live CD3-CD19-MHCII+ cells with controls used to set gates (labelled cells added manually to a lymph node suspension ex vivo). D shows the number of each cell population detected per 1000 MHCII+ cells in each lymph node. Representative experiment shown; treatment groups compared using Wilcoxon matched-pairs sign rank test (***p<0.001).*

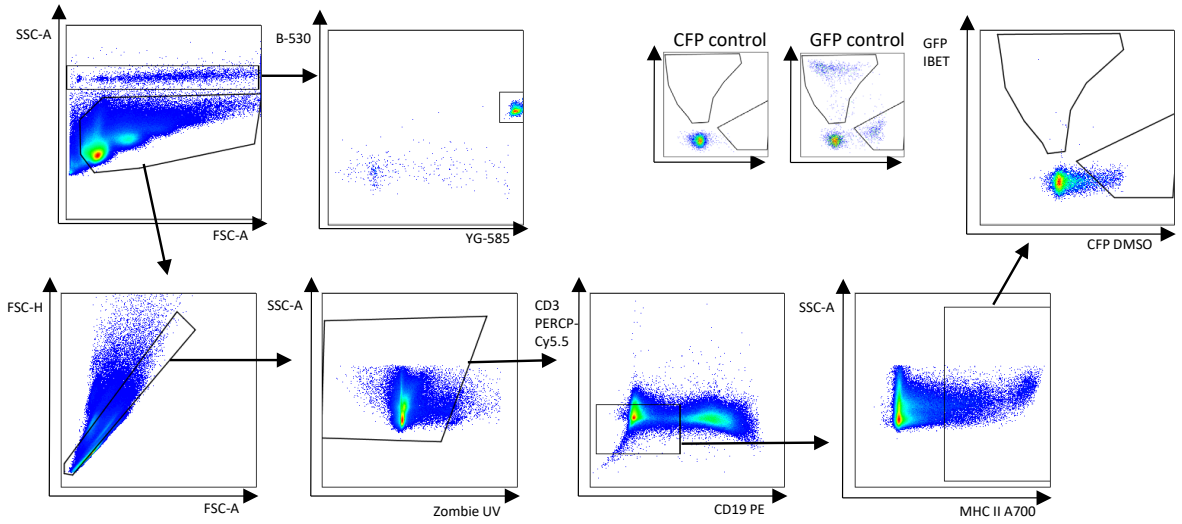


*Figure 100: Representative plots of gating strategy used in an optimised GFP/CFP DC cell transfer experiment*

### 5.3.6 I-BET inhibits co-stimulatory receptor expression

In order to investigate the effect of I-BET on DC's antigen presentation capacity, we measured the surface expression of DC markers and co-stimulatory receptor expression on murine bone marrow derived dendritic cells stimulated with immune complex in the presence and absence of I-BET. GM-CSF murine bone marrow cultures are known to consist of a heterogenous population of CD11c+MHCII+ macrophages and dendritic cells (Figure 101) (Helft 2015). Both undergo maturation upon stimulation with LPS but respond differentially to the stimulus and remain separable entities; $MHCII^{hi}CD11b^{int}$ population of BMDC were of a conventional DC phenotype whereas the $MHCII^{int}CD11b^{hi}$ fraction was shown to be monocyte-derived macrophages. The non-adherent cells at day 6 of culture contain a greater proportion of $MHCII^{hi}CD11b^{int}$ conventional DCs, so we used only non adherent cells at day 6 of culture.

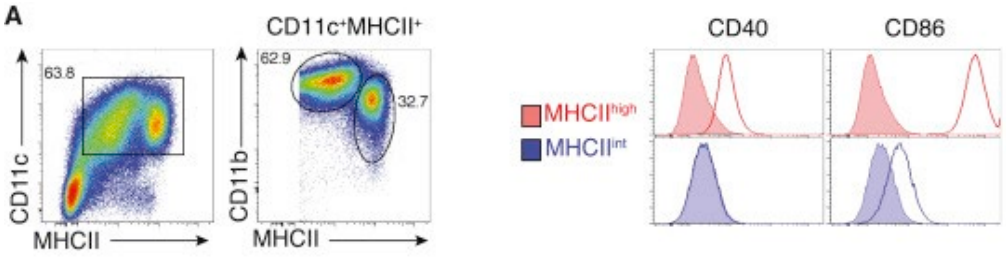

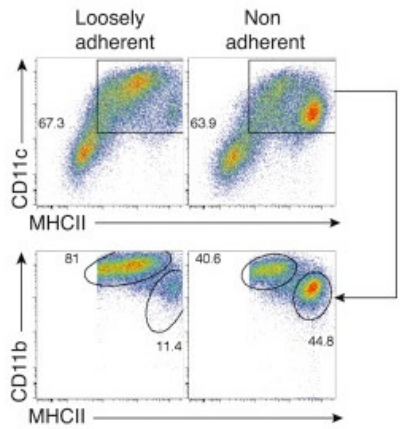


Figure 101. GM-CSF murine bone marrow cultures can be split into MHCII$^{hi}$CD11b$^{int}$ conventional DC and MHCII$^{int}$CD11b$^{hi}$ monocyte derived macrophages. Figure from (Helft 2015)

Both LPS and immune complex were triggers for DC maturation with a trend towards an increased proportion of MHCII+ CD11c+ cells within the BMDC culture compared to cells not given a maturation stimulus (Figure 102A); though LPS induced a greater proportion of MHCII$^{hi}$CD11b$^{int}$ conventional DCs (Figure 102B). I-BET treatment did not affect the proportion of MHCII+ CD11c+ cells (Figure 102A) or the proportion of MHCII$^{hi}$CD11b$^{int}$ conventional DCs for each maturation stimulus (Figure 102B).

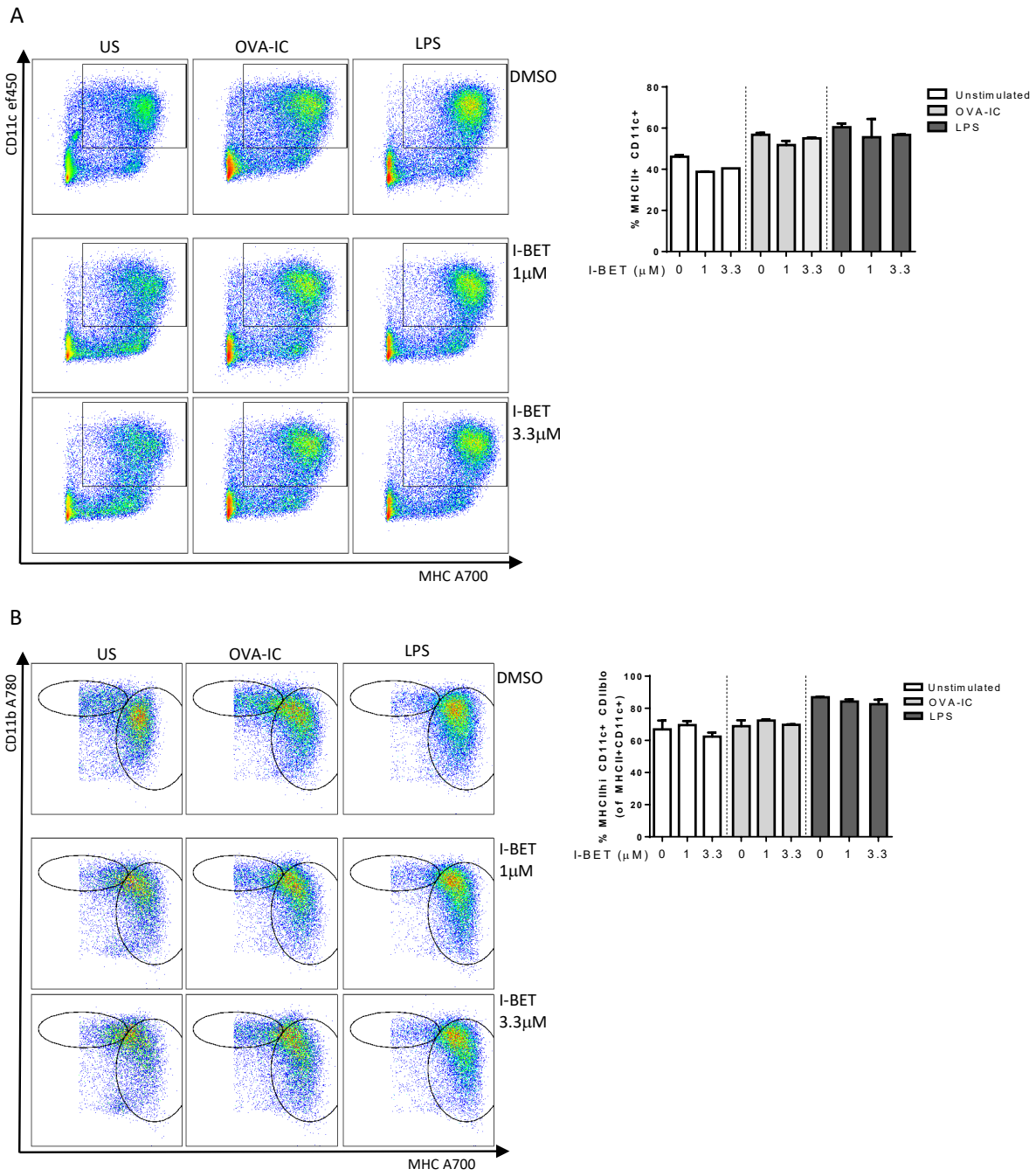


*Figure 100: Quantification of the effect of I-BET on DC maturation using gating as in (Helft 2015). Single experiment with three replicates per condition; representative plots shown and summary data showing median and interquartile range. Due to the small samples numbers trends were observed.*

We went on to quantify the expression of co-stimulatory receptors. Levels of MHC II, as well as CD40, CD80 and CD86 were greatest following LPS maturation (Figure 103Ai-iv). In this experiment we did not see an increase in co-stimulatory receptor expression following FcγR crosslinking, but I-BET treatment led to a concentration dependent reduction in CD80 and CD86 expression,

irrespective of the maturation stimuli used (Figure 103Aiii-iv; B), with a reduction in CD40 on unstimulated cells (Figure 103ii; B).

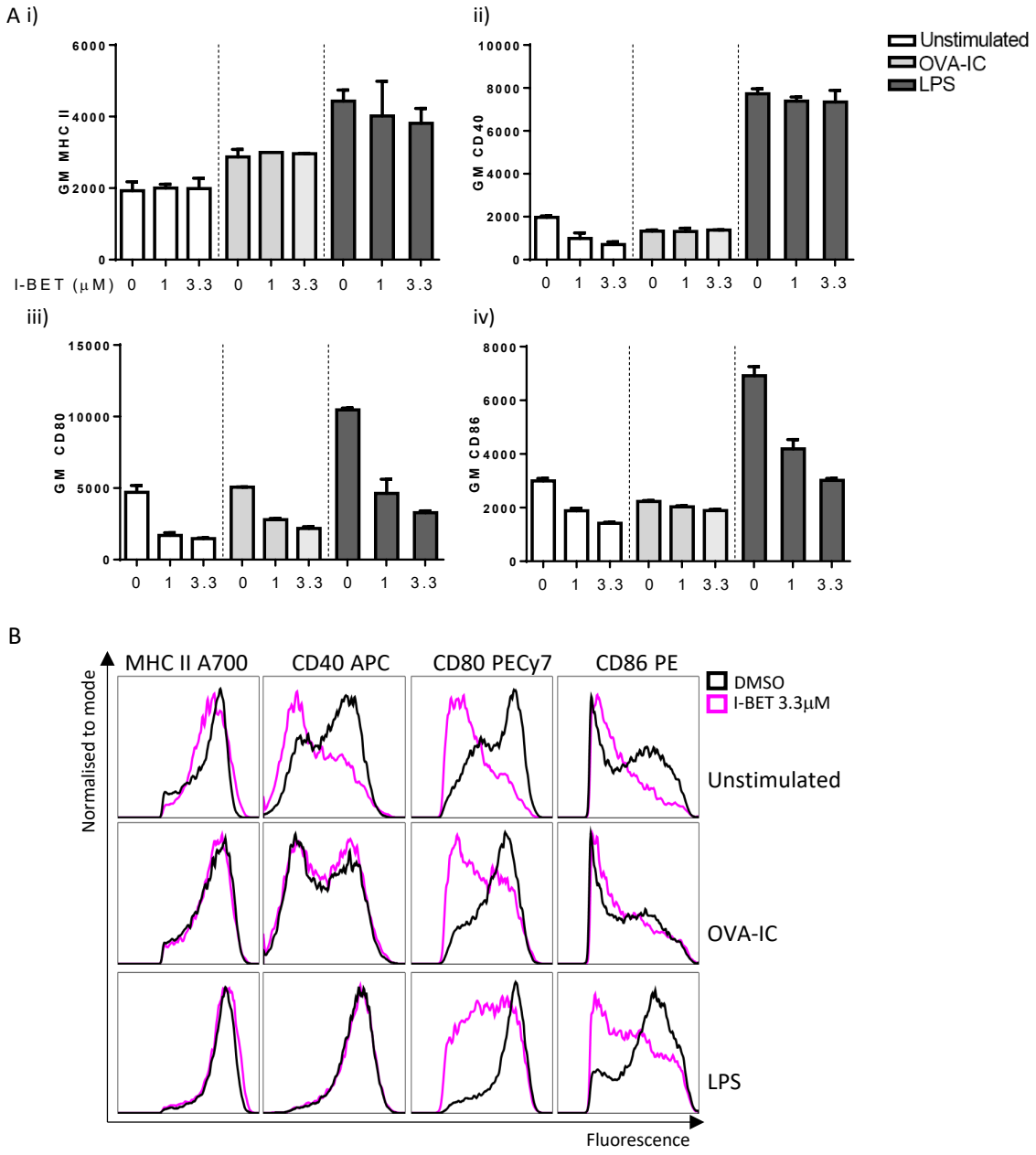


*Figure 103 I-BET inhibits co-stimulatory receptor expression. MHC II and costimulatory receptor expression on live CD11c+MHCII+ cells from a BMDC culture, stimulated for 16 hours with the labelled stimuli at day 7 of culture. Three replicates for each experimental condition; medians with interquartile range displayed in A; representative histograms shown in B.*

Repeat experiments revealed similar trends; though with shorter stimulation times changes in surface expression were less marked. The degree of response to immune complex stimulation was variable between experiments but where increased co-stimulatory receptor expression was seen

with addition of immune complex, the response was in general inhibited by the addition of I-BET (Figure 104).

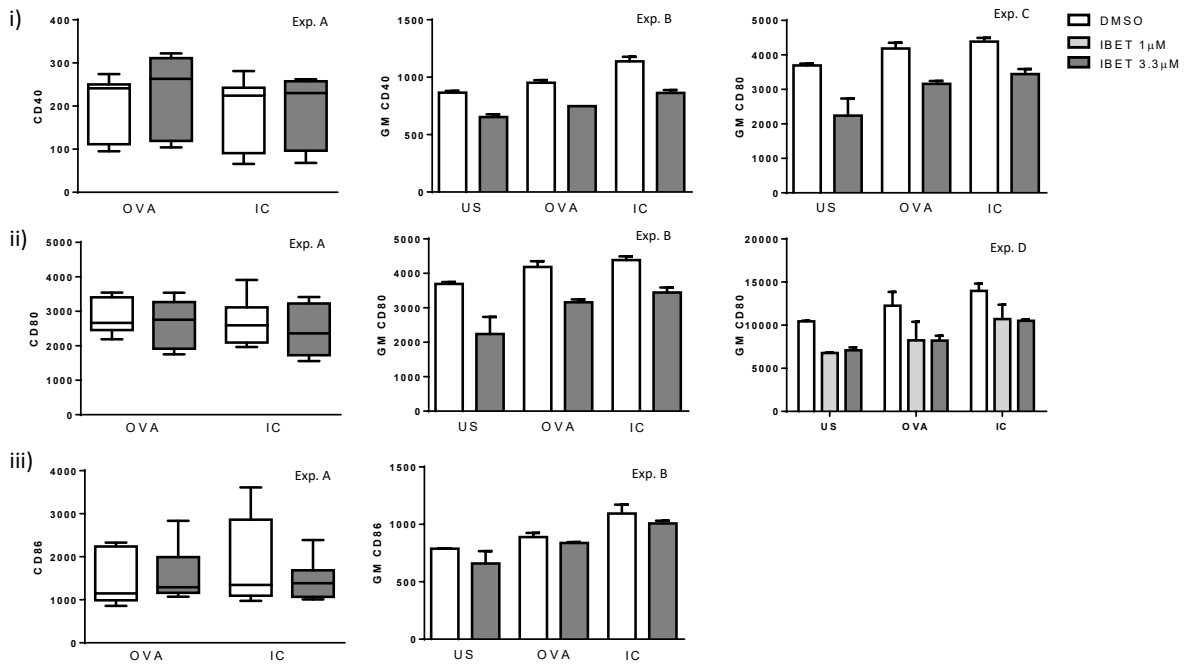


*Figure 104: Further evidence for inhibition of co-stimulatory receptor expression with I-BET. CD40 (i), CD80 (ii) and CD86 (iii) were quantified in a series of experiments on live CD11c+MHCII+ cells from BMDC culture. Experiment A BMDC from five independent mice stimulated for five hours; Experiment B BMDC from a single mouse stimulated for four hours (two replicates per condition); Experiment C and D BMDC stimulated for 12 hours with two (Exp. C) or three (Exp. D) replicates per condition. Medians with interquartile range shown in bar graphs. Box and whiskers plots also show range.*

MHCII levels on CD11c+MHCII+ splenocytes were quantified following 48 hours of I-BET treatment *in vivo* in mice who had undergone FITC painting (Figure 105). Not only were CD11c+MHCII+ DC numbers reduced in the spleen of I-BET treated animals, but those that were present had reduced MHCII expression. Although this result was statistically significant, the reduction in MHCII expression was only marginal so the biological significance is uncertain.

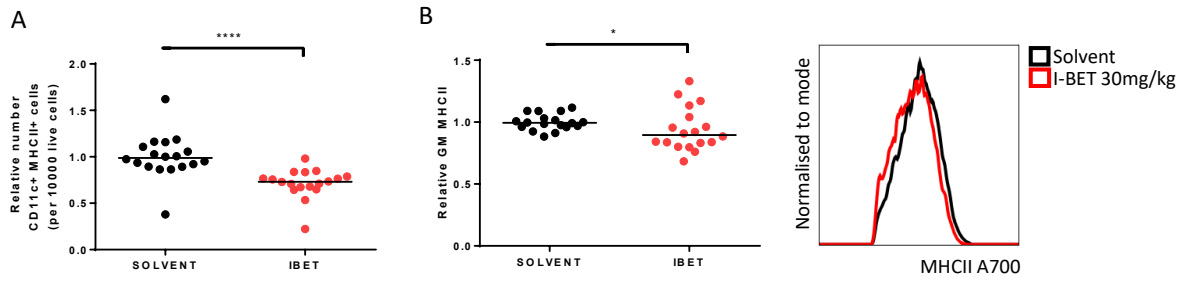

*Figure 105: I-BET treatment led to a reduction in DC numbers and reduced MHCII expression. Results from five independent experiments. Lines represent median values with groups compared using Mann-Whitney test (*p<0.05; ****p<0.0001).*

### 5.3.7 I-BET has little impact on T cell activation by IC-stimulated DCs *in vitro*

We used a DC:T cell co-culture assay in order to assess the ability of I-BET treated DC to activate T cells. Murine BMDC, were pulsed with immune complexed OVA in the presence or absence of I-BET. CD4+ T cells were isolated from OTII splenocytes that express T cell receptors specific for OVA and labelled with CFSE, according to a standard protocol. Following removal of I-BET from the culture, given that it is known to directly affect T cell differentiation, the CFSE labelled CD4+ T cells were added and activation status and proliferation assayed after 96 hours by flow cytometry (Figure 106). T cells cultured with IC stimulated DC's demonstrated increased proliferation and activation (as measured by surface expression of CD25 and CD69). DC treatment with I-BET during antigen capture resulted in a trend towards increased T cell proliferation (Figure 106C) but less activation (Figure 106D-E). However, these were not statistically significant across three independent experiments. I did attempt to assay T cell activation *in vivo* by transferring OTII T cells intravenously at the time of subcutaneous DC transfer, but no T cells were identified in the draining lymph node (data not shown).

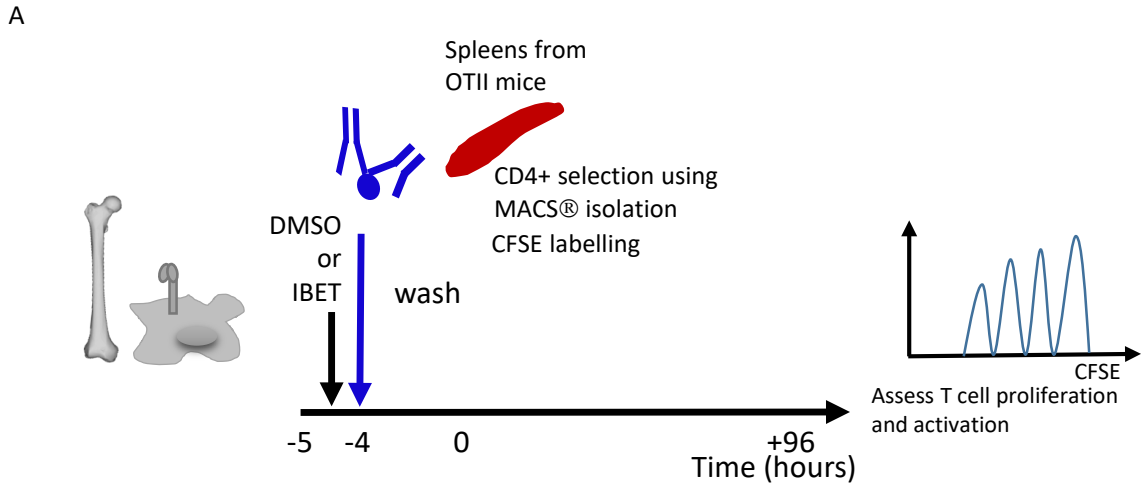

B

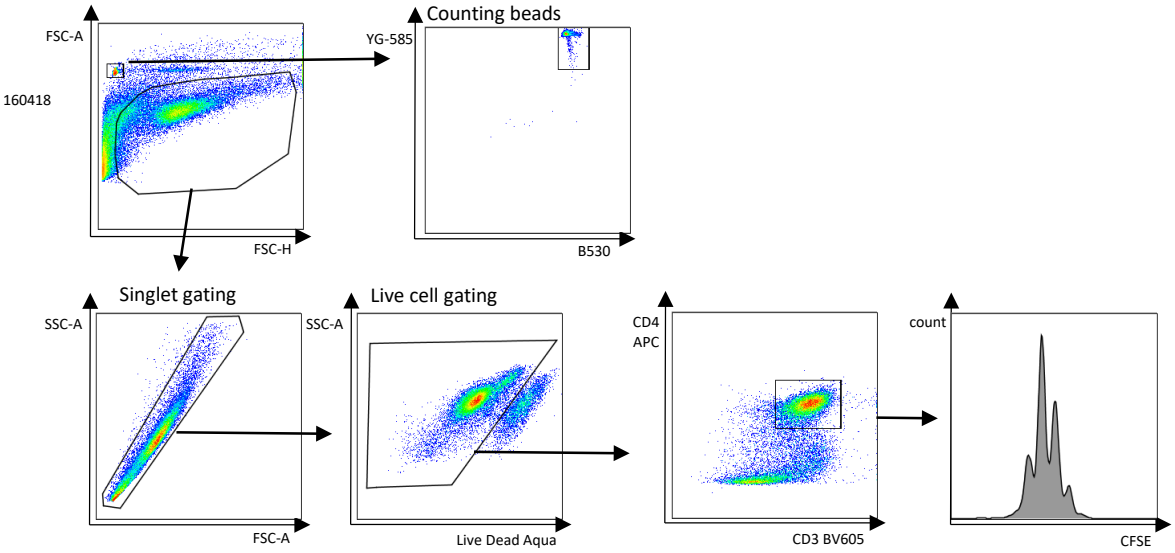
FSC-A
160418
FSC-H
YG-585
Counting beads
B530
Singlet gating
SSC-A
FSC-A
Live cell gating
SSC-A
Live Dead Aqua
CD4
APC
CD3 BV605
count
CFSE

C

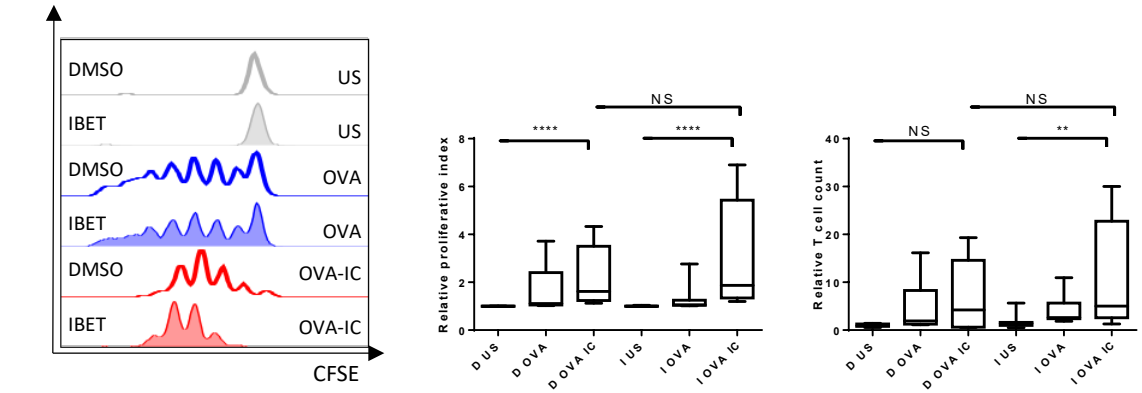
DMSO
US
IBET
US
DMSO
OVA
IBET
OVA
DMSO
OVA-IC
IBET
OVA-IC
CFSE
Relative proliferative index
NS
****
****
D US
D OVA
D OVA IC
I US
I OVA
I OVA IC
Relative T cell count
NS
NS
**

D

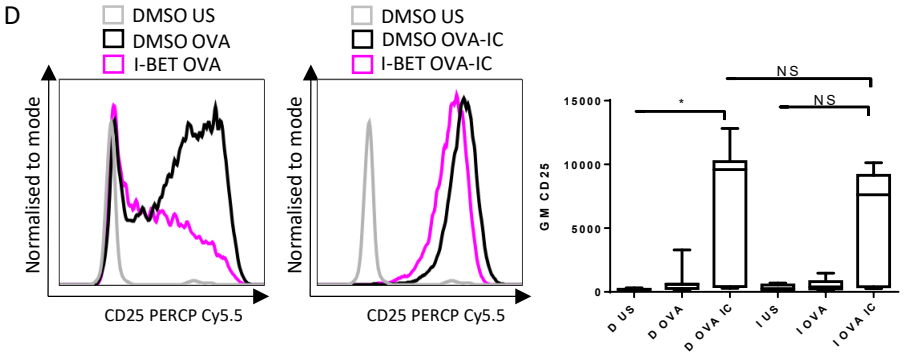
DMSO US
DMSO OVA
I-BET OVA
Normalised to mode
CD25 PERCP Cy5.5
DMSO US
DMSO OVA-IC
I-BET OVA-IC
Normalised to mode
CD25 PERCP Cy5.5
GM CD25
NS
NS
*
D US
D OVA
D OVA IC
I US
I OVA
I OVA IC

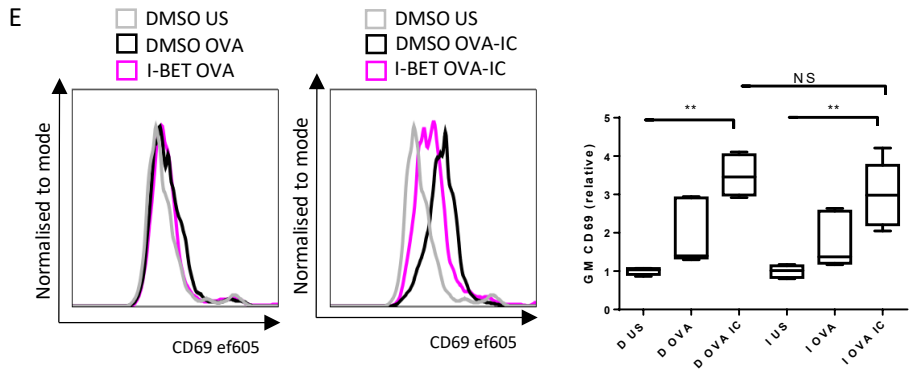


*Figure 106: Antigen presentation by immune complex stimulated DC leads to increased T cell proliferation and activation and is not significantly affected by I-BET treatment. Experimental protocol (A) and representative plots of gating strategy used for a DC:OTII cell co-culture assay. Panel C shows representative CFSE histograms and summary statistics for proliferative index and T cell count. The activation markers CD25 (D) and CD69 (E were measured on the T cells at the end of the co-culture. Five independent experiments with up to four replicates for each experimental condition. Box plots show median, interquartile range and range with representation of all replicates, relative to the mean DMSO US value for the relevant experiment, in C (three experiments) and E (two experiments) and experiment means in D (five individual experiments). Wilcoxon matched-pairs sign rank test used in D; Mann-Whitney test used to compare replicates in C & E. NS p>0.05; *p<0.05; **p<0.01; ****p<0.0001.*

**5.4 Discussion**

Mononuclear phagocytes, including macrophages and DCs respond to stimulation by IgG immune complex; macrophages are specialised for phagocytosis and cytokine production whilst DCs are specialised antigen presenting cells, transporting antigen from the periphery to lymph nodes where they are more likely to encounter naïve T cells to which they can present antigen leading to T cell activation.

In the previous chapter we showed that I-BET reduced the upregulation of many genes following IgG IC stimulation in murine BMDM. Bone marrow-derived MNP populations are known to be heterogenous and those differentiated as 'dendritic cells' using GM-CSF are actually composed of a mixed population of DCs and macrophages (Helft 2015). Although ideally one would base conclusions on the effect of DCs on a study of a pure DC population differentiated *in vivo*, studies in BMDM can still provide a useful experimental system for hypothesis generation and testing. Our microarray study showed that I-BET inhibited pathways upregulated by FcγR signalling relevant to DC phenotype, including cell adhesion pathways as well as antigen processing and presentation pathways (Figure 60). A reduction in FcγR expression was also observed in DCs cultured *in vitro* (Figure 64C) and within splenic DC *in vivo* (Figure 65), potentially reducing their susceptibility to IgG-mediated activation.

I-BET changed the morphology of both macrophages and DCs, resulting in a less adherent phenotype. I-BET treatment led to changes in gene expression in multiple genes that control cell adhesion and migration behaviour. Gene set enrichment analysis showed downregulation of pathways including regulation of actin cytoskeleton, chemokine signalling and cell adhesion molecules, with reduced expression of a number of chemokine receptor genes, as well as genes known to be important for DC migration including cysteinyl leukotriene receptor genes (*Cysltr1, Cysltr2*), critical for the leukotriene mediated induction of capacity for DC to migrate towards CCL19; prostaglandin E receptor 2 (*Ptger2*) known to be important for the induction of *Mmp9;* integrin subunit alpha 4 (*Itga4*), platelet-activating factor receptor (*Ptafr*), PI3K catalytic subunit gamma (*Pi3cg*) and dedicator of cytokinesis 8 (*Dock8*), a crucial CDC42 activator required for the amoeboid migration of DCs. Other important genes were downregulated but did not reach statistical significance including small Rho family GTPases *Cdc42*, *RhoA*, *Rac1* and *Rac2*, components of the Arp2/3 complex (*Arpc2*, *Arpc5*, *Actr2*, *Actr4*), integrin subunit beta 2 (*Itgb2*), *Eps8*, *CCR7* and MMP9.

We were particularly interested in genes that were upregulated with FcγR and impacted by I-BET treatment since these may be particularly important in driving IC-mediated DC migration. The

heatmap in figure 86 identifies numerous genes that appear to fulfil this brief, including Mmp9, Itgb1, Itgb2, Ptafr, Rap1b, Icam1, Cd82, Fscn1, Cmklr1, *Ccr7* and Cd38, although none reached statistical significance when considering both these requirements. In our transcriptomic analysis the effect of I-BET treatment at four hours was greater than that of FcγR crosslinking. Given the small sample size and limited power of our study we may have missed more subtle changes induced by FcγR crosslinking; the fact that I-BET clearly inhibits genes known to drive IC mediated migration is of interest.

These findings prompted us to assess the impact of I-BET treatment on DC migration. The movement of DC's was altered by I-BET treatment. In the absence of a chemokine gradient I-BET treated DC's showed greater track displacement and speed than those treated with DMSO control; likely due to their rounded morphology and reduced adhesion to the collagen matrix. However IgG-IC induced augmentation of DC chemotaxis to CCL19 was abrogated by the addition of I-BET, with a reduced acceleration and chemokine guided migration following addition of IC*. In-vitro* assays are not perfect models given the highly complex regulation of DC migration that is affected my multiple factors including adhesion to the matrix, actin cytoskeletal change, chemokine signalling and matrix composition and degradation. *In vitro* migration assays may not accurately represent the complex *in vivo* milieu in which multiple external environmental factors also impact on DC migration, for example by inducing subtle changes in chemokine gradients (Haessler 2011). Furthermore different processes determine DC migration in 2D and 3D systems; integrin mediated adhesion is critical for migration over 2D surfaces but not required for DC migration in 3D environments (Lammermann 2008).

*In vivo*, two photon imaging showed that systemic I-BET treatment reduced IC-induced dermal DC mobilisation and a FITC paint model showed reduced migration of tissue DCs from I-BET treated animals to draining lymph nodes. We confirmed a DC-intrinsic effect on IgG IC-induced migration by transferring I-BET-treated DCs into the skin and tracking their subsequent trafficking to lymph nodes. We noted reduced numbers of splenic DC in I-BET treated animals injected with subcutaneous IC in the FITC paint model, with under-representation of CD8+ DC. CD8+ DC are a subset of non-migratory tissue resident DC that efficiently cross present exogenous antigens on MHC class I (Schnorrer 2006), holding immunoregulatory properties during steady state but producing IL-12 on activation, stimulating inflammatory responses. During infection with intracellular pathogens, they become major presenters of pathogen antigens promoting CD8+ T-cell responses to the invading pathogens (Shortman 2010). However, a proportion of circulating plasmacytoid DC in the spleen also express CD8α after microbial stimulus (O'Keeffe 2002) and our limited surface staining was insufficient to

fully characterise the subsets effected by I-BET. It appears that I-BET not only impedes the migratory capacity of DC, but may also alter lymphoid tissue resident subsets.

DC maturation following antigen capture induces changes that facilitate migration for example upregulation of CCR7, a process mediated by NF-κB signalling (Baratin 2015). Since starting this work, others have shown that inhibition of bromodomains inhibits LPS driven DC maturation (Sun 2015b, Toniolo 2015, Schilderink 2016), reducing expression of co-stimulatory molecules, inhibiting cytokine and chemokine production and attenuating T cell proliferation. An increase in functionally suppressive CD25+Foxp3+ T cells was hypothesised to result from a failure of maturation of I-BET treated DC or alternatively from an impaired capacity of these DC to uptake and process, or present antigen (Schilderink 2016), although the authors report uptake of dextran particles was not affected by I-BET151. Our work suggests that I-BET does indeed impact DC antigen uptake and processing; in chapter 4 we show that I-BET impacts phagocytosis leading to delayed phagolysosome maturation and IC clearance. Schilderink et al. observed some therapeutic benefit of I-BET151 in a T cell mediated colitis model. Interestingly, their most marked observation was of reduced spleen weight following I-BET treatment; similar to our observation in an immune complex peritonitis model. Sun et al. similarly showed that I-BET reduced LPS induced DC surface co-stimulatory molecule expression and cytokine secretion together with direct effects on T cells, both due to disruption of the association between BRD4 and acetyl-310 RelA of NF-κB, reducing graft versus host disease severity in an MHC-disparate allogeneic bone marrow transplant model (Sun 2015b). Treatment of human monocyte derived DC (Mo-DC) with JQ1 inhibited LPS-induced STAT5 phosphorylation, impairing maturation of Mo-DC. This reduced the ability of Mo-DCs to induce allogeneic CD4+ and CD8+ T cell proliferation and production of proinflammatory cytokines, reducing generation of inflammatory CD8+ T cells and decreasing Th1 differentiation (Toniolo 2015). We studied the effect of I-BET on DC maturation following IC stimulation and show that I-BET similarly inhibited DC co-stimulatory receptor expression. Incomplete maturation of DC is associated with induction of T cell tolerance (Lutz 2002). In limited *in-vitro* co-culture experiments we observed a trend towards increased T cell proliferation with reduced T cell activation following addition of I-BET during DC priming with OVA and OVA-IC. We did not examine T cell polarisation or Foxp3 expression following co-culture; it would be of interest to study the impact of I-BET on DC production of T cell polarizing cytokines following IC challenge.

To our knowledge this is the first account directly implicating bromodomains in the morphology or migration of MNP; though there are supporting reports in other cell types. Malignant cell migration similarly relies on actin polymerisation and molecules that link migratory signals to the actin

cytoskeleton are upregulated in invasive and metastatic cancer cells (Yamaguchi 2007). Furthermore, there are multiple descriptions of bromodomain mediated control of malignant cell migration and invasion (Andrieu 2016b, Wang 2017). Dendritic spines are small protrusions from many types of neuron that share similarities with dendrites of dendritic cells, utilising actin remodelling to drive changes in morphology (Vicente-Manzanares 2009). Bromodomains have been shown to regulate Drosophila dendrite morphology; a loss-of-function mutation in the single Drosophila BET protein encoded by female sterile 1 homeotic [fs(1)h] causes loss of fine, terminal dendritic branches (Bagley 2014). Lung fibroblasts isolated from patients with rapidly progressing idiopathic pulmonary fibrosis exhibit evidence of dysfunctional Brd4 activity with enrichment of Ac-H4K5 and Brd4 at the IL-6 gene locus at baseline; BRD4 inhibition of these fibroblasts with JQ1 *in vitro* attenuated platelet-derived growth factor-BB medicated migration, proliferation, and IL-6 release. JQ1 reduced bleomycin-induced lung fibrosis in an *In vivo* murine model, associated with reduced numbers of infiltrating lymphocytes and macrophages, reversing disease when commenced after onset of fibrosis (Tang 2013). JQ1 reduced the secretion of IL-1β, IL-6, IL-17 and IL-18 from TNFα-stimulated human rheumatoid arthritis fibroblast-like-synoviocytes (RA-FLS), reduced FBS-induced migration and invasion of human RA-FLS and reduced the inflammatory response, autoantibody production and joint damage in a CIA model (Zhang 2015). Similarly, I-BET151 suppressed the inflammatory, matrix-degrading, proliferative and chemoattractive properties of RA-FLS (Klein 2016). BET bromodomain inhibition suppressed the expression of endothelial cell adhesion molecules induced by TNFα or LPS, including ICAM-1, VCAM-1 and E-selectin, and inhibited leukocyte adhesion to activated HUVEC monolayers. In an acute lung inflammation model, *In vivo* treatment with JQ1 attenuated the LPS-induced accumulation of leukocytes and expression of endothelial adhesion molecules in lung tissue (Huang 2017). This report focussed on the effects of bromodomain inhibition on the endothelium, without probing whether it directly influenced leukocyte migration.

It is not surprising that we see I-BET induced changes in both phagocytosis and adhesion/migration since these processes share signalling pathways and cellular components, both reliant on remodelling of the actin cytoskeleton. Maturation of DCs in response to TLR4–MyD88 signalling increases their migration speed and persistence by regulating actin-nucleation machineries; favouring a RhoA-mDia1-dependent actin pool located at the cell's rear, which facilitates forward locomotion; and limiting a Cdc42-Arp2/3-dependent actin pool present at the cell's front, which limits migration but promotes antigen capture (Vargas 2016). Our microarray study showed that I-BET impacts genes within both these pathways; differential effects could cause alterations in the distribution of the actin pool which may account for some of the I-BET driven changes in migration behaviour observed. We observed cell rounding associated with I-BET treatment, a feature observed

in adherent cells during phagocytosis; felt to arise in this setting due to competition for cytoskeletal and membrane components necessary for phagocytosis and adhesion, which become enriched in the phagocytic cup (Aderem 1999). Cell rounding is also described as a feature of pathogens manipulating the host cytoskeleton; the Yersinia species protein YopT is a cysteine protease that inactivates Rho, leading to inhibition of phagocytosis and chemotaxis (Schmidt 2011); the *Vibrio parahaemolyticus* protein VopS inactivates Rho by AMPylation, preventing the interaction of Rho GTPases with downstream effectors, thereby inhibiting actin assembly in infected cells (Yarbrough 2009). In the case of I-BET treatment, rounding could result due to alteration in the dynamics of actin reorganisation following phagocytosis, where we see delayed phagolysosome processing and build-up of phagocytic debris within cells, or via direct effects on Rho GTPases or downstream effectors.

The impact of I-BET on DC migration is likely multifactorial with effects on NF-κB mediated DC maturation, chemokine-chemokine receptor signalling, cell adhesion and motility. Our observations further support the hypothesis that I-BET inhibits the inflammatory response of myeloid cells to IC. I-BET may therefore interfere with the uptake of IgG opsonised antigen by mononuclear phagocytes, antigen processing and DC trafficking to secondary lymphoid tissues, providing mechanistic insight into the potential therapeutic benefit of I-BET in the setting of antibody-associated inflammation.

**Chapter 6: Final discussion**

### 6.1. Summary

In this thesis I explored the impact of two therapeutic agents that influence the immune system, at different stages of clinical development. In the setting of a phase 2 experimental medicine study in kidney transplant recipients, we explored the therapeutic potential of belimumab, an anti-BLyS antibody, as an adjunct to standard immunosuppression. Therapeutic agents that limit humoral alloimmunity in kidney transplant recipients are currently lacking. We hypothesised that blocking BLyS, a cytokine that promotes B cell survival, may be beneficial. We provide the first data on the use of belimumab in kidney transplant recipients, showing no excess risk of infection or rejection and a reduction in naïve B cells, activated memory B cells, circulating plasmablasts, and kidney-specific IgG. We also provide the first data on the impact of belimumab to reduce de novo IgG formation and increase regulatory B cell numbers in the peripheral blood.

Preclinical studies were performed to investigate the potential efficacy of the bromodomain inhibitor I-BET in reducing antibody-mediated immune cell activation. We show that I-BET delays phagolysosome maturation associated with build-up of immune complex whilst selectively inhibiting IC induced cytokine production. I-BET changed MNP morphology, resulting in a less adherent phenotype and altered DC migratory capacity. *In vitro*, in a 3D collagen matrix, IgG-IC induced augmentation of DC chemotaxis to CCL19 was abrogated by the addition of I-BET. *In vivo*, two photon imaging showed that systemic I-BET treatment reduced IC-induced dermal DC mobilisation. Tissue DCs and transferred DC also had reduced migration to draining lymph nodes following I-BET treatment. We found that I-BET treatment led to reduced expression of co-stimulatory receptor expression, though in limited studies were unable to show a significant impact on subsequent T cell activation, but definitive conclusions on this will require further experiments. Together, these data provide mechanistic insights into the potential therapeutic benefit of I-BET in the setting of antibody-associated inflammation.

### 6.2 Therapeutic implications of the BEL114424 study

The BEL114424 study provides a useful platform from which to explore the further use of belimumab in renal transplantation. It gives a clear indication of the potential efficacy of belimumab as an immunomodulatory agent in transplantation that can limit new antibody formation and provides a blueprint for much-needed proof of concept experimental medicine studies in this field where the need for surrogate endpoints and innovative study design has been acknowledged by the community (O'Connell 2017). The knowledge we have gained from this study provides numerous options for future potential studies. In order to progress the drug to the clinic with a licence for use

in transplantation one would need to prove efficacy and demonstrate an effect on clinical outcomes. We hypothesise that by inhibiting new antibody production, limiting memory B cell activation and T cell proliferation and potentiating regulatory B cell function, belimumab would lead to less DSA production and improved graft function and survival. However chronic ABMR and graft loss take a number of years to develop and are therefore difficult to measure in a clinical trial setting. The transplant cohort we used was of low immunological risk and therefore the number likely to develop chronic ABMR and develop graft loss is low. Given the association between pre-transplant BLyS levels and risk of ABMR and the development of DSA, one may be able to stratify a population based on their pre transplant BLyS levels in order to determine those most likely to benefit from belimumab therapy.

Belimumab's effects in lowering activated memory B cells and on preformed IgG highlight an additional potential role in sensitised kidney transplant recipients or in those with antibody-mediated rejection. One could consider using belimumab in a cohort with higher immunological risk who are likely to have a higher event rate and potentially could benefit more from treatment. However, in this subset of patients we currently use alternative immunosuppression approaches including lymphocyte depleting treatment with alemtuzumab or anti-thymocyte globulin (ATG) at induction. The safety of belimumab in combination with these regimes is not known. It is also uncertain if the observed effects would apply in the setting of B cell depletion. Following alemtuzumab treatment, a rise in serum BLyS is observed and this has been associated with rises in DSA (Bloom 2009). It would be interesting to follow treatment with alemtuzumab with belimumab during the reconstitution phase to see if this modulates the reconstituting B cell compartment, leading to a more tolerogenic compartment with increased IL-10/IL-6 cytokine production. The COMBIVAS trial combining rituximab with belimumab treatment is due to start in the setting of vasculitis and it will be interesting to see the effect of belimumab treatment following B cell depletion.

There are currently no proven treatments for chronic ABMR. There is an isolated case report describing the successful use of belimumab in a case of rituximab resistant acute ABMR (Leca 2013). Belimumab treatment is effective in the setting of the autoimmune disease SLE, where preformed antibodies are present. Belimumab may therefore be an effective therapy in the setting of acute or chronic ABMR, an area with limited current therapies due to the difficulties of targeting long lived plasma cells.

We are the first to describe an impact of belimumab on immunoregulatory cytokine release. Our study therefore informs those using belimumab outside of the field of transplantation in SLE. Plans

are in place to use the regulatory B cell assay developed as part of this work in future GSK studies using belimumab.

## 6.3 Outstanding questions regarding the impact of bromodomain inhibition on FcγR mediated MNP activation

### 6.3.1 Epigenetic changes induced by FcγR crosslinking

We describe changes in phenotype induced following I-BET treatment and using a microarray platform with subsequent confirmation by quantitative PCR, in the case of FcγR expression levels, describe changes in gene expression which may account for the phenotypic changes observed. As yet we have not explored the epigenome of MNP; at baseline this may determine the susceptibility of individual genes to I-BET mediated inhibition; a comparison following I-BET treatment may explain the changes observed. To our knowledge no-one has yet studied epigenetic modifications in MNP induced by FcγR crosslinking. We have planned to perform a full analysis of the epigenetic state of MNP using ATACseq technology, focussing on changes induced by FcγR crosslinking in the presence and absence of bromodomain inhibition (Figure 107). We have chosen to use ATACseq analysis to assess epigenetic changes because this allows a broad assessment of the epigenome, in contrast to ChiP-Seq, in which specific histone marks are assayed.

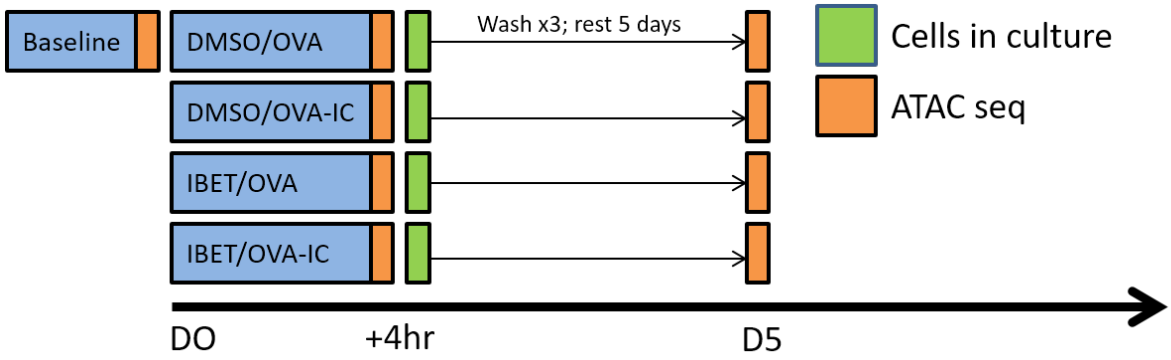


*Figure 107: ATACseq analysis of epigenetic changes induced by FcγR crosslinking and the impact of bromodomain inhibition. BMDM will be cultured and treated with/without I-BET together with immune complexes (IgG opsonised OVA-IC) or control protein (OVA). After four-hours, all stimuli will be removed, the cells washed and some harvested for ATACseq studies. A subset of the cells will be cultured for an additional five days in standard media and then harvested to assess the stability of epigenetic changes induced by IC. For accuracy and reproducibility, three technical replicates will be used for each condition. We will also assay three unstimulated samples to provide information on the baseline epigenetic landscape*

### 6.3.2 Pinpointing the mechanism of bromodomain inhibitor action

Through our work we have identified multiple ways in which bromodomain inhibition alters MNP gene expression and phenotype. The epigenetic study outlined above will further our knowledge of key regulators; we hypothesise that I-BET will impede enhancer and superenhancer landscape remodelling following FcγR crosslinking, similarly to that seen in other settings (Brown 2014), leading to changes in multiple key immune pathways.

Given the multitude of potential effects of bromodomain inhibition and the presence of complex immune regulation networks, *in vivo* models are critical for understanding the implications of bromodomain inhibition. Unfortunately our attempts at setting up a nephrotoxic nephritis model were unsuccessful. We utilised alternative models to test the impact of I-BET. We showed reduced recruitment of mononuclear phagocytes to the kidney and reduced pro-inflammatory gene expression in response to circulating immune complex; using a FITC paint model, two photon microscopy and transfer of DC's treated with I-BET *ex-vivo,* we confirmed that I-BET impedes DC migration. Ideally we would like to dissect the effect of bromodomain inhibition in a more conventional autoimmunity model and have discussed the potential for using a K/BxN serum transfer arthritis (Christensen 2016), where we would be able to assay the effect of I-BET on the MNP immune response to autoantibody, independently from potential effects on B cell autoantibody production itself. We would plan to observe any impact on disease severity within the joints whilst also studying joint draining lymph nodes. With a working model of autoimmune disease, one could then explore changing the timing of therapeutic intervention to see whether I-BET impacts the development and/or maintenance of an established immune response.

Our work suggests that I-BET may have some impact on baseline MNP adhesion and migration independent from changes resulting following FcγR crosslinking, leading to changes in baseline homeostasis; we see alterations in unstimulated BMDM by microarray analysis, for example in cytokine and chemokine signalling pathways; see altered kidney MNP populations even in the absence of IC administration; and observed changes in the size of non draining lymph nodes and splenic DC populations in our FITC paint model. We report that the impact of I-BET on DC migration is likely multifactorial, with effects on NF-κB mediated DC maturation, chemokine-chemokine receptor signalling, cell adhesion and motility. Use of LifeAct–GFP mice would allow the generation of LifeAct–GFP density maps, as in (Vargas 2016), and would confirm whether changes in actin distribution underpin the alterations in adhesion and motility observed. It is important to further characterise changes observed in the absence of IC stimulation since they could have implications for side-effects associated with treatment.

### 6.3.4 Effect of bromodomain inhibition on B cell memory responses

Bromodomain inhibition has been shown to impact the BAFF axis; JQ1 improved survival in a murine lupus model and reduced serum anti-dsDNA antibody, BAFF, IL-1β, IL-6, IL-17 and IFN-γ, whilst increasing the immunoregulatory cytokine IL10. *In vitro,* JQ1 caused similar changes in cytokine release in cultures of splenocytes from diseased MRL-lpr mice and human monocytes stimulated with IC (Wei 2015). The reciprocal change in IL-6 and IL-10 associated with reduced BAFF mirror our findings with belimumab; giving further support for a role of BAFF/BLyS axis in modulating the balance between proinflammatory and immunoregulatory B cell cytokine release; and prompting study of the effects of bromodomain inhibition on B cell subsets. However, Wei and colleagues found that JQ1 inhibits the recruitment of BRD4 and NF-κB p65 at the IL-10 promoter region upon LPS stimulation, inhibiting IL-10 release from LPS stimulated mouse splenocytes in a dose dependent fashion. They found no change in the frequency of $CD1d^{hi}CD5^{+}$ regulatory B cells but JQ1 reduced the differentiation of precursor cells to mature IL-10-producing regulatory B cells (Lee 2017). Published data suggest that BET inhibition can limit the proliferation of malignant B cells, causing a G1 cell cycle arrest (Chapuy 2013). Brd2 binds the cyclin A promoter in B cells, increases cyclin A expression and S-phase progression in *in vitro* mitogen-stimulated non-malignant primary B cells and JQ1 reduces B cell mitogenesis (Belkina 2014). In lymphoma cell lines, BRD4 loading has been noted on the enhancers for a number of transcription factors that determine B cell fate including Bcl6, Pax5 and Irf8 (Chapuy 2013). An increase in BRD4 expression occurs in GC B cells and BRD4 inhibition *in vivo* results in the suppression of GC formation and reduced IgG titres following T-dependent antigen immunisation (Gao 2015). In keeping with this, BET inhibition led to a reduction in Bcl6 expression, the master regulator of GC B cells, and of Irf8, Pax5 and Bach2 (Gao 2015). Brd4 is also critical for non-homologous end-joining repair of activation-induced cytidine deaminase (AID)-induced DNA breaks and BET inhibition reduces class-switch recombination *in vivo* (Stanlie 2014). These data support the potential for BET inhibition as a therapeutic strategy targeting B cells in antibody-mediated diseases. Given that in most autoimmune disease, and in sensitised organ transplant recipients, it is not the primary antibody response that mediates disease but rather an on-going recall response, we would look to determine the role of BET proteins and the efficacy of BET inhibitors in impacting humoral memory, specifically the activation of memory B cells and the generation and maintenance of plasma cells.

### 6.3.3 Applicability as potential treatment in autoimmunity and transplantation

Our work suggests that I-BET may have potential therapeutic benefit in the setting of antibody-associated inflammation; limiting the MNP response to deposited IC and impeding DC migration to

secondary lymphoid organs, resulting in potential attenuation of any subsequent T cell response. However it is uncertain if such a treatment may be effective in people with pre-existing autoimmune disease. When considering use as a therapeutic agent the timing of administration is crucial. Apart from perhaps in the setting of transplantation, when the timing of introduction of the allograft is known; those with autoimmunity in general present following the initiation of the autoimmune response. In our experiments pre-treatment with I-BET shortly prior to IC stimulation was used to maximise the I-BET treatment effect whilst elucidating mechanisms of action. Further experiments where introduction of I-BET following initial stimulation would be of interest.

The targets of bromodomain inhibition are influenced by the baseline epigenetic state of genes and autoimmunity itself can result from epigenetic modifications (Long 2016); there is no guarantee that MNP's from those with autoimmunity will behave similarly to those from healthy controls. Aberrant histone acetylation has been implicated in the pathogenesis of SLE with a global site-specific histone H3 and H4 hypoacetylation detected in CD4+ T cells from patients with SLE, correlating with increased disease activity (Hu 2008), and splenocytes of MRL/lpr lupus mice; with improvement of disease phenotype associated with normalisation of acetylation state following *in vivo* administration of a histone deacetylase inhibitor (Garcia 2005). Increased H4 acetylation at the TNFα locus in monocytes from patients with SLE associates with increased TNFα transcripts and markers of disease severity (Sullivan 2007). Moreover, monocytes from those with SLE show increased promoter H4 acetylation at multiple gene loci; network analysis identified significant nodes as ERK, p38, NFκB, CREB1 and αIFN; the majority of genes with increased H4ac having upstream interferon regulatory factor 1 (IRF1) binding sites and exhibiting the potential to be regulated by IRF1, consistent with the previous knowledge of type-I interferon hyper-responsiveness in SLE (Zhang 2010). Elevated basal levels of H3 and H4 acetylation is associated with an open chromatin state and resistance to I-BET treatment (Nicodeme 2010). The epigenetic changes observed in patients with SLE could therefore render their MNP more resistant to I-BET mediated inhibition. We would wish to expand our *in vitro* work using human monocyte derived macrophages and dendritic cells, ideally including cells from patients with established autoimmune disease. The responses of MNP from those with prior autoimmunity may also differ from those of healthy controls due to the phenomenon of 'trained immunity', whereby innate immune cells show an exaggerated response to secondary stimuli (Netea 2016); a process mediated itself by epigenetic reprogramming (Saeed 2014), driven by a shift in metabolism with an increase in glycolysis dependent on the activation of mammalian target of rapamycin (mTOR) through a dectin-1/Akt/HIF1α (hypoxia-inducible factor-1α) pathway (Cheng 2014). It is unknown whether FcγR crosslinking induces a state of trained immunity; this is something we hope to address using our ATAC-seq experiment.

Bromodomain inhibition has proven efficacy in animal models of autoimmune disease; our research complements those of others, suggesting that this class of drug targets multiple immune effectors, with potential to modulate the development and maintenance of the allo/autoimmune response to IgG (Figure 108). Reducing DC migration at the time of tissue implantation and antigen exposure may suppress the development of alloimmune responses in the setting of transplantation. Impeding presentation of persistent self-antigen that accumulates in SLE, may impact maintenance of autoimmune responses. Reduced MNP activation in response to FcγR crosslinking may attenuate the response to deposited immune complex, giving potential for use in established autoimmune disease and ABMR. Early phase studies of bromodomain inhibitors in solid organ and haematological malignancy are recruiting (clinical trial identifier NCT01587703; NCT01943851); as we gain more experience of their clinical use, if their tolerability is acceptable, it is likely that they will be tested in the field of autoimmunity.

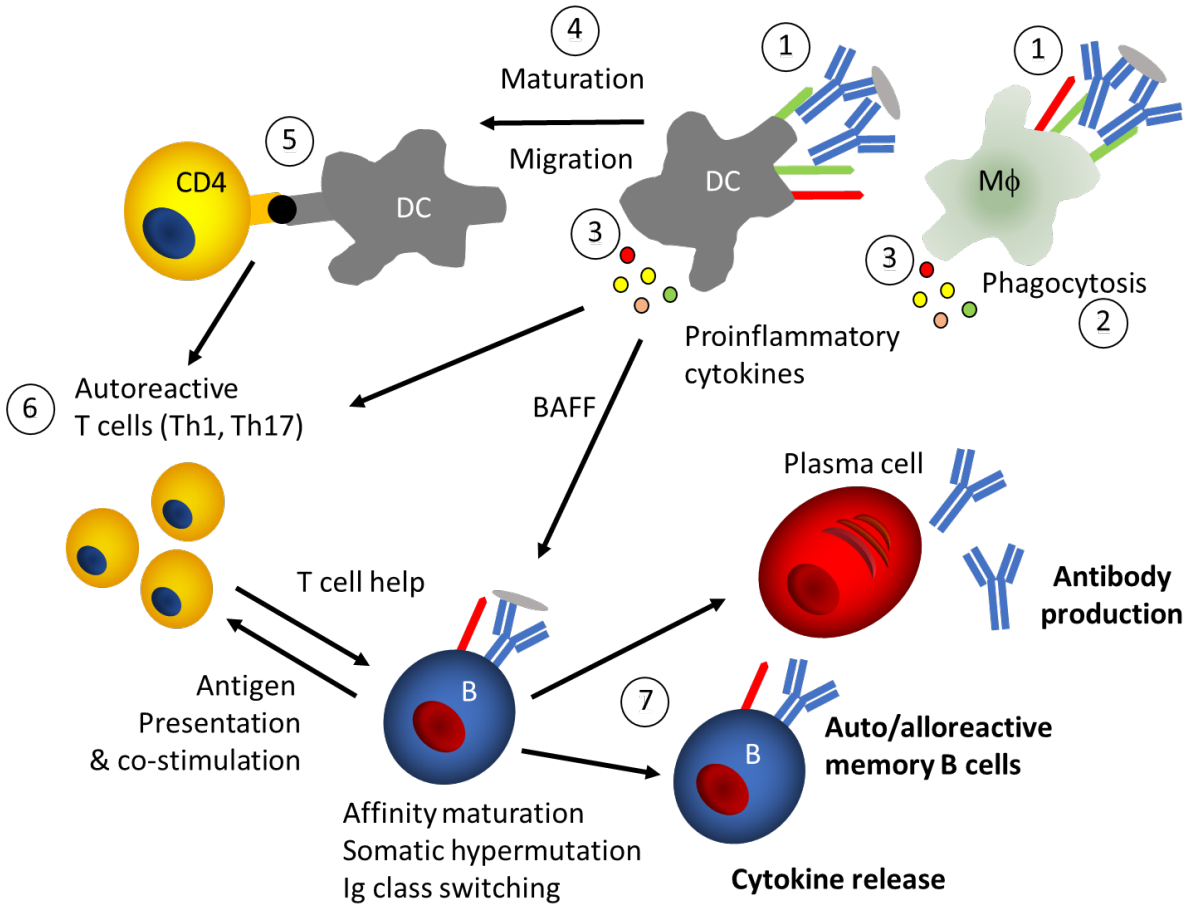


*Figure 108: Bromodomain inhibitors act at multiple sites and are of* potential therapeutic benefit in the setting of antibody-associated inflammation. *I-BET reduces expression of FcγR on macrophages and DC (1). Our in vivo studies suggest a greater reduction in activatory receptors compared to FcγR2b leading to a reduced A/I ratio and increased threshold for cell activation.* I-BET delays

phagolysosome maturation associated with build-up of immune complex (2) whilst selectively inhibiting IC induced cytokine production (3). Following encounter with IC, in the presence of I-BET DC fail to mature fully, expressing reduced levels of costimulatory receptors CD80 and CD86; and migration towards draining lymph nodes is impaired (4). An altered pattern of DC cytokine release associated with reduced expression of co-stimulatory receptors may favour provision of tolerogenic signals to T cells (5) and has been associated with increased numbers of regulatory T cells (Schilderink 2016). I-BET treatment directly effects T cell polarisation, with documented effects of Th1 (Bandukwala 2012) and Th17 subsets (Mele 2013) (6). Reduced secretion of BAFF and proinflammatory cytokines together with direct effects on B cells (Belkina 2014, Stanlie 2014, Gao 2015) may hinder development of autoreactive B cells and antibody (7).

**Acknowledgements**

The work contained in this thesis would not have been possible without the help of a number of colleagues, friends and family who have generously shared their time, expertise and support.

**Professor Lorraine Harper and the Birmingham NIHR funded Academic Clinical Fellow Programme** for allowing me to spend time in Menna Clatworthy's laboratory to gain preliminary data to support my application for a **Wellcome Trust funded Translational Medicine and Theurapeutics (TMAT) PhD Fellowship** (**102728/z/13/z)**.

The **Wellcome Trust** for their generous support.

**GlaxoSmithKline** for funding the BEL114424 study and the microarray portion of the I-BET work together with the proposed ATACseq experiment.

**Ms. Elizabeth McIntyre**, Graduate and Clinical Academic Training Office, School of Clinical Medicine, University of Cambridge for assistance with all TMAT queries.

**Dr. Nick Barry, Dr. Mathias Pasche and Dr. Jonathan Howe** (LMB) for their technical help with microscopy. **Dr. Verena Bröcker** (Addenbrooke's Hospital) for her assistance looking for signs of induced glomerulonephritis in murine kidney sections.

To all my colleagues in the **Clatworthy lab** for your support. In particular **Dr. Miriam Berry** for welcoming me into the laboratory when it was starting out, teaching me the fundamentals and providing ongoing support back in Birmingham. **Mr. Chenzhi Ying** for sharing mice legs and BMDM, and teaching me the basics of R. **Dr. Benjamin Stewart** for bearing with me whilst teaching about tSNE. **Dr. Ondrej Suchanek** for his assistance with peritoneal lavage and general enthusiasm for all things immunology. **Dr. Elizabeth Wlodek** who drew the short straw of sharing a desk (apologies!) and for our discussions about how best to work with industry partners. **Dr. Laurence Lok** for advice and company using Imaris. **Dr. Kirsten Scott** for being an inspiring medic scientist mummy. **Dr. Kevin Loudon** for his friendship and motivation. **Dr. Patrick Trotter** (Department of Surgery) for his support and encouragement on our transplant conference circuit. **Dr. John Ferdinand** for his general guidance, attempting to teach me transcriptomic analysis and then all his hard work redoing it professionally. **Dr. Rebeccah Mathews** for showing me where everything was (and constantly reminding me), for all her help in the mouse house and laboratory, for ensuring microarray samples were processed whilst I was on maternity leave and for generally keeping the laboratory running smoothly.

To all those who assisted with the planning and running of the BEL114424 study. **Dr. Nicholas Torpey** for overseeing the study. **Ms. Anne-Marie O'Sullivan** for her hard work supporting me to enrol subjects and organising their ongoing care. The staff at the **NIHR/Wellcome Trust Clinical Research Facility** for administrating infusions. The pharmacy team for preparing them. All the staff of the Addenbrooke's Transplant Unit for their care of research participants on the ward and beyond. The GSK **BEL114424 study team. Dr Andrew Want**, **Dr Sara Franco** and the **GlaxoSmithKline Clinical Unit Cambridge** for technical support. **Addenbrooke's Hospital Histocompatibility and Immunogenetics laboratory and pathology services** for their assistance with sample processing. **ThermoFisher** for their advice on ProtoArray analysis. **Dr. David Game and colleagues at Guy's and St Thomas' NHS Foundation Trust** for their contribution to subject screening. My most grateful thanks go to all the **patients who participated in the study**, without whom this work would not have been possible.

To all those within the **ImmunoInflammation Therapy Area Unit, GSK, Stevenage, UK.** In particular, **Ms. Adele Gibson** for all her hard work validating the Breg assay to GCP conditions; for keeping me company during the many hours we spent together running patient samples and doing what seemed like endless trial data analysis and QC; for ensuring the upmost data integrity at all times and teaching me how to navigate GSK internal procedures. **Mr. Joseph Chadwick,** an undergraduate student from the University of Bath, who performed the Breg healthy control studies in section 3.4.11; he did incredibly well to complete this work under tight time constraints to GSK GCP standards and I wish him every success with his future studies. **Dr. Shaun Flint,** who started processing BEL114424 samples as a fellow Wellcome Trust TMAT PhD and continued to support the BEL114424 study as a GSK employee, leading the microarray and ProtoArray analyses and assisting Adele and I by pre-processing the exploratory dataset. **Mr. Don Shanahan** for statistical oversight. **Dr. Rachel Jones**, **Dr. Luke Devey, Dr. Anna Richards** and **Prof. Lars-Peter Erwig** for their roles over the course of the study as trial clinicians. **Dr. Robbie Henderson** for his scientific input and supervision. **Prof. Caroline Savage** for providing mentorship.

**Dr. Paul Lyons,** University of Cambridge, for his oversight of the BEL114424 microarray analysis.

To all the **BEL114424 study authors** for your input in preparing abstracts, presentations and manuscripts.

**Dr. Rab Prinjha,** Epinova Epigenetics DPU, GSK, Stevenage for the opportunity to work with I-BET.

**Dr. Nicholas Smithers,** Epinova Epigenetics DPU, GSK, Stevenage for providing oversight within GSK of the I-BET work and for his help arranging additional funds.

On a more personal note, I would like to thank my family for making this work possible. I could not have completed my studies without the huge amount of emotional and practical support offered by my husband **James**. Thank you for supporting me in my decision to return to Cambridge, the numerous journeys up and down the A14, and for being an excellent hands-on daddy enabling us to have two children over the course of my PhD. Thank you to **Joshua** for embracing having two homes and sleeping just enough to allow me to get work done. Thank you to **Francesca** for holding on just long enough and for letting me complete this thesis in your first few months. Hopefully one day you will both look back and be proud of what we achieved.

And finally, to my supervisor **Dr. Menna Clatworthy**, thank you for inspiring me as a medical student; bringing me under your wing and starting off the BAFF journey. Thank you for all your scientific supervision and practical support along the way. Thank you for bearing with me and appreciating my need to work with more flexibility as my family grew.

**References**

Aderem, A. and Underhill, D. M. (1999). "Mechanisms of phagocytosis in macrophages." Annu Rev Immunol **17**: 593-623.

Almond, P. S., Matas, A., Gillingham, K., Dunn, D. L., Payne, W. D., Gores, P., Gruessner, R. and Najarian, J. S. (1993). "Risk factors for chronic rejection in renal allograft recipients." Transplantation **55**(4): 752-756; discussion 756-757.

Andrieu, G., Belkina, A. C. and Denis, G. V. (2016a). "Clinical trials for BET inhibitors run ahead of the science." Drug Discov Today Technol **19**: 45-50.

Andrieu, G., Tran, A. H., Strissel, K. J. and Denis, G. V. (2016b). "BRD4 Regulates Breast Cancer Dissemination through Jagged1/Notch1 Signaling." Cancer Res **76**(22): 6555-6567.

Angeli, V., Ginhoux, F., Llodra, J., Quemeneur, L., Frenette, P. S., Skobe, M., Jessberger, R., Merad, M. and Randolph, G. J. (2006). "B cell-driven lymphangiogenesis in inflamed lymph nodes enhances dendritic cell mobilization." Immunity **24**(2): 203-215.

Aravena, O., Ferrier, A., Menon, M., Mauri, C., Aguillon, J. C., Soto, L. and Catalan, D. (2017). "TIM-1 defines a human regulatory B cell population that is altered in frequency and function in systemic sclerosis patients." Arthritis Res Ther **19**(1): 8.

Avery, D. T., Kalled, S. L., Ellyard, J. I., Ambrose, C., Bixler, S. A., Thien, M., Brink, R., Mackay, F., Hodgkin, P. D. and Tangye, S. G. (2003). "BAFF selectively enhances the survival of plasmablasts generated from human memory B cells." J Clin Invest **112**(2): 286-297.

Baechler, E. C., Batliwalla, F. M., Karypis, G., Gaffney, P. M., Ortmann, W. A., Espe, K. J., Shark, K. B., Grande, W. J., Hughes, K. M., Kapur, V., Gregersen, P. K. and Behrens, T. W. (2003). "Interferon-inducible gene expression signature in peripheral blood cells of patients with severe lupus." Proc Natl Acad Sci U S A **100**(5): 2610-2615.

Bagavant, H. and Fu, S. M. (2009). "Pathogenesis of kidney disease in systemic lupus erythematosus." Curr Opin Rheumatol **21**(5): 489-494.

Bagley, J. A., Yan, Z., Zhang, W., Wildonger, J., Jan, L. Y. and Jan, Y. N. (2014). "Double-bromo and extraterminal (BET) domain proteins regulate dendrite morphology and mechanosensory function." Genes Dev **28**(17): 1940-1956.

Banchereau, J. and Steinman, R. M. (1998). "Dendritic cells and the control of immunity." Nature **392**(6673): 245-252.

Bandukwala, H. S., Gagnon, J., Togher, S., Greenbaum, J. A., Lamperti, E. D., Parr, N. J., Molesworth, A. M., Smithers, N., Lee, K., Witherington, J., Tough, D. F., Prinjha, R. K., Peters, B. and Rao, A. (2012). "Selective inhibition of CD4+ T-cell cytokine production and autoimmunity by BET protein and c-Myc inhibitors." Proc Natl Acad Sci U S A **109**(36): 14532-14537.

Banham-Hall, E., Clatworthy, M. R. and Okkenhaug, K. (2012). "The Therapeutic Potential for PI3K Inhibitors in Autoimmune Rheumatic Diseases." Open Rheumatol J **6**: 245-258.

Banham, G., Prezzi, D., Harford, S., Taylor, C. J., Hamer, R., Higgins, R., Bradley, J. A. and Clatworthy, M. R. (2013). "Elevated pretransplantation soluble BAFF is associated with an increased risk of acute antibody-mediated rejection." Transplantation **96**(4): 413-420.

Banham, G. D., Flint, S. M., Torpey, N., Lyons, P. A., Shanahan, D. N., Gibson, A., Watson, C. J. E., O'Sullivan, A. M., Chadwick, J. A., Foster, K. E., Jones, R. B., Devey, L. R., Richards, A., Erwig, L. P., Savage, C. O., Smith, K. G. C., Henderson, R. B. and Clatworthy, M. R. (2018). "Belimumab in kidney transplantation: an experimental medicine, randomised, placebo-controlled phase 2 trial." Lancet **391**(10140): 2619-2630.

Bannister, A. J. and Kouzarides, T. (2011). "Regulation of chromatin by histone modifications." Cell Res **21**(3): 381-395.

Baratin, M., Foray, C., Demaria, O., Habbeddine, M., Pollet, E., Maurizio, J., Verthuy, C., Davanture, S., Azukizawa, H., Flores-Langarica, A., Dalod, M. and Lawrence, T. (2015). "Homeostatic NF-kappaB Signaling in Steady-State Migratory Dendritic Cells Regulates Immune Homeostasis and Tolerance." Immunity **42**(4): 627-639.

Barnden, M. J., Allison, J., Heath, W. R. and Carbone, F. R. (1998). "Defective TCR expression in transgenic mice constructed using cDNA-based alpha- and beta-chain genes under the control of heterologous regulatory elements." Immunol Cell Biol **76**(1): 34-40.

Barr, T. A., Shen, P., Brown, S., Lampropoulou, V., Roch, T., Lawrie, S., Fan, B., O'Connor, R. A., Anderton, S. M., Bar-Or, A., Fillatreau, S. and Gray, D. (2012). "B cell depletion therapy ameliorates autoimmune disease through ablation of IL-6-producing B cells." J Exp Med **209**(5): 1001-1010.

Belkina, A. C., Blanton, W. P., Nikolajczyk, B. S. and Denis, G. V. (2014). "The double bromodomain protein Brd2 promotes B cell expansion and mitogenesis." J Leukoc Biol **95**(3): 451-460.

Belkina, A. C. and Denis, G. V. (2012). "BET domain co-regulators in obesity, inflammation and cancer." Nat Rev Cancer **12**(7): 465-477.

Belkina, A. C., Nikolajczyk, B. S. and Denis, G. V. (2013). "BET protein function is required for inflammation: Brd2 genetic disruption and BET inhibitor JQ1 impair mouse macrophage inflammatory responses." J Immunol **190**(7): 3670-3678.

Benson, M. J., Dillon, S. R., Castigli, E., Geha, R. S., Xu, S., Lam, K. P. and Noelle, R. J. (2008). "Cutting edge: the dependence of plasma cells and independence of memory B cells on BAFF and APRIL." J Immunol **180**(6): 3655-3659.

Bentall, A., Cornell, L. D., Gloor, J. M., Park, W. D., Gandhi, M. J., Winters, J. L., Chedid, M. F., Dean, P. G. and Stegall, M. D. (2013). "Five-year outcomes in living donor kidney transplants with a positive crossmatch." Am J Transplant **13**(1): 76-85.

Benvenuti, F., Hugues, S., Walmsley, M., Ruf, S., Fetler, L., Popoff, M., Tybulewicz, V. L. and Amigorena, S. (2004). "Requirement of Rac1 and Rac2 expression by mature dendritic cells for T cell priming." Science **305**(5687): 1150-1153.

Bernasconi, N. L., Traggiai, E. and Lanzavecchia, A. (2002). "Maintenance of serological memory by polyclonal activation of human memory B cells." Science **298**(5601): 2199-2202.

Berry, M. R., Mathews, R. J., Ferdinand, J. R., Jing, C., Loudon, K. W., Wlodek, E., Dennison, T. W., Kuper, C., Neuhofer, W. and Clatworthy, M. R. (2017). "Renal Sodium Gradient Orchestrates a Dynamic Antibacterial Defense Zone." Cell **170**(5): 860-874 e819.

Blair, P. A., Chavez-Rueda, K. A., Evans, J. G., Shlomchik, M. J., Eddaoudi, A., Isenberg, D. A., Ehrenstein, M. R. and Mauri, C. (2009). "Selective targeting of B cells with agonistic anti-CD40 is an efficacious strategy for the generation of induced regulatory T2-like B cells and for the suppression of lupus in MRL/lpr mice." J Immunol **182**(6): 3492-3502.

Blair, P. A., Norena, L. Y., Flores-Borja, F., Rawlings, D. J., Isenberg, D. A., Ehrenstein, M. R. and Mauri, C. (2010). "CD19(+)CD24(hi)CD38(hi) B cells exhibit regulatory capacity in healthy individuals but are functionally impaired in systemic Lupus Erythematosus patients." Immunity **32**(1): 129-140.

Blanco, P., Palucka, A. K., Gill, M., Pascual, V. and Banchereau, J. (2001). "Induction of dendritic cell differentiation by IFN-alpha in systemic lupus erythematosus." Science **294**(5546): 1540-1543.

Bloom, D., Chang, Z., Pauly, K., Kwun, J., Fechner, J., Hayes, C., Samaniego, M. and Knechtle, S. (2009). "BAFF is increased in renal transplant patients following treatment with alemtuzumab." Am J Transplant **9**(8): 1835-1845.

Bohl, D. L. and Brennan, D. C. (2007). "BK virus nephropathy and kidney transplantation." Clin J Am Soc Nephrol **2 Suppl 1**: S36-46.

Bolland, S. and Ravetch, J. V. (2000). "Spontaneous autoimmune disease in Fc(gamma)RIIB-deficient mice results from strain-specific epistasis." Immunity **13**(2): 277-285.

Bolton, W. K. (1996). "Goodpasture's syndrome." Kidney Int **50**(5): 1753-1766.

Bork, P., Holm, L. and Sander, C. (1994). "The immunoglobulin fold. Structural classification, sequence patterns and common core." J Mol Biol **242**(4): 309-320.

Boross, P., Arandhara, V. L., Martin-Ramirez, J., Santiago-Raber, M. L., Carlucci, F., Flierman, R., van der Kaa, J., Breukel, C., Claassens, J. W., Camps, M., Lubberts, E., Salvatori, D., Rastaldi, M. P., Ossendorp, F., Daha, M. R., Cook, H. T., Izui, S., Botto, M. and Verbeek, J. S. (2011). "The inhibiting Fc receptor for IgG, FcgammaRIIB, is a modifier of autoimmune susceptibility." J Immunol **187**(3): 1304-1313.

Boruchov, A. M., Heller, G., Veri, M. C., Bonvini, E., Ravetch, J. V. and Young, J. W. (2005). "Activating and inhibitory IgG Fc receptors on human DCs mediate opposing functions." J Clin Invest **115**(10): 2914-2923.

Bosello, S., Youinou, P., Daridon, C., Tolusso, B., Bendaoud, B., Pietrapertosa, D., Morelli, A. and Ferraccioli, G. (2008). "Concentrations of BAFF correlate with autoantibody levels, clinical disease activity, and response to treatment in early rheumatoid arthritis." J Rheumatol **35**(7): 1256-1264.

Bossen, C. and Schneider, P. (2006). "BAFF, APRIL and their receptors: structure, function and signaling." Semin Immunol **18**(5): 263-275.

Braza, F., Chesne, J., Durand, M., Dirou, S., Brosseau, C., Mahay, G., Cheminant, M. A., Magnan, A. and Brouard, S. (2015). "A regulatory CD9(+) B-cell subset inhibits HDM-induced allergic airway inflammation." Allergy **70**(11): 1421-1431.

Brown, J. D., Lin, C. Y., Duan, Q., Griffin, G., Federation, A. J., Paranal, R. M., Bair, S., Newton, G., Lichtman, A. H., Kung, A. L., Yang, T., Wang, H., Luscinskas, F. W., Croce, K. J., Bradner, J. E. and Plutzky, J. (2014). "NF-kappaB directs dynamic super enhancer formation in inflammation and atherogenesis." Mol Cell **56**(2): 219-231.

Brownlie, R. J., Lawlor, K. E., Niederer, H. A., Cutler, A. J., Xiang, Z., Clatworthy, M. R., Floto, R. A., Greaves, D. R., Lyons, P. A. and Smith, K. G. (2008). "Distinct cell-specific control of autoimmunity and infection by FcgammaRIIb." J Exp Med **205**(4): 883-895.

Carvalho, B. S. and Irizarry, R. A. (2010). "A framework for oligonucleotide microarray preprocessing." Bioinformatics **26**(19): 2363-2367.

Castigli, E., Wilson, S. A., Garibyan, L., Rachid, R., Bonilla, F., Schneider, L. and Geha, R. S. (2005a). "TACI is mutant in common variable immunodeficiency and IgA deficiency." Nat Genet **37**(8): 829-834.

Castigli, E., Wilson, S. A., Scott, S., Dedeoglu, F., Xu, S., Lam, K. P., Bram, R. J., Jabara, H. and Geha, R. S. (2005b). "TACI and BAFF-R mediate isotype switching in B cells." J Exp Med **201**(1): 35-39.

Cera, M. R., Del Prete, A., Vecchi, A., Corada, M., Martin-Padura, I., Motoike, T., Tonetti, P., Bazzoni, G., Vermi, W., Gentili, F., Bernasconi, S., Sato, T. N., Mantovani, A. and Dejana, E. (2004). "Increased DC trafficking to lymph nodes and contact hypersensitivity in junctional adhesion molecule-A-deficient mice." J Clin Invest **114**(5): 729-738.

Chan, C. H., Fang, C., Yarilina, A., Prinjha, R. K., Qiao, Y. and Ivashkiv, L. B. (2014). "BET bromodomain inhibition suppresses transcriptional responses to cytokine-Jak-STAT signaling in a gene-specific manner in human monocytes." Eur J Immunol.

Chan, O. and Shlomchik, M. J. (1998). "A new role for B cells in systemic autoimmunity: B cells promote spontaneous T cell activation in MRL-lpr/lpr mice." J Immunol **160**(1): 51-59.

Chan, O. T., Hannum, L. G., Haberman, A. M., Madaio, M. P. and Shlomchik, M. J. (1999). "A novel mouse with B cells but lacking serum antibody reveals an antibody-independent role for B cells in murine lupus." J Exp Med **189**(10): 1639-1648.

Chandraker, A., Kobashigawa, J., Stehlik, J., Givertz, M., Pierson, r., Pinney, S., Joren, M., Nissen, S., Guleria, I., Morrison, Y., Armstrong, B., Bridges, N., Sayegh, M. H. and Starling, R. (2016). "Rituximab Induction in Cardiac Transplantation Is Associated with

Accelerated Coronary Artery Vasculopathy: CTOT11." American Journal of Transplantation **16**(Supplement S3): 403.

Chapuy, B., McKeown, M. R., Lin, C. Y., Monti, S., Roemer, M. G., Qi, J., Rahl, P. B., Sun, H. H., Yeda, K. T., Doench, J. G., Reichert, E., Kung, A. L., Rodig, S. J., Young, R. A., Shipp, M. A. and Bradner, J. E. (2013). "Discovery and characterization of super-enhancer-associated dependencies in diffuse large B cell lymphoma." Cancer Cell **24**(6): 777-790.

Cheng, S. C., Quintin, J., Cramer, R. A., Shepardson, K. M., Saeed, S., Kumar, V., Giamarellos-Bourboulis, E. J., Martens, J. H., Rao, N. A., Aghajanirefah, A., Manjeri, G. R., Li, Y., Ifrim, D. C., Arts, R. J., van der Veer, B. M., Deen, P. M., Logie, C., O'Neill, L. A., Willems, P., van de Veerdonk, F. L., van der Meer, J. W., Ng, A., Joosten, L. A., Wijmenga, C., Stunnenberg, H. G., Xavier, R. J. and Netea, M. G. (2014). "mTOR- and HIF-1alpha-mediated aerobic glycolysis as metabolic basis for trained immunity." Science **345**(6204): 1250684.

Cherukuri, A., Rothstein, D. M., Clark, B., Carter, C. R., Davison, A., Hernandez-Fuentes, M., Hewitt, E., Salama, A. D. and Baker, R. J. (2014). "Immunologic human renal allograft injury associates with an altered IL-10/TNF-alpha expression ratio in regulatory B cells." J Am Soc Nephrol **25**(7): 1575-1585.

Cherukuri, A., Salama, A., Carter, C., Clark, B., Rothstein, D. and Baker, R. (2013). "Human Regulatory B Cells (BRegs) Are Characterised by Both IL-10 and TNF-α Expression and Are Reduced in Numbers with Altered Function in Renal Transplant Recipients with Immunological Graft Injury." American Journal of Transplantation **13**(s5, A645): 229.

Chesneau, M., Pallier, A., Braza, F., Lacombe, G., Le Gallou, S., Baron, D., Giral, M., Danger, R., Guerif, P., Aubert-Wastiaux, H., Neel, A., Michel, L., Laplaud, D. A., Degauque, N., Soulillou, J. P., Tarte, K. and Brouard, S. (2014). "Unique B cell differentiation profile in tolerant kidney transplant patients." Am J Transplant **14**(1): 144-155.

Cheung, K., Lu, G., Sharma, R., Vincek, A., Zhang, R., Plotnikov, A. N., Zhang, F., Zhang, Q., Ju, Y., Hu, Y., Zhao, L., Han, X., Meslamani, J., Xu, F., Jaganathan, A., Shen, T., Zhu, H., Rusinova, E., Zeng, L., Zhou, J., Yang, J., Peng, L., Ohlmeyer, M., Walsh, M. J., Zhang, D. Y., Xiong, H. and Zhou, M. M. (2017). "BET N-terminal bromodomain inhibition selectively blocks Th17 cell differentiation and ameliorates colitis in mice." Proc Natl Acad Sci U S A **114**(11): 2952-2957.

Choi, J., Aubert, O., Vo, A., Loupy, A., Haas, M., Puliyanda, D., Kim, I., Louie, S., Kang, A., Peng, A., Kahwaji, J., Reinsmoen, N., Toyoda, M. and Jordan, S. C. (2017). "Assessment of Tocilizumab (Anti-Interleukin-6 Receptor Monoclonal) as a Potential Treatment for Chronic Antibody-Mediated Rejection and Transplant Glomerulopathy in HLA-Sensitized Renal Allograft Recipients." Am J Transplant.

Christensen, A. D., Haase, C., Cook, A. D. and Hamilton, J. A. (2016). "K/BxN Serum-Transfer Arthritis as a Model for Human Inflammatory Arthritis." Front Immunol **7**: 213.

Clark, M. R., Campbell, K. S., Kazlauskas, A., Johnson, S. A., Hertz, M., Potter, T. A., Pleiman, C. and Cambier, J. C. (1992). "The B cell antigen receptor complex: association of Ig-alpha and Ig-beta with distinct cytoplasmic effectors." Science **258**(5079): 123-126.

Clatworthy, M. R. (2011). "Targeting B cells and antibody in transplantation." Am J Transplant **11**(7): 1359-1367.

Clatworthy, M. R., Aronin, C. E., Mathews, R. J., Morgan, N. Y., Smith, K. G. and Germain, R. N. (2014a). "Immune complexes stimulate CCR7-dependent dendritic cell migration to lymph nodes." Nat Med **20**(12): 1458-1463.

Clatworthy, M. R., Harford, S. K., Mathews, R. J. and Smith, K. G. (2014b). "FcgammaRIIb inhibits immune complex-induced VEGF-A production and intranodal lymphangiogenesis." Proc Natl Acad Sci U S A **111**(50): 17971-17976.

Clatworthy, M. R. and Smith, K. G. (2004). "FcgammaRIIb balances efficient pathogen clearance and the cytokine-mediated consequences of sepsis." J Exp Med **199**(5): 717-723.

Clatworthy, M. R., Watson, C. J., Plotnek, G., Bardsley, V., Chaudhry, A. N., Bradley, J. A. and Smith, K. G. (2009). "B-cell-depleting induction therapy and acute cellular rejection." N Engl J Med **360**(25): 2683-2685.

Craig, S. W. and Chen, H. (2003). "Lamellipodia protrusion: moving interactions of vinculin and Arp2/3." Curr Biol **13**(6): R236-238.

Craxton, A., Draves, K. E., Gruppi, A. and Clark, E. A. (2005). "BAFF regulates B cell survival by downregulating the BH3-only family member Bim via the ERK pathway." J Exp Med **202**(10): 1363-1374.

Crispin, J. C., Vargas-Rojas, M. I., Monsivais-Urenda, A. and Alcocer-Varela, J. (2012). "Phenotype and function of dendritic cells of patients with systemic lupus erythematosus." Clin Immunol **143**(1): 45-50.

Crotty, S. (2011). "Follicular helper CD4 T cells (TFH)." Annu Rev Immunol **29**: 621-663.

Cyster, J. G. (1999). "Chemokines and the homing of dendritic cells to the T cell areas of lymphoid organs." J Exp Med **189**(3): 447-450.

Dang, I., Gorelik, R., Sousa-Blin, C., Derivery, E., Guerin, C., Linkner, J., Nemethova, M., Dumortier, J. G., Giger, F. A., Chipysheva, T. A., Ermilova, V. D., Vacher, S., Campanacci, V., Herrada, I., Planson, A. G., Fetics, S., Henriot, V., David, V., Oguievetskaia, K., Lakisic, G., Pierre, F., Steffen, A., Boyreau, A., Peyrieras, N., Rottner, K., Zinn-Justin, S., Cherfils, J., Bieche, I., Alexandrova, A. Y., David, N. B., Small, J. V., Faix, J., Blanchoin, L. and Gautreau, A. (2013). "Inhibitory signalling to the Arp2/3 complex steers cell migration." Nature **503**(7475): 281-284.

Darce, J. R., Arendt, B. K., Wu, X. and Jelinek, D. F. (2007). "Regulated expression of BAFF-binding receptors during human B cell differentiation." J Immunol **179**(11): 7276-7286.

Dawson, M. A., Prinjha, R. K., Dittmann, A., Giotopoulos, G., Bantscheff, M., Chan, W. I., Robson, S. C., Chung, C. W., Hopf, C., Savitski, M. M., Huthmacher, C., Gudgin, E., Lugo, D., Beinke, S., Chapman, T. D., Roberts, E. J., Soden, P. E., Auger, K. R., Mirguet, O., Doehner, K., Delwel, R., Burnett, A. K., Jeffrey, P., Drewes, G., Lee, K., Huntly, B. J. and Kouzarides, T. (2011). "Inhibition of BET recruitment to chromatin as an effective treatment for MLL-fusion leukaemia." Nature **478**(7370): 529-533.

de Noronha, S., Hardy, S., Sinclair, J., Blundell, M. P., Strid, J., Schulz, O., Zwirner, J., Jones, G. E., Katz, D. R., Kinnon, C. and Thrasher, A. J. (2005). "Impaired dendritic-cell homing in vivo in the absence of Wiskott-Aldrich syndrome protein." Blood **105**(4): 1590-1597.

Decker, P., Kotter, I., Klein, R., Berner, B. and Rammensee, H. G. (2006). "Monocyte-derived dendritic cells over-express CD86 in patients with systemic lupus erythematosus." Rheumatology (Oxford) **45**(9): 1087-1095.

Dhalluin, C., Carlson, J. E., Zeng, L., He, C., Aggarwal, A. K. and Zhou, M. M. (1999). "Structure and ligand of a histone acetyltransferase bromodomain." Nature **399**(6735): 491-496.

Dhodapkar, K. M., Banerjee, D., Connolly, J., Kukreja, A., Matayeva, E., Veri, M. C., Ravetch, J. V., Steinman, R. M. and Dhodapkar, M. V. (2007). "Selective blockade of the inhibitory Fcgamma

receptor (FcgammaRIIB) in human dendritic cells and monocytes induces a type I interferon response program." J Exp Med **204**(6): 1359-1369.

Ding, D., Mehta, H., McCune, W. J. and Kaplan, M. J. (2006). "Aberrant phenotype and function of myeloid dendritic cells in systemic lupus erythematosus." J Immunol **177**(9): 5878-5889.

Ding, N., Hah, N., Yu, R. T., Sherman, M. H., Benner, C., Leblanc, M., He, M., Liddle, C., Downes, M. and Evans, R. M. (2015). "BRD4 is a novel therapeutic target for liver fibrosis." Proc Natl Acad Sci U S A **112**(51): 15713-15718.

Ding, Q., Yeung, M., Camirand, G., Zeng, Q., Akiba, H., Yagita, H., Chalasani, G., Sayegh, M. H., Najafian, N. and Rothstein, D. M. (2011). "Regulatory B cells are identified by expression of TIM-1 and can be induced through TIM-1 ligation to promote tolerance in mice." J Clin Invest **121**(9): 3645-3656.

Dragun, D., Muller, D. N., Brasen, J. H., Fritsche, L., Nieminen-Kelha, M., Dechend, R., Kintscher, U., Rudolph, B., Hoebeke, J., Eckert, D., Mazak, I., Plehm, R., Schonemann, C., Unger, T., Budde, K., Neumayer, H. H., Luft, F. C. and Wallukat, G. (2005). "Angiotensin II type 1-receptor activating antibodies in renal-allograft rejection." N Engl J Med **352**(6): 558-569.

Duan, Q., McMahon, S., Anand, P., Shah, H., Thomas, S., Salunga, H. T., Huang, Y., Zhang, R., Sahadevan, A., Lemieux, M. E., Brown, J. D., Srivastava, D., Bradner, J. E., McKinsey, T. A. and Haldar, S. M. (2017). "BET bromodomain inhibition suppresses innate inflammatory and profibrotic transcriptional networks in heart failure." Sci Transl Med **9**(390).

Eisenbarth, S. C., Williams, A., Colegio, O. R., Meng, H., Strowig, T., Rongvaux, A., Henao-Mejia, J., Thaiss, C. A., Joly, S., Gonzalez, D. G., Xu, L., Zenewicz, L. A., Haberman, A. M., Elinav, E., Kleinstein, S. H., Sutterwala, F. S. and Flavell, R. A. (2016). "Corrigendum: NLRP10 is a NOD-like receptor essential to initiate adaptive immunity by dendritic cells." Nature **530**(7591): 504.

Eleftheriadis, T., Pissas, G., Antoniadi, G., Liakopoulos, V. and Stefanidis, I. (2014). "Factors affecting effectiveness of vaccination against hepatitis B virus in hemodialysis patients." World J Gastroenterol **20**(34): 12018-12025.

Emlen, W., Niebur, J. and Kadera, R. (1994). "Accelerated in vitro apoptosis of lymphocytes from patients with systemic lupus erythematosus." J Immunol **152**(7): 3685-3692.

Epelman, S., Lavine, K. J. and Randolph, G. J. (2014). "Origin and functions of tissue macrophages." Immunity **41**(1): 21-35.

Evans, J. G., Chavez-Rueda, K. A., Eddaoudi, A., Meyer-Bahlburg, A., Rawlings, D. J., Ehrenstein, M. R. and Mauri, C. (2007). "Novel suppressive function of transitional 2 B cells in experimental arthritis." J Immunol **178**(12): 7868-7878.

Farh, K. K., Marson, A., Zhu, J., Kleinewietfeld, M., Housley, W. J., Beik, S., Shoresh, N., Whitton, H., Ryan, R. J., Shishkin, A. A., Hatan, M., Carrasco-Alfonso, M. J., Mayer, D., Luckey, C. J., Patsopoulos, N. A., De Jager, P. L., Kuchroo, V. K., Epstein, C. B., Daly, M. J., Hafler, D. A. and Bernstein, B. E. (2015). "Genetic and epigenetic fine mapping of causal autoimmune disease variants." Nature **518**(7539): 337-343.

Fearon, D. T. and Carter, R. H. (1995). "The CD19/CR2/TAPA-1 complex of B lymphocytes: linking natural to acquired immunity." Annu Rev Immunol **13**: 127-149.

Filippakopoulos, P., Qi, J., Picaud, S., Shen, Y., Smith, W. B., Fedorov, O., Morse, E. M., Keates, T., Hickman, T. T., Felletar, I., Philpott, M., Munro, S., McKeown, M. R., Wang, Y., Christie, A. L., West, N., Cameron, M. J., Schwartz, B., Heightman, T. D., La Thangue, N., French, C. A., Wiest, O., Kung, A. L., Knapp, S. and Bradner, J. E. (2010). "Selective inhibition of BET bromodomains." Nature **468**(7327): 1067-1073.

Fillatreau, S., Sweenie, C. H., McGeachy, M. J., Gray, D. and Anderton, S. M. (2002). "B cells regulate autoimmunity by provision of IL-10." Nat Immunol **3**(10): 944-950.

Flores-Borja, F., Bosma, A., Ng, D., Reddy, V., Ehrenstein, M. R., Isenberg, D. A. and Mauri, C. (2013). "CD19+CD24hiCD38hi B cells maintain regulatory T cells while limiting TH1 and TH17 differentiation." Sci Transl Med **5**(173): 173ra123.

Floto, R. A., Clatworthy, M. R., Heilbronn, K. R., Rosner, D. R., MacAry, P. A., Rankin, A., Lehner, P. J., Ouwehand, W. H., Allen, J. M., Watkins, N. A. and Smith, K. G. C. (2005). "Loss of function of a lupus-associated FcgammaRIIb polymorphism through exclusion from lipid rafts." Nat Med **11**(10): 1056-1058.

Forster, R., Schubel, A., Breitfeld, D., Kremmer, E., Renner-Muller, I., Wolf, E. and Lipp, M. (1999). "CCR7 coordinates the primary immune response by establishing functional microenvironments in secondary lymphoid organs." Cell **99**(1): 23-33.

Frittoli, E., Matteoli, G., Palamidessi, A., Mazzini, E., Maddaluno, L., Disanza, A., Yang, C., Svitkina, T., Rescigno, M. and Scita, G. (2011). "The signaling adaptor Eps8 is an essential actin capping protein for dendritic cell migration." Immunity **35**(3): 388-399.

Fu, W., Farache, J., Clardy, S. M., Hattori, K., Mander, P., Lee, K., Rioja, I., Weissleder, R., Prinjha, R. K., Benoist, C. and Mathis, D. (2014). "Epigenetic modulation of type-1 diabetes via a dual effect on pancreatic macrophages and beta cells." Elife **3**: e04631.

Fu, Y. X., Huang, G., Wang, Y. and Chaplin, D. D. (1998). "B lymphocytes induce the formation of follicular dendritic cell clusters in a lymphotoxin alpha-dependent fashion." J Exp Med **187**(7): 1009-1018.

Furie, R., Petri, M., Zamani, O., Cervera, R., Wallace, D. J., Tegzova, D., Sanchez-Guerrero, J., Schwarting, A., Merrill, J. T., Chatham, W. W., Stohl, W., Ginzler, E. M., Hough, D. R., Zhong, Z. J., Freimuth, W., van Vollenhoven, R. F. and Group, B.-S. (2011). "A phase III, randomized, placebo-controlled study of belimumab, a monoclonal antibody that inhibits B lymphocyte stimulator, in patients with systemic lupus erythematosus." Arthritis Rheum **63**(12): 3918-3930.

Gao, F., Yang, Y., Wang, Z., Gao, X. and Zheng, B. (2015). "BRAD4 plays a critical role in germinal center response by regulating Bcl-6 and NF-kappaB activation." Cell Immunol **294**(1): 1-8.

Garcia, B. A., Busby, S. A., Shabanowitz, J., Hunt, D. F. and Mishra, N. (2005). "Resetting the epigenetic histone code in the MRL-lpr/lpr mouse model of lupus by histone deacetylase inhibition." J Proteome Res **4**(6): 2032-2042.

Geissler, E. K. (2012). "The ONE Study compares cell therapy products in organ transplantation: introduction to a review series on suppressive monocyte-derived cells." Transplant Res **1**(1): 11.

Geissmann, F., Gordon, S., Hume, D. A., Mowat, A. M. and Randolph, G. J. (2010). "Unravelling mononuclear phagocyte heterogeneity." Nat Rev Immunol **10**(6): 453-460.

Giles, J. R., Kashgarian, M., Koni, P. A. and Shlomchik, M. J. (2015). "B Cell-Specific MHC Class II Deletion Reveals Multiple Nonredundant Roles for B Cell Antigen Presentation in Murine Lupus." J Immunol **195**(6): 2571-2579.

Ginhoux, F. and Jung, S. (2014). "Monocytes and macrophages: developmental pathways and tissue homeostasis." Nat Rev Immunol **14**(6): 392-404.

Goenka, R., Matthews, A. H., Zhang, B., O'Neill, P. J., Scholz, J. L., Migone, T. S., Leonard, W. J., Stohl, W., Hershberg, U. and Cancro, M. P. (2014). "Local BLyS production by T follicular cells mediates retention of high affinity B cells during affinity maturation." J Exp Med **211**(1): 45-56.

Golovkina, T. V., Shlomchik, M., Hannum, L. and Chervonsky, A. (1999). "Organogenic role of B lymphocytes in mucosal immunity." Science **286**(5446): 1965-1968.

Gonzalez, M., Mackay, F., Browning, J. L., Kosco-Vilbois, M. H. and Noelle, R. J. (1998). "The sequential role of lymphotoxin and B cells in the development of splenic follicles." J Exp Med **187**(7): 997-1007.

Goodnow, C. C., Sprent, J., Fazekas de St Groth, B. and Vinuesa, C. G. (2005). "Cellular and genetic mechanisms of self tolerance and autoimmunity." Nature **435**(7042): 590-597.

Gordan, S., Biburger, M. and Nimmerjahn, F. (2015). "bIgG time for large eaters: monocytes and macrophages as effector and target cells of antibody-mediated immune activation and repression." Immunol Rev **268**(1): 52-65.

Gordon, S., Pluddemann, A. and Martinez Estrada, F. (2014). "Macrophage heterogeneity in tissues: phenotypic diversity and functions." Immunol Rev **262**(1): 36-55.

Gray, M., Miles, K., Salter, D., Gray, D. and Savill, J. (2007). "Apoptotic cells protect mice from autoimmune inflammation by the induction of regulatory B cells." Proc Natl Acad Sci U S A **104**(35): 14080-14085.

Greenwald, R. J., Tumang, J. R., Sinha, A., Currier, N., Cardiff, R. D., Rothstein, T. L., Faller, D. V. and Denis, G. V. (2004). "E mu-BRD2 transgenic mice develop B-cell lymphoma and leukemia." Blood **103**(4): 1475-1484.

Griffin, D. O., Holodick, N. E. and Rothstein, T. L. (2011). "Human B1 cells in umbilical cord and adult peripheral blood express the novel phenotype CD20+ CD27+ CD43+ CD70." J Exp Med **208**(1): 67-80.

Gross, J. A., Johnston, J., Mudri, S., Enselman, R., Dillon, S. R., Madden, K., Xu, W., Parrish-Novak, J., Foster, D., Lofton-Day, C., Moore, M., Littau, A., Grossman, A., Haugen, H., Foley, K., Blumberg, H., Harrison, K., Kindsvogel, W. and Clegg, C. H. (2000). "TACI and BCMA are receptors for a TNF homologue implicated in B-cell autoimmune disease." Nature **404**(6781): 995-999.

Gunawan, M., Venkatesan, N., Loh, J. T., Wong, J. F., Berger, H., Neo, W. H., Li, L. Y., La Win, M. K., Yau, Y. H., Guo, T., See, P. C., Yamazaki, S., Chin, K. C., Gingras, A. R., Shochat, S. G., Ng, L. G., Sze, S.

K., Ginhoux, F. and Su, I. H. (2015). "The methyltransferase Ezh2 controls cell adhesion and migration through direct methylation of the extranuclear regulatory protein talin." Nat Immunol **16**(5): 505-516.

Haas, M. (2016). "The Revised (2013) Banff Classification for Antibody-Mediated Rejection of Renal Allografts: Update, Difficulties, and Future Considerations." Am J Transplant **16**(5): 1352-1357.

Haas, M., Sis, B., Racusen, L. C., Solez, K., Glotz, D., Colvin, R. B., Castro, M. C., David, D. S., David-Neto, E., Bagnasco, S. M., Cendales, L. C., Cornell, L. D., Demetris, A. J., Drachenberg, C. B., Farver, C. F., Farris, A. B., 3rd, Gibson, I. W., Kraus, E., Liapis, H., Loupy, A., Nickeleit, V., Randhawa, P., Rodriguez, E. R., Rush, D., Smith, R. N., Tan, C. D., Wallace, W. D., Mengel, M. and Banff meeting report writing, c. (2014). "Banff 2013 meeting report: inclusion of c4d-negative antibody-mediated rejection and antibody-associated arterial lesions." Am J Transplant **14**(2): 272-283.

Haessler, U., Pisano, M., Wu, M. and Swartz, M. A. (2011). "Dendritic cell chemotaxis in 3D under defined chemokine gradients reveals differential response to ligands CCL21 and CCL19." Proc Natl Acad Sci U S A **108**(14): 5614-5619.

Hah, N., Benner, C., Chong, L. W., Yu, R. T., Downes, M. and Evans, R. M. (2015). "Inflammation-sensitive super enhancers form domains of coordinately regulated enhancer RNAs." Proc Natl Acad Sci U S A **112**(3): E297-302.

Harada, Y., Tanaka, Y., Terasawa, M., Pieczyk, M., Habiro, K., Katakai, T., Hanawa-Suetsugu, K., Kukimoto-Niino, M., Nishizaki, T., Shirouzu, M., Duan, X., Uruno, T., Nishikimi, A., Sanematsu, F., Yokoyama, S., Stein, J. V., Kinashi, T. and Fukui, Y. (2012). "DOCK8 is a Cdc42 activator critical for interstitial dendritic cell migration during immune responses." Blood **119**(19): 4451-4461.

Hargreaves, D. C., Horng, T. and Medzhitov, R. (2009). "Control of inducible gene expression by signal-dependent transcriptional elongation." Cell **138**(1): 129-145.

Harris, D. P., Goodrich, S., Gerth, A. J., Peng, S. L. and Lund, F. E. (2005a). "Regulation of IFN-gamma production by B effector 1 cells: essential roles for T-bet and the IFN-gamma receptor." J Immunol **174**(11): 6781-6790.

Harris, D. P., Goodrich, S., Mohrs, K., Mohrs, M. and Lund, F. E. (2005b). "Cutting edge: the development of IL-4-producing B cells (B effector 2 cells) is controlled by IL-4, IL-4 receptor alpha, and Th2 cells." J Immunol **175**(11): 7103-7107.

Hashimoto, D., Chow, A., Noizat, C., Teo, P., Beasley, M. B., Leboeuf, M., Becker, C. D., See, P., Price, J., Lucas, D., Greter, M., Mortha, A., Boyer, S. W., Forsberg, E. C., Tanaka, M., van Rooijen, N., Garcia-Sastre, A., Stanley, E. R., Ginhoux, F., Frenette, P. S. and Merad, M. (2013). "Tissue-resident macrophages self-maintain locally throughout adult life with minimal contribution from circulating monocytes." Immunity **38**(4): 792-804.

Hawiger, D., Inaba, K., Dorsett, Y., Guo, M., Mahnke, K., Rivera, M., Ravetch, J. V., Steinman, R. M. and Nussenzweig, M. C. (2001). "Dendritic cells induce peripheral T cell unresponsiveness under steady state conditions in vivo." J Exp Med **194**(6): 769-779.

Heinz, S., Romanoski, C. E., Benner, C. and Glass, C. K. (2015). "The selection and function of cell type-specific enhancers." Nat Rev Mol Cell Biol **16**(3): 144-154.

Helft, J., Bottcher, J., Chakravarty, P., Zelenay, S., Huotari, J., Schraml, B. U., Goubau, D. and Reis e Sousa, C. (2015). "GM-CSF Mouse Bone Marrow Cultures Comprise a Heterogeneous Population of CD11c(+)MHCII(+) Macrophages and Dendritic Cells." Immunity **42**(6): 1197-1211.

Herrmann, M., Voll, R. E., Zoller, O. M., Hagenhofer, M., Ponner, B. B. and Kalden, J. R. (1998). "Impaired phagocytosis of apoptotic cell material by monocyte-derived macrophages from patients with systemic lupus erythematosus." Arthritis Rheum **41**(7): 1241-1250.

Hilkens, C. M. and Isaacs, J. D. (2013). "Tolerogenic dendritic cell therapy for rheumatoid arthritis: where are we now?" Clin Exp Immunol **172**(2): 148-157.

Hu, N., Qiu, X., Luo, Y., Yuan, J., Li, Y., Lei, W., Zhang, G., Zhou, Y., Su, Y. and Lu, Q. (2008). "Abnormal histone modification patterns in lupus CD4+ T cells." J Rheumatol **35**(5): 804-810.

Huang, B., Yang, X. D., Zhou, M. M., Ozato, K. and Chen, L. F. (2009). "Brd4 coactivates transcriptional activation of NF-kappaB via specific binding to acetylated RelA." Mol Cell Biol **29**(5): 1375-1387.

Huang, M., Zeng, S., Zou, Y., Shi, M., Qiu, Q., Xiao, Y., Chen, G., Yang, X., Liang, L. and Xu, H. (2017). "The suppression of bromodomain and extra-terminal domain inhibits vascular inflammation by blocking NF-kappaB and MAPK activation." Br J Pharmacol **174**(1): 101-115.

Ichiyasu, H., McCormack, J. M., McCarthy, K. M., Dombkowski, D., Preffer, F. I. and Schneeberger, E. E. (2004). "Matrix metalloproteinase-9-deficient dendritic cells have impaired migration through tracheal epithelial tight junctions." Am J Respir Cell Mol Biol **30**(6): 761-770.

Iijima, N., Yanagawa, Y., Clingan, J. M. and Onoe, K. (2005). "CCR7-mediated c-Jun N-terminal kinase activation regulates cell migration in mature dendritic cells." Int Immunol **17**(9): 1201-1212.

Inaba, A. and Clatworthy, M. R. (2016). "Novel immunotherapeutic strategies to target alloantibody-producing B and plasma cells in transplantation." Curr Opin Organ Transplant **21**(4): 419-426.

Irizarry, R. A., Bolstad, B. M., Collin, F., Cope, L. M., Hobbs, B. and Speed, T. P. (2003). "Summaries of Affymetrix GeneChip probe level data." Nucleic Acids Res **31**(4): e15.

Iwata, Y., Matsushita, T., Horikawa, M., Dilillo, D. J., Yanaba, K., Venturi, G. M., Szabolcs, P. M., Bernstein, S. H., Magro, C. M., Williams, A. D., Hall, R. P., St Clair, E. W. and Tedder, T. F. (2011). "Characterization of a rare IL-10-competent B-cell subset in humans that parallels mouse regulatory B10 cells." Blood **117**(2): 530-541.

Jackson, A. M., Sigdel, T. K., Delville, M., Hsieh, S. C., Dai, H., Bagnasco, S., Montgomery, R. A. and Sarwal, M. M. (2015). "Endothelial cell antibodies associated with novel targets and increased rejection." J Am Soc Nephrol **26**(5): 1161-1171.

Janeway CA Jr, T. P., Walport M, et al. (2001). Immunobiology: The Immune System in Health and Disease. New York, Garland Science.

Jawdat, D. M., Albert, E. J., Rowden, G., Haidl, I. D. and Marshall, J. S. (2004). "IgE-mediated mast cell activation induces Langerhans cell migration in vivo." J Immunol **173**(8): 5275-5282.

Jeannet, M., Pinn, V. W., Flax, M. H., Winn, H. J. and Russell, P. S. (1970). "Humoral antibodies in renal allotransplantation in man." N Engl J Med **282**(3): 111-117.

Jonsson, M. V., Szodoray, P., Jellestad, S., Jonsson, R. and Skarstein, K. (2005). "Association between circulating levels of the novel TNF family members APRIL and BAFF and lymphoid organization in primary Sjogren's syndrome." J Clin Immunol **25**(3): 189-201.

Jordan, S. C., Choi, J., Kim, I., Wu, G., Toyoda, M., Shin, B. and Vo, A. (2017). "Interleukin-6, A Cytokine Critical to Mediation of Inflammation, Autoimmunity and Allograft Rejection: Therapeutic Implications of IL-6 Receptor Blockade." Transplantation **101**(1): 32-44.

Jordan, S. C., Vo, A., Tyan, D. and Toyota, M. (2006). "Desensitization therapy with intravenous gammaglobulin (IVIG): applications in solid organ transplantation." Trans Am Clin Climatol Assoc **117**: 199-211; discussion 211.

Kagoya, Y., Nakatsugawa, M., Yamashita, Y., Ochi, T., Guo, T., Anczurowski, M., Saso, K., Butler, M. O., Arrowsmith, C. H. and Hirano, N. (2016). "BET bromodomain inhibition enhances T cell persistence and function in adoptive immunotherapy models." J Clin Invest **126**(9): 3479-3494.

Kaikkonen, M. U., Spann, N. J., Heinz, S., Romanoski, C. E., Allison, K. A., Stender, J. D., Chun, H. B., Tough, D. F., Prinjha, R. K., Benner, C. and Glass, C. K. (2013). "Remodeling of the enhancer landscape during macrophage activation is coupled to enhancer transcription." Mol Cell **51**(3): 310-325.

Kaplan, D. H. (2010). "In vivo function of Langerhans cells and dermal dendritic cells." Trends Immunol **31**(12): 446-451.

Karsten, C. M. and Kohl, J. (2012). "The immunoglobulin, IgG Fc receptor and complement triangle in autoimmune diseases." Immunobiology **217**(11): 1067-1079.

Khan, A. R., Hams, E., Floudas, A., Sparwasser, T., Weaver, C. T. and Fallon, P. G. (2015). "PD-L1hi B cells are critical regulators of humoral immunity." Nat Commun **6**: 5997.

Khare, S. D., Sarosi, I., Xia, X. Z., McCabe, S., Miner, K., Solovyev, I., Hawkins, N., Kelley, M., Chang, D., Van, G., Ross, L., Delaney, J., Wang, L., Lacey, D., Boyle, W. J. and Hsu, H. (2000). "Severe B cell hyperplasia and autoimmune disease in TALL-1 transgenic mice." Proc Natl Acad Sci U S A **97**(7): 3370-3375.

Klein, K., Kabala, P. A., Grabiec, A. M., Gay, R. E., Kolling, C., Lin, L. L., Gay, S., Tak, P. P., Prinjha, R. K., Ospelt, C. and Reedquist, K. A. (2016). "The bromodomain protein inhibitor I-BET151 suppresses expression of inflammatory genes and matrix degrading enzymes in rheumatoid arthritis synovial fibroblasts." Ann Rheum Dis **75**(2): 422-429.

Kobayashi, Y., Matsumoto, M., Kotani, M. and Makino, T. (1999). "Possible involvement of matrix metalloproteinase-9 in Langerhans cell migration and maturation." J Immunol **163**(11): 5989-5993.

Kometani, K. and Kurosaki, T. (2015). "Differentiation and maintenance of long-lived plasma cells." Curr Opin Immunol **33**: 64-69.

Kono, H., Kyogoku, C., Suzuki, T., Tsuchiya, N., Honda, H., Yamamoto, K., Tokunaga, K. and Honda, Z. (2005). "FcgammaRIIB Ile232Thr transmembrane polymorphism associated with human systemic lupus erythematosus decreases affinity to lipid rafts and attenuates inhibitory effects on B cell receptor signaling." Hum Mol Genet **14**(19): 2881-2892.

Kono, H. and Rock, K. L. (2008). "How dying cells alert the immune system to danger." Nat Rev Immunol **8**(4): 279-289.

Korganow, A. S., Ji, H., Mangialaio, S., Duchatelle, V., Pelanda, R., Martin, T., Degott, C., Kikutani, H., Rajewsky, K., Pasquali, J. L., Benoist, C. and Mathis, D. (1999). "From systemic T cell self-reactivity to organ-specific autoimmune disease via immunoglobulins." Immunity **10**(4): 451-461.

Krishnaswamy, J. K., Singh, A., Gowthaman, U., Wu, R., Gorrepati, P., Sales Nascimento, M., Gallman, A., Liu, D., Rhebergen, A. M., Calabro, S., Xu, L., Ranney, P., Srivastava, A., Ranson, M., Gorham, J. D., McCaw, Z., Kleeberger, S. R., Heinz, L. X., Muller, A. C., Bennett, K. L., Superti-Furga, G., Henao-Mejia, J., Sutterwala, F. S., Williams, A., Flavell, R. A. and Eisenbarth, S. C. (2015). "Coincidental loss of DOCK8 function in NLRP10-deficient and C3H/HeJ mice results in defective dendritic cell migration." Proc Natl Acad Sci U S A **112**(10): 3056-3061.

Kumar, V., Scandella, E., Danuser, R., Onder, L., Nitschke, M., Fukui, Y., Halin, C., Ludewig, B. and Stein, J. V. (2010). "Global lymphoid tissue remodeling during a viral infection is orchestrated by a B cell-lymphotoxin-dependent pathway." Blood **115**(23): 4725-4733.

Kwun, J., Page, E., Hong, J. J., Gibby, A., Yoon, J., Farris, A. B., Villinger, F. and Knechtle, S. (2015). "Neutralizing BAFF/APRIL with atacicept prevents early DSA formation and AMR development in T cell depletion induced nonhuman primate AMR model." Am J Transplant **15**(3): 815-822.

Lammermann, T., Bader, B. L., Monkley, S. J., Worbs, T., Wedlich-Soldner, R., Hirsch, K., Keller, M., Forster, R., Critchley, D. R., Fassler, R. and Sixt, M. (2008). "Rapid leukocyte migration by integrin-independent flowing and squeezing." Nature **453**(7191): 51-55.

Langfelder, P. and Horvath, S. (2008). "WGCNA: an R package for weighted correlation network analysis." BMC Bioinformatics **9**: 559.

Lanzavecchia, A. and Sallusto, F. (2007). "Toll-like receptors and innate immunity in B-cell activation and antibody responses." Curr Opin Immunol **19**(3): 268-274.

Lauffenburger, D. A. and Horwitz, A. F. (1996). "Cell migration: a physically integrated molecular process." Cell **84**(3): 359-369.

Lebre, M. C., Kalinski, P., Das, P. K. and Everts, V. (1999). "Inhibition of contact sensitizer-induced migration of human Langerhans cells by matrix metalloproteinase inhibitors." Arch Dermatol Res **291**(7-8): 447-452.

Leca, N. M., K. (2013). "Belimumab (Anti-BAFF/BLyS) Effective in a Case of Resistant Antibody Mediated Rejection " Am J Transplant **13 (suppl 5)**.

Lee, M. B., Lee, J. H., Hong, S. H., You, J. S., Nam, S. T., Kim, H. W., Park, Y. H., Lee, D., Min, K. Y., Park, Y. M., Kim, Y. M., Kim, H. S. and Choi, W. S. (2017). "JQ1, a BET inhibitor, controls TLR4-induced IL-10 production in regulatory B cells by BRD4-NF-kappaB axis." BMB Rep **50**(12): 640-646.

Lefaucheur, C., Loupy, A., Hill, G. S., Andrade, J., Nochy, D., Antoine, C., Gautreau, C., Charron, D., Glotz, D. and Suberbielle-Boissel, C. (2010). "Preexisting donor-specific HLA antibodies predict outcome in kidney transplantation." J Am Soc Nephrol **21**(8): 1398-1406.

Lefaucheur, C., Loupy, A., Vernerey, D., Duong-Van-Huyen, J. P., Suberbielle, C., Anglicheau, D., Verine, J., Beuscart, T., Nochy, D., Bruneval, P., Charron, D., Delahousse, M., Empana, J. P., Hill, G. S., Glotz, D., Legendre, C. and Jouven, X. (2013). "Antibody-mediated vascular rejection of kidney allografts: a population-based study." Lancet **381**(9863): 313-319.

LeRoy, G., Rickards, B. and Flint, S. J. (2008). "The double bromodomain proteins Brd2 and Brd3 couple histone acetylation to transcription." Mol Cell **30**(1): 51-60.

Lesley, R., Xu, Y., Kalled, S. L., Hess, D. M., Schwab, S. R., Shu, H. B. and Cyster, J. G. (2004). "Reduced competitiveness of autoantigen-engaged B cells due to increased dependence on BAFF." Immunity **20**(4): 441-453.

Li, L., Wadia, P., Chen, R., Kambham, N., Naesens, M., Sigdel, T. K., Miklos, D. B., Sarwal, M. M. and Butte, A. J. (2009). "Identifying compartment-specific non-HLA targets after renal transplantation by integrating transcriptome and "antibodyome" measures." Proc Natl Acad Sci U S A **106**(11): 4148-4153.

Lindquist, R. L., Shakhar, G., Dudziak, D., Wardemann, H., Eisenreich, T., Dustin, M. L. and Nussenzweig, M. C. (2004). "Visualizing dendritic cell networks in vivo." Nat Immunol **5**(12): 1243-1250.

Liu, Y., Masuda, E., Blank, M. C., Kirou, K. A., Gao, X., Park, M. S. and Pricop, L. (2005). "Cytokine-mediated regulation of activating and inhibitory Fc gamma receptors in human monocytes." J Leukoc Biol **77**(5): 767-776.

Loder, F., Mutschler, B., Ray, R. J., Paige, C. J., Sideras, P., Torres, R., Lamers, M. C. and Carsetti, R. (1999). "B cell development in the spleen takes place in discrete steps and is determined by the quality of B cell receptor-derived signals." J Exp Med **190**(1): 75-89.

Long, H., Yin, H., Wang, L., Gershwin, M. E. and Lu, Q. (2016). "The critical role of epigenetics in systemic lupus erythematosus and autoimmunity." J Autoimmun **74**: 118-138.

Loupy, A., Lefaucheur, C., Vernerey, D., Prugger, C., Duong van Huyen, J. P., Mooney, N., Suberbielle, C., Fremeaux-Bacchi, V., Mejean, A., Desgrandchamps, F., Anglicheau, D., Nochy, D., Charron, D., Empana, J. P., Delahousse, M., Legendre, C., Glotz, D., Hill, G. S., Zeevi, A. and Jouven, X. (2013). "Complement-binding anti-HLA antibodies and kidney-allograft survival." N Engl J Med **369**(13): 1215-1226.

Lucas, M., Zhang, X., Prasanna, V. and Mosser, D. M. (2005). "ERK activation following macrophage FcgammaR ligation leads to chromatin modifications at the IL-10 locus." J Immunol **175**(1): 469-477.

Lund, F. E. (2008). "Cytokine-producing B lymphocytes-key regulators of immunity." Curr Opin Immunol **20**(3): 332-338.

Lutz, M. B. and Schuler, G. (2002). "Immature, semi-mature and fully mature dendritic cells: which signals induce tolerance or immunity?" Trends Immunol **23**(9): 445-449.

Lyons, P. A., Koukoulaki, M., Hatton, A., Doggett, K., Woffendin, H. B., Chaudhry, A. N. and Smith, K. G. (2007). "Microarray analysis of human leucocyte subsets: the advantages of positive selection and rapid purification." BMC Genomics **8**: 64.

Mackay, F., Schneider, P., Rennert, P. and Browning, J. (2003). "BAFF AND APRIL: a tutorial on B cell survival." Annu Rev Immunol **21**: 231-264.

Mackay, F., Woodcock, S. A., Lawton, P., Ambrose, C., Baetscher, M., Schneider, P., Tschopp, J. and Browning, J. L. (1999). "Mice transgenic for BAFF develop lymphocytic disorders along with autoimmune manifestations." J Exp Med **190**(11): 1697-1710.

MacNeill, S. J., Casula, A., Shaw, C. and Castledine, C. (2016). "UK Renal Registry 18th Annual Report: Chapter 2 UK Renal Replacement Therapy Prevalence in 2014: National and Centre-specific Analyses." Nephron **132 Suppl 1**: 41-68.

Maddaluno, L., Verbrugge, S. E., Martinoli, C., Matteoli, G., Chiavelli, A., Zeng, Y., Williams, E. D., Rescigno, M. and Cavallaro, U. (2009). "The adhesion molecule L1 regulates transendothelial migration and trafficking of dendritic cells." J Exp Med **206**(3): 623-635.

Mandell, K. J., Babbin, B. A., Nusrat, A. and Parkos, C. A. (2005). "Junctional adhesion molecule 1 regulates epithelial cell morphology through effects on beta1 integrins and Rap1 activity." J Biol Chem **280**(12): 11665-11674.

Mantchev, G. T., Cortesao, C. S., Rebrovich, M., Cascalho, M. and Bram, R. J. (2007). "TACI is required for efficient plasma cell differentiation in response to T-independent type 2 antigens." J Immunol **179**(4): 2282-2288.

Manzi, S., Sanchez-Guerrero, J., Merrill, J. T., Furie, R., Gladman, D., Navarra, S. V., Ginzler, E. M., D'Cruz, D. P., Doria, A., Cooper, S., Zhong, Z. J., Hough, D., Freimuth, W., Petri, M. A., Bliss and Groups, B.-S. (2012). "Effects of belimumab, a B lymphocyte stimulator-specific inhibitor, on disease activity across multiple organ domains in patients with systemic lupus erythematosus: combined results from two phase III trials." Ann Rheum Dis **71**(11): 1833-1838.

Maritzen, T., Zech, T., Schmidt, M. R., Krause, E., Machesky, L. M. and Haucke, V. (2012). "Gadkin negatively regulates cell spreading and motility via sequestration of the actin-nucleating ARP2/3 complex." Proc Natl Acad Sci U S A **109**(26): 10382-10387.

Martin, F., Oliver, A. M. and Kearney, J. F. (2001). "Marginal zone and B1 B cells unite in the early response against T-independent blood-borne particulate antigens." Immunity **14**(5): 617-629.

Matsumoto, M., Baba, A., Yokota, T., Nishikawa, H., Ohkawa, Y., Kayama, H., Kallies, A., Nutt, S. L., Sakaguchi, S., Takeda, K., Kurosaki, T. and Baba, Y. (2014). "Interleukin-10-producing plasmablasts exert regulatory function in autoimmune inflammation." Immunity **41**(6): 1040-1051.

Mauri, C., Gray, D., Mushtaq, N. and Londei, M. (2003). "Prevention of arthritis by interleukin 10-producing B cells." J Exp Med **197**(4): 489-501.

Mauri, C. and Menon, M. (2015). "The expanding family of regulatory B cells." Int Immunol **27**(10): 479-486.

Mauri, C. and Menon, M. (2017). "Human regulatory B cells in health and disease: therapeutic potential." J Clin Invest **127**(3): 772-779.

Maxfield, S. J., Taylor, C. J., Kosmoliaptsis, V., Broecker, V., Watson, C. J., Bradley, J. A. and Peacock, S. (2015). "Transfer of HLA-Specific Allosensitization From a Highly Sensitized Deceased Organ Donor to the Recipients of Each Kidney." Am J Transplant **15**(9): 2501-2506.

Maynard, C. L. and Weaver, C. T. (2008). "Diversity in the contribution of interleukin-10 to T-cell-mediated immune regulation." Immunol Rev **226**: 219-233.

Mele, D. A., Salmeron, A., Ghosh, S., Huang, H. R., Bryant, B. M. and Lora, J. M. (2013). "BET bromodomain inhibition suppresses TH17-mediated pathology." J Exp Med **210**(11): 2181-2190.

Meng, S., Zhang, L., Tang, Y., Tu, Q., Zheng, L., Yu, L., Murray, D., Cheng, J., Kim, S. H., Zhou, X. and Chen, J. (2014). "BET Inhibitor JQ1 Blocks Inflammation and Bone Destruction." J Dent Res **93**(7): 657-662.

Menon, M., Blair, P. A., Isenberg, D. A. and Mauri, C. (2016). "A Regulatory Feedback between Plasmacytoid Dendritic Cells and Regulatory B Cells Is Aberrant in Systemic Lupus Erythematosus." Immunity **44**(3): 683-697.

Merad, M., Sathe, P., Helft, J., Miller, J. and Mortha, A. (2013). "The dendritic cell lineage: ontogeny and function of dendritic cells and their subsets in the steady state and the inflamed setting." Annu Rev Immunol **31**: 563-604.

Mirguet, O., Lamotte, Y., Donche, F., Toum, J., Gellibert, F., Bouillot, A., Gosmini, R., Nguyen, V. L., Delannee, D., Seal, J., Blandel, F., Boullay, A. B., Boursier, E., Martin, S., Brusq, J. M., Krysa, G., Riou, A., Tellier, R., Costaz, A., Huet, P., Dudit, Y., Trottet, L., Kirilovsky, J. and Nicodeme, E. (2012). "From ApoA1 upregulation to BET family bromodomain inhibition: discovery of I-BET151." Bioorg Med Chem Lett **22**(8): 2963-2967.

Miyara, M., Ito, Y. and Sakaguchi, S. (2014). "TREG-cell therapies for autoimmune rheumatic diseases." Nat Rev Rheumatol **10**(9): 543-551.

Mizoguchi, A., Mizoguchi, E., Takedatsu, H., Blumberg, R. S. and Bhan, A. K. (2002). "Chronic intestinal inflammatory condition generates IL-10-producing regulatory B cell subset characterized by CD1d upregulation." Immunity **16**(2): 219-230.

Moher, D., Schulz, K. F. and Altman, D. G. (2001). "The CONSORT statement: revised recommendations for improving the quality of reports of parallel-group randomised trials." Lancet **357**(9263): 1191-1194.

Montgomery, R. A., Lonze, B. E., King, K. E., Kraus, E. S., Kucirka, L. M., Locke, J. E., Warren, D. S., Simpkins, C. E., Dagher, N. N., Singer, A. L., Zachary, A. A. and Segev, D. L. (2011). "Desensitization in HLA-incompatible kidney recipients and survival." N Engl J Med **365**(4): 318-326.

Morelli, A. E. and Thomson, A. W. (2007). "Tolerogenic dendritic cells and the quest for transplant tolerance." Nat Rev Immunol **7**(8): 610-621.

Mosser, D. M. and Edwards, J. P. (2008). "Exploring the full spectrum of macrophage activation." Nat Rev Immunol **8**(12): 958-969.

Mujtaba, M. A., Komocsar, W. J., Nantz, E., Samaniego, M. D., Henson, S. L., Hague, J. A., Lobashevsky, A. L., Higgins, N. G., Czader, M., Book, B. K., Anderson, M. D., Pescovitz, M. D. and Taber, T. E. (2016). "Effect of Treatment With Tabalumab, a B Cell-Activating Factor Inhibitor, on Highly Sensitized Patients With End-Stage Renal Disease Awaiting Transplantation." Am J Transplant.

Munoz, L. E., Gaipl, U. S., Franz, S., Sheriff, A., Voll, R. E., Kalden, J. R. and Herrmann, M. (2005). "SLE--a disease of clearance deficiency?" Rheumatology (Oxford) **44**(9): 1101-1107.

Munoz, L. E., Lauber, K., Schiller, M., Manfredi, A. A. and Herrmann, M. (2010). "The role of defective clearance of apoptotic cells in systemic autoimmunity." Nat Rev Rheumatol **6**(5): 280-289.

Naji, A. "One Year Exploratory Study to Evaluate the Efficacy and Safety of Belimumab for Normalization of Alloantibody Levels in Sensitized Patients Awaiting Kidney Transplantation." Clinicaltrials.gov **NCT01025193**.

Navarra, S. V., Guzman, R. M., Gallacher, A. E., Hall, S., Levy, R. A., Jimenez, R. E., Li, E. K., Thomas, M., Kim, H. Y., Leon, M. G., Tanasescu, C., Nasonov, E., Lan, J. L., Pineda, L., Zhong, Z. J., Freimuth, W., Petri, M. A. and Group, B.-S. (2011). "Efficacy and safety of belimumab in patients with active systemic lupus erythematosus: a randomised, placebo-controlled, phase 3 trial." Lancet **377**(9767): 721-731.

Netea, M. G., Joosten, L. A., Latz, E., Mills, K. H., Natoli, G., Stunnenberg, H. G., O'Neill, L. A. and Xavier, R. J. (2016). "Trained immunity: A program of innate immune memory in health and disease." Science **352**(6284): aaf1098.

Newell, K. A., Asare, A., Kirk, A. D., Gisler, T. D., Bourcier, K., Suthanthiran, M., Burlingham, W. J., Marks, W. H., Sanz, I., Lechler, R. I., Hernandez-Fuentes, M. P., Turka, L. A., Seyfert-Margolis, V. L.

and Immune Tolerance Network, S. T. S. G. (2010). "Identification of a B cell signature associated with renal transplant tolerance in humans." J Clin Invest **120**(6): 1836-1847.

Nicodeme, E., Jeffrey, K. L., Schaefer, U., Beinke, S., Dewell, S., Chung, C. W., Chandwani, R., Marazzi, I., Wilson, P., Coste, H., White, J., Kirilovsky, J., Rice, C. M., Lora, J. M., Prinjha, R. K., Lee, K. and Tarakhovsky, A. (2010). "Suppression of inflammation by a synthetic histone mimic." Nature **468**(7327): 1119-1123.

Nielsen, C. H., Hegedus, L. and Leslie, R. G. (2004). "Autoantibodies in autoimmune thyroid disease promote immune complex formation with self antigens and increase B cell and CD4+ T cell proliferation in response to self antigens." Eur J Immunol **34**(1): 263-272.

Nimmerjahn, F. and Ravetch, J. V. (2007a). "The antiinflammatory activity of IgG: the intravenous IgG paradox." J Exp Med **204**(1): 11-15.

Nimmerjahn, F. and Ravetch, J. V. (2007b). "Fc-receptors as regulators of immunity." Adv Immunol **96**: 179-204.

Nimmerjahn, F. and Ravetch, J. V. (2008). "Fcgamma receptors as regulators of immune responses." Nat Rev Immunol **8**(1): 34-47.

Nitschke, L. (2005). "The role of CD22 and other inhibitory co-receptors in B-cell activation." Curr Opin Immunol **17**(3): 290-297.

Nobes, C. D. and Hall, A. (1995). "Rho, rac, and cdc42 GTPases regulate the assembly of multimolecular focal complexes associated with actin stress fibers, lamellipodia, and filopodia." Cell **81**(1): 53-62.

Nurieva, R. I., Chung, Y., Martinez, G. J., Yang, X. O., Tanaka, S., Matskevitch, T. D., Wang, Y. H. and Dong, C. (2009). "Bcl6 mediates the development of T follicular helper cells." Science **325**(5943): 1001-1005.

Nutt, S. L., Hodgkin, P. D., Tarlinton, D. M. and Corcoran, L. M. (2015). "The generation of antibody-secreting plasma cells." Nat Rev Immunol **15**(3): 160-171.

O'Connell, P. J., Kuypers, D. R., Mannon, R. B., Abecassis, M., Chadban, S. J., Gill, J. S., Murphy, B., Nickerson, P. W., Schold, J. D., Stock, P. G., Seron, D., Alloway, R. R., Bromberg, J. S., Budde, K., Jordan, S. C., Legendre, C., Lefaucheur, C., Sarwall, M., Segev, D. L., Stegall, M. D., Tullius, S. G., Wong, G., Woodle, E. S., Ascher, N. and Morris, R. E. (2017). "Clinical Trials for Immunosuppression

in Transplantation: The Case for Reform and Change in Direction." Transplantation **101**(7): 1527-1534.

O'Connor, B. P., Raman, V. S., Erickson, L. D., Cook, W. J., Weaver, L. K., Ahonen, C., Lin, L. L., Mantchev, G. T., Bram, R. J. and Noelle, R. J. (2004). "BCMA is essential for the survival of long-lived bone marrow plasma cells." J Exp Med **199**(1): 91-98.

O'Keeffe, M., Hochrein, H., Vremec, D., Caminschi, I., Miller, J. L., Anders, E. M., Wu, L., Lahoud, M. H., Henri, S., Scott, B., Hertzog, P., Tatarczuch, L. and Shortman, K. (2002). "Mouse plasmacytoid cells: long-lived cells, heterogeneous in surface phenotype and function, that differentiate into CD8(+) dendritic cells only after microbial stimulus." J Exp Med **196**(10): 1307-1319.

Ou, X., Xu, S. and Lam, K. P. (2012). "Deficiency in TNFRSF13B (TACI) expands T-follicular helper and germinal center B cells via increased ICOS-ligand expression but impairs plasma cell survival." Proc Natl Acad Sci U S A **109**(38): 15401-15406.

Pallier, A., Hillion, S., Danger, R., Giral, M., Racape, M., Degauque, N., Dugast, E., Ashton-Chess, J., Pettre, S., Lozano, J. J., Bataille, R., Devys, A., Cesbron-Gautier, A., Braudeau, C., Larrose, C., Soulillou, J. P. and Brouard, S. (2010). "Patients with drug-free long-term graft function display increased numbers of peripheral B cells with a memory and inhibitory phenotype." Kidney Int **78**(5): 503-513.

Parsons, R. F., Vivek, K., Redfield, R. R., 3rd, Migone, T. S., Cancro, M. P., Naji, A. and Noorchashm, H. (2010). "B-lymphocyte homeostasis and BLyS-directed immunotherapy in transplantation." Transplant Rev (Orlando) **24**(4): 207-221.

Parsons, R. F., Yu, M., Vivek, K., Zekavat, G., Rostami, S. Y., Ziaie, A. S., Luo, Y., Koeberlein, B., Redfield, R. R., Ward, C. D., Migone, T. S., Cancro, M. P., Naji, A. and Noorchashm, H. (2012). "Murine islet allograft tolerance upon blockade of the B-lymphocyte stimulator, BLyS/BAFF." Transplantation **93**(7): 676-685.

Partida-Sanchez, S., Goodrich, S., Kusser, K., Oppenheimer, N., Randall, T. D. and Lund, F. E. (2004). "Regulation of dendritic cell trafficking by the ADP-ribosyl cyclase CD38: impact on the development of humoral immunity." Immunity **20**(3): 279-291.

Pasare, C. and Medzhitov, R. (2005). "Control of B-cell responses by Toll-like receptors." Nature **438**(7066): 364-368.

Patel, R. and Terasaki, P. I. (1969). "Significance of the positive crossmatch test in kidney transplantation." N Engl J Med **280**(14): 735-739.

Peperzak, V., Vikstrom, I., Walker, J., Glaser, S. P., LePage, M., Coquery, C. M., Erickson, L. D., Fairfax, K., Mackay, F., Strasser, A., Nutt, S. L. and Tarlinton, D. M. (2013). "Mcl-1 is essential for the survival of plasma cells." Nat Immunol **14**(3): 290-297.

Poe, J. C., Hasegawa, M. and Tedder, T. F. (2001). "CD19, CD21, and CD22: multifaceted response regulators of B lymphocyte signal transduction." Int Rev Immunol **20**(6): 739-762.

Price, A. A., Cumberbatch, M., Kimber, I. and Ager, A. (1997). "alpha 6 integrins are required for Langerhans cell migration." Adv Exp Med Biol **417**: 129-132.

Pricop, L., Redecha, P., Teillaud, J. L., Frey, J., Fridman, W. H., Sautes-Fridman, C. and Salmon, J. E. (2001). "Differential modulation of stimulatory and inhibitory Fc gamma receptors on human monocytes by Th1 and Th2 cytokines." J Immunol **166**(1): 531-537.

Prinjha, R. K., Witherington, J. and Lee, K. (2012). "Place your BETs: the therapeutic potential of bromodomains." Trends Pharmacol Sci **33**(3): 146-153.

Radbruch, A., Muehlinghaus, G., Luger, E. O., Inamine, A., Smith, K. G., Dorner, T. and Hiepe, F. (2006). "Competence and competition: the challenge of becoming a long-lived plasma cell." Nat Rev Immunol **6**(10): 741-750.

Raftopoulou, M. and Hall, A. (2004). "Cell migration: Rho GTPases lead the way." Dev Biol **265**(1): 23-32.

Rajewsky, K. (1996). "Clonal selection and learning in the antibody system." Nature **381**(6585): 751-758.

Randolph, G. J., Angeli, V. and Swartz, M. A. (2005). "Dendritic-cell trafficking to lymph nodes through lymphatic vessels." Nat Rev Immunol **5**(8): 617-628.

Randolph, G. J., Ochando, J. and Partida-Sanchez, S. (2008). "Migration of dendritic cell subsets and their precursors." Annu Rev Immunol **26**: 293-316.

Ratzinger, G., Stoitzner, P., Ebner, S., Lutz, M. B., Layton, G. T., Rainer, C., Senior, R. M., Shipley, J. M., Fritsch, P., Schuler, G. and Romani, N. (2002). "Matrix metalloproteinases 9 and 2 are necessary for

the migration of Langerhans cells and dermal dendritic cells from human and murine skin." J Immunol **168**(9): 4361-4371.

Reboldi, A., Arnon, T. I., Rodda, L. B., Atakilit, A., Sheppard, D. and Cyster, J. G. (2016). "IgA production requires B cell interaction with subepithelial dendritic cells in Peyer's patches." Science **352**(6287): aaf4822.

Reinke, P., Fietze, E., Ode-Hakim, S., Prosch, S., Lippert, J., Ewert, R. and Volk, H. D. (1994). "Late-acute renal allograft rejection and symptomless cytomegalovirus infection." Lancet **344**(8939-8940): 1737-1738.

Reis e Sousa, C. (2006). "Dendritic cells in a mature age." Nat Rev Immunol **6**(6): 476-483.

Rickert, P., Weiner, O. D., Wang, F., Bourne, H. R. and Servant, G. (2000). "Leukocytes navigate by compass: roles of PI3Kgamma and its lipid products." Trends Cell Biol **10**(11): 466-473.

Riley, J. L., June, C. H. and Blazar, B. R. (2009). "Human T regulatory cell therapy: take a billion or so and call me in the morning." Immunity **30**(5): 656-665.

Riol-Blanco, L., Sanchez-Sanchez, N., Torres, A., Tejedor, A., Narumiya, S., Corbi, A. L., Sanchez-Mateos, P. and Rodriguez-Fernandez, J. L. (2005). "The chemokine receptor CCR7 activates in dendritic cells two signaling modules that independently regulate chemotaxis and migratory speed." J Immunol **174**(7): 4070-4080.

Ritchie, M. E., Phipson, B., Wu, D., Hu, Y., Law, C. W., Shi, W. and Smyth, G. K. (2015). "limma powers differential expression analyses for RNA-sequencing and microarray studies." Nucleic Acids Res **43**(7): e47.

Roake, J. A., Rao, A. S., Morris, P. J., Larsen, C. P., Hankins, D. F. and Austyn, J. M. (1995). "Dendritic cell loss from nonlymphoid tissues after systemic administration of lipopolysaccharide, tumor necrosis factor, and interleukin 1." J Exp Med **181**(6): 2237-2247.

Robbiani, D. F., Finch, R. A., Jager, D., Muller, W. A., Sartorelli, A. C. and Randolph, G. J. (2000). "The leukotriene C(4) transporter MRP1 regulates CCL19 (MIP-3beta, ELC)-dependent mobilization of dendritic cells to lymph nodes." Cell **103**(5): 757-768.

Rodriguez-Pinto, D. (2005). "B cells as antigen presenting cells." Cell Immunol **238**(2): 67-75.

Ronnblom, L. and Pascual, V. (2008). "The innate immune system in SLE: type I interferons and dendritic cells." Lupus **17**(5): 394-399.

Rosser, E. C. and Mauri, C. (2015). "Regulatory B cells: origin, phenotype, and function." Immunity **42**(4): 607-612.

Rosser, E. C., Oleinika, K., Tonon, S., Doyle, R., Bosma, A., Carter, N. A., Harris, K. A., Jones, S. A., Klein, N. and Mauri, C. (2014). "Regulatory B cells are induced by gut microbiota-driven interleukin-1beta and interleukin-6 production." Nat Med **20**(11): 1334-1339.

Saeed, S., Quintin, J., Kerstens, H. H., Rao, N. A., Aghajanirefah, A., Matarese, F., Cheng, S. C., Ratter, J., Berentsen, K., van der Ent, M. A., Sharifi, N., Janssen-Megens, E. M., Ter Huurne, M., Mandoli, A., van Schaik, T., Ng, A., Burden, F., Downes, K., Frontini, M., Kumar, V., Giamarellos-Bourboulis, E. J., Ouwehand, W. H., van der Meer, J. W., Joosten, L. A., Wijmenga, C., Martens, J. H., Xavier, R. J., Logie, C., Netea, M. G. and Stunnenberg, H. G. (2014). "Epigenetic programming of monocyte-to-macrophage differentiation and trained innate immunity." Science **345**(6204): 1251086.

Sallusto, F., Schaerli, P., Loetscher, P., Schaniel, C., Lenig, D., Mackay, C. R., Qin, S. and Lanzavecchia, A. (1998). "Rapid and coordinated switch in chemokine receptor expression during dendritic cell maturation." Eur J Immunol **28**(9): 2760-2769.

Salzer, U., Chapel, H. M., Webster, A. D., Pan-Hammarstrom, Q., Schmitt-Graeff, A., Schlesier, M., Peter, H. H., Rockstroh, J. K., Schneider, P., Schaffer, A. A., Hammarstrom, L. and Grimbacher, B. (2005). "Mutations in TNFRSF13B encoding TACI are associated with common variable immunodeficiency in humans." Nat Genet **37**(8): 820-828.

Sanchez, R. and Zhou, M. M. (2009). "The role of human bromodomains in chromatin biology and gene transcription." Curr Opin Drug Discov Devel **12**(5): 659-665.

Sango, C., Merino, D., San Segundo, D., Rodrigo, E., Lopez-Hoyos, M., Benito, A., Angeles Ramos, M., Gomez-Roman, J. and Arias, M. (2016). "B-Cell-Activating Factor Levels Are Associated With Antibody-Mediated Histological Damage in Kidney Transplantation." Transplant Proc **48**(9): 2910-2912.

Savill, J. (1997). "Recognition and phagocytosis of cells undergoing apoptosis." Br Med Bull **53**(3): 491-508.

Schachtner, H., Weimershaus, M., Stache, V., Plewa, N., Legler, D. F., Hopken, U. E. and Maritzen, T. (2015). "Loss of Gadkin Affects Dendritic Cell Migration In Vitro." PLoS One **10**(12): e0143883.

Schaefer, B. C., Schaefer, M. L., Kappler, J. W., Marrack, P. and Kedl, R. M. (2001). "Observation of antigen-dependent CD8+ T-cell/ dendritic cell interactions in vivo." Cell Immunol **214**(2): 110-122.

Schaefer, U. (2014). "Pharmacological inhibition of bromodomain-containing proteins in inflammation." Cold Spring Harb Perspect Biol **6**(6).

Schiemann, B., Gommerman, J. L., Vora, K., Cachero, T. G., Shulga-Morskaya, S., Dobles, M., Frew, E. and Scott, M. L. (2001). "An essential role for BAFF in the normal development of B cells through a BCMA-independent pathway." Science **293**(5537): 2111-2114.

Schilderink, R., Bell, M., Reginato, E., Patten, C., Rioja, I., Hilbers, F. W., Kabala, P. A., Reedquist, K. A., Tough, D. F., Tak, P. P., Prinjha, R. K. and de Jonge, W. J. (2016). "BET bromodomain inhibition reduces maturation and enhances tolerogenic properties of human and mouse dendritic cells." Mol Immunol **79**: 66-76.

Schlosser, H. A., Thelen, M., Dieplinger, G., von Bergwelt-Baildon, A., Garcia-Marquez, M., Reuter, S., Shimabukuro-Vornhagen, A., Wennhold, K., Haustein, N., Buchner, D., Heiermann, N., Kleinert, R., Wahba, R., Ditt, V., Kurschat, C., Cingoz, T., Becker, J., Stippel, D. L. and von Bergwelt-Baildon, M. (2016). "Prospective analyses of circulating B-cell subsets in AB0-compatible and AB0-incompatible kidney transplant recipients." Am J Transplant.

Schmidt, G. (2011). "Yersinia enterocolitica outer protein T (YopT)." Eur J Cell Biol **90**(11): 955-958.

Schmidt, S. V., Krebs, W., Ulas, T., Xue, J., Bassler, K., Gunther, P., Hardt, A. L., Schultze, H., Sander, J., Klee, K., Theis, H., Kraut, M., Beyer, M. and Schultze, J. L. (2016). "The transcriptional regulator network of human inflammatory macrophages is defined by open chromatin." Cell Res **26**(2): 151-170.

Schmittgen, T. D. and Livak, K. J. (2008). "Analyzing real-time PCR data by the comparative C(T) method." Nat Protoc **3**(6): 1101-1108.

Schnorrer, P., Behrens, G. M., Wilson, N. S., Pooley, J. L., Smith, C. M., El-Sukkari, D., Davey, G., Kupresanin, F., Li, M., Maraskovsky, E., Belz, G. T., Carbone, F. R., Shortman, K., Heath, W. R. and Villadangos, J. A. (2006). "The dominant role of CD8+ dendritic cells in cross-presentation is not dictated by antigen capture." Proc Natl Acad Sci U S A **103**(28): 10729-10734.

Schroder, S., Cho, S., Zeng, L., Zhang, Q., Kaehlcke, K., Mak, L., Lau, J., Bisgrove, D., Schnolzer, M., Verdin, E., Zhou, M. M. and Ott, M. (2012). "Two-pronged binding with bromodomain-containing protein 4 liberates positive transcription elongation factor b from inactive ribonucleoprotein complexes." J Biol Chem **287**(2): 1090-1099.

Schulz, C., Gomez Perdiguero, E., Chorro, L., Szabo-Rogers, H., Cagnard, N., Kierdorf, K., Prinz, M., Wu, B., Jacobsen, S. E., Pollard, J. W., Frampton, J., Liu, K. J. and Geissmann, F. (2012). "A lineage of myeloid cells independent of Myb and hematopoietic stem cells." Science **336**(6077): 86-90.

Schwarzenberger, K. and Udey, M. C. (1996). "Contact allergens and epidermal proinflammatory cytokines modulate Langerhans cell E-cadherin expression in situ." J Invest Dermatol **106**(3): 553-558.

Seal, J., Lamotte, Y., Donche, F., Bouillot, A., Mirguet, O., Gellibert, F., Nicodeme, E., Krysa, G., Kirilovsky, J., Beinke, S., McCleary, S., Rioja, I., Bamborough, P., Chung, C. W., Gordon, L., Lewis, T., Walker, A. L., Cutler, L., Lugo, D., Wilson, D. M., Witherington, J., Lee, K. and Prinjha, R. K. (2012). "Identification of a novel series of BET family bromodomain inhibitors: binding mode and profile of I-BET151 (GSK1210151A)." Bioorg Med Chem Lett **22**(8): 2968-2972.

Sela-Culang, I., Kunik, V. and Ofran, Y. (2013). "The structural basis of antibody-antigen recognition." Front Immunol **4**: 302.

Shabir, S., Girdlestone, J., Briggs, D., Kaul, B., Smith, H., Daga, S., Chand, S., Jham, S., Navarrete, C., Harper, L., Ball, S. and Borrows, R. (2015). "Transitional B lymphocytes are associated with protection from kidney allograft rejection: a prospective study." Am J Transplant **15**(5): 1384-1391.

Sharp, P. E., Martin-Ramirez, J., Mangsbo, S. M., Boross, P., Pusey, C. D., Touw, I. P., Cook, H. T., Verbeek, J. S. and Tarzi, R. M. (2013). "FcgammaRIIb on myeloid cells and intrinsic renal cells rather than B cells protects from nephrotoxic nephritis." J Immunol **190**(1): 340-348.

Shen, P. and Fillatreau, S. (2015). "Antibody-independent functions of B cells: a focus on cytokines." Nat Rev Immunol **15**(7): 441-451.

Shen, P., Roch, T., Lampropoulou, V., O'Connor, R. A., Stervbo, U., Hilgenberg, E., Ries, S., Dang, V. D., Jaimes, Y., Daridon, C., Li, R., Jouneau, L., Boudinot, P., Wilantri, S., Sakwa, I., Miyazaki, Y., Leech, M. D., McPherson, R. C., Wirtz, S., Neurath, M., Hoehlig, K., Meinl, E., Grutzkau, A., Grun, J. R., Horn, K., Kuhl, A. A., Dorner, T., Bar-Or, A., Kaufmann, S. H., Anderton, S. M. and Fillatreau, S. (2014). "IL-35-

producing B cells are critical regulators of immunity during autoimmune and infectious diseases." Nature **507**(7492): 366-370.

Shortman, K. and Heath, W. R. (2010). "The CD8+ dendritic cell subset." Immunol Rev **234**(1): 18-31.

Sigdel, T. K., Li, L., Tran, T. Q., Khatri, P., Naesens, M., Sansanwal, P., Dai, H., Hsieh, S. C. and Sarwal, M. M. (2012). "Non-HLA antibodies to immunogenic epitopes predict the evolution of chronic renal allograft injury." J Am Soc Nephrol **23**(4): 750-763.

Sis, B., Mengel, M., Haas, M., Colvin, R. B., Halloran, P. F., Racusen, L. C., Solez, K., Baldwin, W. M., 3rd, Bracamonte, E. R., Broecker, V., Cosio, F., Demetris, A. J., Drachenberg, C., Einecke, G., Gloor, J., Glotz, D., Kraus, E., Legendre, C., Liapis, H., Mannon, R. B., Nankivell, B. J., Nickeleit, V., Papadimitriou, J. C., Randhawa, P., Regele, H., Renaudin, K., Rodriguez, E. R., Seron, D., Seshan, S., Suthanthiran, M., Wasowska, B. A., Zachary, A. and Zeevi, A. (2010). "Banff '09 meeting report: antibody mediated graft deterioration and implementation of Banff working groups." Am J Transplant **10**(3): 464-471.

Slifka, M. K., Antia, R., Whitmire, J. K. and Ahmed, R. (1998). "Humoral immunity due to long-lived plasma cells." Immunity **8**(3): 363-372.

Smith, K. G. C. and Clatworthy, M. R. (2010). "FcgammaRIIB in autoimmunity and infection: evolutionary and therapeutic implications." Nat Rev Immunol **10**(5): 328-343.

Stadanlick, J. E., Kaileh, M., Karnell, F. G., Scholz, J. L., Miller, J. P., Quinn, W. J., 3rd, Brezski, R. J., Treml, L. S., Jordan, K. A., Monroe, J. G., Sen, R. and Cancro, M. P. (2008). "Tonic B cell antigen receptor signals supply an NF-kappaB substrate for prosurvival BLyS signaling." Nat Immunol **9**(12): 1379-1387.

Stamatiades, E. G., Tremblay, M. E., Bohm, M., Crozet, L., Bisht, K., Kao, D., Coelho, C., Fan, X., Yewdell, W. T., Davidson, A., Heeger, P. S., Diebold, S., Nimmerjahn, F. and Geissmann, F. (2016). "Immune Monitoring of Trans-endothelial Transport by Kidney-Resident Macrophages." Cell **166**(4): 991-1003.

Stanlie, A., Yousif, A. S., Akiyama, H., Honjo, T. and Begum, N. A. (2014). "Chromatin reader Brd4 functions in Ig class switching as a repair complex adaptor of nonhomologous end-joining." Mol Cell **55**(1): 97-110.

Stavnezer, J., Guikema, J. E. and Schrader, C. E. (2008). "Mechanism and regulation of class switch recombination." Annu Rev Immunol **26**: 261-292.

Steinman, R. M. (2012). "Decisions about dendritic cells: past, present, and future." Annu Rev Immunol **30**: 1-22.

Steinman, R. M., Hawiger, D. and Nussenzweig, M. C. (2003). "Tolerogenic dendritic cells." Annu Rev Immunol **21**: 685-711.

Steri, M., Orru, V., Idda, M. L., Pitzalis, M., Pala, M., Zara, I., Sidore, C., Faa, V., Floris, M., Deiana, M., Asunis, I., Porcu, E., Mulas, A., Piras, M. G., Lobina, M., Lai, S., Marongiu, M., Serra, V., Marongiu, M., Sole, G., Busonero, F., Maschio, A., Cusano, R., Cuccuru, G., Deidda, F., Poddie, F., Farina, G., Dei, M., Virdis, F., Olla, S., Satta, M. A., Pani, M., Delitala, A., Cocco, E., Frau, J., Coghe, G., Lorefice, L., Fenu, G., Ferrigno, P., Ban, M., Barizzone, N., Leone, M., Guerini, F. R., Piga, M., Firinu, D., Kockum, I., Lima Bomfim, I., Olsson, T., Alfredsson, L., Suarez, A., Carreira, P. E., Castillo-Palma, M. J., Marcus, J. H., Congia, M., Angius, A., Melis, M., Gonzalez, A., Alarcon Riquelme, M. E., da Silva, B. M., Marchini, M., Danieli, M. G., Del Giacco, S., Mathieu, A., Pani, A., Montgomery, S. B., Rosati, G., Hillert, J., Sawcer, S., D'Alfonso, S., Todd, J. A., Novembre, J., Abecasis, G. R., Whalen, M. B., Marrosu, M. G., Meloni, A., Sanna, S., Gorospe, M., Schlessinger, D., Fiorillo, E., Zoledziewska, M. and Cucca, F. (2017). "Overexpression of the Cytokine BAFF and Autoimmunity Risk." N Engl J Med **376**(17): 1615-1626.

Stohl, W., Hiepe, F., Latinis, K. M., Thomas, M., Scheinberg, M. A., Clarke, A., Aranow, C., Wellborne, F. R., Abud-Mendoza, C., Hough, D. R., Pineda, L., Migone, T. S., Zhong, Z. J., Freimuth, W. W., Chatham, W. W., Group, B.-S. and Group, B.-S. (2012). "Belimumab reduces autoantibodies, normalizes low complement levels, and reduces select B cell populations in patients with systemic lupus erythematosus." Arthritis Rheum **64**(7): 2328-2337.

Stohl, W., Schwarting, A., Okada, M., Scheinberg, M., Doria, A., Hammer, A. E., Kleoudis, C., Groark, J., Bass, D., Fox, N. L., Roth, D. and Gordon, D. (2017). "Efficacy and Safety of Subcutaneous Belimumab in Systemic Lupus Erythematosus: A Fifty-Two-Week Randomized, Double-Blind, Placebo-Controlled Study." Arthritis Rheumatol **69**(5): 1016-1027.

Stolp, J., Turka, L. A. and Wood, K. J. (2014). "B cells with immune-regulating function in transplantation." Nat Rev Nephrol **10**(7): 389-397.

Struhl, K. (1998). "Histone acetylation and transcriptional regulatory mechanisms." Genes Dev **12**(5): 599-606.

Suarez-Alvarez, B., Morgado-Pascual, J. L., Rayego-Mateos, S., Rodriguez, R. M., Rodrigues-Diez, R., Cannata-Ortiz, P., Sanz, A. B., Egido, J., Tharaux, P. L., Ortiz, A., Lopez-Larrea, C. and Ruiz-Ortega, M. (2017). "Inhibition of Bromodomain and Extraterminal Domain Family Proteins Ameliorates Experimental Renal Damage." J Am Soc Nephrol **28**(2): 504-519.

Subramanian, A., Tamayo, P., Mootha, V. K., Mukherjee, S., Ebert, B. L., Gillette, M. A., Paulovich, A., Pomeroy, S. L., Golub, T. R., Lander, E. S. and Mesirov, J. P. (2005). "Gene set enrichment analysis: a knowledge-based approach for interpreting genome-wide expression profiles." Proc Natl Acad Sci U S A **102**(43): 15545-15550.

Sullivan, K. E., Suriano, A., Dietzmann, K., Lin, J., Goldman, D. and Petri, M. A. (2007). "The TNFalpha locus is altered in monocytes from patients with systemic lupus erythematosus." Clin Immunol **123**(1): 74-81.

Sun, J., Wang, J., Pefanis, E., Chao, J., Rothschild, G., Tachibana, I., Chen, J. K., Ivanov, II, Rabadan, R., Takeda, Y. and Basu, U. (2015a). "Transcriptomics Identify CD9 as a Marker of Murine IL-10-Competent Regulatory B Cells." Cell Rep **13**(6): 1110-1117.

Sun, Y., Wang, Y., Toubai, T., Oravecz-Wilson, K., Liu, C., Mathewson, N., Wu, J., Rossi, C., Cummings, E., Wu, D., Wang, S. and Reddy, P. (2015b). "BET bromodomain inhibition suppresses graft-versus-host disease after allogeneic bone marrow transplantation in mice." Blood **125**(17): 2724-2728.

Tamoutounour, S., Henri, S., Lelouard, H., de Bovis, B., de Haar, C., van der Woude, C. J., Woltman, A. M., Reyal, Y., Bonnet, D., Sichien, D., Bain, C. C., Mowat, A. M., Reis e Sousa, C., Poulin, L. F., Malissen, B. and Guilliams, M. (2012). "CD64 distinguishes macrophages from dendritic cells in the gut and reveals the Th1-inducing role of mesenteric lymph node macrophages during colitis." Eur J Immunol **42**(12): 3150-3166.

Tang, X., Peng, R., Phillips, J. E., Deguzman, J., Ren, Y., Apparsundaram, S., Luo, Q., Bauer, C. M., Fuentes, M. E., DeMartino, J. A., Tyagi, G., Garrido, R., Hogaboam, C. M., Denton, C. P., Holmes, A. M., Kitson, C., Stevenson, C. S. and Budd, D. C. (2013). "Assessment of Brd4 inhibition in idiopathic pulmonary fibrosis lung fibroblasts and in vivo models of lung fibrosis." Am J Pathol **183**(2): 470-479.

Teichmann, L. L., Cullen, J. L., Kashgarian, M., Dong, C., Craft, J. and Shlomchik, M. J. (2015). "Local triggering of the ICOS coreceptor by CD11c(+) myeloid cells drives organ inflammation in lupus." Immunity **42**(3): 552-565.

Teichmann, L. L., Ols, M. L., Kashgarian, M., Reizis, B., Kaplan, D. H. and Shlomchik, M. J. (2010). "Dendritic cells in lupus are not required for activation of T and B cells but promote their expansion, resulting in tissue damage." Immunity **33**(6): 967-978.

Thaunat, O., Patey, N., Gautreau, C., Lechaton, S., Fremeaux-Bacchi, V., Dieu-Nosjean, M. C., Cassuto-Viguier, E., Legendre, C., Delahousse, M., Lang, P., Michel, J. B. and Nicoletti, A. (2008). "B cell survival in intragraft tertiary lymphoid organs after rituximab therapy." Transplantation **85**(11): 1648-1653.

Thibault-Espitia, A., Foucher, Y., Danger, R., Migone, T., Pallier, A., Castagnet, S., C, G. G., Devys, A., A, C. G., Giral, M., Soulillou, J. P. and Brouard, S. (2012). "BAFF and BAFF-R levels are associated with risk of long-term kidney graft dysfunction and development of donor-specific antibodies." Am J Transplant **12**(10): 2754-2762.

Thien, M., Phan, T. G., Gardam, S., Amesbury, M., Basten, A., Mackay, F. and Brink, R. (2004). "Excess BAFF rescues self-reactive B cells from peripheral deletion and allows them to enter forbidden follicular and marginal zone niches." Immunity **20**(6): 785-798.

Thievessen, I., Fakhri, N., Steinwachs, J., Kraus, V., McIsaac, R. S., Gao, L., Chen, B. C., Baird, M. A., Davidson, M. W., Betzig, E., Oldenbourg, R., Waterman, C. M. and Fabry, B. (2015). "Vinculin is required for cell polarization, migration, and extracellular matrix remodeling in 3D collagen." FASEB J **29**(11): 4555-4567.

Thompson, J. S., Bixler, S. A., Qian, F., Vora, K., Scott, M. L., Cachero, T. G., Hession, C., Schneider, P., Sizing, I. D., Mullen, C., Strauch, K., Zafari, M., Benjamin, C. D., Tschopp, J., Browning, J. L. and Ambrose, C. (2001). "BAFF-R, a newly identified TNF receptor that specifically interacts with BAFF." Science **293**(5537): 2108-2111.

Thompson, S. A., Jones, J. L., Cox, A. L., Compston, D. A. and Coles, A. J. (2010). "B-cell reconstitution and BAFF after alemtuzumab (Campath-1H) treatment of multiple sclerosis." J Clin Immunol **30**(1): 99-105.

Tiegs, S. L., Russell, D. M. and Nemazee, D. (1993). "Receptor editing in self-reactive bone marrow B cells." J Exp Med **177**(4): 1009-1020.

Tonelli, M., Wiebe, N., Knoll, G., Bello, A., Browne, S., Jadhav, D., Klarenbach, S. and Gill, J. (2011). "Systematic review: kidney transplantation compared with dialysis in clinically relevant outcomes." Am J Transplant **11**(10): 2093-2109.

Toniolo, P. A., Liu, S., Yeh, J. E., Moraes-Vieira, P. M., Walker, S. R., Vafaizadeh, V., Barbuto, J. A. and Frank, D. A. (2015). "Inhibiting STAT5 by the BET bromodomain inhibitor JQ1 disrupts human dendritic cell maturation." J Immunol **194**(7): 3180-3190.

Toong, C., Adelstein, S. and Phan, T. G. (2011). "Clearing the complexity: immune complexes and their treatment in lupus nephritis." Int J Nephrol Renovasc Dis **4**: 17-28.

Tough, D. F. and Prinjha, R. K. (2017). "Immune disease-associated variants in gene enhancers point to BET epigenetic mechanisms for therapeutic intervention." Epigenomics **9**(4): 573-584.

Tsokos, G. C. (2011). "Systemic lupus erythematosus." N Engl J Med **365**(22): 2110-2121.

Tumanov, A., Kuprash, D., Lagarkova, M., Grivennikov, S., Abe, K., Shakhov, A., Drutskaya, L., Stewart, C., Chervonsky, A. and Nedospasov, S. (2002). "Distinct role of surface lymphotoxin expressed by B cells in the organization of secondary lymphoid tissues." Immunity **17**(3): 239-250.

Tumanov, A. V., Kuprash, D. V., Mach, J. A., Nedospasov, S. A. and Chervonsky, A. V. (2004). "Lymphotoxin and TNF produced by B cells are dispensable for maintenance of the follicle-associated epithelium but are required for development of lymphoid follicles in the Peyer's patches." J Immunol **173**(1): 86-91.

Tussiwand, R., Bosco, N., Ceredig, R. and Rolink, A. G. (2009). "Tolerance checkpoints in B-cell development: Johnny B good." Eur J Immunol **39**(9): 2317-2324.

Tyden, G., Ekberg, H., Tufveson, G. and Mjornstedt, L. (2012). "A randomized, double-blind, placebo-controlled study of single dose rituximab as induction in renal transplantation: a 3-year follow-up." Transplantation **94**(3): e21-22.

Tyden, G., Genberg, H., Tollemar, J., Ekberg, H., Persson, N. H., Tufveson, G., Wadstrom, J., Gabel, M. and Mjornstedt, L. (2009). "A randomized, doubleblind, placebo-controlled, study of single-dose rituximab as induction in renal transplantation." Transplantation **87**(9): 1325-1329.

Vallerskog, T., Gunnarsson, I., Widhe, M., Risselada, A., Klareskog, L., van Vollenhoven, R., Malmstrom, V. and Trollmo, C. (2007). "Treatment with rituximab affects both the cellular and the humoral arm of the immune system in patients with SLE." Clin Immunol **122**(1): 62-74.

van de Veen, W., Stanic, B., Yaman, G., Wawrzyniak, M., Sollner, S., Akdis, D. G., Ruckert, B., Akdis, C. A. and Akdis, M. (2013). "IgG4 production is confined to human IL-10-producing regulatory B cells that suppress antigen-specific immune responses." J Allergy Clin Immunol **131**(4): 1204-1212.

van den Hoogen, M. W., Kamburova, E. G., Baas, M. C., Steenbergen, E. J., Florquin, S., HJ, M. K., Joosten, I. and Hilbrands, L. B. (2015). "Rituximab as induction therapy after renal transplantation: a randomized, double-blind, placebo-controlled study of efficacy and safety." Am J Transplant **15**(2): 407-416.

van Lent, P., Nabbe, K. C., Boross, P., Blom, A. B., Roth, J., Holthuysen, A., Sloetjes, A., Verbeek, S. and van den Berg, W. (2003). "The inhibitory receptor FcgammaRII reduces joint inflammation and destruction in experimental immune complex-mediated arthritides not only by inhibition of FcgammaRI/III but also by efficient clearance and endocytosis of immune complexes." Am J Pathol **163**(5): 1839-1848.

van Montfoort, N., t Hoen, P. A., Mangsbo, S. M., Camps, M. G., Boross, P., Melief, C. J., Ossendorp, F. and Verbeek, J. S. (2012). "Fcgamma receptor IIb strongly regulates Fcgamma receptor-facilitated T cell activation by dendritic cells." J Immunol **189**(1): 92-101.

Vanholder, R. and Ringoir, S. (1993). "Infectious morbidity and defects of phagocytic function in end-stage renal disease: a review." J Am Soc Nephrol **3**(9): 1541-1554.

Vargas, P., Maiuri, P., Bretou, M., Saez, P. J., Pierobon, P., Maurin, M., Chabaud, M., Lankar, D., Obino, D., Terriac, E., Raab, M., Thiam, H. R., Brocker, T., Kitchen-Goosen, S. M., Alberts, A. S., Sunareni, P., Xia, S., Li, R., Voituriez, R., Piel, M. and Lennon-Dumenil, A. M. (2016). "Innate control of actin nucleation determines two distinct migration behaviours in dendritic cells." Nat Cell Biol **18**(1): 43-53.

Vicente-Manzanares, M., Hodges, J. and Horwitz, A. R. (2009). "Dendritic Spines: Similarities with Protrusions and Adhesions in Migrating Cells." Open Neurosci J **3**: 87-96.

von Willebrand, E., Pettersson, E., Ahonen, J. and Hayry, P. (1986). "CMV infection, class II antigen expression, and human kidney allograft rejection." Transplantation **42**(4): 364-367.

Wang, L., Wu, X., Wang, R., Yang, C., Li, Z., Wang, C., Zhang, F. and Yang, P. (2017). "BRD4 inhibition suppresses cell growth, migration and invasion of salivary adenoid cystic carcinoma." Biol Res **50**(1): 19.

Wang, R. X., Yu, C. R., Dambuza, I. M., Mahdi, R. M., Dolinska, M. B., Sergeev, Y. V., Wingfield, P. T., Kim, S. H. and Egwuagu, C. E. (2014). "Interleukin-35 induces regulatory B cells that suppress autoimmune disease." Nat Med **20**(6): 633-641.

Wang, Z., Shi, B. Y., Qian, Y. Y., Cai, M. and Wang, Q. (2009). "Short-term anti-CD25 monoclonal antibody administration down-regulated CD25 expression without eliminating the neogenetic functional regulatory T cells in kidney transplantation." Clin Exp Immunol **155**(3): 496-503.

Warnatz, K., Salzer, U., Rizzi, M., Fischer, B., Gutenberger, S., Bohm, J., Kienzler, A. K., Pan-Hammarstrom, Q., Hammarstrom, L., Rakhmanov, M., Schlesier, M., Grimbacher, B., Peter, H. H. and Eibel, H. (2009). "B-cell activating factor receptor deficiency is associated with an adult-onset antibody deficiency syndrome in humans." Proc Natl Acad Sci U S A **106**(33): 13945-13950.

Wei, S., Sun, Y. and Sha, H. (2015). "Therapeutic targeting of BET protein BRD4 delays murine lupus." Int Immunopharmacol **29**(2): 314-319.

Weiss, J. M., Sleeman, J., Renkl, A. C., Dittmar, H., Termeer, C. C., Taxis, S., Howells, N., Hofmann, M., Kohler, G., Schopf, E., Ponta, H., Herrlich, P. and Simon, J. C. (1997). "An essential role for CD44 variant isoforms in epidermal Langerhans cell and blood dendritic cell function." J Cell Biol **137**(5): 1137-1147.

Weyand, C. M., Seyler, T. M. and Goronzy, J. J. (2005). "B cells in rheumatoid synovitis." Arthritis Res Ther **7 Suppl 3**: S9-12.

Whyte, W. A., Orlando, D. A., Hnisz, D., Abraham, B. J., Lin, C. Y., Kagey, M. H., Rahl, P. B., Lee, T. I. and Young, R. A. (2013). "Master transcription factors and mediator establish super-enhancers at key cell identity genes." Cell **153**(2): 307-319.

Wiebe, C., Gibson, I. W., Blydt-Hansen, T. D., Karpinski, M., Ho, J., Storsley, L. J., Goldberg, A., Birk, P. E., Rush, D. N. and Nickerson, P. W. (2012). "Evolution and clinical pathologic correlations of de novo donor-specific HLA antibody post kidney transplant." Am J Transplant **12**(5): 1157-1167.

Wienerroither, S., Rauch, I., Rosebrock, F., Jamieson, A. M., Bradner, J., Muhar, M., Zuber, J., Muller, M. and Decker, T. (2014). "Regulation of NO synthesis, local inflammation, and innate immunity to pathogens by BET family proteins." Mol Cell Biol **34**(3): 415-427.

Willcocks, L. C., Carr, E. J., Niederer, H. A., Rayner, T. F., Williams, T. N., Yang, W., Scott, J. A., Urban, B. C., Peshu, N., Vyse, T. J., Lau, Y. L., Lyons, P. A. and Smith, K. G. (2010). "A defunctioning polymorphism in FCGR2B is associated with protection against malaria but susceptibility to systemic lupus erythematosus." Proc Natl Acad Sci U S A **107**(17): 7881-7885.

Wolf, S. D., Dittel, B. N., Hardardottir, F. and Janeway, C. A., Jr. (1996). "Experimental autoimmune encephalomyelitis induction in genetically B cell-deficient mice." J Exp Med **184**(6): 2271-2278.

Wood, K. J., Bushell, A. and Hester, J. (2012). "Regulatory immune cells in transplantation." Nat Rev Immunol **12**(6): 417-430.

Xiong, C., Masucci, M. V., Zhou, X., Liu, N., Zang, X., Tolbert, E., Zhao, T. C. and Zhuang, S. (2016). "Pharmacological targeting of BET proteins inhibits renal fibroblast activation and alleviates renal fibrosis." Oncotarget **7**(43): 69291-69308.

Xu, H., He, X., Sun, J., Shi, D., Zhu, Y. and Zhang, X. (2009). "The expression of B-cell activating factor belonging to tumor necrosis factor superfamily (BAFF) significantly correlated with C4D in kidney allograft rejection." Transplant Proc **41**(1): 112-116.

Yamaguchi, H. and Condeelis, J. (2007). "Regulation of the actin cytoskeleton in cancer cell migration and invasion." Biochim Biophys Acta **1773**(5): 642-652.

Yanaba, K., Bouaziz, J. D., Haas, K. M., Poe, J. C., Fujimoto, M. and Tedder, T. F. (2008). "A regulatory B cell subset with a unique CD1dhiCD5+ phenotype controls T cell-dependent inflammatory responses." Immunity **28**(5): 639-650.

Yarbrough, M. L., Li, Y., Kinch, L. N., Grishin, N. V., Ball, H. L. and Orth, K. (2009). "AMPylation of Rho GTPases by Vibrio VopS disrupts effector binding and downstream signaling." Science **323**(5911): 269-272.

Ye, Q., Wang, L., Wells, A. D., Tao, R., Han, R., Davidson, A., Scott, M. L. and Hancock, W. W. (2004). "BAFF binding to T cell-expressed BAFF-R costimulates T cell proliferation and alloresponses." Eur J Immunol **34**(10): 2750-2759.

Yen, J. H., Khayrullina, T. and Ganea, D. (2008). "PGE2-induced metalloproteinase-9 is essential for dendritic cell migration." Blood **111**(1): 260-270.

Yilmaz-Elis, A. S., Ramirez, J. M., Asmawidjaja, P., van der Kaa, J., Mus, A. M., Brem, M. D., Claassens, J. W., Breukel, C., Brouwers, C., Mangsbo, S. M., Boross, P., Lubberts, E. and Verbeek, J. S. (2014). "FcgammaRIIb on myeloid cells rather than on B cells protects from collagen-induced arthritis." J Immunol **192**(12): 5540-5547.

Yuseff, M. I., Pierobon, P., Reversat, A. and Lennon-Dumenil, A. M. (2013). "How B cells capture, process and present antigens: a crucial role for cell polarity." Nat Rev Immunol **13**(7): 475-486.

Zhang, Q., Davis, J. C., Lamborn, I. T., Freeman, A. F., Jing, H., Favreau, A. J., Matthews, H. F., Davis, J., Turner, M. L., Uzel, G., Holland, S. M. and Su, H. C. (2009). "Combined immunodeficiency associated with DOCK8 mutations." N Engl J Med **361**(21): 2046-2055.

Zhang, Q. and Reed, E. F. (2016). "The importance of non-HLA antibodies in transplantation." Nat Rev Nephrol **12**(8): 484-495.

Zhang, Q. G., Qian, J. and Zhu, Y. C. (2015). "Targeting bromodomain-containing protein 4 (BRD4) benefits rheumatoid arthritis." Immunol Lett **166**(2): 103-108.

Zhang, W., Prakash, C., Sum, C., Gong, Y., Li, Y., Kwok, J. J., Thiessen, N., Pettersson, S., Jones, S. J., Knapp, S., Yang, H. and Chin, K. C. (2012). "Bromodomain-containing protein 4 (BRD4) regulates RNA polymerase II serine 2 phosphorylation in human CD4+ T cells." J Biol Chem **287**(51): 43137-43155.

Zhang, Z., Song, L., Maurer, K., Petri, M. A. and Sullivan, K. E. (2010). "Global H4 acetylation analysis by ChIP-chip in systemic lupus erythematosus monocytes." Genes Immun **11**(2): 124-133.

Zhou, B., Mu, J., Gong, Y., Lu, C., Zhao, Y., He, T. and Qin, Z. (2017). "Brd4 inhibition attenuates unilateral ureteral obstruction-induced fibrosis by blocking TGF-beta-mediated Nox4 expression." Redox Biol **11**: 390-402.

Zhubanchaliyev, A., Temirbekuly, A., Kongrtay, K., Wanshura, L. C. and Kunz, J. (2016). "Targeting Mechanotransduction at the Transcriptional Level: YAP and BRD4 Are Novel Therapeutic Targets for the Reversal of Liver Fibrosis." Front Pharmacol **7**: 462.

Zou, Y., Stastny, P., Susal, C., Dohler, B. and Opelz, G. (2007). "Antibodies against MICA antigens and kidney-transplant rejection." N Engl J Med **357**(13): 1293-1300.

**Appendix A**

Banham, G. D., Flint, S. M., Torpey, N., Lyons, P. A., Shanahan, D. N., Gibson, A., Watson, C. J. E., O'Sullivan, A.-M., Chadwick, J. A., Foster, K. E., Jones, R. B., Devey, L. R., Richards, A., Erwig, L.-P., Savage, C. O., Smith, K. G. C., Henderson, R. B. and Clatworthy, M. R. (2018). "Belimumab in kidney transplantation: an experimental medicine, randomised, placebo-controlled phase 2 trial."

Title: A Phase 2 Experimental Medicine Randomised Placebo Controlled Trial of Belimumab in Kidney Transplantation (BEL114424)

Gemma D. Banham MRCP(UK)*[1,5], Shaun M. Flint FRACP*[1,3,5], Nicholas Torpey FRCP[2,5], Paul A. Lyons PhD[1,5], Don N. Shanahan MSc[3], Adele Gibson BSc[3], Prof. Christopher J.E. Watson FRCS[4,5], Ann-Marie O'Sullivan MRes[2,5], Joseph A. Chadwick[3], Katie E. Foster PhD[3], Rachel B. Jones FRCP[1,3,5], Luke R. Devey MRCSEd[3], Anna Richards MRCP(UK)[3], Prof. Lars-Peter Erwig MD[3], Prof. Caroline O. Savage FMedSci[3], Prof. Kenneth G.C. Smith FMedSci[1,5], Robert B. Henderson PhD*[3], Menna R. Clatworthy FRCP*[1,5]

1. Department of Medicine, University of Cambridge School of Clinical Medicine, Cambridge, UK

2. Cambridge University Hospitals NHS Foundation Trust, Cambridge, UK

3. ImmunoInflammation Therapy Area Unit, GlaxoSmithKline (GSK), Stevenage, UK

4. Department of Surgery, University of Cambridge School of Clinical Medicine, Cambridge, UK

5. NIHR Cambridge Biomedical Research Centre, Cambridge, UK

*authors contributed equally to this work

Correspondence to:

Dr Menna R Clatworthy, Molecular Immunity Unit, Department of Medicine, University of Cambridge, Cambridge, CB2 0QQ, UK. mrc38@cam.ac.uk

Summary:

Background: B cells produce alloantibodies and activate alloreactive T cells, negatively affecting kidney transplant survival. In contrast, regulatory B cells are associated with transplant tolerance. There is an unmet need for immunotherapies that inhibit B cell effector function, including antibody secretion, whilst sparing regulators and minimising infection risk. B lymphocyte stimulator (BLyS) is a cytokine that promotes B cell activation, and has not previously been targeted in kidney transplant recipients.

Aim: We sought to examine the safety and activity (the latter measured by a reduction in naïve B cells from baseline to week 24) of an anti-BLyS antibody, belimumab, in addition to standard of care immunosuppression in adult kidney transplant recipients. We utilised an experimental medicine study design with multiple secondary and exploratory endpoints to gain further insight into the effect of belimumab on the generation of *de novo* IgG and on the regulatory B cell compartment.

Methods: We conducted a phase 2 double-blind randomised placebo-controlled trial of belimumab, in addition to standard of care immunosuppression (basiliximab, mycophenolate mofetil, tacrolimus and prednisolone), in adults aged 18-75 receiving a kidney transplant. Subjects were randomised at a single centre, Addenbrooke's Hospital (UK), stratified according to receipt of a living or deceased donor organ. Within each stratum subjects were randomised by telephone in a 1:1 ratio to receive intravenous belimumab 10mg/kg or placebo (day 0, 14, 28 and every four weeks thereafter for a total of seven infusions). Co-primary endpoints were safety and change in naïve B cells from baseline to Week 24. This trial has completed and is registered as ClinicalTrials.gov number NCT01536379 and EudraCT number 2011-006215-56.

Findings: 28 kidney transplant recipients were randomised to belimumab (n=14) or placebo (n=14) treatment between 13th September 2013 and 8th February 2015. Twelve belimumab and 13 placebo patients were transplanted and went on to receive at least one dose of

belimumab/placebo (modified intention to treat (MITT) population). We observed similar rates of adverse events in belimumab and placebo groups, including serious infection (1/12 (8%) and 5/13 (38%) respectively during the six month on-treatment phase; 0/13 (0%) and 2/13 (15%) during the six month post-treatment follow-up phase). There was one death in the on-treatment phase in a patient in the placebo group. The co-primary endpoint of a reduction in naïve B cells from baseline to week 24 was not met; treatment with belimumab resulted in a trend towards, but not a statistically significant reduction in naïve B cells from baseline to week 24 (adjusted mean difference -34·4 cells/$mm^3$ (95% confidence interval (CI) -109·5 to 40·7)).

Interpretation: Treatment with belimumab in addition to standard of care immunosuppression in low immunological risk renal transplant recipients was not associated with an adverse safety signal nor an increased risk of infection.

Funding: GlaxoSmithKline

Panel: Research in context

Evidence before this study

Therapeutic agents that limit humoral alloimmunity in kidney transplant recipients are currently lacking. B lymphocyte stimulator (BLyS; also known as BAFF) is a cytokine that promotes B cell survival, and we hypothesised that this pathway may represent a useful therapeutic target in transplantation. We searched PubMed using the terms 'BAFF' and 'kidney transplantation' and 'Clinical trial' and Clinicaltrials.gov using the terms 'kidney transplantation and 'BAFF' to establish the current clinical evidence-base in this area. Of the six studies identified in this search, only two included agents that targeted the BAFF/BLyS pathway, using monoclonal antibodies that bind BAFF/BLyS (tabalumab and belimumab), and only one of these was completed and published (Mujtaba *et al.* 2016). In fact, neither of these studies attempted BAFF/BLyS blockade in kidney transplant recipients. Both used an anti-BAFF/BLyS antibody as monotherapy in patients with end-stage kidney failure, with the aim of reducing pre-formed HLA antibodies to a level that permitted safe transplantation, but observed little effect. No trial to date has addressed the question of whether blockade of BAFF/BLyS could be a useful addition to current maintenance immunosuppressive agents following kidney transplantation.

Added value of this study

This study adds value to the existing evidence base by delivering the first data on the use of belimumab in kidney transplant recipients, showing no excess risk of infection and a reduction in naïve B cells, activated memory B cells, circulating plasmablasts, and kidney-specific IgG. We also provide the first data on the impact of belimumab to reduce *de novo* IgG formation and increase regulatory B cell numbers in the peripheral blood. Our study informs clinical trials modulating the BLyS/BAFF axis in transplant recipients, and those using belimumab outside of the field of transplantation in systemic lupus erythematosus (SLE).

Implications of all the available evidence

Our data suggest that belimumab may be a useful therapeutic strategy in standard immunological risk kidney transplant recipients to prevent *de novo* donor-specific antibody formation. The observed lowering of activated memory B cells and preformed IgG suggest an additional potential role in sensitised kidney transplant recipients or in those with antibody-mediated rejection. Therefore, the use of belimumab warrants further study in these patient groups, in the context of larger randomised controlled trials.

Introduction

Transplantation is the optimal renal replacement therapy for most patients with end-stage renal failure (ESRF). Current immunosuppressive regimens carry an increased risk of infection but limit T cell activation such that T cell mediated rejection (TCMR) occurs in less than 20% of kidney transplant recipients and is largely treatable. In contrast, there remain significant challenges in the field of humoral alloimmunity. *De-novo* donor-specific human leucocyte antigen (HLA)–specific immunoglobulin G (IgG) antibodies (DSA) and some non-HLA IgG antibodies are associated with acute antibody-mediated rejection (ABMR) and allograft loss[1-3]. Furthermore, sensitised patients with pre-formed DSA have an elevated risk of acute and chronic ABMR, reducing graft survival[4]. B cells are not only the precursors of antibody-producing plasma cells, but act as antigen presenting cells and secrete pro-inflammatory cytokines, including interleukin (IL)-6, that can activate T cells driving TCMR. Indeed, the presence of B cells in TCMR biopsies is a negative prognostic factor associated with steroid resistance[5]. Hence, there is an urgent unmet need in solid organ transplantation for immunotherapeutic strategies that target B cells and plasma cells[6], ideally without increasing infectious complications.

Efforts to inhibit pathological humoral immunity are complicated by the fact that B cells may also regulate immune responses via IL-10 production[7,8]. These regulatory B cells are enriched in transitional ($CD24/CD38^{high}$)[7] and memory ($CD24^{high}/CD27^{+}$) B cell compartments in humans[8]. Several lines of evidence suggest that regulatory B cells may be important in transplantation. Firstly, although a single dose of the anti-CD20 antibody rituximab at induction had no impact on transplant outcomes[9,10], the use of a second dose within one to two weeks of transplantation was associated with TCMR in kidney transplant recipients[11] and cardiac allograft vasculopathy[12]. Secondly, B cell transcripts and IL-10 producing B cells are increased in the peripheral blood of tolerant kidney transplant recipients[13-15]. Finally, kidney transplant recipients with a higher number of transitional B cells have reduced rejection[16]. Similarly, patients with a higher B cell IL-10:TNF$\alpha$ ratio have a slower decline in transplant

function and reduced allograft loss[17,18]. In contrast, patients with rejection following ABO incompatible transplantation had fewer $CD24^{high}/CD27^{+}$ memory B cells[19]. Together, these data show that B cells can play both a positive and negative role in transplantation and highlight the need to identify immunosuppressants that preserve the immunoregulatory aspect of B cell function.

B lymphocyte stimulator (BLyS; also known as BAFF) is a cytokine that enhances B cell survival and proliferation[20] and contributes to the plasma cell niche[21]. The humanised anti-BLyS IgG1 antibody, belimumab, is licenced for use in patients with SLE[22], a disease characterised by high circulating BLyS[23]. In renal transplant recipients, elevated serum BLyS is associated with the development of *de novo* DSA[24], high-titre HLA antibodies[25], and an increased frequency of ABMR[26]. Experimental models suggest that BLyS neutralisation may be effective in preventing rejection[27,28]. BLyS inhibition, used as monotherapy, had little impact on HLA antibody titres in sensitised subjects on the transplant waiting list[29,30], but to date, this axis has not been targeted in human transplant recipients.

Currently, only 10% of compounds entering clinical trials reach patients as medicines. Experimental medicine seeks to improve this by '*identify(ing) mechanisms of pathophysiology or disease, or … demonstrat(ing) proof-of-concept evidence of the validity and importance of new discoveries or treatments'* (UK Medical Research Council), thus providing detailed, mechanistic phenotypic data that precedes and informs late phase clinical development.

We undertook a phase 2 randomised, double-blind, placebo-controlled experimental medicine trial of belimumab in addition to standard of care immunosuppression in renal transplant recipients to assess its safety and activity, as measured by a reduction in naïve B cells from baseline to week 24, and its effect on a number of exploratory endpoints. The use of belimumab was not associated with increased infection but led to a reduction in naïve B cells and activated memory B cells. The residual B cell compartment in belimumab-treated

subjects was skewed towards cells with a regulatory phenotype, with an increased capacity to produce IL-10 relative to IL-6. Following belimumab treatment, whole blood gene expression and protein microarray analysis indicated fewer circulating plasmablasts, reduced *de novo* IgG antibody formation and a reduction in kidney and endothelial cell-specific antibodies known to negatively impact graft outcome. In addition, belimumab treatment had a significant effect on the CD4 T cell transcriptome, with a marked reduction in cell cycle gene expression. Our data suggest that belimumab may be a useful therapeutic strategy to explore further in standard immunological risk kidney transplant recipients.

## METHODS

### STUDY DESIGN:

In this phase IIA, randomised, double-blind, sponsor unblind study, subjects were recruited at a single UK transplant centre (Addenbrooke's Hospital, Cambridge). The study was approved by the local Research Ethics Committee (East of England - Cambridge East). The study protocol is available at www.gsk-clinicalstudyregister.com

### STUDY PATIENTS:

Patients aged 18 to 75 years receiving a kidney transplant were eligible for inclusion. Exclusion criteria included donor age <5 or >70 years, ABO blood type incompatibility, 0-0-0 HLA mismatch, a positive T and/or B cell cross-match, and previous recipient exposure to B cell targeted therapy (full eligibility criteria are in study protocol, supplementary material). All patients provided written informed consent.

### RANDOMISATION AND MASKING:

Subjects were stratified according to whether the recipient received a living or deceased donor organ. Within each stratum, subjects were randomised in a 1:1 ratio to either belimumab or placebo. Randomisation was performed by the investigators using the

GlaxoSmithKline telephone based Registration and Medication Ordering System (RAMOS). This was a double-blind study in which the investigator, patient and sponsor (with the exception of statistics personnel unblinded for interim/sample size re-estimation) were blinded to the treatment assignment. An unblinded pharmacist prepared the infusion according to the subject's randomised treatment.

PROCEDURES:

Subjects received seven doses of belimumab 10mg/kg (GlaxoSmithKline, Rockville, MD, USA) or placebo (0.9% sodium chloride solution) by intravenous infusion over one hour at days 0, 14, 28 and then every four weeks to week 20, in addition to basiliximab (20mg IV days 0 and 3), tacrolimus (0.15mg/kg daily: target trough level 6-10µg/L first six months post transplantation, 5-8µg/L thereafter), mycophenolate mofetil (500mg twice daily) and prednisolone (20mg daily initially, weaning to 5mg daily in month 1-2). Patients received infection prophylaxis with nystatin (1st month), co-trimoxazole (months 1-6) and valganciclovir (months 1-6), and were followed for 12 months (see study protocol in supplementary material).

For adverse event reporting the on-treatment phase commenced from the start of the first infusion of belimumab/placebo and ended 28 days after the last dose. The post-treatment phase began the following day. For other primary and secondary endpoints the on-treatment phase ended 35 days after the last dose to allow inclusion of the On-Trt Week 24 visit on day 168 +/- 7 days. Details of visit windows can be found in the supplementary appendix.

OUTCOMES:

The first co-primary endpoint was safety assessed by: review of AEs and SAEs, classified using the Medical Dictionary for Regulatory Activities (MedDRA) and including AEs of special interest; and change from baseline and number of subjects outside the normal range for vital

signs and safety laboratory assessments, including immunoglobulin levels and white cell count.

The second co-primary endpoint was change in naïve B cells from baseline to Week 24, a measure of functional BLyS neutralisation validated in patients with SLE[31].

Secondary and exploratory endpoints included pharmacodynamics, immunological biomarkers (e.g. regulatory B cells, assessment of peripheral blood transcriptional profiles, and non-HLA antibodies) and clinical endpoints. Full details of the secondary and exploratory endpoints can be found in the supplementary appendix and study protocol.

B CELL STIMULATION ASSAYS:

Frozen peripheral blood mononuclear cells (PBMC) were thawed and cultured *in vitro* with CpG DNA Oligodeoxynucleotides (100nM; Hycult Biotech) and CD40L (1µg/ml; R&D Systems). Phorbol 12-myristate 13-acetate (PMA) (50ng/ml; Sigma-Aldrich), ionomycin (500ng/ml; Sigma-Aldrich) and brefeldin A (5µg/ml; BioLegend) were added for the last five hours of culture and IL-6 and IL-10 quantified by flow cytometry.

MICROARRAY ANALYSES:

RNA was extracted from whole blood or from purified leukocyte subsets as described previously[32], and hybridised to Human Gene ST 2.1 microarrays (Affymetrix). Microarray data are available in the ArrayExpress database (http://www.ebi.ac.uk/arrayexpress) under accession number E-MTAB-5906.

Patient serum was hybridised to ProtoArray (Invitrogen) protein microarrays according to manufacturer's instructions.

Details of gene expression and protein array analyses are in the supplementary appendix.

STATISTICAL ANALYSIS:

Primary analyses were undertaken using a pre-specified modified intention to treat population (MITT) including all patients randomised who received at least one infusion of belimumab/placebo. Secondary and exploratory biomarker outputs were undertaken using a pre-specified per protocol population (PP) that included all MITT subjects who received at least five infusions of belimumab/placebo, were followed up beyond week 24 and received no prohibited medications or plasma exchange (referred to as PP1 population in the study protocol).

No formal statistical hypotheses were defined in the reporting and analysis plan (RAP). For the primary and secondary biomarker endpoints, a mixed model for repeated measures (MMRM) approach was used to produce adjusted mean differences between belimumab and placebo with corresponding 95% confidence intervals (details in supplementary appendix). For each of the primary and secondary endpoints, error diagnostics from the residuals were examined to ensure that the model did not depart from the assumptions underlying analysis of variance. If the assumptions were seriously violated, then non-parametric alternatives were performed as defined in the RAP. Non-parametric statistical analyses were performed on exploratory endpoints *post hoc* and these are marked as such.

The target sample size of 20 evaluable subjects was informed by feasibility assessment but calculated with the aim of achieving a reduction in naïve B cell count from baseline to 24 weeks. Assumptions for the sample size calculation are provided in the supplemental methods.

Interim re-estimations of sample size were performed in November 2014 and February 2015. An extended safety review team, consisting at a minimum of a safety physician, a clinical development physician and a statistician, oversaw the study.

Analyses were performed using SAS version 9.3 except for transcriptomic and protein microarray analyses, which were performed using R version 3.3.1.

ClinicalTrials.gov number NCT01536379; EudraCT number 2011-006215-56

ROLE OF THE FUNDING SOURCE:

The study was designed by the sponsor, GlaxoSmithKline, in close collaboration with principal investigators at Addenbrooke's Hospital. Authors affiliated to GlaxoSmithKline, Addenbrooke's Hospital and the University of Cambridge were jointly responsible for trial design, data collection, analysis and interpretation, report writing and the decision to submit the paper for publication.

## RESULTS

Twenty-eight subjects were randomised to belimumab (n=14) or placebo (n=14) between 13th September 2013 and 8th February 2015. Twelve belimumab and 13 placebo patients went on to receive at least one dose of belimumab/placebo (Fig. 1) in addition to standard immunosuppression (Table S3). Baseline patient characteristics were comparable between groups (Table 1). Belimumab pharmacokinetic (PK) parameters were similar to those observed in SLE[22] and were not affected by ESRF (Fig. S1A; Table S12). Belimumab effectively removed circulating BLyS, and levels remained suppressed up to week 12 post-treatment, rebounding thereafter (Fig. S1B).

The first co-primary endpoint was safety. We observed AE in 11/12 (92%) belimumab-treated subjects and 10/13 (77%) placebo-treated subjects during the 6 month on-treatment phase and 10/12 (83%) and 9/13 (69%) respectively during the 6 month post-treatment follow-up phase. AE occurring in more than one subject with a higher incidence in the belimumab group were diarrhoea, urinary tract infection, dizziness and vomiting (on treatment) and nasopharyngitis, urinary tract infection and type two diabetes (post treatment). For each event, the difference in frequency compared to placebo was no more than two subjects and

not considered to represent a new safety signal. The number of patients experiencing serious AE were similar (5/12 (42%) of belimumab-treated and 7/13 (54%) of placebo-treated subjects during the 6 month on-treatment phase and 2/12 (17%) and 2/13 (15%) respectively during the 6 month post-treatment follow-up phase). A key question we wished to address in this study was whether the use of belimumab in renal transplantation might be associated with an excess risk of infection. Belimumab has previously been used in patients with autoimmune diseases, in combination with steroids, and in some cases, an anti-proliferative agent (e.g., azathioprine, MMF or methotrexate)[22]. This is the first study to use belimumab with basiliximab induction and with triple maintenance immunosuppression (tacrolimus, MMF and prednisolone) in patients with ESRF at baseline, a condition known to be associated with a heightened susceptibility to infection[33]. Therefore, post-transplant infection was an important end-point, particularly given its association with an increased risk of rejection and allograft loss[34]. At 6 and 12 month follow-up, we observed no excess serious infection events in the belimumab group (1/12 (8%) and 5/13 (38%) in belimumab and placebo-treated patients respectively during the 6 month on-treatment phase and 0/13 (0%) and 2/13 (15%) respectively in the 6 month post-treatment follow-up phase). We also found no excess frequency of BK virus and cytomegalovirus (CMV) infection in belimumab-treated subjects (Table 2). There were no new diagnoses of malignancy in either group during the follow up period and one death, from a cardiovascular cause, in the placebo group (Table 2). In summary, in this preliminary study, belimumab was not associated with an excess risk of serious infection or malignancy when used with standard transplant immunosuppression.

BLyS is known to support the survival of transitional and naïve B cells[20]. Therefore, we assessed naïve B cell count as a co-primary endpoint. This co-primary endpoint of a reduction in naïve B cells from baseline to Week 24 was not met. When considering the MITT population, there was a trend towards a reduction, but no statistically significant difference in naïve B cells (adjusted mean difference naïve B cells from baseline to week 24 -34·4 cells/mm$^3$ (95% CI -109·5 to 40·7)) (Fig. 2A; Table S4). At later time points in the PP

population that included all MITT subjects who received at least five infusions of belimumab/placebo, significant differences in naïve B cell count were observed; adjusted mean difference naïve B cells from baseline to post treatment week 28 was -61.6 cells/mm$^3$ (95% CI -122.6 to -0·7) (Fig S1D; Table S4). A pre-specified non-parametric sensitivity analysis on the MITT population showed a greater reduction from baseline naïve B cell count with belimumab at post treatment week 12 and 28 (median difference at post treatment week 28 -48.3 cells/mm$^3$ (95% CI -144.7 to -13.0)) (Fig. S1E; Table S5).

Biopsy proven TCMR (Banff grade I-III) occurs with a frequency of 15.3% in the 6 months post-transplant, in those receiving basiliximab-based induction therapy[35]. B cell depletion with the anti-CD20 antibody rituximab has been associated with increased TCMR[11] and cardiac allograft vasculopathy[12]. Since belimumab also depletes some B cell subsets, we sought to confirm that its use was not associated with an increase in alloimmune responses. The overall frequency of TCMR (including borderline episodes, Banff classification) was similar in belimumab (n=1/12 (16.7%)) and placebo-treated subjects (n=3/13 (23%), Table 1). One additional subject was randomised to the belimumab group and received a single dose at day 0 but was withdrawn from the study due to a positive B lymphocyte flow cytometry cross-match (an exclusion criterion), the results of which became available post-transplant. This subject subsequently developed Banff IIA TCMR rejection with features suspicious of early acute humoral rejection (day 6), with a further biopsy during treatment demonstrating grade II ABMR (day 34), both of which resolved following treatment with methylprednisolone (day 3-5), plasma exchange (day 8 & 38-52) and anti-thymocyte globulin (day 8-21) (details in supplementary appendix). In the context of pre-formed HLA antibodies and suboptimal induction immunosuppression their rejection episode was not unexpected; however given there was also one further episode of Banff grade IIA cellular rejection in the belimumab PP treatment group and only three Banff ‘borderline’ rejections in the placebo treated group (one was treated with corticosteroids), close monitoring for rejection episodes in larger studies will be required to better understand this observation. Overall, transplant function at one year,

graft and patient survival were not negatively affected by the addition of belimumab to standard of care immunosuppression (Table 1 & 2).

Total B cell numbers were comparable throughout the study (Fig. S1C; Table S13). We observed fewer transitional ($CD24^{br}CD38^{br}IgD^{+}$) B cells at post-treatment week 12 (adjusted mean difference -9156 cells/ml (95% CI -18307 to -6) (Fig. S1F; Table S14) with relative sparing of memory ($CD20^{+}CD27^{+}$) B cells (Fig. S1G; Table S15) such that the proportion of memory B cells was increased throughout the treatment and follow up period (maximal adjusted mean difference 25.7% (95% CI 16.0 to 35.5) at post-treatment week 12; post hoc analysis) (Fig. 2B, C; Table S7). In contrast to the effect of belimumab on the total memory B cell pool, activated memory ($CD95^{+}CD27^{+}$) B cells were decreased from post-treatment week 12 to 28 (Fig. 2D, S1H; Table S16) (adjusted mean difference -14538.52 cells/ml (95% CI -24875.4 to -4201.6) at post-treatment week 12). There was also a reduction in circulating $CD19^{+}CD27^{+}CD38^{hi}$ plasmablasts measured by flow cytometry at post-treatment week 12 (adjusted mean difference -1055.5 count/ml (95% CI -1889.7 to -221.2; post hoc analysis) (Fig. S1I; Table S17). In order to further understand the impact of belimumab on B cell activation and differentiation into antibody-secreting cells, we assessed the whole blood transcriptome. Weighted gene co-expression network analysis identified a B cell gene expression module, identified as such based on the overrepresentation of genes annotated as part of the BCR signaling pathway in the Gene Ontology (Fig. S1L), with attenuated expression in belimumab-treated subjects (post hoc analysis; Fig. 2E). The most attenuated genes in this module coded for IgG, suggesting a strong effect on antibody-secreting cells and complementing our observation of fewer circulating plasmablasts and reduced *de novo* non-HLA antibody formation (described below).

Eight study participants had anti-HLA antibodies (non donor-specific) at transplantation (3/12 in the belimumab group and 5/13 in the placebo group, Table 1). We observed a variable reduction in pre-existing HLA class I and II antibody levels, but the small sample size precludes any definitive conclusions on the effect of belimumab (Fig. S2). Two patients

recruited to the study developed *de novo* DSA during follow-up; both had been withdrawn following a single dose of belimumab for reasons unrelated to antibody development (Fig S2C; see appendix for details).

*De novo* HLA and non-HLA IgG autoantibodies can have a deleterious effect on allograft function[2,3,36]. In order to sensitively measure the ability of belimumab to inhibit the development of *de novo* IgG antibodies, we compared antibody binding to a human protein array in serum samples taken at time zero and week 24. This demonstrated that the addition of belimumab to standard of care immunosuppression significantly reduced *de novo* IgG antibody formation (median number new antibody specificities binding above threshold 55.5 placebo vs 15.5 belimumab; post hoc analysis p=0.0474) (Fig. 2G; Table S8). In addition to effects on *de novo* antibodies, we also observed an effect on pre-formed non-HLA antibodies that have been implicated in allograft damage; at week 24 we saw a trend towards reduced IgG specific for kidney antigens[37] following belimumab treatment (median number antibodies binding kidney specific antigen above threshold 12.5 placebo vs 8.0 belimumab; post hoc analysis p=0.0524 (Fig. 2H; Table S8); median mean protoarray signal 1307.3 placebo vs 983.5 belimumab; post hoc analysis p=0.065 (Fig. S2D; Table S8), and a significant reduction in anti-EDIL3 (EGF-like repeats and discoidin I-like domains 3) antibodies at week 24 (median of mean protoarray signal 353.6 placebo vs 261.9 belimumab; post hoc analysis p=0.0379) (Fig. S2E; Table S8), an endothelial cell-specific antibody associated with post-transplant glomerulopathy[36]. The presence of antibodies to glial cell-derived neurotrophic factor (GDNF) at the time of transplantation has been associated with more severe chronic allograft injury (interstitial fibrosis and tubular atrophy) on 24 month biopsies[3]; we observed a reduction in the number of subjects with detectable anti-GDNF antibodies at week 24 compared with time 0 in the belimumab group (6/8 and 2/8 at time 0 and 24 weeks respectively), in contrast to the placebo group (6/8 and 6/8 at time 0 and week 24 respectively; post hoc analysis) (Fig. S2F). Together, these data emphasise that belimumab modulates a clinically important aspect of B cell function post-transplant.

Transitional B cells have been associated with good outcomes in renal transplant, and this has been proposed to be due to their enrichment with IL-10 producing regulatory B cells[15-18]. IL-10 producing B cells have also been identified within memory subsets[8]. We sought to address how belimumab treatment affects B cell cytokine production post-transplant. PBMC were stimulated *ex vivo* with CpG and CD40L, and B cell IL-10 and IL-6 production assessed (Fig. 3A, B; Table S9). Despite reductions in transitional B cells (Fig. S1F; Table S14), at week 12 post-treatment subjects receiving belimumab had a reduction in IL-6-producing B cells (median 42.62% placebo vs. 29.18% belimumab; post hoc analysis p=0.0379) and an increase in IL-10+ B cells (median 2.46% placebo vs. 4.56% belimumab; post hoc analysis p=0.0499) (Fig. 3A, B; Table S9), skewing the cytokine ratio toward a more regulatory profile compared with controls (median 0.059 placebo vs. 0.127 belimumab; post hoc analysis p=0.0070) (Fig. 3C). This skewing of cytokine production towards IL-10 was observed in both transitional and memory B-cell subsets (Fig. 3D; Table S10). To validate our findings and confirm that the effect of belimumab on B cell cytokine production was B cell intrinsic we cultured PBMC enriched for memory B cells from healthy controls with BLyS in the presence or absence of belimumab. This demonstrated that BLyS stimulation significantly decreased B cell IL-10 relative to IL-6 (mean % change from baseline with 100ng/ml BLyS -22.90% (95%CI -36.52, -9.28); post hoc analysis p=0.0029) and was abrogated by the addition of belimumab (mean % change from baseline with 100ng/ml BLyS + 15nM belimumab 0.63% (95%CI -18.28, 19.54); post hoc analysis p=0.9377) (Fig. 3E; Table S11) providing new insights for Breg biology.

We also investigated whether T cell activation was altered by belimumab treatment, since B cells are potent antigen presenting cells and IL-6 may augment T cell activation[38] whilst IL-10 can regulate T cell responses[39]. There was no difference in the number of circulating T cells by treatment (Fig. S1J-K); Table S18-19) but transcriptomic analysis of purified circulating CD4 T cells revealed reduced expression of cell-cycle genes in belimumab-treated subjects

(post hoc analysis; Fig. 3F, Table S2) suggesting that BLyS neutralisation may also inhibit T cell proliferation.

## DISCUSSION

A key goal of this study was to determine the safety profile of belimumab in combination with standard transplant immunosuppression. Although belimumab has previously been used in patients with SLE with renal involvement, it has not been used in those with established ESRF, which in itself confers an increased risk of infection[33]. Despite this, and a significantly greater burden of concomitant immunosuppression than used previously, we observed no excess infections with the addition of belimumab. Observed AEs were consistent with that expected for the underlying population, concurrent medications and known safety profile of belimumab.

The co-primary endpoint of a reduction in naïve B cells from baseline to week 24 was not met in the MITT population, due to the impact of subjects that received only one dose of belimumab on a group with limited sample size. However, sensitivity and pre-specified analyses performed on the PP population that included subjects who received at least five doses of belimumab/placebo, confirmed that belimumab did have a significant biological effect, greatest at post treatment week 12. Sample size calculation relied on data from studies of belimumab in SLE; it is likely that the more intense immunosuppression given in the immediate post-transplant period masked earlier differences.

Although the co-primary endpoint of a reduction in naïve B cells from baseline to week 24 was not met, data from secondary and mechanistic end-points suggest but do not definitely prove, potential beneficial effects of belimumab post-transplant. Despite depletion by belimumab of the transitional B cell subset known to contain regulatory B cells, remaining B cells after belimumab treatment demonstrated an increased capacity to produce the immunoregulatory cytokine IL-10 relative to IL-6. Since B cells are the major source of IL-6 in secondary lymphoid organs[40], this observation is significant and of potential clinical benefit in

transplantation: IL-6 promotes B cell differentiation into antibody-forming plasma cells, contributes to the plasma cell niche[41], enhances T follicular helper cell differentiation (critical for the germinal centre response), and inhibits the generation of regulatory T cells[38]. Indeed, an IL-6R antagonist has been used to treat patients with chronic ABMR[42].

We present flow cytometry, transcriptomic and protein microarray data suggesting that BLyS neutralisation reduced antibody-forming cells and resulted in a lower incidence of *de novo* non-HLA autoantibody formation post-transplant. In particular, observed trends in kidney and endothelial specific IgG raise the possibility of improved longer-term transplant outcomes[2,3,36]. Our study also highlights the role of BLyS in memory B cell activation. Belimumab-treated subjects had fewer circulating activated (CD95+) memory B cells, suggesting a rationale for using belimumab as a longer-term adjuvant in sensitised transplant subjects with pre-existing donor-specific memory B cells, in addition to lymphocyte depletion and antibody removal. This strategy is currently being studied in a recently established clinical trial using belimumab in combination with bortezomib, plasma exchange and rituximab as a desensitisation therapy (ClinicalTrials.gov Identifier: NCT02500251). Finally, a decrease in T cell proliferation markers demonstrates the potential for belimumab to modulate both cellular and humoral alloimmunity.

Our study has several limitations; the sample size was not powered for clinical endpoints, limiting the broader interpretation of our findings. Early phase studies with modest numbers cannot provide definitive data on safety; with this caveat we report no major adverse safety signal. Despite modest numbers, we were able to implement a range of assays measuring both clinical and immunological parameters so that our major findings are backed by multiple independent readouts, for example flow cytometry, transcriptional differences and antibody array, which together support robust and clinically useful effects on the B cell compartment post-transplant.

The study population (standard immunological risk transplant recipients without DSA) was selected in light of previous studies in SLE showing a significant effect of belimumab on naïve B cells; we therefore hypothesised that the depletion and inhibition of naïve B cells may prevent the development of de novo HLA antibodies in low risk patients. However, these patients have a low risk of developing DSA (around 10% per annum) and a trial powered to detect a difference would need several thousand patients, unfeasible for a Phase 2 experimental medicine study. The transplant community has acknowledged that the unmet need for novel effective therapies for ABMR and to improve long-term graft outcomes may be best addressed through non-traditional trial designs that include surrogate endpoints[43].

Although our study did not include sensitised subjects at greatest risk of ABMR and graft loss, the occurrence of ABMR in the sensitised subject that was inadvertently included in the study provides valuable information for the design of future trials in this area, suggesting that such patients may well need antibody removal and pan-lymphocyte depletion in addition to belimumab. Further studies will be required to evaluate the safety and efficacy of belimumab alongside lymphocyte depleting treatments including thymoglobulin or alemtuzumab, agents that previously associated with an increase in serum BLyS[44]. Whether belimumab would have the same pro-regulatory effect on the reconstituted B cell pool when used in combination with lymphocyte-depletion remains to be determined. An observed rebound in serum BLyS following cessation of belimumab raises the question of whether belimumab should be administered for a more extended period post-transplant, with graduated discontinuation alongside monitoring of serum BLyS.

This study exemplifies an experimental medicine approach and suggests potential efficacy of belimumab as an immunomodulatory agent in transplantation that can limit new antibody formation, providing a useful platform to support design of future clinical studies to explore the further use of belimumab in renal transplantation. In addition, our study provides new insights into BLyS biology and the mechanism of action of belimumab, including novel

preliminary data on its effect on the regulatory B cell compartment and autoantibody production, which are also of relevance in autoimmunity.

CONTRIBUTORS:

GDB, SMF, NT, PAL, DNS, AG, CJEW, RBJ, LRD, COS, KGCS, RBH and MRC were involved in study design.

GDB, NT, AOS and MRC recruited participants.

GDB, SMF, NT, PAL, AG, CJEW, AOS, JAC, KEF, AR, LPE, RBH and MRC collected data.

GDB, SMF, PAL, DNS, AG, JAC, KEF and AR were involved in data analysis.

DNS performed statistical analysis.

GDB, SMF, NT, PAL, DNS, AG, AR, LPE, COS, KGCS, RBH and MRC interpreted the data

GDB, SMF and DNS produced figures.

MRC and GDB wrote the first draft of the manuscript; all authors contributed to its revision and approved the final version.

DISCLOSURES

GDB was funded by a Wellcome Trust Translational Medicine and Therapeutics (TMAT) PhD grant (102728/z/13/z). SMF received funding from GlaxoSmithKline (GSK) for a GSK-Wellcome Trust TMAT PhD. SMF, DNS, AG, KEF, AR, L-PE, COS, and RBH are employees of and hold stock in GSK. JAC is employed by a recruitment agency, working on contract at GSK. RBJ did a secondment to GSK, funded by the company. LRD is a previous employee and a stockholder of GSK, and employee and stockholder of Celgene Corporation. GDB, PAL, and MRC have received grants from GSK outside the submitted work. NT has received support to attend clinical meetings from Astellas Pharma and Alexion Pharmaceuticals.

CJEW has received support to attend clinical meetings from Organ Assist and reports consultancy fees from GSK. KGCS reports consultancy fees from MedImmune, UCB, and Kymab. MRC is funded by a Medical Research Council New Investigator Research Grant (MR/N024907/1) and an Arthritis Research UK Cure Challenge Research Grant (21777), and also receives support from the National Institute of Health Research Cambridge Biomedical Research Centre. RBH has a patent PB65956 pending. AR has a patent issued for recombinant factor H and variants and conjugates thereof (US20150139975 A1), and an EU application pending (WO2011077102 A1). AR's spouse David Kavanagh is head of the National Renal Complement Therapeutics Centre, UK; Chief Investigator for NCT02949128, Alexion Pharmaceuticals; founding board member and scientific adviser to Gyroscope Therapeutics (stock options; consultancy fees paid to Newcastle University, Newcastle, UK); and consults for Alexion Pharmaceuticals and Akari Therapeutics (Newcastle University, Newcastle, UK, receives consulting fees). A-MO declares no competing interests.

ACKNOWLEDGMENTS

Study funded by GlaxoSmithKline; ClinicalTrials.gov number NCT01536379; EudraCT number 2011-006215-56.

CJEW and MRC are supported by the National Institute of Health Research (NIHR) Cambridge Biomedical Research Centre and the NIHR Blood and Transplant Research Unit. We thank all the patients who participated in the study, without whom this work would not have been possible. We also thank the Wellcome trust for their role in funding GDB, A J Want, S S Franco, P A Wilson, the GSK Clinical Unit Cambridge for technical support, Addenbrooke's Hospital Histocompatibility and Immunogenetics laboratory and pathology services for their assistance with sample processing, ThermoFisher for their advice on ProtoArray analysis, and D Game and colleagues at Guy's and St Thomas' National Health Service (NHS) Foundation Trust for their contribution to patient screening..

Table 1. Baseline Demographics and Clinical Outcomes.

| | Placebo (n=13) | Belimumab 10mg/kg (n=12) |
|---|---|---|
| Baseline demographic data, n | 13 | 12 |
| Age (years), Mean (SD) | 51.0 (14.0) | 54.3 (11.0) |
| Range | 24-73 | 32-72 |
| Sex, n (%) | | |
| - Female | 4 (31) | 7 (58) |
| - Male | 9 (69) | 5 (42) |
| Race, n (%) | | |
| - White/Caucasian | 12 (92) | 11 (92) |
| - Asian | 1 (8) | 1 (8) |
| Mean number (SD) of HLA-A/B/DR mismatches | | |
| - HLA-A | 1.7 (0.5) | 1.8 (0.5) |
| - HLA-B | 0.9 (0.6) | 1.1 (0.3) |
| - HLA-DR | 0.6 (0.5) | 0.8 (0.6) |
| Number of previous kidney transplants, n (%) | | |
| - 0 | 11 (85) | 11 (92) |
| - 1 | 2 (15) | 1 (8) |
| Pre-transplant renal replacement modality, n (%) | | |
| - None | 3 (23) | 2 (17) |
| - Haemodialysis | 7 (54) | 7 (58) |
| - Peritoneal dialysis | 3 (23) | 3 (25) |
| HLA antibody at baseline (MFI>2000)[3], n (%) | | |
| - Non-DSA | 5 (38) | 3 (25) |
| - DSA [2] | 0 | 1 (8) |
| Donor type, n (%) | | |
| - Living | 3 (23) | 4 (33) |

| | | | | |
|---|---|---|---|---|
| - Donation after circulatory death | 7 (54) | | 5 (42) | |
| - Donation after brain death | 3 (23) | | 3 (25) | |
| Donor age (years) | | | | |
| Mean (SD) | 52.9 (8.8) | | 58.3 (8.1) | |
| Range | 37-68 | | 47-69 | |
| Donor creatinine-last value prior to transplant (µmol/L) | | | | |
| Mean (SD) | 64.8 (17.5) | | 84.3 (30.7) | |
| Median (Min, Max) | 66.0 (37-92) | | 78.0 (51-167) | |
| Clinical outcome data[1], n | 8 | | 8 | |
| Acute transplant rejection by week 52[2], n (%) | | | | |
| - Borderline, not treated | 2 (25) | | 0 | |
| - Borderline, treated | 1 (12.5) | | 0 | |
| - Type IIa, treated | 0 | | 1 (12.5) | |
| Cumulative HLA class I (MFI >500)[3] | Sub 22 | Sub 28 | Sub 8 | Sub 27 |
| Before treatment | 39612 | 20046 | 127392 | 4894 |
| On treatment Wk 2 | 24658 | 14731 | 56453 | 4493 |
| On treatment Wk 4 | 26129 | 21466 | 33810 | 3438 |
| On treatment Wk 8 | 28930 | 19528 | 34420 | 4632 |
| On treatment Wk 12 | 26709 | 26500 | 25985 | 6320 |
| On treatment Wk 24 | 23152 | 18376 | 26491 | 8103 |
| Post treatment Wk 28 | 19204 | 18892 | 24607 | 4349 |
| Cumulative HLA class II (MFI >500)[3] | Sub 4 | | Sub 1 | |
| Before treatment | 2382 | | 16009 | |
| On treatment Wk 2 | 916 | | 9305 | |
| On treatment Wk 4 | 1211 | | 12346 | |
| On treatment Wk 8 | 768 | | 12553 | |
| On treatment Wk 12 | 606 | | 10540 | |

| | | |
|---|---|---|
| On treatment Wk 24 | 577 | 13408 |
| Post treatment Wk 28 | 785 | 9075 |
| Graft survival, n (%) | 8 (100) | 8 (100) |
| Creatinine at 52 weeks (μmol/L) | | |
| Mean (SD) | 142.5 (65.7) | 110.6 (43.6) |
| Median (Min, Max) | 114 (86-282) | 94 (68-201) |
| eGFR at 52 weeks (ml/min/1.73m$^2$), | | |
| Mean (SD) | 53.00 (22.10) | 57.42 (15.08) |
| Median (Min, Max) | 54.03 (20.41-86.63) | 56.77 (30.25-81.93) |

[1]Clinical outcome data described for the per protocol population.

[2]Acute rejection was defined on biopsy according to Banff 2009 criteria: Acute antibody mediated rejection (Grade I, II or III) or acute T cell mediated rejection (Borderline, Type IA, Type IB, Type IIA, Type IIB, Type III). An additional subject randomised to belimumab had a positive pre-transplant MHC class II flow crossmatch (fulfilling an exclusion criterion but unknown at the time of enrolment and transplant). They experienced Type IIA acute cellular rejection (day 6) and grade II antibody mediated rejection (day 34). They were withdrawn once the crossmatch was recognised following a single dose of belimumab.

[3]A cut-off of MFI>2000 was used to define preformed HLA antibody at baseline, since this is the threshold for clinical significance determined by the tissue-typing laboratory. Cumulative HLA class I and class II MFI calculated by summing the normalised MFI values for any single antigen bead with a value above the level of detection (500). An additional subject in the belimumab group underwent adoptive transfer of donor HLA-specific allosensitization following kidney transplantation from a highly sensitized donor.

SD standard deviation, n number of subjects, HLA human leukocyte antigen, MFI mean fluorescence intensity measured by Luminex assay, DSA Donor specific antibody, Min minimum, Max maximum, and eGFR estimated glomerular filtration rate.

Table 2. Safety Findings During On-treatment and Post-treatment Phases, by Treatment Group.

| | On treatment [1] | | Post-treatment | |
|---|---|---|---|---|
| | Number (%) Subjects | | Number (%) Subjects | |
| | Placebo (n=13) | Belimumab (n=12) | Placebo (n=13) | Belimumab (n=12) |
| Any adverse event (AE) | 10 (77) | 11 (92) | 9 (69) | 10 (83) |
| Any serious AE (SAE) | 7 (54) | 5 (42) | 2 (15) | 2 (17) |
| Any severe AE | 6 (46) | 8 (67) | 3 (23) | 3 (25) |
| Deaths [2] | 1 (8) | 0 | 0 | 0 |
| Most common AE [3] | | | | |
| - Leukopenia | 4 (31) | 4 (33) | 3 (23) | 3 (25) |
| - Diarrhoea | 3 (23) | 5 (42) | 1 (8) | 1 (8) |
| - Urinary tract infection [4] | 3 (23) | 4 (33) | 1 (8) | 2 (17) |
| - Anaemia [5] | 4 (31) | 3 (25) | 0 | 1 (8) |
| - Lower respiratory tract infection [6] | 2 (15) | 2 (17) | 2 (15) | 0 |
| - Dyspepsia[7] | 2 (15) | 2 (17) | 2 (15) | 0 |
| - Nasopharyngitis | 2 (15) | 1 (8) | 1 (8) | 2 (17) |
| - Alanine aminotransferase increased | 2 (15) | 2 (17) | 0 | 0 |
| - Diabetes Mellitus[8] | 1 (8) | 1 (8) | 0 | 2 (17) |
| - Endoscopic evidence upper GI inflammation[9] | 2 (15) | 1 (8) | 0 | 0 |
| - Dizziness | 0 | 2 (17) | 0 | 1 (8) |
| - Vomiting | 0 | 2 (17) | 0 | 0 |
| Infections | | | | |
| - All | 7 (54) | 5 (42) | 8 (62) | 6 (50) |
| - Serious infections (n≥1) | 5 (38) | 1 (8) | 2 (15) | 0 |

| | | | | |
|---|---|---|---|---|
| - Severe infections (n≥1) | 5 (38) | 2 (17) | 3 (23) | 0 |
| - Opportunistic infections | 3 (23) | 2 (17) | 3 (23) | 3 (25) |
| - BK viraemia | 2 (15) | 1 (8) | 1 (8) | 1 (8) |
| - BK viraemia-associated nephropathy | 0 | 1 (8) | 1 (8) | 0 |
| - Cytomegalovirus (CMV) viraemia[10] | 1 (8) | 0 | 1 (8) | 2 (17) |
| Malignant neoplasm | 0 | 0 | 0 | 0 |
| Depression/Suicide/Self injury | 0 | 0 | 0 | 0 |
| Post infusion systemic reaction[11] | 0 | 1 (8) | NA | NA |
| Recurrence of focal segmental glomerulonephritis[12] | 1 (8) | 1 (8) | 0 | 0 |
| Hypogammaglobulinemia of grade ≥3 (<4.0g/L) | 2 (15) | 3 (25) | 0 | 0 |

[1]The on-treatment phase commences from the start of the first infusion of randomised study drug and ends 28 days after the last dose. The post-treatment phase begins the following day.

[2]Death due to fatal myocardial infarction and acute cardiac failure.

[3]Includes all AEs (by grouped MedDRA preferred terms) occurring in more than one subject during the study not including opportunistic infections (listed separately), ordered by overall frequency.

[4]Grouped preferred terms include urinary tract infection, Escherichia urinary tract infection, urinary tract infection enterococcal and urosepsis.

[5]Grouped preferred terms include anaemia, anaemia vitamin B12 deficiency and iron deficiency anaemia.

[6]Grouped preferred terms include pneumonia and lower respiratory tract infection.

[7]Grouped preferred terms include dyspepsia and gastrooesophageal reflux disease.

[8]Grouped preferred terms include diabetes mellitus and type two diabetes mellitus; one post treatment AE was worsening of diabetes, onset on treatment, in context of steroids for SAE (colitis)

[9]Grouped preferred terms include oesophagitis, duodenal ulcer, duodenitis and ulcerative gastritis.

[10]Grouped preferred terms include cytomegalovirus test positive, cytomegalovirus viraemia, culture positive (verbatim term CMV).

[11]The infusion reaction reported was mild, settled spontaneously and did not recur on subsequent infusions.

[12]Grouped preferred terms include focal segmental glomerulosclerosis (FSGS) and glomerulonephritis (recurrence of FSGS verbatim term). NA denotes not applicable.

Figure 1. Enrolment, Randomisation and Follow-up.

The randomised treatment was given in addition to standard immunosuppression consisting of basiliximab, mycophenolate mofetil, tacrolimus and corticosteroids (see methods for full details).

[1]260 at Addenbrooke's Hospital, Cambridge (28 randomised); 43 at Guy's and St Thomas' NHS Foundation Trust, London (0 randomised).

[2]Reasons for not meeting inclusion criteria shown in Supplementary Table 1. Logistical reasons included unavailability of study staff or randomised study drug, insufficient time for consent and recipient resident out of region.

[3]The pre-specified per protocol (PP) population used for biomarker and clinical endpoint analysis consisted of all subjects in the modified intention to treat (MITT) population who received at least five infusions of belimumab/placebo, no prohibited medications or plasma exchange and at least 24 weeks follow-up.

FSGS Focal Segmental Glomerulosclerosis, SAE Serious Adverse Event

Figure 2. Belimumab Affects Naïve B Cells, Activated Memory B Cells and Circulating Plasmablasts, and Reduces Allo/Auto-antibody Generation.

Panel A shows the adjusted mean (95% CI) change from baseline in naïve ($CD20^{+}CD27^{-}$) B cell count (cells/$mm^3$), by visit and treatment.

Panel B is a radar plot summarising the median difference from baseline to week 24 compared to baseline (i.e. percentage at week 24 – percentage at week 0) for the labelled B cell populations by belimumab or placebo, where each B-cell population is expressed as a percentage of total B cells.

Panel C shows memory ($CD20^+CD27^+$) B cells expressed as a percentage of B cells by visit and treatment group.

Panel D shows the relationship between memory B cell count (cells/$mm^3$) and activated memory B cell ($CD95^+CD27^+$) percentage at the post treatment week 12 timepoint for individual subjects labelled by treatment group.

Panel E shows expression (arbitrary units) of a B cell whole blood gene expression module by treatment group at baseline, end of on-treatment phase (Week 24) and end of follow-up (Week 52). Horizontal lines correspond to median and interquartile ranges.

Panel F shows a heat map of differential gene expression (belimumab versus placebo groups) for genes in the B cell module at baseline, week 24 and week 52. Genes are ordered by fold-change at week 24 and immunoglobulin-coding transcripts are highlighted. Colour corresponds to $log_2$-fold change, with blue indicating higher expression in the placebo group (Placebo) relative to the belimumab group (Belimumab).

Panel G shows the number of unique ProtoArray antigen specificities with significant antibody binding at Week 24 but not at baseline. Horizontal lines on boxplot (left) correspond to median and interquartile ranges. Ordered individual participant data are also shown (right), with participants coloured by treatment group. The Wilcoxon rank-sum test was used to compare the belimumab treatment group (BEL) and placebo treatment group (PBO); * denotes $p<0.05$.

Panel H shows the number of kidney-specific unique ProtoArray antigen specificities (as defined in [37]) with significant antibody binding at Week 24. Horizontal lines on boxplot (left) correspond to median and interquartile ranges. Ordered individual participant data are also shown (right), with participants coloured by treatment group. The Wilcoxon rank-sum test was used to compare the belimumab treatment group (BEL) and placebo treatment group (PBO); exact p value displayed.

Panel A uses the MITT population. Panels B, C, D, G and H use the PP population. Panels E and F use the MITT population for baseline and the PP population thereafter. C shows raw values at baseline for comparison and adjusted mean estimate with 95% confidence intervals at subsequent timepoints. Adjusted mean estimates and 95% confidence intervals are obtained from MMRM model, with fixed categorical effects of treatment, visit, donor type and treatment-by-visit interaction and fixed continuous covariates of baseline and baseline-by-visit interaction. A compound symmetry variance structure was used to model the within-patient errors, shared across treatments. # indicates that the 95% confidence interval of the treatment difference does not include zero. D shows data for individual PP subjects labelled by treatment group. Panels B, C, D, E, F, G and H represent analyses performed *post hoc*.

Figure 3. Memory B Cell IL-10/IL-6 Ratio is BLyS Dependent. Belimumab Treatment Increases Regulatory B Cells and is Associated with Reduced T cell Proliferation.

Peripheral blood mononuclear cells (PBMC) were stimulated *ex vivo* for 5 hours and intracellular cytokine production quantified by flow cytometry (Panel A-D). Individual data points represent individual subjects with horizontal lines signifying the median for each treatment group. Wilcoxon rank-sum tests were performed to compare samples by treatment and visit.

Panel A shows representative flow cytometry plots for IL-6 (upper) and the percentage of CD19+ B cells expressing IL-6 (lower).

Panel B shows representative flow cytometry plots for IL-10 (upper) and the percentage of CD19+ B cells expressing IL-10 by treatment group and timepoint (lower).

Panel C shows the calculated ratio of IL-10/IL-6 with higher values indicating a more anti-inflammatory cytokine milieu.

Panel D shows the IL-10/IL-6 ratio for individual subsets of naïve (CD27-), transitional ($CD24^{hi}CD38^{hi}IgD^{+}$), $CD24^{+}CD27^{+}$ memory, switched memory ($CD27^{+}IgD^{-}$), and non switched memory ($CD27^{+}IgD^{+}$) B cells at post treatment Wk 12.

Panel E shows the mean IL-10/IL-6 ratio (relative to 0ng/mL BLyS) with 95% confidence intervals for PBMC from healthy volunteers enriched for CD27+ memory B cells and stimulated for 48 hours with increasing quantities of BLyS. In the presence of increasing quantities of BLyS a more inflammatory cytokine milieu was observed. This change was blocked by the addition of belimumab. N, number of healthy volunteers tested for each experimental condition. T-tests were performed to determine whether the mean percentage changes from baseline differed significantly from 0 for each experimental condition.

Panel F shows a heatmap of differential gene expression in circulating CD4+ T-cells for the most downregulated genes at week 24 in the belimumab group relative to the placebo group, with genes ordered by unsupervised hierarchical clustering. Genes annotated to the cell-cycle (GO:0007049) are highlighted. Colour corresponds to $\log_2$-fold change, with blue indicating higher expression in the placebo group (Placebo) relative to the belimumab group (Belimumab).

Panels A-D use the PP population and Panel F uses the MITT population for baseline and PP population thereafter. P-values in Panels A-D were calculated using Wilcoxon rank-sum tests and indicated where significant; in all other cases the values are not statistically significantly different. P-values in Panel E were calculated using Student's t-test. * $p<0.05$, ** $p<0.01$, *** $p<0.001$, NS not significant ($p\geq0.05$). All analyses were performed *post hoc*.

## References


1. Lefaucheur C, Loupy A, Vernerey D, et al. Antibody-mediated vascular rejection of kidney allografts: a population-based study. *Lancet* 2013; **381**(9863): 313-9.
2. Dragun D, Muller DN, Brasen JH, et al. Angiotensin II type 1-receptor activating antibodies in renal-allograft rejection. *N Engl J Med* 2005; **352**(6): 558-69.
3. Sigdel TK, Li L, Tran TQ, et al. Non-HLA antibodies to immunogenic epitopes predict the evolution of chronic renal allograft injury. *J Am Soc Nephrol* 2012; **23**(4): 750-63.
4. Bentall A, Cornell LD, Gloor JM, et al. Five-year outcomes in living donor kidney transplants with a positive crossmatch. *Am J Transplant* 2013; **13**(1): 76-85.
5. Sarwal M, Chua MS, Kambham N, et al. Molecular heterogeneity in acute renal allograft rejection identified by DNA microarray profiling. *N Engl J Med* 2003; **349**(2): 125-38.
6. Inaba A, Clatworthy MR. Novel immunotherapeutic strategies to target alloantibody-producing B and plasma cells in transplantation. *Curr Opin Organ Transplant* 2016; **21**(4): 419-26.
7. Blair PA, Norena LY, Flores-Borja F, et al. CD19(+)CD24(hi)CD38(hi) B cells exhibit regulatory capacity in healthy individuals but are functionally impaired in systemic Lupus Erythematosus patients. *Immunity* 2010; **32**(1): 129-40.
8. Iwata Y, Matsushita T, Horikawa M, et al. Characterization of a rare IL-10-competent B-cell subset in humans that parallels mouse regulatory B10 cells. *Blood* 2011; **117**(2): 530-41.
9. Tyden G, Ekberg H, Tufveson G, Mjornstedt L. A randomized, double-blind, placebo-controlled study of single dose rituximab as induction in renal transplantation: a 3-year follow-up. *Transplantation* 2012; **94**(3): e21-2.
10. van den Hoogen M, Kamburova EG, Baas MC, et al. Rituximab as induction therapy after renal transplantation: a randomized, double-blind, placebo-controlled study of efficacy and safety. *Am J Transplant* 2015; **15**(2): 407-16.
11. Clatworthy MR, Watson CJ, Plotnek G, et al. B-cell-depleting induction therapy and acute cellular rejection. *N Engl J Med* 2009; **360**(25): 2683-5.
12. Chandraker A, Kobashigawa J, Stehlik J, et al. Rituximab Induction in Cardiac Transplantation Is Associated with Accelerated Coronary Artery Vasculopathy: CTOT11. *American Journal of Transplantation* 2016; **16**(Supplement S3): 403.
13. Pallier A, Hillion S, Danger R, et al. Patients with drug-free long-term graft function display increased numbers of peripheral B cells with a memory and inhibitory phenotype. *Kidney Int* 2010; **78**(5): 503-13.
14. Newell KA, Asare A, Kirk AD, et al. Identification of a B cell signature associated with renal transplant tolerance in humans. *J Clin Invest* 2010; **120**(6): 1836-47.
15. Chesneau M, Pallier A, Braza F, et al. Unique B cell differentiation profile in tolerant kidney transplant patients. *Am J Transplant* 2014; **14**(1): 144-55.
16. Shabir S, Girdlestone J, Briggs D, et al. Transitional B lymphocytes are associated with protection from kidney allograft rejection: a prospective study. *Am J Transplant* 2015; **15**(5): 1384-91.
17. Cherukuri A, Salama A, Carter C, Clark B, Rothstein D, Baker R. Human Regulatory B Cells (BRegs) Are Characterised by Both IL-10 and TNF-α Expression and Are Reduced in Numbers with Altered Function in Renal Transplant Recipients with Immunological Graft Injury. *American Journal of Transplantation* 2013; **13**(s5, A645): 229.
18. Cherukuri A, Rothstein DM, Clark B, et al. Immunologic human renal allograft injury associates with an altered IL-10/TNF-alpha expression ratio in regulatory B cells. *J Am Soc Nephrol* 2014; **25**(7): 1575-85.
19. Schlosser HA, Thelen M, Dieplinger G, et al. Prospective analyses of circulating B-cell subsets in AB0-compatible and AB0-incompatible kidney transplant recipients. *Am J Transplant* 2016.
20. Mackay F, Schneider P, Rennert P, Browning J. BAFF AND APRIL: a tutorial on B cell survival. *Annu Rev Immunol* 2003; **21**: 231-64.
21. Avery DT, Kalled SL, Ellyard JI, et al. BAFF selectively enhances the survival of plasmablasts generated from human memory B cells. *J Clin Invest* 2003; **112**(2): 286-97.

22. Navarra SV, Guzman RM, Gallacher AE, et al. Efficacy and safety of belimumab in patients with active systemic lupus erythematosus: a randomised, placebo-controlled, phase 3 trial. *Lancet* 2011; **377**(9767): 721-31.
23. Steri M, Orru V, Idda ML, et al. Overexpression of the Cytokine BAFF and Autoimmunity Risk. *N Engl J Med* 2017; **376**(17): 1615-26.
24. Thibault-Espitia A, Foucher Y, Danger R, et al. BAFF and BAFF-R levels are associated with risk of long-term kidney graft dysfunction and development of donor-specific antibodies. *Am J Transplant* 2012; **12**(10): 2754-62.
25. Snanoudj R, Candon S, Roelen DL, et al. Peripheral B-cell phenotype and BAFF levels are associated with HLA immunization in patients awaiting kidney transplantation. *Transplantation* 2014; **97**(9): 917-24.
26. Banham G, Prezzi D, Harford S, et al. Elevated pretransplantation soluble BAFF is associated with an increased risk of acute antibody-mediated rejection. *Transplantation* 2013; **96**(4): 413-20.
27. Parsons RF, Yu M, Vivek K, et al. Murine islet allograft tolerance upon blockade of the B-lymphocyte stimulator, BLyS/BAFF. *Transplantation* 2012; **93**(7): 676-85.
28. Kwun J, Page E, Hong JJ, et al. Neutralizing BAFF/APRIL with atacicept prevents early DSA formation and AMR development in T cell depletion induced nonhuman primate AMR model. *Am J Transplant* 2015; **15**(3): 815-22.
29. Mujtaba MA, Komocsar WJ, Nantz E, et al. Effect of Treatment With Tabalumab, a B Cell-Activating Factor Inhibitor, on Highly Sensitized Patients With End-Stage Renal Disease Awaiting Transplantation. *Am J Transplant* 2016.
30. Naji A. One Year Exploratory Study to Evaluate the Efficacy and Safety of Belimumab for Normalization of Alloantibody Levels in Sensitized Patients Awaiting Kidney Transplantation. *Clinicaltrialsgov*; **NCT01025193**.
31. Stohl W, Hiepe F, Latinis KM, et al. Belimumab reduces autoantibodies, normalizes low complement levels, and reduces select B cell populations in patients with systemic lupus erythematosus. *Arthritis Rheum* 2012; **64**(7): 2328-37.
32. Lyons PA, Koukoulaki M, Hatton A, et al. Microarray analysis of human leucocyte subsets: the advantages of positive selection and rapid purification. *BMC Genomics* 2007; **8**: 64.
33. Vanholder R, Ringoir S. Infectious morbidity and defects of phagocytic function in end-stage renal disease: a review. *J Am Soc Nephrol* 1993; **3**(9): 1541-54.
34. Almond PS, Matas A, Gillingham K, et al. Risk factors for chronic rejection in renal allograft recipients. *Transplantation* 1993; **55**(4): 752-6; discussion 6-7.
35. Group CSC, Haynes R, Harden P, et al. Alemtuzumab-based induction treatment versus basiliximab-based induction treatment in kidney transplantation (the 3C Study): a randomised trial. *Lancet* 2014; **384**(9955): 1684-90.
36. Jackson AM, Sigdel TK, Delville M, et al. Endothelial cell antibodies associated with novel targets and increased rejection. *J Am Soc Nephrol* 2015; **26**(5): 1161-71.
37. Li L, Wadia P, Chen R, et al. Identifying compartment-specific non-HLA targets after renal transplantation by integrating transcriptome and "antibodyome" measures. *Proc Natl Acad Sci U S A* 2009; **106**(11): 4148-53.
38. Jordan SC, Choi J, Kim I, et al. Interleukin-6, A Cytokine Critical to Mediation of Inflammation, Autoimmunity and Allograft Rejection: Therapeutic Implications of IL-6 Receptor Blockade. *Transplantation* 2017; **101**(1): 32-44.
39. Maynard CL, Weaver CT. Diversity in the contribution of interleukin-10 to T-cell-mediated immune regulation. *Immunol Rev* 2008; **226**: 219-33.
40. Barr TA, Shen P, Brown S, et al. B cell depletion therapy ameliorates autoimmune disease through ablation of IL-6-producing B cells. *J Exp Med* 2012; **209**(5): 1001-10.
41. Kometani K, Kurosaki T. Differentiation and maintenance of long-lived plasma cells. *Curr Opin Immunol* 2015; **33**: 64-9.

42. Choi J, Aubert O, Vo A, et al. Assessment of Tocilizumab (Anti-Interleukin-6 Receptor Monoclonal) as a Potential Treatment for Chronic Antibody-Mediated Rejection and Transplant Glomerulopathy in HLA-Sensitized Renal Allograft Recipients. *Am J Transplant* 2017.
43. O'Connell PJ, Kuypers DR, Mannon RB, et al. Clinical Trials for Immunosuppression in Transplantation: The Case for Reform and Change in Direction. *Transplantation* 2017; **101**(7): 1527-34.
44. Bloom D, Chang Z, Pauly K, et al. BAFF is increased in renal transplant patients following treatment with alemtuzumab. *Am J Transplant* 2009; **9**(8): 1835-45.

Figure1: Enrolment, Randomisation and Follow-up.

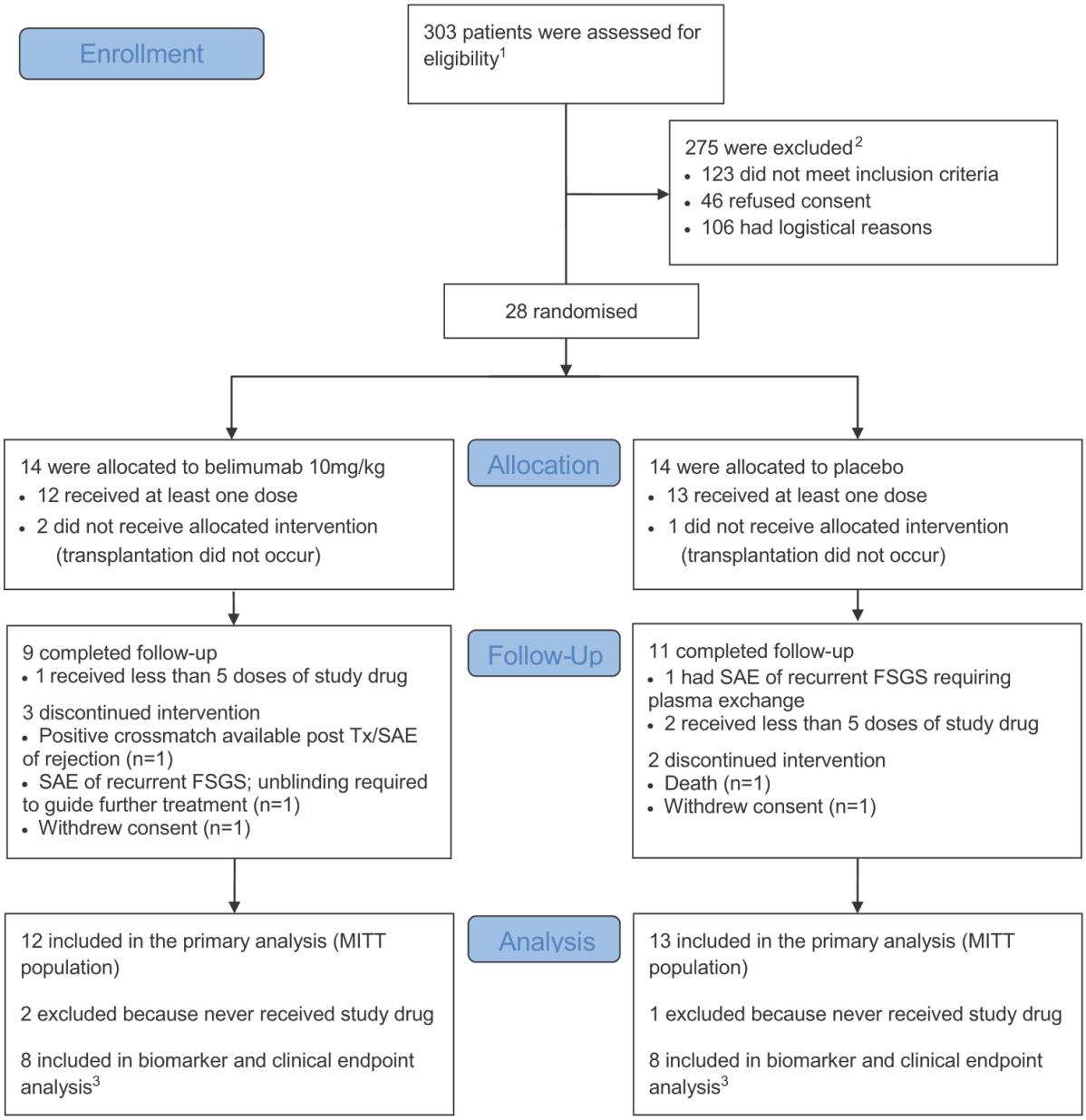

Figure 2. Belimumab Affects Naïve B Cells, Activated Memory B Cells and Circulating Plasmablasts, and Reduces Allo/Auto-antibody Generation.

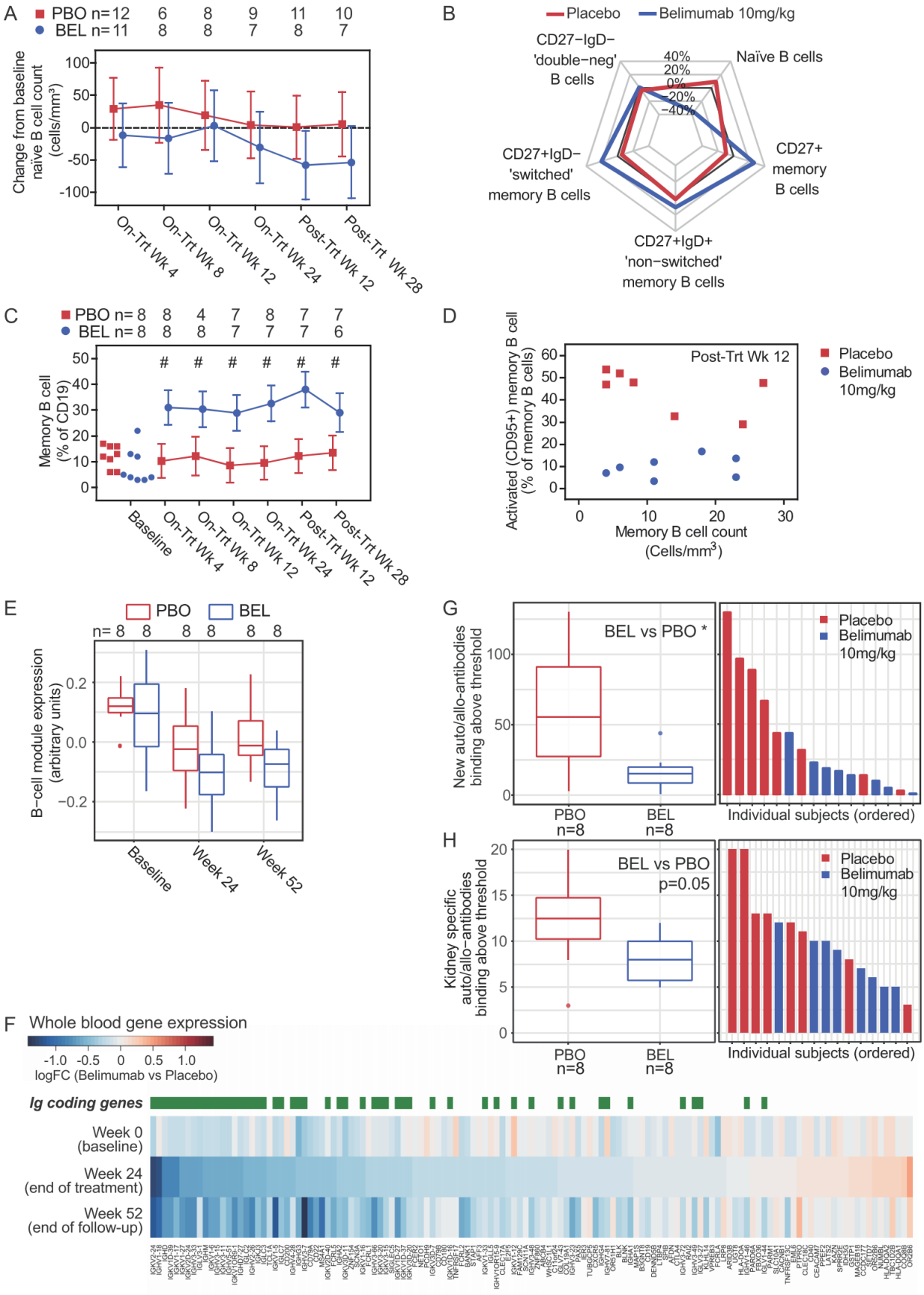

Figure 3. Memory B cell IL-10/IL-6 Ratio is BLyS Dependent. Belimumab Treatment Increases Regulatory B cells and is Associated with Reduced T cell Proliferation.

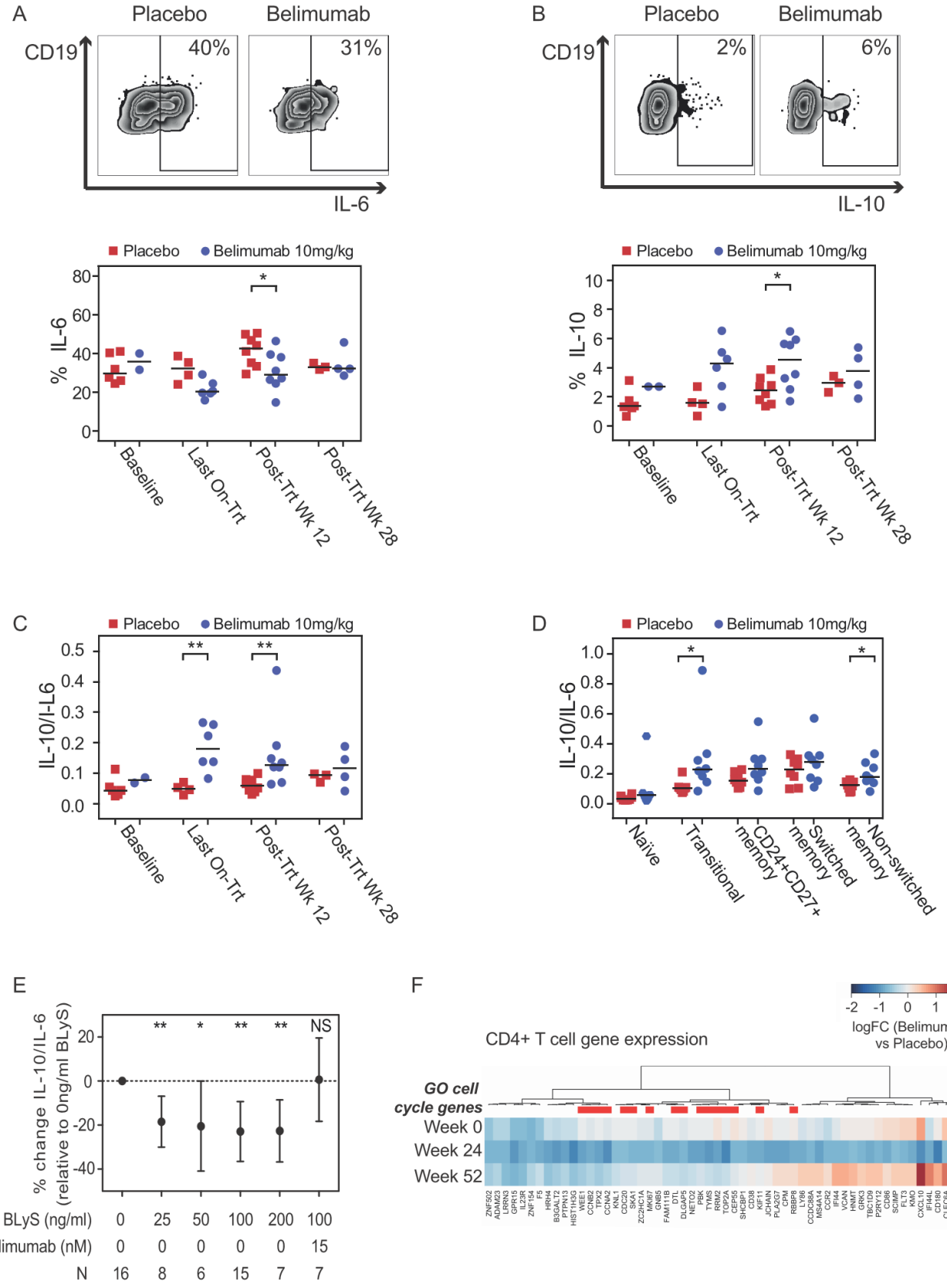

## Supplementary Appendix

# A Phase 2 Experimental Medicine Randomised Placebo Controlled Trial of Belimumab in Kidney Transplantation (BEL114424)

Gemma D. Banham*, Shaun M. Flint*, Nicholas Torpey, Paul A. Lyons, Don N. Shanahan, Adele Gibson, Christopher J.E. Watson, Ann-Marie O'Sullivan, Joseph A. Chadwick, Katie E. Foster, Rachel B. Jones, Luke R. Devey, Anna Richards, Lars-Peter Erwig, Caroline O. Savage, Kenneth G.C. Smith, Robert B. Henderson*, Menna R. Clatworthy* (*authors contributed equally to this work)

**Contents:**

**BEL114424 eligibility criteria and study protocol**

The BEL114424 study protocol, including full eligibility criteria is included as a separate file and will also be published at www.gsk-clinicalstudyregister.com.

The original protocol excluded donation after circulatory death (DCD) donors aged > 60 years old, or > 50 if they had died from a stroke, had a history of high blood pressure, or had a serum creatinine greater than 135µmol/L at the time of donation (i.e. extended criteria DCDs). An amendment to widen eligibility criteria was sought (protocol amendment 4, dated 16 October 2013), with the aim of increasing recruitment. The reasons for subjects not meeting inclusion criteria are listed in Table S1.

**Table S1: Reasons for subjects not meeting inclusion criteria.**

| Reason not meeting inclusion criteria | Number |
|---|---|
| Donor characteristic | 36 |
| Alternative immunosuppression planned | 21 |
| 0-0-0 mismatch | 16 |
| HLAi or ABOi transplant | 15 |
| Other disease/condition judged unsuitable by PI | 12 |
| Prior therapy | 8 |
| Transplant other than kidney | 3 |
| Recipient hepatitis | 3 |
| Donor hepatitis | 2 |
| Recipient unable to consent due to learning difficulties | 2 |
| Recipient HIV+ | 2 |
| Drug sensitivity | 1 |
| Prior malignancy | 1 |
| Poor venous access | 1 |
| **Total** | **123** |

**Visit windows**

Assessments were assigned to visit windows (slots) according to the date of assessment (for study schedule see study protocol).

For adverse events the on-treatment phase commenced from the start of the first infusion of belimumab/placebo and ended 28 days after the last dose. The post-treatment phase began the following day. For other primary and secondary endpoints, the on-treatment phase ended 35 days after the last dose to allow incorporation of the On-Trt Week 24 visit on day 168 +/- 7 days.

The visit slotting intervals for the Pre-Treatment and On-Treatment (On-Trt) phases for biomarker endpoints were as follows:

| Week | Day relative to first infusion | Day | Visit Window |
|---|---|---|---|
| Baseline | ≤0 | ≤0 | ≤0 |
| On-Trt Week 4 | 28 | 28 - 27 Days or + 14 Days | Days 1 to 42 |
| On-Trt Week 8 | 56 | 56 - 13 Days or + 14 Days | Days 43 to 70 |
| On-Trt Week 12 | 84 | 84 - 13 Days + 42 Days | Days 71 to 126 |
| On-Trt Week 24 | 168 | 168 - 41 Days +7 Days | Days 127 to 175 |

The visit slotting intervals for the Post-Treatment (Post-Trt) phase for biomarker endpoints were as follows:

| Week | Day relative to (last infusion + 35 Days) | Day relative to last infusion | Day | Visit Window |
|---|---|---|---|---|
| Post-Trt Week 12 | 84 | 119 | 84 – 83 Days or + 56 Days | Days 1 to 140 |
| Post-Trt Week 28 | 196 | 231 | 196 – 55 Days or + 154 Days | Days 141 to 350 |

If more than one assessment fell within the same visit window, the assessment nearest to the scheduled time point was used. If two assessments were equally close, the latter was used. Samples for transcriptomic and protoarray analysis were collected at baseline, at week 24 (+/- 7 days) and at week 52 (+/- 7 days) according to the study schedule, irrespective of the last dose of study drug given, so data for these endpoints are presented without window fitting. On-treatment samples for the B cell stimulation assay were limited so the last available on-treatment result is displayed ('Last On-Trt').

**Study objectives and endpoints**

| Objectives | Endpoints |
|---|---|
| **Co-primary** | |
| **Efficacy:** To estimate the change in naive B cells following belimumab 10 mg/kg (or placebo) in addition to standard of care immunosuppressants in renal transplant patients from the time of transplantation up to 24 weeks | Change from baseline in naïve B cells from baseline to Week 24. |
| **Safety:** To assess the safety and tolerability of belimumab 10 mg/kg (or placebo) in renal transplant patients in addition to standard of care immunosuppressants. | AEs and SAEs, including AEs of special interest (opportunistic infections, malignancies, hypersensitivity and infusion reactions, all cause mortality and suicidality)<br>Incidence and severity of infections<br>Change from baseline and number of subjects outside the normal range for blood pressure, heart rate, and temperature<br>Change from baseline and number of subjects outside the normal range for clinical chemistry and haematology parameters, with particular attention to white blood cell count and immunoglobulin levels |
| **Secondary** | |
| To further assess the pharmacodynamic effect of belimumab in addition to standard of care immunosuppressants in renal transplant patients at 24 weeks | Percent change from baseline in memory B cells, Activated memory B cells, Transitional B cells |
| To assess the phenotype and tolerogenic profile of the repopulating B cells after belimumab therapy at Week 52. | |
| To further assess the potential for efficacy of belimumab in addition to standard of care immunosuppressants in reducing the incidence of renal allograft rejection using biomarker and clinical outcomes. | Activated T cells, regulatory T cells, and ratio of activated: regulatory T cells<br>All HLA-specific and donor HLA-specific antibody levels<br>Proportion of subjects with episodes of acute rejection<br>Serum creatinine<br>Estimated glomerular filtration rate (eGFR)<br>Immunosuppressant/corticosteroid use |
| **Exploratory** | |
| To further assess the potential for efficacy of belimumab in addition to standard of care immunosuppressants in reducing the incidence of renal allograft rejection using exploratory biomarkers. | Exploratory endpoints may include analyses of transcriptomic signatures, non-HLA antibody profiles, cytokine profiles and additional leukocyte subsets |
| **Other** | |
| To determine immunogenicity and pharmacokinetic profile of belimumab, and to characterize genetic variability that may affect efficacy or safety endpoints in renal transplant patients. | Incidence, titers, and specificity of anti-belimumab antibodies<br>Serum concentrations of belimumab<br>Characterize genetic variability (e.g., HLA typing) |

**Statistical methods**

There were no formal statistical hypotheses tested in this study. An estimation approach was used to investigate the magnitude of the difference in the selected primary and secondary endpoints following treatment with belimumab relative to placebo. Because the study included no prospectively defined formal hypothesis testing, no adjustment for multiplicity was required for the primary and secondary endpoints.

The primary and, where specified, secondary analyses utilised a mixed model for repeated measures (MMRM) approach with fixed categorical effects of treatment, visit, donor organ status (coded as live donor, donated after brain death, donated after circulatory death) and treatment-by-visit interaction and fixed continuous covariates of baseline values and baseline values-by-visit interaction. A compound symmetry variance structure was used to model the within-patient errors, shared across treatments.

All post hoc analyses are labelled as such. Analyses were performed using SAS version 9.3 except for transcriptomic and protein microarray analyses, which were performed using R version 3.3.1.

Enabling work in transplant patients (n=93 renal transplant recipients at the Cambridge Transplant Unit (unpublished data)) found that naive B cell counts at baseline in transplant patients were similar to SLE patients (Phase III BLISS-76 study[1]) after removing the top 5th percentile of SLE patients with highest baseline counts. By adjusting the SLE data in this way, and assuming transplant patients will vary in a similar way to SLE patients a standard deviation (SD) of 63.24 cells/$mm^3$ was observed. Assuming a sample size of 10 per group, and mean difference of -59 cells/$mm^3$ (observed in BLISS-76) we predicted a 95% confidence interval around the mean difference of (-114.43, -3.57).

Interim re-estimations of sample size were performed in November 2014 and February 2015 to take into account drop-outs and inform the potential benefit and requirement for further study enrolment. An unblinded statistician examined the variability in naive B-cells and compared to BLISS-76, looking for trends over time with subject profile plots. The observed treatment difference of the change from baseline in naïve B cells at Week 8 was used to make a predictive probability statement about the probability of achieving success at Week 24 for a particular total sample size. The predictive probability assessment suggested that "the benefit of recruiting an additional 10 evaluable subjects (30 evaluable overall) on the outcome of the study was negligible"

**Microarray analysis**

Leukocyte subsets were purified from whole blood then lysed as previously described [2]. Lysates (CD4+ T-cell) and PAXgene tubes (whole blood) were stored at -80°C until required. RNA was extracted from CD4+ T-cell lysates using an AllPrep Kit (Qiagen) and from whole blood using the PAXgene system (Qiagen). RNA was processed and hybridised to Human Gene ST 2.1 microarrays (Affymetrix) according to the manufacturer's instructions.

Affymetrix CEL files were imported into R/Bioconductor, normalised and summarised at the transcript cluster level using the oligo package (rma function, target = "core"). Transcript clusters were annotated using Ensembl biomaRt and manufacturer's own annotation and Affymetrix control probes were removed. Non-protein coding probes were also removed.

Weighted gene coexpression network analysis (WGCNA) was undertaken of the whole blood gene expression data using the WGCNA package in R/Bioconductor. One of the resulting whole blood gene expression modules was identified as representing a B-cell transcriptional programme on the basis of a unique overlap of module genes with the Gene Ontology class 'GO:0050853 BCR signalling pathway' (Supplementary Figure 1L). Module expression was determined as the value of the first principal component calculated from module gene expression, along standard analysis lines for WGCNA and using functions in the WGCNA package.

Differential gene expression analyses were performed using the limma package in R/Bioconductor. The model incorporated time-point and treatment group interaction terms and accounted for the repeated measures nature of the analysis (study participants contributed gene expression samples at three different timepoints) using the duplicateCorrelation function. Contrasts were defined for differential expression at baseline, 24 weeks and 52 weeks (Belimumab – Placebo at each timepoint). Estimates were adjusted using the eBayes function.

Where there was more than one transcript cluster per gene, differential expression was summarised into a single gene measure using the mean log-fold change. Immunoglobulin coding genes were identified from their Ensembl Biotype annotation. Cell cycle genes were identified using the Gene Ontology class 'GO:0007049 Cell cycle'.

**Table S2: Top 100 differentially expressed genes (by fold-change) in CD4+ T-cells comparing belimumab treated subjects and placebo at Week 24. P-values are unadjusted. Cell cycle column denotes whether a gene is annotated with GO:0007049 cell cycle in the Gene Ontology**

| | | Week 0 (Baseline) | | Week 24 | | Week 52 | | |
|---|---|---|---|---|---|---|---|---|
| **Affymetrix ID** | **Gene Symbol** | **log(2) FC** | **P-value** | **log(2) FC** | **P-value** | **log(2) FC** | **P-value** | **Cell cycle gene** |
| 16996813 | CD180 | 0.104 | 0.668 | -1.081 | 0.018 | 0.615 | 0.125 | |
| 16844312 | TOP2A | 0.049 | 0.733 | -1.032 | 0.028 | -0.194 | 0.539 | cell_cycle |
| 17016403 | HIST1H3G | -0.224 | 0.245 | -0.973 | 0.110 | -0.460 | 0.407 | |
| 16850477 | TYMS | -0.014 | 0.915 | -0.967 | 0.035 | -0.215 | 0.503 | cell_cycle |
| 16976644 | JCHAIN | 0.106 | 0.651 | -0.907 | 0.096 | 0.041 | 0.905 | |
| 16979515 | CCNA2 | -0.089 | 0.496 | -0.895 | 0.073 | -0.302 | 0.386 | cell_cycle |
| 16697471 | B3GALT2 | -0.332 | 0.283 | -0.882 | 0.036 | -0.445 | 0.225 | |
| 16977052 | CXCL10 | 0.679 | 0.012 | -0.882 | 0.225 | 1.433 | 0.034 | |
| 17019728 | PLA2G7 | 0.044 | 0.912 | -0.882 | 0.022 | 0.265 | 0.533 | |
| 16826230 | NETO2 | -0.037 | 0.730 | -0.850 | 0.001 | -0.252 | 0.333 | |
| 16877019 | RRM2 | 0.136 | 0.274 | -0.848 | 0.054 | -0.277 | 0.358 | cell_cycle |
| 17075776 | PBK | -0.011 | 0.918 | -0.845 | 0.003 | -0.159 | 0.416 | cell_cycle |
| 17101531 | TLR7 | 0.264 | 0.271 | -0.838 | 0.049 | 0.651 | 0.111 | |
| 16943181 | GPR15 | -0.595 | 0.074 | -0.827 | 0.024 | -0.629 | 0.086 | |
| 16912379 | TPX2 | 0.033 | 0.827 | -0.826 | 0.062 | -0.427 | 0.106 | cell_cycle |
| 16965268 | CD38 | -0.129 | 0.204 | -0.821 | 0.021 | 0.031 | 0.883 | |
| 16767335 | CPM | 0.045 | 0.796 | -0.813 | 0.011 | 0.199 | 0.496 | |
| 16980096 | TBC1D9 | 0.078 | 0.666 | -0.804 | 0.018 | 0.413 | 0.301 | |
| 16986913 | VCAN | 0.082 | 0.844 | -0.771 | 0.224 | 0.665 | 0.261 | |
| 16707468 | KIF11 | -0.003 | 0.985 | -0.771 | 0.036 | 0.012 | 0.957 | cell_cycle |
| 16944618 | CD86 | 0.221 | 0.356 | -0.770 | 0.100 | 0.194 | 0.647 | |
| 16725227 | MS4A14 | -0.199 | 0.424 | -0.770 | 0.017 | 0.340 | 0.376 | |
| 16968529 | PTPN13 | -0.257 | 0.188 | -0.765 | 0.016 | -0.339 | 0.133 | |
| 16851618 | HRH4 | -0.239 | 0.355 | -0.764 | 0.043 | -0.465 | 0.047 | |
| 16851397 | RBBP8 | 0.064 | 0.713 | -0.759 | 0.010 | 0.224 | 0.351 | cell_cycle |
| 16721835 | WEE1 | -0.049 | 0.768 | -0.758 | 0.011 | -0.447 | 0.062 | cell_cycle |
| 16801557 | CCNB2 | -0.116 | 0.379 | -0.757 | 0.056 | -0.341 | 0.311 | cell_cycle |
| 16677201 | DTL | -0.081 | 0.319 | -0.724 | 0.096 | -0.194 | 0.483 | cell_cycle |
| 16843627 | CCL3L3 | -0.163 | 0.261 | -0.714 | 0.093 | 0.200 | 0.460 | |
| 16719515 | MKI67 | -0.120 | 0.273 | -0.706 | 0.043 | -0.079 | 0.729 | cell_cycle |
| 16992744 | FAM153B | -0.732 | 0.002 | -0.704 | 0.012 | -0.089 | 0.704 | |
| 16707551 | CEP55 | 0.094 | 0.381 | -0.700 | 0.033 | -0.036 | 0.868 | cell_cycle |
| 16679349 | KMO | 0.290 | 0.203 | -0.699 | 0.078 | 0.366 | 0.368 | |
| 17004518 | LY86 | -0.117 | 0.600 | -0.696 | 0.054 | 0.351 | 0.345 | |
| 16696187 | F5 | -0.538 | 0.007 | -0.693 | 0.009 | -0.209 | 0.424 | |

| | | | | | | | | |
|---|---|---|---|---|---|---|---|---|
| 16875997 | ZNF154 | -0.719 | 0.001 | -0.693 | 0.003 | -0.357 | 0.105 | |
| 16725041 | FAM111B | -0.004 | 0.977 | -0.692 | 0.100 | -0.195 | 0.421 | |
| 16960577 | P2RY12 | 0.168 | 0.318 | -0.686 | 0.042 | 0.503 | 0.210 | |
| 16666509 | IFI44 | -0.065 | 0.809 | -0.685 | 0.034 | 0.611 | 0.027 | |
| 16666326 | ST6GALNAC3 | 0.157 | 0.225 | -0.684 | 0.001 | -0.099 | 0.723 | |
| 16852312 | SKA1 | -0.009 | 0.947 | -0.683 | 0.048 | -0.143 | 0.525 | cell_cycle |
| 16875467 | LILRA4 | -0.216 | 0.435 | -0.681 | 0.270 | -0.028 | 0.943 | |
| 16940172 | CCR2 | -0.315 | 0.127 | -0.677 | 0.007 | 0.196 | 0.508 | |
| 16826160 | SHCBP1 | 0.089 | 0.505 | -0.669 | 0.015 | 0.041 | 0.850 | |
| 16840245 | SCIMP | 0.186 | 0.427 | -0.664 | 0.090 | 0.197 | 0.617 | |
| 16665878 | IL23R | -0.554 | 0.066 | -0.652 | 0.066 | -0.503 | 0.070 | |
| 17070229 | ZC2HC1A | -0.096 | 0.638 | -0.650 | 0.003 | -0.059 | 0.718 | |
| 16928428 | GRK3 | 0.063 | 0.801 | -0.645 | 0.032 | 0.355 | 0.288 | |
| 16793225 | DLGAP5 | -0.121 | 0.191 | -0.645 | 0.100 | -0.297 | 0.230 | cell_cycle |
| 17094893 | ALDH1A1 | 0.253 | 0.378 | -0.644 | 0.168 | 0.686 | 0.228 | |
| 16747958 | CLEC6A | 0.468 | 0.221 | -0.641 | 0.188 | 1.090 | 0.040 | |
| 17050350 | LRRN3 | -0.313 | 0.202 | -0.640 | 0.089 | -0.594 | 0.132 | |
| 16886105 | HNMT | 0.128 | 0.533 | -0.636 | 0.091 | 0.540 | 0.161 | |
| 16663514 | CDC20 | -0.044 | 0.718 | -0.635 | 0.037 | -0.131 | 0.602 | cell_cycle |
| 16828886 | GINS2 | 0.067 | 0.703 | -0.624 | 0.094 | -0.153 | 0.491 | cell_cycle |
| 16949625 | CCDC50 | -0.094 | 0.626 | -0.621 | 0.051 | -0.011 | 0.973 | |
| 16777685 | FLT3 | 0.317 | 0.043 | -0.620 | 0.096 | 0.503 | 0.263 | |
| 16789334 | TDRD9 | -0.292 | 0.288 | -0.617 | 0.141 | 0.012 | 0.975 | cell_cycle |
| 16677425 | CENPF | -0.147 | 0.200 | -0.613 | 0.003 | -0.148 | 0.331 | cell_cycle |
| 16671139 | S100A9 | 0.340 | 0.334 | 0.609 | 0.331 | 0.705 | 0.165 | |
| 16813206 | ANPEP | 0.202 | 0.499 | 0.609 | 0.254 | 0.603 | 0.285 | |
| 16940444 | CAMP | 0.044 | 0.711 | 0.612 | 0.013 | 0.242 | 0.301 | |
| 16743816 | PDGFD | 0.386 | 0.145 | 0.619 | 0.015 | 0.002 | 0.996 | |
| 16872978 | CD177 | 0.035 | 0.824 | 0.624 | 0.491 | 0.853 | 0.079 | |
| 16660360 | CDA | 0.348 | 0.198 | 0.636 | 0.267 | 0.473 | 0.371 | |
| 16983451 | BASP1 | 0.144 | 0.473 | 0.636 | 0.314 | 0.646 | 0.205 | |
| 16672462 | FCRL6 | 0.621 | 0.139 | 0.640 | 0.137 | 0.047 | 0.927 | |
| 16784760 | DACT1 | 0.371 | 0.320 | 0.645 | 0.111 | 0.407 | 0.272 | |
| 16865540 | FCAR | 0.269 | 0.133 | 0.677 | 0.309 | 0.796 | 0.077 | |
| 17012582 | ARG1 | 0.063 | 0.628 | 0.681 | 0.235 | 0.374 | 0.206 | |
| 16933766 | OSM | 0.271 | 0.086 | 0.689 | 0.014 | 0.150 | 0.450 | |
| 17052550 | MGAM2 | 0.109 | 0.393 | 0.701 | 0.007 | 0.059 | 0.743 | |
| 16947173 | MME | 0.335 | 0.184 | 0.721 | 0.186 | 0.023 | 0.958 | |
| 16761617 | MANSC1 | 0.076 | 0.576 | 0.723 | 0.056 | 0.275 | 0.448 | |
| 16819563 | ADGRG3 | 0.314 | 0.093 | 0.728 | 0.265 | 0.442 | 0.358 | |
| 16686040 | SVBP | 0.697 | 0.004 | 0.740 | 0.009 | 0.663 | 0.011 | |
| 16695715 | FCGR3B | 0.386 | 0.083 | 0.743 | 0.105 | 0.613 | 0.185 | |
| 16747969 | CLEC4D | 0.378 | 0.055 | 0.744 | 0.324 | 1.162 | 0.052 | |
| 17101698 | BMX | 0.166 | 0.050 | 0.745 | 0.180 | 0.498 | 0.124 | |
| 16792859 | PYGL | 0.266 | 0.234 | 0.757 | 0.191 | 0.674 | 0.161 | |
| 16660436 | ALPL | 0.375 | 0.026 | 0.758 | 0.215 | 0.234 | 0.567 | |

| | | | | | | | |
|---|---|---|---|---|---|---|---|
| 16660059 | PADI4 | 0.310 | 0.169 | 0.767 | 0.248 | 0.585 | 0.204 |
| 16820937 | HP | -0.034 | 0.860 | 0.795 | 0.401 | 1.116 | 0.100 |
| 16681278 | UTS2 | 0.729 | 0.062 | 0.805 | 0.097 | 0.668 | 0.146 |
| 16922759 | KCNJ15 | 0.376 | 0.090 | 0.823 | 0.124 | 0.607 | 0.279 |
| 16998551 | SLCO4C1 | 0.757 | 0.085 | 0.844 | 0.217 | 0.962 | 0.137 |
| 17052425 | MGAM | 0.549 | 0.044 | 0.850 | 0.275 | 0.633 | 0.328 |
| 16974529 | FGFBP2 | 0.984 | 0.079 | 0.906 | 0.156 | -0.129 | 0.847 |
| 16743686 | MMP8 | -0.086 | 0.809 | 0.914 | 0.398 | 1.323 | 0.068 |
| 16968213 | ANXA3 | 0.129 | 0.530 | 0.932 | 0.235 | 0.853 | 0.130 |
| 16873501 | PGLYRP1 | 0.187 | 0.181 | 0.947 | 0.140 | 0.649 | 0.173 |
| 16919547 | SLPI | 0.070 | 0.525 | 0.983 | 0.145 | 0.340 | 0.482 |
| 16956213 | PROK2 | 0.376 | 0.254 | 0.984 | 0.109 | 0.330 | 0.553 |
| 17019877 | CRISP3 | 0.174 | 0.421 | 0.999 | 0.352 | 0.896 | 0.120 |
| 16849400 | SOCS3 | 0.314 | 0.320 | 1.022 | 0.005 | 0.485 | 0.173 |
| 17099463 | ABO | 0.680 | 0.225 | 1.030 | 0.101 | 0.410 | 0.454 |
| 16697370 | PTGS2 | 0.384 | 0.332 | 1.041 | 0.153 | 0.361 | 0.590 |
| 16914395 | MMP9 | 0.366 | 0.062 | 1.539 | 0.098 | 0.786 | 0.232 |
| 17017885 | HLA-DRB5 | 1.863 | 0.125 | 1.548 | 0.181 | 1.218 | 0.320 |
| 17017900 | HLA-DRB1 | 1.566 | 0.192 | 1.706 | 0.151 | 1.534 | 0.224 |

**ProtoArray (Invitrogen) protein microarrays**

Serum samples were stored at -80°C until required. ProtoArray Human Protein Microarray 5.1 slides were blocked in blocking buffer (50 mM HEPES, 200 mM NaCl, 0.01% Triton X-100, 25% glycerol, 20 mM reduced glutathione, 1.0 mM DTT, 1X Synthetic Block) at 4 °C for 1 hour. After blocking, arrays were rinsed once with freshly prepared PBST buffer (1X PBS, 0.1% Tween 20, and 1 X Synthetic Block). Arrays were then probed with a 1:500 dilution of each sample diluted in 5 mL of PBST buffer. Arrays were incubated for 90 minutes at 4°C in QuadriPERM 4-well trays (Greiner) with gentle agitation. After incubation, slides were washed five times (5 minutes per wash) in 5 ml PBST Buffer in 4-well trays. An Alexa Fluor®647-conjugated goat anti-human IgG antibody diluted in 5 ml PBST buffer to a 1.0 µg/ml final concentration was added to each array and allowed to incubate with gentle shaking at 4°C for 90 minutes. After incubation, the secondary antibody was removed, and arrays were washed as described above. Arrays were dried by spinning in a table top centrifuge equipped with a plate rotor at 200x gravity for 2 minutes. Arrays were then scanned using a Tecan PowerScanner™ fluorescent microarray scanner.

GenePix 7 software was used to overlay the mapping of human proteins in the array list file to each array image with a fixed feature size of 130 µm (diameter). After aligning each of the 48 subarrays using spots from the AlexaFluor®-conjugated and murine antibodies printed in each subarray, the features were resized by the GenePix software to best fit the feature. Pixel intensities for each spot on the array were determined. Arrays were normalised and a signal for each spot on the array calculated by subtracting the local background signal. Microarray hybridisation and these initial processing steps were performed by ThermoFisher.

After removing data from control group spots and TNFSF13B (as bound by belimumab) the signal from duplicate spots was combined (mean) to give one value per unique antigen. This dataset was used to define a global threshold for 'significant' antibody binding (10,750) by maximising the signal-to-noise ratio for the comparison of number of antigen with a signal above threshold in samples at baseline (no immunosuppression) versus Week 24 (maximal immunosuppression). This approach avoided defining a threshold based on the parameter of interest (treatment group), relying on the biologically plausible hypothesis that there would be differences in circulating auto-/allo-antibody pre- and post-transplant.

This threshold was used to determine whether an individual antigen specificity had significant antibody binding (yes/no). New antigenic specificities post-transplant were defined as antigenic specificities with significant binding at Week 24 post-transplant not observed at baseline (Week 0). Kidney specific antigens were defined as those identified as such in [3] (Table S2).

**Immunophenotyping**

Immunophenotyping was performed by flow cytometry with absolute cell numbers calculated using TBNK counts.

**Healthy control B cell stimulation assay**

CD19+CD27+ memory B cells were enriched from PBMCs of 16 healthy donors using a human memory B cell isolation kit (Miltenyi Biotec) and cultured in vitro in the presence of CpG (100nM; Hycult Biotech) and CD40L (1µg/ml; R&D Systems) with 0 to 200ng/ml BLyS (GSK) for 48 hours. Phorbol 12-myristate 13-acetate (PMA) (50ng/ml; Sigma-Aldrich), ionomycin (500ng/ml; Sigma-Aldrich) and brefeldin A (5µg/ml; BioLegend) were added for the last 5 hours of culture and IL-6 and IL-10 quantified by flow cytometry. In 7 of these healthy donors, 15nM belimumab (GSK) was added in addition to 100ng/ml BLyS.

**Subject with retrospective flow positive crossmatch**

A single subject (subject 5) in the belimumab treatment group was found to have a positive flow cytometry cross-match with donor specific antibodies to DP1 and DP6 at baseline. This subject was receiving a second transplant and known to be sensitized against multiple HLA DP antigens. The HLA DP type of the donor was not known at the time of transplantation, and T and B lymphocyte CDC cross-match tests were negative. Both the donor DP type and flow cytometry cross-match result became available following transplantation. Had this information been available the subject would have been deemed ineligible for the study and given lymphocyte depleting induction therapy in view of his increased immunological risk. This subject experienced Banff IIA acute cellular rejection with features suspicious for early humoral rejection (day 6) associated with a rise in the titre of DP DSA and development of *de novo* DSA to HLA-A11 and HLA-B18. A further biopsy (day 34) demonstrated overt antibody mediated rejection. They were withdrawn from the study following a single dose of belimumab and the rejection responded to treatment with methlyprednisolone, plasma exchange and anti-thymocyte globulin.

**Donor specific and anti-MICA antibodies**

Two patients recruited to the study developed *de novo* DSA during follow-up; neither were part of the PP population having been withdrawn following a single dose of study drug (belimumab). Subject 5 was withdrawn due to a positive cross-match; subject 13 withdrew consent for study drug (Fig. S2C).

One patient in each group had positive anti-MICA antibodies at baseline; subject 19 received one dose of placebo and had positive levels throughout the first year post transplant; subject 27 received 5 doses of belimumab and antibody levels fell below the positive threshold. Subject 13 received a single dose of belimumab and developed *de novo* anti-MIC antibodies in addition to low level *de novo* DSA.

**Subject with adoptive transfer of donor HLA specific allosensitization**

Subject 21 had no HLA antibodies detectable at baseline but received a kidney from a sensitised donor. Post-transplant, high levels de novo IgG HLA class I- and class II-specific antibodies were measurable with no antibodies to donor HLA. A similar antibody profile was found in the recipient of the paired deceased donor kidney (not part of this study) and in stored donor serum[4].

**Figure S1: Belimumab Pharmacokinetics and Impact on Peripheral B and T Cell Subsets**

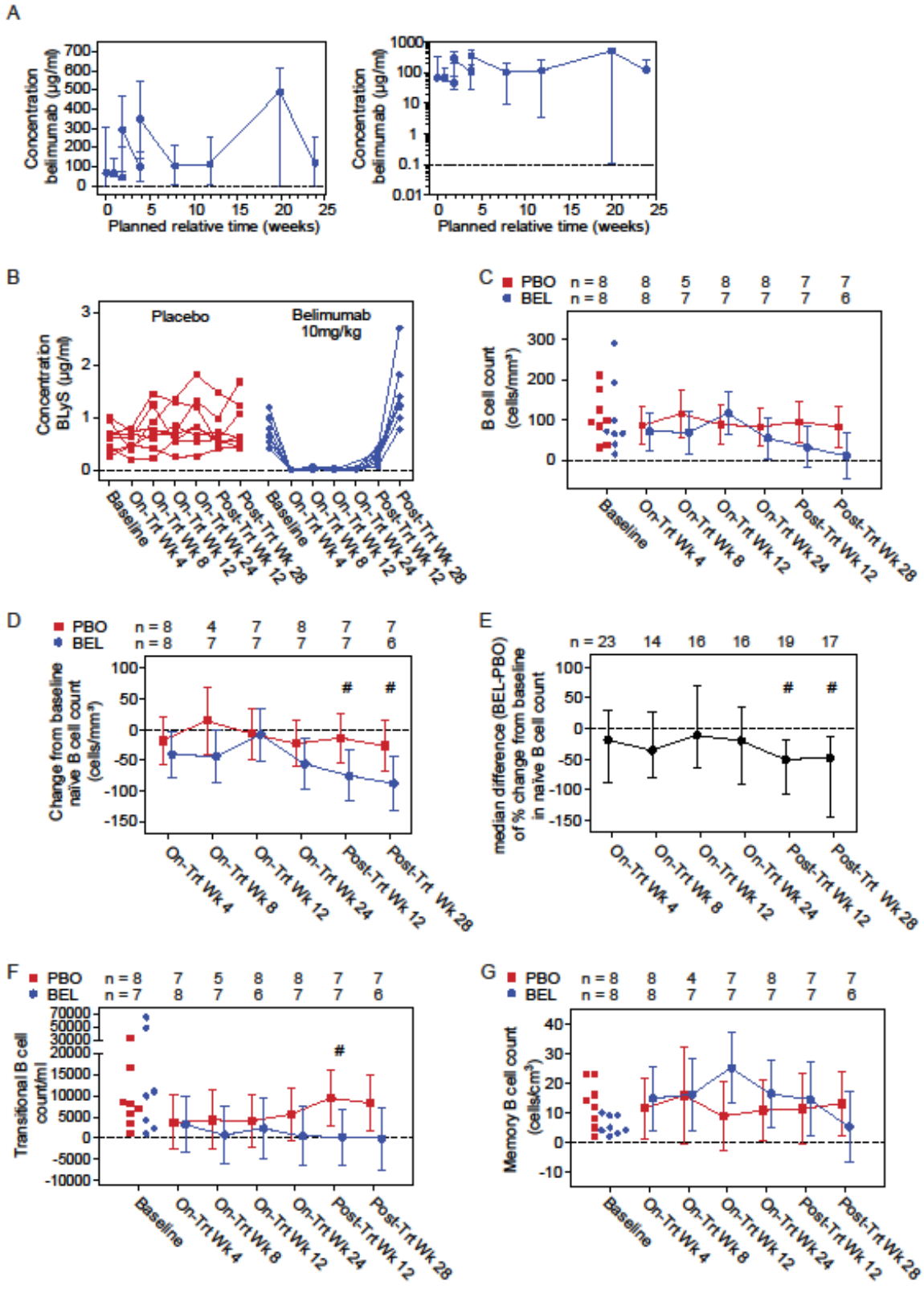

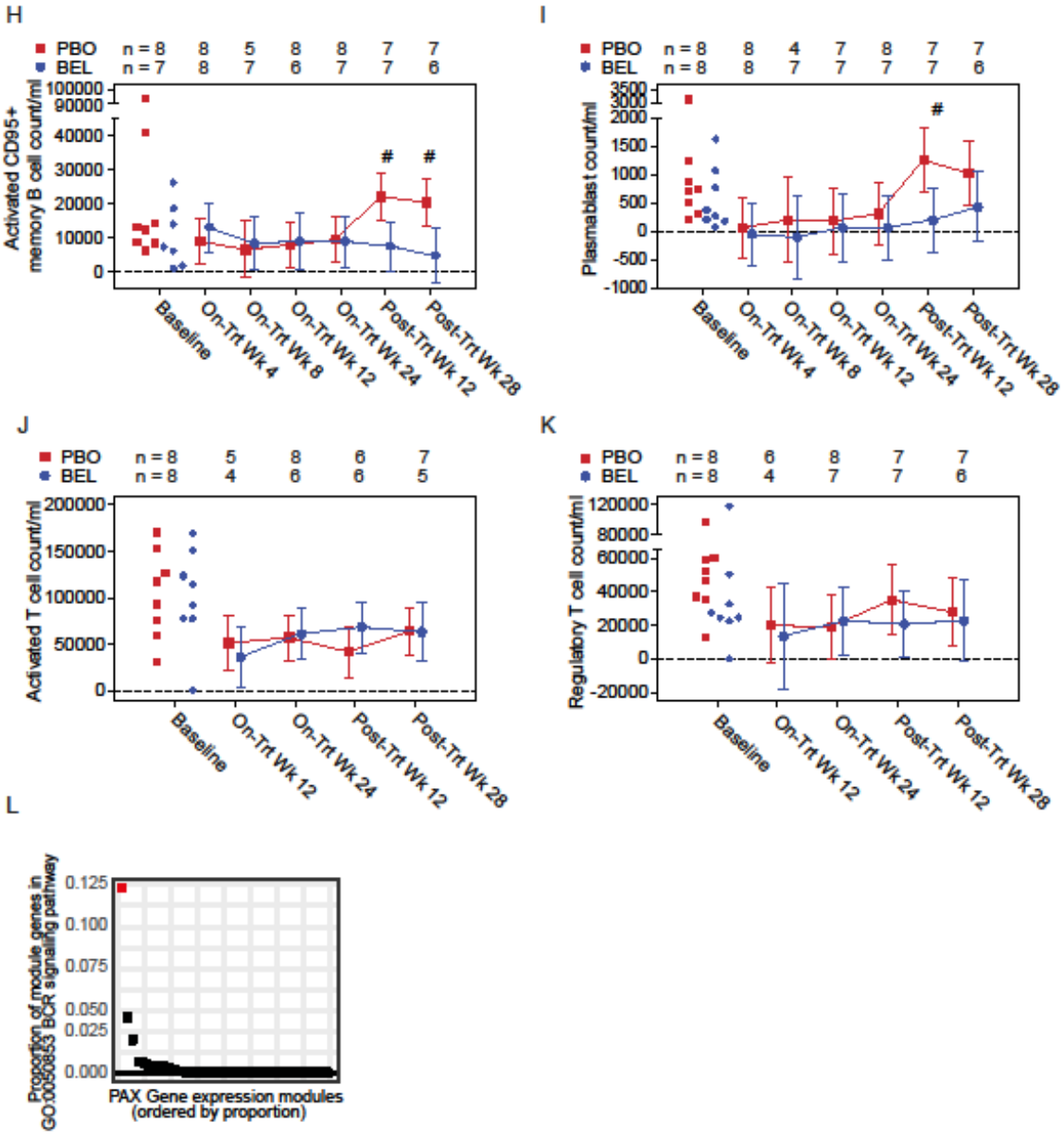


Panel A shows the median serum concentration of belimumab over time (left panel linear scale; right panel logarithmic scale). The lower limit of detection of 100ng/ml is marked with a dotted line. Error bars indicate range. Pharmacokinetics (PK) population that consisted of all subjects randomised to belimumab treatment that were treated with at least one dose and had a PK sample that was analysed (N=12).

Panel B shows serial measurements of serum BLyS concentration (µg/ml) in individual subjects.

Panel C shows B cell count (cells/mm$^3$).

Panel D shows the adjusted mean (95% CI) change from baseline in naïve (CD20+CD27-) B cell count, by visit and treatment in the PP population.

Panel E shows the Hodges Lehman estimates and 95% CI for median difference (belimumab 10mg/kg (BEL) – placebo (PBO)) of percent change from baseline in naïve B-cell (CD20+CD27-) count by visit in the MITT population (sensitivity analysis of primary endpoint).

Panel F shows transitional ($CD24^{br}CD38^{br}IgD^{+}$) B cell count/ml.

Panel G shows memory ($CD20^{+}CD27^{+}$) B cell count (cells/$cm^3$).

Panel H shows activated memory ($CD95^{+}CD27^{+}$) B cell count (cells/ml) by visit and treatment group.

Panel I shows plasmablast ($CD19^{+}CD27^{+}CD38^{+}$) count/ml.

Panel J shows activated T cell ($CD4^{+}CD25^{hi}CD45RA^{-}$IL $7R^{hi}$) count/ml

Panel K shows regulatory T cell ($CD4^{+}CD25^{hi}$IL-$7R^{lo}$) count/ml

B-D and F-K performed on PP population. E performed on MITT population. C and F-K show raw values at baseline for comparison and adjusted mean estimate with 95% confidence intervals, obtained from the same MMRM model as used for the primary endpoint, at subsequent timepoints. # indicates that the 95% confidence interval of the treatment difference does not include zero. In J and K weeks 4 and 8 excluded due to known effects of basiliximab on CD25 surface expression. C, G and I represent analyses performed *post hoc.* Where n numbers are displayed, these represent the number of subjects assayed at each timepoint.

Panel L shows the proportion of module genes within each module identified during weighted correlation network analysis of whole blood RNA in the GO:0050853 BCR signalling pathway. A single module (coloured red) was enriched for BCR signalling and analysed further for the effects of belimumab treatment. Analysis performed on MITT population at baseline and PP thereafter.

**Figure S2: HLA and Non-HLA Antibodies**

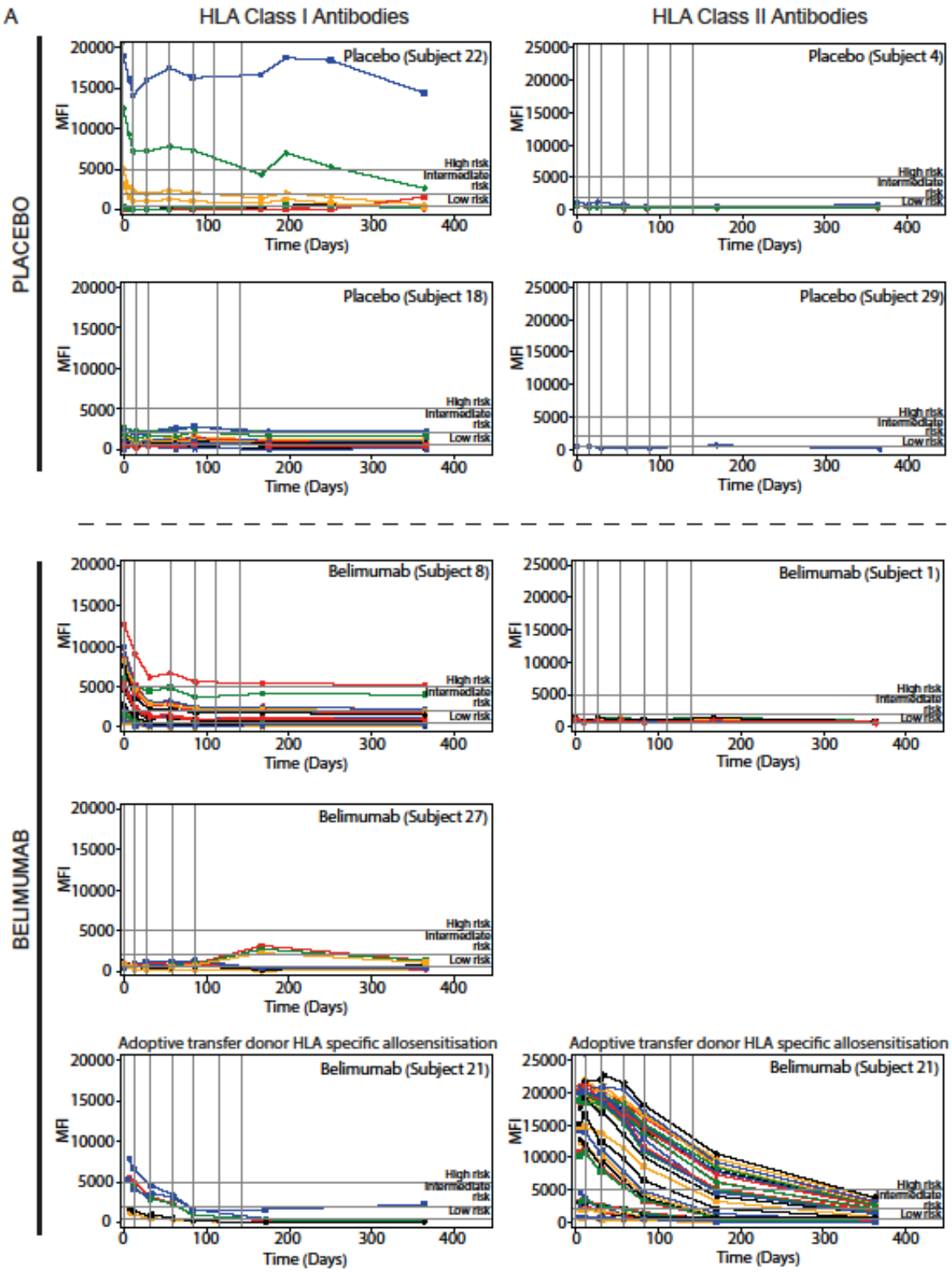

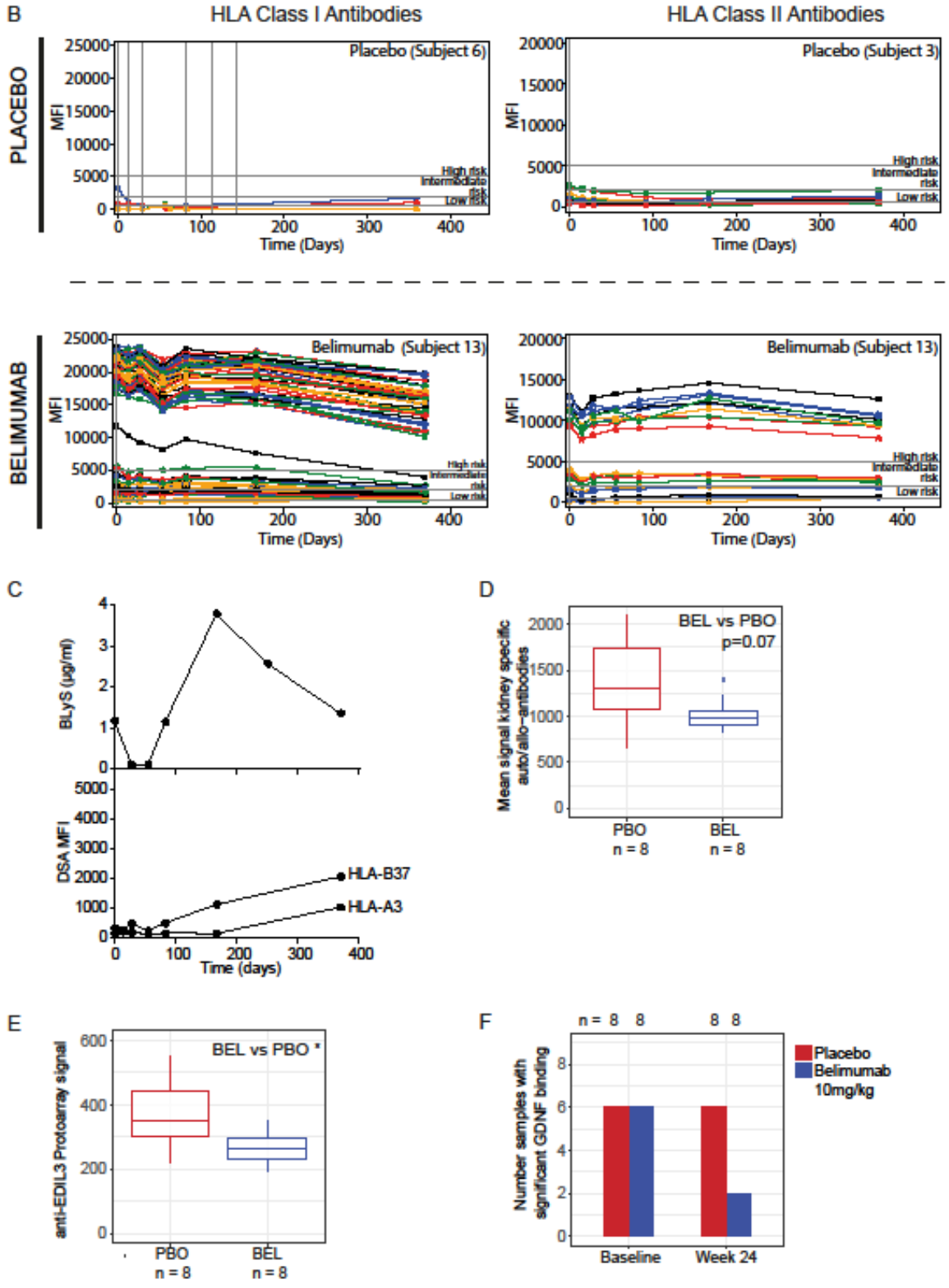


Serum samples before and after treatment were screened for HLA antibodies using Luminex HLA class I and class II antibody detection beads (LABScreen™ Mixed, One Lambda) and HLA antibody specificities were determined using Luminex single antigen HLA-specific antibody detection beads (LABScreen Single Antigen HLA Class I and Class II, One Lambda). The normalized mean fluorescence intensity (MFI) for each single antigen bead with an MFI above the detection limit of 500 at any timepoint is shown in individuals from the PP population (A) and those not in the PP population (B). Vertical lines show when doses of study drug were received. Subject 6 received plasma exchange for FSGS between days 31 and 64. Subjects 3 and 13 withdrew

consent for study drug following a single dose. Adoptive transfer donor HLA specific allosensitization as described in [4].

Panel C shows the relationship between serum BLyS and *de novo* donor-specific HLA antibody over time for subject 13 who received a single dose of belimumab on day 0 prior to withdrawal of consent for study drug. Serum was sampled for BLyS levels at Day 0, week (W) 4, W8, W16, W24, W36 and W52. The first increase in serum BLyS was detected at W24, with a fall in levels thereafter to baseline by W52. Antibodies were measured using Luminex single antigen HLA-specific antibody detection beads (LABScreen Single Antigen HLA Class I and Class II, One Lambda); donor specificity was determined manually by comparison of donor and recipient HLA-types. A low MFI MHC class I B37 antibody became detectable at W24, and a further A3 antibody at W52, the latter in the context of a falling serum BLyS level.

Panel D shows the mean protoarray signal from kidney specific antigens (defined in [3]) at week 24. Horizontal lines on boxplot correspond to median and interquartile ranges. Patients are coloured by treatment group. The Wilcoxon rank-sum test was used to compare the belimumab treatment group (BEL) and placebo treatment group (PBO); exact p value displayed.

Panel E shows the distribution of the mean protoarray signal from two antigens on the array annotated to EGF-like repeats and discoidin I-like domains 3 (EDIL3) (BC053656.1; BC030828.1) by treatment group at week 24. Horizontal lines on boxplot correspond to median and interquartile ranges. PP population. The Wilcoxon rank-sum test was used to compare the belimumab and placebo treatment groups; * denotes $p<0.05$.

Panel F shows the number of subjects in each treatment group with above threshold protoarray binding to glial cell-derived neurotrophic factor (GDNF) at baseline and week 24. PP population; Eight subjects were tested at each timepoint for both treatment groups.

D, E and F represent *post hoc* analyses. Where n numbers are displayed, these represent the number of subjects assayed at each timepoint.

**Table S3: Concomitant maintenance immunosuppression (*post hoc* analysis).**
1. In addition, for treatment of rejection (week 2), one subject in the placebo group received 500mg x 3 pulsed iv methylprednisolone and one subject in the belimumab group received 1000mg x 3 pulsed iv methylprednisolone.
2. One subject in the placebo arm switched to mycophenolate sodium (Myfortic) at week 52; one subject in the belimumab group switched at week 4. mycophenolate sodium 720mg approximately equivalent to mycophenolate mofetil 1g. One subject in the belimumab group was on azathioprine 50mg on day 231 through to week 52, having stopped MMF on day 120.

| | Placebo (N=8) | | | Belimumab 10mg/kg (N=8) | | |
|---|---|---|---|---|---|---|
| | n | Mean (SD) | Median(Range) | n | Mean (SD) | Median (Range) |
| Daily prednisolone dose (mg)[1] | | | | | | |
| week 1 | 8 | 20.0 (0.0) | 20.0 (20.0-20.0) | 8 | 20.0 (0.0) | 20.0 (20.0-20.0) |
| week 4 | 8 | 8.8 (3.3) | 8.8 (5.0 -15.0) | 8 | 8.4 (2.3) | 10.0 (5.0-10.0) |
| week 12 | 8 | 5.0 (1.3) | 5.0 (2.5-7.5) | 8 | 4.7 (0.9) | 5.0 (2.5-5.0) |
| week 24 | 8 | 5.3 (2.1) | 5.0 (2.5-10.0) | 8 | 6.9 (5.8) | 5.0 (2.5-20.0) |
| week 52 | 8 | 4.3 (1.8) | 5.0 (0.0-5.0) | 8 | 4.7 (1.6) | 5.0 (2.5-7.5) |
| Tacrolimus daily dose (mg) | | | | | | |
| week 1 | 8 | 10.3 (3.1) | 8.5 (8-15) | 7 | 7.8 (4.6) | 6.5 (0-13) |
| week 4 | 8 | 12.1 (5.8) | 11.5 (5-24) | 8 | 9.6 (3.7) | 11.5 (4-14) |
| week 12 | 8 | 9.6 (6.3) | 9.0 (4-24) | 8 | 8.3 (4.0) | 8.0 (3-15) |
| week 24 | 8 | 7.5 (3.9) | 6.5 (4-16) | 8 | 7.1 (4.1) | 7.0 (3-15) |
| week 52 | 8 | 6.1 (1.5) | 6.0 (4-8) | 8 | 6.1 (2.9) | 7.0 (2.5-10) |
| Tacrolimus level (µg/L) | | | | | | |
| week 1 | 8 | 5.6 (2.8) | 4.4 (2.8-10.5) | 8 | 7.3 (1.8) | 6.9 (4.9-10.8) |
| week 4 | 7 | 10.7 (5.8) | 9.3 (4.5 - 22.8) | 7 | 8.3 (2.4) | 8.7 (3.3-10.3) |

| | | | | | | |
|---|---|---|---|---|---|---|
| week 12 | 8 | 7.9 (2.1) | 8.5 (3.7 - 10.5) | 7 | 8.6 (2.1) | 7.4 (6.2-11.6) |
| week 24 | 7 | 6.6 (1.0) | 7.0 (4.5 - 7.6) | 6 | 8.4 (3.5) | 8.5 (3.5 - 13.0) |
| week 52 | 5 | 4.8 (3.0) | 6.0 (0.0 - 7.4) | 8 | 6.1 (1.8) | 5.9 (3.7 - 9.4) |
| MMF equivalent dose (mg)[2] | | | | | | |
| week 1 | 8 | 937.5 (176.8) | 1000 (500-1000) | 8 | 1062.5 (176.8) | 1000 (1000-1500) |
| week 4 | 8 | 1062.5 (176.8) | 1000 (1000-1500) | 8 | 1062.5 (267.3) | 1000 (500-1500) |
| week 12 | 8 | 812.5 (530.3) | 1000 (0-1500) | 8 | 875 (517.5) | 1000 (0-1500) |
| week 24 | 8 | 750 (534.5) | 1000 (0-1500) | 8 | 687.5 (530.3) | 750 (0-1500) |
| week 52 | 8 | 625 (443.2) | 750 (0-1000) | 8 | 687.5 (530.3) | 750 (0-1000) |

**Table S4: Analysis for change from baseline in naïve B cell count by visit (MITT and PP populations).**

1. Adjusted Mean Differences(treatment-placebo) and 95% confidence intervals for differences are obtained from MMRM model, with fixed categorical effects of treatment, visit, donor type and treatment-by-visit interaction and fixed continuous covariates of baseline and baseline-by-visit interaction. A compound symmetry variance structure was used to model the within-patient errors, shared across treatments. Naïve B cell count = CD20+CD27- cells/mm$^3$. This data is represented visually in Figure 2A (MITT population) and Figure S1D (PP population)

**MITT Population: Unadjusted baseline values naïve B cell count (cells/mm$^3$)**

| Treatment | Visit | N | n | Mean | SD | Median | Min | Max |
|---|---|---|---|---|---|---|---|---|
| Placebo | Baseline | 13 | 13 | 97.5 | 58.22 | 84 | 25 | 196 |
| Belimumab 10mg/kg | Baseline | 12 | 12 | 119.2 | 104.87 | 78.5 | 11 | 357 |

**MITT Population: Change from baseline in naïve B cell count by visit**

| Treatment | Visit | N | n | Adjusted mean (SE) | 95% CI of adjusted mean | Adjusted mean difference (SE)[1] | 95% CI of difference |
|---|---|---|---|---|---|---|---|
| Placebo | On-Trt Wk4 | 13 | 12 | 29.0 (23.65) | (-19.2, 77.2) | | |
| Belimumab 10mg/kg | | 12 | 11 | -11.7 (24.24) | (-61.0, 37.7) | -40.7 (33.79) | (-109.5, 28.1) |
| Placebo | On-Trt Wk8 | 13 | 6 | 35.0 (29.14) | (-23.4, 93.4) | | |
| Belimumab 10mg/kg | | 12 | 8 | -16.5(27.35) | (-71.5, 38.6) | -51.5 (40.58) | (-132.9, 29.9) |
| Placebo | On-Trt Wk12 | 13 | 8 | 19.4 (26.54) | (-34.1, 72.8) | | |
| Belimumab 10mg/kg | | 12 | 8 | 3.1 (27.31) | (-51.9, 58.0) | -16.3 (38.45) | (-93.6, 61.0) |
| Placebo | On-Trt Wk24 | 13 | 9 | 4.0 (25.55) | (-47.7, 55.6) | | |
| Belimumab 10mg/kg | | 12 | 7 | -30.4 (27.50) | (-85.8, 24.9) | -34.4 (37.24) | (-109.5, 40.7) |
| Placebo | Post-Trt Wk12 | 13 | 11 | 0.8 (24.11) | (-48.3, 49.8) | | |
| Belimumab 10mg/kg | | 12 | 8 | -58.0 (26.52) | (-111.5, -4.5) | -58.7 (35.72) | (-131.0, 13.6) |
| Placebo | Post-Trt Wk28 | 13 | 10 | 5.4 (24.67) | (-44.6, 55.5) | | |
| Belimumab 10mg/kg | | 12 | 7 | -53.8 (27.83) | (-109.7, 2.1) | -59.3 (37.12) | (-134.1, 15.6) |

**PP Population: Unadjusted baseline values naïve B cell count (cells/mm$^3$)**

| Treatment | Visit | N | n | Mean | SD | Median | Min | Max |
|---|---|---|---|---|---|---|---|---|
| Placebo | Baseline | 8 | 8 | 91.9 | 56.26 | 79.5 | 25 | 184 |
| Belimumab 10mg/kg | Baseline | 8 | 8 | 96.1 | 87.55 | 61.0 | 11 | 274 |

**PP Population: Change from baseline in naïve B cell count by visit**

| Treatment | Visit | N | n | Adjusted mean (SE) | 95% CI of adjusted mean | Adjusted mean difference (SE)[1] | 95% CI of difference |
|---|---|---|---|---|---|---|---|
| Placebo | On-Trt Wk4 | 8 | 8 | -18.4 (19.11) | (-56.6, 19.9) | | |
| Belimumab 10mg/kg | | 8 | 8 | -40.5 (19.02) | (-78.6, -2.5) | -22.2 (26.75) | (-75.7, 31.4) |
| Placebo | On-Trt Wk8 | 8 | 4 | 14.2 (27.38) | (-40.5, 68.9) | | |
| Belimumab 10mg/kg | | 8 | 7 | -44.3 (21.66) | (-87.6, -0.9) | -58.5 (35.75) | (-129.9, 13.0) |
| Placebo | On-Trt Wk12 | 8 | 7 | -7.1 (20.44) | (-48.0, 33.8) | -0.9 (29.93) | (-60.7, 59.0) |

| | | | | | | | |
|---|---|---|---|---|---|---|---|
| Belimumab 10mg/kg | | 8 | 7 | -8.0 (21.53) | (-51.1, 35.1) | | |
| Placebo | On-Trt Wk24 | 8 | 8 | -22.9 (19.11) | (-61.1, 15.4) | | |
| Belimumab 10mg/kg | | 8 | 7 | -56.2 (20.47) | (-97.1, -15.2) | -33.3 (27.64) | (-88.6, 22.0) |
| Placebo | Post-Trt Wk12 | 8 | 7 | -14.0 (20.44) | (-55.0, 26.9) | | |
| Belimumab 10mg/kg | | 8 | 7 | -75.3 (20.44) | (-116.2, -34.4) | -61.2 (29.08) | (-119.4, -3.0) |
| Placebo | Post-Trt Wk28 | 8 | 7 | -26.7 (20.37) | (-67.4, 14.1) | | |
| Belimumab 10mg/kg | | 8 | 6 | -88.3 (22.82) | (-133.9, -42.7) | -61.6 (30.49) | (-122.6, -0.7) |

**Table S5: Non-parametric analysis of percent change from baseline in naïve B cell count.**

1. Median difference and 95% CI of difference obtained using the Hodges-Lehman method. Naïve B cell count = CD20+CD27- cells/mm$^3$. This data is represented visually in Figure S1E.

**MITT population**

| Comparison | N | Visit | n | Median difference % change from baseline naïve B cell count[1] | 95% CI of median difference |
|---|---|---|---|---|---|
| Belimumab 10mg/kg vs placebo | 25 | On-Trt Wk4 | 23 | -18.7 | (-88.8, 30.8) |
| | | On-Trt Wk8 | 14 | -36.1 | (-81.4, 27.2) |
| | | On-Trt Wk12 | 16 | -11.5 | (-65.5, 70.1) |
| | | On-Trt Wk24 | 16 | -20.1 | (-90.9, 34.5) |
| | | Post-Trt Wk12 | 19 | -50.4 | (-107.0, -18.0) |
| | | Post-Trt Wk28 | 17 | -48.3 | (-144.7, -13.0) |

**Table S6: B cell populations at week 24 expressed as percentage of total B-cells (*post hoc* analysis).** Median difference from baseline to week 24 (percentage at week 24 – percentage at week 0) in the labelled B cell populations by treatment group with each population expressed as a percentage of B cells. This data is represented visually in Figure 2B.

| | Placebo (N=8) | | | | Belimumab 10mg/kg (N=8) | | | |
|---|---|---|---|---|---|---|---|---|
| Subset | n | Median difference (%) | IQR | Range | n | Median difference (%) | IQR | Range |
| Naïve | 8 | 9.277 | (4.036, 10.503) | (-65.407, 12.67) | 8 | -36.231 | (-50.492, -29.662) | (-69.66, 52.963) |
| Memory | 8 | -9.451 | (-12.14, -6.752) | (-12.912, -2.497) | 8 | 26.284 | (12.117, 40.853) | (-58.19, 48.231) |
| Non switched memory | 8 | 1.081 | (-0.53, 2.602) | (-1.709, 72.622) | 8 | 10.953 | (8.632, 17.545) | (5.227, 21.429) |
| Switched memory | 8 | -5.518 | (-7.392, -4.074) | (-9.417, -2.113) | 8 | 20.653 | (13.785, 34.642) | (-57.145, 49.29) |
| DN memory | 8 | -3.598 | (-5.195, -0.386) | (-8.947, 2.285) | 8 | 0.883 | (-1.082, 6.538) | (-2.566, 9.761) |

**Table S7: Analysis of memory B cell (%CD19) by visit.**

1. Adjusted mean differences (treatment-placebo) and 95% confidence intervals for differences obtained from MMRM model, with fixed categorical effects of treatment, visit, donor type and treatment-by-visit interaction and fixed continuous covariates of baseline and baseline-by-visit interaction. A compound symmetry variance structure was used to model the within-patient errors, shared across treatments. This data is represented visually in Figure 2C.

**PP Population: Unadjusted baseline values**

| Treatment | Visit | N | n | Mean | SD | Median | Min | Max |
|---|---|---|---|---|---|---|---|---|
| Placebo | Baseline | 8 | 8 | 12.1 | 4.32 | 12.5 | 6 | 17 |
| Belimumab 10mg/kg | Baseline | 8 | 8 | 8.3 | 6.84 | 4.5 | 3 | 22 |

**PP Population: Change from baseline in memory B cell count by visit**

| Treatment | Visit | N | n | Adjusted mean (SE) | 95% CI of adjusted mean | Adjusted mean difference (SE)[1] | 95% CI of difference |
|---|---|---|---|---|---|---|---|
| Placebo | On-Trt Wk4 | 8 | 8 | 10.3 (3.13) | (3.8, 16.9) | | |
| Belimumab 10mg/kg | | 8 | 8 | 31.0 (3.25) | (24.2, 37.8) | 20.7 (4.62) | (11.0, 30.3) |
| Placebo | On-Trt Wk8 | 8 | 4 | 12.2 (3.68) | (4.8, 19.7) | | |
| Belimumab 10mg/kg | | 8 | 8 | 30.4 (3.25) | (23.5, 37.2) | 18.1 (5.00) | (7.8, 28.4) |
| Placebo | On-Trt Wk12 | 8 | 7 | 8.6 (3.20) | (2.0, 15.2) | | |
| Belimumab 10mg/kg | | 8 | 7 | 28.9 (3.31) | (22.0, 35.8) | 20.3 (4.67) | (10.6, 30.0) |
| Placebo | On-Trt Wk24 | 8 | 8 | 9.6 (3.13) | (3.1, 16.1) | | |
| Belimumab 10mg/kg | | 8 | 7 | 32.6 (3.36) | (25.6, 39.6) | 23.0 (4.70) | (13.2, 32.8) |
| Placebo | Post-Trt Wk12 | 8 | 7 | 12.3 (3.20) | (5.6, 18.9) | | |
| Belimumab 10mg/kg | | 8 | 7 | 38.0 (3.31) | (31.1, 44.9) | 25.7 (4.69) | (16.0, 35.5) |
| Placebo | Post-Trt Wk28 | 8 | 7 | 13.5 (3.23) | (6.8, 20.1) | | |
| Belimumab 10mg/kg | | 8 | 6 | 29.0 (3.68) | (21.5, 36.5) | 15.5 (5.10) | (5.1, 26.0) |

**Table S8: Analysis of non-HLA antibodies via ProtoArray (*post hoc* analysis)**

Patient serum from baseline and week 24 was hybridised to ProtoArray (Invitrogen) protein microarrays. P values relate to Wilcoxon rank-sum tests used to compare the belimumab and placebo treatment groups. Kidney specific auto/allo-antibodies were defined in (Li 2009). IQR interquartile range; EDIL3 - EGF-like repeats and discoidin I-like domains 3 (EDIL3) (mean signal of two probes annotated to EDIL3 on array (BC053656.1; BC030828.1)); GDNF - Glial glial cell-derived neurotrophic factor (GDNF). This data is represented visually in Figure 2G-H; S2D-F.

| | Placebo (n=8) | Belimumab 10mg/kg (n=8) | P-value |
|---|---|---|---|
| Number new auto/allo-antibodies above threshold (median (IQR)(range)) | 55.5 (27.5-91) (3-130) | 15.5 (8.75-20) (1-44) | 0.0474 |
| Number new kidney specific auto/allo-antibodies above threshold (median (IQR)(range)) | 12.5 (10.25-14.75) (3-20) | 8.0 (5.75 - 10.0) (5-12) | 0.0524 |
| Mean signal of kidney specific auto/allo-antibodies (median (IQR)(range)) | 1307.3 (1076-1743) (662-2096) | 983.5 (914-1064) (823-1396) | 0.0650 |
| EDIL3 protoarray signal at week 24 (median (IQR)(range)) | 353.6 (305-442) (221-550) | 261.9 (232-296) (191 - 350) | 0.0379 |
| Number of samples with above threshold GDNF binding | | | |
| - baseline | 6 | 6 | |
| - week 24 | 6 | 2 | |

**Table S9: Analysis of B cell intracellular cytokine production following *ex-vivo* stimulation (*post hoc* analysis).** PBMC were stimulated *ex vivo* for 5 hours and intracellular cytokine production quantified by flow cytometry**.** IL-6 and IL-10 secreting B cells are expressed as a percentage of CD19+ cells. Wilcoxon rank-sum tests were performed to compare samples by treatment and visit. This data is represented visually in Figure 3A-C.

| Treatment | Visit | N | n | Endpoint | Median | p value |
|---|---|---|---|---|---|---|
| Placebo | Baseline | 8 | 6 | IL-6 secreting B cells | 29.833 | |
| Belimumab 10mg/kg | | 8 | 2 | IL-6 secreting B cells | 35.833 | 0.8571 |
| Placebo | Last On-Trt | 8 | 4 | IL-6 secreting B cells | 32.183 | |
| Belimumab 10mg/kg | | 8 | 6 | IL-6 secreting B cells | 20.250 | 0.0667 |
| Placebo | Post-Trt Wk12 | 8 | 8 | IL-6 secreting B cells | 42.617 | |
| Belimumab 10mg/kg | | 8 | 8 | IL-6 secreting B cells | 29.175 | 0.0379 |
| Placebo | Post-Trt Wk28 | 8 | 3 | IL-6 secreting B cells | 33.067 | |
| Belimumab 10mg/kg | | 8 | 4 | IL-6 secreting B cells | 32.183 | 0.8571 |
| Placebo | Baseline | 8 | 6 | IL-10 secreting B cells | 1.352 | |
| Belimumab 10mg/kg | | 8 | 2 | IL-10 secreting B cells | 2.702 | 0.2857 |
| Placebo | Last On-Trt | 8 | 4 | IL-10 secreting B cells | 1.575 | |
| Belimumab 10mg/kg | | 8 | 6 | IL-10 secreting B cells | 4.307 | 0.0667 |
| Placebo | Post-Trt Wk12 | 8 | 8 | IL-10 secreting B cells | 2.458 | |
| Belimumab 10mg/kg | | 8 | 8 | IL-10 secreting B cells | 4.555 | 0.0499 |
| Placebo | Post-Trt Wk28 | 8 | 3 | IL-10 secreting B cells | 2.960 | |
| Belimumab 10mg/kg | | 8 | 4 | IL-10 secreting B cells | 3.750 | 0.8571 |
| Placebo | Baseline | 8 | 6 | Ratio of IL-10/IL-6 | 0.043 | |
| Belimumab 10mg/kg | | 8 | 2 | Ratio of IL-10/IL-6 | 0.076 | 0.2857 |
| Placebo | Last On-Trt | 8 | 4 | Ratio of IL-10/IL-6 | 0.049 | |
| Belimumab 10mg/kg | | 8 | 6 | Ratio of IL-10/IL-6 | 0.180 | 0.0095 |
| Placebo | Post-Trt Wk12 | 8 | 8 | Ratio of IL-10/IL-6 | 0.059 | |
| Belimumab 10mg/kg | | 8 | 8 | Ratio of IL-10/IL-6 | 0.127 | 0.0070 |
| Placebo | Post-Trt Wk28 | 8 | 3 | Ratio of IL-10/IL-6 | 0.093 | |
| Belimumab 10mg/kg | | 8 | 4 | Ratio of IL-10/IL-6 | 0.117 | 0.8571 |

**Table S10: Analysis of B cell subset intracellular cytokine production following *ex-vivo* stimulation (*post hoc* analysis).** Peripheral blood mononuclear cells were stimulated *ex vivo* for 5 hours and intracellular cytokine production quantified by flow cytometry**.** The IL-10/IL-6 ratio for individual subsets of naïve (CD27-), transitional (CD24hiCD38hiIgD+), CD24+CD27+ memory, switched memory (CD27+IgD-), and non switched memory (CD27+IgD+) B cells at post treatment Wk 12. Wilcoxon rank-sum tests were performed to compare samples by treatment. This data is represented visually in Figure 3D.

| | Median IL-10/IL-6 at post Trt Week 12 | | |
|---|---|---|---|
| Subset | Placebo (n=8) | Belimumab 10mg/kg (n=8) | P-value |
| Naïve | 0.035 | 0.060 | 0.1327 |
| TrB | 0.100 | 0.225 | 0.0109 |
| CD34+CD27+ memory | 0.150 | 0.230 | 0.0780 |
| Switched memory | 0.225 | 0.275 | 0.4880 |
| Non-switched memory | 0.120 | 0.180 | 0.0185 |

**Table S11: Summary of percent change from baseline of IL10:IL6 ratio (relative to 0ng/mL BLyS) in PBMC from healthy volunteers enriched for CD27+ memory B cells and stimulated for 48 hours with increasing quantities of BLyS (*post hoc* analysis).** In the presence of increasing quantities of BLyS a more inflammatory cytokine milieu was observed. This change was blocked by the addition of belimumab. N, number of healthy volunteers tested for each experimental condition. T-tests were performed to determine

whether the mean percentage changes from baseline differed significantly from 0 for each experimental condition. This data is represented visually in Figure 3E.

| BLyS (ng/ml) | Belimumab (nM) | n | Mean change from baseline (%) | SD | 95% CI of mean | p value |
|---|---|---|---|---|---|---|
| 25 | 0 | 8 | -18.47 | 13.850 | -30.05, -6.89 | 0.0070 |
| 50 | 0 | 6 | -20.47 | 19.447 | -40.88, -0.06 | 0.0495 |
| 100 | 0 | 15 | -22.90 | 24.595 | -36.52, -9.28 | 0.0029 |
| 200 | 0 | 7 | -22.64 | 15.218 | -36.72, -8.57 | 0.0077 |
| 100 | 15 | 7 | 0.63 | 20.448 | -18.28, 19.54 | 0.9377 |

**Table S12: Median serum concentration of belimumab over time.** The lower limit of detection of 100ng. Pharmacokinetics (PK) population that consisted of all subjects randomised to belimumab treatment that were treated with at least one dose and had a PK sample that was analysed. Values at day 0 pre IV dose were imputed. This data is represented visually in Figure S1A-B.

| Time | N | n | median serum concentration of belimumab (µg/ml) | minimum serum concentration of belimumab (µg/ml) | maximum serum concentration of belimumab (µg/ml) |
|---|---|---|---|---|---|
| Day 0 (pre IV dose) | 12 | 12 | 0.00 | 0.00 | 0.00 |
| Day 0 (post IV dose) | 12 | 12 | 212.63 | 134.40 | 309.60 |
| Week 1 | 12 | 12 | 67.06 | 49.98 | 140.98 |
| Week 2 (pre IV dose) | 12 | 12 | 45.76 | 28.56 | 73.10 |
| Week 2 (post IV dose) | 12 | 9 | 291.94 | 207.19 | 468.23 |
| Week 4 (pre IV dose) | 12 | 10 | 100.08 | 26.23 | 177.61 |
| Week 4 (post IV dose) | 12 | 8 | 349.29 | 141.54 | 550.07 |
| Week 8 (pre IV dose) | 12 | 10 | 103.19 | 9.55 | 210.42 |
| Week 12 (pre IV dose) | 12 | 10 | 113.79 | 3.34 | 257.04 |
| Week 20 (post IV dose) | 12 | 8 | 489.89 | 0.11 | 616.84 |
| Week 24 | 12 | 11 | 119.37 | 0.00 | 253.97 |

**Table S13: Analysis of B cell count by visit (*post hoc* analysis).**

1. Adjusted Mean Difference (treatment-placebo) and 95% confidence intervals for differences are obtained from MMRM model, with fixed categorical effects of treatment, visit, donor type and treatment-by-visit interaction and fixed continuous covariates of baseline and baseline-by-visit interaction. A compound symmetry variance structure was used to model the within-patient errors, shared across treatments. B cell count = CD19+ cells/$mm^3$. This data is represented visually in Figure S1C.

**PP Population: Unadjusted baseline values B cell count (cells/$mm^3$)**

| Treatment | Visit | N | n | Mean | SD | Median | Min | Max |
|---|---|---|---|---|---|---|---|---|
| Placebo | Baseline | 8 | 8 | 107.6 | 62.33 | 96 | 32 | 211 |
| Belimumab 10mg/kg | Baseline | 8 | 8 | 105.8 | 91.41 | 70 | 16 | 291 |

**PP Population: Change from baseline in B cell count by visit**

| Treatment | Visit | N | n | Adjusted mean | 95% CI of adjusted mean | Adjusted mean difference (SE)[1] | 95% CI of difference |
|---|---|---|---|---|---|---|---|
| Placebo | On-Trt Wk4 | 8 | 8 | 86.4 | (39.4, 133.5) | | |
| Belimumab 10mg/kg | | 8 | 8 | 71.2 | (24.4, 118.0) | -15.2 (33.01) | (-81.2, 50.7) |
| Placebo | On-Trt Wk8 | 8 | 5 | 115.8 | (56.0, 175.7) | | |
| Belimumab 10mg/kg | | 8 | 7 | 70.3 | (17.4, 123.2) | -45.5 (39.90) | (-125.3, 34.2) |
| Placebo | On-Trt Wk12 | 8 | 8 | 89.2 | (42.1, 136.2) | | |
| Belimumab 10mg/kg | | 8 | 7 | 117.1 | (64.3, 169.9) | 27.9 (35.19) | (-42.4, 98.2) |
| Placebo | On-Trt Wk24 | 8 | 8 | 83.5 | (36.4, 130.6) | | |
| Belimumab 10mg/kg | | 8 | 7 | 55.6 | (5.2, 105.9) | -27.9 (34.02) | (-95.9, 40.0) |

| | | | | | | | |
|---|---|---|---|---|---|---|---|
| Placebo | Post-Trt Wk12 | 8 | 7 | 96.2 | (45.4, 147.0) | | |
| Belimumab 10mg/kg | | 8 | 7 | 32.6 | (-18.0, 83.2) | -63.6 (36.28) | (-136.1, 8.9) |
| Placebo | Post-Trt Wk28 | 8 | 7 | 84 | (33.7, 134.2) | | |
| Belimumab 10mg/kg | | 8 | 6 | 12.1 | (-44.2, 68.4) | -71.9 (37.58) | (-147.0, 3.2) |

**Table S14: Analysis of transitional B cell count by visit.**

1. Adjusted mean difference (treatment-placebo) and 95% confidence intervals for differences are obtained from MMRM model, with fixed categorical effects of treatment, visit, donor type and treatment-by-visit interaction and fixed continuous covariates of baseline and baseline-by-visit interaction. A compound symmetry variance structure was used to model the within-patient errors, shared across treatments. Transitional B cell count = CD19+CD24b+CD38b+IgD+ cells/ml. This data is represented visually in Figure S1F.

**PP Population: Unadjusted baseline values transitional B cell count (cells/ml)**

| Treatment | Visit | N | n | Mean | SD | Median | Min | Max |
|---|---|---|---|---|---|---|---|---|
| Placebo | Baseline | 8 | 8 | 10437.19 | 10071.917 | 7592.85 | 1233.2 | 32697.0 |
| Belimumab 10mg/kg | Baseline | 8 | 7 | 20380.89 | 25680.973 | 9931.33 | 1005.2 | 64790.5 |

**PP Population: Change from baseline in transitional B cell count by visit**

| Treatment | Visit | N | n | Adjusted mean (SE) | 95% CI of adjusted mean | Adjusted mean difference (SE)[1] | 95% CI of difference |
|---|---|---|---|---|---|---|---|
| Placebo | On-Trt Wk4 | 8 | 7 | 3738 (3123.2) | (-2720, 10197) | | |
| Belimumab 10mg/kg | | 8 | 8 | 3240 (3178.6) | (-3350, 9831) | -498 (4433.1) | (-9658, 8663) |
| Placebo | On-Trt Wk8 | 8 | 5 | 4309 (3429.8) | (-2692, 11311) | | |
| Belimumab 10mg/kg | | 8 | 7 | 779 (3283.7) | (-5993, 7550) | -3531 (4677.9) | (-13120, 6059) |
| Placebo | On-Trt Wk12 | 8 | 8 | 4092 (3055.0) | (-2251, 10434) | | |
| Belimumab 10mg/kg | | 8 | 6 | 2315 (3446.5) | (-4743, 9373) | -1777 (4544.2) | (-11129, 7576) |
| Placebo | On-Trt Wk24 | 8 | 8 | 5586 (3031.6) | (-717, 11890) | | |
| Belimumab 10mg/kg | | 8 | 7 | 452 (3371.0) | (-6469, 7374) | -5134 (4519.6) | (-14442, 4174) |
| Placebo | Post-Trt Wk12 | 8 | 7 | 9464 (3119.9) | (3012, 15917) | | |
| Belimumab 10mg/kg | | 8 | 7 | 308 (3178.8) | (-6283, 6899) | -9156 (4427.7) | (-18307, -6) |
| Placebo | Post-Trt Wk28 | 8 | 7 | 8348 (3141.0) | | | |
| Belimumab 10mg/kg | | 8 | 6 | -33 (3614.9) | (-7396, 7329) | -8382 (4847.8) | (-18276, 1513) |

**Table S15: Analysis of memory B cell count by visit (*post hoc* analysis).**

1. Adjusted mean difference (treatment-placebo) and 95% confidence intervals for differences are obtained from MMRM model, with fixed categorical effects of treatment, visit, donor type and treatment-by-visit interaction and fixed continuous covariates of baseline and baseline-by-visit interaction. A compound symmetry variance structure was used to model the within-patient errors, shared across treatments. Memory B cell count = CD20+CD27+ cells/$mm^3$. This data is represented visually in Figure S1G.

**PP Population: Unadjusted baseline values memory B cell count (cells/mm³)**

| Treatment | Visit | N | n | Mean | SD | Median | Min | Max |
|---|---|---|---|---|---|---|---|---|
| Placebo | Baseline | 8 | 8 | 12.9 | 7.75 | 13.0 | 2 | 23 |
| Belimumab 10mg/kg | Baseline | 8 | 8 | 5.8 | 3.11 | 4.5 | 2 | 10 |

**PP Population: Change from baseline in memory B cell count by visit**

| Treatment | Visit | N | n | Adjusted mean (SE) | 95% CI of adjusted mean | Adjusted mean difference (SE)[1] | 95% CI of difference |
|---|---|---|---|---|---|---|---|
| Placebo | On-Trt Wk4 | 8 | 8 | 11.5 (5.12) | (1.2, 21.7) | | |
| Belimumab 10mg/kg | | 8 | 8 | 14.9 (5.40) | (4.1, 25.7) | 3.4 (8.16) | (-12.9, 19.7) |
| Placebo | On-Trt Wk8 | 8 | 4 | 15.8 (8.20) | (-0.6, 32.2) | | |
| Belimumab 10mg/kg | | 8 | 7 | 16.1 (6.06) | (4.0, 28.2) | 0.3 (11.71) | (-23.1, 23.7) |
| Placebo | On-Trt Wk12 | 8 | 7 | 8.9 (5.92) | (-2.9, 20.8) | | |
| Belimumab 10mg/kg | | 8 | 7 | 25.1 (5.97) | (13.2, 37.1) | 16.2 (9.57) | (-2.9, 35.3) |
| Placebo | On-Trt Wk24 | 8 | 8 | 10.7 (5.12) | (0.5, 20.9) | | |
| Belimumab 10mg/kg | | 8 | 7 | 16.4 (5.60) | (5.2, 27.6) | 5.7 (8.22) | (-10.7, 22.2) |
| Placebo | Post-Trt Wk12 | 8 | 7 | 11.4 (5.98) | (-0.6, 23.3) | | |
| Belimumab 10mg/kg | | 8 | 7 | 14.5 (6.16) | (2.2, 26.9) | 3.2 (9.91) | (-16.7, 23.0) |
| Placebo | Post-Trt Wk28 | 8 | 7 | 13.0 (5.31) | (2.4, 23.7) | | |
| Belimumab 10mg/kg | | 8 | 6 | 5.3 (6.04) | (-6.8, 17.4) | -7.8 (8.59) | (-25.0, 9.4) |

**Table S16: Analysis of activated memory B cell (CD95%+) count by visit.**

1. Adjusted mean difference (treatment-placebo) and 95% confidence intervals for differences are obtained from MMRM model, with fixed categorical effects of treatment, visit, donor type and treatment-by-visit interaction and fixed continuous covariates of baseline and baseline-by-visit interaction. A compound symmetry variance structure was used to model the within-patient errors, shared across treatments. Activated memory B cell count = CD19+ CD27+ CD95+ cells/ml. This data is represented visually in Figure S1H.

**PP Population: Unadjusted baseline values activated memory B cell count (cells/ml)**

| Treatment | Visit | N | n | Mean | SD | Median | Min | Max |
|---|---|---|---|---|---|---|---|---|
| Placebo | Baseline | 8 | 8 | 24516.5 | 29798.59 | 12610.3 | 6091 | 93078 |
| Belimumab 10mg/kg | Baseline | 8 | 7 | 10535.3 | 9295.42 | 7131.4 | 876 | 25999 |

**PP Population: Change from baseline in activated memory B cell count by visit**

| Treatment | Visit | N | n | Adjusted mean (SE) | 95% CI of adjusted mean | Adjusted mean difference (SE)[1] | 95% CI of difference |
|---|---|---|---|---|---|---|---|
| Placebo | On-Trt Wk4 | 8 | 8 | 8839.1 (3293.27) | (2151.0, 15527.1) | | |
| Belimumab 10mg/kg | | 8 | 8 | 12900.5 (3556.85) | (5677.0, 20124.0) | 4061.48 (4940.18) | (-5965.7, 14088.6) |
| Placebo | On-Trt Wk8 | 8 | 5 | 6396.7 (4196.14) | (-2029.2, 14822.7) | | |
| Belimumab 10mg/kg | | 8 | 7 | 8189.6 (3850.17) | (411.1, 15968.1) | 1792.88 (5983.11) | (-10234.5, 13820.2) |
| Placebo | On-Trt Wk12 | 8 | 8 | 7696.3 (3293.38) | (1008.1, 14384.5) | | |
| Belimumab 10mg/kg | | 8 | 6 | 8833.6 (4112.07) | (550.4, 17116.8) | 1137.35 (5391.68) | (-9747.1, 12021.8) |
| Placebo | | 8 | 8 | 9266.8 (3295.62) | (2574.4, 15959.2) | | |

| | | | | | | | |
|---|---|---|---|---|---|---|---|
| Belimumab 10mg/kg | On-Trt Wk24 | 8 | 7 | 8735.3 (3720.62) | (1203.8, 16266.8) | -531.55 (5029.91) | (-10727.4, 9664.3) |
| Placebo | Post-Trt Wk12 | 8 | 7 | 21892.8 (3479.10) | (14854.1, 28931.5) | - 14538.52 (5104.63) | (-24875.4, -4201.6) |
| Belimumab 10mg/kg | | 8 | 7 | 7354.3 (3560.25) | (124.4, 14584.1) | | |
| Placebo | Post-Trt Wk28 | 8 | 7 | 20274.1 (3420.31) | (13347.0, 27201.3) | - 15749.48 (5372.70) | (-26595.5, -4903.5) |
| Belimumab 10mg/kg | | 8 | 6 | 4524.7 (4053.36) | (-3642.2, 12691.5) | | |

**Table S17: Analysis of plasmablast count by visit (*post hoc* analysis)**.

1. Adjusted mean difference (treatment-placebo) and 95% confidence intervals for differences are obtained from MMRM model, with fixed categorical effects of treatment, visit, donor type and treatment-by-visit interaction and fixed continuous covariates of baseline and baseline-by-visit interaction. A compound symmetry variance structure was used to model the within-patient errors, shared across treatments. Plasmablast count = CD27+CD38+CD19+ (EVENTS). Values for this rare subset have been normalised and converted to count/mL using the formula: normalised count/mL = [(event count) / (CD19+ event count)] * (CD19+ count per $mm^3$) * 1000 cells/ml. This data is represented visually in Figure S1I.

**PP Population: Unadjusted baseline values plasmablast count (cells/$mm^3$)**

| Treatment | Visit | N | n | Mean | SD | Median | Min | Max |
|---|---|---|---|---|---|---|---|---|
| Placebo | Baseline | 8 | 8 | 973.2 | 935.50 | 726.9 | 218 | 3143 |
| Belimumab 10mg/kg | Baseline | 8 | 8 | 575.7 | 542.24 | 324.6 | 80 | 1629 |

**PP Population: Change from baseline in plasmablast count by visit**

| Treatment | Visit | N | n | Adjusted mean (SE) | 95% CI of adjusted mean | Adjusted mean difference (SE)[1] | 95% CI of difference |
|---|---|---|---|---|---|---|---|
| Placebo | On-Trt Wk4 | 8 | 8 | 63.5 (270.58) | (-479.6, 606.7) | | |
| Belimumab 10mg/kg | | 8 | 8 | -50.2 (269.52) | (-591.4, 491.1) | -113.7 (386.43) | (-889.3, 661.9) |
| Placebo | On-Trt Wk8 | 8 | 4 | 206.4 (376.37) | (-546.1, 958.9) | | |
| Belimumab 10mg/kg | | 8 | 7 | -100.8 (368.77) | (-838.3, 636.7) | -307.2 (479.12) | (-1265.9, 651.4) |
| Placebo | On-Trt Wk12 | 8 | 7 | 187.0 (289.06) | (-392.5, 766.5) | | |
| Belimumab 10mg/kg | | 8 | 7 | 70.3 (297.79) | (-526.5, 667.1) | -116.7 (427.98) | (-974.1, 740.7) |
| Placebo | On-Trt Wk24 | 8 | 8 | 307.7 (270.90) | (-236.0, 851.5) | | |
| Belimumab 10mg/kg | | 8 | 7 | 74.7 (283.62) | (-494.1, 643.6) | -233.0 (393.20) | (-1021.8, 555.8) |
| Placebo | Post-Trt Wk12 | 8 | 7 | 1259.1 (288.55) | (680.6, 1837.7) | | |
| Belimumab 10mg/kg | | 8 | 7 | 203.7 (286.98) | (-371.8, 779.1) | -1055.5 (416.23) | (-1889.7, -221.2) |
| Placebo | Post-Trt Wk28 | 8 | 7 | 1032.8 (287.02) | (457.3, 1608.2) | | |
| Belimumab 10mg/kg | | 8 | 6 | 432.2 (308.99) | (-186.5, 1051.0) | -600.6 (425.67) | (-1453.2, 252.1) |

**Table S18: Analysis of activated T Cell count by visit**.

1. Adjusted mean difference (treatment-placebo) and 95% confidence intervals for differences are obtained from MMRM model, with fixed categorical effects of treatment, visit, donor type and treatment-by-visit interaction and fixed continuous covariates of baseline and baseline-by-visit interaction. A compound symmetry variance structure was used to model the within-patient errors, shared across treatments. Activated T-cell count= CD4+ CD25hi CD45RA- IL7Rhi cells/ml. This data is represented visually in Figure S1J.

**PP Population: Unadjusted baseline values activated T cell count (cells/ml)**

| Treatment | Visit | N | n | Mean | SD | Median | Min | Max |
|---|---|---|---|---|---|---|---|---|
| Placebo | Baseline | 8 | 8 | 103344.1 | 47314.16 | 105357.3 | 31488 | 170276 |
| Belimumab 10mg/kg | Baseline | 8 | 8 | 100793.4 | 52470.57 | 103341.5 | 542 | 169844 |

**PP Population: Activated T cell count by visit**

| Treatment | Visit | N | n | Adjusted mean (SE) | 95% CI of adjusted mean | Adjusted mean difference (SE)[1] | 95% CI of difference |
|---|---|---|---|---|---|---|---|
| Placebo | On-Trt Wk12 | 8 | 5 | 51203.4 (14618.11) | (21342.6, 81064.2) | -15043.8 (21896.18) | (-59669.7, 29582.0) |
| Belimumab 10mg/kg | | 8 | 4 | 36159.5 (16350.26) | (2849.4, 69469.7) | | |
| Placebo | On-Trt Wk24 | 8 | 8 | 57278.7 (11872.54) | (32803.8, 81753.5) | 3881.2 (17477.72) | (-31954.2, 39716.7) |
| Belimumab 10mg/kg | | 8 | 6 | 61159.9 (13288.02) | (33935.5, 88384.3) | | |
| Placebo | Post-Trt Wk12 | 8 | 6 | 41835.9 (13483.91) | (14211.7, 69460.1) | 26387.0 (18975.60) | (-12451.7, 65225.7) |
| Belimumab 10mg/kg | | 8 | 6 | 68222.9 (13529.41) | (40540.1, 95905.8) | | |
| Placebo | Post-Trt Wk28 | 8 | 7 | 63901.1 (12475.65) | (38257.5, 89544.7) | -650.8 (19371.60) | (-40233.6, 38932.0) |
| Belimumab 10mg/kg | | 8 | 5 | 63250.3 15250.65) | (32152.3, 94348.4) | | |

**Table S19: Analysis of regulatory T cell count by visit**.

1. Adjusted mean difference (treatment-placebo) and 95% confidence intervals for differences are obtained from MMRM model, with fixed categorical effects of treatment, visit, donor type and treatment-by-visit interaction and fixed continuous covariates of baseline and baseline-by-visit interaction. A compound symmetry variance structure was used to model the within-patient errors, shared across treatments. Regulatory T-cell count = CD4+ CD25hi IL-7Rlo cells/ml. This data is represented visually in Figure S1K

**PP Population: Unadjusted baseline values regulatory T cell count (cells/ml)**

| Treatment | Visit | N | n | Mean | SD | Median | Min | Max |
|---|---|---|---|---|---|---|---|---|
| Placebo | Baseline | 8 | 8 | 50119.4 | 24537.03 | 49473.7 | 12884 | 97360 |
| Belimumab 10mg/kg | Baseline | 8 | 8 | 37496.1 | 35027.59 | 26074.9 | 192 | 117226 |

**PP Population: Regulatory T cell count by visit**

| Treatment | Visit | N | n | Adjusted mean (SE) | 95% CI of adjusted mean | Adjusted mean difference (SE)[1] | 95% CI of difference |
|---|---|---|---|---|---|---|---|
| Placebo | On-Trt Wk12 | 8 | 6 | 19855.8 (11089.98) | (-2594.7, 42306.3) | -6357.8 (20260.67) | (-47373.3, 34657.8) |
| Belimumab 10mg/kg | | 8 | 4 | 13498.0 (15530.96) | (-17942.7, 44938.8) | | |
| Placebo | On-Trt Wk24 | 8 | 8 | 19196.7 (9437.89) | (90.7, 38302.7) | 3486.5 (13654.12) | (-24154.8, 31127.8) |
| Belimumab 10mg/kg | | 8 | 7 | 22683.3 (9933.17) | (2574.6, 42791.9) | | |
| Placebo | Post-Trt Wk12 | 8 | 7 | 35047.0 (10367.51) | (14059.1, 56034.9) | -14278.4 (14198.12) | (-43021.0, 14464.2) |
| Belimumab 10mg/kg | | 8 | 7 | 20768.6 (9794.01) | (941.6, 40595.5) | | |
| Placebo | Post-Trt Wk28 | 8 | 7 | 27998.4 (10183.27) | (7383.4, 48613.3) | -5143.3 (16598.08) | (-38744.3, 28457.8) |
| Belimumab 10mg/kg | | 8 | 6 | 22855.1 (12004.05) | (-1445.8, 47156.0) | | |

**References**

1. Stohl W, Hiepe F, Latinis KM, et al. Belimumab reduces autoantibodies, normalizes low complement levels, and reduces select B cell populations in patients with systemic lupus erythematosus. *Arthritis Rheum* 2012; **64**(7): 2328-37.

2. Lyons PA, Koukoulaki M, Hatton A, et al. Microarray analysis of human leucocyte subsets: the advantages of positive selection and rapid purification. *BMC Genomics* 2007; **8**: 64.

3. Li L, Wadia P, Chen R, et al. Identifying compartment-specific non-HLA targets after renal transplantation by integrating transcriptome and "antibodyome" measures. *Proc Natl Acad Sci U S A* 2009; **106**(11): 4148-53.

4. Maxfield SJ, Taylor CJ, Kosmoliaptsis V, et al. Transfer of HLA-Specific Allosensitization From a Highly Sensitized Deceased Organ Donor to the Recipients of Each Kidney. *Am J Transplant* 2015; **15**(9): 2501-6.